

NASA Technical Memorandum 80066

(NASA-TM-80066) AN EXPERIMENTAL
INVESTIGATION OF THE EFFECT OF ROTOR TIP
SHAPE ON HELICOPTER BLADE-SLAP NOISE (NASA)
464 p HC A20/MF A01

CSCL 20A

N79-25844

Unclass
G3/71 26036

AN EXPERIMENTAL INVESTIGATION OF THE EFFECT OF ROTOR TIP SHAPE ON HELICOPTER BLADE-SLAP NOISE

Danny R. Hoad

May 1979



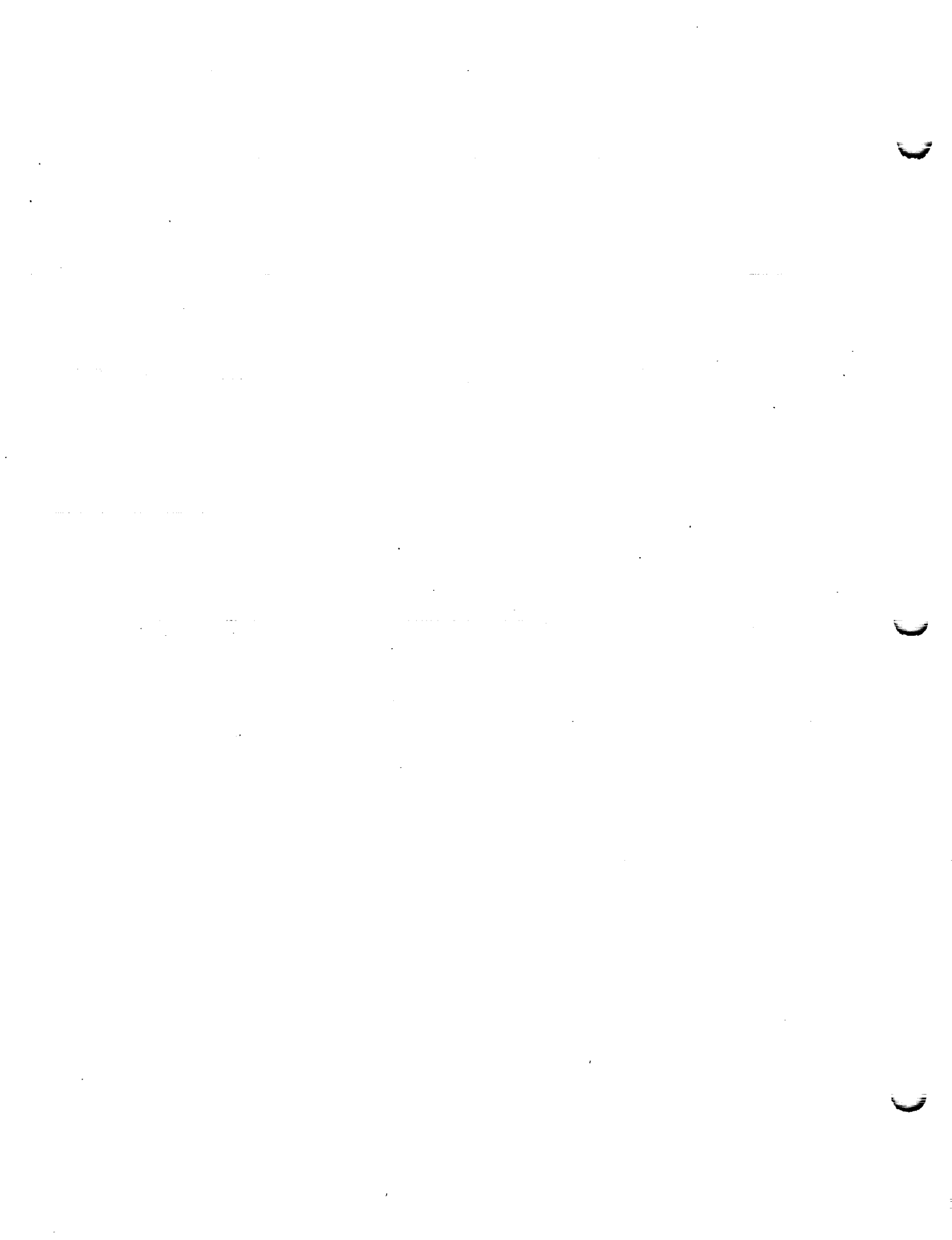
National Aeronautics and
Space Administration

Langley Research Center
Hampton, Virginia 23665





1. Report No. TM 80066	2. Government Accession No.	3. Recipient's Catalog No.	
4. Title and Subtitle AN EXPERIMENTAL INVESTIGATION OF THE EFFECT OF ROTOR TIP SHAPE ON HELICOPTER BLADE-SLAP NOISE		5. Report Date May 1979	6. Performing Organization Code
7. Author(s) Danny R. Hoad		8. Performing Organization Report No.	
9. Performing Organization Name and Address Structures Laboratory USARTL (AVRADCOM) NASA Langley Research Center Hampton, VA 23665		10. Work Unit No. 505-10-23-05	11. Contract or Grant No.
12. Sponsoring Agency Name and Address National Aeronautics and Space Administration Washington, DC 20546 and U.S. Army Aviation R&D Command, St. Louis, MO 63166		13. Type of Report and Period Covered Technical Memorandum	
14. Sponsoring Agency Code			
15. Supplementary Notes			
16. Abstract <p>An experimental investigation of the effect of tip-shape modification on blade-vortex interaction-induced helicopter blade-slap noise has been conducted. The general rotor model system (GRMS) with a 3.148-m (10.33-ft) diameter, four-bladed fully articulated rotor was installed in the Langley V/STOL wind tunnel. The tunnel was operated in the open-throat configuration with treatment to improve the semi-anechoic characteristics of the test chamber.</p> <p>Based on previous investigations, four promising tips (ogee, sub-wing, 60° swept-tapered, and end-plate) were used along with a standard square tip as a baseline configuration. This investigation provided detailed aerodynamic and acoustical data on the same rotor system of the relative applicability of the various tip configurations for blade-slap noise reduction. There data are presented without analysis or discussion.</p>			
17. Key Words (Suggested by Author(s)) Helicopter impulsive noise Blade vortex interaction Wind-tunnel test Aerodynamics		18. Distribution Statement Unclassified - Unlimited Subject Category 71	
19. Security Classif. (of this report) Unclassified	20. Security Classif. (of this page) Unclassified	21. No. of Pages 462	22. Price* \$14.50



SUMMARY

An experimental investigation of the effect of tip-shape modification on blade-vortex interaction-induced helicopter blade-slap noise has been conducted. The general rotor model system (GRMS) with a 3.148-m (10.33-ft) diameter, four-bladed fully articulated rotor was installed in the Langley V/STOL wind tunnel. The tunnel was operated in the open-throat configuration with treatment to improve the semi-anechoic characteristics of the test chamber.

Based on previous investigations, four promising tips (ogee, sub-wing, 60° swept-tapered, and end-plate) were used along with a standard square tip as a baseline configuration. This investigation provided detailed aerodynamic and acoustical data on the same rotor system of the relative applicability of the various tip configurations for blade-slap noise reduction. These data are presented without analysis or discussion.

INTRODUCTION

Helicopter rotor noise is typically separated into categories, such as rotational noise, broadband turbulent interaction noise, and impulsive noise. When present, impulsive noise is usually the most objectionable for the community (refs. 1 and 2) and represents a significant problem for reducing ground detectability of military helicopters. It can occur during high-speed flight as a result of the relatively high advancing blade tip Mach numbers or during partial power descent as a result of the interaction of a blade with a vortex generated by a prior blade passage.

Four promising tip configurations for reducing the peak velocity, or strength, of the generated tip vortex were chosen along with a standard square tip to be compared on a realistically scaled model rotor system in a semi-anechoic facility both in performance and acoustics. These tip configurations were: (1) an ogee tip (refs. 3 and 4); (2) a sub-wing tip (refs. 5 and 6); (3) a swept-tapered tip (ref. 7); and (4) an end-plate tip (ref. 8). (See figs. 1 and 2.)

SYMBOLS

The axes used for the aerodynamic data presented for this investigation are presented in figures 3 and 4. The units for the physical quantities defined in this paper are presented in both the International System of Units (SI), and where appropriate, parenthetically in U.S. Customary Units. Conversion factors used for these units are given in reference 9.

a_{1s} first harmonic of rotor lateral flapping, deg

a_0 rotor coning angle, deg

A_1	rotor longitudinal cyclic, measured at 75-percent R, deg
b_{1s}	first harmonic of rotor longitudinal flapping, deg
B_1	rotor lateral cyclic, measured at 75-percent R, deg
c	blade chord, 10.77 cm (4.24 in.)
C_Q	rotor torque coefficient, $\frac{\text{Torque}}{4 \int_0^R \frac{1}{2} \rho(\Omega r)^2 c(r) r dr}$
C_T	rotor thrust coefficient, $\frac{\text{Thrust}}{4 \int_0^R \frac{1}{2} \rho(\Omega r)^2 c(r) dr}$
D	rotor drag, N (lb)
L	rotor lift, N (lb)
r	local blade span, m (ft)
R	rotor radius with square tip, m (ft)
R'	rotor radius with any tip, m (ft)
V_T	rotor tip speed, m/sec (ft/sec)
V_∞	free-stream velocity, m/sec (ft/sec)
α_c	rotor shaft angle of attack, deg
α_{TPP}	rotor tip-path-plane attitude, referenced to tunnel geometric centerline, deg
γ	descent angle, $\tan^{-1}(D/L)$, deg
θ_c	rotor collective, measured at 75-percent R, deg
μ	advance ratio, V_∞/V_T
ρ	free-stream density, kg/m^3 (slugs/ft^3)
Ω	rotor rotational speed, 1200 rpm

Notation:

BVI	blade vortex interaction
rpm	revolutions per minute
SPL	sound pressure level, dB

HELICOPTER MODEL AND TEST FACILITY

Helicopter Model

The general rotor model system (GRMS) in the Langley V/STOL tunnel was used for this investigation (ref. 10). The fuselage was an arbitrary shape, one rotor diameter in length, designed to enclose the basic model, transmission, and controls for the rotor system. A sketch of the helicopter model is provided in figure 4.

The main rotor used in this investigation had four blades on a fully articulated hub. Rotor blade construction was a graphite composite spar with balsa-ribbed trailing surfaces wrapped by fiberglass and kevlar skins. The baseline blade configuration (square tip) had a revolved tip cap with a overall baseline rotor radius (R) of 157.4 cm (61.98 in.), blade chord of 10.77 cm (4.24 in.), and a NACA 0012 airfoil section. The baseline rotor (square tip) had a solidity (bc/R) of 0.0871, a root cutout of 20 percent, and -8° of linear twist. Each blade tip had interchangeable tip fittings with four available tip configurations. (See figs. 1 and 2.) Tangler's sub-wing (ref. 5) was used with a span of 0.3538 blade chords and a chord of 0.20 blade chords. It was positioned 0.56 cm (0.22 in.) behind the blade leading edge and 0.20 cm (0.08 in.) above the blade chord line. It had 0° incidence, 0° dihedral referenced to the blade chord at the tip, and a NACA 0012 airfoil section. Maximum blade radius was increased 2.02 percent for this tip configuration. White's end plate (ref. 8) which included a vertical fin on the upper-surface tip trailing edge with 22.29° leading-edge sweep was tested. The end-plate leading-edge apex intersection with blade chord was at 60-percent blade chord station. Its chord line was perpendicular to blade chord with 90° dihedral and had a NACA 0012 airfoil section. The ogee-tip configuration (refs. 3 and 4) was tested with a NACA 0012 airfoil maintained to the tip. The chord distribution for this tip configuration is presented in table 1. Maximum blade radius was increased by 4.74 percent in order to maintain blade area consistency with the square-tip configuration. The swept-tapered tip was designed with maximum blade radius consistent with the square tip. Blade thickness was linearly tapered from the NACA 0012 airfoil section at 94.09-percent radius to a NACA 0010 airfoil section at the 96.06-percent radius--beginning of 60° sweep on leading edge. The thickness was further tapered linearly to a NACA 0006 airfoil section at the tip.

The rotor hub was fully articulated with cyclic and collective pitch on the blades controlled by a swashplate driven by remotely controlled actuators. Blade-flapping and lead-lag angles were measured at the flapping-hinge offset which was 7.71 cm (3.04 in.) radius from the rotor axis. The rotor was driven by twin 67-kW (90-hp) electric motors driving a common transmission. These variable-speed electric motors were water cooled through an umbilical from an external water source. The transmission was cooled and lubricated by oil pumped into the model through the umbilical. The entire system--rotor, transmission, and motor--was mounted on a six-component strain-gage balance within the model to measure rotor forces and moments. Even though the fuselage was on a separate balance and the complete model was balance mounted for other purposes, the performance data presented in this report are based on measurements obtained from the rotor balance.

Wind-Tunnel Facility

The model investigation was conducted in the Langley V/STOL tunnel. The variable-wall configuration of the facility includes an open-throat test chamber, accomplished by raising the side walls and the ceiling. The dimensions of the rectangular jet entrance to the test chamber are 4.42 m (14.50 ft) high by 6.63 m (21.75 ft) wide. The ceiling height in the configuration is approximately 7.50 m (24.60 ft) above the test chamber floor. An evaluation of the feasibility of obtaining realistic free-field noise measurements in this facility in the open-throat configuration was conducted by Ver (ref. 11). He found that the test chamber was semireverberant and suggested a model study to ascertain the amount and kind of acoustical treatment needed to improve the free-field measurement capability of the facility. The results of this modeling study are available in reference 12. It was found that 12.7-cm (5.0-in.) thick aluminum panels filled with fiberglass on the raised ceiling and the test-section floor below it constituted the most effective method in increasing the anechoic characteristics of the facility. The recommended treatment to the floor was installed; however, practical aspects of interchangeability of test-section configuration precluded using the suggested ceiling treatment. Open-cell polyurethane (10.16-cm (4.00-in.) thick) pads were installed on the ceiling for this purpose. After each acoustic investigation, this treatment could be easily removed. A follow-on evaluation of the effectiveness of this treatment was conducted and reported in reference 13. Results indicated that the hall radius was increased substantially and that accurate free-field measurements would be obtained up to about 0.3 m (1.0 ft) from any tunnel surface.

Instrumentation

The acoustic transducers used for this investigation were 1.27-cm (0.50-in.) diameter condensor microphones fitted with standard Brüel and Kjaer (B&K) nose cones. Seven microphones were positioned in the flow around the model as presented in figure 5. A photograph of the model installed in the V/STOL tunnel with floor treatment and microphones is presented in figure 6. The location of these microphones relative to the rotor hub with the model at 0° angle of attack are presented in table II. Three microphones (nos. 1, 2, and 3) were mounted on the fuselage in locations shown to be relatively sensitive to blade vortex interaction (BVI) blade slap (refs. 14 and 15). Three microphones (nos. 5, 6, and 7) were mounted ahead of the model as far as possible from the rotor--yet in the free-field environment of the facility--at about 30° off rotor tip-path plane. The directivity of the BVI blade slap has been shown experimentally (refs. 1, 16, and 17) and theoretically (ref. 18) to be a maximum in this direction. One microphone (no. 4) was positioned in the tip-path plane to measure thickness noise at high tip speeds. Signals from each microphone were fed through an amplifier-attenuator and into a 14-channel frequency-modulated (FM) tape recorder operating at 76.2 cm/sec (30.0 in./sec) tape speed along with a blade azimuth indicator and time code.

OPERATING PROCEDURES AND DATA REDUCTION

Operating Procedures

Realistic representation of helicopter flight at model scale is difficult. Flight parameters most sensitive to model scale testing have been studied (ref. 19) concluding that rotor tip speed, advance ratio, thrust coefficient, blade elasticity, rotor solidity, and Reynolds number are important. Since this investigation was not concerned with exact duplication of a flight vehicle, primary concern was obtaining a typical rotor-wake deflection in flight. Rotor-tip speed, advance ratio, and thrust coefficient are prime factors in this regard. A tip speed of about 198 m/sec (650 ft/sec) and a thrust coefficient of about 0.36 was chosen. This thrust coefficient was not computed as is typically done for helicopters. The nondimensionalizing factor used will be discussed later.

A typical flight envelope for the occurrence of BVI blade slap (ref. 14) is presented in figure 7. This figure was the result of an observer's assessment in the cabin of an AH-1G helicopter (ref. 14). It has been shown that this observation does not always provide a real assessment of the propagation or occurrence of blade slap. It does, however, provide an indication of the flight conditions required to bracket the envelope of blade-slap intensity.

The procedure used to establish each flight condition was to set a constant tunnel velocity equal to the desired flight speed, thus setting advance ratio ($\mu = V_\infty/V_T$). Adjusting collective, cyclics, and model angle of attack to obtain desired rotor lift (in this case, 1.78 kN (400 lbs)) and balanced rotor pitching moment and rolling moment. At the same time, the rotor tip-path plane was varied primarily by model angle of attack to obtain the desired descent angle ($\gamma = \tan^{-1}(D/L)$). With the rotor system at the desired condition (μ , lift, pitching moment, rolling moment, and γ), 30 seconds of information from the microphones were recorded on the FM tape recorder. Corresponding model and tunnel information was recorded on the tunnel computer data acquisition system coincidentally.

Critical to comparison of the noise radiated due to tip shape is model position and attitude consistency at each matched test condition. Special consideration was given to carefully setting each test condition of the various tips to that conducted with the square tip. Cyclic control and collective settings may have been different due to performance differences, but model angle of attack, lift, pitching and rolling moments, advanced ratio, and most importantly, tip-path-plane attitude were carefully matched between tip tests as much as possible. The tip-path-plane attitude was computed from the rotor shaft angle (referenced to tunnel geometric centerline) and the longitudinal flapping angle. This tip-path-plane attitude must remain consistent between tip configurations at identical model operating conditions to minimize ambiguity related to directivity characteristics of the noise source. At each tunnel velocity tested, background noise measurements were made with blades off and rotor hub turning at the test condition (1200 rpm).

Data Reduction, Correction, and Presentation

Corrections due to jet boundary and blockage effects have been made to the aerodynamic data presented herein--except the tip-path-plane angle (α_{TPP}). These corrections in an open-throat tunnel primarily affect angle of attack (ref. 20).

The blade-tip configurations when installed were not consistent in blade area and radius (tip speed) for reasons mentioned before. Because of this situation, it was felt that the traditional nondimensionalization of rotor forces and moments (rotor disk area and tip speed) would bias the performance analysis of some tips. Therefore, this nondimensionalization factor was developed by obtaining the integral of local area and velocity as function of blade span (γ):

$$C_T = \frac{\text{Thrust}}{4 \int_0^R \frac{1}{2} \rho(\Omega r)^2 c(r) dr}$$

$$C_Q = \frac{\text{Torque}}{4 \int_0^R \frac{1}{2} \rho(\Omega r)^2 c(r) r dr}$$

where ρ = free-stream density; r = local blade span; $c(r)$ = local blade chord function of blade span; and R = total blade span.

These factors are effective thrust-weighted solidity and torque weighted solidity. They were constant throughout the test except for variations in density. However, assuming standard density--for example, these factors would be:

	$4 \int_0^R \frac{1}{2} \rho(\Omega r)^2 c(r) dr$	$4 \int_0^R \frac{1}{2} \rho(\Omega r)^2 c(r) r dr$		
	N	(lb)	m-N	(in., -lb)
Square & end plate	5382.57	(1210.05)	6397.8	(56,625)
Ogee	5410.64	(1216.36)	6448.5	(57,074)
Sub-wing	5446.67	(1224.46)	6499.7	(57,527)
Swept-tapered	5081.69	(1142.41)	5930.2	(52,487)

Before and after the tests, "pink" and "white" noise signals were recorded to verify that the complete system (excluding the microphones) had a flat frequency response over the range of interest (50-10,000 Hz). All microphones were calibrated with a 125-dB piston-phone at 250 Hz before and after each series of tests.

The acoustic data were analyzed for one-third-octave and narrowband sound pressure levels (SPL) and flight-scaled dBA weighted overall sound pressure levels (OASPL). The analysis used is described in reference 21. Absolute values of peak-to-peak amplitude of the BVI impulses were determined. The one-third-octave and narrowband analyses were obtained from a 2-second (40-rotor revolutions) digital record of each test condition. Each acoustic record was band-pass filtered at 50-10,000 Hz and digitized at the rate of 20,000 samples per second. Each record was divided into a number of blocks each corresponding to one rotor revolution (0.05 sec) and triggered at the instant in time when the instrumented blade passed over the tail of the fuselage. This, with the digitizing rate of 20,000 samples per second, resulted in a constant bandwidth of 19.5 Hz.

The aerodynamic results of this investigation have been presented in coefficient form. Complete helicopter performance analysis can be obtained in reference 22. The rotor forces and moments are resolved in the stability-axis system and about a center of gravity on the rotor shaft axis near the vertical center of the body (fig. 4). Pertinent aerodynamic performance data are provided in Tables III to VII.

Aerodynamic results are presented in the following order without analysis:

	<u>Figure</u>
Performance comparison of rotor-tip configurations in hover.....	8
Performance comparison of rotor tip configurations at various forward speeds.....	9

The acoustic data obtained during the investigation have been analyzed in one-third-octave centerband frequency and selected narrowband analyses. Each one-third-octave figure presented herein was acquired at constant rotor lift (1.78 kN (400 lb)) and balanced pitching and rolling moments. On each figure, one-third-octave spectra are presented for various descent angles all at constant tunnel velocities. Background noise one-third-octave spectra are provided for similar tunnel velocities as it was acquired with blades off and hub turning.

Sample pressure-time histories and narrowband analyses are included for selected microphones. Two are presented for selected one-third-octave figures--one with light or no discernible blade slap and one with the most intense blade slap. The time scale on the pressure-time histories are presented in terms of one rotor revolution. These data are presented in the following order without analysis:

	<u>Figure</u>
Tunnel velocity \approx 51 knots	
A. Square tip, $V_\infty = 51.4$ knots.....	10
1. One-third octave, microphone no. 1.....	(a)
2. Pressure-time histories, microphone no. 1.....	(b)
3. Narrowband analysis, microphone no. 1, $\gamma = -4.49^\circ$	(c)

Figure

- 4. Narrowband analysis, microphone no. 1, $\gamma = 4.23^\circ$ (d)
 - 5. One-third octave, microphone no. 2..... (e)
 - 6. Pressure-time histories, microphone no. 2..... (f)
 - 7. Narrowband analysis, microphone no. 2, $\gamma = -4.49^\circ$ (g)
 - 8. Narrowband analysis, microphone no. 2, $\gamma = 2.15^\circ$ (h)
 - 9. One-third octave, microphone no. 3..... (i)
 - 10. Pressure time histories, microphone no. 3..... (j)
 - 11. Narrowband analysis, microphone no. 3, $\gamma = -4.49^\circ$ (k)
 - 12. Narrowband analysis, microphone no. 3, $\gamma = 2.15^\circ$ (l)
 - 13. One-third octave, microphone no. 4..... (m)
 - 14. Pressure-time histories, microphone no. 4..... (n)
 - 15. Narrowband analysis, microphone no. 4, $\gamma = -2.47^\circ$ (o)
 - 16. Narrowband analysis, microphone no. 4, $\gamma = 6.41^\circ$ (p)
 - 17. One-third octave, microphone no. 5..... (q)
 - 18. Pressure-time histories, microphone no. 5..... (r)
 - 19. Narrowband analysis, microphone no. 5, $\gamma = -4.49^\circ$ (s)
 - 20. Narrowband analysis, microphone no. 5, $\gamma = 4.23^\circ$ (t)
 - 21. One-third octave, microphone no. 6..... (u)
 - 22. Pressure-time histories, microphone no. 6..... (v)
 - 23. Narrowband analysis, microphone no. 6, $\gamma = -1.12^\circ$ (w)
 - 24. Narrowband analysis, microphone no. 6, $\gamma = 4.23^\circ$ (x)
 - 25. One-third octave, microphone no. 7..... (y)
 - 26. Pressure-time histories, microphone no. 7..... (z)
 - 27. Narrowband analysis, microphone no. 7, $\gamma = -1.12^\circ$ (aa)
 - 28. Narrowband analysis, microphone no. 7, $\gamma = 4.23^\circ$ (bb)
- B. Ogee tip, $V_\infty = 51.0$ knots..... 11
- 1. One third octave, microphone no. 1..... (a)
 - 2. Pressure-time histories, microphone no. 1..... (b)
 - 3. Narrowband analysis, microphone no. 1, $\gamma = -1.08^\circ$ (c)
 - 4. Narrowband analysis, microphone no. 1, $\gamma = 2.07^\circ$ (d)
 - 5. One-third octave, microphone no. 2..... (e)
 - 6. Pressure-time histories, microphone no. 2..... (f)
 - 7. Narrowband analysis, microphone no. 2, $\gamma = -1.08^\circ$ (g)
 - 8. Narrowband analysis, microphone no. 2, $\gamma = 2.07^\circ$ (h)
 - 9. One-third octave, microphone no. 3..... (i)
 - 10. Pressure time histories, microphone no. 3..... (j)
 - 11. Narrowband analysis, microphone no. 3, $\gamma = -1.08^\circ$ (k)
 - 12. Narrowband analysis, microphone no. 3, $\gamma = 2.07^\circ$ (l)
 - 13. One-third octave, microphone no. 4..... (m)
 - 14. Pressure-time histories, microphone no. 4..... (n)
 - 15. Narrowband analysis, microphone no. 4, $\gamma = -1.08^\circ$ (o)
 - 16. Narrowband analysis, microphone no. 4, $\gamma = 6.45^\circ$ (p)
 - 17. One-third octave, microphone no. 5..... (q)
 - 18. Pressure-time histories, microphone no. 5..... (r)
 - 19. Narrowband analysis, microphone no. 5, $\gamma = -1.08^\circ$ (s)
 - 20. Narrowband analysis, microphone no. 5, $\gamma = 4.24^\circ$ (t)
 - 21. One-third octave, microphone no. 6..... (u)
 - 22. Pressure-time histories, microphone no. 6..... (v)

Figure

23.	Narrowband analysis, microphone no. 6, $\gamma = -1.08^\circ$	(w)
24.	Narrowband analysis, microphone no. 6, $\gamma = 4.24^\circ$	(x)
25.	One-third octave, microphone no. 7.....	(y)
26.	Pressure-time histories, microphone no. 7.....	(z)
27.	Narrowband analysis, microphone no. 7, $\gamma = -1.08^\circ$	(aa)
28.	Narrowband analysis, microphone no. 7, $\gamma = 4.24^\circ$	(bb)
C.	Sub-wing tip, $V_\infty = 51.1$ knots.....	12
1.	One third octave, microphone no. 1.....	(a)
2.	Pressure-time histories, microphone no. 1.....	(b)
3.	Narrowband analysis, microphone no. 1, $\gamma = -2.16^\circ$	(c)
4.	Narrowband analysis, microphone no. 1, $\gamma = 2.15^\circ$	(d)
5.	One-third octave, microphone no. 3.....	(e)
6.	Pressure-time histories, microphone no. 3.....	(f)
7.	Narrowband analysis, microphone no. 3, $\gamma = -2.16^\circ$	(g)
8.	Narrowband analysis, microphone no. 3, $\gamma = 1.11^\circ$	(h)
9.	One-third octave, microphone no. 4.....	(i)
10.	Pressure time histories, microphone no. 4.....	(j)
11.	Narrowband analysis, microphone no. 4, $\gamma = -2.16^\circ$	(k)
12.	Narrowband analysis, microphone no. 4, $\gamma = 4.23^\circ$	(l)
13.	One-third octave, microphone no. 5.....	(m)
14.	Pressure-time histories, microphone no. 5.....	(n)
15.	Narrowband analysis, microphone no. 5, $\gamma = -2.16^\circ$	(o)
16.	Narrowband analysis, microphone no. 5, $\gamma = 2.15^\circ$	(p)
17.	One-third octave, microphone no. 6.....	(q)
18.	Pressure-time histories, microphone no. 6.....	(r)
19.	Narrowband analysis, microphone no. 6, $\gamma = -2.16^\circ$	(s)
20.	Narrowband analysis, microphone no. 6, $\gamma = 2.15^\circ$	(t)
21.	One-third octave, microphone no. 7.....	(u)
22.	Pressure-time histories, microphone no. 7.....	(v)
23.	Narrowband analysis, microphone no. 7, $\gamma = -2.16^\circ$	(w)
24.	Narrowband analysis, microphone no. 7, $\gamma = 2.15^\circ$	(x)
D.	Swept-tapered tip, $V_\infty = 50.6$ knots.....	13
1.	One third octave, microphone no. 1.....	(a)
2.	Pressure-time histories, microphone no. 1.....	(b)
3.	Narrowband analysis, microphone no. 1, $\gamma = -2.30^\circ$	(c)
4.	Narrowband analysis, microphone no. 1, $\gamma = 2.24^\circ$	(d)
5.	One-third octave, microphone no. 2.....	(e)
6.	Pressure-time histories, microphone no. 2.....	(f)
7.	Narrowband analysis, microphone no. 2, $\gamma = -2.30^\circ$	(g)
8.	Narrowband analysis, microphone no. 2, $\gamma = 2.24^\circ$	(h)
9.	One-third octave, microphone no. 3.....	(i)
10.	Pressure time histories, microphone no. 3.....	(j)
11.	Narrowband analysis, microphone no. 3, $\gamma = -2.30^\circ$	(k)
12.	Narrowband analysis, microphone no. 3, $\gamma = 2.24^\circ$	(l)
13.	One-third octave, microphone no. 4.....	(m)
14.	Pressure-time histories, microphone no. 4.....	(n)
15.	Narrowband analysis, microphone no. 4, $\gamma = -2.30^\circ$	(o)

Figure

16.	Narrowband analysis, microphone no. 4, $\gamma = 4.13^\circ$	(p)
17.	One-third octave, microphone no. 5.....	(q)
18.	Pressure-time histories, microphone no. 5.....	(r)
19.	Narrowband analysis, microphone no. 5, $\gamma = -2.30^\circ$	(s)
20.	Narrowband analysis, microphone no. 5, $\gamma = 4.13^\circ$	(t)
21.	One-third octave, microphone no. 6.....	(u)
22.	Pressure-time histories, microphone no. 6.....	(v)
23.	Narrowband analysis, microphone no. 6, $\gamma = -2.30^\circ$	(w)
24.	Narrowband analysis, microphone no. 6, $\gamma = 4.13^\circ$	(x)
25.	One-third octave, microphone no. 7.....	(y)
26.	Pressure-time histories, microphone no. 7.....	(z)
27.	Narrowband analysis, microphone no. 7, $\gamma = -2.30^\circ$	(aa)
28.	Narrowband analysis, microphone no. 7, $\gamma = 4.13^\circ$	(bb)
E.	End-plate tip, $V_\infty = 50.4$ knots.....	14
1.	One third octave, microphone no. 1.....	(a)
2.	Pressure-time histories, microphone no. 1.....	(b)
3.	Narrowband analysis, microphone no. 1, $\gamma = -2.21^\circ$	(c)
4.	Narrowband analysis, microphone no. 1, $\gamma = 2.14^\circ$	(d)
5.	One-third octave, microphone no. 2.....	(e)
6.	Pressure-time histories, microphone no. 2.....	(f)
7.	Narrowband analysis, microphone no. 2, $\gamma = -2.21^\circ$	(g)
8.	Narrowband analysis, microphone no. 2, $\gamma = 1.01^\circ$	(h)
9.	One-third octave, microphone no. 3.....	(i)
10.	Pressure time histories, microphone no. 3.....	(j)
11.	Narrowband analysis, microphone no. 3, $\gamma = -2.21^\circ$	(k)
12.	Narrowband analysis, microphone no. 3, $\gamma = 4.28^\circ$	(l)
13.	One-third octave, microphone no. 4.....	(m)
14.	Pressure-time histories, microphone no. 4.....	(n)
15.	Narrowband analysis, microphone no. 4, $\gamma = -2.21^\circ$	(o)
16.	Narrowband analysis, microphone no. 4, $\gamma = 4.48^\circ$	(p)
17.	One-third octave, microphone no. 5.....	(q)
18.	Pressure-time histories, microphone no. 5.....	(r)
19.	Narrowband analysis, microphone no. 5, $\gamma = -2.21^\circ$	(s)
20.	Narrowband analysis, microphone no. 5, $\gamma = 4.48^\circ$	(t)
21.	One-third octave, microphone no. 6.....	(u)
22.	Pressure-time histories, microphone no. 6.....	(v)
23.	Narrowband analysis, microphone no. 6, $\gamma = -2.21^\circ$	(w)
24.	Narrowband analysis, microphone no. 6, $\gamma = 1.01^\circ$	(x)
25.	One-third octave, microphone no. 7.....	(y)
26.	Pressure-time histories, microphone no. 7.....	(z)
27.	Narrowband analysis, microphone no. 7, $\gamma = -2.21^\circ$	(aa)
28.	Narrowband analysis, microphone no. 7, $\gamma = 1.01^\circ$	(bb)

Tunnel velocity ≈ 56 knots

A.	Square tip, $V_\infty = 56.2$ knots.....	15
1.	One-third octave, microphone no. 1.....	(a)
2.	One-third octave, microphone no. 2.....	(b)
3.	Pressure-time histories, microphone no. 2.....	(c)
4.	One-third octave, microphone no. 3.....	(d)

Figure

5. Pressure-time histories, microphone no. 3.....	(e)
6. One-third octave, microphone no. 4.....	(f)
7. One-third octave, microphone no. 5.....	(g)
8. Pressure-time histories, microphone no. 5.....	(h)
9. One-third octave, microphone no. 6.....	(i)
10. One-third octave, microphone no. 7.....	(j)
 B. Ogee tip, $V_\infty = 55.9$ knots.....	16
1. One-third octave, microphone no. 1.....	(a)
2. One-third octave, microphone no. 2.....	(b)
3. Pressure-time histories, microphone no. 2.....	(c)
4. One-third octave, microphone no. 3.....	(d)
5. Pressure-time histories, microphone no. 3.....	(e)
6. One-third octave, microphone no. 4.....	(f)
7. One-third octave, microphone no. 5.....	(g)
8. Pressure-time histories, microphone no. 5.....	(h)
9. One-third octave, microphone no. 6.....	(i)
10. One-third octave, microphone no. 7.....	(j)
 C. Sub-wing tip, $V_\infty = 55.8$ knots.....	17
1. One-third octave, microphone no. 1.....	(a)
2. One-third octave, microphone no. 2.....	(b)
3. Pressure-time histories, microphone no. 2.....	(c)
4. One-third octave, microphone no. 3.....	(d)
5. Pressure-time histories, microphone no. 3.....	(e)
6. One-third octave, microphone no. 4.....	(f)
7. One-third octave, microphone no. 5.....	(g)
8. Pressure-time histories, microphone no. 5.....	(h)
9. One-third octave, microphone no. 6.....	(i)
10. One-third octave, microphone no. 7.....	(j)
 D. Swept-tapered tip, $V_\infty = 55.8$ knots.....	18
1. One-third octave, microphone no. 1.....	(a)
2. One-third octave, microphone no. 2.....	(b)
3. Pressure-time histories, microphone no. 2.....	(c)
4. One-third octave, microphone no. 3.....	(d)
5. Pressure-time histories, microphone no. 3.....	(e)
6. One-third octave, microphone no. 4.....	(f)
7. One-third octave, microphone no. 5.....	(g)
8. Pressure-time histories, microphone no. 5.....	(h)
9. One-third octave, microphone no. 6.....	(i)
10. One-third octave, microphone no. 7.....	(j)
 E. End-plate tip, $V_\infty = 55.3$ knots.....	19
1. One-third octave, microphone no. 1.....	(a)
2. One-third octave, microphone no. 2.....	(b)
3. Pressure-time histories, microphone no. 2.....	(c)
4. One-third octave, microphone no. 3.....	(d)
5. Pressure-time histories, microphone no. 3.....	(e)

Figure

6.	One-third octave, microphone no. 4.....	(f)
7.	One-third octave, microphone no. 5.....	(g)
8.	Pressure-time histories, microphone no. 5.....	(h)
9.	One-third octave, microphone no. 6.....	(i)
10.	One-third octave, microphone no. 7.....	(j)

Tunnel velocity \approx 61 knots

A.	Square tip, $V_\infty = 61.3$ knots.....	20
1.	One-third octave, microphone no. 1.....	(a)
2.	One-third octave, microphone no. 2.....	(b)
3.	Pressure-time histories, microphone no. 2.....	(c)
4.	One-third octave, microphone no. 3.....	(d)
5.	Pressure-time histories, microphone no. 3.....	(e)
6.	One-third octave, microphone no. 4.....	(f)
7.	One-third octave, microphone no. 5.....	(g)
8.	Pressure-time histories, microphone no. 5.....	(h)
9.	One-third octave, microphone no. 6.....	(i)
10.	One-third octave, microphone no. 7.....	(j)
B.	Ogee tip, $V_\infty = 61.2$ knots.....	21
1.	One-third octave, microphone no. 1.....	(a)
2.	One-third octave, microphone no. 2.....	(b)
3.	Pressure-time histories, microphone no. 2.....	(c)
4.	One-third octave, microphone no. 3.....	(d)
5.	Pressure-time histories, microphone no. 3.....	(e)
6.	One-third octave, microphone no. 4.....	(f)
7.	One-third octave, microphone no. 5.....	(g)
8.	Pressure-time histories, microphone no. 5.....	(h)
9.	One-third octave, microphone no. 6.....	(i)
10.	One-third octave, microphone no. 7.....	(j)
C.	Sub-wing tip, $V_\infty = 60.9$ knots.....	22
1.	One-third octave, microphone no. 1.....	(a)
2.	One-third octave, microphone no. 2.....	(b)
3.	Pressure-time histories, microphone no. 2.....	(c)
4.	One-third octave, microphone no. 3.....	(d)
5.	Pressure-time histories, microphone no. 3.....	(e)
6.	One-third octave, microphone no. 4.....	(f)
7.	One-third octave, microphone no. 5.....	(g)
8.	Pressure-time histories, microphone no. 5.....	(h)
9.	One-third octave, microphone no. 6.....	(i)
10.	One-third octave, microphone no. 7.....	(j)
D.	Swept-tapered tip, $V_\infty = 60.6$ knots.....	23
1.	One-third octave, microphone no. 1.....	(a)
2.	One-third octave, microphone no. 2.....	(b)
3.	Pressure-time histories, microphone no. 2.....	(c)
4.	One-third octave, microphone no. 3.....	(d)
5.	Pressure-time histories, microphone no. 3.....	(e)
6.	One-third octave, microphone no. 4.....	(f)

Figure

7. One-third octave, microphone no. 5.....	(g)
8. Pressure-time histories, microphone no. 5.....	(h)
9. One-third octave, microphone no. 6.....	(i)
10. One-third octave, microphone no. 7.....	(j)
E. End-plate tip, $V_\infty = 62.3$ knots.....	24
1. One-third octave, microphone no. 1.....	(a)
2. One-third octave, microphone no. 2.....	(b)
3. Pressure-time histories, microphone no. 2.....	(c)
4. One-third octave, microphone no. 3.....	(d)
5. Pressure-time histories, microphone no. 3.....	(e)
6. One-third octave, microphone no. 4.....	(f)
7. One-third octave, microphone no. 5.....	(g)
8. Pressure-time histories, microphone no. 5.....	(h)
9. One-third octave, microphone no. 6.....	(i)
10. One-third octave, microphone no. 7.....	(j)
Tunnel velocity ≈ 66 knots	
A. Square tip, $V_\infty = 65.7$ knots.....	25
1. One-third octave, microphone no. 1.....	(a)
2. One-third octave, microphone no. 2.....	(b)
3. Pressure-time histories, microphone no. 2.....	(c)
4. One-third octave, microphone no. 3.....	(d)
5. Pressure-time histories, microphone no. 3.....	(e)
6. One-third octave, microphone no. 4.....	(f)
7. One-third octave, microphone no. 5.....	(g)
8. Pressure-time histories, microphone no. 5.....	(h)
9. One-third octave, microphone no. 6.....	(i)
10. One-third octave, microphone no. 7.....	(j)
B. Ogee tip, $V_\infty = 66.7$ knots.....	26
1. One-third octave, microphone no. 1.....	(a)
2. One-third octave, microphone no. 2.....	(b)
3. Pressure-time histories, microphone no. 2.....	(c)
4. One-third octave, microphone no. 3.....	(d)
5. Pressure-time histories, microphone no. 3.....	(e)
6. One-third octave, microphone no. 4.....	(f)
7. One-third octave, microphone no. 5.....	(g)
8. Pressure-time histories, microphone no. 5.....	(h)
9. One-third octave, microphone no. 6.....	(i)
10. One-third octave, microphone no. 7.....	(j)
C. Sub-wing tip, $V_\infty = 66.2$ knots.....	27
1. One-third octave, microphone no. 1.....	(a)
2. One-third octave, microphone no. 2.....	(b)
3. Pressure-time histories, microphone no. 2.....	(c)
4. One-third octave, microphone no. 3.....	(d)
5. Pressure-time histories, microphone no. 3.....	(e)
6. One-third octave, microphone no. 4.....	(f)
7. One-third octave, microphone no. 5.....	(g)

Figure

8. Pressure-time histories, microphone no. 5.....	(h)
9. One-third octave, microphone no. 6.....	(i)
10. One-third octave, microphone no. 7.....	(j)
D. Swept-tapered tip, $V_\infty = 66.2$ knots.....	28
1. One-third octave, microphone no. 1.....	(a)
2. One-third octave, microphone no. 2.....	(b)
3. Pressure-time histories, microphone no. 2.....	(c)
4. One-third octave, microphone no. 3.....	(d)
5. Pressure-time histories, microphone no. 3.....	(e)
6. One-third octave, microphone no. 4.....	(f)
7. One-third octave, microphone no. 5.....	(g)
8. Pressure-time histories, microphone no. 5.....	(h)
9. One-third octave, microphone no. 6.....	(i)
10. One-third octave, microphone no. 7.....	(j)
E. End-plate tip, $V_\infty = 66.7$ knots.....	29
1. One-third octave, microphone no. 1.....	(a)
2. One-third octave, microphone no. 2.....	(b)
3. Pressure-time histories, microphone no. 2.....	(c)
4. One-third octave, microphone no. 3.....	(d)
5. Pressure-time histories, microphone no. 3.....	(e)
6. One-third octave, microphone no. 4.....	(f)
7. One-third octave, microphone no. 5.....	(g)
8. Pressure-time histories, microphone no. 5.....	(h)
9. One-third octave, microphone no. 6.....	(i)
10. One-third octave, microphone no. 7.....	(j)

Tunnel velocity ≈ 71 knots

A. Square tip, $V_\infty = 71.1$ knots.....	30
1. One-third octave, microphone no. 1.....	(a)
2. One-third octave, microphone no. 2.....	(b)
3. Pressure-time histories, microphone no. 2.....	(c)
4. One-third octave, microphone no. 3.....	(d)
5. Pressure-time histories, microphone no. 3.....	(e)
6. One-third octave, microphone no. 4.....	(f)
7. One-third octave, microphone no. 5.....	(g)
8. Pressure-time histories, microphone no. 5.....	(h)
9. One-third octave, microphone no. 6.....	(i)
10. One-third octave, microphone no. 7.....	(j)
B. Ogee tip, $V_\infty = 70.7$ knots.....	31
1. One-third octave, microphone no. 1.....	(a)
2. One-third octave, microphone no. 2.....	(b)
3. Pressure-time histories, microphone no. 2.....	(c)
4. One-third octave, microphone no. 3.....	(d)
5. Pressure-time histories, microphone no. 3.....	(e)
6. One-third octave, microphone no. 4.....	(f)
7. One-third octave, microphone no. 5.....	(g)
8. Pressure-time histories, microphone no. 5.....	(h)

Figure

9. One-third octave, microphone no. 6.....	(i)
10. One-third octave, microphone no. 7.....	(j)
C. Sub-wing tip, $V_{\infty} = 71.2$ knots.....	32
1. One-third octave, microphone no. 1.....	(a)
2. One-third octave, microphone no. 2.....	(b)
3. Pressure-time histories, microphone no. 2.....	(c)
4. One-third octave, microphone no. 3.....	(d)
5. Pressure-time histories, microphone no. 3.....	(e)
6. One-third octave, microphone no. 4.....	(f)
7. One-third octave, microphone no. 5.....	(g)
8. Pressure-time histories, microphone no. 5.....	(h)
9. One-third octave, microphone no. 6.....	(i)
10. One-third octave, microphone no. 7.....	(j)
D. Swept-tapered, tip, $V_{\infty} = 70.9$ knots.....	33
1. One-third octave, microphone no. 1.....	(a)
2. One-third octave, microphone no. 2.....	(b)
3. Pressure-time histories, microphone no. 2.....	(c)
4. One-third octave, microphone no. 3.....	(d)
5. Pressure-time histories, microphone no. 3.....	(e)
6. One-third octave, microphone no. 4.....	(f)
7. One-third octave, microphone no. 5.....	(g)
8. Pressure-time histories, microphone no. 5.....	(h)
9. One-third octave, microphone no. 6.....	(i)
10. One-third octave, microphone no. 7.....	(j)
E. End-plate tip, $V_{\infty} = 71.2$ knots.....	34
1. One-third octave, microphone no. 1.....	(a)
2. One-third octave, microphone no. 2.....	(b)
3. Pressure-time histories, microphone no. 2.....	(c)
4. One-third octave, microphone no. 3.....	(d)
5. Pressure-time histories, microphone no. 3.....	(e)
6. One-third octave, microphone no. 4.....	(f)
7. One-third octave, microphone no. 5.....	(g)
8. Pressure-time histories, microphone no. 5.....	(h)
9. One-third octave, microphone no. 6.....	(i)
10. One-third octave, microphone no. 7.....	(j)
Tunnel velocity ≈ 76 knots	
A. Square tip, $V_{\infty} = 75.9$ knots.....	35
1. One-third octave, microphone no. 1.....	(a)
2. One-third octave, microphone no. 2.....	(b)
3. Pressure-time histories, microphone no. 2.....	(c)
4. One-third octave, microphone no. 3.....	(d)
5. Pressure-time histories, microphone no. 3.....	(e)
6. One-third octave, microphone no. 4.....	(f)
7. One-third octave, microphone no. 5.....	(g)
8. Pressure-time histories, microphone no. 5.....	(h)
9. One-third octave, microphone no. 6.....	(i)
10. One-third octave, microphone no. 7.....	(j)

Figure

B.	Ogee tip, $V_\infty = 76.0$ knots.....	36
1.	One-third octave, microphone no. 1.....	(a)
2.	One-third octave, microphone no. 2.....	(b)
3.	Pressure-time histories, microphone no. 2.....	(c)
4.	One-third octave, microphone no. 3.....	(d)
5.	Pressure-time histories, microphone no. 3.....	(e)
6.	One-third octave, microphone no. 4.....	(f)
7.	One-third octave, microphone no. 5.....	(g)
8.	Pressure-time histories, microphone no. 5.....	(h)
9.	One-third octave, microphone no. 6.....	(i)
10.	One-third octave, microphone no. 7.....	(j)
C.	Sub-wing tip, $V_\infty = 75.9$ knots.....	37
1.	One-third octave, microphone no. 1.....	(a)
2.	One-third octave, microphone no. 2.....	(b)
3.	Pressure-time histories, microphone no. 2.....	(c)
4.	One-third octave, microphone no. 3.....	(d)
5.	Pressure-time histories, microphone no. 3.....	(e)
6.	One-third octave, microphone no. 4.....	(f)
7.	One-third octave, microphone no. 5.....	(g)
8.	Pressure-time histories, microphone no. 5.....	(h)
9.	One-third octave, microphone no. 6.....	(i)
10.	One-third octave, microphone no. 7.....	(j)
D.	Swept-tapered tip, $V_\infty = 75.9$ knots.....	38
1.	One-third octave, microphone no. 1.....	(a)
2.	One-third octave, microphone no. 2.....	(b)
3.	Pressure-time histories, microphone no. 2.....	(c)
4.	One-third octave, microphone no. 3.....	(d)
5.	Pressure-time histories, microphone no. 3.....	(e)
6.	One-third octave, microphone no. 4.....	(f)
7.	One-third octave, microphone no. 5.....	(g)
8.	Pressure-time histories, microphone no. 5.....	(h)
9.	One-third octave, microphone no. 6.....	(i)
10.	One-third octave, microphone no. 7.....	(j)

Tunnel velocity ≈ 82 knots

A.	Square tip, $V_\infty = 81.8$ knots.....	39
1.	One-third octave, microphone no. 1.....	(a)
2.	One-third octave, microphone no. 2.....	(b)
3.	Pressure-time histories, microphone no. 2.....	(c)
4.	One-third octave, microphone no. 3.....	(d)
5.	Pressure-time histories, microphone no. 3.....	(e)
B.	Ogee tip, $V_\infty = 81.8$ knots.....	40
1.	One-third octave, microphone no. 1.....	(a)
2.	One-third octave, microphone no. 2.....	(b)
3.	Pressure-time histories, microphone no. 2.....	(c)
4.	One-third octave, microphone no. 3.....	(d)
5.	Pressure-time histories, microphone no. 3.....	(e)

Figure

C. Sub-wing tip, $V_\infty = 82.0$ knots.....	41
1. One-third octave, microphone no. 1.....	(a)
2. One-third octave, microphone no. 2.....	(b)
3. Pressure-time histories, microphone no. 2.....	(c)
4. One-third octave, microphone no. 3.....	(d)
5. Pressure-time histories, microphone no. 3.....	(e)
D. Swept-tapered tip, $V_\infty = 81.6$ knots.....	42
1. One-third octave, microphone no. 1.....	(a)
2. One-third octave, microphone no. 2.....	(b)
3. Pressure-time histories, microphone no. 2.....	(c)
4. One-third octave, microphone no. 3.....	(d)
5. Pressure-time histories, microphone no. 3.....	(e)
Tunnel velocity ≈ 91 knots	
A. Square tip, $V_\infty = 91.5$ knots.....	43
1. One-third octave, microphone no. 1.....	(a)
2. One-third octave, microphone no. 2.....	(b)
3. Pressure-time histories, microphone no. 2.....	(c)
4. One-third octave, microphone no. 3.....	(d)
5. Pressure-time histories, microphone no. 3.....	(e)
B. Sub-wing tip, $V_\infty = 91.6$ knots.....	44
1. One-third octave, microphone no. 1.....	(a)
2. One-third octave, microphone no. 2.....	(b)
3. Pressure-time histories, microphone no. 2.....	(c)
4. One-third octave, microphone no. 3.....	(d)
5. Pressure-time histories, microphone no. 3.....	(e)
C. Swept-tapered tip, $V_\infty = 91.1$ knots.....	45
1. One-third octave, microphone no. 1.....	(a)
2. One-third octave, microphone no. 2.....	(b)
3. Pressure-time histories, microphone no. 2.....	(c)
4. One-third octave, microphone no. 3.....	(d)
5. Pressure-time histories, microphone no. 3.....	(e)

The presence of blade slap is not evident in the pressure-time histories for microphone numbers 1 and 4 as it is in the data for microphone numbers 2, 3, 5, 6, and 7 even though the characteristic hump existed in the one-third-octave spectra. Microphone number 6 and 7 were very similar in waveform and blade-slap impulse character, except for peak amplitude, to that for microphone number 5. For these reasons, sample pressure-time histories are not presented in the data for velocities higher than 51 knots for microphone numbers 1, 4, 6, and 7.

Background data indicate that the helicopter noise measured on microphones 2 and 3 were well above the background levels for all tunnel velocities tested except at frequencies below 400 Hz (see, for example, figs. 43(b) and 43(d)), and only at frequencies other than multiples of blade passage (80 Hz). The helicopter noise measured at microphone number 1 is heavily contaminated

with background noise for tunnel velocities over 80 knots (see, for example, fig. 39(a)). Helicopter noise measured by microphone numbers 4, 5, 6, and 7 are seriously affected by background noise for tunnel velocities greater than 70 knots (see, for example, figs. 30(f), 30(g), 30(i), and 30(j)), and they are not even presented for tunnel velocities greater than 80 knots. Background noise spectra for microphone number 4, which was mounted on a tall streamlined stand, show evidence of a pure tone at mid-frequency dependent on tunnel velocity (see, for example, fig. 30(f)). This has been attributed to vortex shedding from a guy wire supporting this stand. This particular noise source limits the acceptability of the helicopter noise measured at 70 knots and higher for this microphone. The reader should be careful in interpreting the generated helicopter noise at high tunnel velocities and consider the effect of the background noise levels.

REFERENCES

1. Lowson, M. V.; and Ollerhead, J. B.: Studies of Helicopter Rotor Noise. USSAAVLABS Tech. Rep. 68-60, U.S. Army Aviation Labs., 1969
2. Langenbucher, V.: Noise Phenomena With Helicopter Rotors and Possibilities of Noise Reduction. ESA-TT-244, European Space Agency, 1976
3. Mantay, Wayne R.; Campbell, Richard L.; and Shidler, Phillip A.: Full-Scale Testing of an Ogee Tip Rotor. NASA CP-2052, 1978, pp. 277-308
4. Landgrebe, Anton J.; and Bellinger, E. Dean: Experimental Investigations of Model Variable-Geometry and Ogee Tip Rotors. NASA CR-2275, 1974
5. Tangler, James L.: The Design and Testing of a Tip to Reduce Blade Slap. Proc. 31st American Helicopter Soc. Forum, Washington, D.C., 1975
6. Tangler, James L.: Experimental Investigation of the Subwing Tip and Its Vortex Structure. NASA CR-3058, 1978
7. Tangler, James L.; Wohlfeld, Robert M.; and Miley, Stan J.: An Experimental Investigation of Vortex Stability, Tip Shapes, Compressibility, and Noise for Hovering Model Rotors. NASA CR-2305, 1973
8. White, Richard P., Jr.: Vortex Dissipation. U.S. Patent 3,845,918, 1974
9. Mechtly, E. A.: The International System of Units--Physical Constants and Conversion Factors (Second Revision). NASA SP-7012, 1973
10. Wilson, John C.: A General Rotor Model Systm for Wind-Tunnel Investigations. J. Aircraft, vol. 14, no. 7, July 1977, pp. 639-643
11. Ver, I. L.: Acoustical Evaluation of the NASA Langley V/STOL Wind Tunnel. NASA CR-145087, 1976

12. Ver, I. L.; Anderson, D. W.; and Bliss, D. B.: Acoustic Modeling Study of the Open Test Section of the NASA Langley V/STOL Wind Tunnel. NASA CR-145005, 1976
13. Theobald, M. A.: Evaluation of the Acoustic Measurement Capability of the NASA Langley V/STOL Wind-Tunnel Open Test Section With Acoustically Absorbent Ceiling and Floor Treatment. Rep. 3820, Bolt, Beranek, and Newman, May 1978
14. Cox, C. R.: Helicopter Rotor Aerodynamic and Aeroacoustic Environments. AIAA Paper 77-1338, 1977
15. Hoad, Danny R.; and Greene, George C.: Helicopter Noise Research at the Langley V/STOL Tunnel. NASA CP-2052, 1978, pp. 181-204
16. Wright, S. E.: Discrete Radiation from Rotating Periodic Sources. J. Sound Vibration, vol. 17, no. 4, 1971, pp. 437-498
17. Schmitz, F. H.; and Boxwell, D. A.: In-Flight Far-Field Measurement of Helicopter Impulsive Noise. Proc. 32nd Annual American Helicopter Soc. Forum, Washington, D.C., 1976
18. Widnall, Sheila: Helicopter Noise Due to Blade-Vortex Interaction. J. Acoust. Soc. America, vol. 50, no. 1, pt. 2, 1971, pp. 354-365
19. Yeager, William T., Jr.; and Mantay, Wayne R.: Correlation of Full-Scale Helicopter Rotor Performance in Air With Model-Scale Freon Data. NASA TN D-8328, 1976
20. Heyson, Harry H.: Use of Superposition in Digital Computers to Obtain Wind-Tunnel Interference Factors for Arbitrary Configurations, With Particular Reference to V/STOL Models. NASA TR R-302, 1969
21. Brown, Thomas J.; Brown, Christine G.; and Hardin, Jay C.: Program for the Analysis of Time Series. NASA TM X-2983, 1974
22. Mineck, Raymond E.: Effect of Rotor Blade Tip Shape on the Performance of an Articulated Rotor Model. NASA TM 80080, 1979

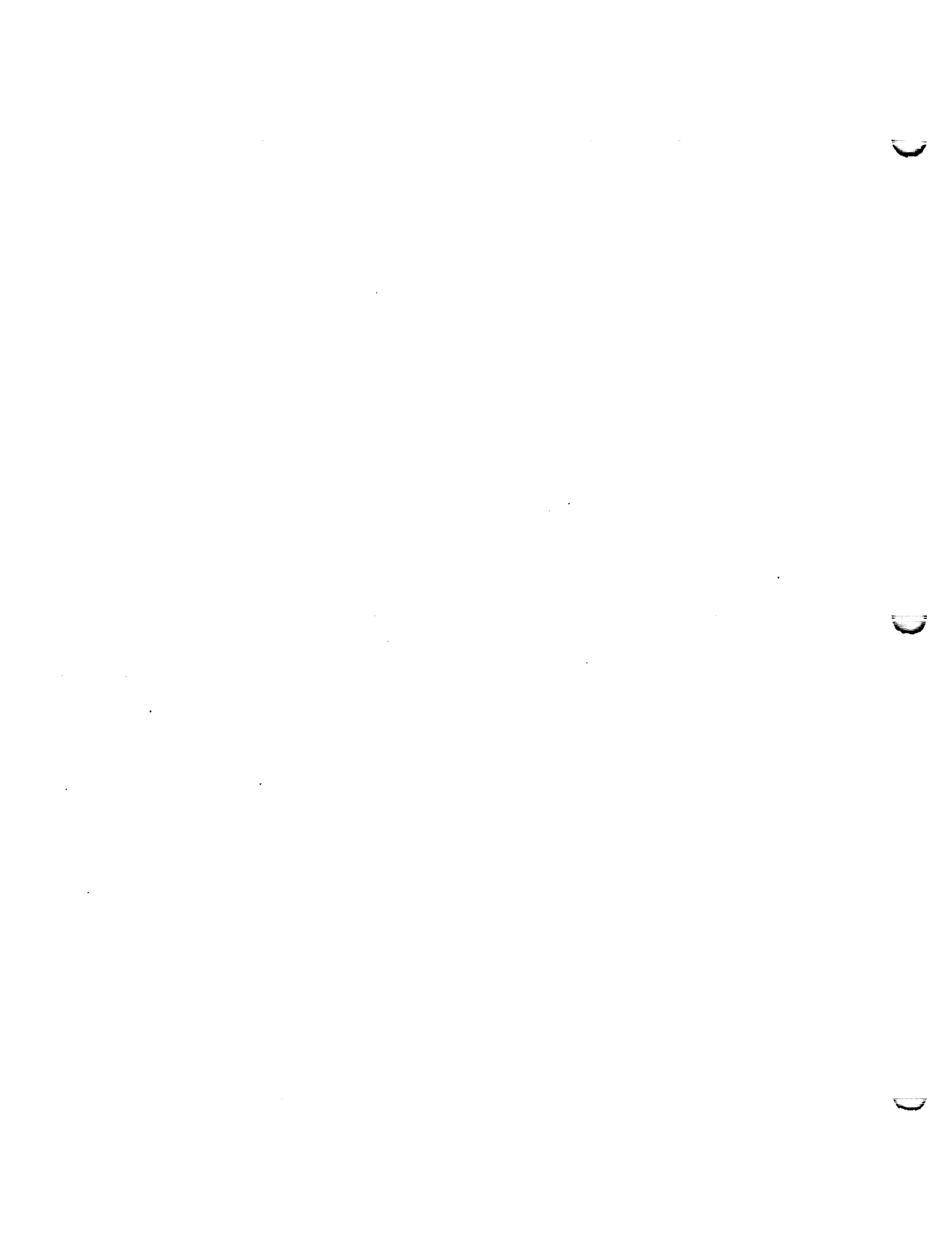
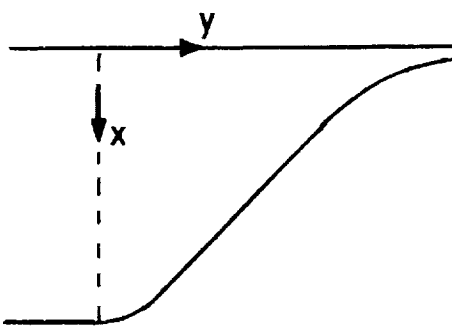


TABLE I.- OGEE PLANFORM COORDINATES



x/c	y/c
1.000	0
.990	.090
.970	.140
.950	.180
.920	.215
.900	.235
.850	.285
.800	.335
.750	.385
.700	.435
.650	.485
.600	.535
.550	.585
.500	.635
.450	.685
.400	.735
.350	.785

x/c	y/c
.300	.835
.250	.885
.225	.915
.200	.950
.175	.985
.150	1.025
.125	1.070
.115	1.100
.100	1.130
.090	1.160
.080	1.180
.070	1.210
.060	1.250
.050	1.290
.040	1.350
.020	1.370
0	1.350

TABLE II
MICROPHONE LOCATIONS RELATIVE TO ROTOR HUB

Microphone system	r	δ , deg	ϕ , deg
1	0.438 R	88.2	-85.3
2	0.876 R	20.6	3.6
3	0.448 R	87.8	88.0
4	2.789 R	-1.3	36.4
5	2.735 R	31.0	19.3
6	2.616 R	31.0	-0.7
7	2.734 R	31.2	-20.0

Table III. ROTOR OPERATING CONDITIONS - Square Tip

a. AVERAGE TUNNEL VELOCITY = 51.4 KTS

α , deg	α_{TPP} , deg	θ_C , deg	A_1 , deg	B_1 , deg	a_0 , deg	a_{1S} , deg	b_{1S} , deg	μ	γ , deg	C_T	C_Q
-2.14	-2.82	5.91	-1.99	2.50	1.34	-1.08	-.09	.135	-4.49	.3428	.02370
-.17	-.90	5.48	-2.04	2.28	1.50	-1.11	-.17	.133	-2.47	.3395	.02147
.93	.43	5.19	-2.10	1.98	1.52	-.88	-.20	.134	-1.05	.3419	.01988
2.15	1.48	5.09	-2.12	2.19	1.56	-1.06	-.17	.133	-.12	.3488	.01963
3.23	2.66	4.69	-2.08	1.98	1.51	-.94	-.16	.133	1.12	.3463	.01800
4.37	3.70	4.38	-2.06	1.98	1.51	-1.02	-.17	.134	2.15	.3458	.01656
6.63	5.84	3.99	-2.05	1.99	1.58	-1.13	-.15	.133	4.23	.3551	.01455
8.94	8.11	3.27	-1.94	2.01	1.20	-1.15	-.03	.133	6.41	.3536	.01172

b. AVERAGE TUNNEL VELOCITY = 56.2 KTS

α , deg	α_{TPP} , deg	θ_C , deg	A_1 , deg	B_1 , deg	a_0 , deg	a_{1S} , deg	b_{1S} , deg	μ	γ , deg	C_T	C_Q
-2.08	-2.93	5.98	-2.01	2.68	1.89	-1.19	-.22	.145	-4.53	.3436	.02272
2.02	1.38	4.89	-2.00	2.28	1.89	-.96	-.17	.146	-.08	.3462	.01775
3.00	2.28	4.58	-2.02	2.29	1.85	-1.03	-.21	.148	.86	.3461	.01647
4.04	3.27	4.34	-1.98	2.19	1.87	-1.08	-.18	.146	1.79	.3457	.01521
6.10	5.26	3.79	-1.93	2.19	1.89	-1.13	-.17	.147	3.78	.3503	.01262
5.10	4.36	3.92	-1.99	2.20	1.66	-1.03	-.13	.146	2.80	.3433	.01356
7.10	6.37	3.59	-1.88	1.98	1.93	-1.01	-.14	.147	5.02	.3575	.01167

Table III. Continued.

c. AVERAGE TUNNEL VELOCITY = 61.3 KTS

α , deg	α_{TPP} , deg	θ_C , deg	A_1 , deg	B_1 , deg	a_0 , deg	a_{1S} , deg	b_{1S} , deg	μ	γ , deg	C_T	C_Q
1.84	1.02	4.69	-1.87	2.48	1.85	-1.09	-.19	.159	-.33	.3416	.01692
.86	.12	4.99	-1.93	2.48	1.87	-1.00	-.21	.159	-1.20	.3428	.01813
2.77	2.10	4.28	-1.91	2.40	1.55	-.93	-.09	.161	.71	.3458	.01549
3.78	3.09	4.20	-1.82	2.28	1.89	-.95	-.12	.160	1.77	.3506	.01437
4.75	3.91	3.99	-1.83	2.38	1.92	-1.09	-.15	.160	2.56	.3537	.01324
5.66	4.75	3.75	-1.85	2.38	1.91	-1.17	-.18	.159	3.35	.3521	.01228

d. AVERAGE TUNNEL VELOCITY = 65.7 KTS

α , deg	α_{TPP} , deg	θ_C , deg	A_1 , deg	B_1 , deg	a_0 , deg	a_{1S} , deg	b_{1S} , deg	μ	γ , deg	C_T	C_Q
-.27	-1.14	5.14	-1.89	2.73	1.54	-1.09	-.32	.171	-2.18	.3372	.01954
-.27	-1.09	5.14	-1.78	2.73	1.52	-1.04	-.23	.171	-2.10	.3362	.01965
1.52	.70	4.70	-1.19	2.64	1.55	-1.04	.31	.170	-.43	.3423	.01794
2.37	1.48	4.39	-1.19	2.64	1.52	-1.11	.28	.171	.32	.3367	.01658
3.31	2.44	4.20	-1.19	2.53	1.56	-1.09	.31	.171	1.29	.3462	.01568
4.17	3.24	4.00	-1.19	2.56	1.56	-1.14	.29	.170	2.11	.3462	.01458

e. AVERAGE TUNNEL VELOCITY = 71.1 KTS

α , deg	α_{TPP} , deg	θ_C , deg	A_1 , deg	B_1 , deg	a_0 , deg	a_{1S} , deg	b_{1S} , deg	μ	γ , deg	C_T	C_Q
-.10	-1.19	5.28	-1.08	3.28	1.56	-1.29	.32	.185	-2.26	.3427	.01864
.42	-.52	5.08	-1.08	2.97	1.53	-1.13	.32	.186	-1.41	.3426	.01787
1.39	.43	4.79	-1.08	2.97	1.54	-1.16	.32	.185	-.62	.3476	.01619
1.88	1.06	4.53	-1.08	2.72	1.44	-1.01	.31	.185	.16	.3409	.01497
2.87	1.92	4.21	-1.08	2.78	1.43	-1.14	.30	.185	.91	.3440	.01349
3.64	2.62	3.99	-1.08	2.78	1.43	-1.21	.28	.185	1.66	.3443	.01240
4.37	3.52	3.79	-1.08	2.58	1.46	-1.03	.29	.184	2.59	.3486	.01122

Table III. Concluded.

f. AVERAGE TUNNEL VELOCITY = 75.9 KTS

α , deg	α_{TPP} , deg	θ_c , deg	A_1 , deg	B_1 , deg	a_0 , deg	a_{1S} , deg	b_{1S} , deg	μ	γ , deg	c_t	c_q
-2.03	-2.02	5.43	-11.00	2.11	1.43	-1.16	.39	.198	-2.25	.3417	.01899
-1.31	-1.21	5.19	-1.00	1.93	1.46	-.07	.40	.198	-1.45	.3456	.01755
-.56	-.45	4.88	-1.00	1.79	1.45	-.05	.39	.197	-.68	.3438	.01609
.20	.36	4.68	-1.00	1.68	1.47	-.01	.40	.197	.13	.3467	.01501
.91	1.12	4.38	-1.00	1.59	1.46	.04	.39	.198	.92	.3484	.01331
1.68	1.88	4.08	-1.00	1.49	1.45	.04	.37	.197	1.70	.3456	.01187
2.38	2.58	3.83	-1.00	1.38	1.44	.04	.36	.196	2.38	.3455	.01090

g. AVERAGE TUNNEL VELOCITY = 81.8 KTS

α , deg	α_{TPP} , deg	θ_c , deg	A_1 , deg	B_1 , deg	a_0 , deg	a_{1S} , deg	b_{1S} , deg	μ	γ , deg	c_t	c_q
-2.19	-2.16	5.59	-.99	2.39	1.75	-.13	.41	.214	-2.23	.3489	.02136
-1.13	-1.28	5.22	-.99	2.48	1.74	-.30	.38	.213	-1.51	.3465	.01968
-.09	-.36	4.87	-1.00	2.53	1.72	-.42	.37	.212	-.68	.3447	.01793
.90	.40	4.58	-1.00	2.68	1.71	-.64	.35	.213	-.01	.3437	.01661
1.85	1.23	4.18	-1.00	2.68	1.70	-.77	.32	.212	.69	.3438	.01492
2.79	2.02	4.07	-1.00	2.88	1.75	-.92	.35	.212	1.41	.3523	.01424

h. AVERAGE TUNNEL VELOCITY = 91.5 KTS

α , deg	α_{TPP} , deg	θ_c , deg	A_1 , deg	B_1 , deg	a_0 , deg	a_{1S} , deg	b_{1S} , deg	μ	γ , deg	c_t	c_q
2.84	2.19	3.73	-1.00	2.88	1.71	-.76	.26	.238	2.16	.3442	.01239
1.41	1.99	4.27	-1.00	2.78	1.72	-.53	.30	.238	1.01	.3451	.01462
.44	.24	4.57	-.99	2.62	1.73	-.32	.31	.238	.35	.3484	.01612
-.59	-.63	4.88	-1.00	2.48	1.72	-.16	.32	.238	-.39	.3452	.01756
-1.50	-1.22	5.19	-.99	2.28	1.74	.15	.37	.238	-.87	.3493	.01875
-2.03	-1.81	5.37	-1.00	2.38	1.70	.10	.35	.237	-1.45	.3419	.01982

Table IV. ROTOR OPERATING CONDITIONS - Ogee Tip

a. AVERAGE TUNNEL VELOCITY = 51.0 KTS

α , deg	α_{TPP} , deg	θ_C , deg	A_1 , deg	B_1 , deg	a_0 , deg	a_{1S} , deg	b_{1S} , deg	μ	γ , deg	C_T	C_Q
-.13	-.56	5.25	-1.45	2.00	2.10	-.81	.30	.127	-2.10	.3798	.02279
.96	.47	4.95	-1.44	2.00	2.04	-.86	.28	.127	-1.08	.3735	.02129
2.26	1.59	4.74	-1.45	2.19	2.07	-1.02	.27	.129	-.06	.3832	.02039
3.27	2.64	4.53	-1.45	2.10	2.07	-.99	.30	.127	.98	.3846	.01919
4.47	3.76	4.22	-1.45	2.11	2.06	-1.06	.31	.127	2.07	.3832	.01773
6.77	5.94	3.82	-1.45	2.11	2.09	-1.17	.31	.125	4.24	.3906	.01552
9.12	8.12	3.33	-1.45	2.10	2.10	-1.32	.21	.124	6.45	.3912	.01284

b. AVERAGE TUNNEL VELOCITY = 55.9 KTS

α , deg	α_{TPP} , deg	θ_C , deg	A_1 , deg	B_1 , deg	a_0 , deg	a_{1S} , deg	b_{1S} , deg	μ	γ , deg	C_T	C_Q
-2.10	-2.82	5.65	-1.19	2.48	2.10	-1.04	.31	.140	-4.27	.3855	.02539
2.13	1.33	4.64	-1.20	2.37	2.09	-1.10	.36	.140	-.23	.3856	.02001
3.05	2.23	4.35	-1.20	2.28	2.07	-1.12	.33	.140	.72	.3809	.01840
4.13	3.32	4.04	-1.18	2.17	2.05	-1.10	.33	.139	1.85	.3778	.01680
5.20	4.31	3.79	-1.18	2.17	2.06	-1.18	.30	.138	2.87	.3808	.01556
6.22	5.29	3.64	-1.19	2.18	2.08	-1.21	.32	.138	3.79	.3874	.01464
7.23	6.27	3.44	-1.19	2.17	2.11	-1.24	.30	.138	4.78	.3913	.01351

c. AVERAGE TUNNEL VELOCITY = 61.2 KTS

α , deg	α_{TPP} , deg	θ_C , deg	A_1 , deg	B_1 , deg	a_0 , deg	a_{1S} , deg	b_{1S} , deg	μ	γ , deg	C_T	C_Q
.86	.14	4.84	-1.04	2.47	2.42	-.98	.43	.153	-1.11	.3838	.02151
1.85	1.06	4.55	-1.05	2.49	2.40	-1.05	.41	.152	-.25	.3811	.01990
2.78	2.09	4.29	-1.05	2.30	2.42	-.95	.44	.152	.21	.3846	.01826
3.86	3.05	4.13	-1.05	2.40	2.46	-1.06	.45	.152	1.70	.3952	.01753
4.92	3.91	3.84	-1.06	2.50	2.42	-1.21	.41	.152	2.59	.3896	.01600
5.82	4.62	3.63	-1.06	2.70	2.42	-1.40	.39	.151	3.19	.3893	.01503

Table IV. - Continued.

d. AVERAGE TUNNEL VELOCITY = 66.7 KTS

α , deg	α_{TPP} , deg	θ_C , deg	A_1 , deg	B_1 , deg	a_0 , deg	a_{1S} , deg	b_{1S} , deg	μ	γ , deg	C_T	C_Q
-.26	-.94	4.85	-.97	2.77	1.93	-.89	.53	.166	-2.32	.3759	.02019
1.52	.84	4.36	-.94	2.37	1.92	-.90	.35	.166	-.33	.3759	.01710
2.44	1.67	4.05	-.92	2.39	1.89	-.99	.31	.166	.52	.3698	.01552
3.53	2.55	3.85	-.92	2.59	1.92	-1.21	.30	.165	1.28	.3751	.01441
4.26	3.32	3.43	-.98	2.66	1.87	-1.14	.48	.165	1.88	.3702	.01326

e. AVERAGE TUNNEL VELOCITY = 70.7 KTS

α , deg	α_{TPP} , deg	θ_C , deg	A_1 , deg	B_1 , deg	a_0 , deg	a_{1S} , deg	b_{1S} , deg	μ	γ , deg	C_T	C_Q
-.18	-1.11	4.84	-.83	2.90	1.99	-1.13	.36	.176	-2.09	.3698	.02080
.33	-.55	4.64	-.84	2.80	2.01	-1.07	.40	.175	-1.55	.3738	.01986
1.30	.53	4.34	-.86	2.83	2.05	-.97	.58	.176	-.64	.3808	.01854
1.83	1.17	4.02	-.87	2.65	2.01	-.85	.59	.175	.08	.3703	.01699
2.81	2.10	3.73	-.87	2.65	2.01	-.90	.58	.176	.98	.3752	.01571
3.62	2.85	3.52	-.87	2.65	2.02	-.95	.58	.175	1.69	.3771	.01448
4.31	3.56	3.31	-.87	2.56	2.02	-.94	.56	.175	2.47	.3769	.01356

f. AVERAGE TUNNEL VELOCITY = 76.0 KTS

α , deg	α_{TPP} , deg	θ_C , deg	A_1 , deg	B_1 , deg	a_0 , deg	a_{1S} , deg	b_{1S} , deg	μ	γ , deg	C_T	C_Q
2.42	2.55	3.51	-1.09	1.71	2.07	-.04	.40	.188	2.04	.3810	.01337
1.70	1.84	3.60	-1.09	1.71	2.00	-.02	.39	.189	1.39	.3719	.01444
.87	1.09	3.90	-1.09	1.72	2.01	.05	.41	.188	.62	.3740	.01595
.14	.35	4.15	-1.09	1.82	2.03	.04	.44	.189	-.15	.3779	.01704
-.62	-.40	4.41	-1.09	1.87	2.00	.05	.43	.188	-.89	.3728	.01849
-1.32	-1.03	4.70	-1.09	1.87	2.05	.11	.47	.188	-1.49	.3796	.01982
-2.12	-1.91	4.91	-1.10	2.02	1.99	.04	.42	.189	-2.34	.3728	.02133

Table IV. - Concluded.

g. AVERAGE TUNNEL VELOCITY = 81.8 KTS

α , deg	α_{TPP} , deg	θ_C , deg	A_1 , deg	B_1 , deg	a_0 , deg	a_{1S} , deg	b_{1S} , deg	μ	γ , deg	C_T	C_Q
-2.20	-2.15	5.16	-.84	2.04	2.12	-.10	.31	.203	-2.14	.3787	.02166
-1.12	-1.31	4.86	-.84	2.25	2.09	-.34	.28	.203	-1.45	.3737	.02002
-.13	-.39	4.57	-.84	2.25	2.11	-.41	.27	.203	-.57	.3770	.01833
.89	.38	4.27	-.84	2.45	2.08	-.66	.25	.204	.11	.3730	.01692
1.90	1.16	4.07	-.84	2.66	2.11	-.88	.25	.203	.70	.3792	.01565
2.89	2.07	3.77	-.83	2.65	2.12	-.97	.22	.203	1.60	.3796	.01397

h. AVERAGE TUNNEL VELOCITY = 96.8 KTS

α , deg	α_{TPP} , deg	θ_C , deg	A_1 , deg	B_1 , deg	a_0 , deg	a_{1S} , deg	b_{1S} , deg	μ	γ , deg	C_T	C_Q
-1.94	-2.01	5.29	-.65	2.80	2.08	-.18	.46	.240	-1.50	.3727	.02140
-1.43	-1.45	5.08	-.66	2.71	2.10	-.13	.49	.240	-1.02	.3780	.02018
-.58	-.70	4.73	-.65	2.71	2.09	-.22	.46	.241	-.28	.3785	.01854
.48	.19	4.32	-.66	2.80	2.07	-.40	.45	.241	.53	.3737	.01656
1.40	.94	4.03	-.65	2.90	2.06	-.56	.42	.240	1.23	.3727	.01491

Table V. ROTOR OPERATING CONDITIONS - Sub-Wing Tip

a. AVERAGE TUNNEL VELOCITY = 51.1 KTS

α , deg	α_{TPP} , deg	θ_C , deg	A_1 , deg	B_1 , deg	a_0 , deg	a_{1S} , deg	b_{1S} , deg	μ	γ , deg	C_T	C_Q
-1.13	-7.75	5.41	-1.35	2.11	2.35	-9.99	.30	.132	-2.16	.3552	.02298
.98	.39	5.14	-1.41	2.16	2.32	-9.95	.36	.131	-1.09	.3544	.02167
2.28	1.49	4.91	-1.37	2.24	2.36	-1.13	.32	.131	-0.08	.3569	.02054
3.28	2.62	4.61	-1.36	2.03	2.33	-1.01	.32	.131	1.11	.3561	.01917
4.46	3.68	4.34	-1.36	2.02	2.34	-1.12	.30	.130	2.15	.3567	.01791
6.78	5.81	3.91	-1.36	2.12	2.36	-1.29	.30	.129	4.23	.3595	.01588
9.07	7.94	3.37	-1.36	2.12	2.36	-1.45	.21	.128	6.34	.3589	.01312

b. AVERAGE TUNNEL VELOCITY = 55.8 KTS

α , deg	α_{TPP} , deg	θ_C , deg	A_1 , deg	B_1 , deg	a_0 , deg	a_{1S} , deg	b_{1S} , deg	μ	γ , deg	C_T	C_Q
-2.09	-2.89	5.67	-1.44	2.73	1.78	-1.12	.20	.144	-4.27	.3544	.02471
2.10	1.36	4.57	-1.45	2.38	1.78	-1.04	.23	.143	-0.10	.3530	.01940
2.99	2.22	4.32	-1.45	2.38	1.76	-1.06	.24	.142	.75	.3508	.01827
4.10	3.25	4.07	-1.45	2.38	1.77	-1.13	.23	.143	1.76	.3562	.01710
5.22	4.24	3.77	-1.45	2.43	1.75	-1.27	.20	.143	2.75	.3519	.01564
6.24	5.29	3.58	-1.45	2.33	1.78	-1.24	.21	.141	3.80	.3562	.01460
7.24	6.35	3.37	-1.45	2.18	1.80	-1.16	.19	.141	4.92	.3595	.01343

c. AVERAGE TUNNEL VELOCITY = 60.9 KTS

α , deg	α_{TPP} , deg	θ_C , deg	A_1 , deg	B_1 , deg	a_0 , deg	a_{1S} , deg	b_{1S} , deg	μ	γ , deg	C_T	C_Q
.83	.03	5.02	-1.20	2.25	2.15	-1.06	.11	.156	-1.12	.3583	.01949
1.86	.90	4.73	-1.21	2.37	2.14	-1.21	.11	.156	-0.33	.3589	.01835
2.81	1.93	4.53	-1.21	2.27	2.16	-1.14	.12	.156	.70	.3630	.01734
3.86	2.89	4.22	-1.21	2.27	2.15	-1.23	.11	.155	1.61	.3625	.01586
4.84	3.79	4.02	-1.20	2.26	2.18	-1.30	.11	.155	2.53	.3661	.01471
5.76	4.60	3.82	-1.21	2.37	2.17	-1.42	.09	.154	3.27	.3653	.01374

Table V. - Continued.

d. AVERAGE TUNNEL VELOCITY = 66.2 KTS

α , deg	α_{TPP} , deg	θ_C , deg	A_1 , deg	B_1 , deg	a_0 , deg	a_{1S} , deg	b_{1S} , deg	μ	γ , deg	C_T	C_Q
-.31	-.34	5.07	-1.03	2.71	1.49	-.26	1.07	.170	-2.23	.3555	.02185
1.49	1.49	4.58	-1.03	2.51	1.53	-.23	1.10	.169	-.47	.3608	.01914
2.37	2.32	4.29	-1.03	2.51	1.52	-.27	1.09	.169	.34	.3585	.01790
3.36	3.26	3.97	-1.06	2.57	1.49	-.32	1.11	.169	1.23	.3579	.01644
4.18	3.90	3.68	-1.03	2.61	1.46	-.49	1.04	.168	1.87	.3497	.01527

e. AVERAGE TUNNEL VELOCITY = 71.2 KTS

α , deg	α_{TPP} , deg	θ_C , deg	A_1 , deg	B_1 , deg	a_0 , deg	a_{1S} , deg	b_{1S} , deg	μ	γ , deg	C_T	C_Q
-.22	-1.23	5.01	-1.13	3.18	1.79	-1.21	.25	.180	-2.26	.3526	.02138
.31	-.38	4.77	-1.13	2.78	1.82	-.89	.29	.183	-1.27	.3610	.02015
1.30	.39	4.36	-1.13	2.88	1.76	-1.10	.24	.182	-.57	.3505	.01830
1.81	1.12	4.26	-1.13	2.58	1.83	-.88	.28	.182	.25	.3597	.01749
2.75	1.85	3.86	-1.13	2.68	1.75	-1.09	.23	.181	.93	.3482	.01595
3.58	2.67	3.67	-1.13	2.68	1.77	-1.09	.23	.180	1.71	.3502	.01472
4.30	3.43	3.47	-1.13	2.58	1.80	-1.05	.24	.182	2.56	.3587	.01365

f. AVERAGE TUNNEL VELOCITY = 75.9 KTS

α , deg	α_{TPP} , deg	θ_C , deg	A_1 , deg	B_1 , deg	a_0 , deg	a_{1S} , deg	b_{1S} , deg	μ	γ , deg	C_T	C_Q
-2.10	-2.02	5.22	-1.05	2.08	1.78	-.10	.39	.194	-2.33	.3556	.02174
-1.33	-1.19	4.86	-1.05	1.89	1.76	-.03	.39	.194	-1.47	.3547	.02015
-.62	-.45	4.57	-1.05	1.79	1.76	-.00	.39	.194	-.78	.3549	.01873
.16	.26	4.38	-1.05	1.79	1.79	-.07	.39	.193	-.11	.3582	.01770
.88	1.08	4.08	-1.05	1.59	1.77	.03	.38	.194	.83	.3532	.01625
1.67	1.89	3.78	-1.05	1.49	1.75	.06	.37	.193	1.67	.3505	.01478
2.35	2.51	3.58	-1.05	1.49	1.78	-.00	.37	.194	2.29	.3553	.01389

Table V. - Concluded.

g. AVERAGE TUNNEL VELOCITY = 82.0 KTS

α , deg	α_{TPP} , deg	θ_C , deg	A_1 , deg	B_1 , deg	a_0 , deg	a_{1S} , deg	b_{1S} , deg	μ	γ , deg	C_T	C_Q
-2.22	-2.08	5.37	-1.13	2.28	1.86	-.01	.28	.211	-2.09	.3647	.02214
-1.15	-1.32	4.96	-1.13	2.48	1.80	-.32	.21	.209	-1.45	.3543	.02039
-.14	-.42	4.61	-1.13	2.48	1.82	-.43	.20	.208	-.66	.3564	.01871
.86	.36	4.27	-1.13	2.63	1.78	-.64	.17	.209	.06	.3536	.01728
1.83	1.17	3.96	-1.13	2.73	1.77	-.80	.15	.208	.80	.3503	.01580
2.88	2.04	3.71	-1.13	2.88	1.80	-.99	.14	.208	1.55	.3548	.01444

h. AVERAGE TUNNEL VELOCITY = 91.6 KTS

α , deg	α_{TPP} , deg	θ_C , deg	A_1 , deg	B_1 , deg	a_0 , deg	a_{1S} , deg	b_{1S} , deg	μ	γ , deg	C_T	C_Q
-1.94	-1.76	5.28	-.94	2.47	1.89	.06	.41	.233	-1.45	.3628	.02123
-1.48	-1.32	4.97	-.94	2.37	1.85	.04	.38	.234	-.99	.3565	.01975
-.57	-.58	4.68	-.94	2.47	1.82	-.13	.36	.233	-.30	.3534	.01844
.43	.16	4.37	-.94	2.67	1.82	-.38	.31	.233	.39	.3524	.01694
1.37	.97	4.07	-.94	2.77	1.83	-.51	.29	.234	1.10	.3569	.01560

Table VI. ROTOR OPERATING CONDITIONS - Swept-Tapered Tip

a. AVERAGE TUNNEL VELOCITY = 50.6 KTS

α , deg	α_{TPP} , deg	θ_C , deg	A_1 , deg	B_1 , deg	a_0 , deg	a_{1S} , deg	b_{1S} , deg	μ	γ , deg	C_T	C_Q
-12	.43	6.05	-1.61	2.47	3.16	.17	-.09	.132	-2.30	.3667	.02311
.95	1.60	5.80	-1.59	2.34	3.17	.28	-.09	.134	-1.15	.3721	.02204
2.26	2.74	5.50	-1.59	2.44	3.17	.12	-.08	.132	-.05	.3703	.02078
3.26	3.80	5.24	-1.59	2.30	3.17	.19	-.07	.132	1.03	.3686	.01936
4.46	5.02	4.95	-1.59	2.24	3.17	.21	-.08	.132	2.24	.3720	.01804
6.78	6.99	4.39	-1.59	2.40	3.18	-.12	-.15	.131	4.13	.3728	.01540
9.08	9.11	3.84	-1.59	2.40	3.17	-.29	-.24	.130	6.31	.3701	.01282

b. AVERAGE TUNNEL VELOCITY = 55.8 KTS

α , deg	α_{TPP} , deg	θ_C , deg	A_1 , deg	B_1 , deg	a_0 , deg	a_{1S} , deg	b_{1S} , deg	μ	γ , deg	C_T	C_Q
-2.16	-2.76	6.38	-1.41	2.77	2.63	-.92	.46	.146	-4.16	.3646	.02443
1.99	1.17	5.38	-1.63	2.82	2.64	-1.12	.30	.146	-.32	.3704	.01944
2.90	2.05	5.08	-1.63	2.77	2.62	-1.15	.30	.146	.58	.3693	.01800
3.98	3.03	4.77	-1.63	2.77	2.60	-1.24	.27	.145	1.56	.3637	.01665
5.05	4.01	4.43	-1.64	2.77	2.61	-1.32	.25	.145	2.55	.3664	.01506
6.07	5.07	4.18	-1.64	2.62	2.60	-1.28	.24	.144	3.63	.3681	.01373
7.08	6.19	3.98	-1.64	2.37	2.64	-1.16	.22	.144	4.86	.3730	.01251

c. AVERAGE TUNNEL VELOCITY = 60.6 KTS

α , deg	α_{TPP} , deg	θ_C , deg	A_1 , deg	B_1 , deg	a_0 , deg	a_{1S} , deg	b_{1S} , deg	μ	γ , deg	C_T	C_Q
.80	.11	5.39	-1.51	2.77	2.61	-.96	.32	.159	-1.16	.3651	.01944
1.76	1.01	5.08	-1.51	2.77	2.59	-1.00	.32	.159	-.31	.3659	.01799
2.63	1.90	4.82	-1.51	2.67	2.59	-.98	.31	.158	.61	.3652	.01665
3.73	2.90	4.58	-1.69	2.67	2.60	-1.09	.14	.157	1.55	.3667	.01559
4.73	3.84	4.27	-1.69	2.67	2.59	-1.14	.12	.157	2.53	.3666	.01416
5.60	4.60	4.09	-1.48	2.72	2.60	-1.25	.29	.157	3.33	.3686	.01306

Table VI.~ Continued.

d. AVERAGE TUNNEL VELOCITY = 66.2 KTS

α , deg	α_{TPP} , deg	θ_C , deg	A_1 , deg	B_1 , deg	a_0 , deg	a_{1S} , deg	b_{1S} , deg	μ	γ , deg	C_T	C_Q
-.38	-1.13	5.68	-1.31	3.07	2.39	-.97	.40	.173	-2.08	.3620	.02058
1.39	.56	5.28	-1.43	3.07	2.37	-1.06	.34	.172	-.49	.3729	.01835
2.26	1.37	4.93	-1.45	3.07	2.33	-1.11	.29	.173	.37	.3689	.01692
3.25	2.20	4.68	-1.45	3.18	2.32	-1.26	.28	.172	1.13	.3698	.01582
4.03	2.91	4.43	-1.39	3.18	2.29	-1.33	.31	.172	1.87	.3664	.01456

e. AVERAGE TUNNEL VELOCITY = 70.9 KTS

α , deg	α_{TPP} , deg	θ_C , deg	A_1 , deg	B_1 , deg	a_0 , deg	a_{1S} , deg	b_{1S} , deg	μ	γ , deg	C_T	C_Q
-.33	-1.29	5.68	-1.26	3.47	2.23	-1.16	.39	.184	-2.18	.3656	.02054
.22	-.62	5.43	-1.26	3.27	2.24	-1.04	.39	.185	-1.43	.3635	.01923
1.18	.30	5.18	-1.26	3.27	2.19	-1.08	.40	.184	-.56	.3650	.01783
1.68	.83	4.98	-1.26	3.18	2.19	-1.05	.39	.186	.01	.3701	.01689
2.66	1.71	4.69	-1.26	3.18	2.20	-1.15	.38	.184	.87	.3704	.01535
3.44	2.45	4.43	-1.26	3.17	2.17	-1.18	.37	.184	1.59	.3694	.01428
4.13	3.14	4.23	-1.26	3.07	2.14	-1.18	.37	.184	2.32	.3728	.01309

f. AVERAGE TUNNEL VELOCITY = 75.9 KTS

α , deg	α_{TPP} , deg	θ_C , deg	A_1 , deg	B_1 , deg	a_0 , deg	a_{1S} , deg	b_{1S} , deg	μ	γ , deg	C_T	C_Q
-2.02	-1.66	5.77	-1.24	2.03	2.24	.18	.45	.197	-1.93	.3626	.02042
-1.27	-1.09	5.57	-1.24	2.18	2.26	.01	.45	.196	-1.49	.3656	.01936
-.58	-.35	5.33	-1.24	2.08	2.27	.06	.44	.198	-.70	.3680	.01816
.22	.42	5.07	-1.24	2.08	2.28	.03	.44	.198	.02	.3695	.01687
.90	1.07	4.77	-1.24	2.03	2.27	.00	.42	.198	.67	.3661	.01537
1.68	1.81	4.47	-1.24	1.98	2.25	-.03	.40	.197	1.44	.3635	.01397
2.38	2.45	4.17	-1.24	1.94	2.22	-.09	.36	.199	2.12	.3618	.01262

Table VI. - Concluded.

g. AVERAGE TUNNEL VELOCITY = 81.6 KTS

α , deg	α_{TPP} , deg	θ_C , deg	A_1 , deg	B_1 , deg	α_0 , deg	α_{1S} , deg	b_{1S} , deg	μ	γ , deg	c_Q
-2.14	-1.98	5.82	-1.14	2.48	2.24	.00	.48	.211	-2.16	.02035
-1.08	-1.11	5.42	-1.14	2.63	2.20	-.17	.42	.213	-1.29	.01898
-1.12	-.29	5.17	-1.14	2.73	2.23	-.32	.43	.212	-.62	.01741
.84	.47	4.82	-1.15	2.88	2.24	-.51	.38	.213	.10	.01580
1.77	1.15	4.52	-1.14	3.07	2.21	-.77	.35	.213	.78	.01463
2.71	1.88	4.27	-1.15	3.22	2.23	-.97	.35	.212	1.46	.01345

h. AVERAGE TUNNEL VELOCITY = 91.1 KTS

α , deg	α_{TPP} , deg	θ_C , deg	A_1 , deg	B_1 , deg	α_0 , deg	α_{1S} , deg	b_{1S} , deg	μ	γ , deg	c_Q
-1.87	-1.75	5.67	-1.40	2.78	2.13	.00	.17	.237	-1.45	.01968
-1.35	-1.10	5.53	-1.09	2.63	2.20	.13	.46	.238	-.82	.01853
-.54	-.48	5.09	-1.12	2.76	2.01	-.05	.44	.237	-.23	.01687
.55	.32	4.82	-1.10	2.98	2.13	-.35	.36	.237	.45	.01535
1.40	.92	4.53	-1.10	3.18	2.06	-.60	.31	.237	1.06	.01423
2.84	2.21	4.03	-1.09	3.17	2.13	-.74	.29	.237	2.33	.01180

Table VII. ROTOR OPERATING CONDITIONS - End-Plate Tip

a. AVERAGE TUNNEL VELOCITY = 50.4 KTS

α , deg	α_{TPP} , deg	θ_C , deg	A_1 , deg	B_1 , deg	a_0 , deg	a_{1S} , deg	b_{1S} , deg	μ	γ , deg	C_T	C_Q
-.30	-.98	5.62	-1.65	2.58	2.65	-1.05	.36	.132	-2.21	.3424	.02174
.83	.12	5.30	-1.65	2.59	2.61	-1.06	.37	.132	-1.11	.3388	.02037
2.11	1.31	5.06	-1.67	2.71	2.62	-1.16	.41	.131	-.02	.3408	.01929
3.10	2.30	4.75	-1.67	2.61	2.61	-1.14	.40	.131	1.01	.3393	.01795
4.29	3.43	4.46	-1.67	2.60	2.62	-1.20	.37	.132	2.14	.3430	.01660
6.58	5.61	3.92	-1.67	2.61	2.62	-1.30	.37	.130	4.28	.3447	.01440
8.87	7.72	3.33	-1.65	2.49	2.61	-1.46	.24	.129	6.50	.3416	.01180

b. AVERAGE TUNNEL VELOCITY = 55.3 KTS

α , deg	α_{TPP} , deg	θ_C , deg	A_1 , deg	B_1 , deg	a_0 , deg	a_{1S} , deg	b_{1S} , deg	μ	γ , deg	C_T	C_Q
1.92	1.00	4.85	-1.36	2.99	2.62	-1.23	.55	.145	-.20	.3412	.01854
2.83	2.00	4.52	-1.37	2.81	2.61	-1.12	.58	.145	.83	.3421	.01712
3.92	2.84	4.43	-1.26	2.66	2.68	-1.37	.34	.144	1.82	.3440	.01611
5.01	3.85	4.14	-1.26	2.65	2.68	-1.45	.33	.143	2.84	.3425	.01478
5.99	4.79	3.82	-1.26	2.57	2.66	-1.48	.27	.143	3.83	.3395	.01351
7.01	5.73	3.75	-1.22	2.39	2.73	-1.56	.12	.143	4.92	.3458	.01232

c. AVERAGE TUNNEL VELOCITY = 62.3 KTS

α , deg	α_{TPP} , deg	θ_C , deg	A_1 , deg	B_1 , deg	a_0 , deg	a_{1S} , deg	b_{1S} , deg	μ	γ , deg	C_T	C_Q
.70	-.26	5.12	-1.40	3.41	2.63	-1.20	.54	.162	-1.19	.3476	.02007
1.70	.66	4.72	-1.40	3.41	2.59	-1.28	.52	.163	-.28	.3427	.01818
2.61	1.52	4.53	-1.39	3.40	2.61	-1.34	.51	.162	.57	.3469	.01715
3.72	2.55	4.10	-1.40	3.42	2.53	-1.41	.50	.162	1.61	.3369	.01542
4.66	3.25	4.01	-1.41	3.63	2.60	-1.64	.50	.162	2.25	.3476	.01509
5.54	4.00	3.69	-1.40	3.71	2.56	-1.77	.46	.162	2.99	.3426	.01371

Table VII.~ Concluded.

d. AVERAGE TUNNEL VELOCITY = 66.7 KTS

$\alpha,$ deg	$\alpha_{TPP},$ deg	$\theta_C,$ deg	$A_1,$ deg	$B_1,$ deg	$a_0,$ deg	$a_{1S},$ deg	$b_{1S},$ deg	μ	$\gamma,$ deg	C_T	C_Q
- .47	-1.55	5.46	-1.38	3.26	2.60	-1.31	.12	.173	-2.15	.3425	.02108
1.31	.21	4.83	-1.47	3.39	2.48	-1.31	.25	.174	-.50	.3471	.01878
2.22	1.08	4.50	-1.48	3.41	2.47	-1.35	.27	.173	.28	.3433	.01730
3.23	1.93	4.26	-1.44	3.34	2.52	-1.51	.16	.173	1.24	.3443	.01585
4.01	2.52	4.15	-1.33	3.17	2.59	-1.70	-.06	.174	1.97	.3501	.01497

e. AVERAGE TUNNEL VELOCITY = 71.2 KTS

$\alpha,$ deg	$\alpha_{TPP},$ deg	$\theta_C,$ deg	$A_1,$ deg	$B_1,$ deg	$a_0,$ deg	$a_{1S},$ deg	$b_{1S},$ deg	μ	$\gamma,$ deg	C_T	C_Q
- .39	-1.68	5.29	-1.12	3.72	2.51	-1.49	.33	.185	-2.10	.3398	.02078
.14	-1.03	5.21	-1.11	3.54	2.54	-1.36	.33	.185	-1.43	.3440	.02017
1.11	-.12	4.90	-1.10	3.52	2.55	-1.42	.35	.185	-.56	.3461	.01871
1.62	.46	4.59	-1.09	3.28	2.16	-1.34	.30	.185	.15	.3406	.01738
2.57	1.30	4.37	-1.10	3.39	2.20	-1.46	.33	.185	.88	.3484	.01629
3.41	2.04	4.08	-1.10	3.39	2.19	-1.56	.30	.185	1.60	.3477	.01485
4.13	2.85	3.86	-1.10	3.26	2.16	-1.46	.32	.184	2.42	.3472	.01385

ORIGINAL PAGE IS
OF POOR QUALITY

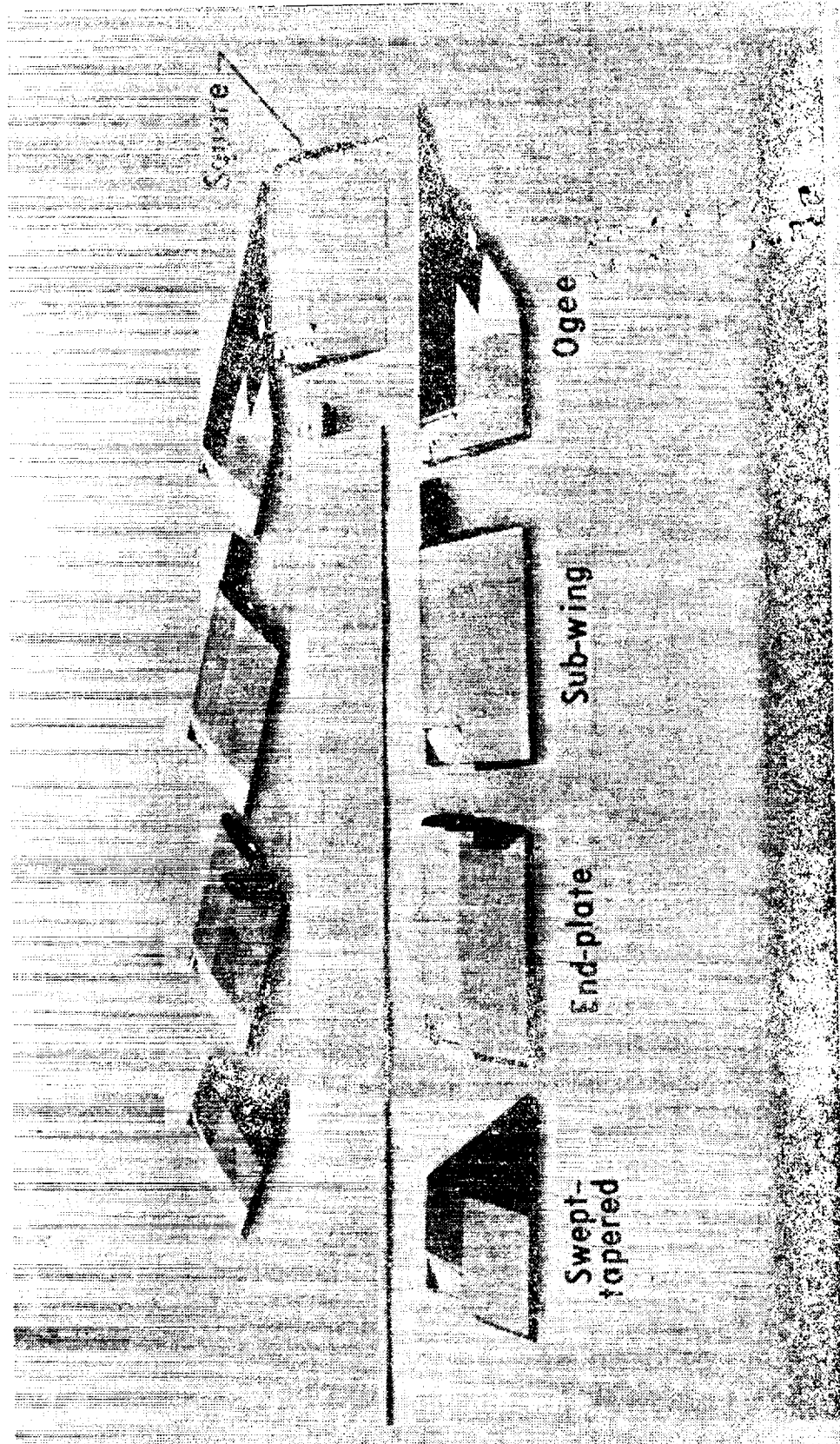


Figure 1. - Photograph of one rotor blade and five tip configurations tested.

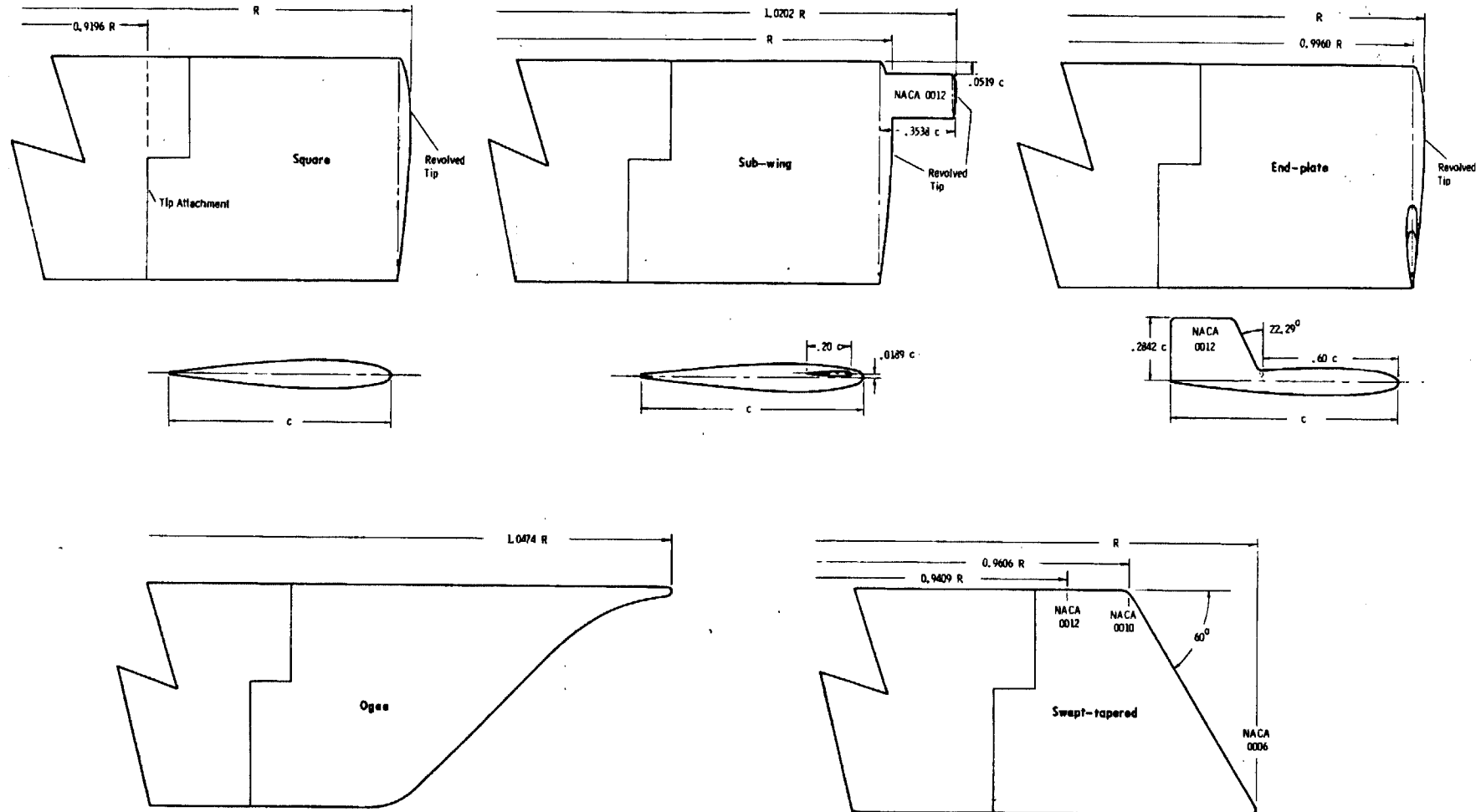
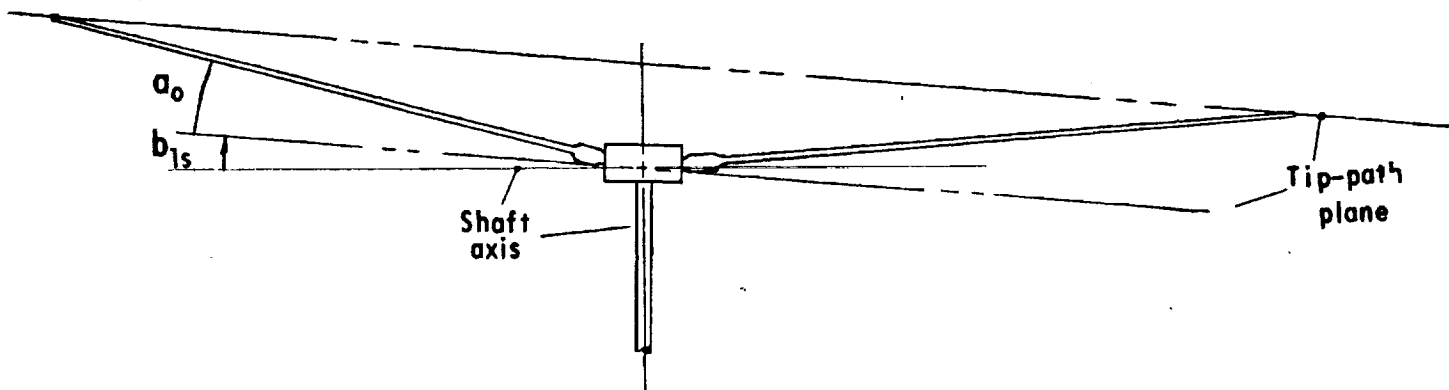
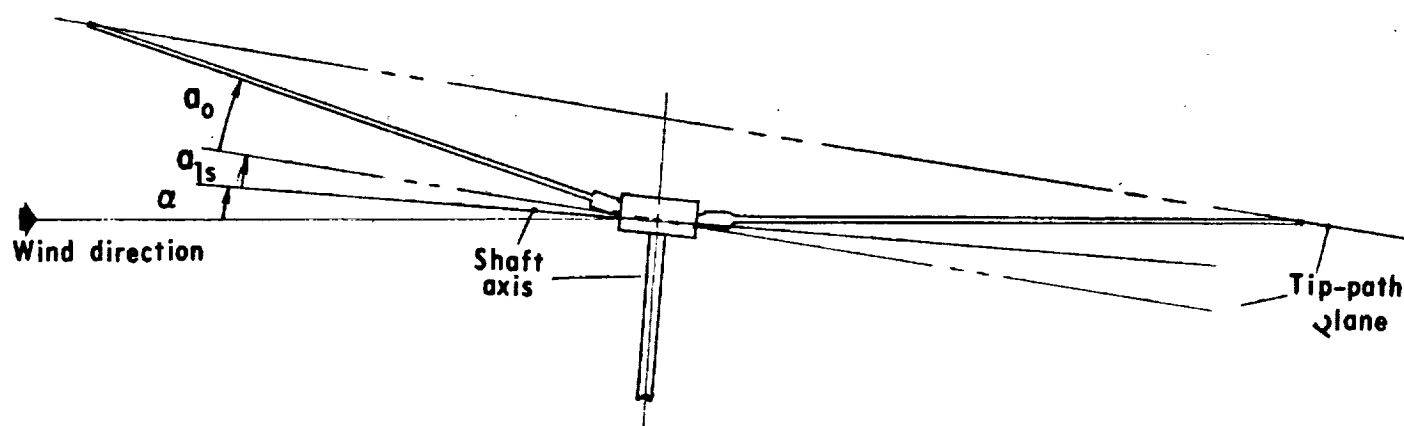


Figure 2. - Sketch of tip configurations tested.



View from rear



View from left

Figure 3. Rotor coordinate system.

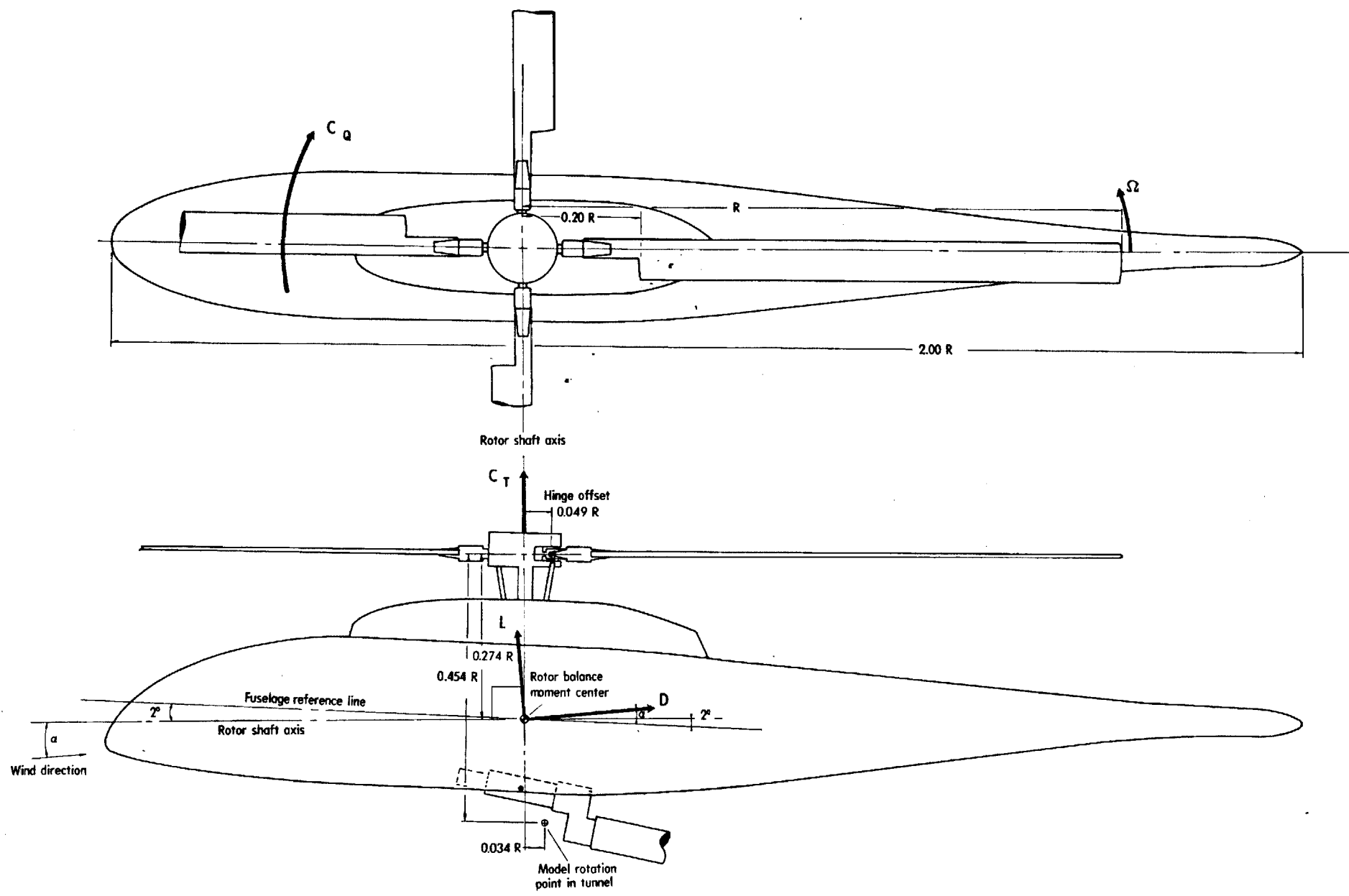
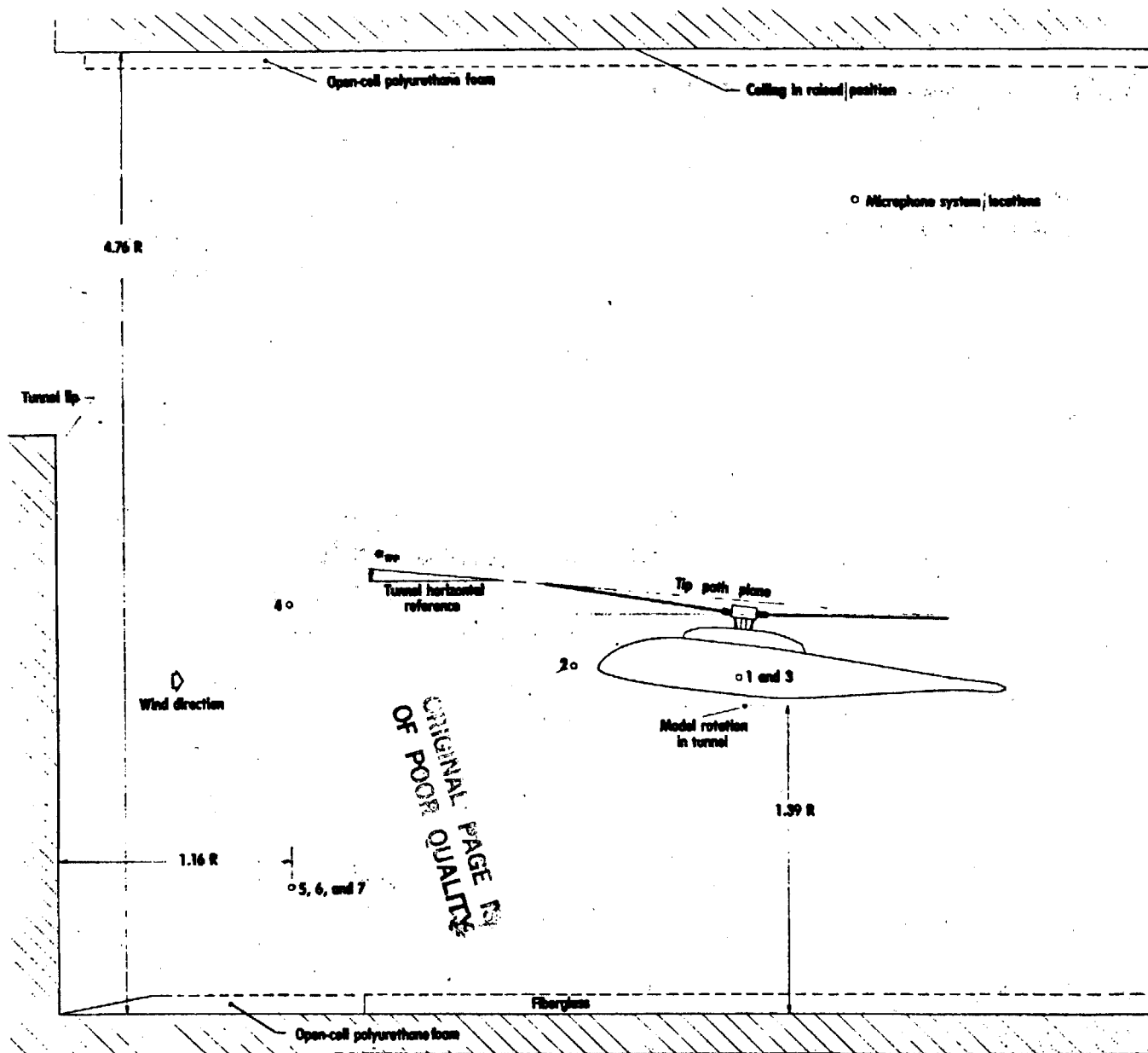
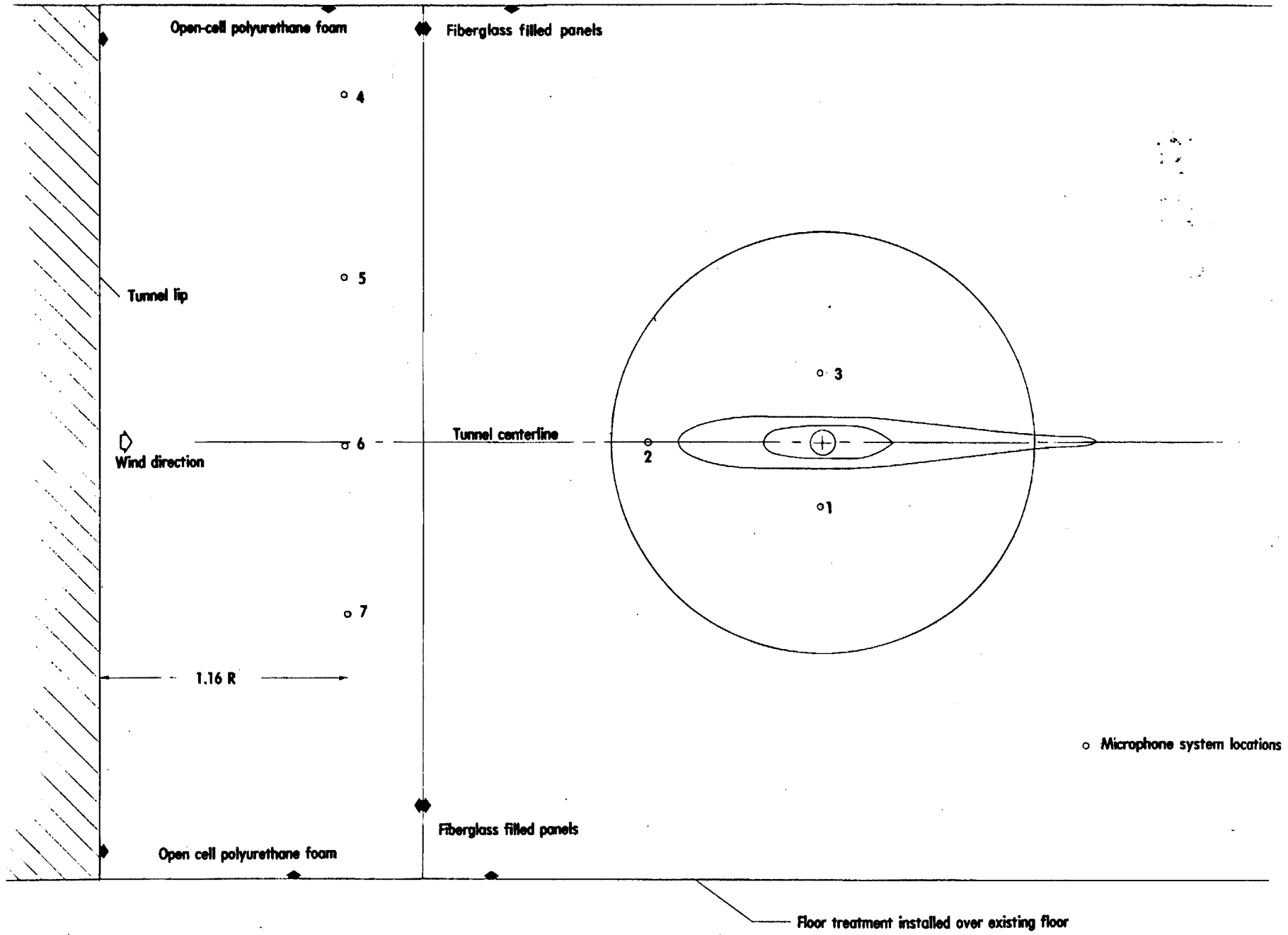


Figure 4. - Sketch of the helicopter model with square tips installed.



(a) Side view

Figure 5. - Sketch of relative positions of model and microphones in the tunnel.



(b) Top view

Figure 5. - Concluded.

ORIGINAL PAGE IS
OF POOR QUALITY

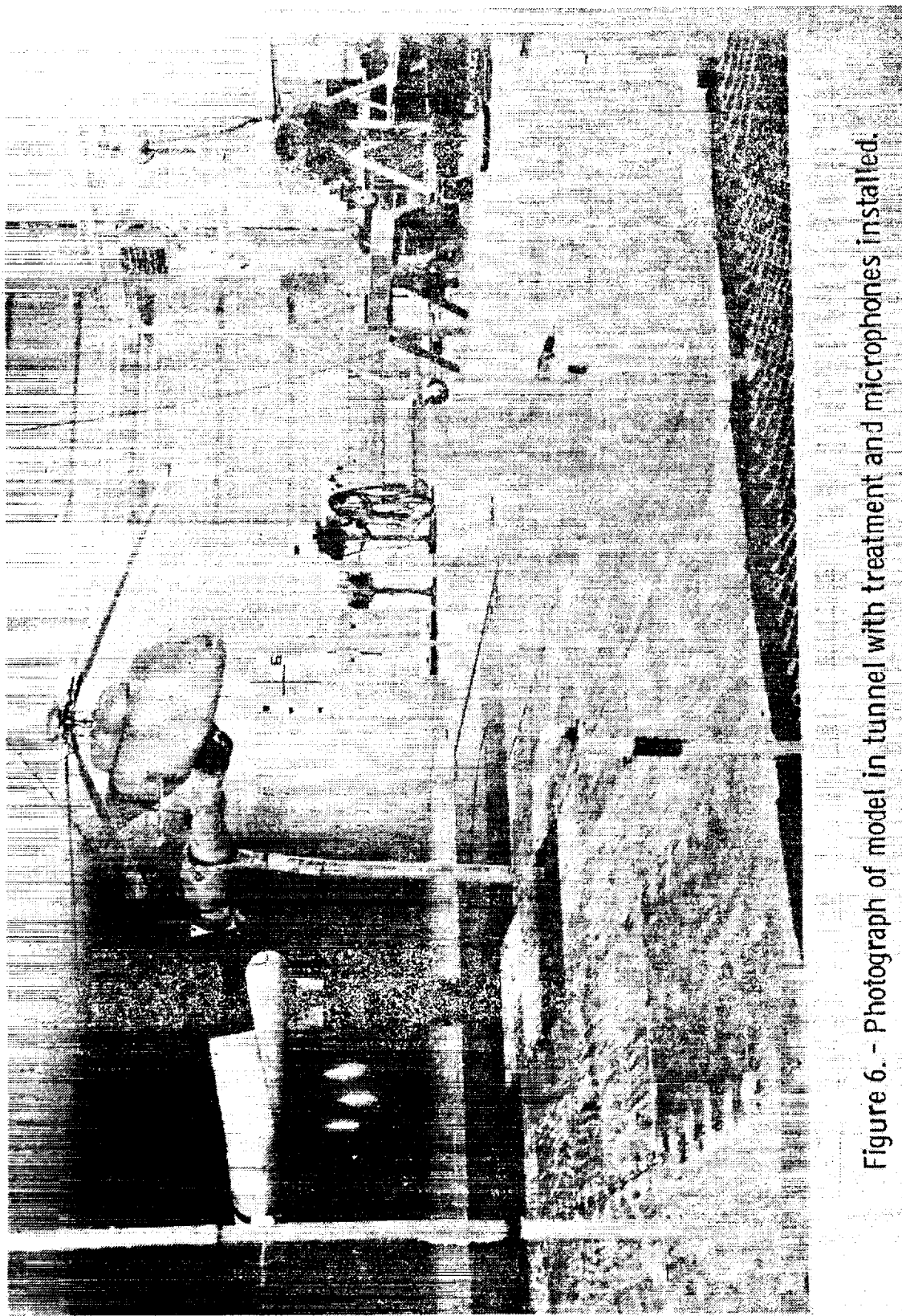


Figure 6. - Photograph of model in tunnel with treatment and microphones installed.

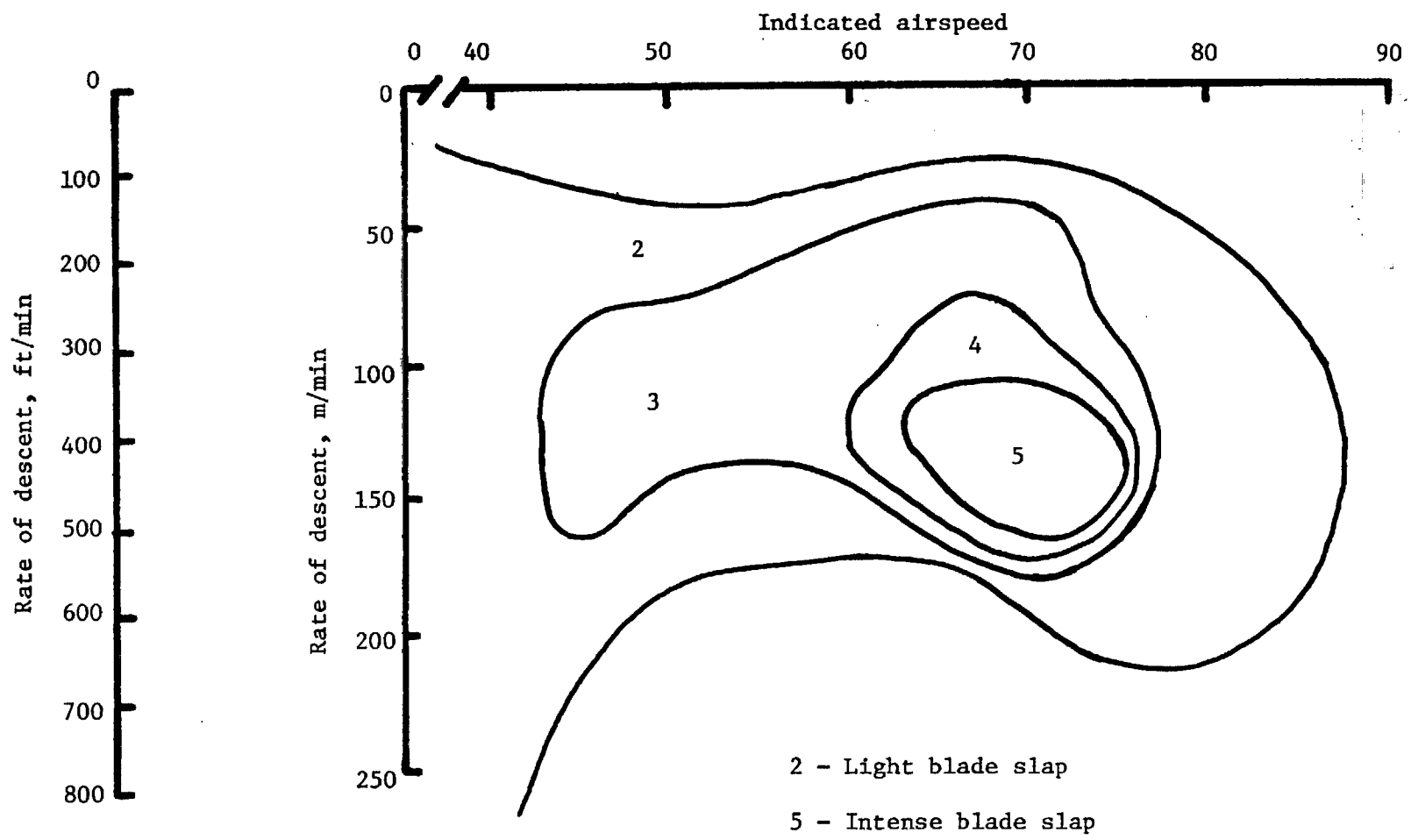


Figure 7. - Internal blade slap noise, observer subjective response - flight test.

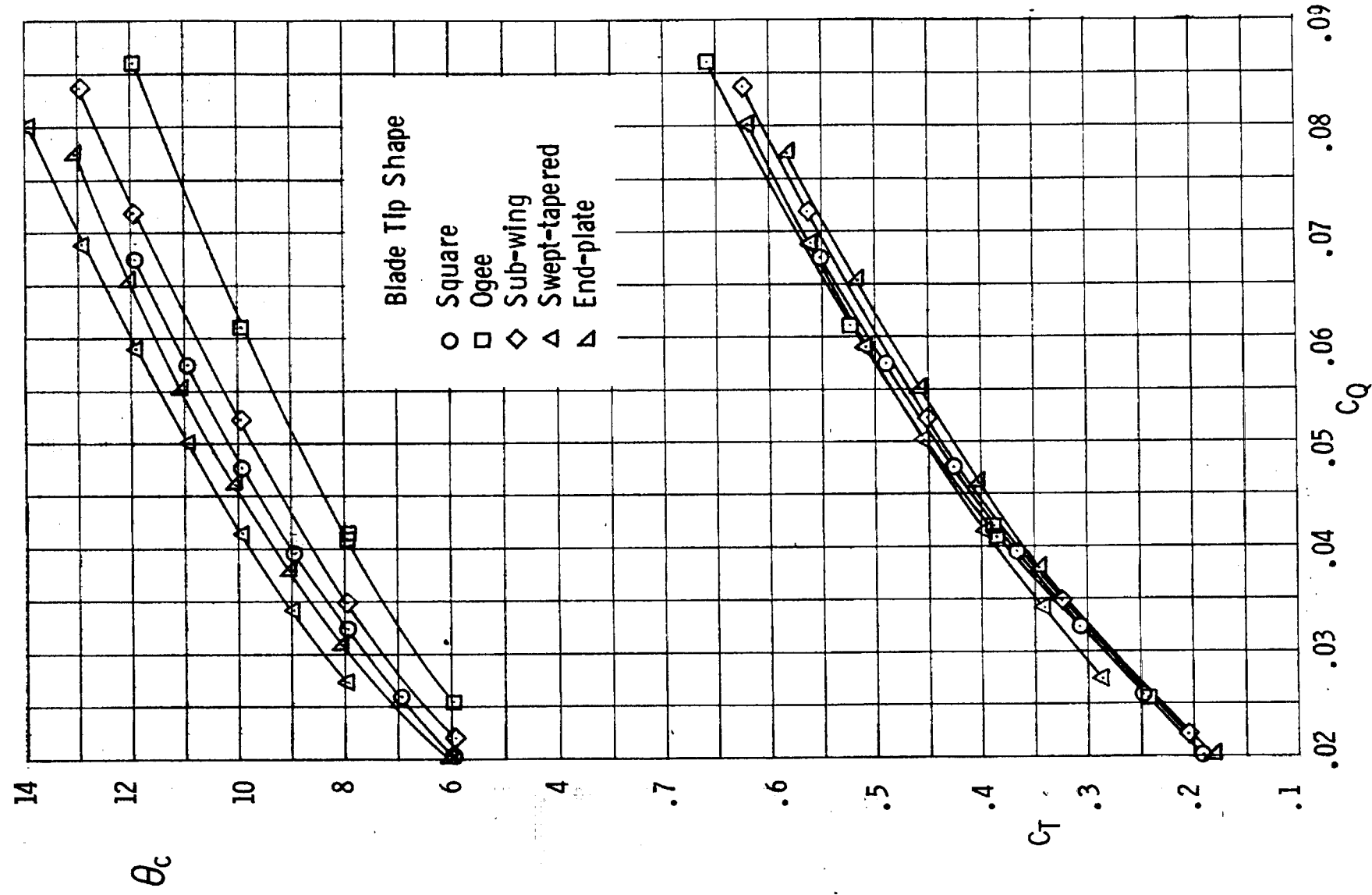
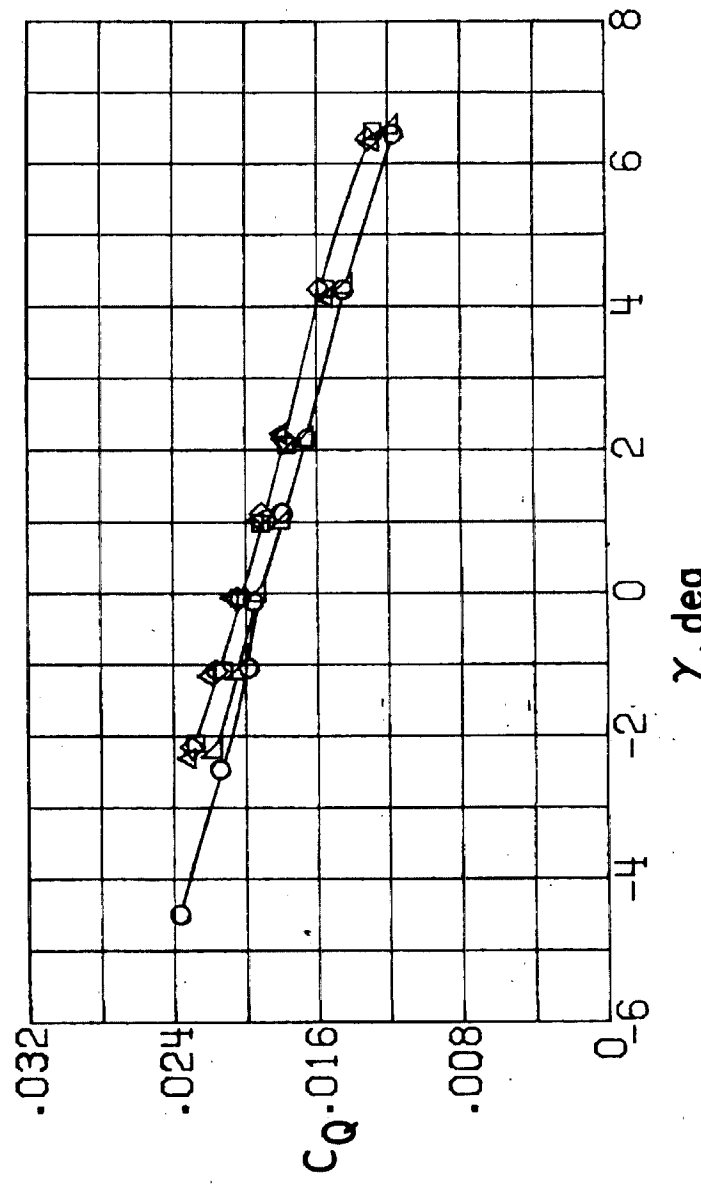
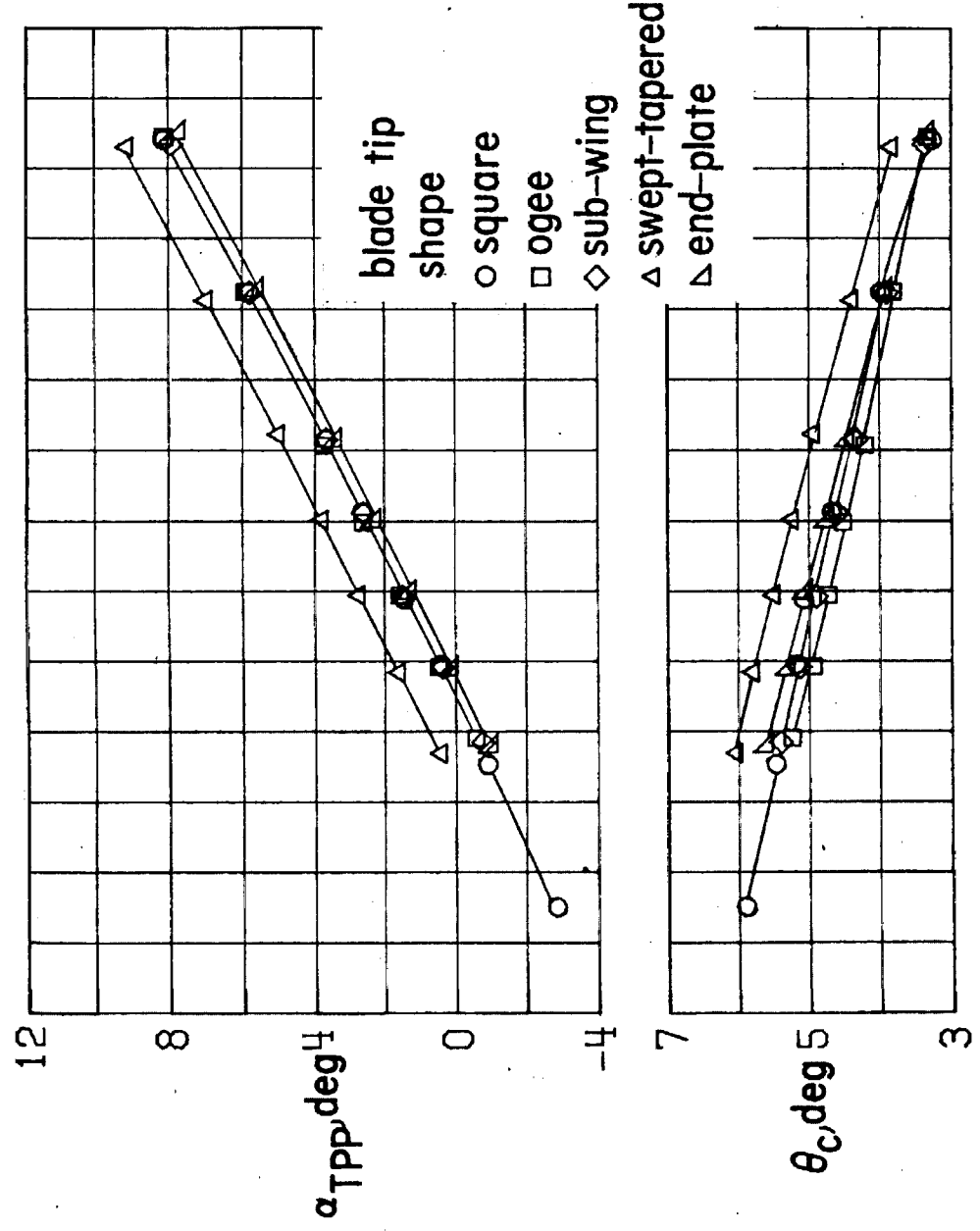


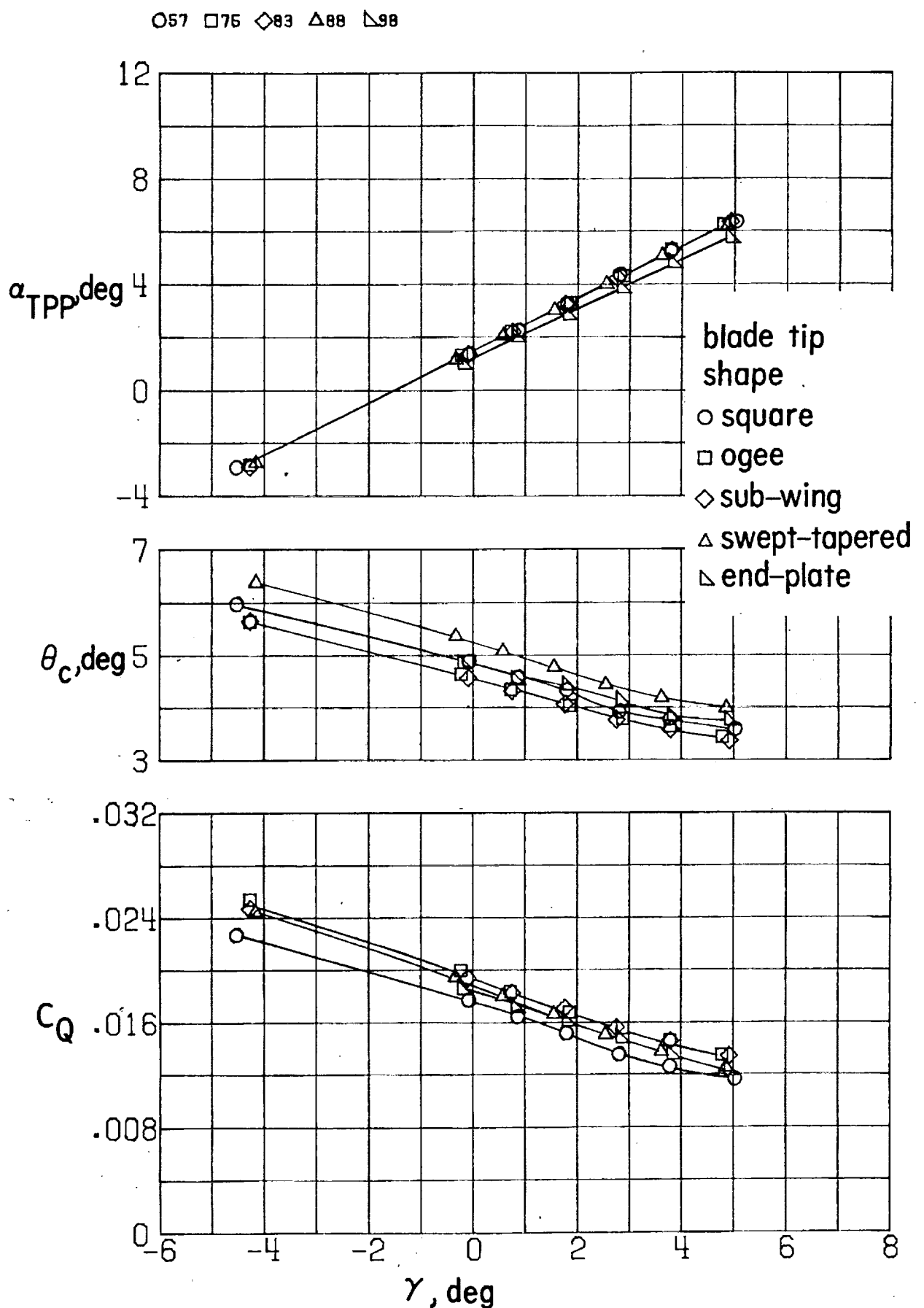
Figure 8. - Performance of rotor tip configurations in hover.

○ 56 □ 74 ◇ 78 Δ 87 ▲ 97



(a) Forward velocity \approx 51 knots

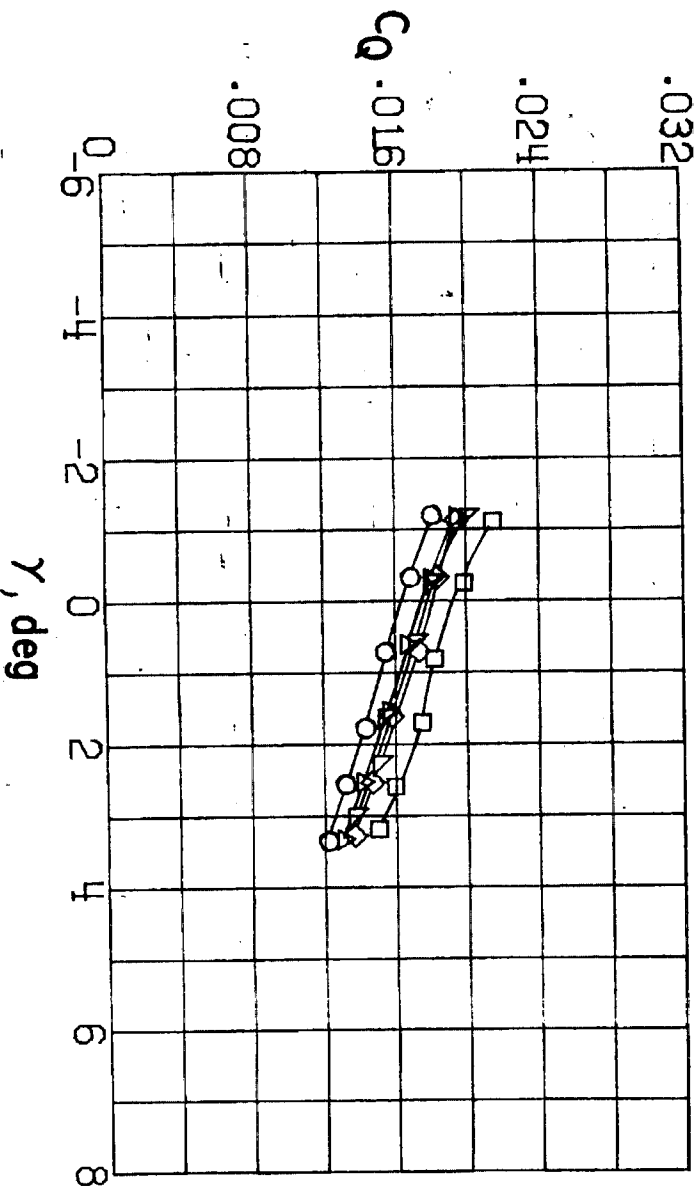
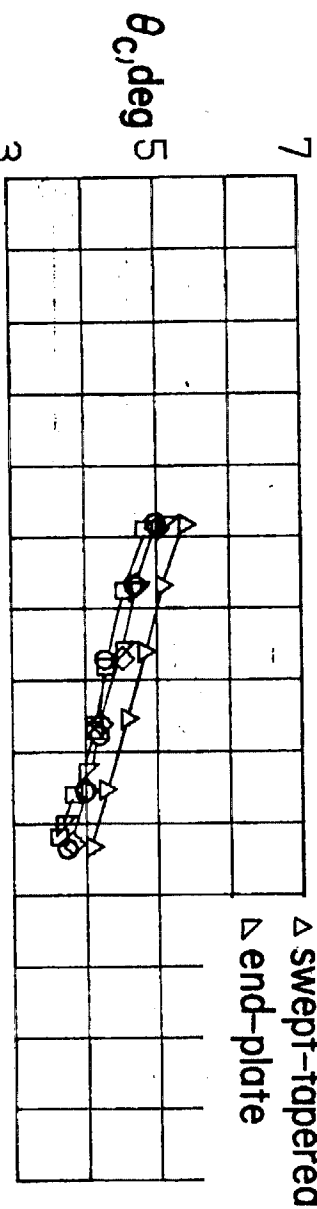
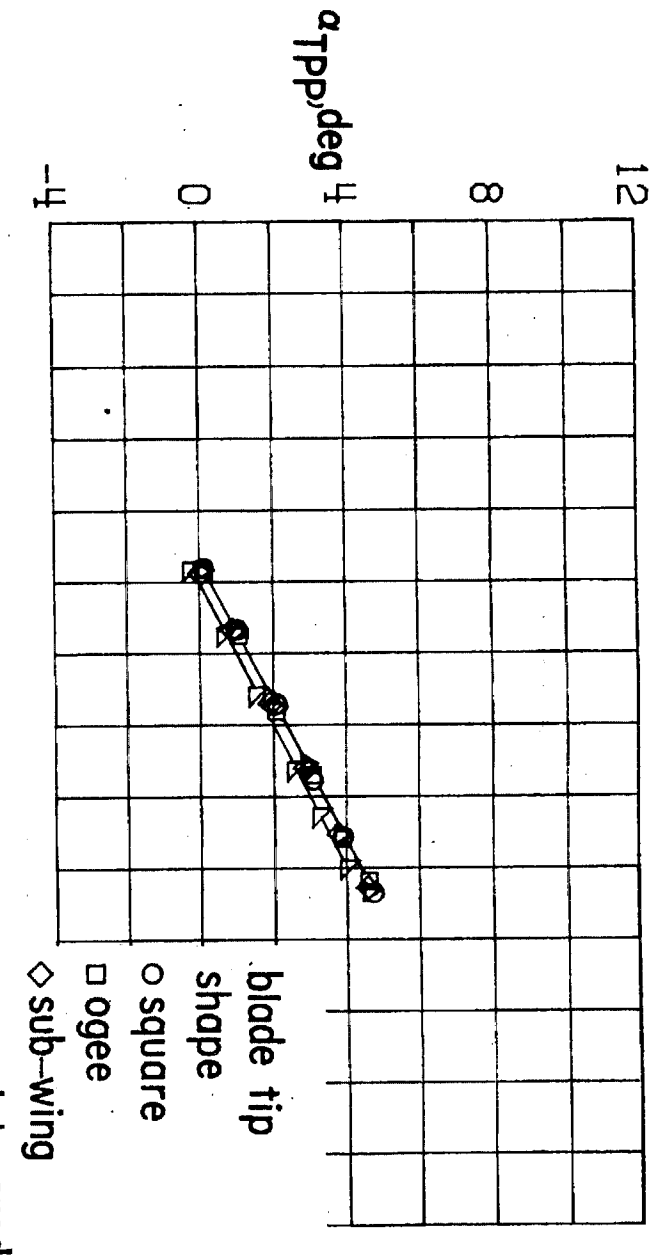
Figure 9.- Performance comparisons of rotor tip configurations at various forward speeds.



(b) Forward velocity \approx 56 knots

Figure 9. - Continued.

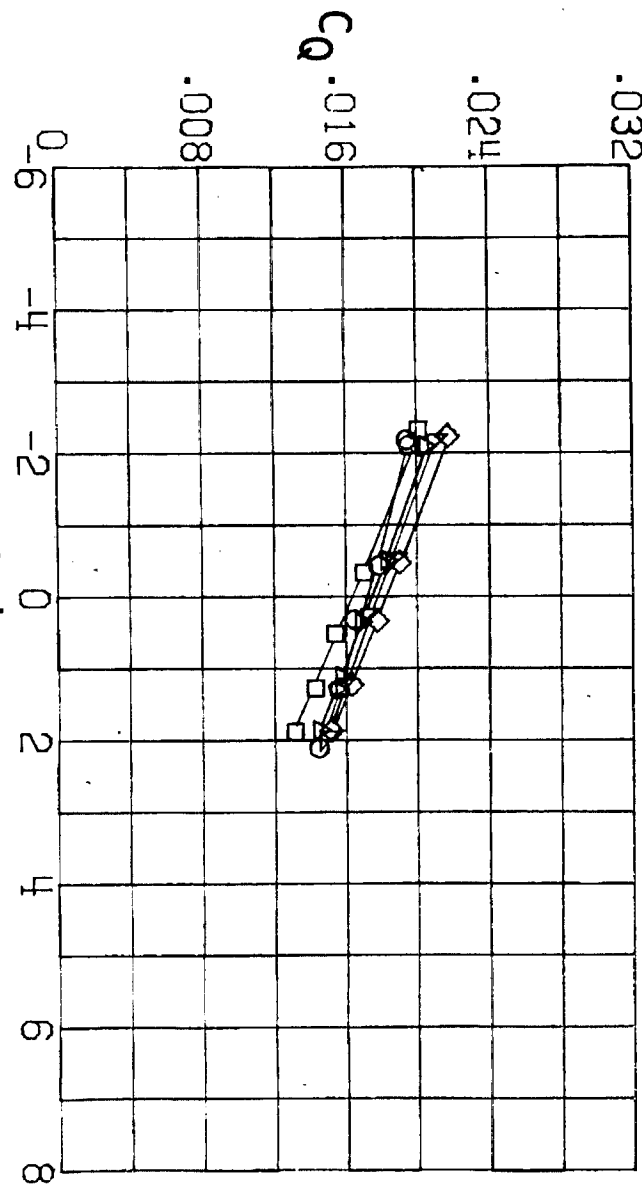
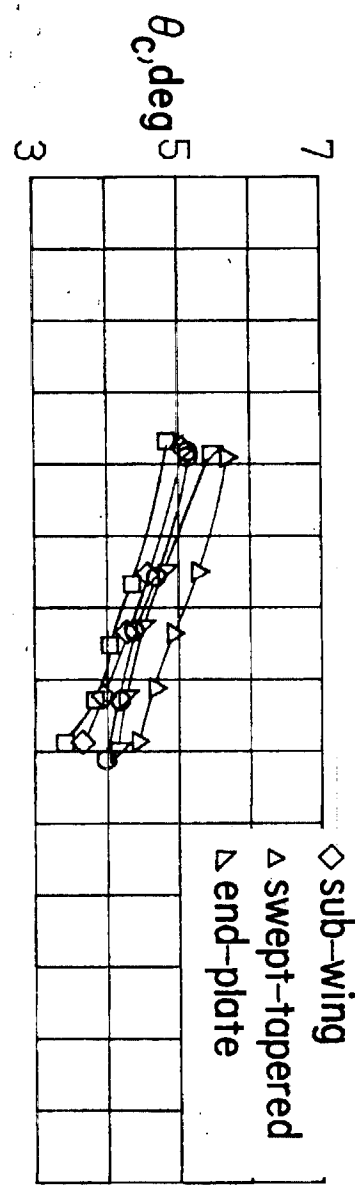
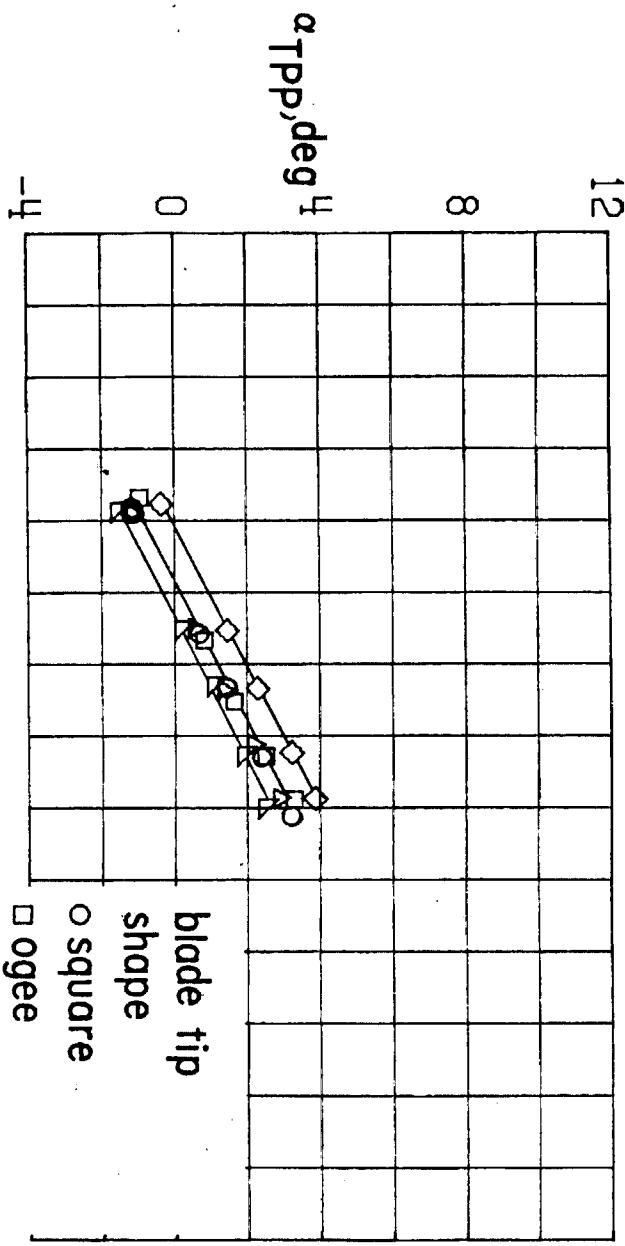
○58 □76 ◇79 △89 ▲99



(c) Forward velocity ≈ 61 knots

Figure 9. - Continued.

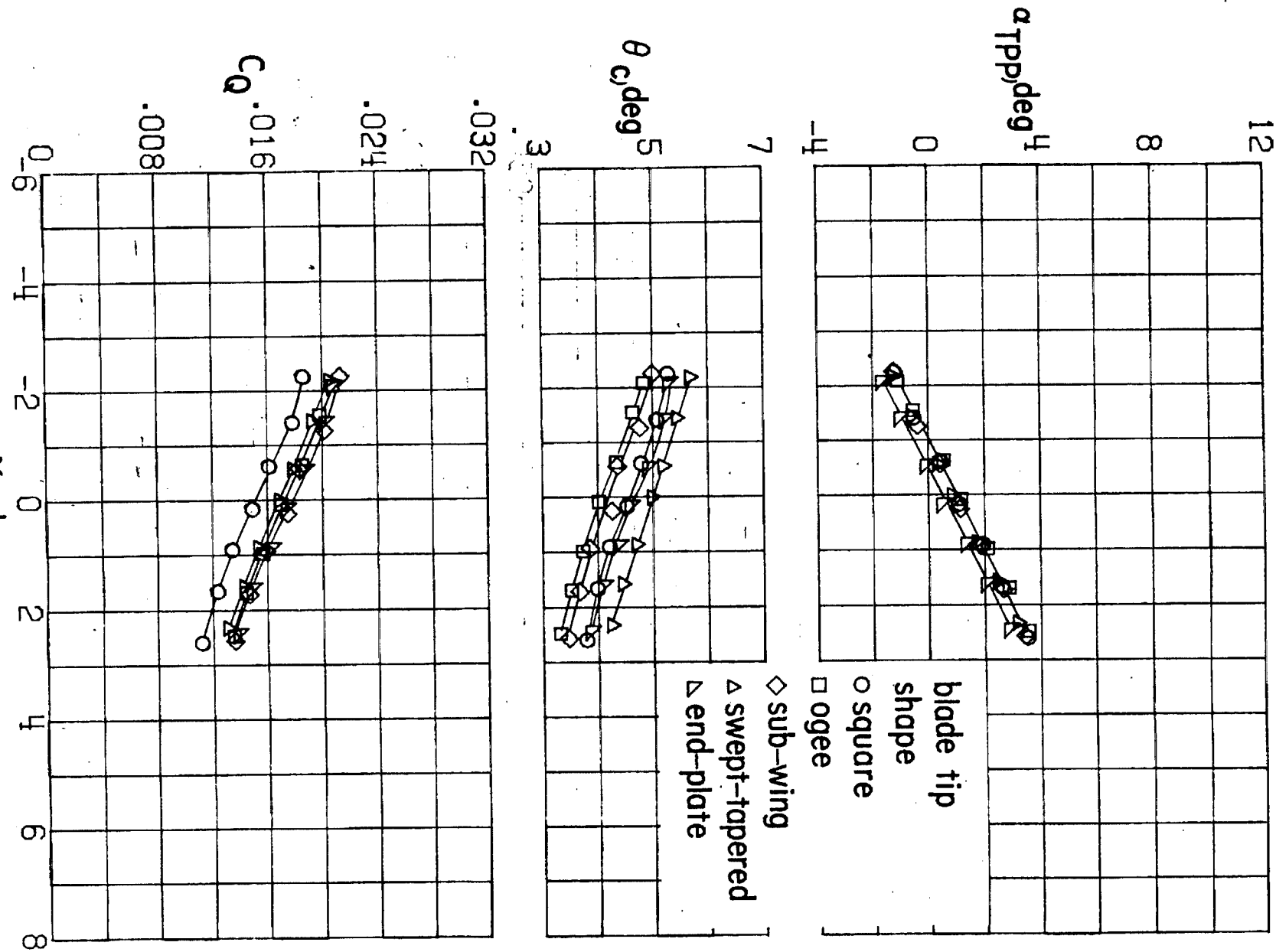
069 □ 69 ◇ 80 Δ 90 △ 100



(d) Forward velocity \approx 66 knots

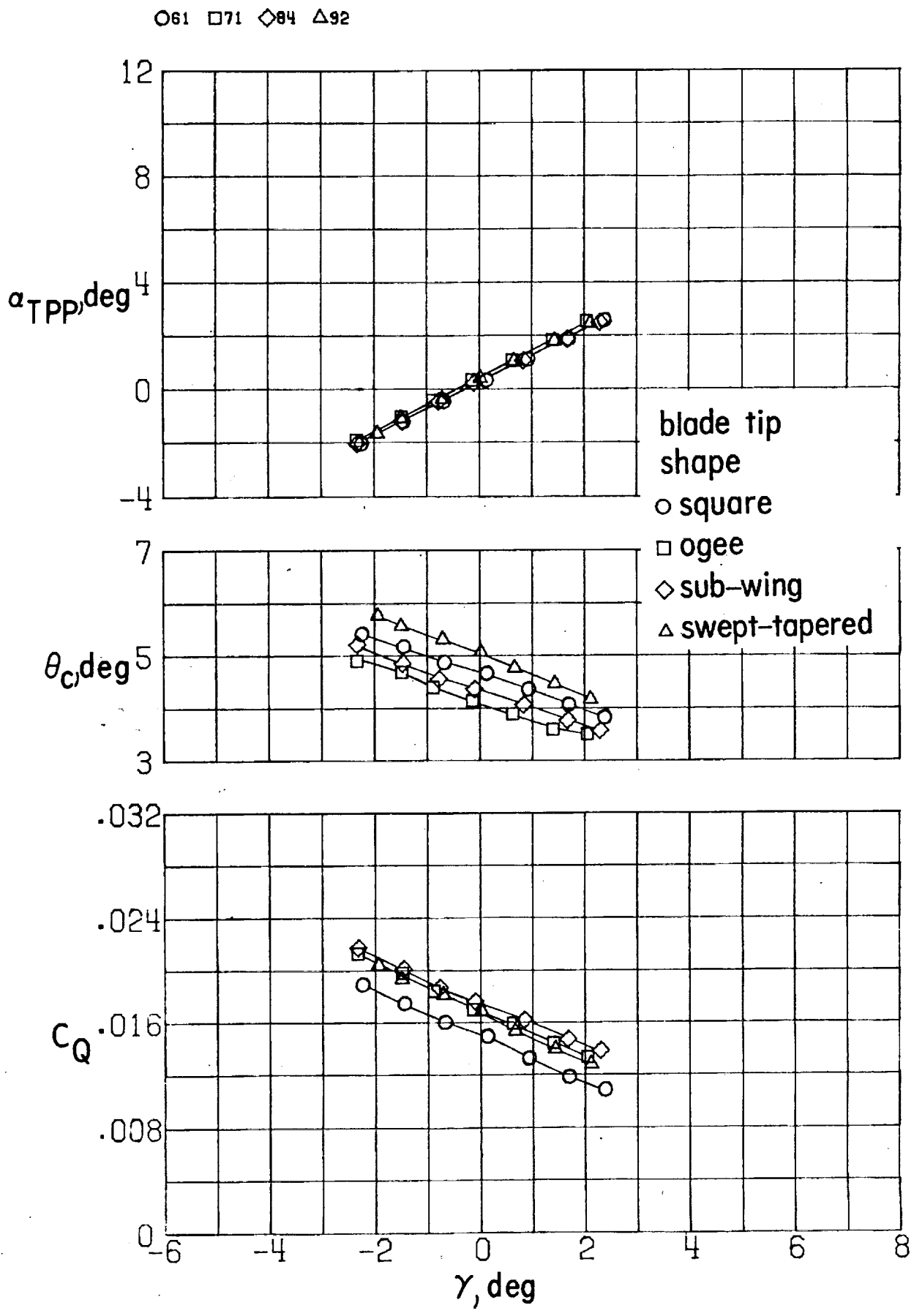
Figure 9. - Continued.

O60 □70 ◇82 Δ91 ▲101



(e) Forward velocity \approx 71 knots

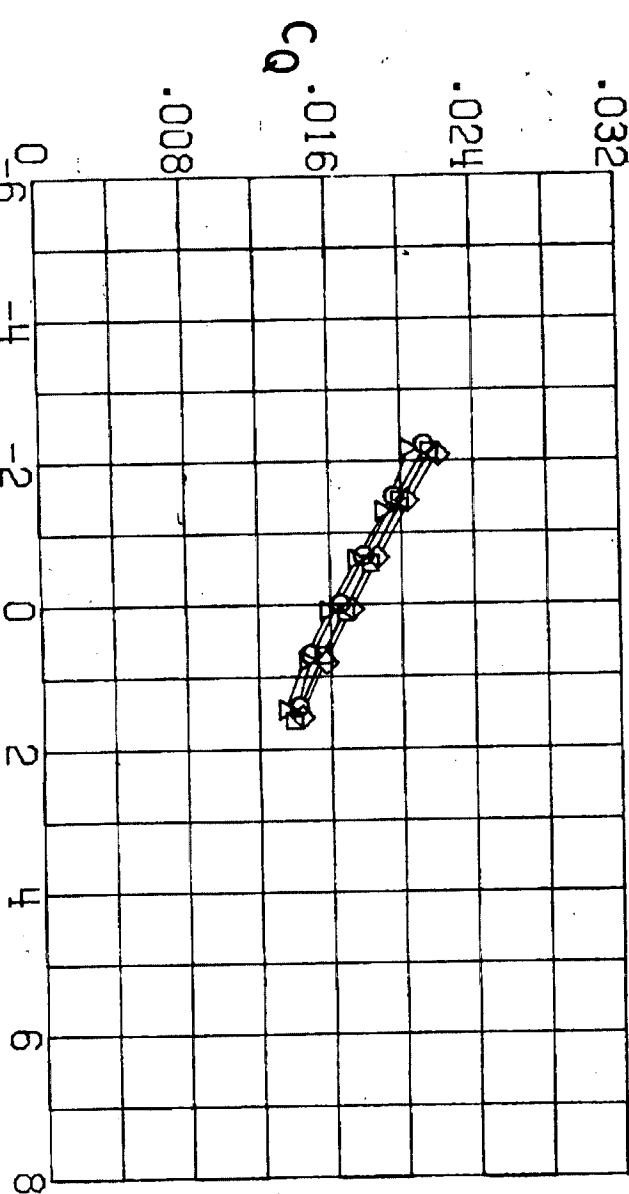
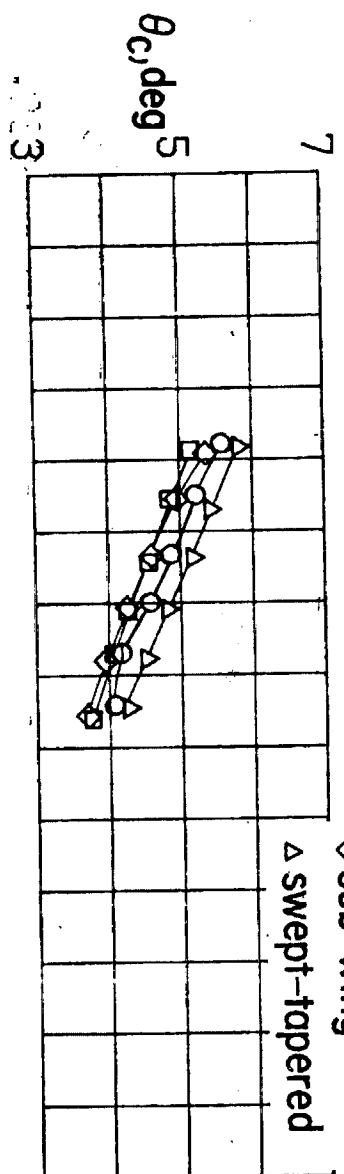
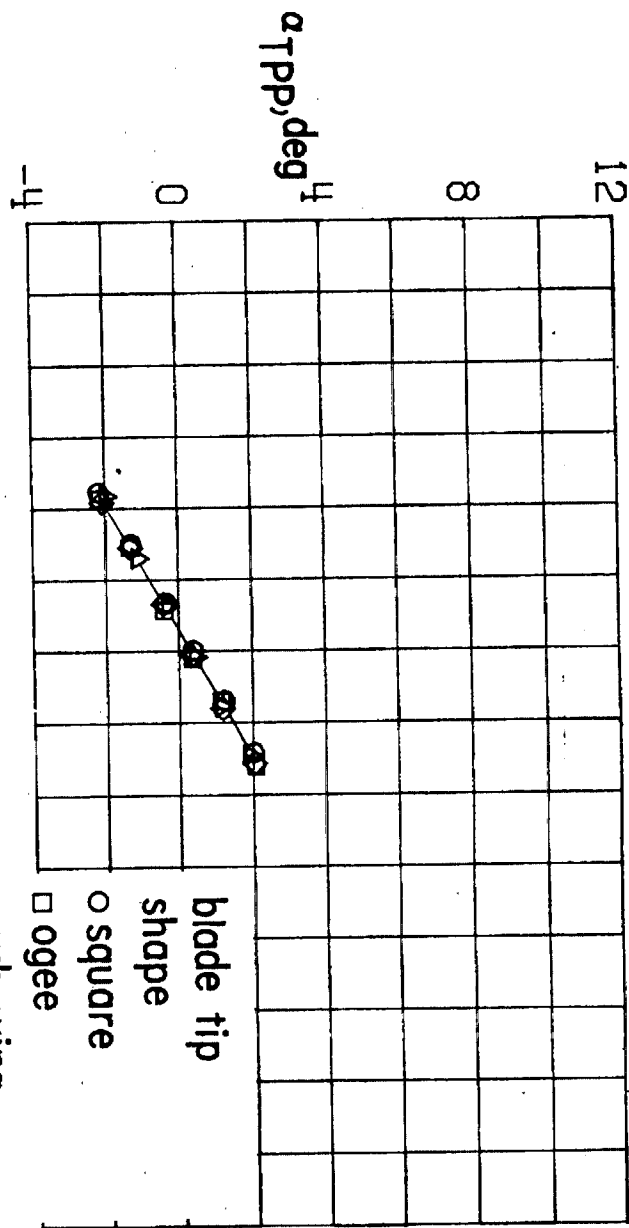
Figure 9. - Continued.



(f) Forward velocity ≈ 76 knots

Figure 9. - Continued.

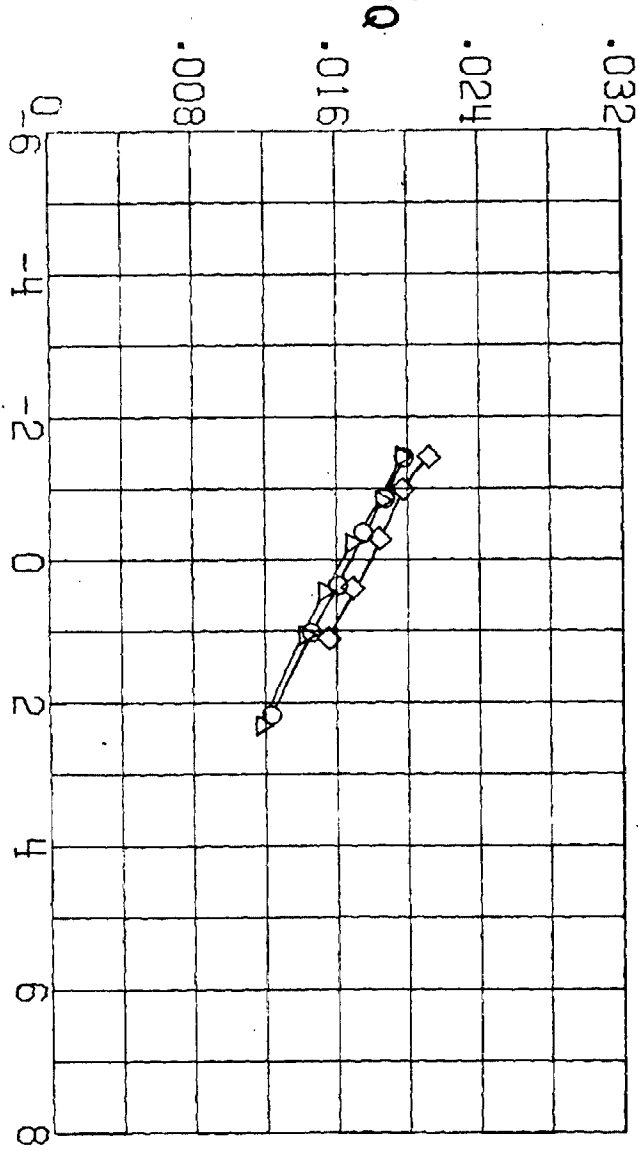
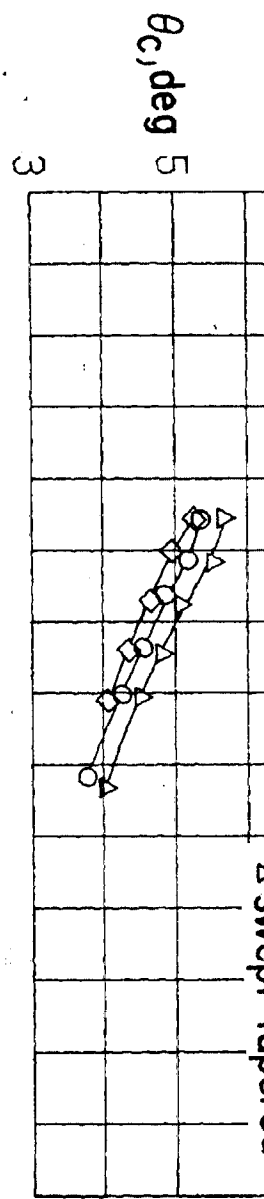
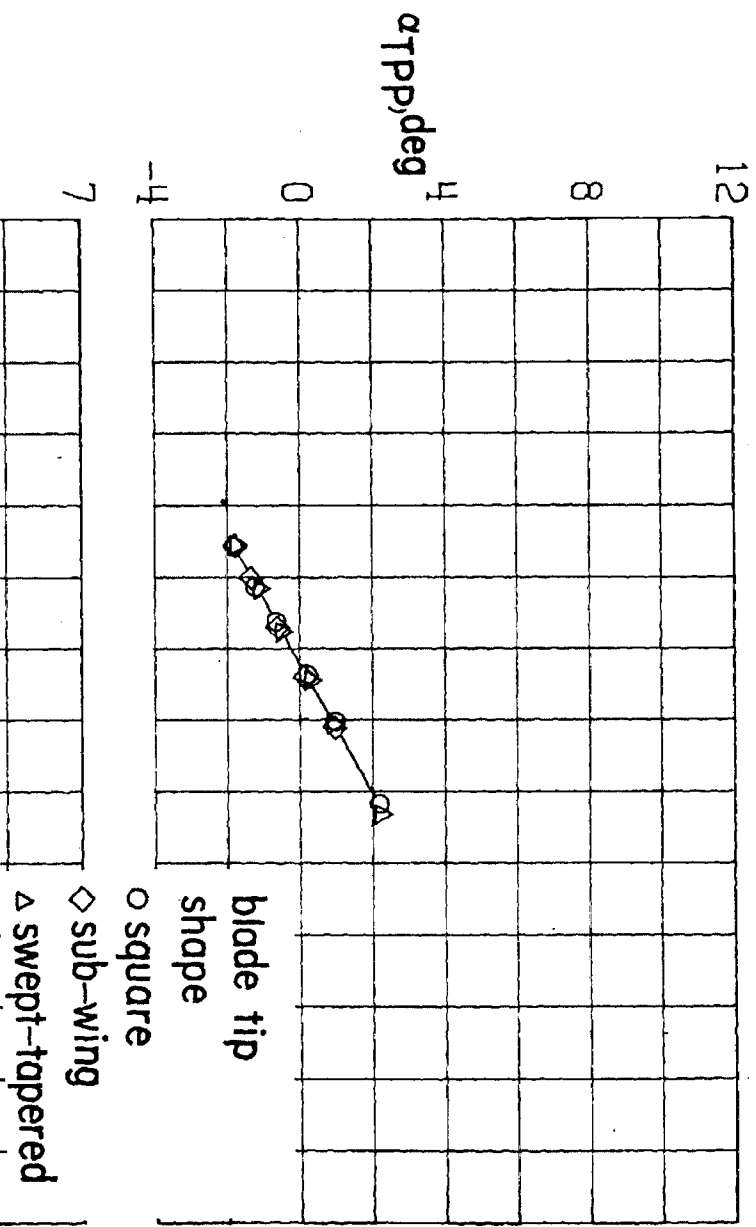
062 □ 72 ◇ 81 Δ 93



(g) Forward velocity ≈ 82 knots

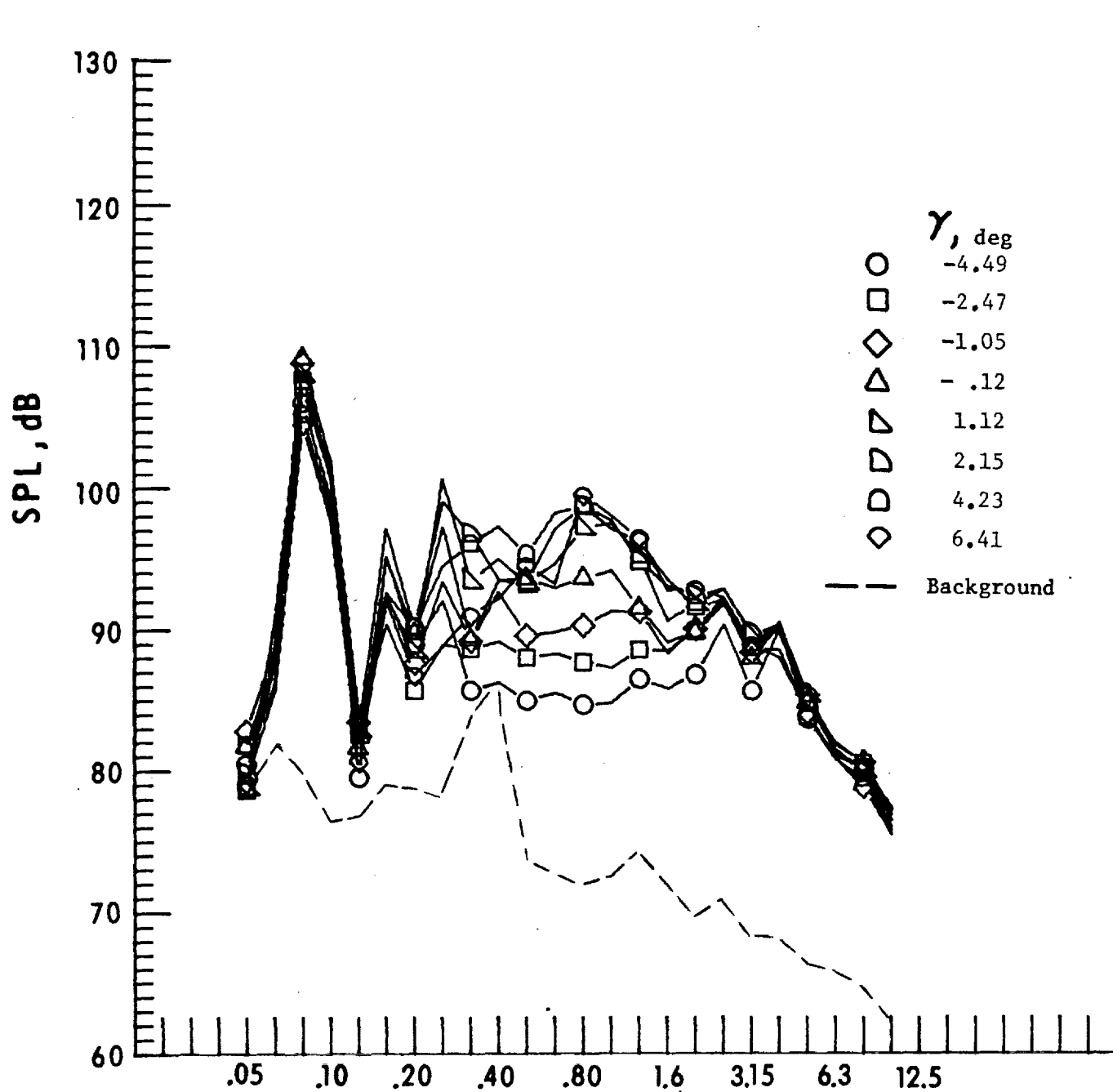
Figure 9. - Continued.

O 63 □ 73 ◇ 85 △ 94



(h) Forward velocity \approx 91 knots

Figure 9. - Concluded.



One-third-octave-band center frequency, kHz

a. Mic. no. 1.

Figure 10. - Effect of descent angle variation on noise generated by helicopter model with square tips installed. $V_\infty = 51.4$ knots.

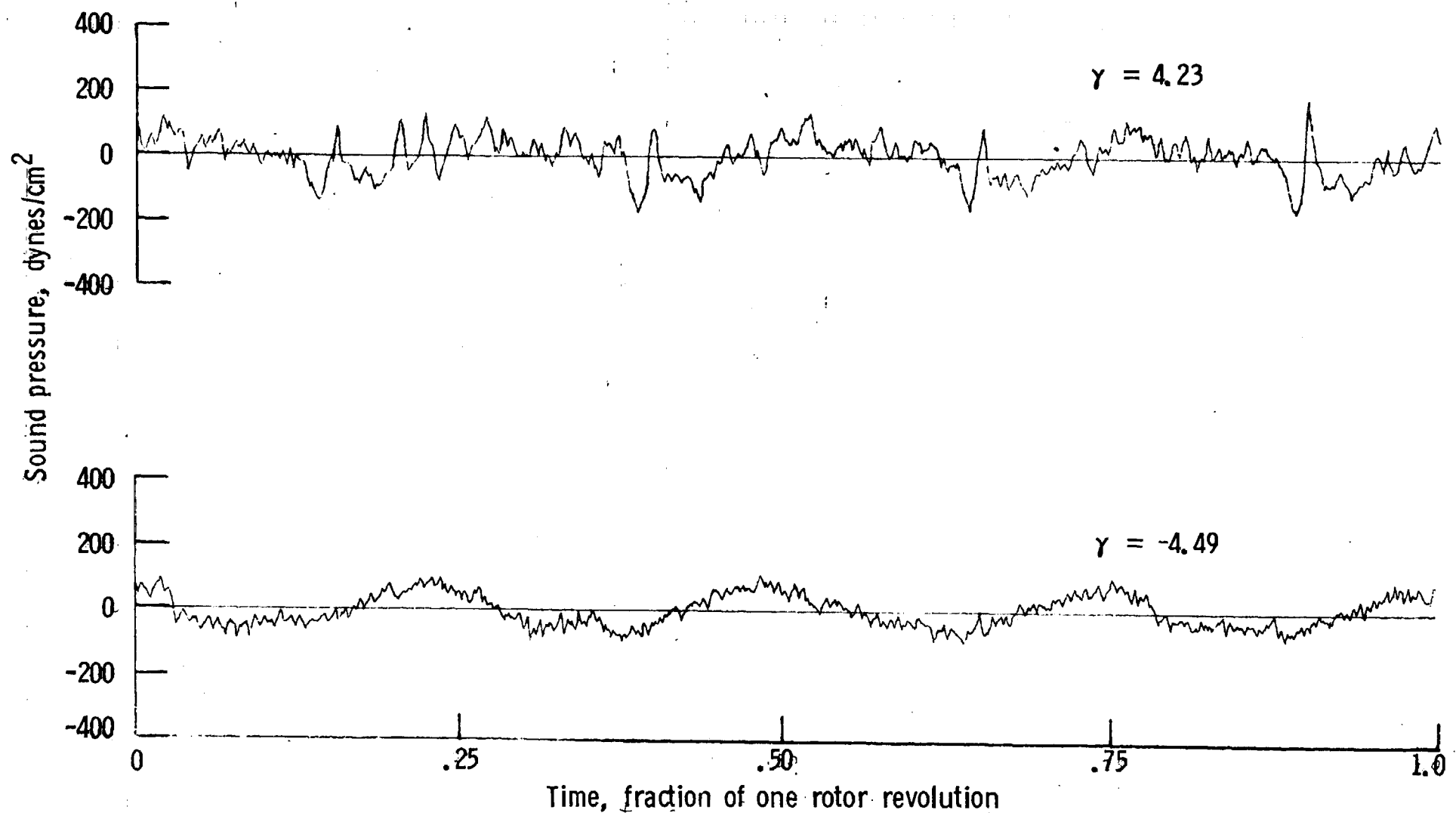
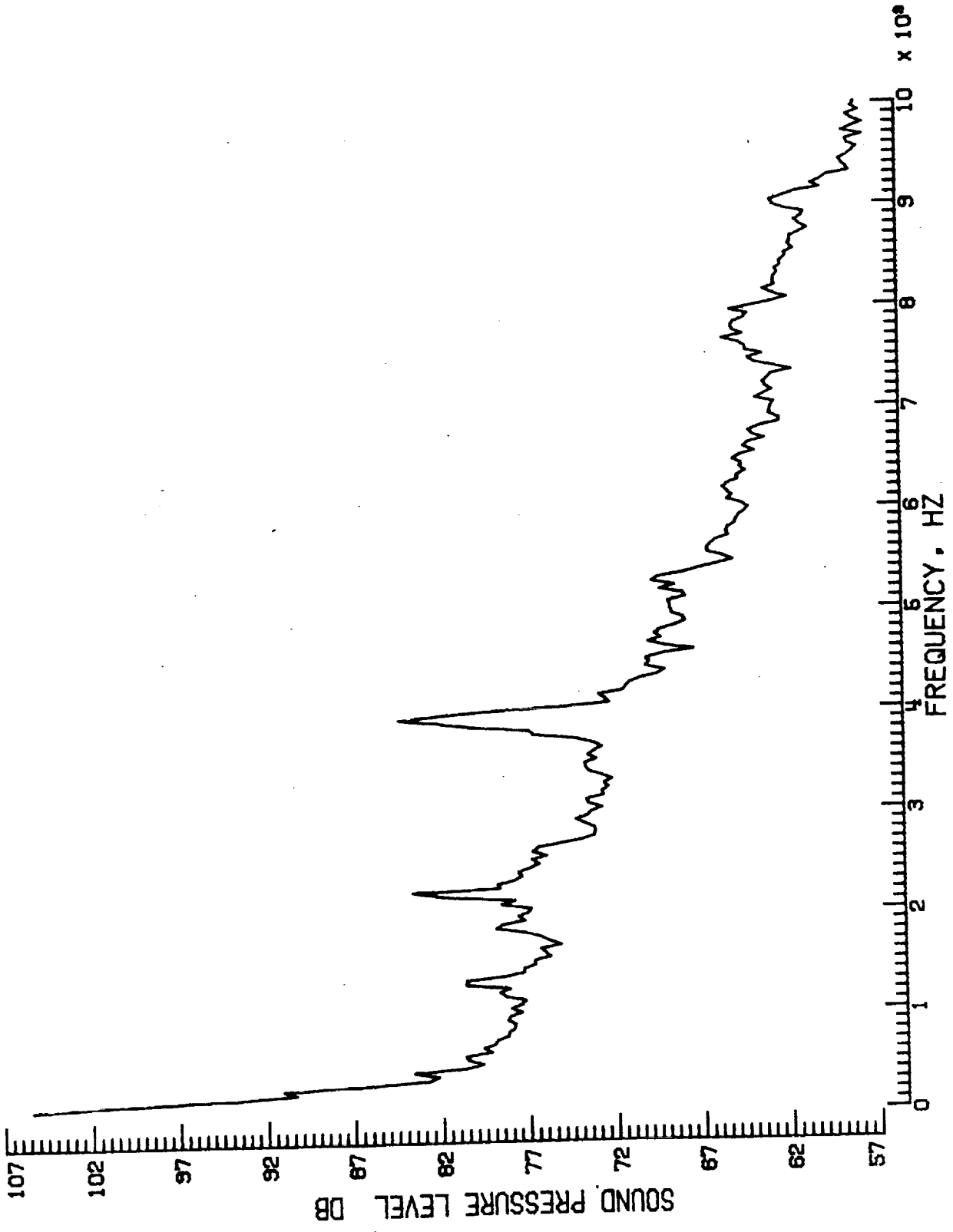
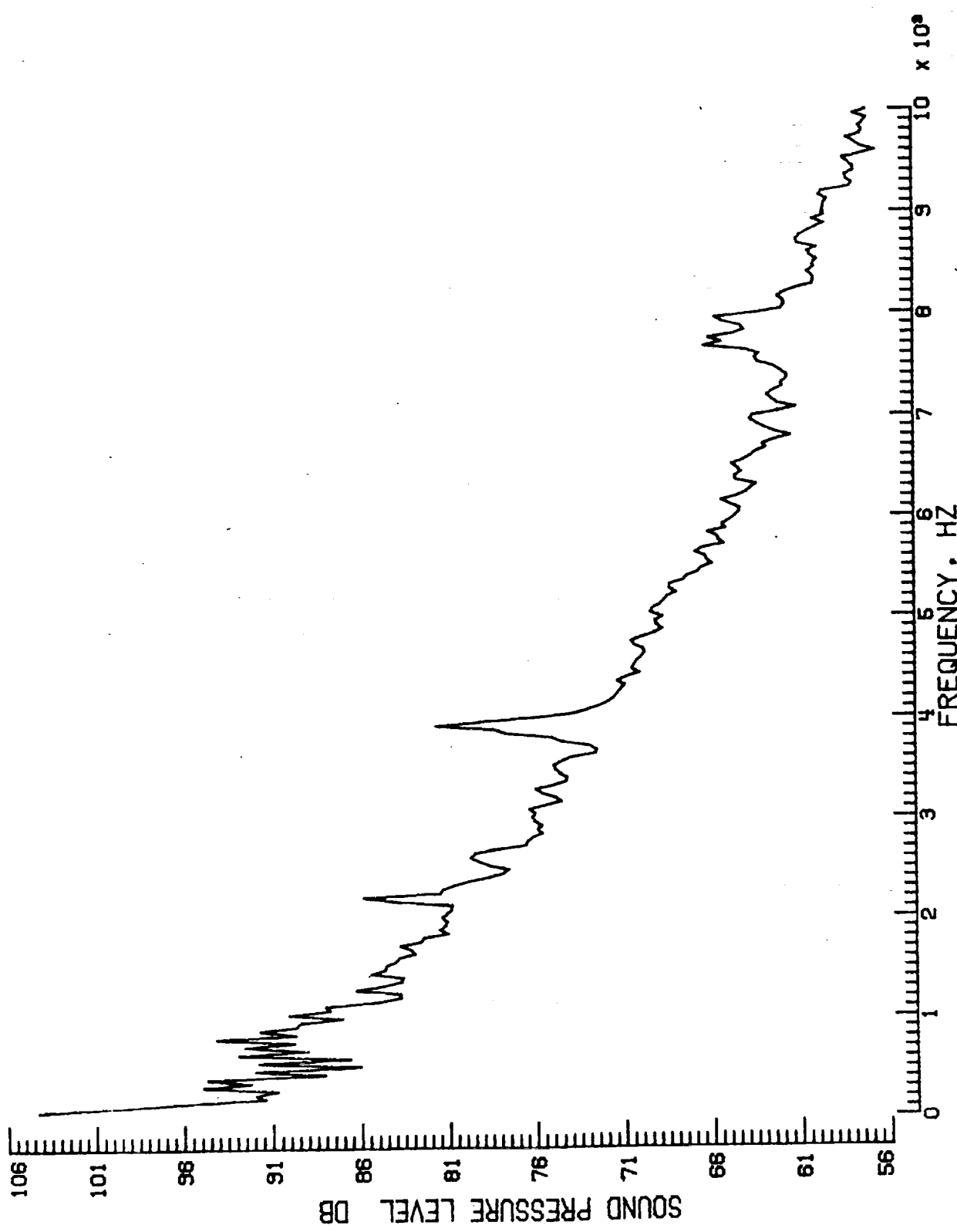


Figure 10. - Continued.



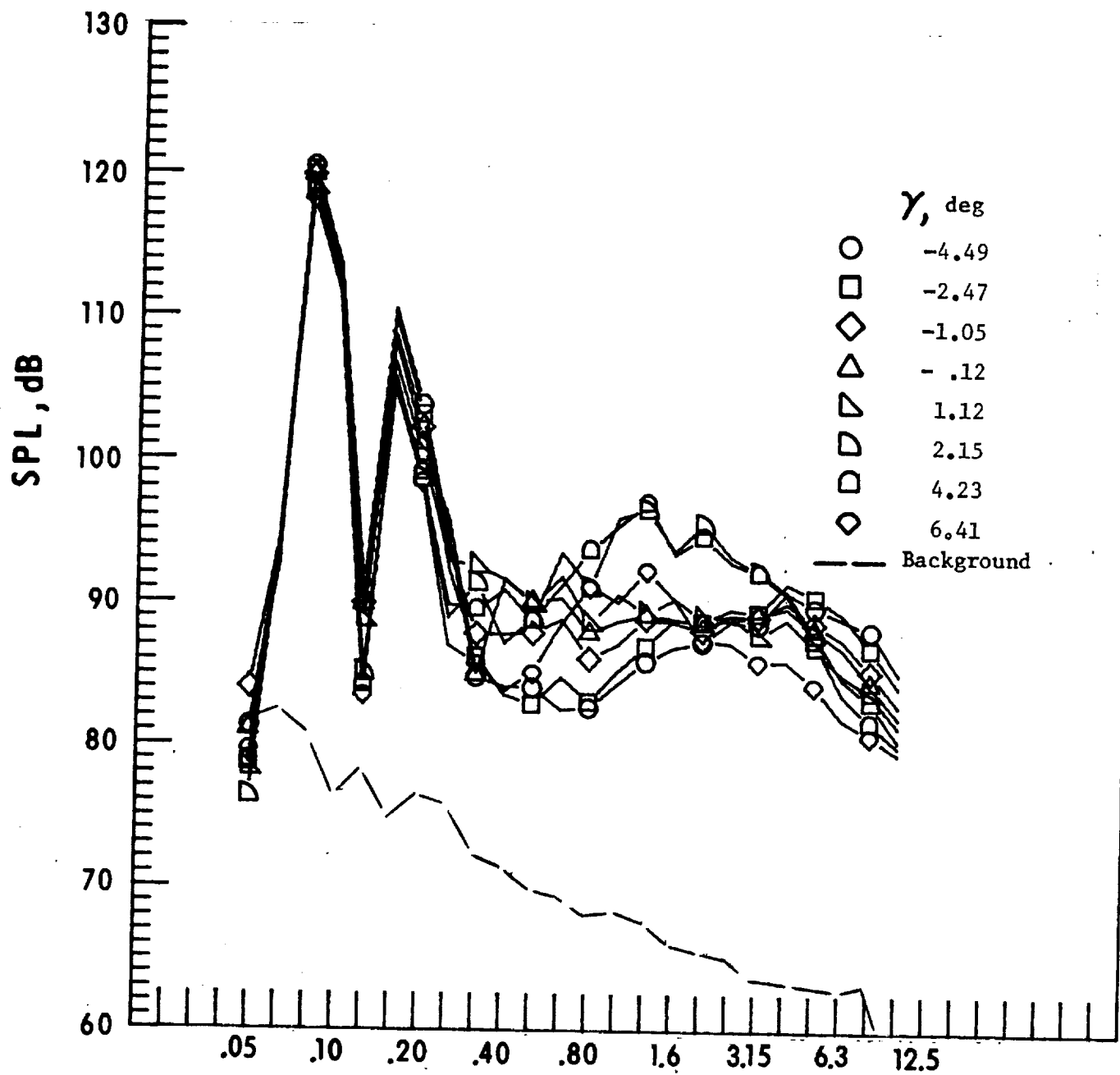
c. Narrow band analysis, Mic. no. 1, $\gamma = -4.49^{\circ}$.

Figure 10. - Continued.



d. Narrow band analysis, Mic. no. 1, $\gamma = 4.23^0$.

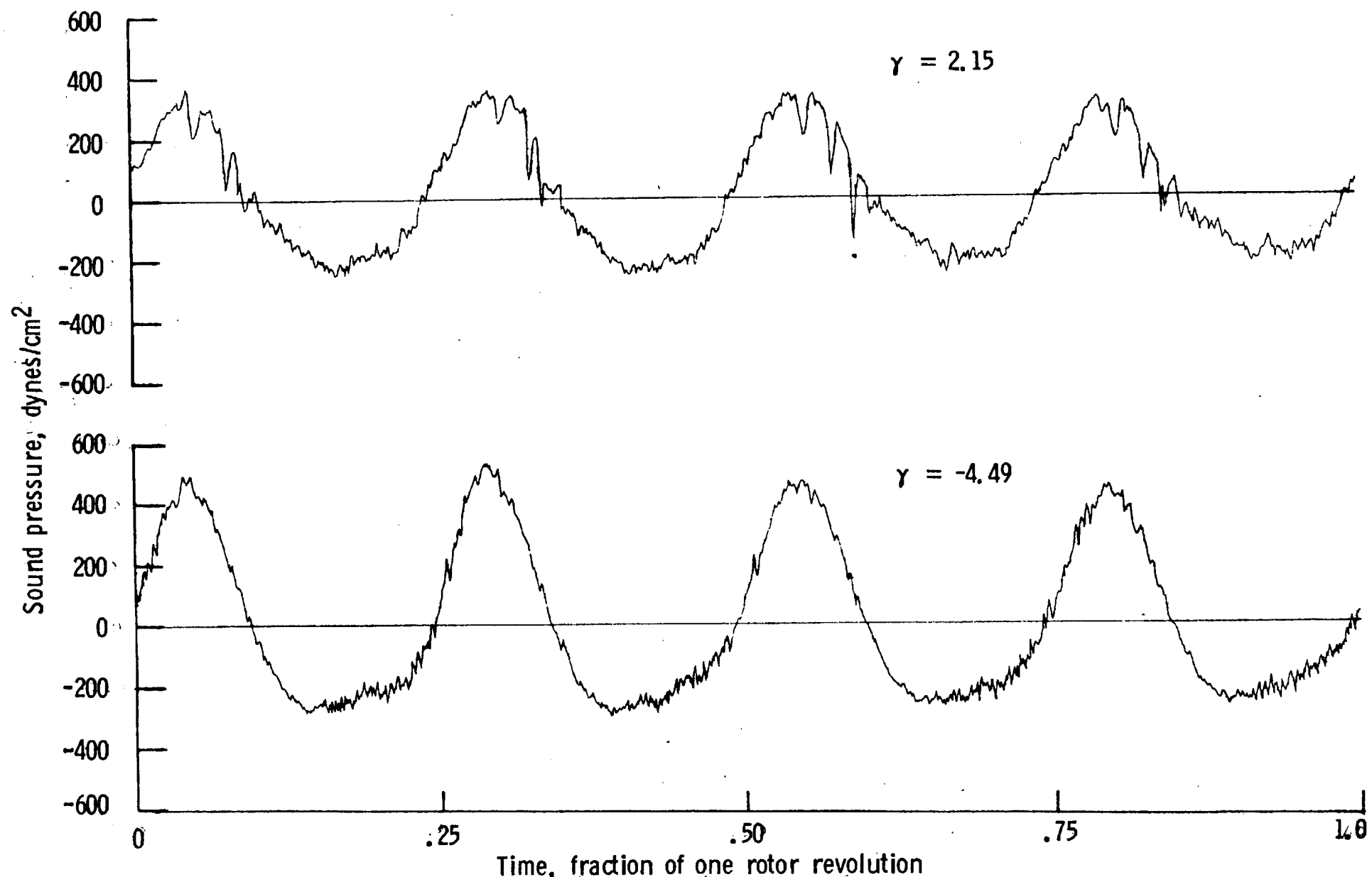
Figure 10. - Continued.



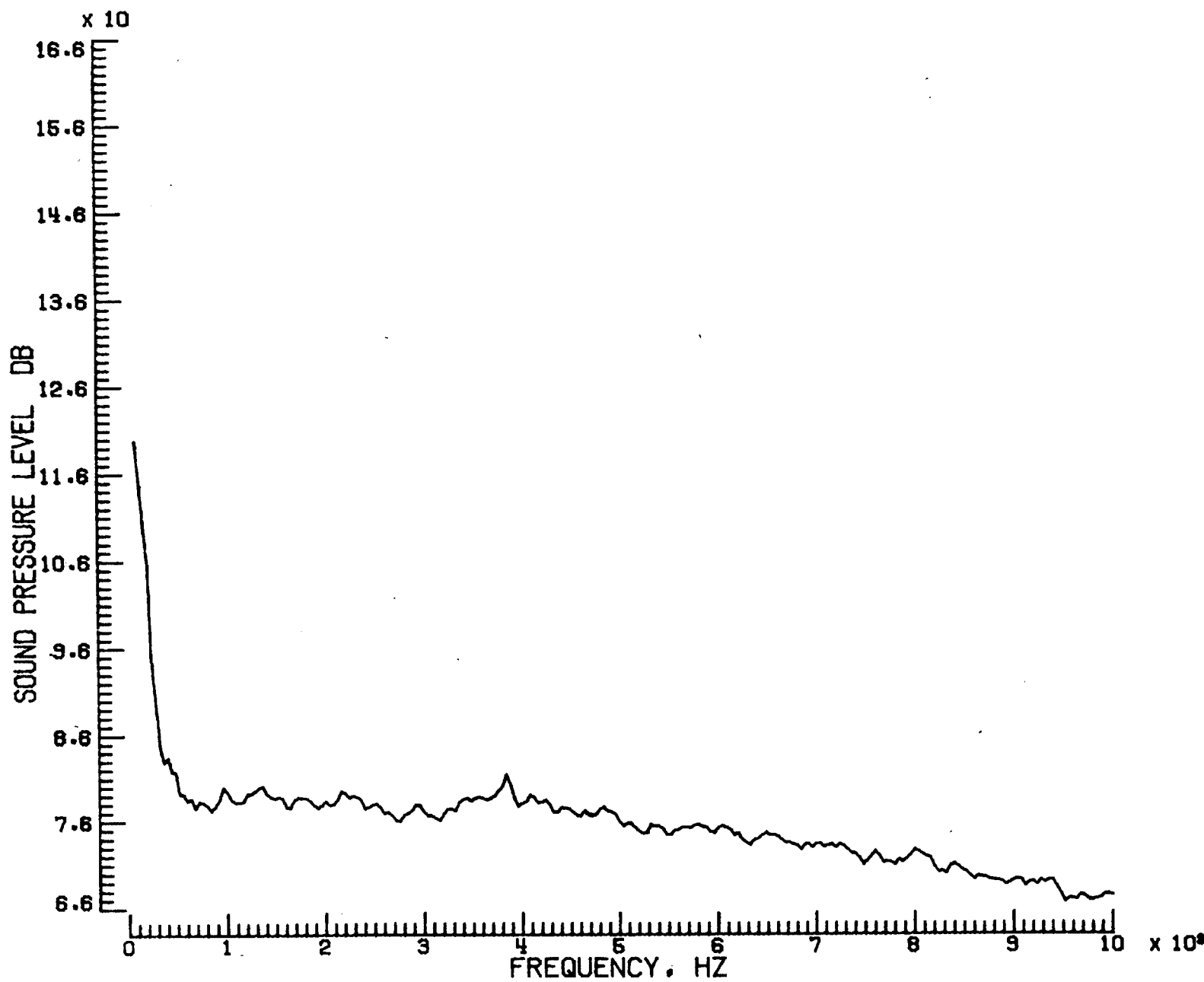
One-third-octave-band center frequency, kHz

e. Mic. no. 2.

Figure 10. - Continued.

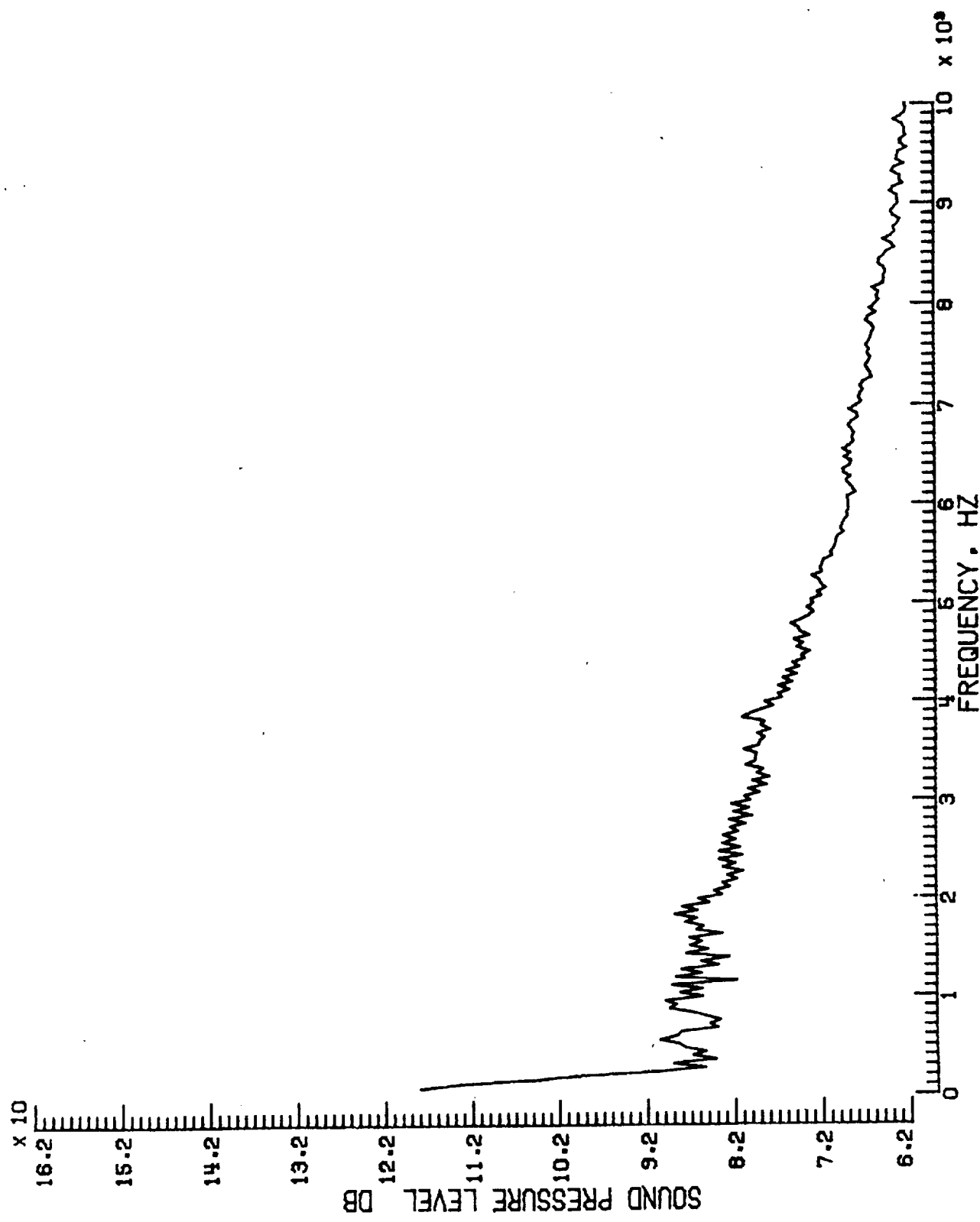


f. Pressure-time histories, Mic. no. 2.



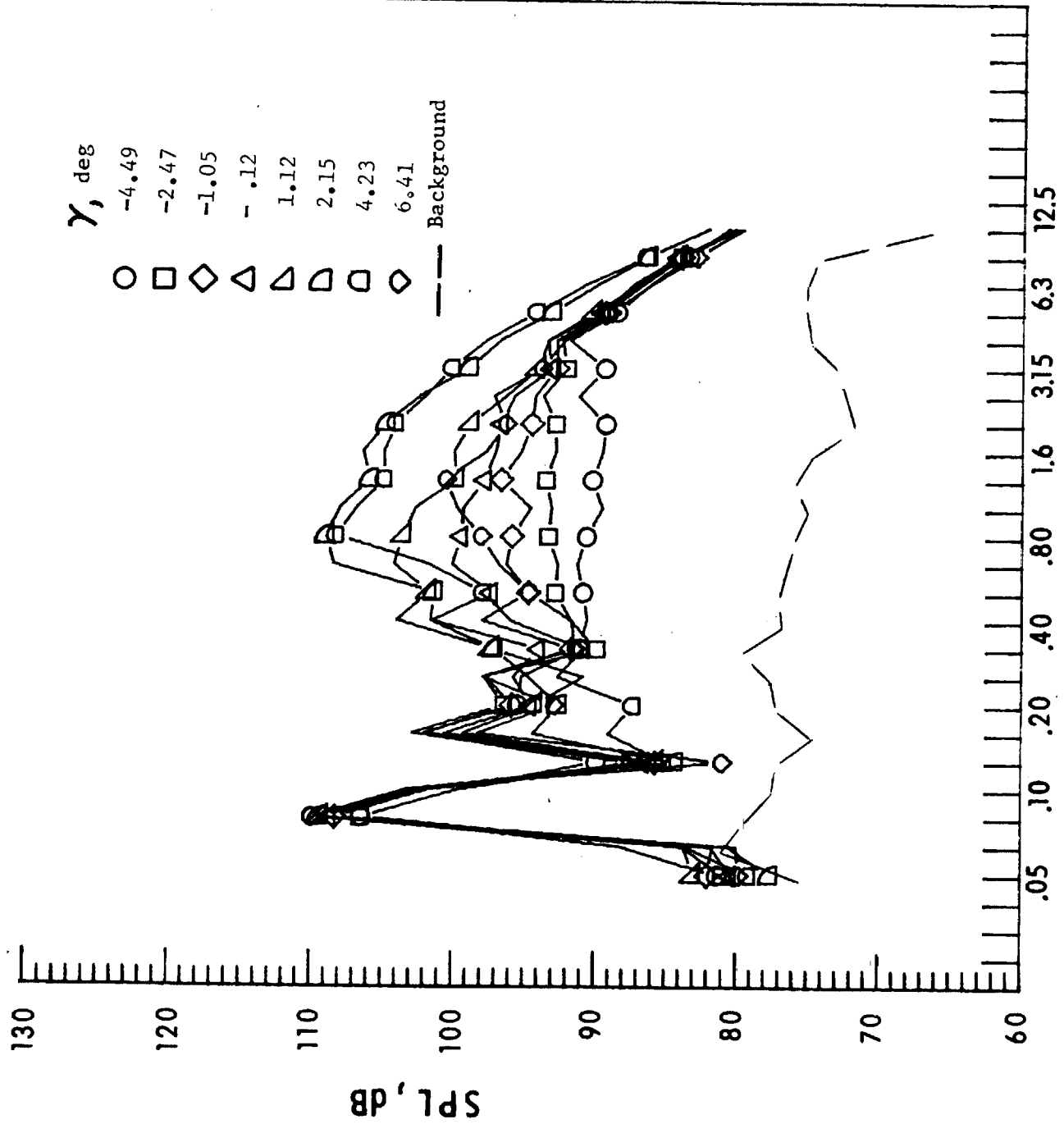
g. Narrow band analysis, Mic. no. 2, $\gamma = -4.49^0$.

Figure 10. - Continued.



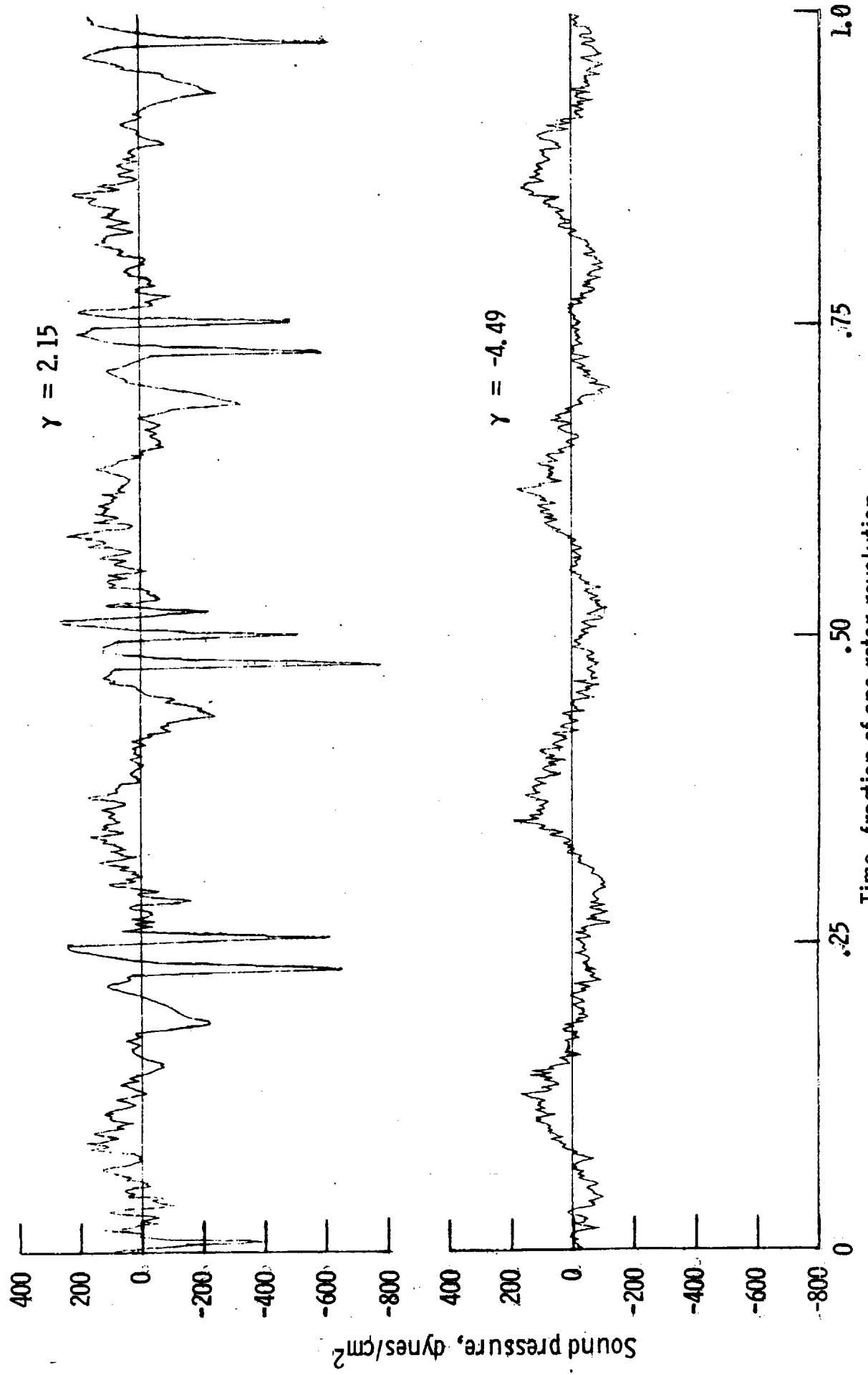
h. Narrow band analysis. Mic. no. 2. $\gamma = 2.15^{\circ}$.

Figure 10. - Continued.



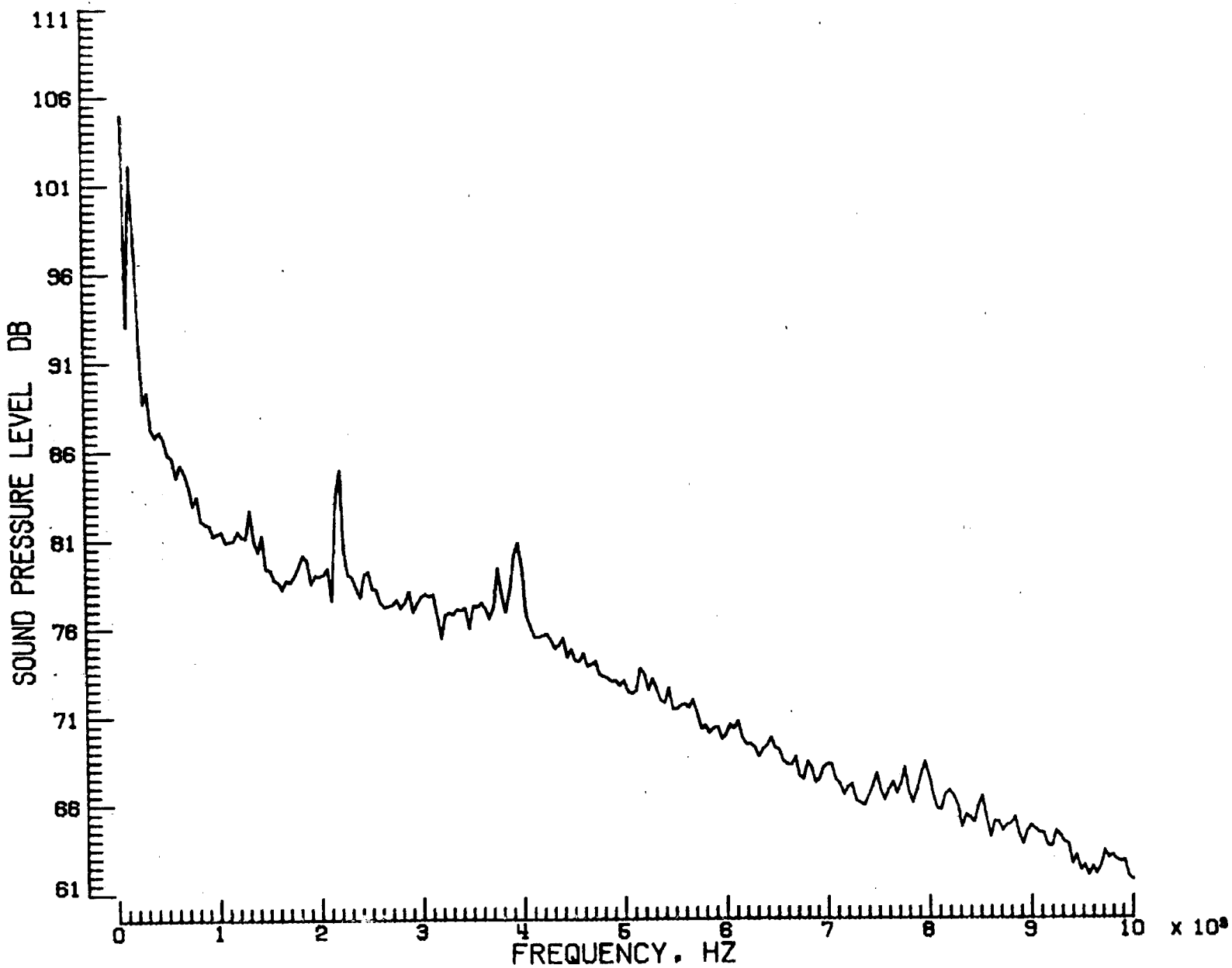
i. Mic. no. 3.

Figure 10. - Continued.



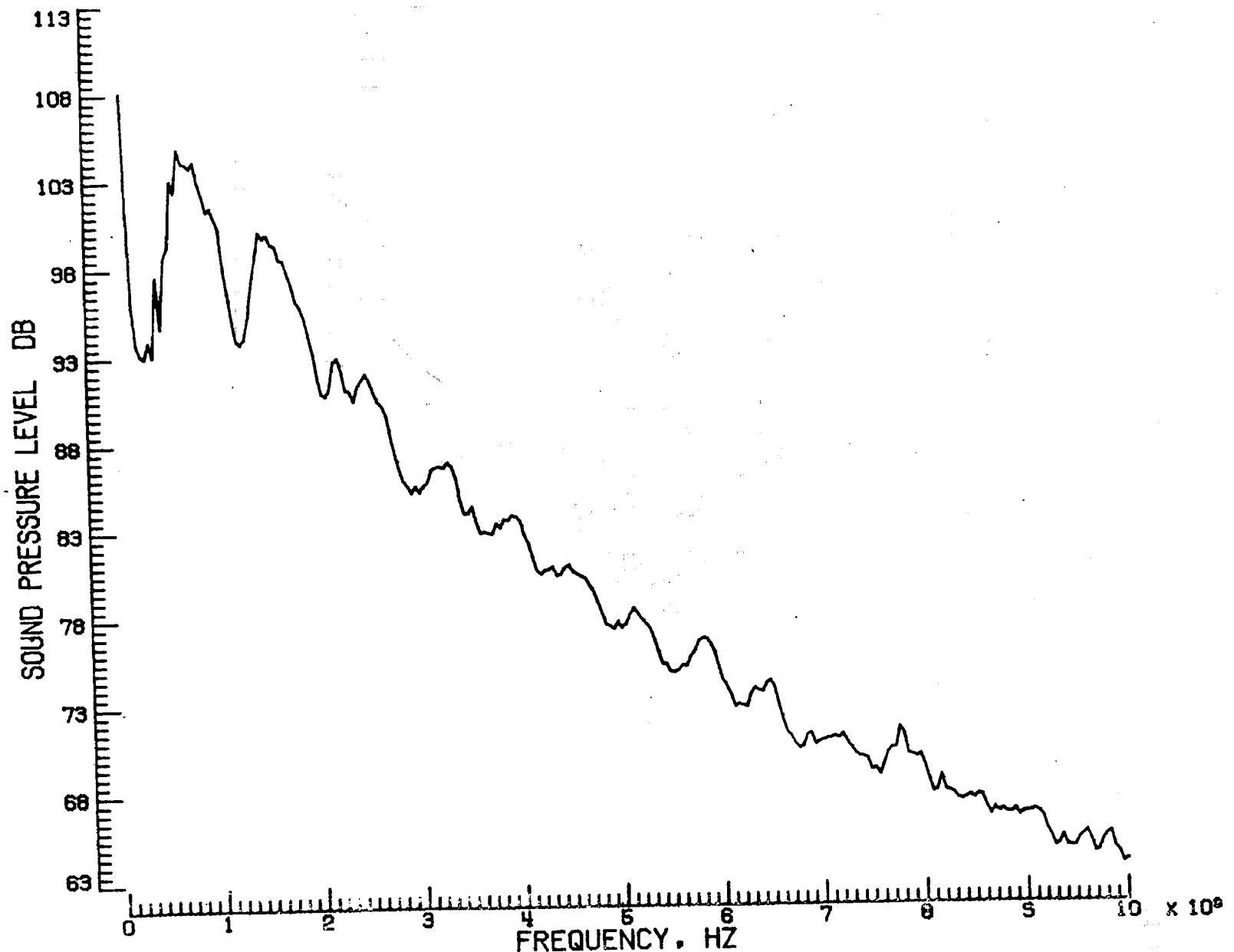
j. Pressure-time histories, Mic. no. 3.

Figure 10. - Continued.



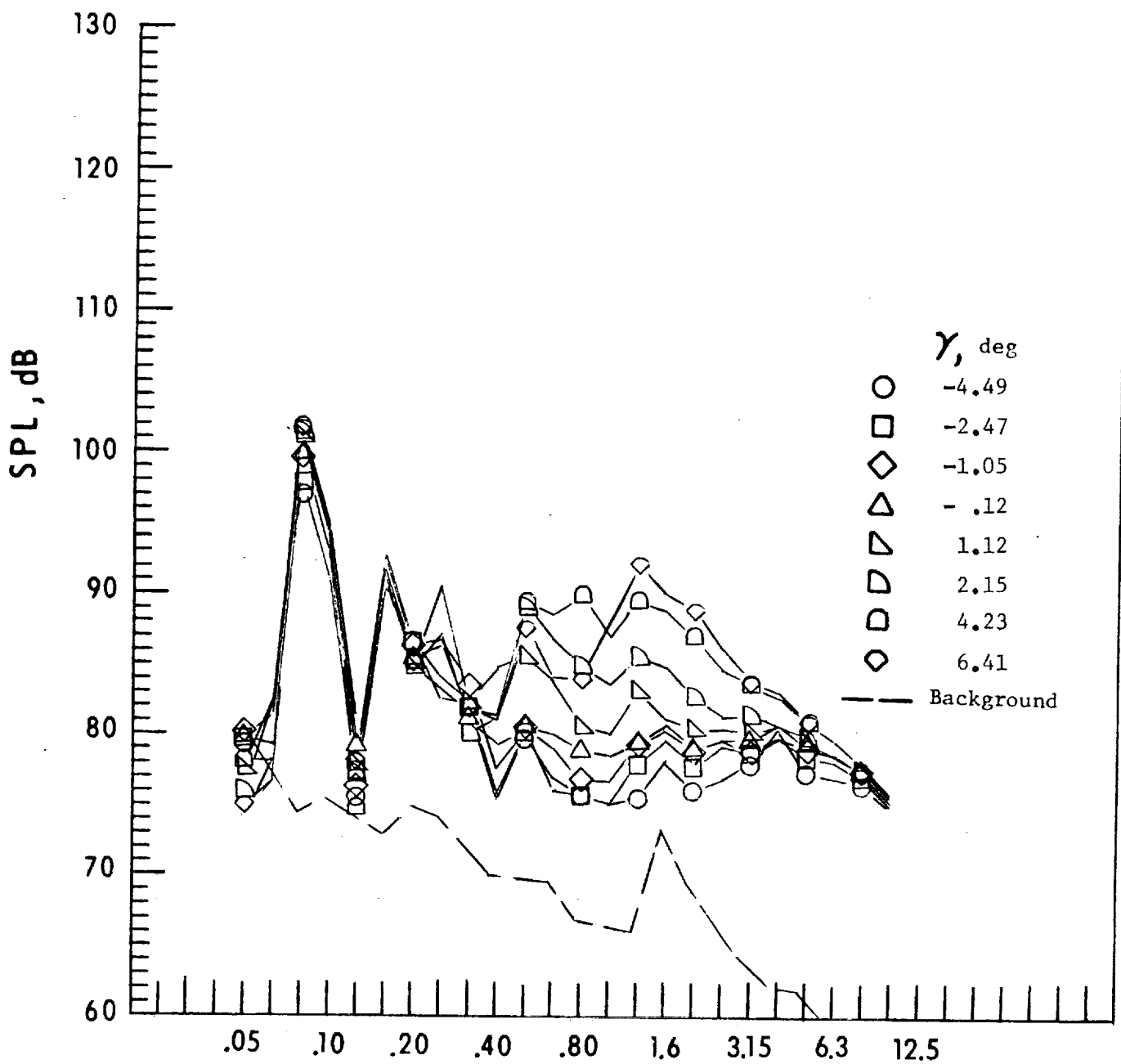
k. Narrow band analysis, Mic. no. 3, $\gamma = 4.49^0$.

Figure 10. - Continued.



i. Narrow band analysis, Mic. no. 3, $\gamma = 2.15^0$.

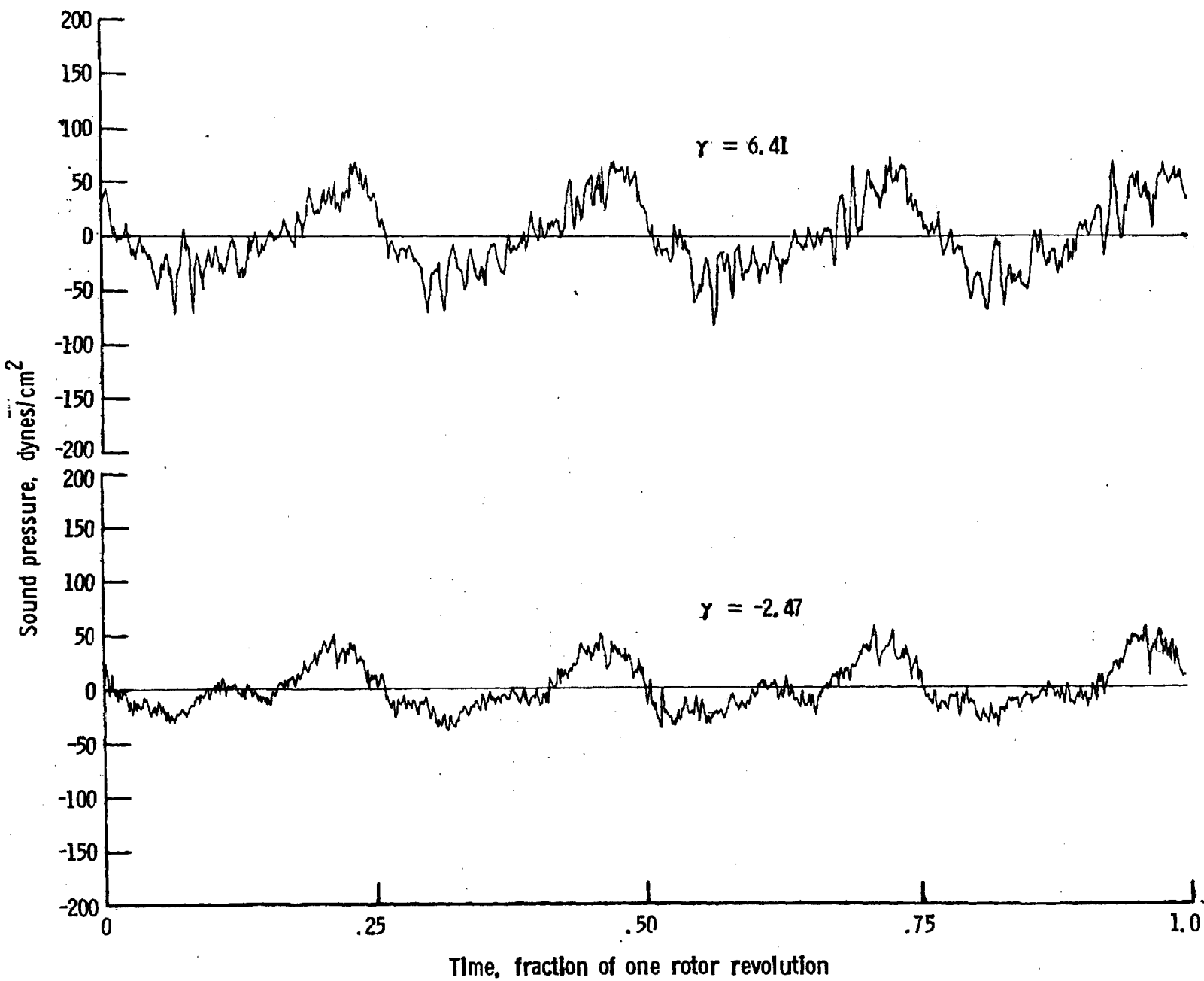
Figure 10. - Continued.



One-third-octave-band center frequency, kHz

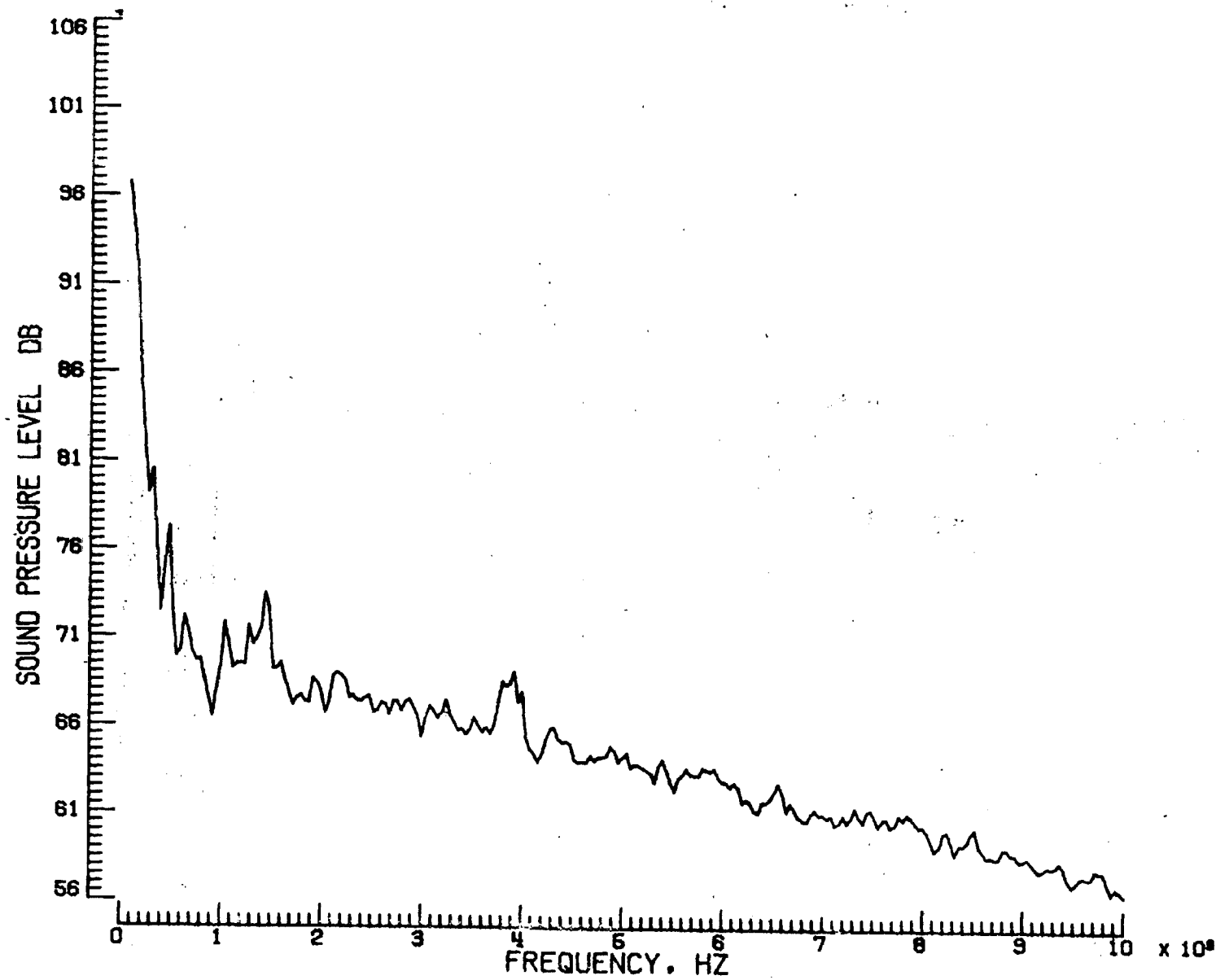
m. Mic. no. 4.

Figure 10. - Continued.



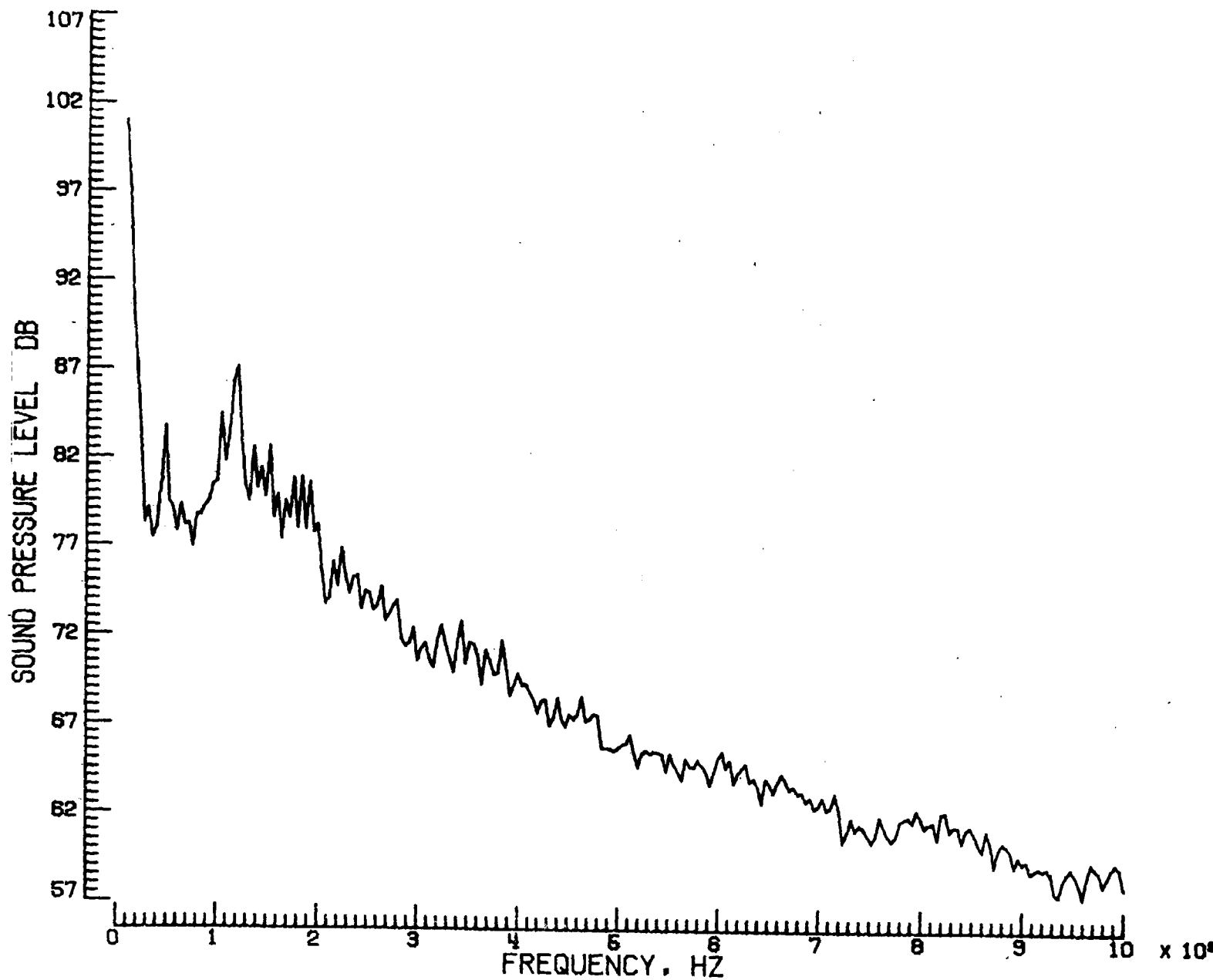
n. Pressure-time histories, Mic. no. 4.

Figure 10. - Continued.



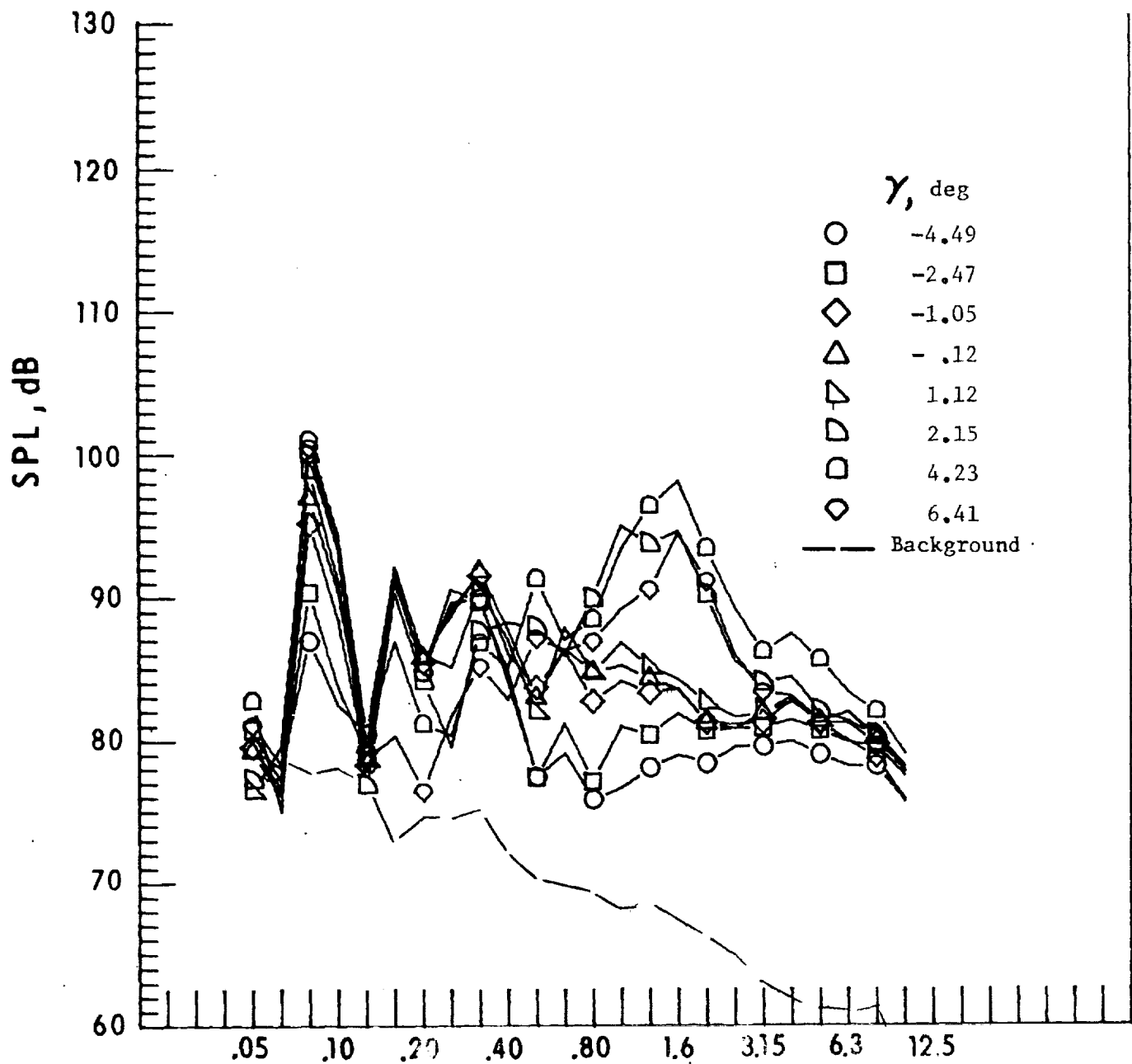
o. Narrow band analysis, Mic. no. 4, $\gamma = 2.470$

Figure 10. - Continued.



p. Narrow band analysis, Mic. no. 4, $\gamma = 6.41^0$.

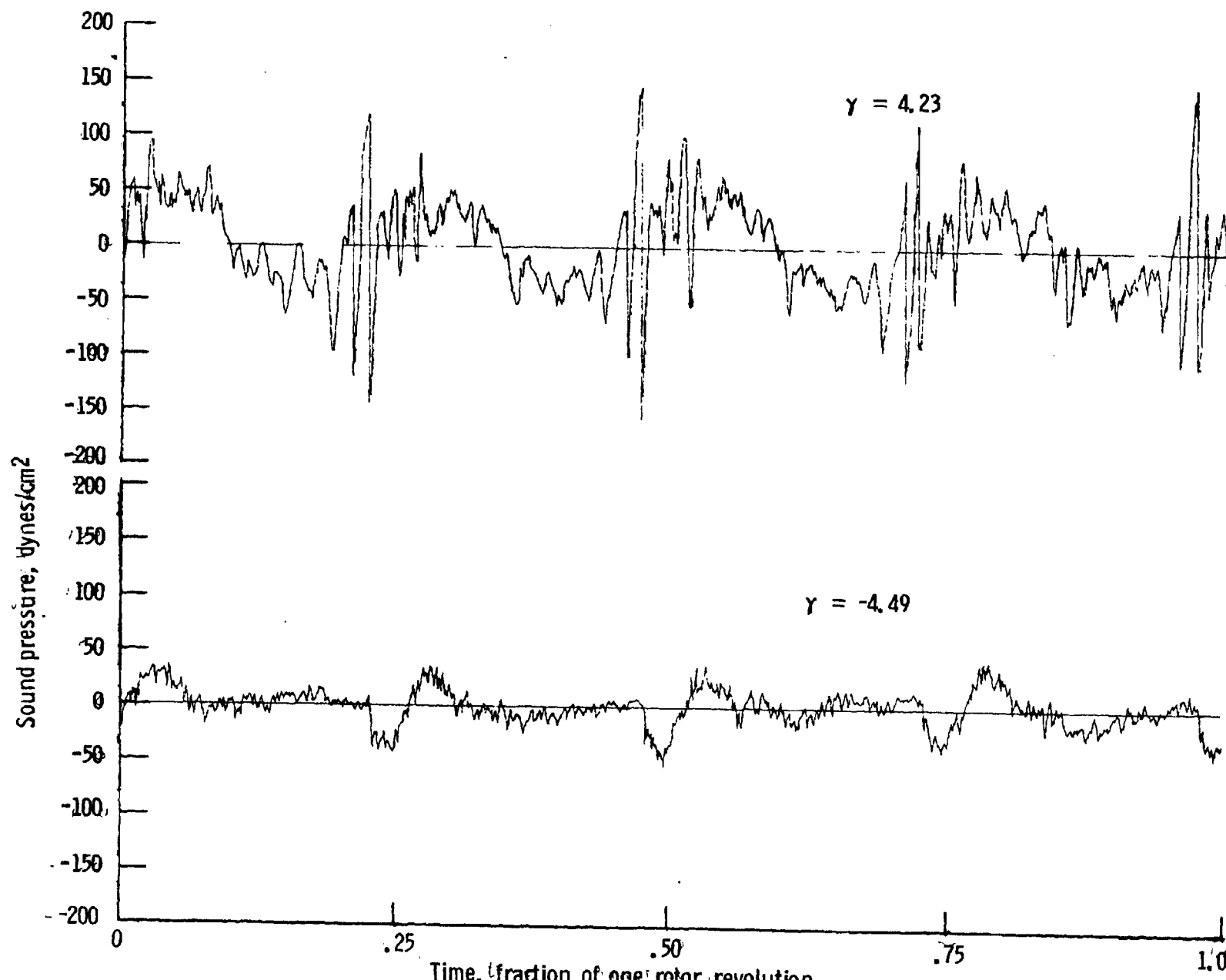
Figure 10. - Continued.



One-third-octave-band center frequency, kHz

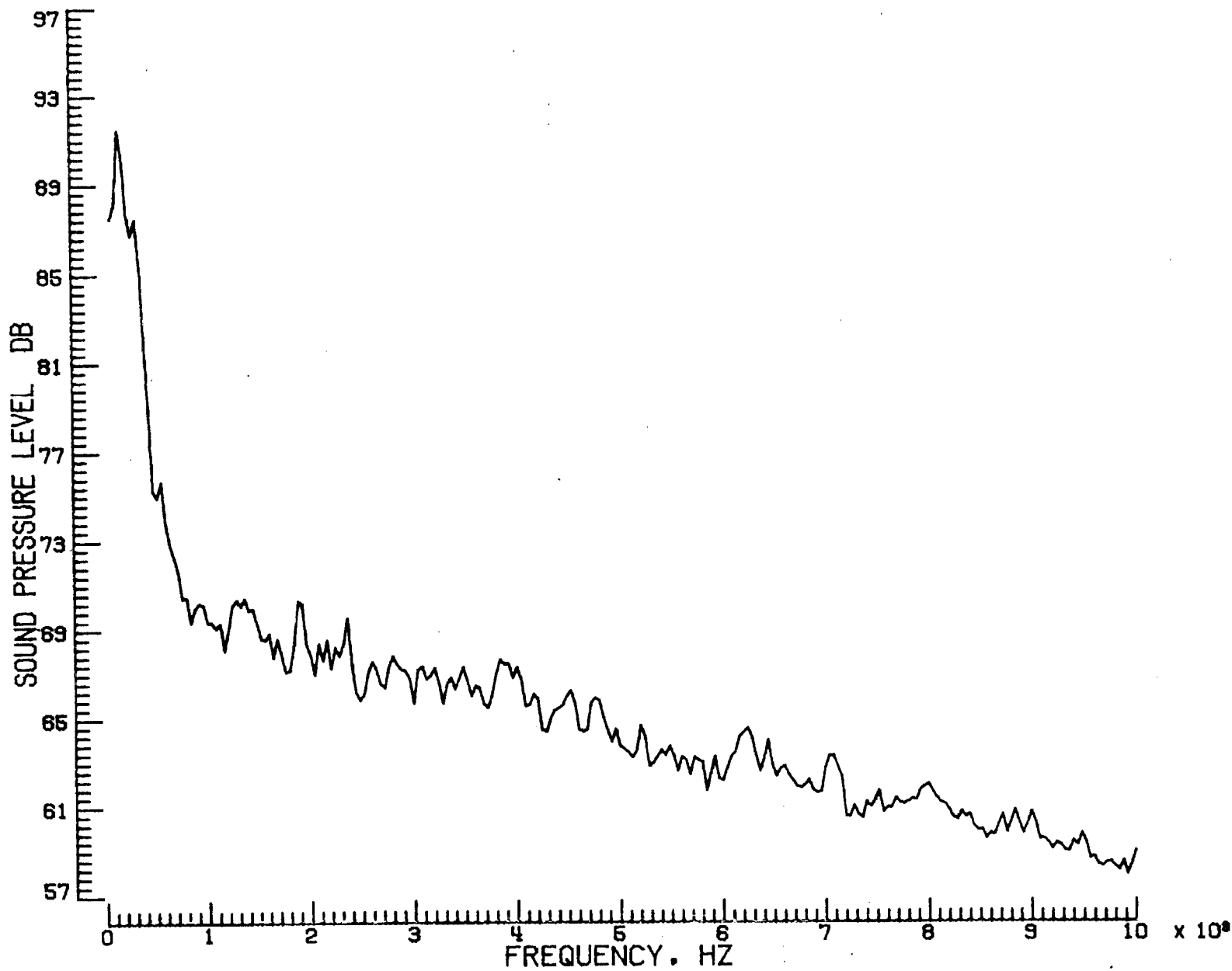
q. Mic. no. 5.

Figure 10. - Continued.



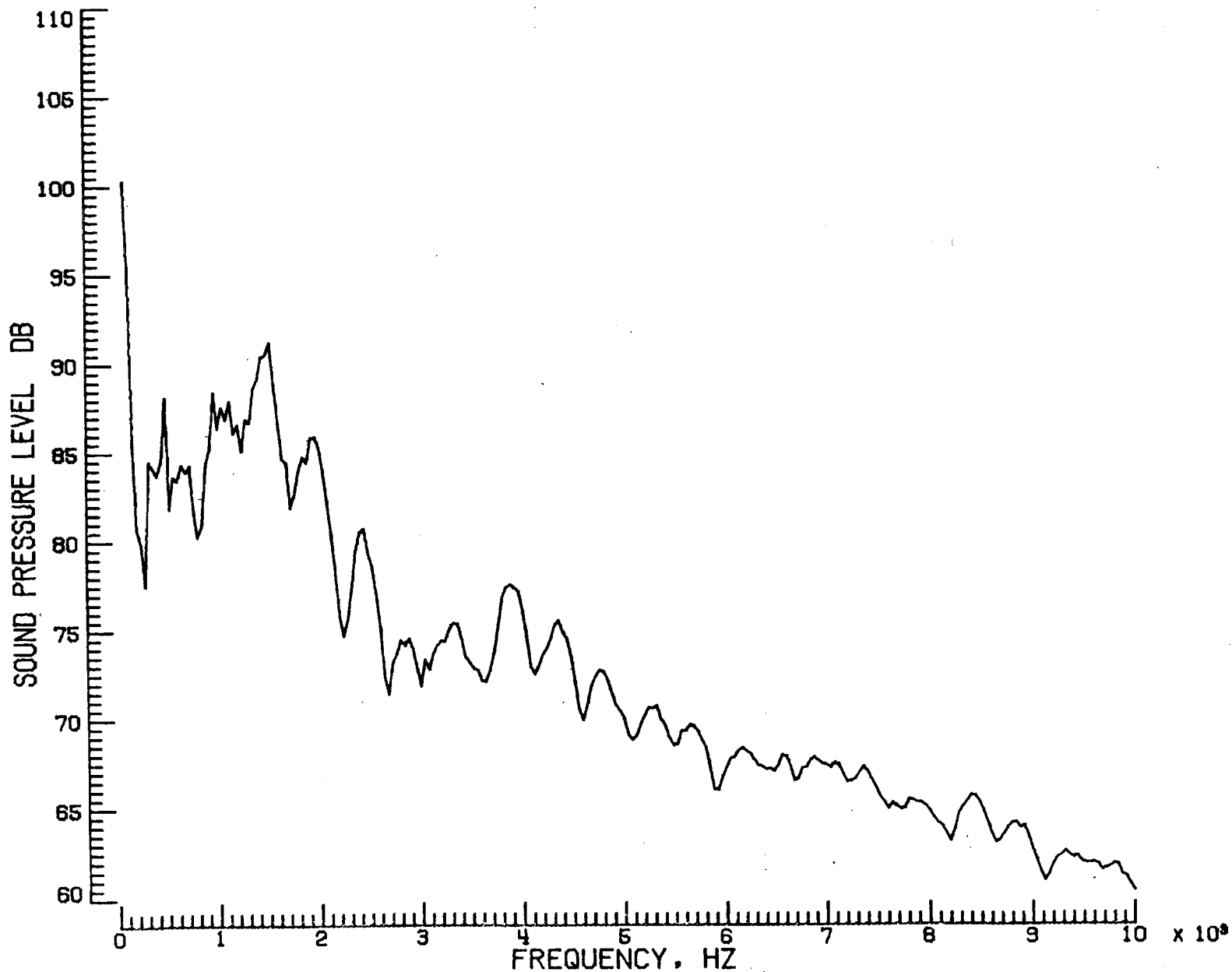
r. Pressure-time histories, Mic. no. 5.

Figure 10. - Continued.

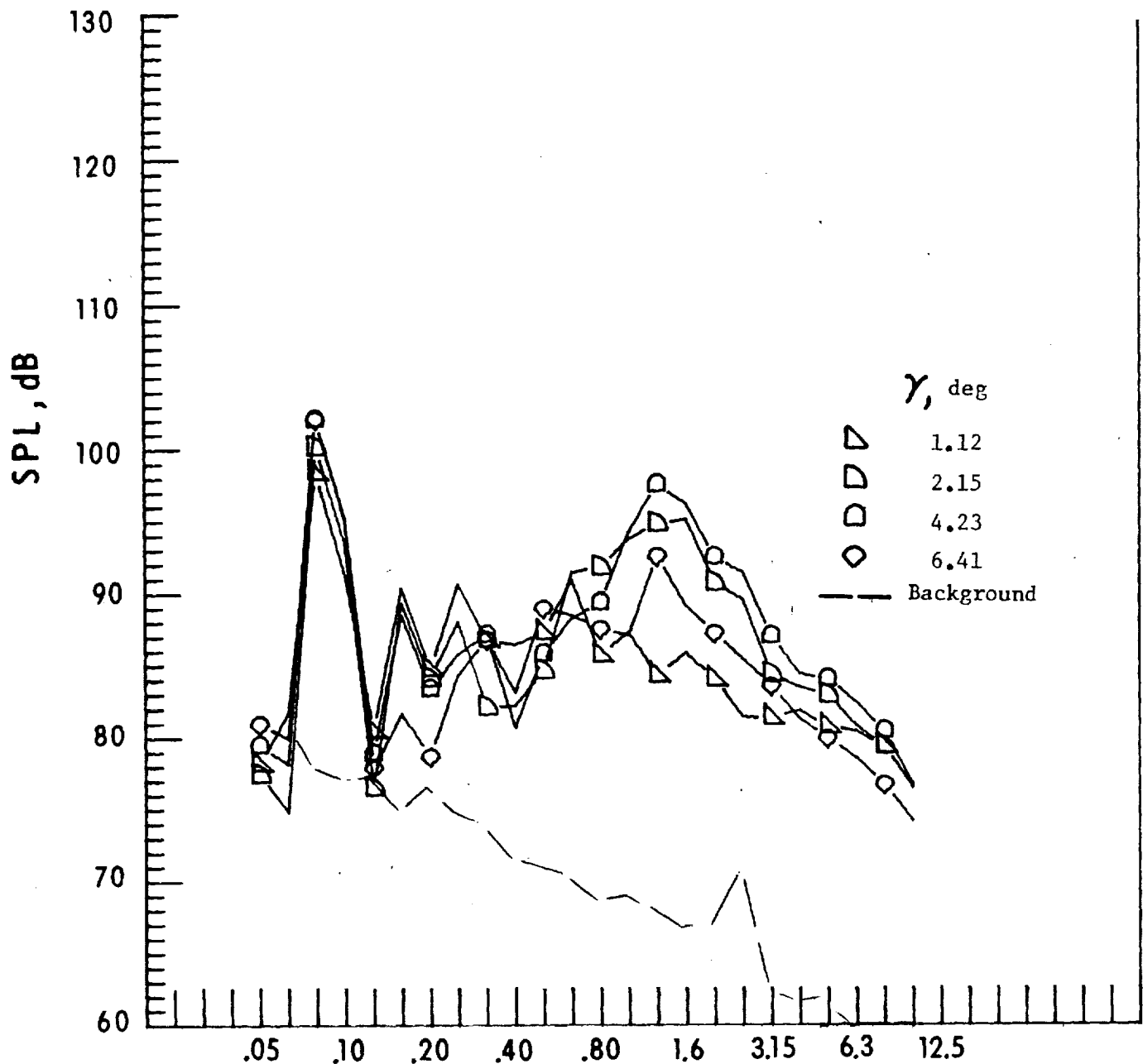


s. Narrow band analysis, Mic. no. 5, $\gamma = -4.49^0$.

Figure 10. - Continued.



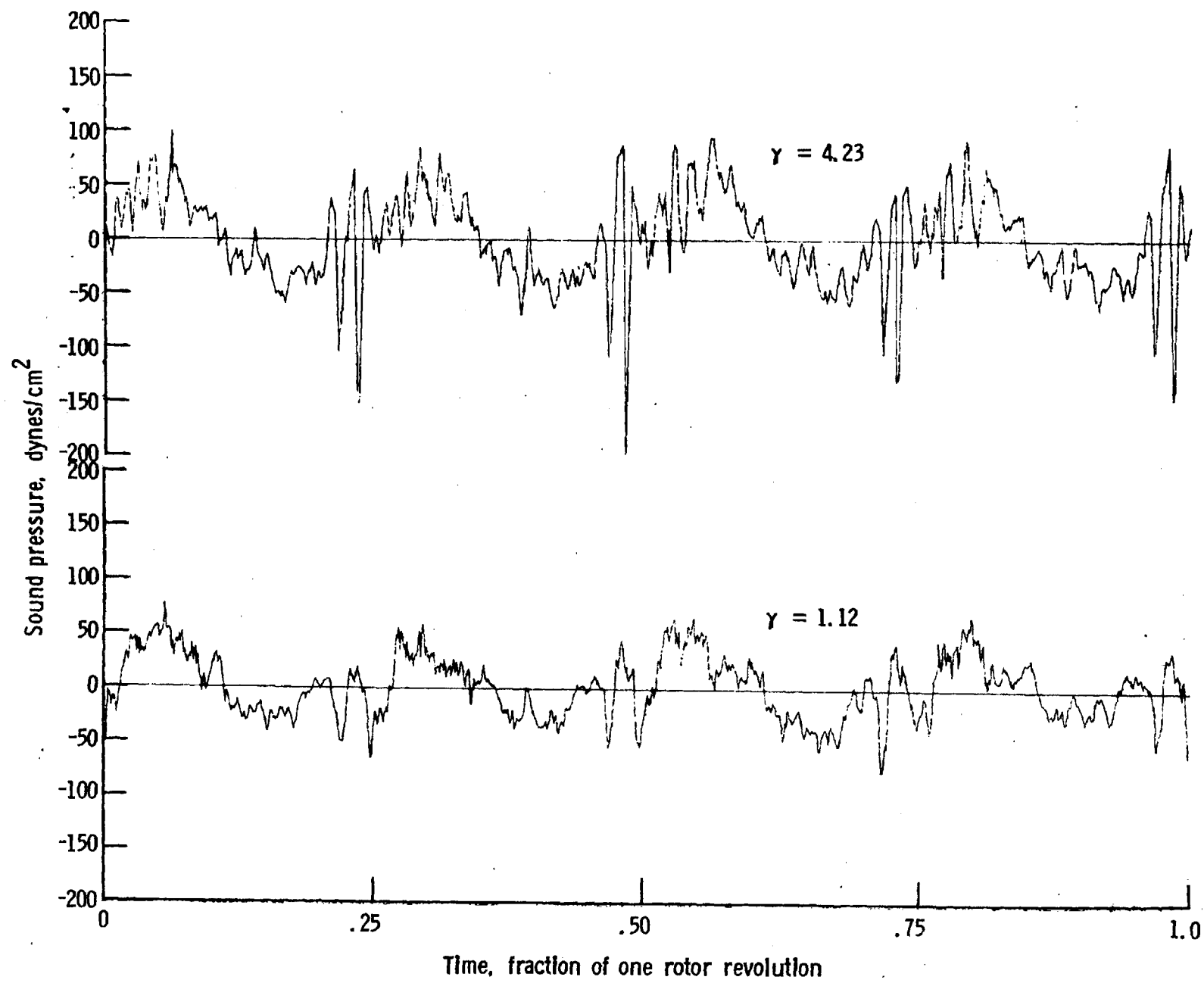
t. Narrow band analysis. Mic. no. 5, $\gamma = 4.23^\circ$.



One-third-octave-band center frequency, kHz

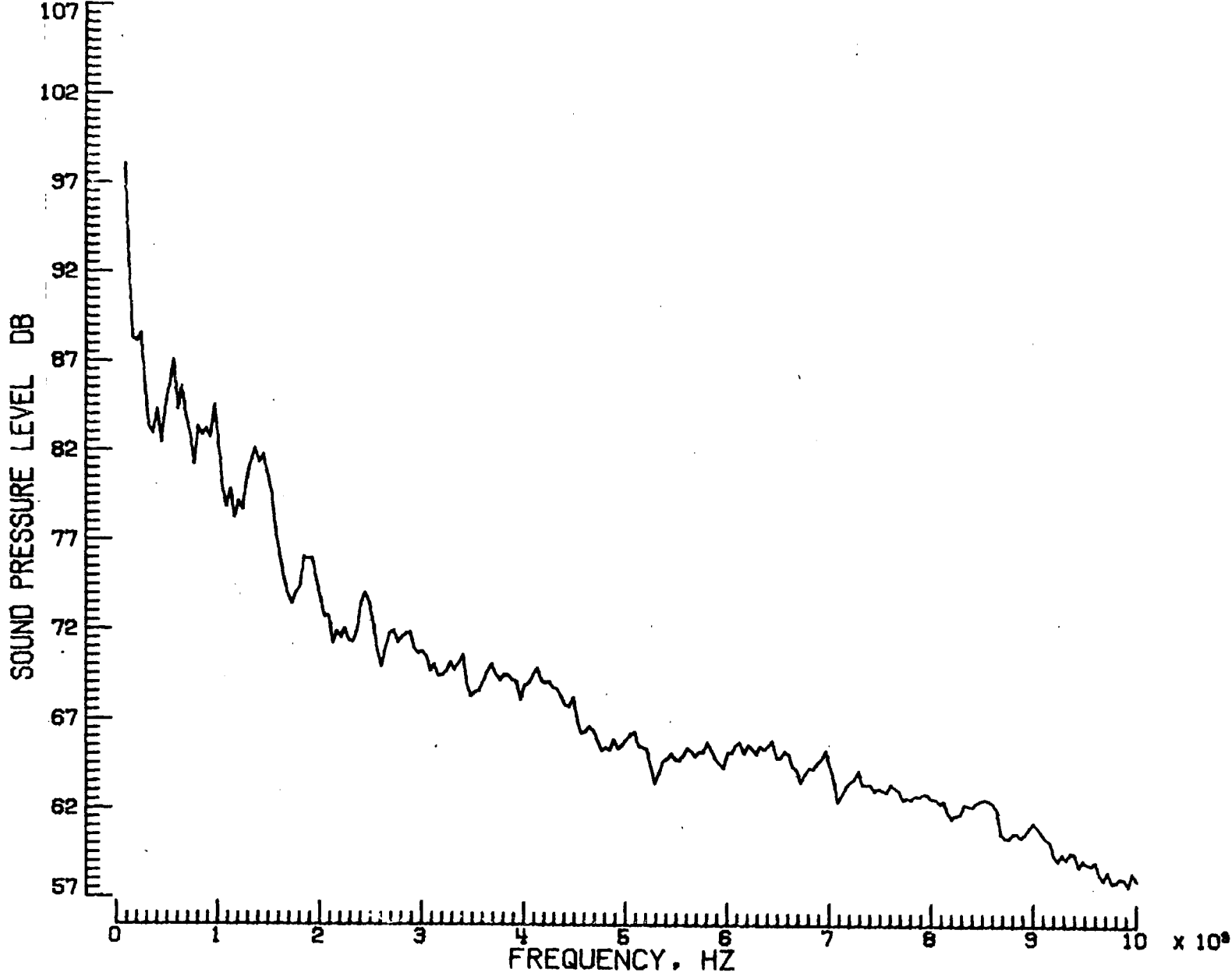
u. Mic. no. 6.

Figure 10. - Continued.



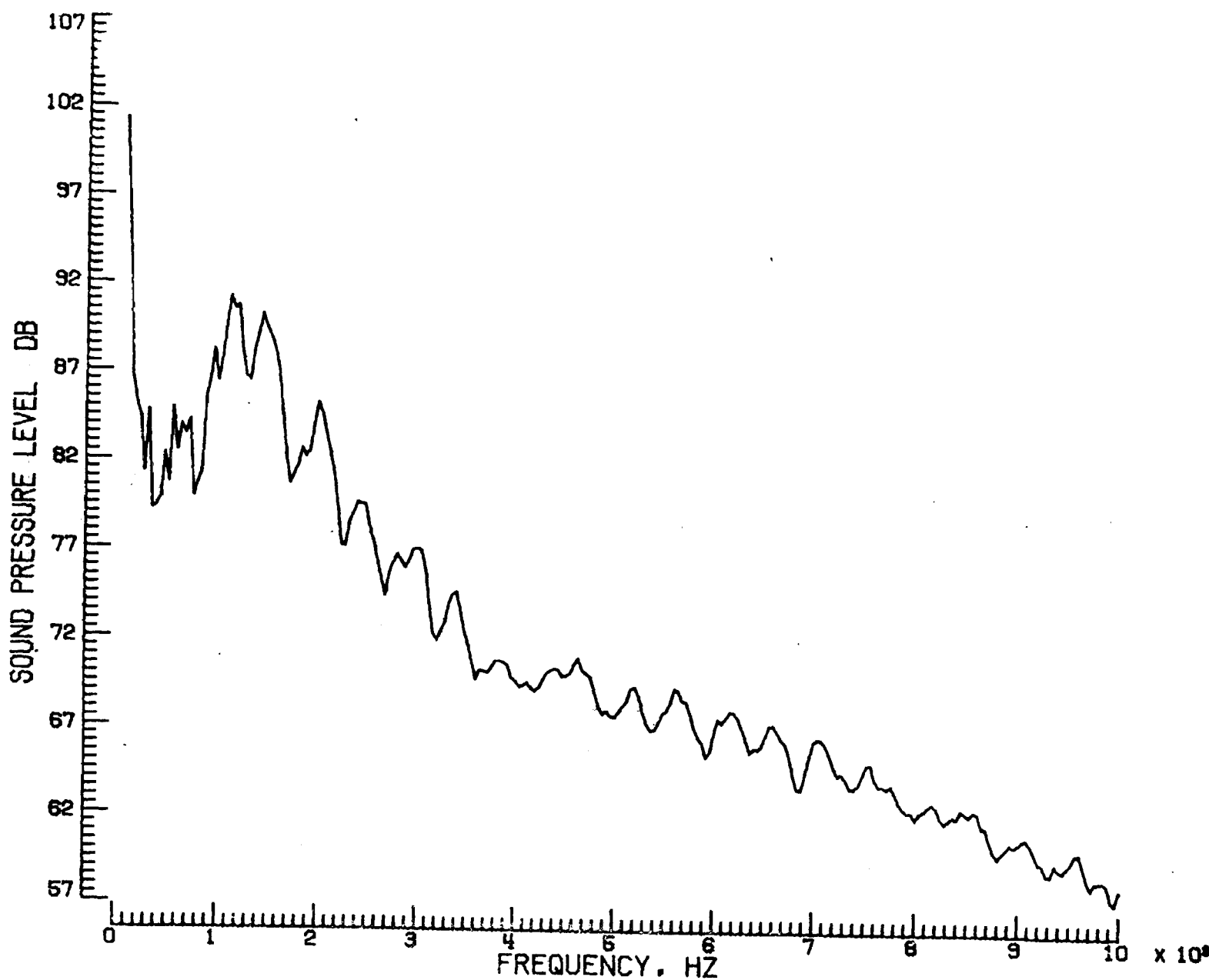
v. Pressure-time histories, Mic. no. 6.

Figure 10. - Continued.

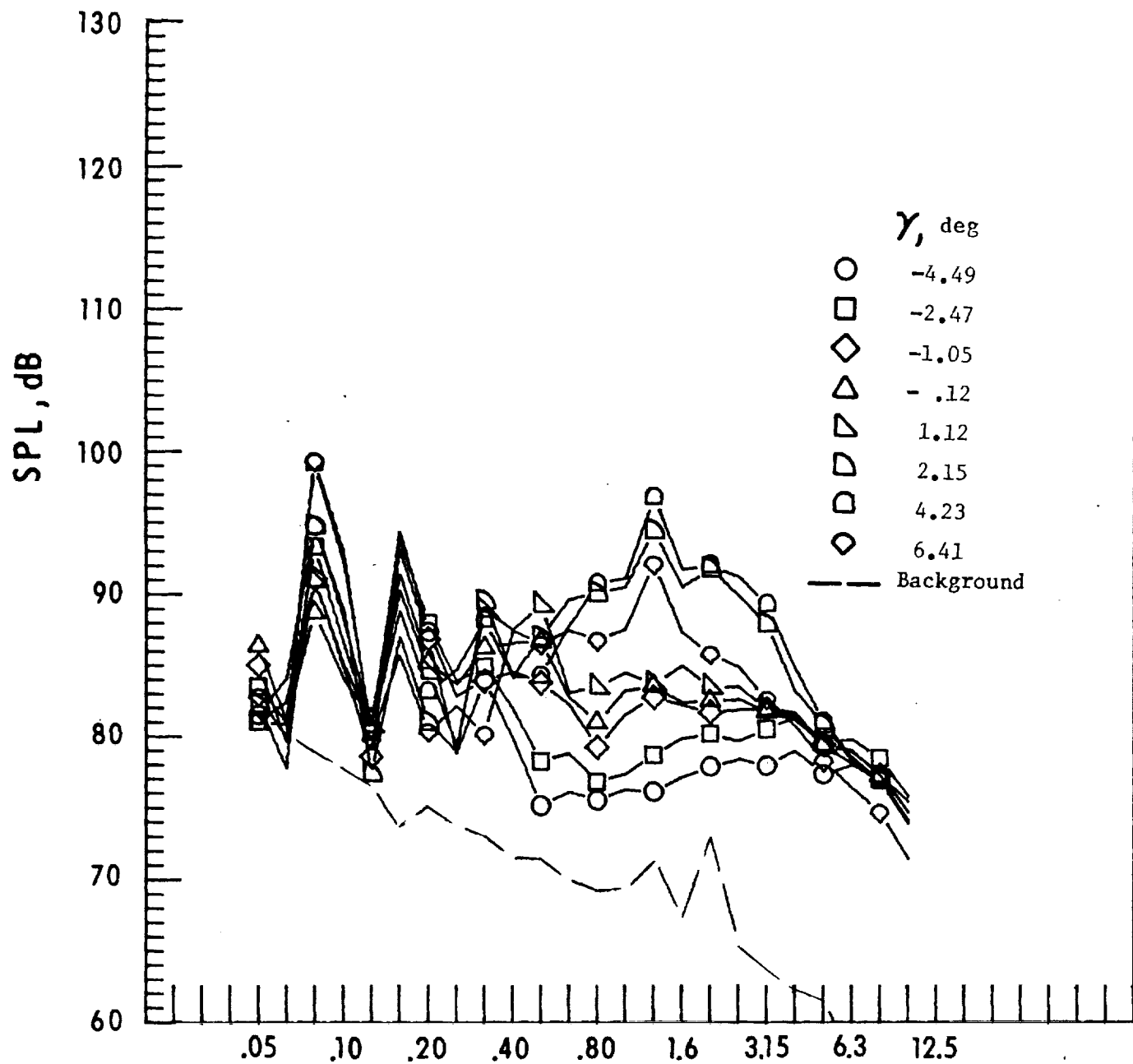


w. Narrow band analysis, Mic. no. 6, $\gamma = 1.12^0$.

Figure 10. - Continued.



x. Narrow band analysis, Mic. no. 6; $\gamma = 4.23^0$.



One-third-octave-band center frequency, kHz

y. Mic. no. 7.

Figure 10. - Continued.

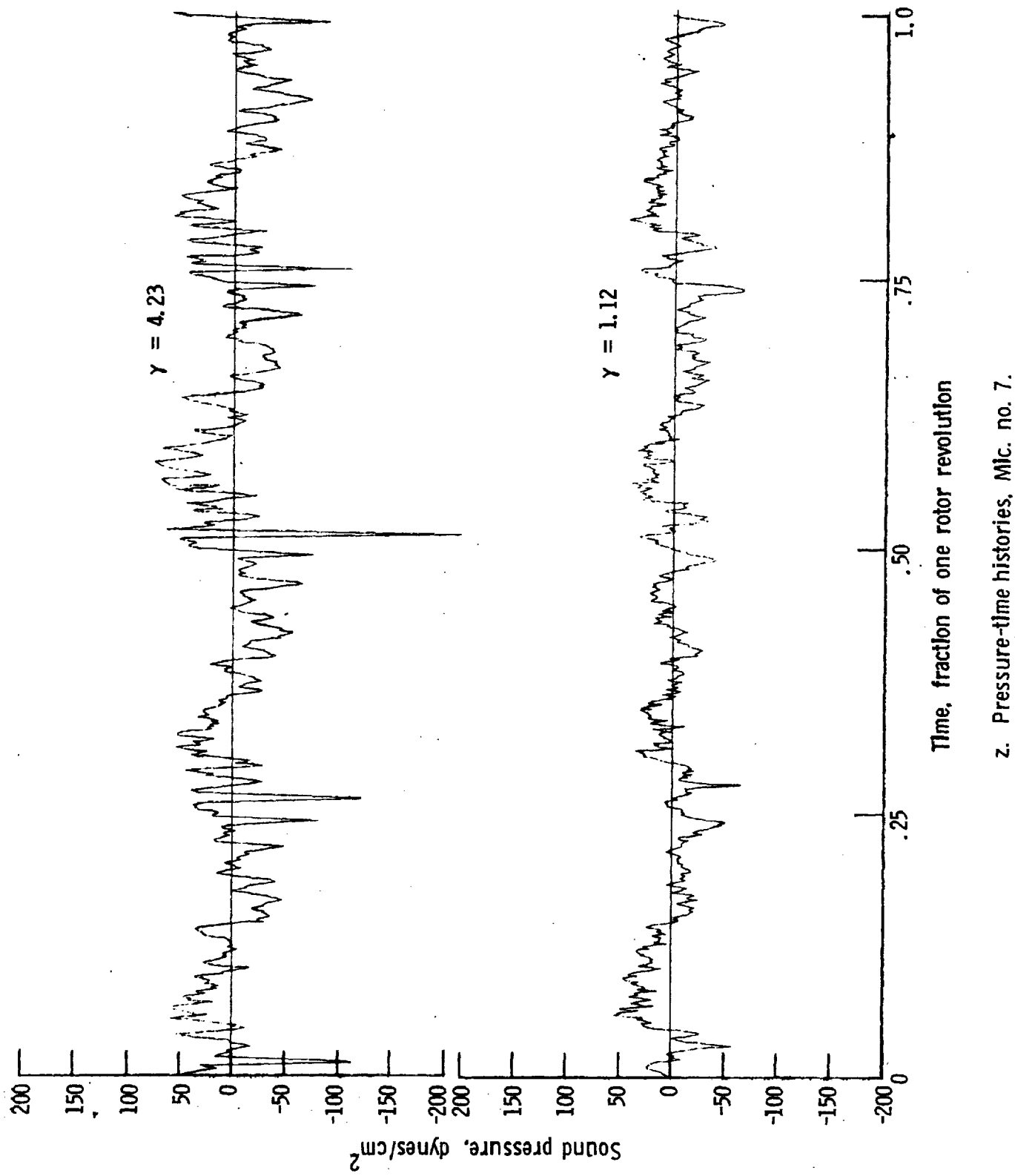
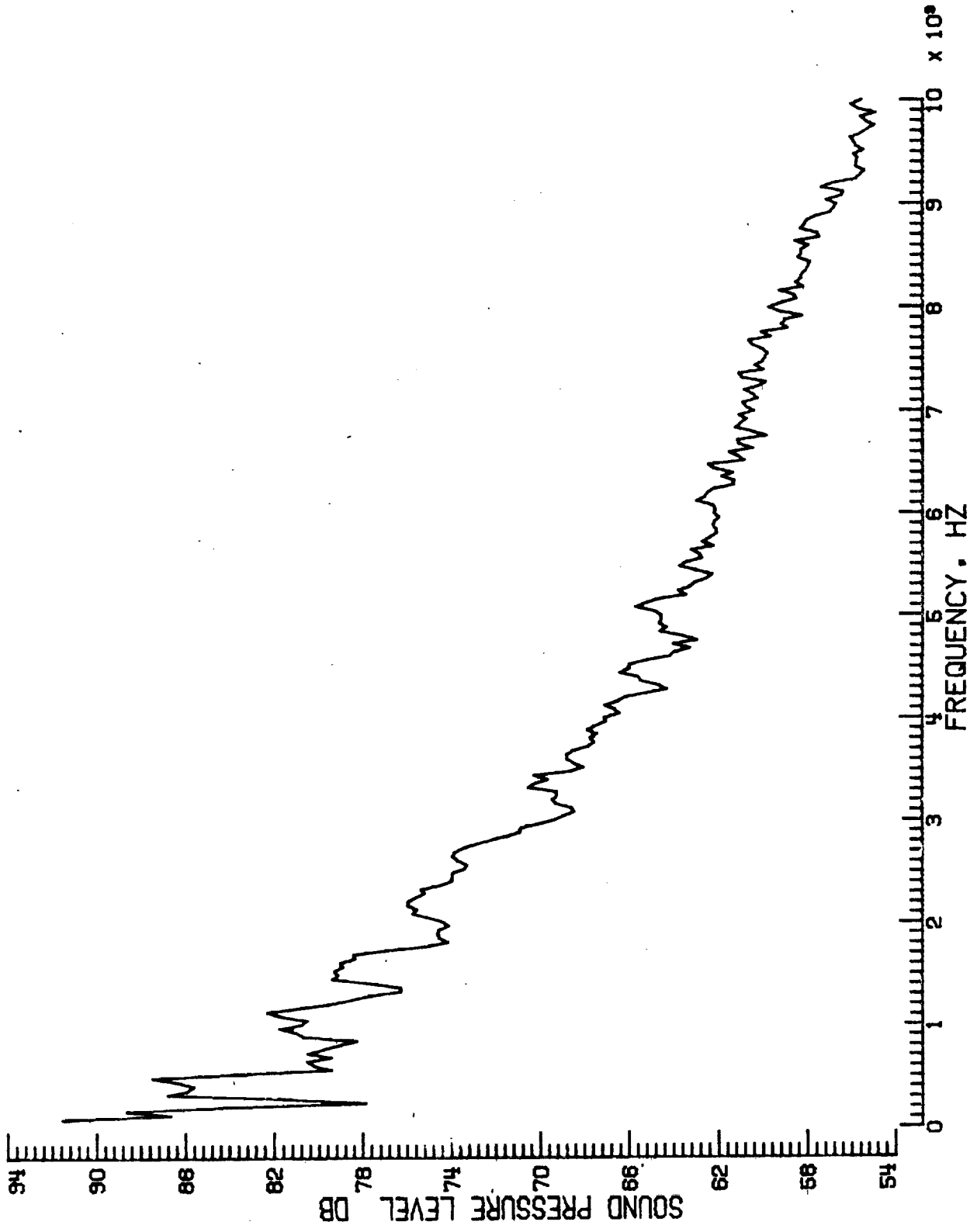


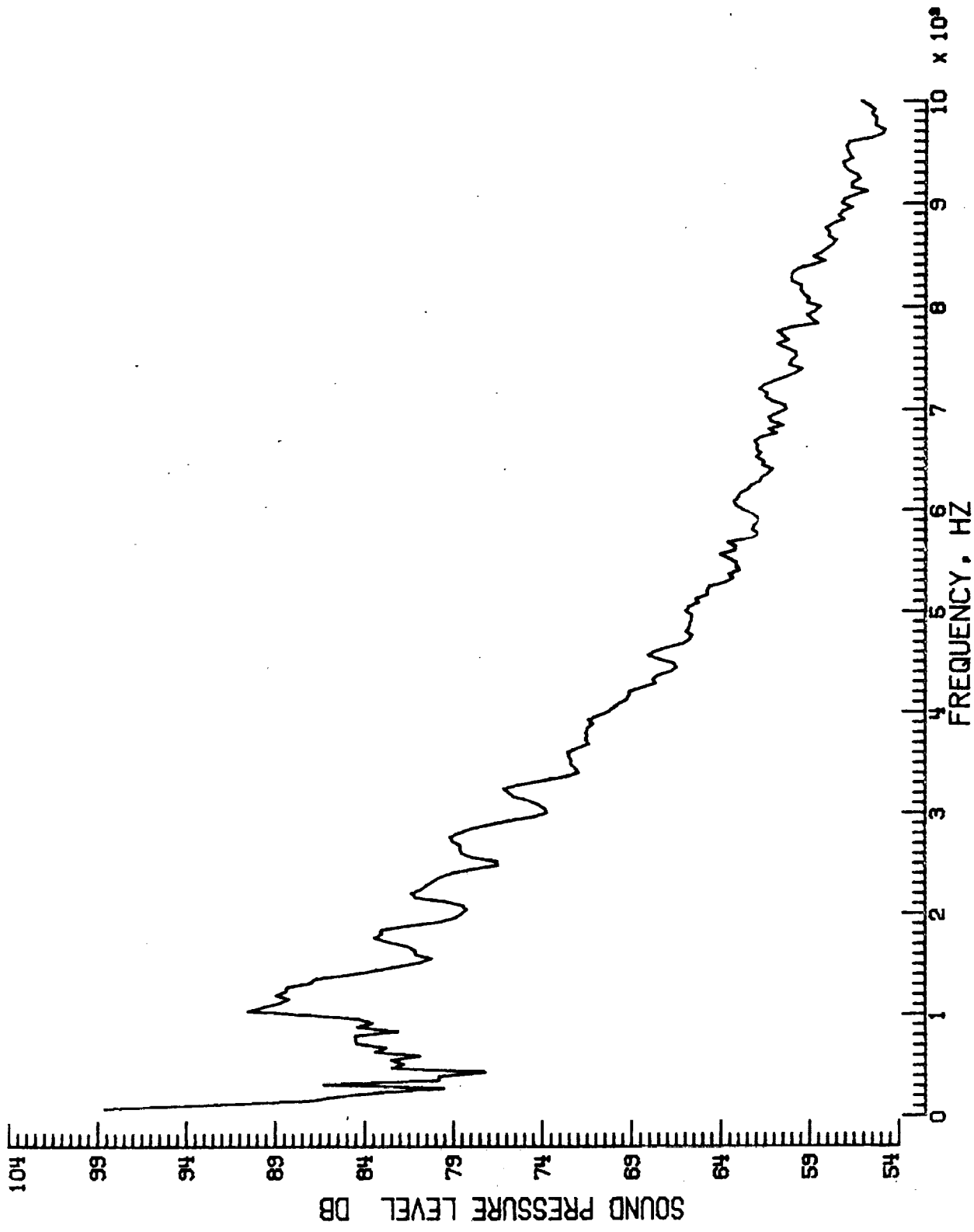
Figure 10. - Continued.

z. Pressure-time histories. Mic. no. 7.



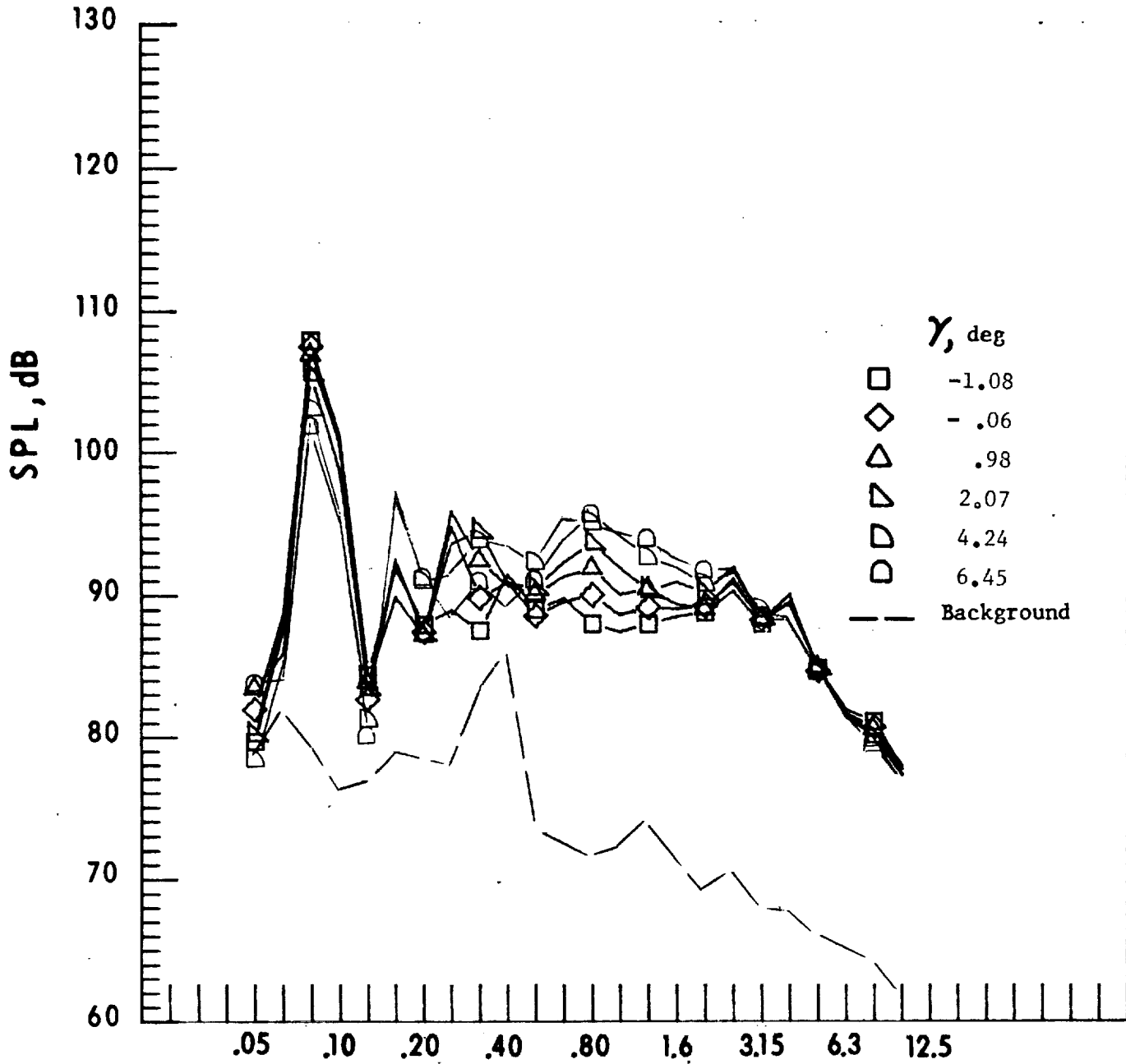
aa Narrow band analysis, Mic. no. 7. $\gamma = 1.12^0$.

Figure 10. - Continued.



bb. Narrow band analysis. Mic. no. 7. $\gamma = 4.23^0$.

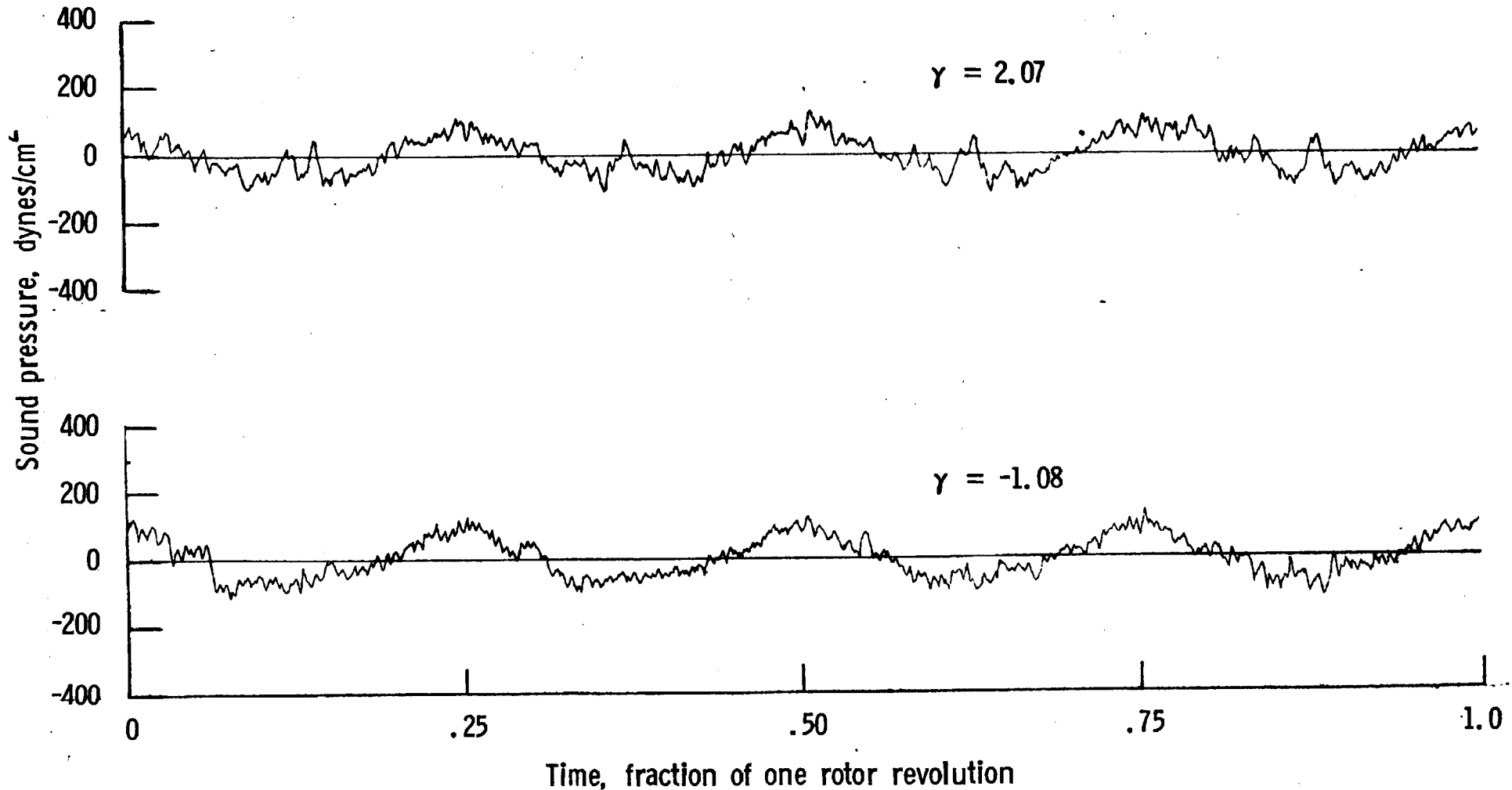
Figure 10. - Concluded.



One-third-octave-band center frequency, kHz

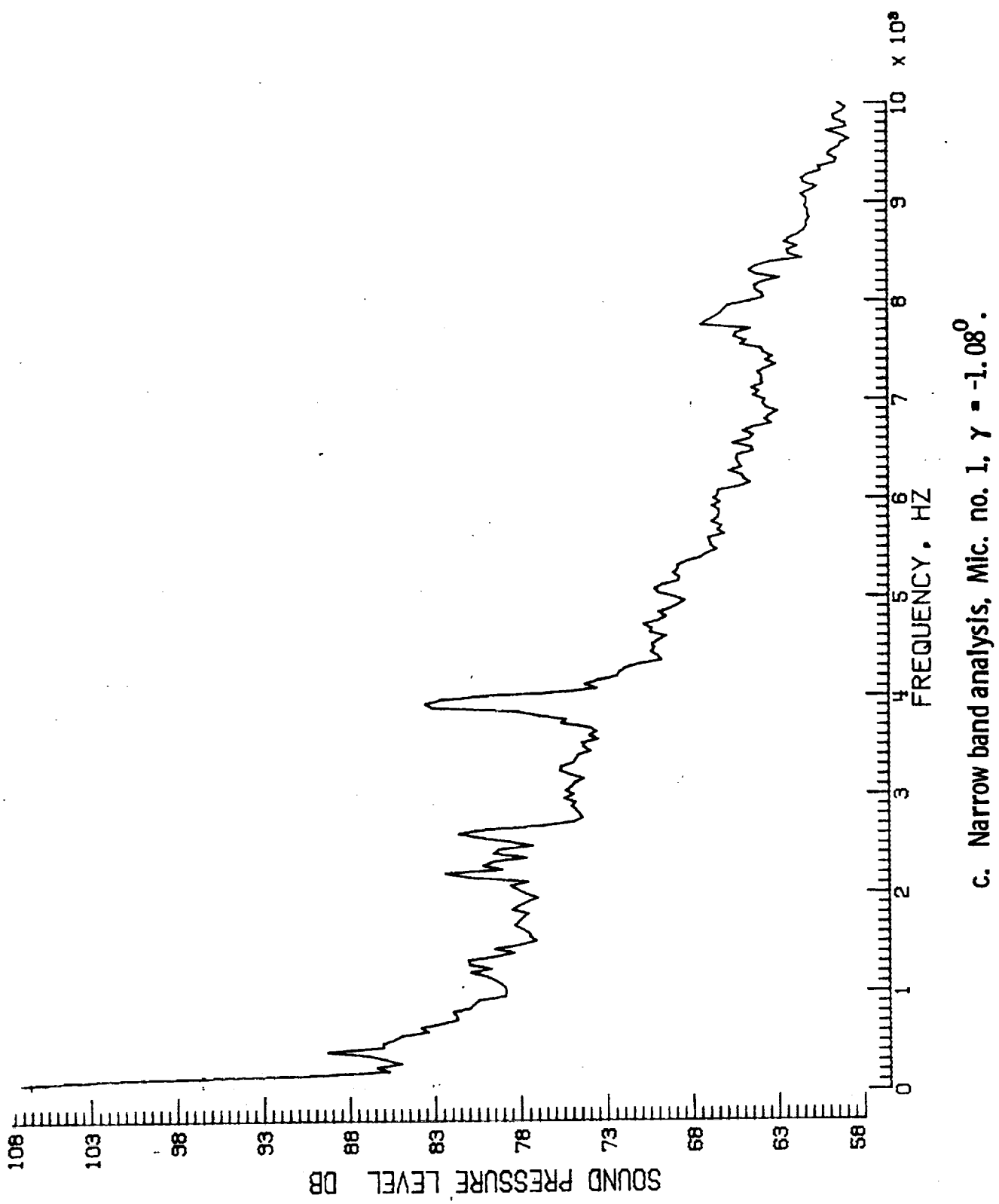
a. Mic. no. 1.

Figure 11. - Effect of descent angle variation on noise generated by helicopter model with ogee tips installed. $V_{\infty} = 51.0$ kts.



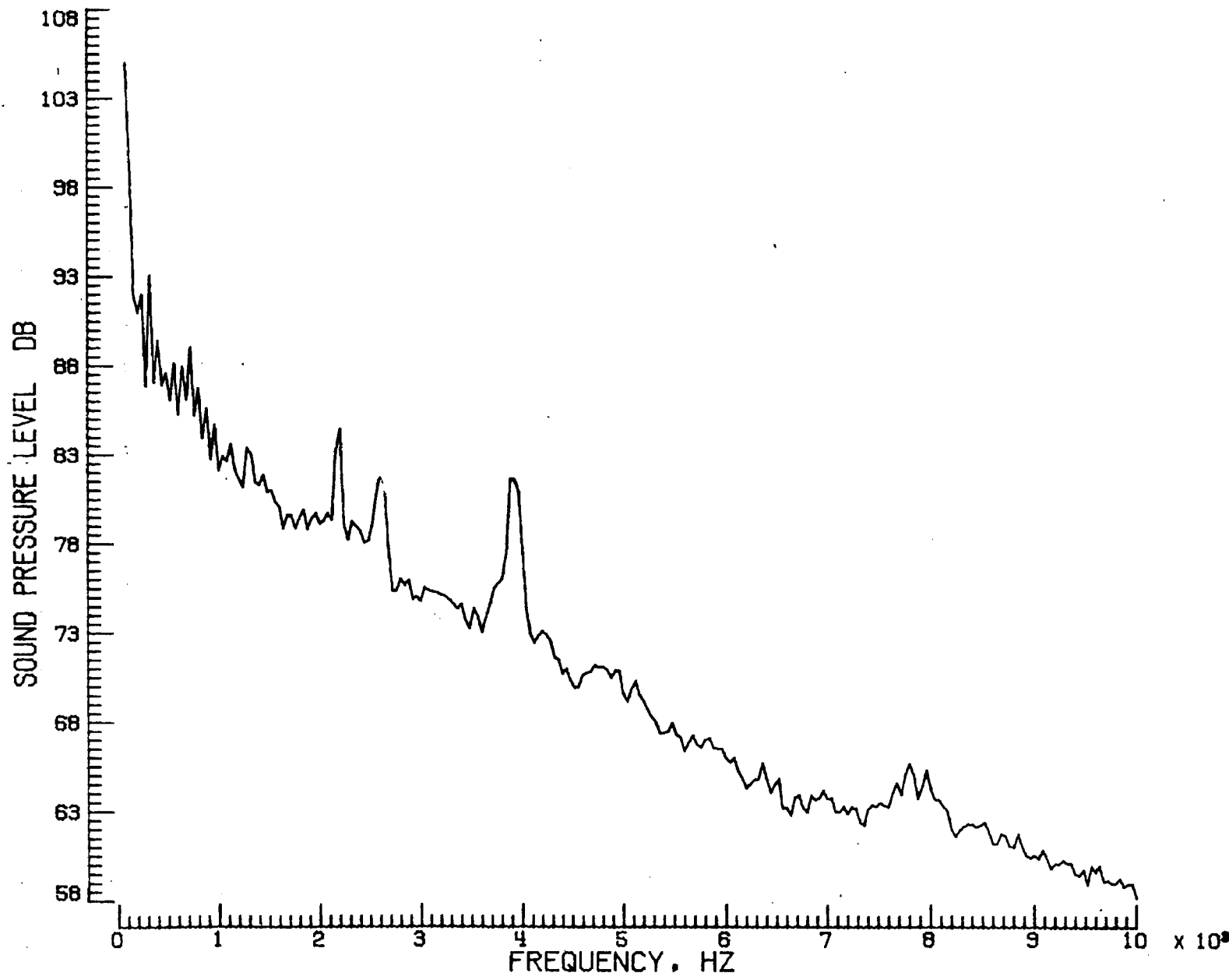
b. Pressure-time histories, Mic. no. 1.

Figure 11. - Continued.



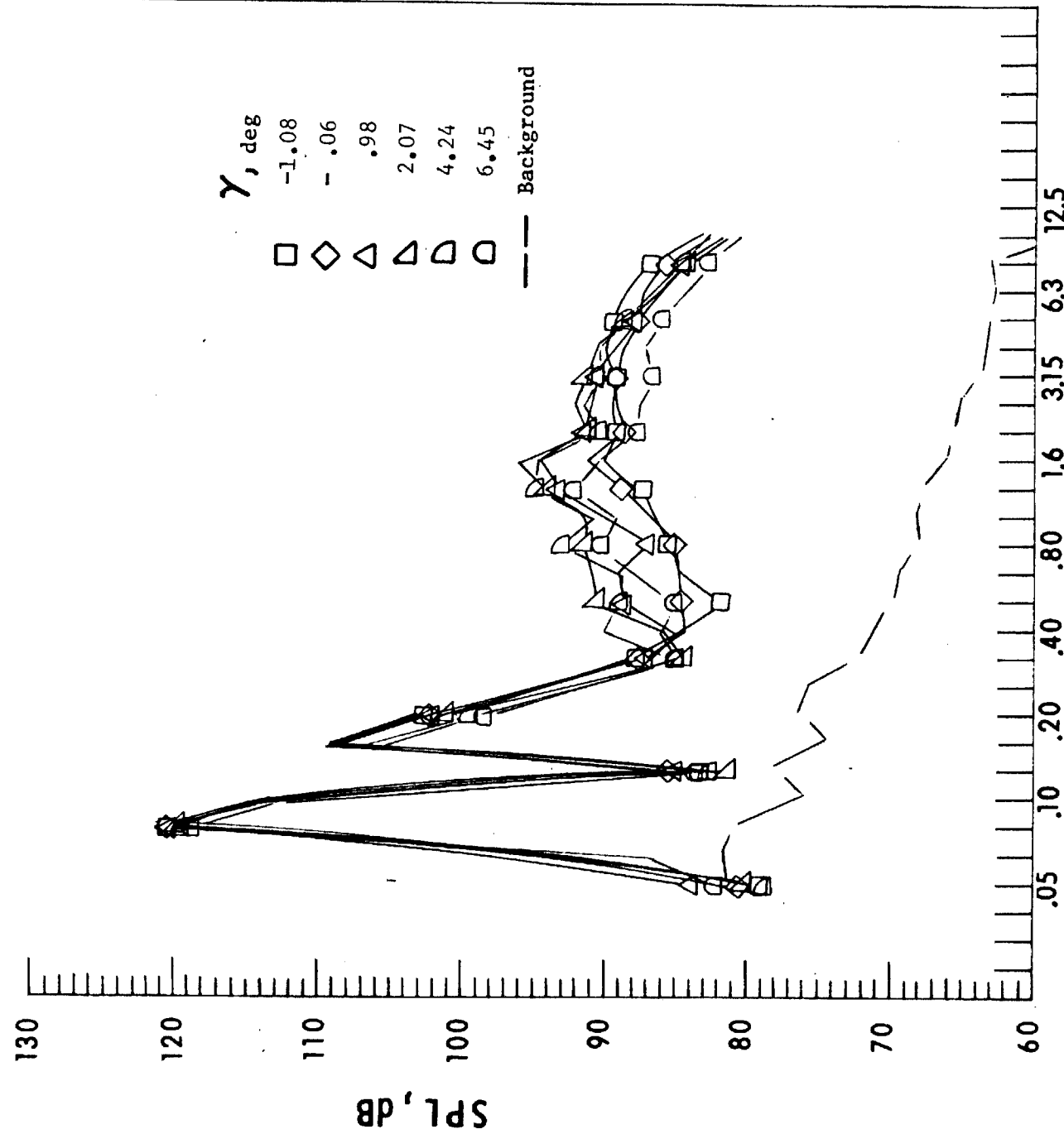
c. Narrow band analysis. Mic. no. 1. $\gamma = -1.08^0$.

Figure 11. - Continued.



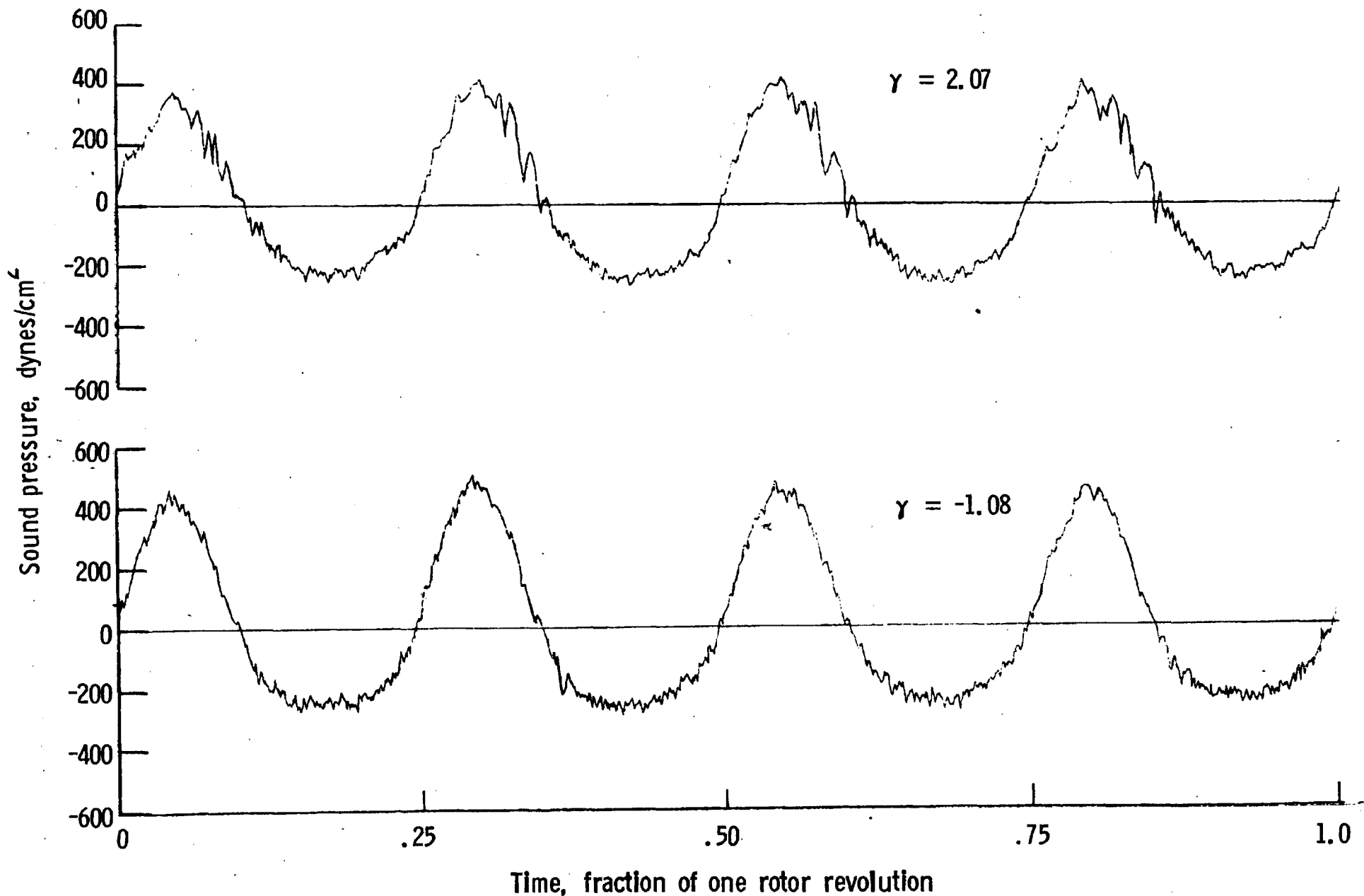
d. Narrow band analysis, Mic. no. 1, $\gamma = 2.07^0$.

Figure 11. - Continued.



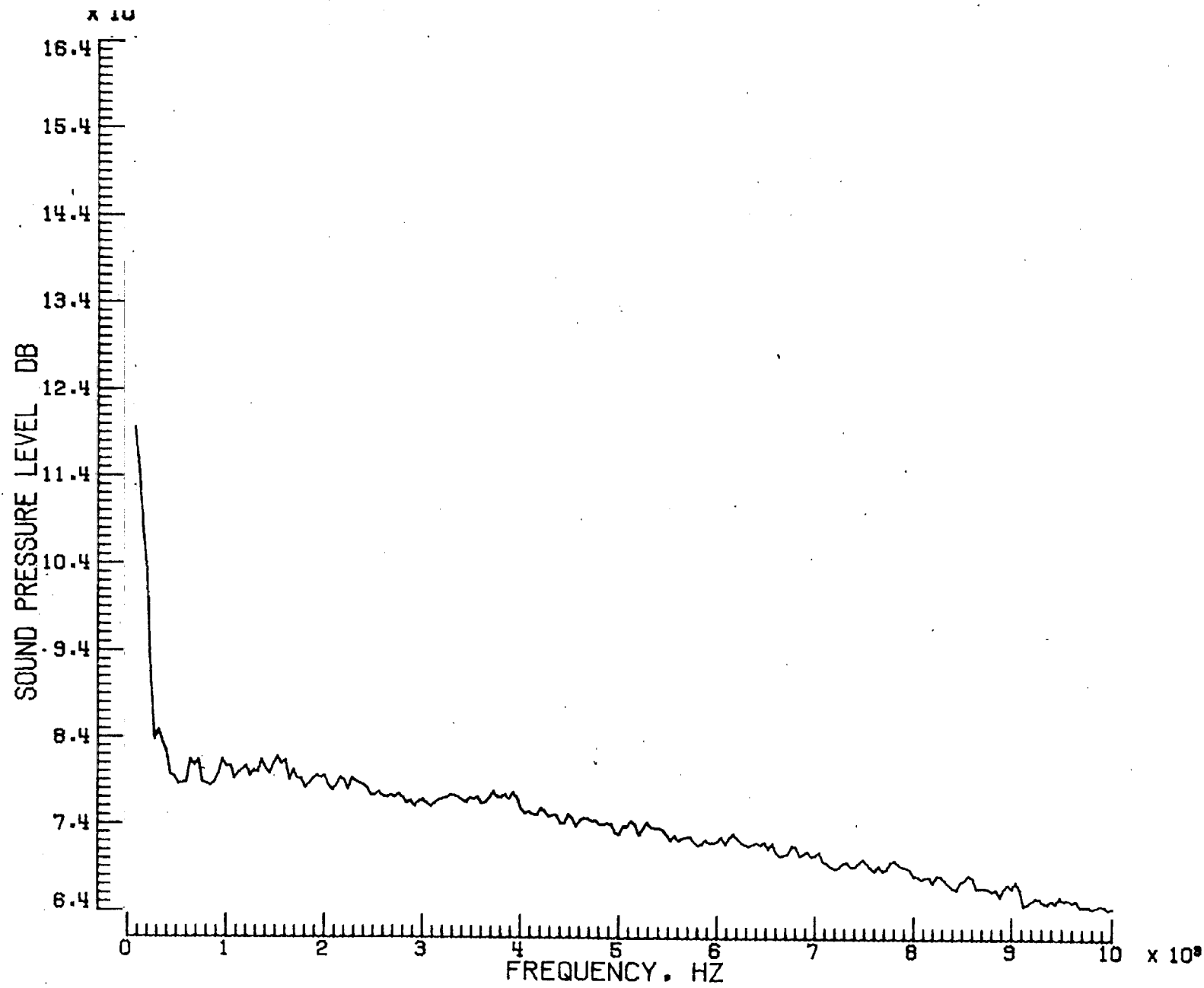
e. Mic. no. 2.

Figure 11. - Continued.



f. Pressure-time histories, Mic. no. 2.

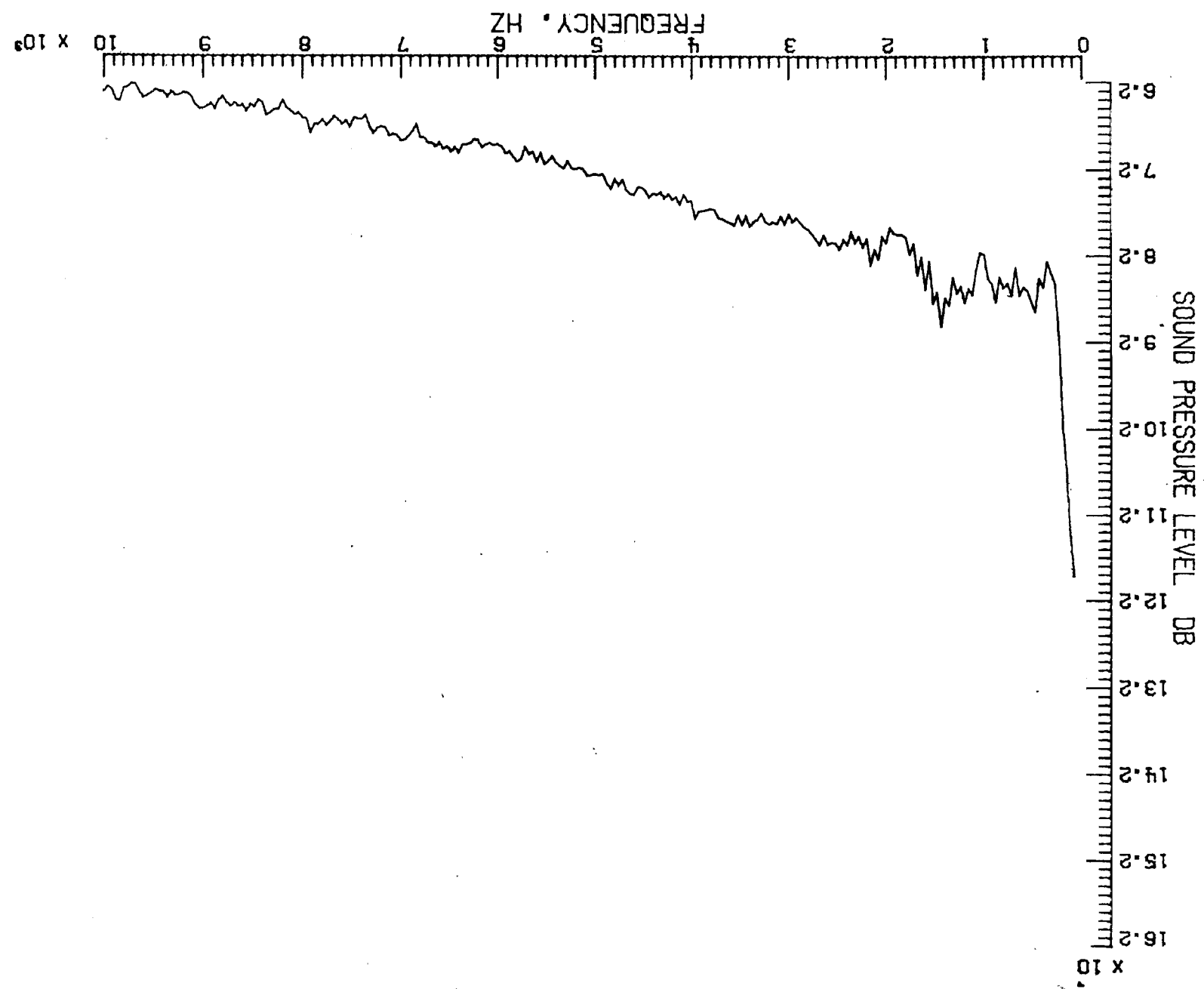
Figure 11. - Continued.

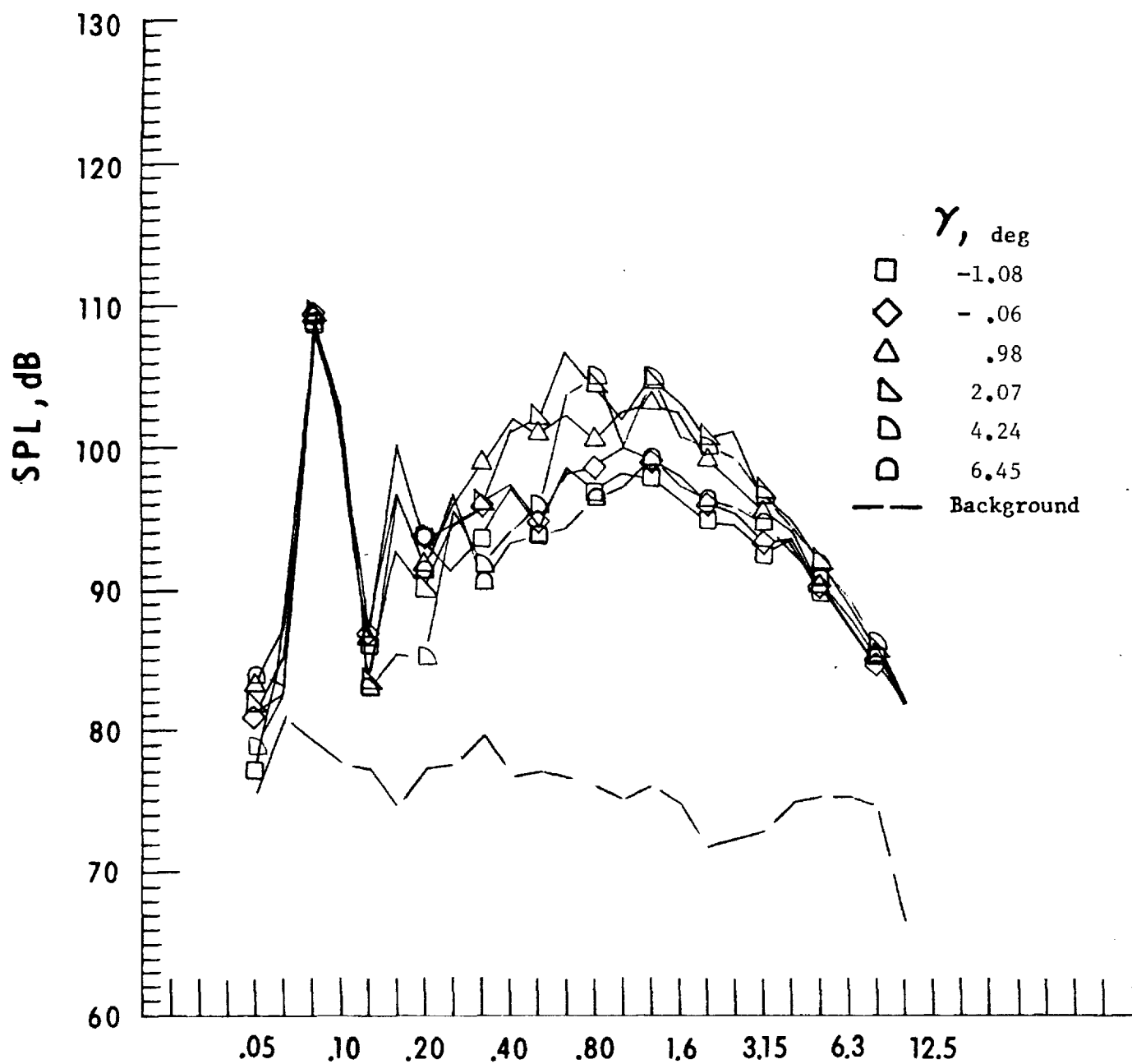


g. Narrow band analysis, Mic. no. 2, $\gamma = -1.08^0$.

Figure 11. - Continued.

Figure 11. - Continued.

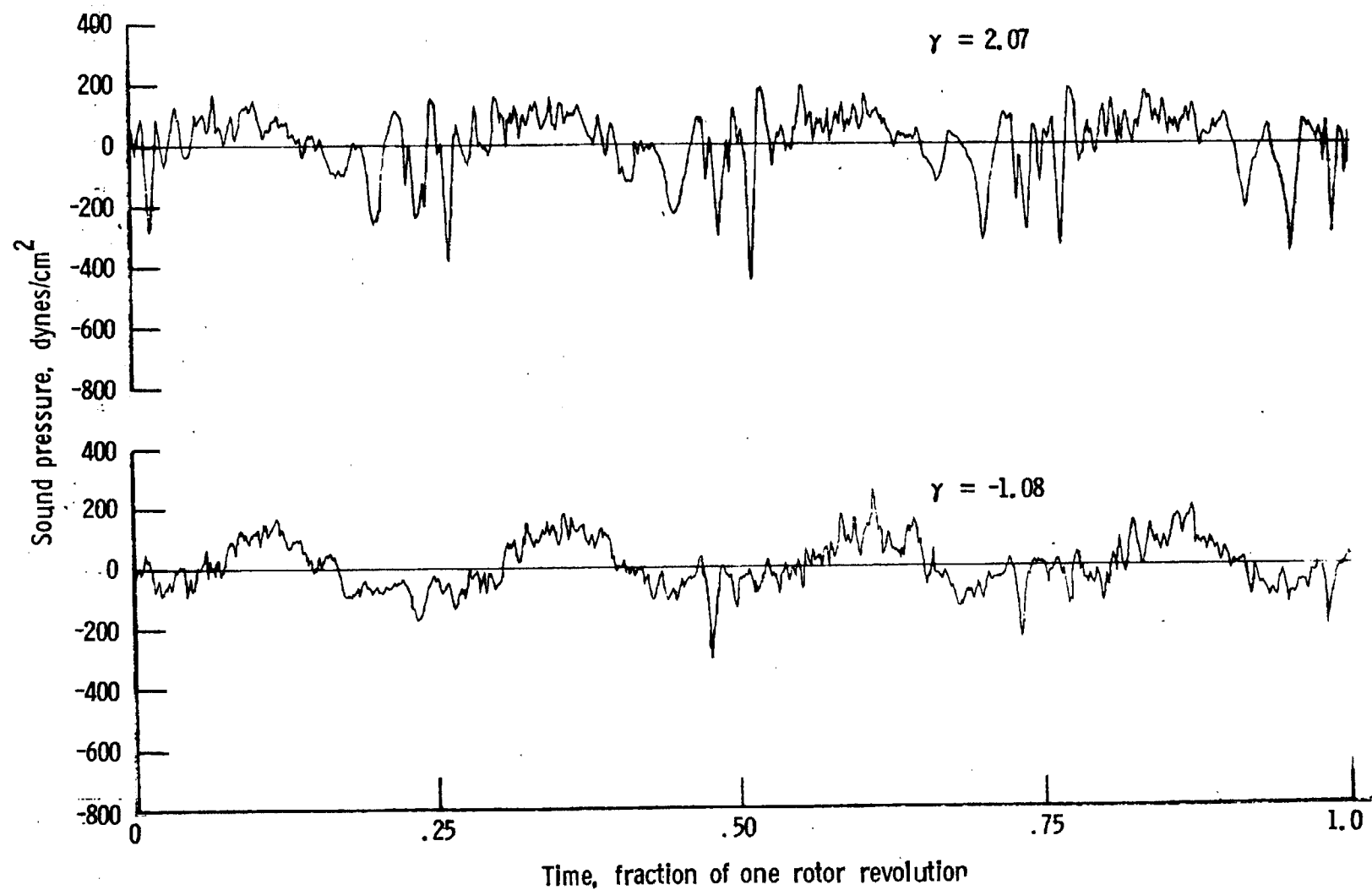
h. Narrow band analysis, Mic. no. 2, $y = 2.07^0$.



One-third-octave-band center frequency, kHz

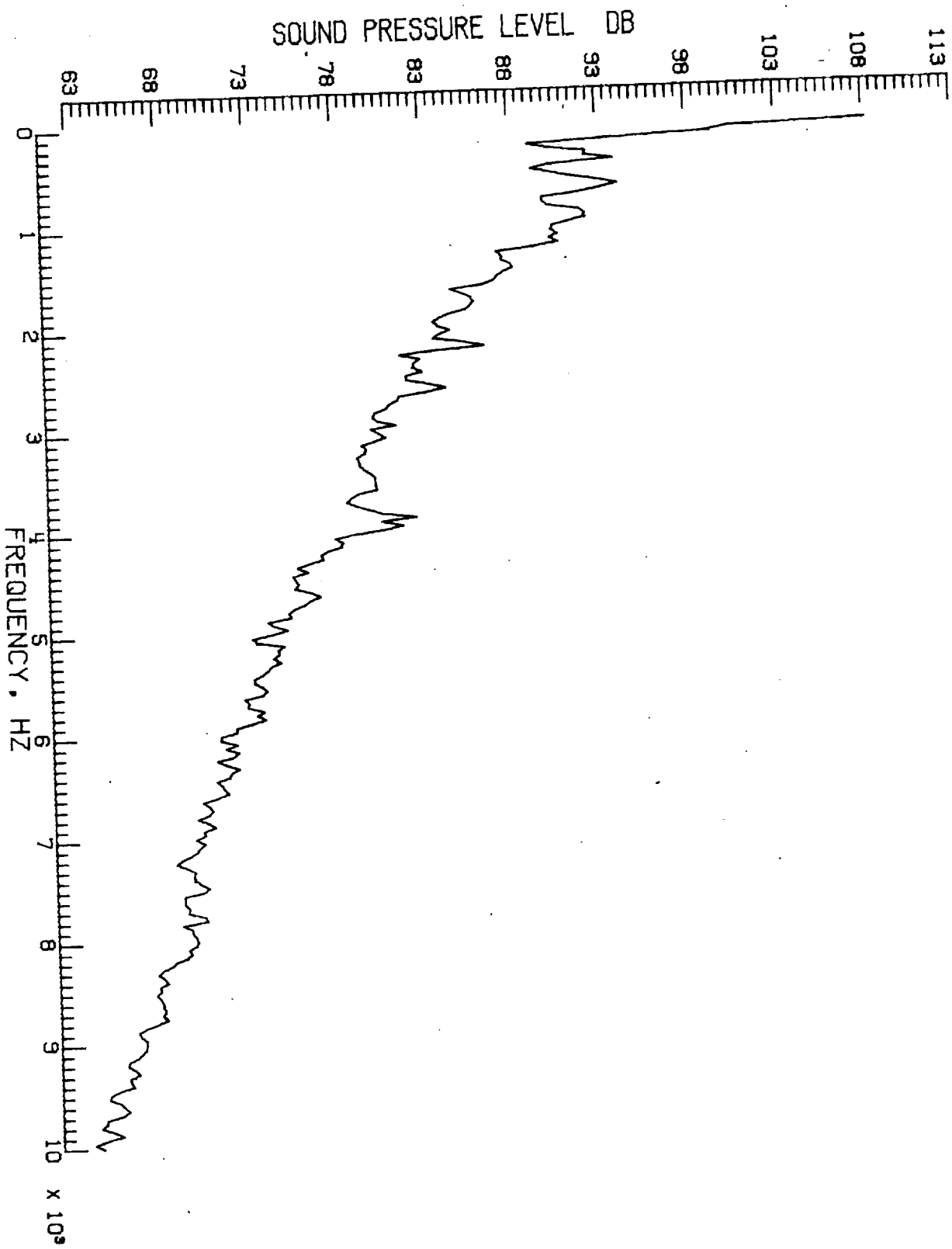
i. Mic. no. 3.

Figure 11. - Continued.



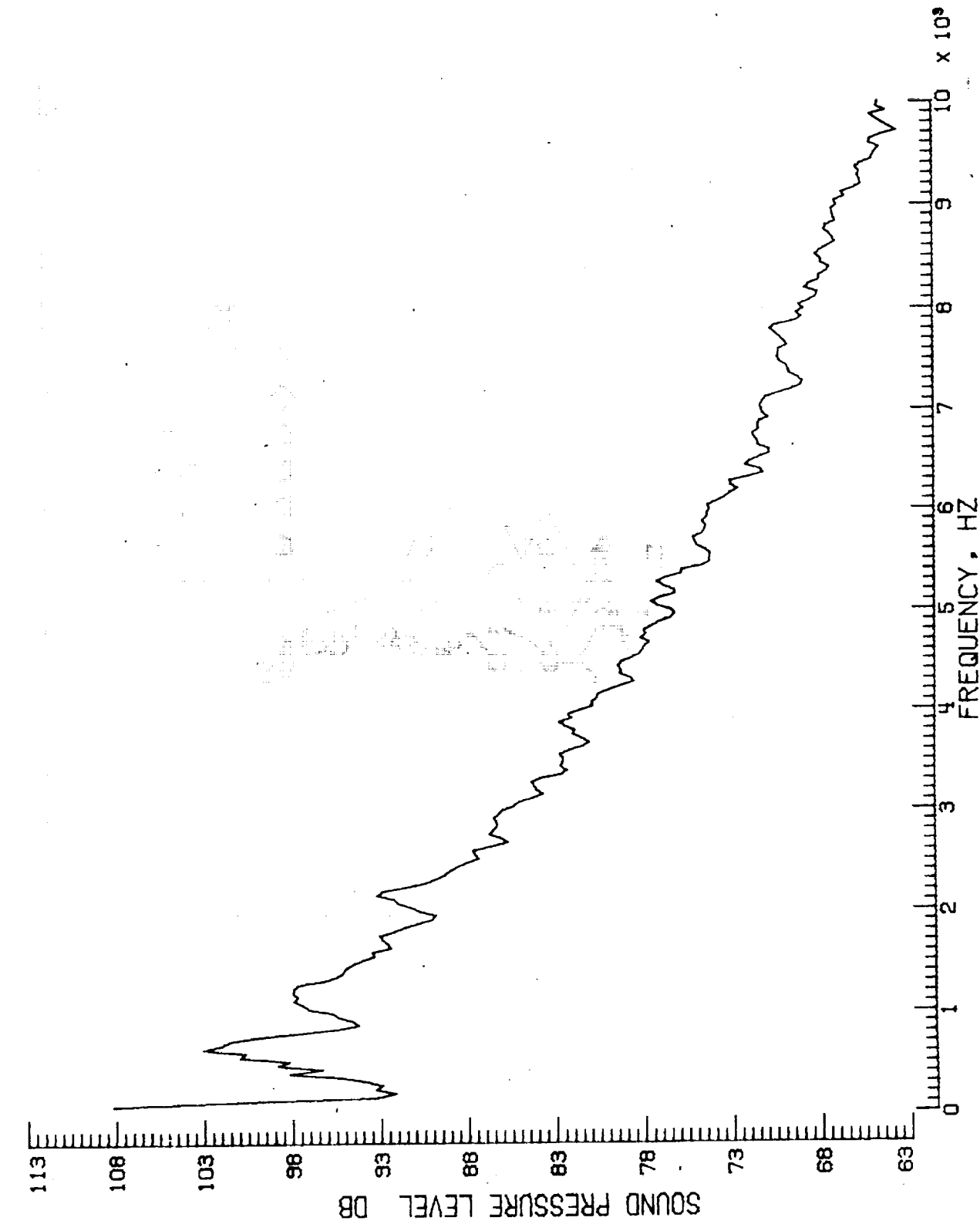
j. Pressure-time histories, Mic. no. 3.

Figure 11. - Continued.



k. Narrow band analysis, Mic. no. 3, $\gamma = -1.08^0$.

Figure 11. - Continued.



I. Narrow band analysis. Mic. no. 3, $\gamma = 2.07^0$.

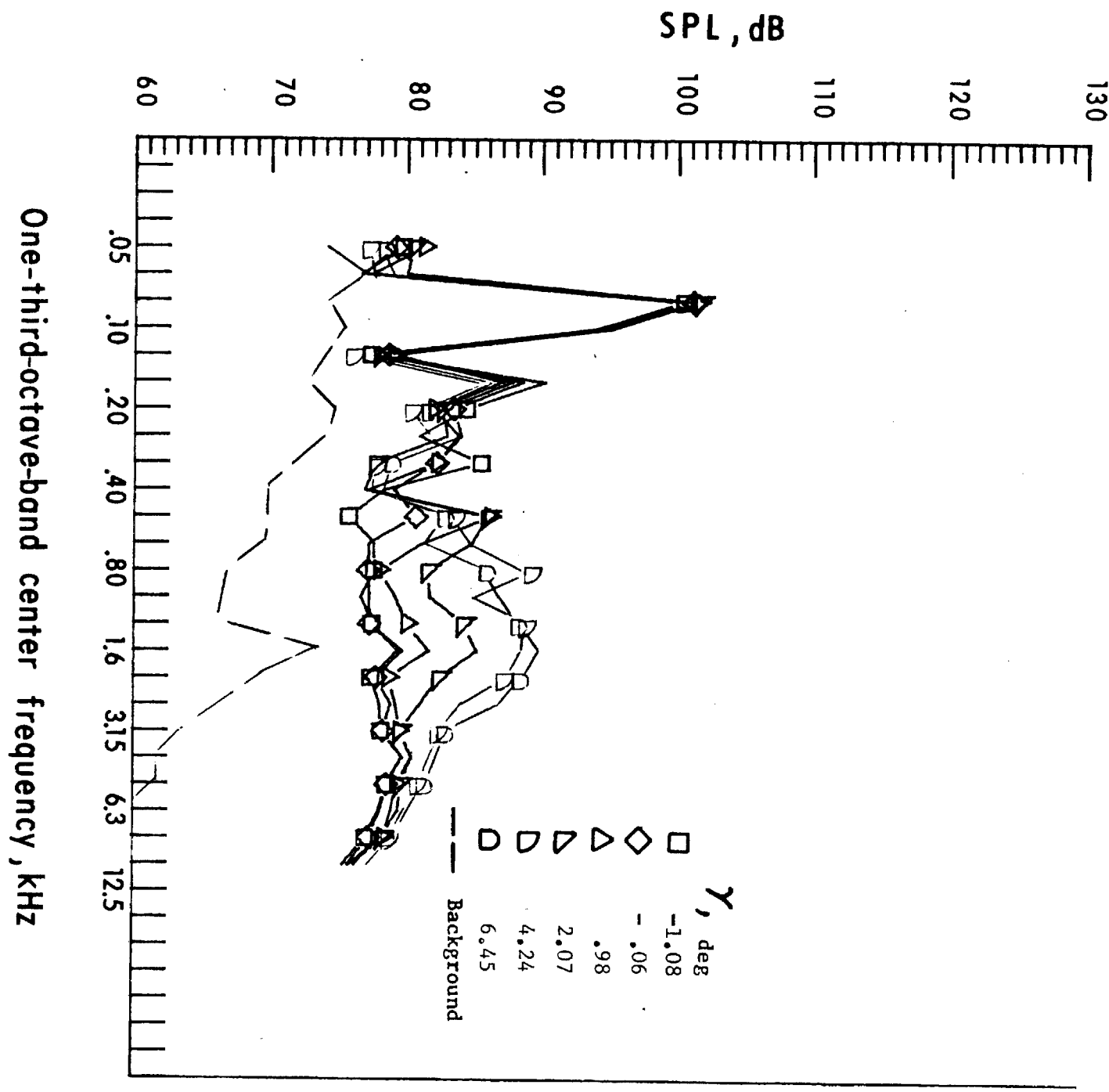
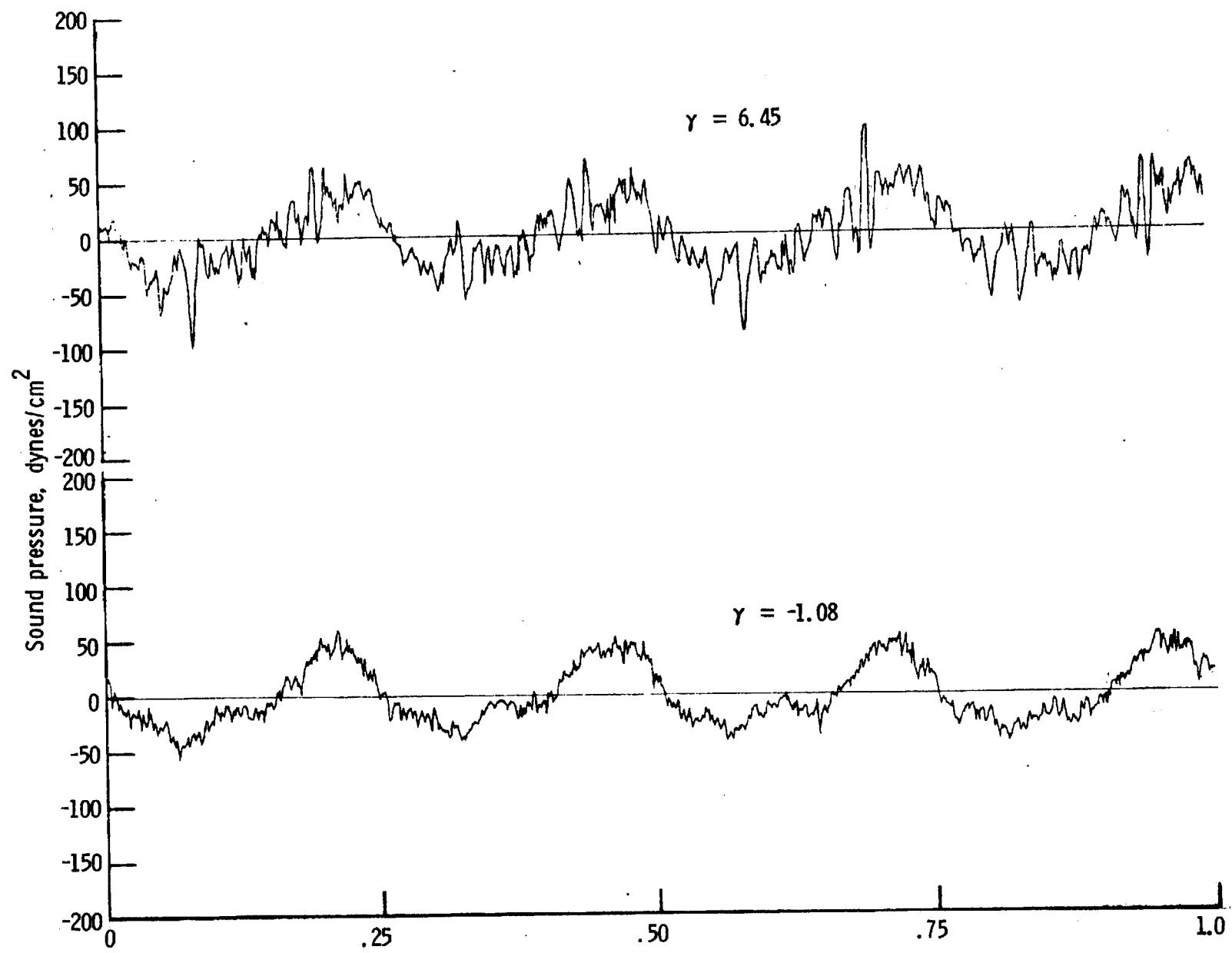
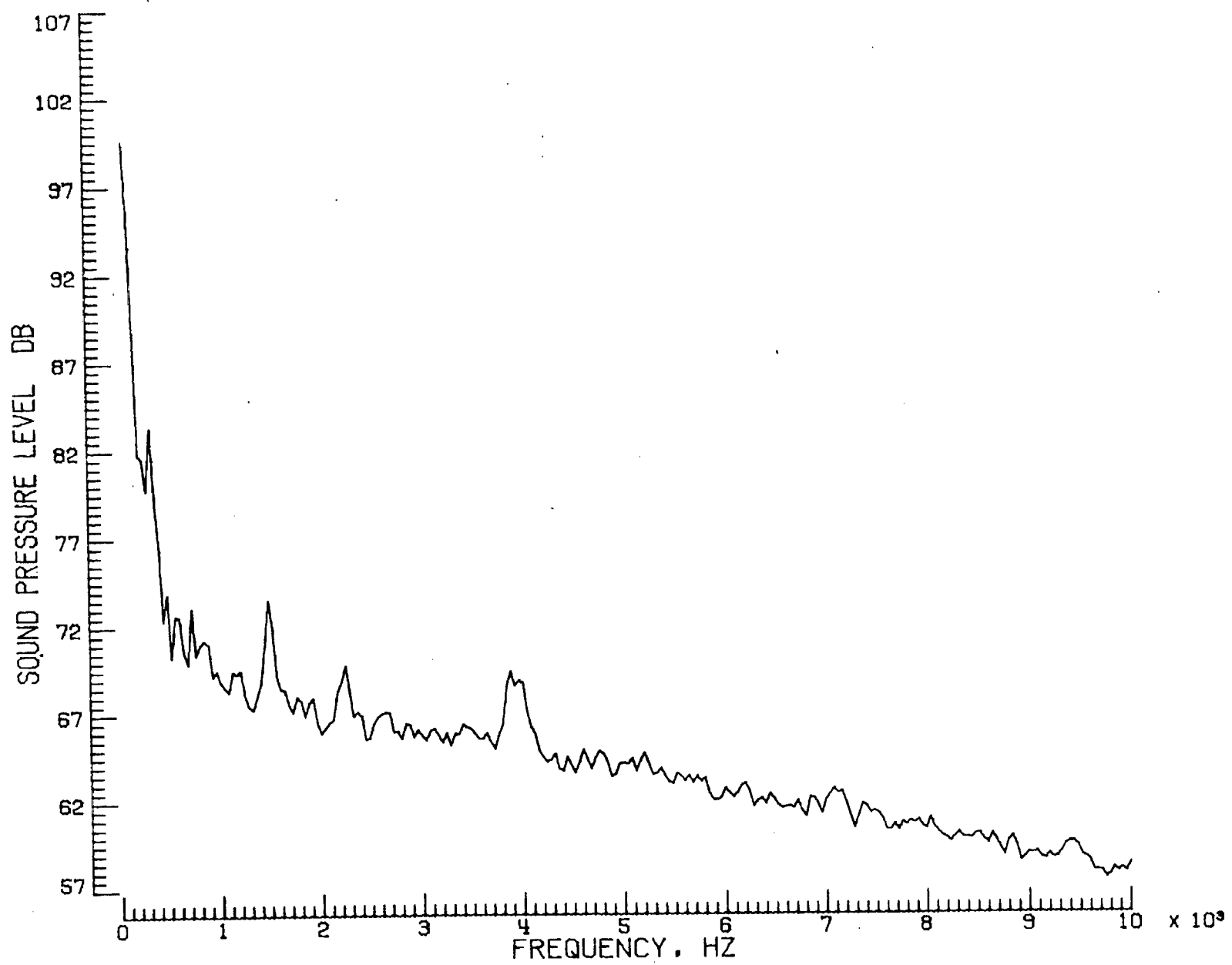


Figure 11. - Continued.

m. Mic. no. 4.

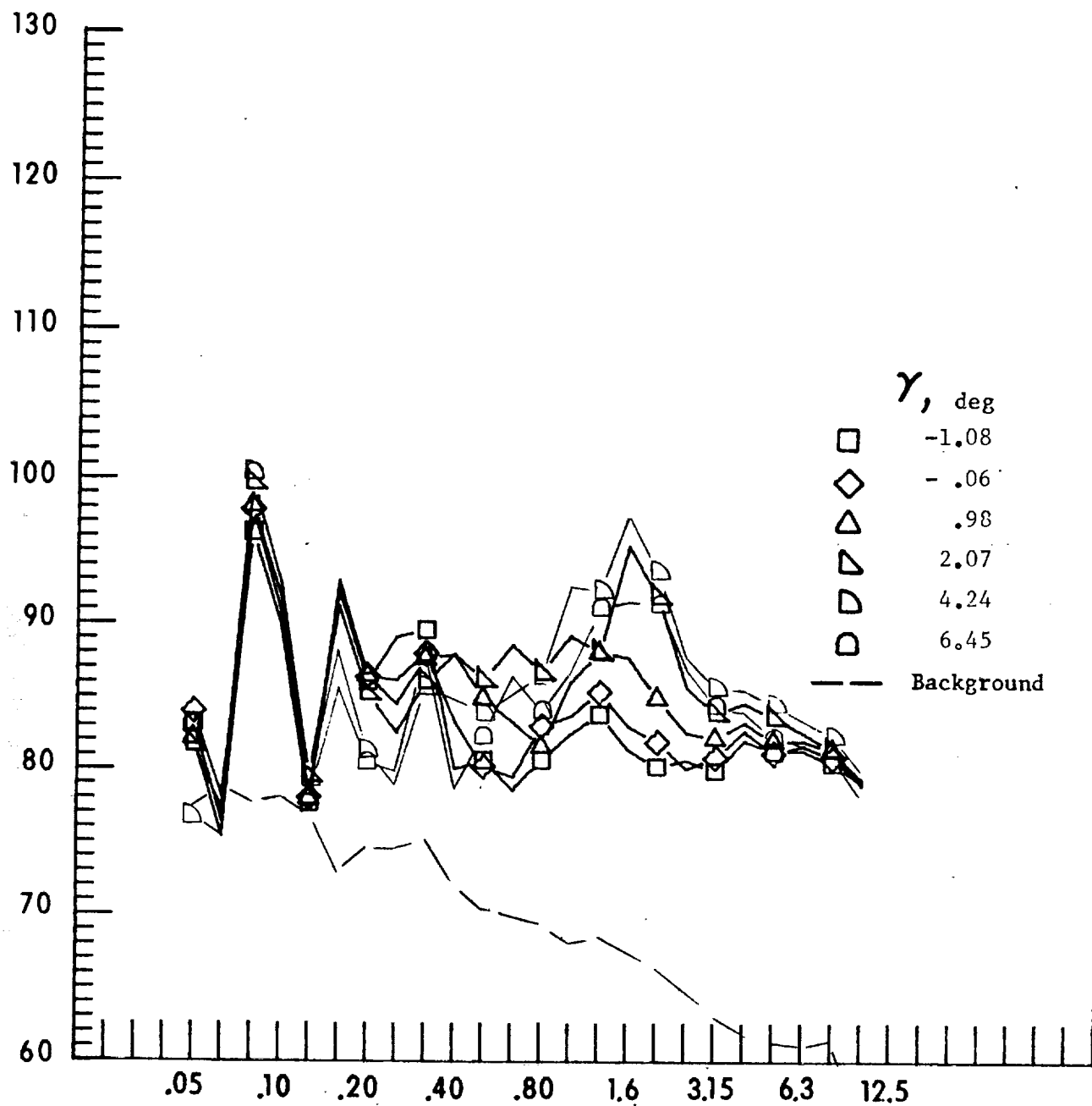


n. Pressure-time histories, Mic. no. 4.



o. Narrow band analysis, Mic. no. 4, $\gamma = -1.08^0$.

Figure 11. - Continued.

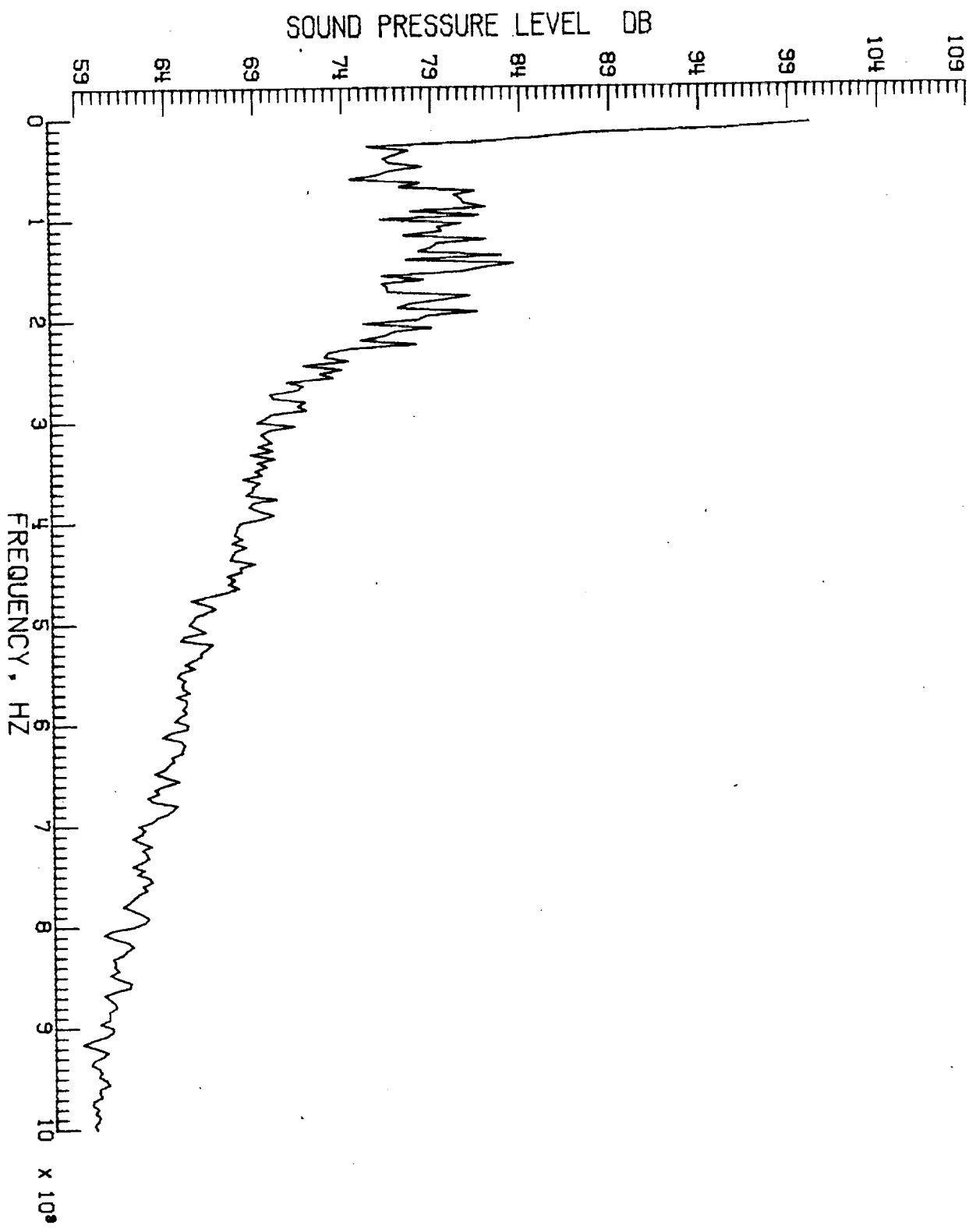


One-third-octave-band center frequency, kHz

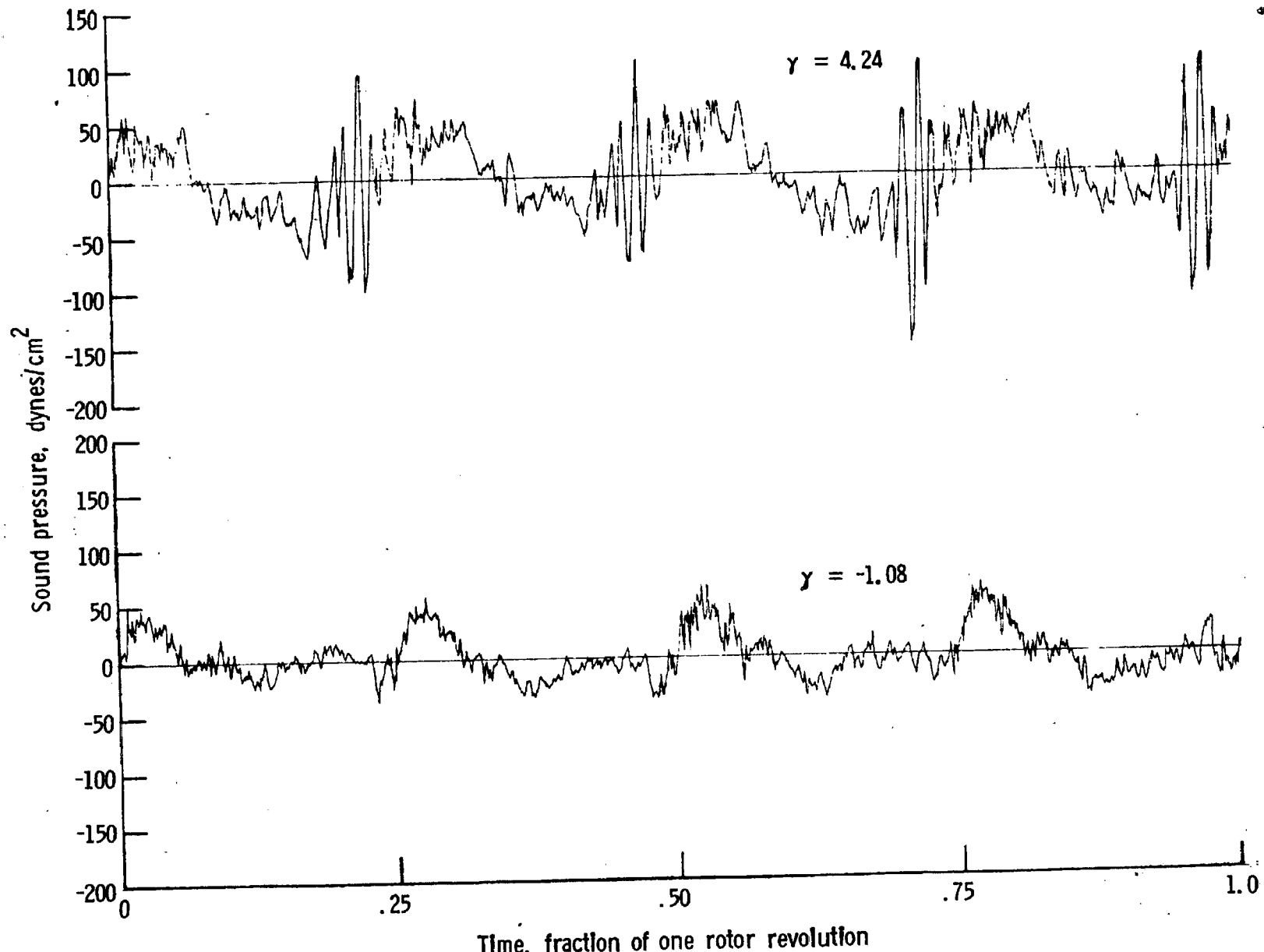
q. Mic. no. 5.

Figure 11. - Continued.

C-2

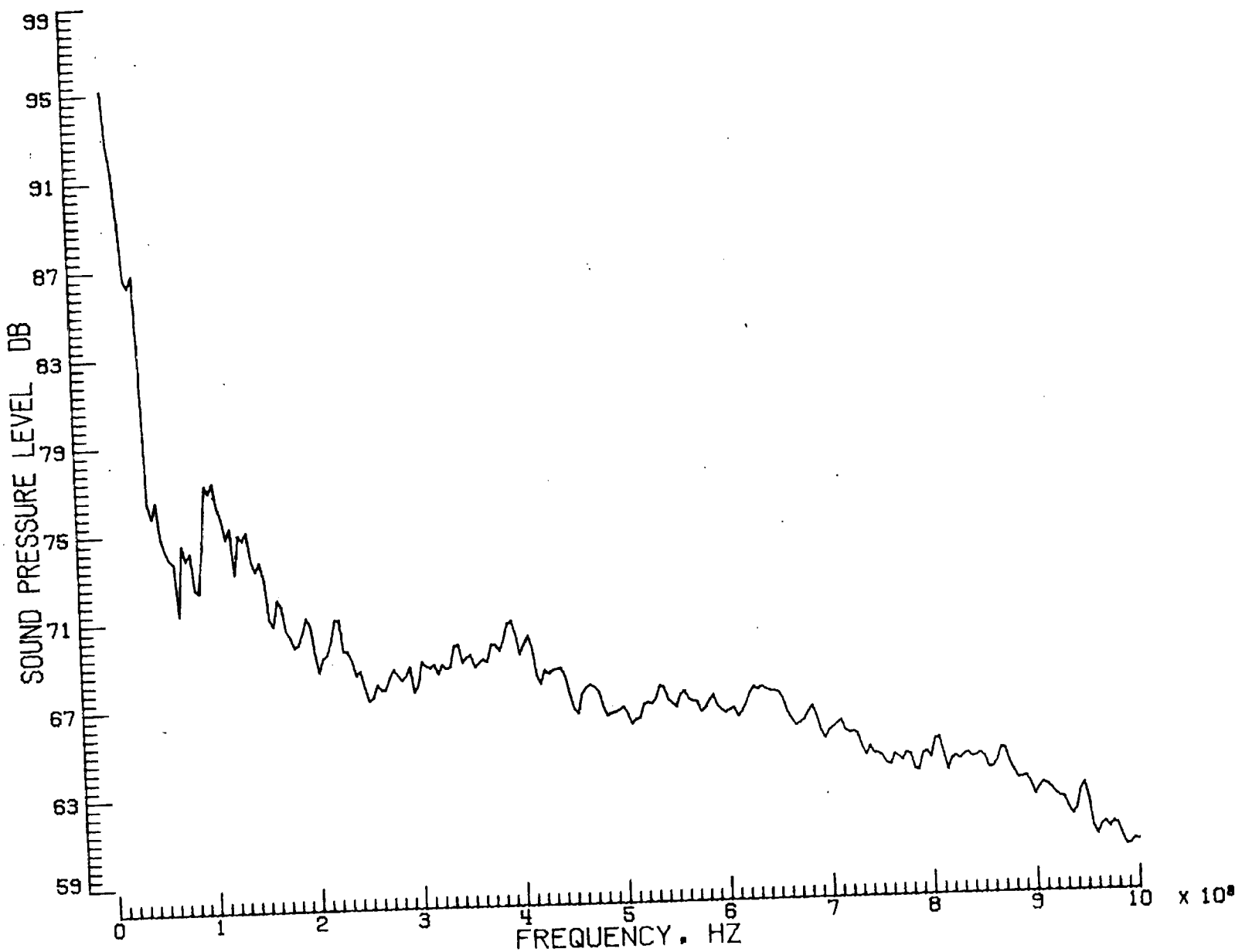


p. Narrow band analysis, Mic. no. 4, $\gamma = 6.45^\circ$.



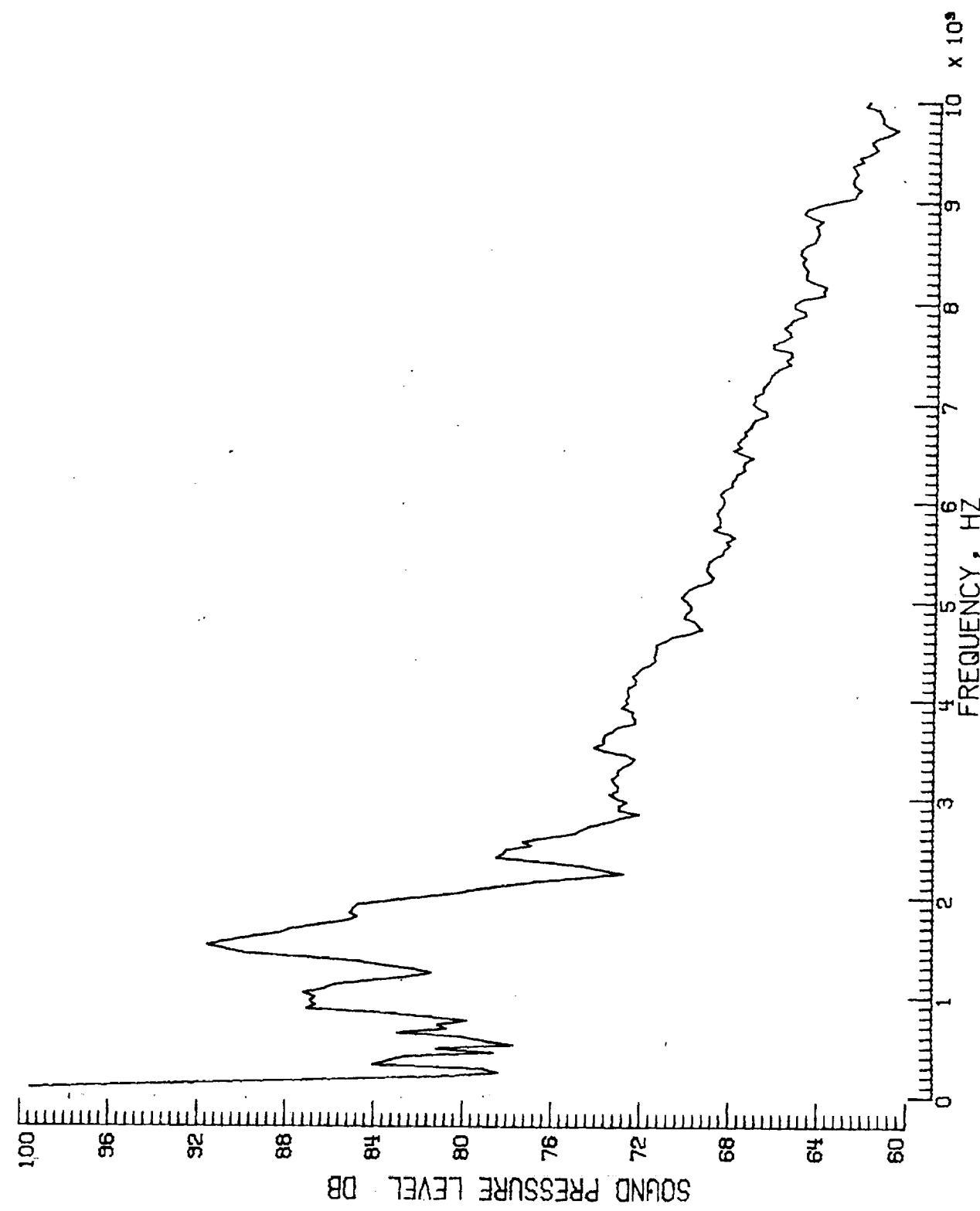
r. Pressure-time histories, Mic. no. 5.

Figure 11. - Continued.

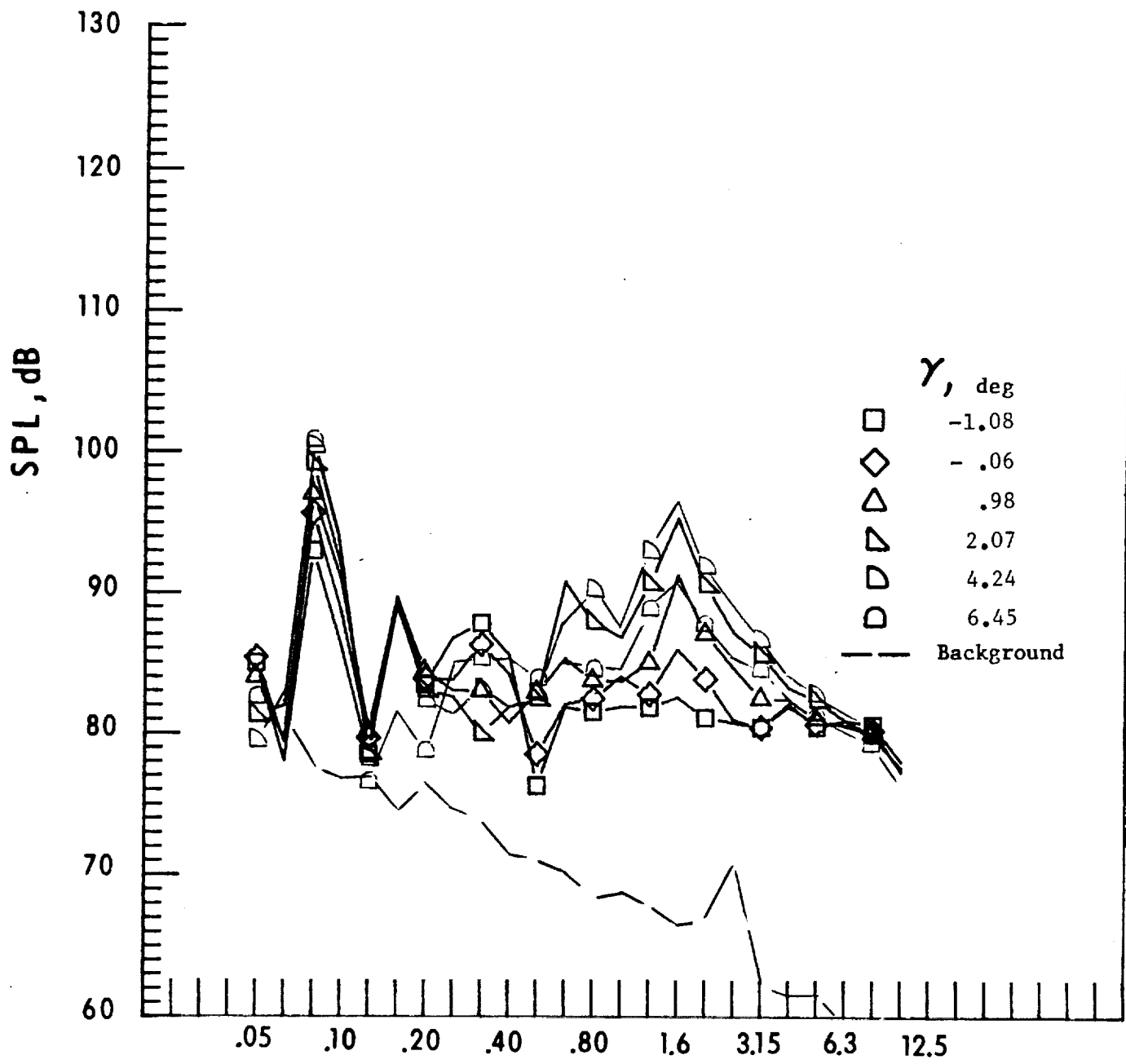


s. Narrow band analysis, Mic. no. 5, $\gamma = -1.08^0$.

Figure 11. - Continued.



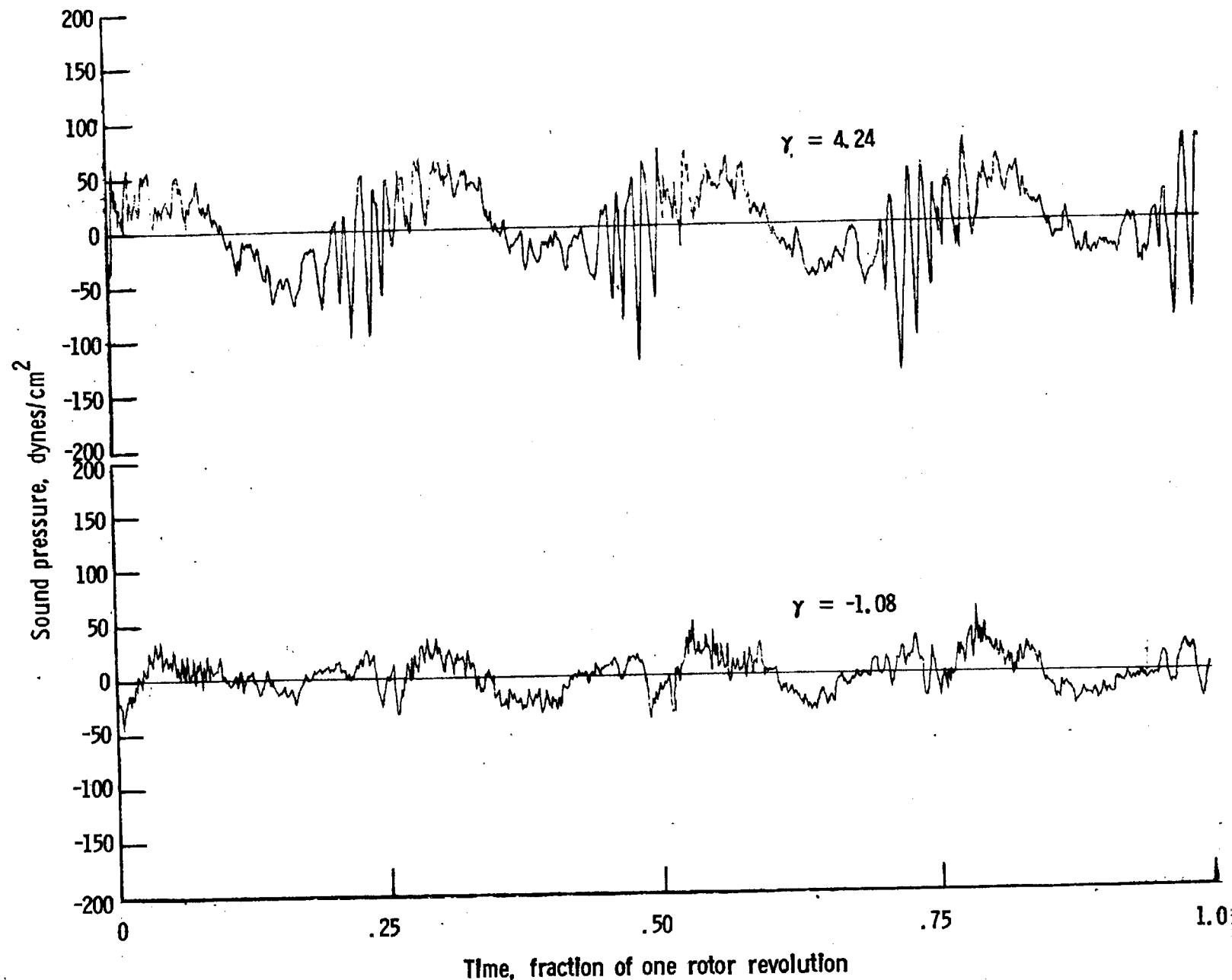
t. Narrow band analysis, Mic. no. 5, $\gamma = 4.24^0$.



One-third-octave-band center frequency, kHz

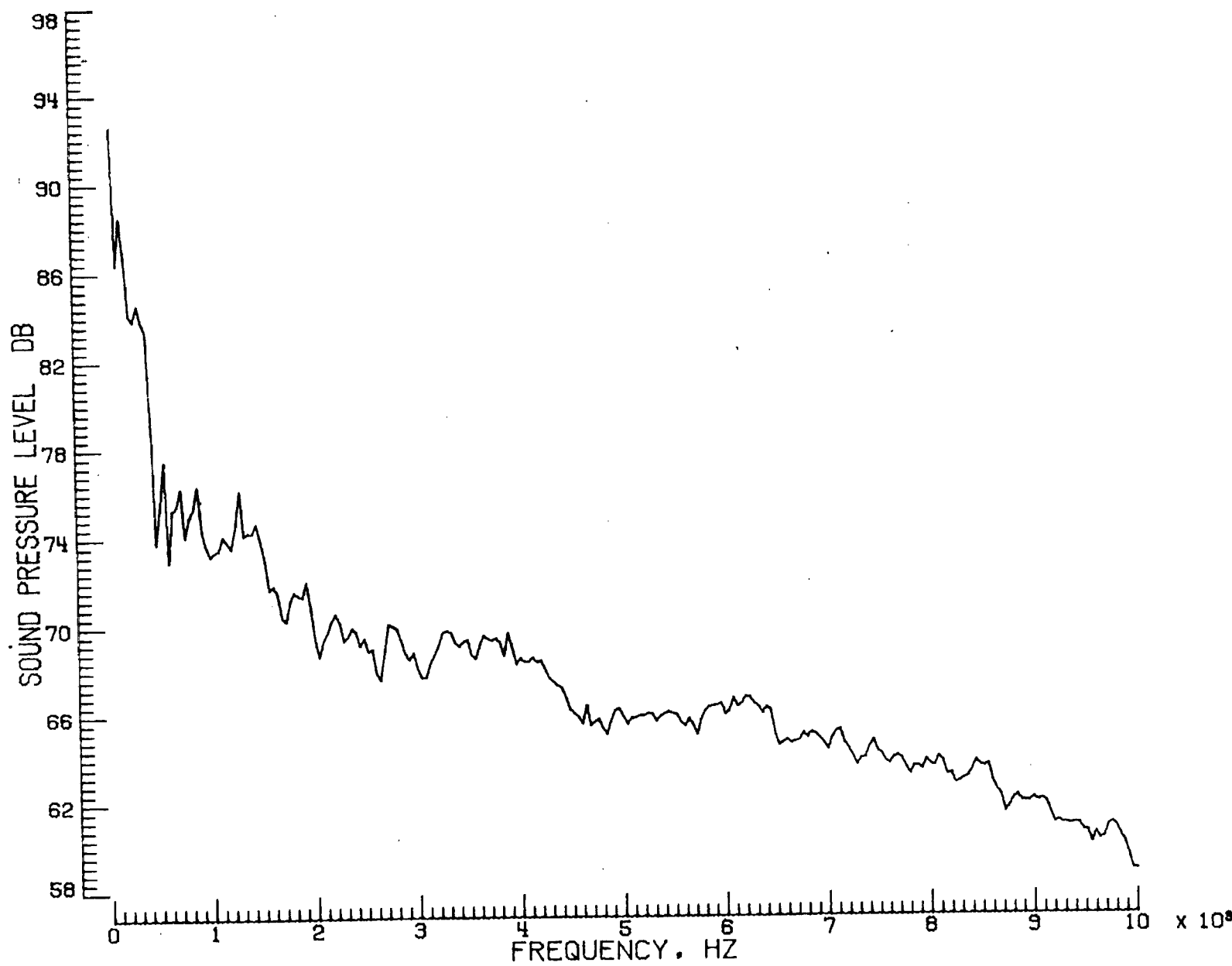
u. Mic. no. 6.

Figure 11. - Continued.



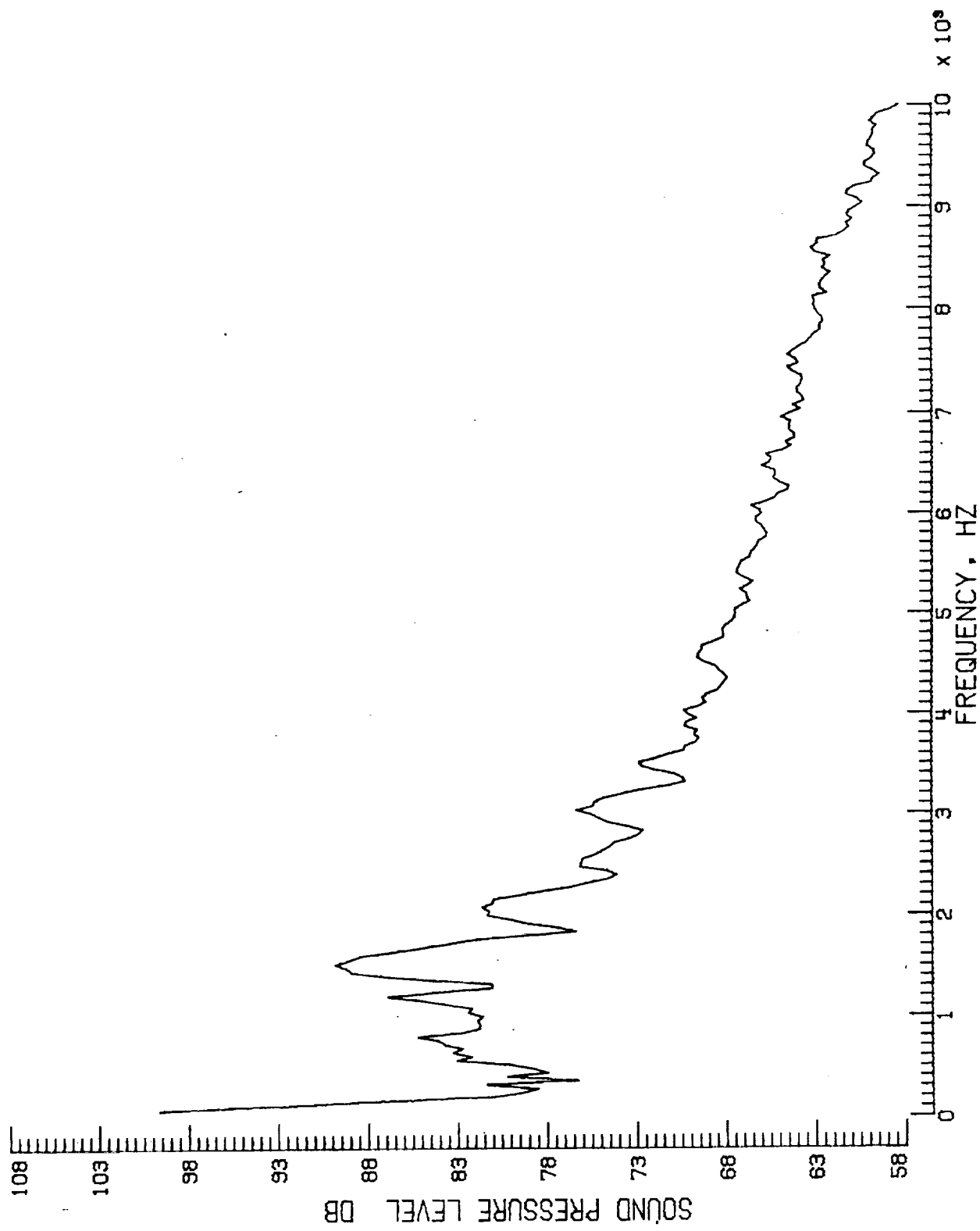
v. Pressure-time histories, Mic. no. 6.

Figure 11. - Continued.



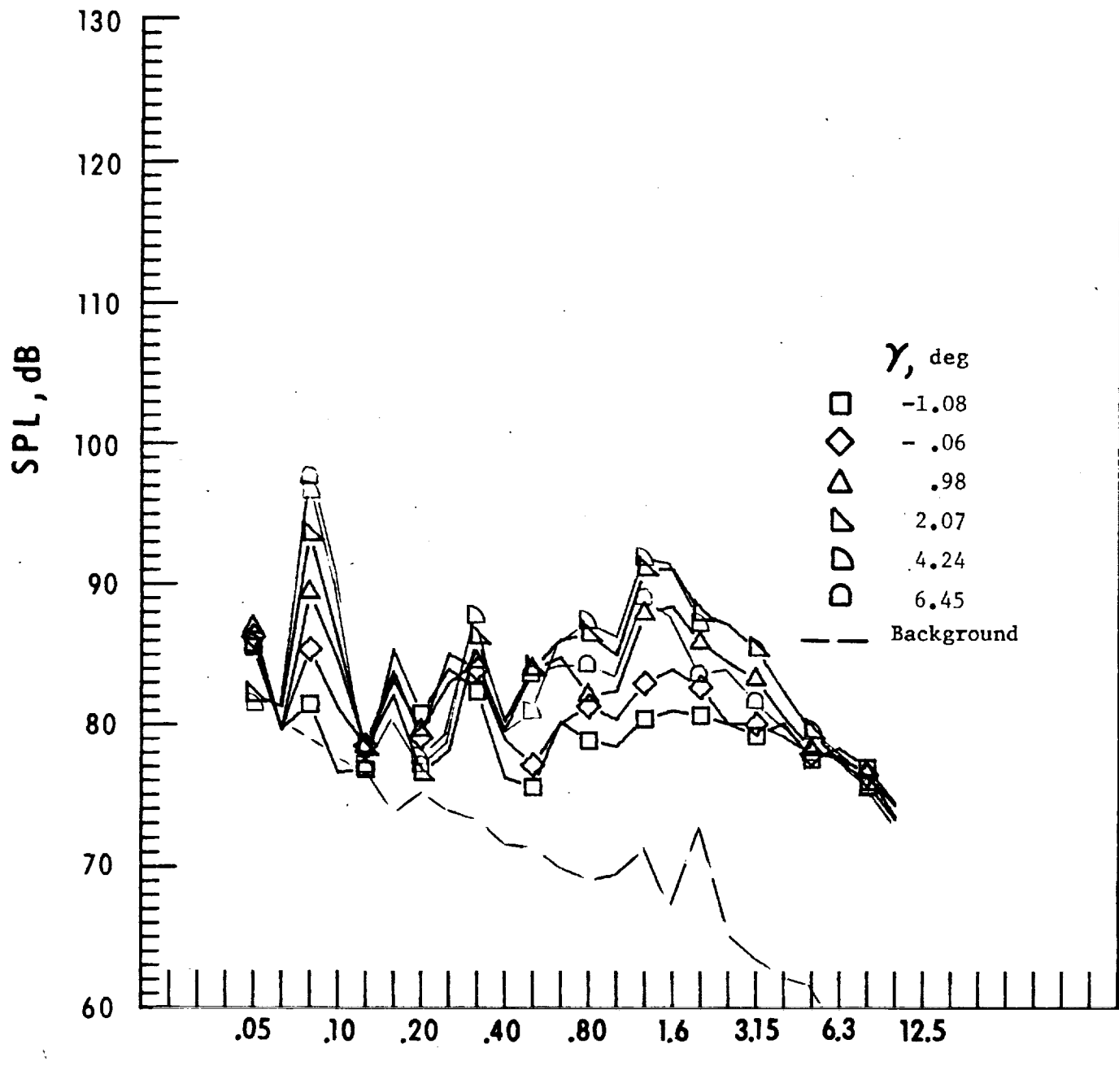
w. Narrow band analysis, Mic. no. 6, $\gamma = -1.08^0$.

Figure 11. - Continued.



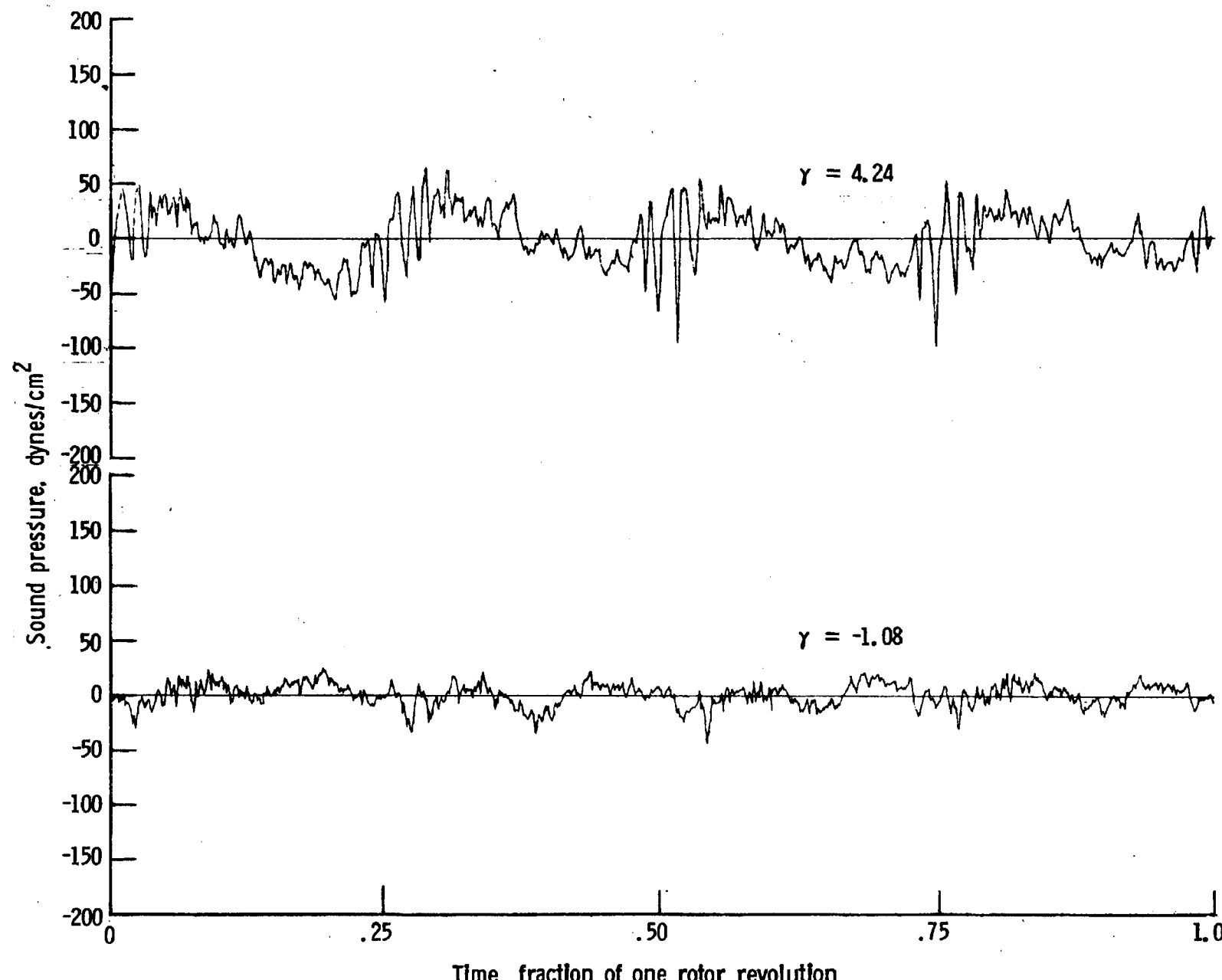
x. Narrow band analysis, Mic. no. 6, $\gamma = 4.24^0$.

Figure 11. - Continued.



y. Mic. no. 7.

Figure 11. - Continued.



z. Pressure-time histories, Mic. no. 7.

Figure 11. - Continued.

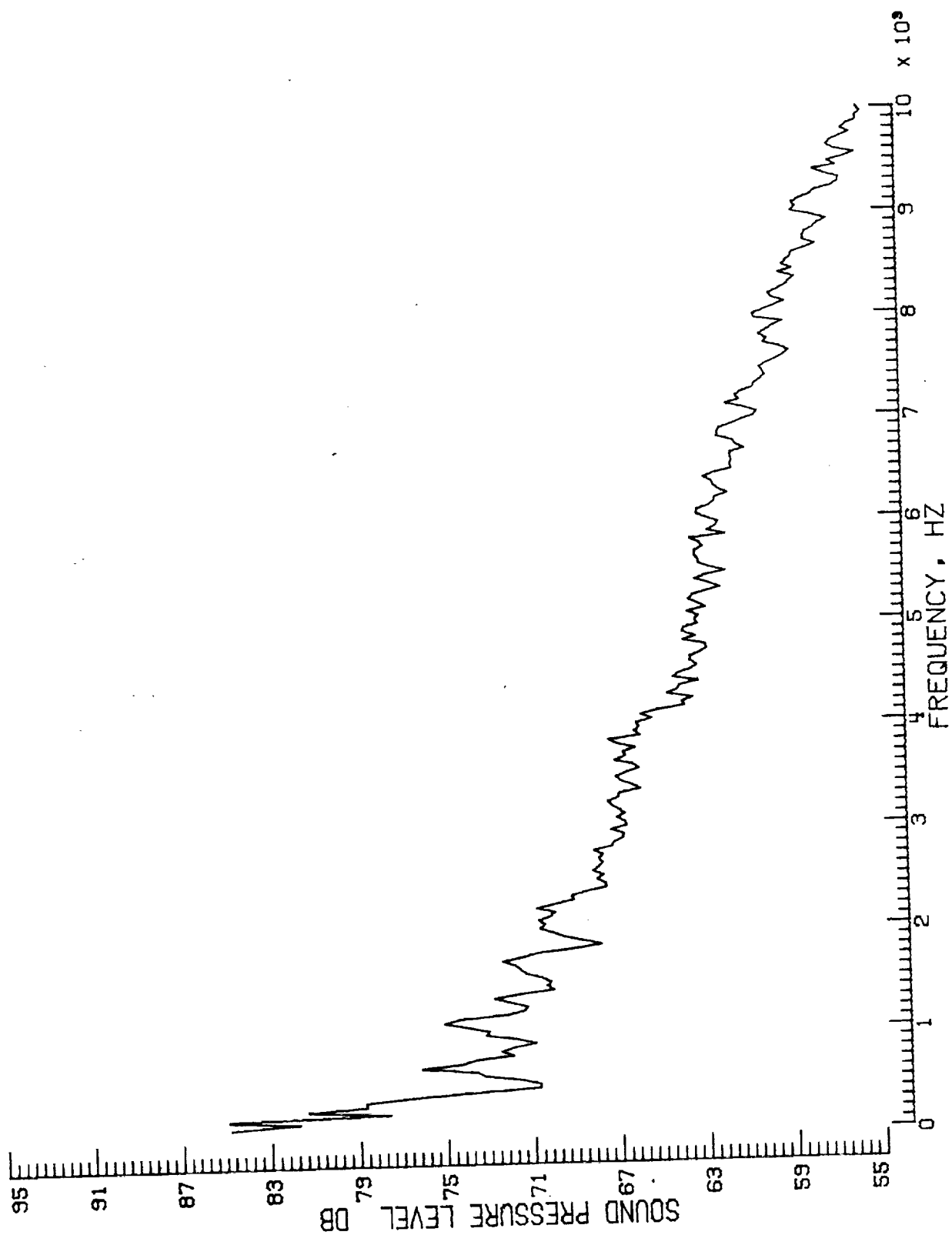
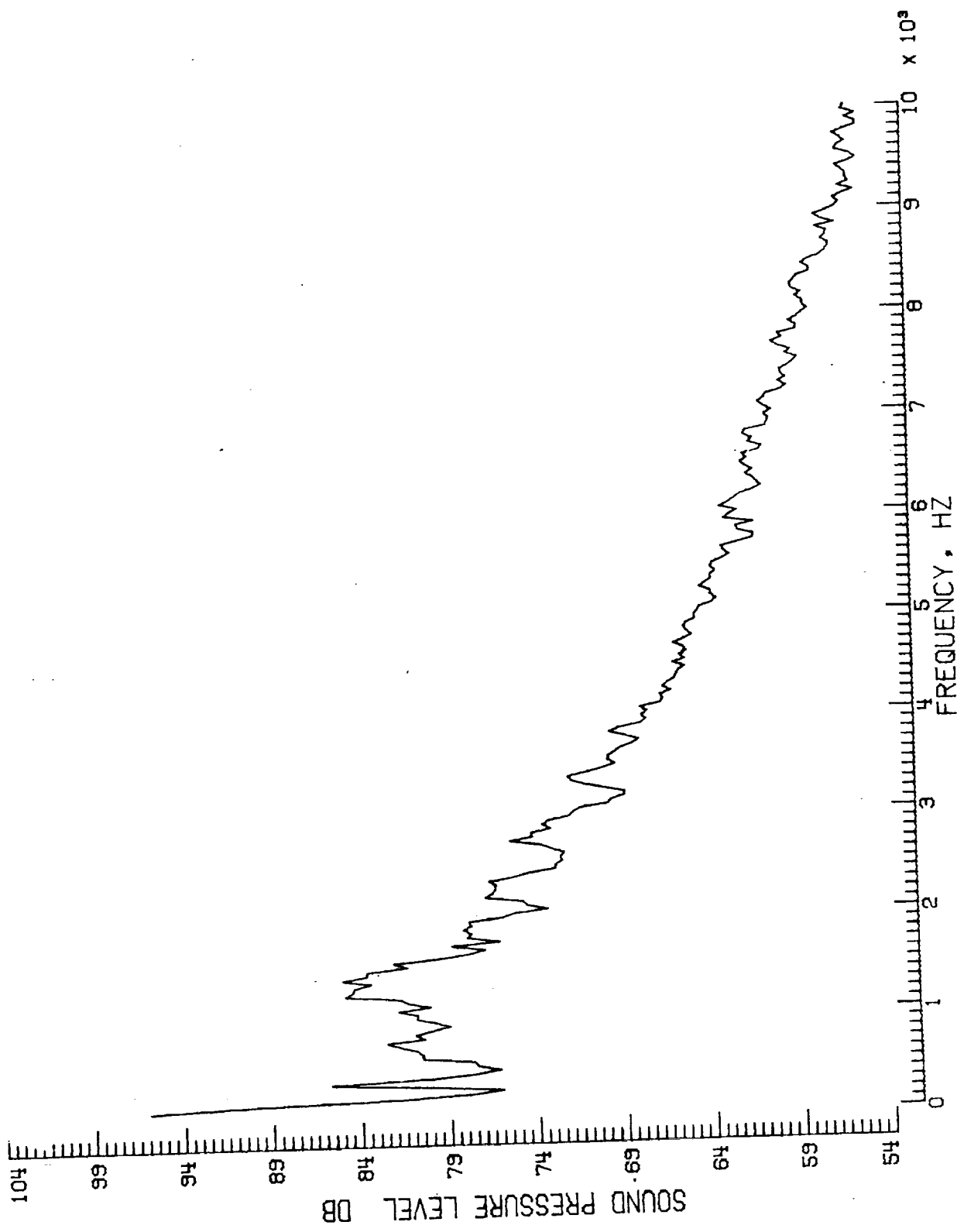
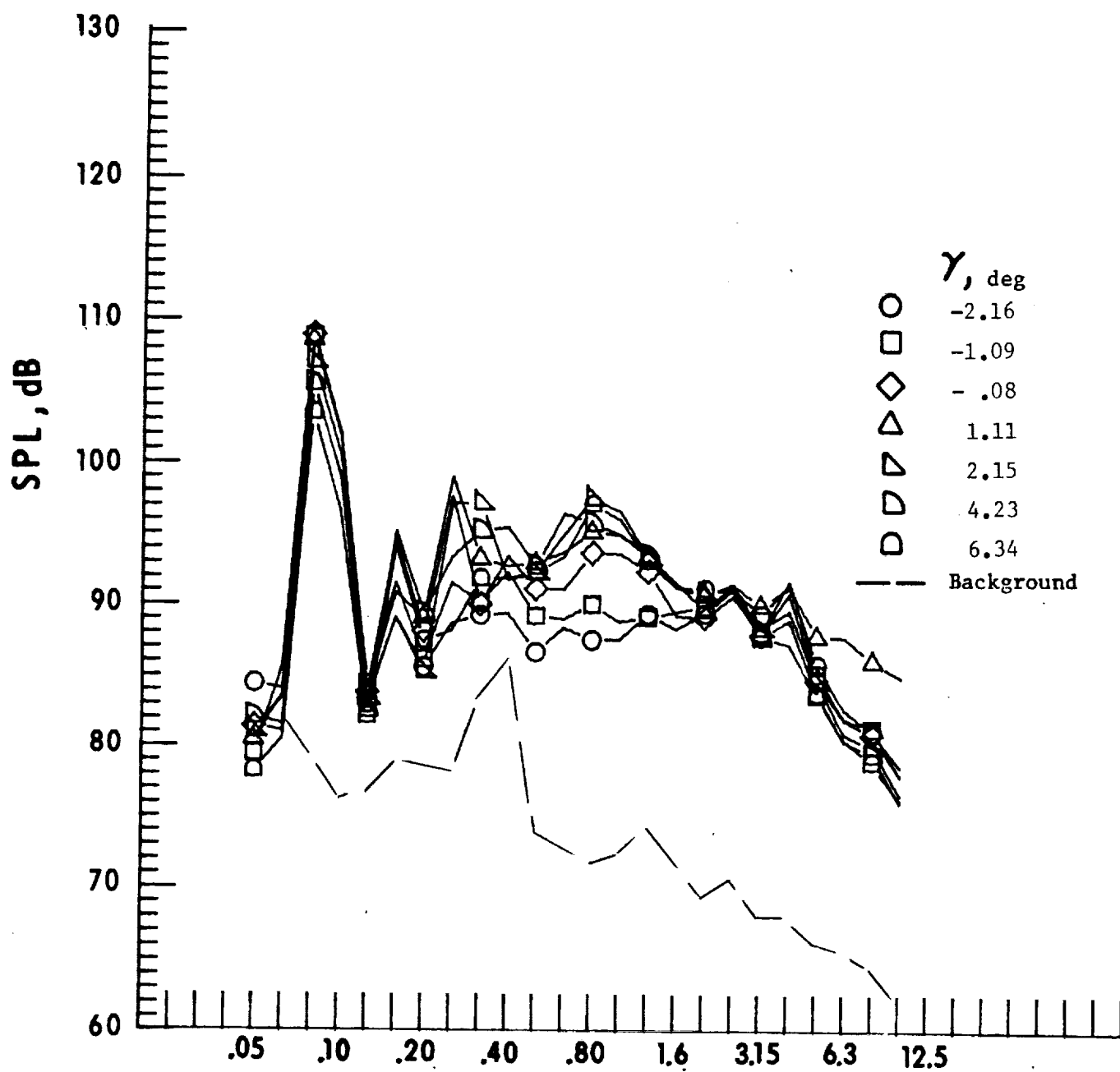


Figure 11. - Continued.



bb. Narrow band analysis, Mic. no. 7, $\gamma = 4.24^{\circ}$.

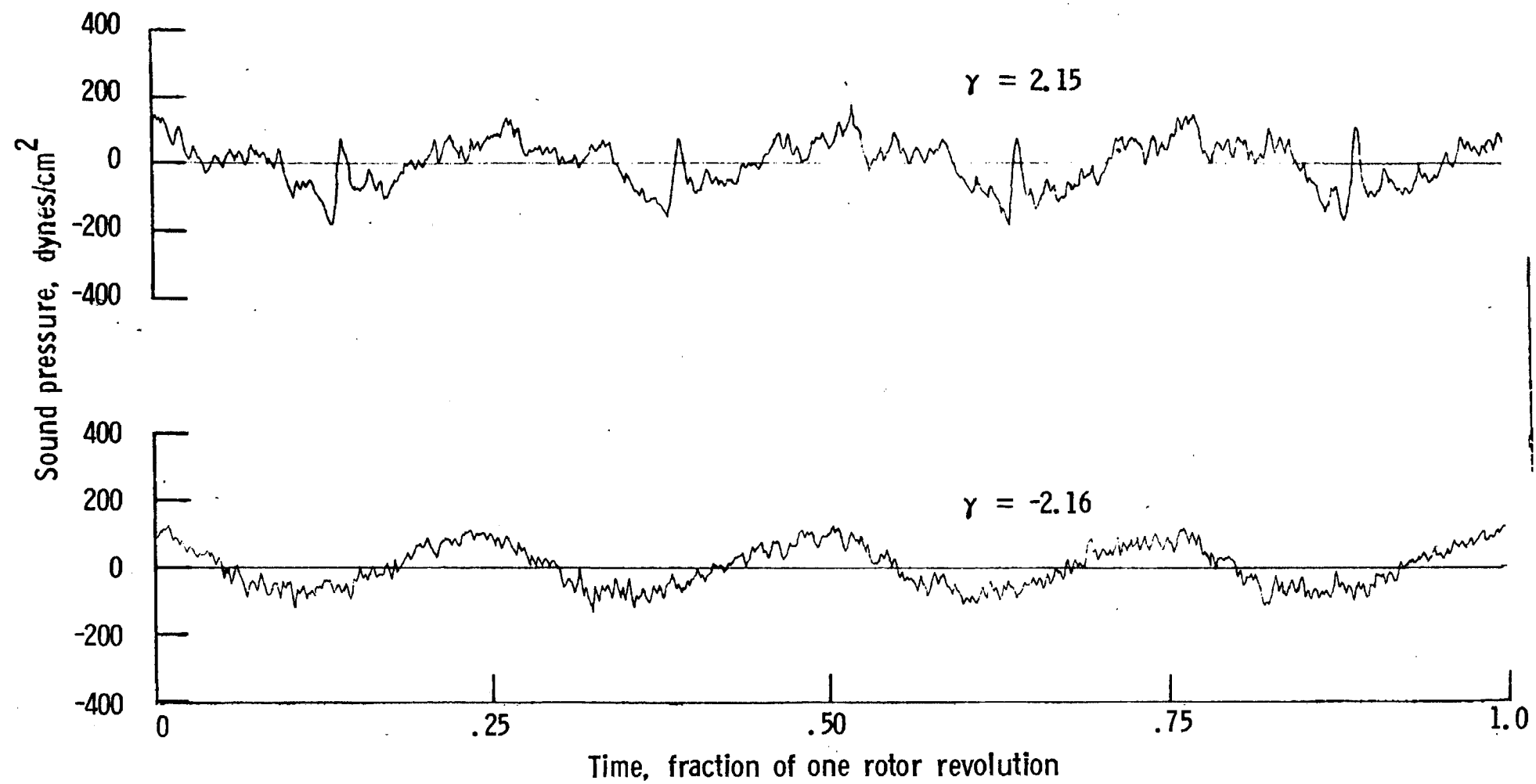
Figure 11. - Concluded.



One-third-octave-band center frequency, kHz

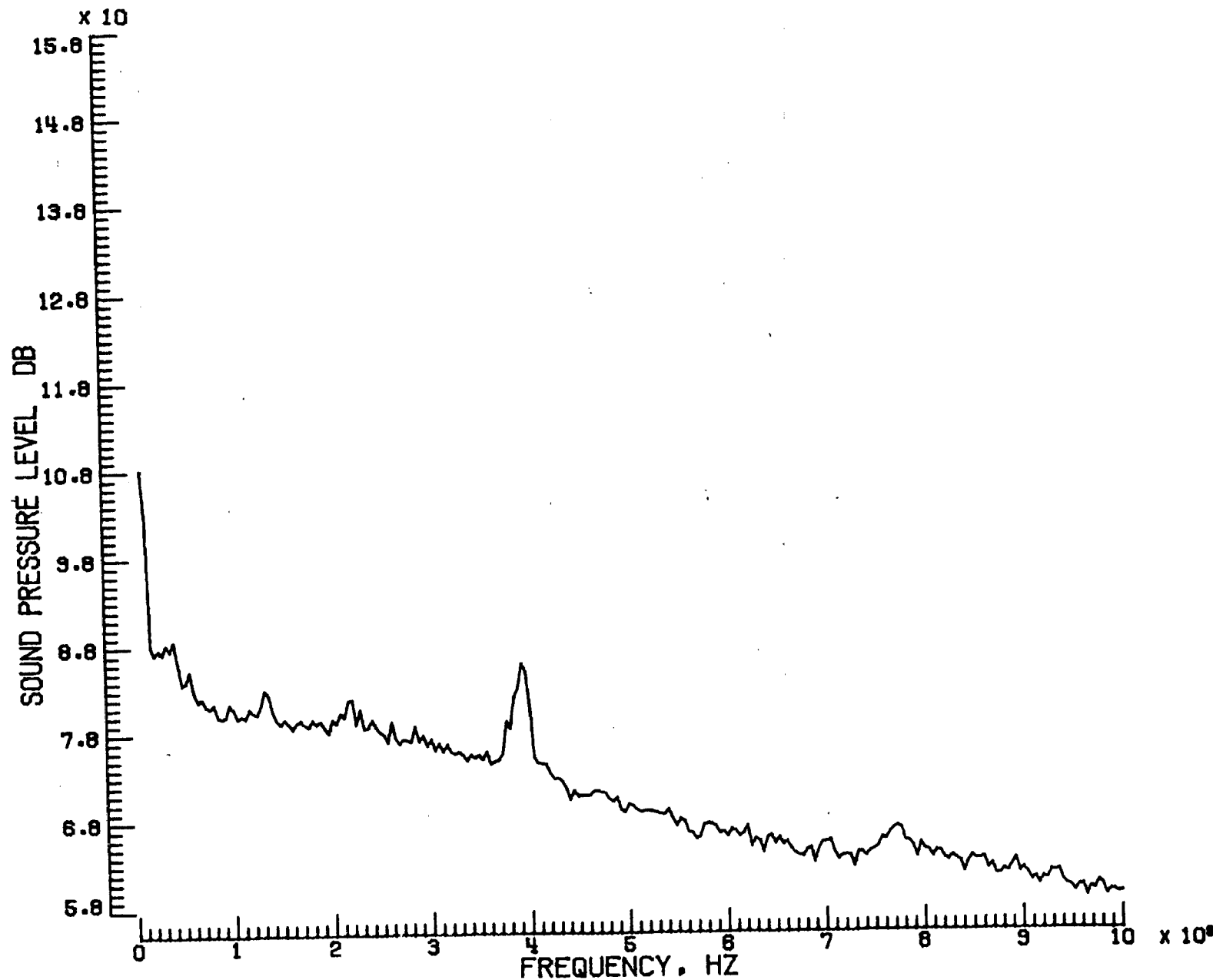
a. Mic. no. 1.

Figure 12. - Effect of descent angle variation on noise generated by helicopter model with sub-wing tips installed. $V_{\infty} = 51.1$ knots.



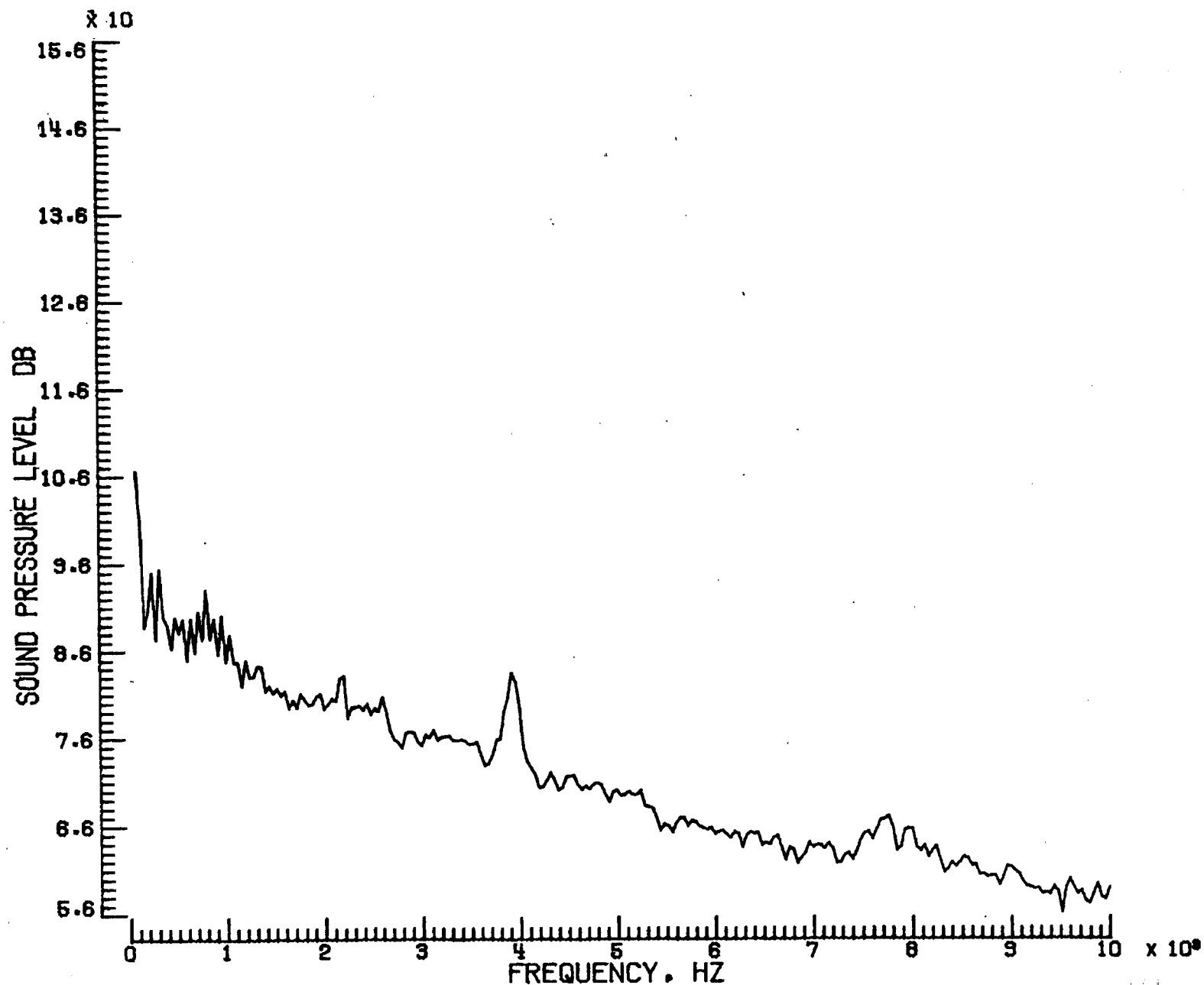
b. Pressure time histories, Mic. no. 2.

Figure 12. - Continued.



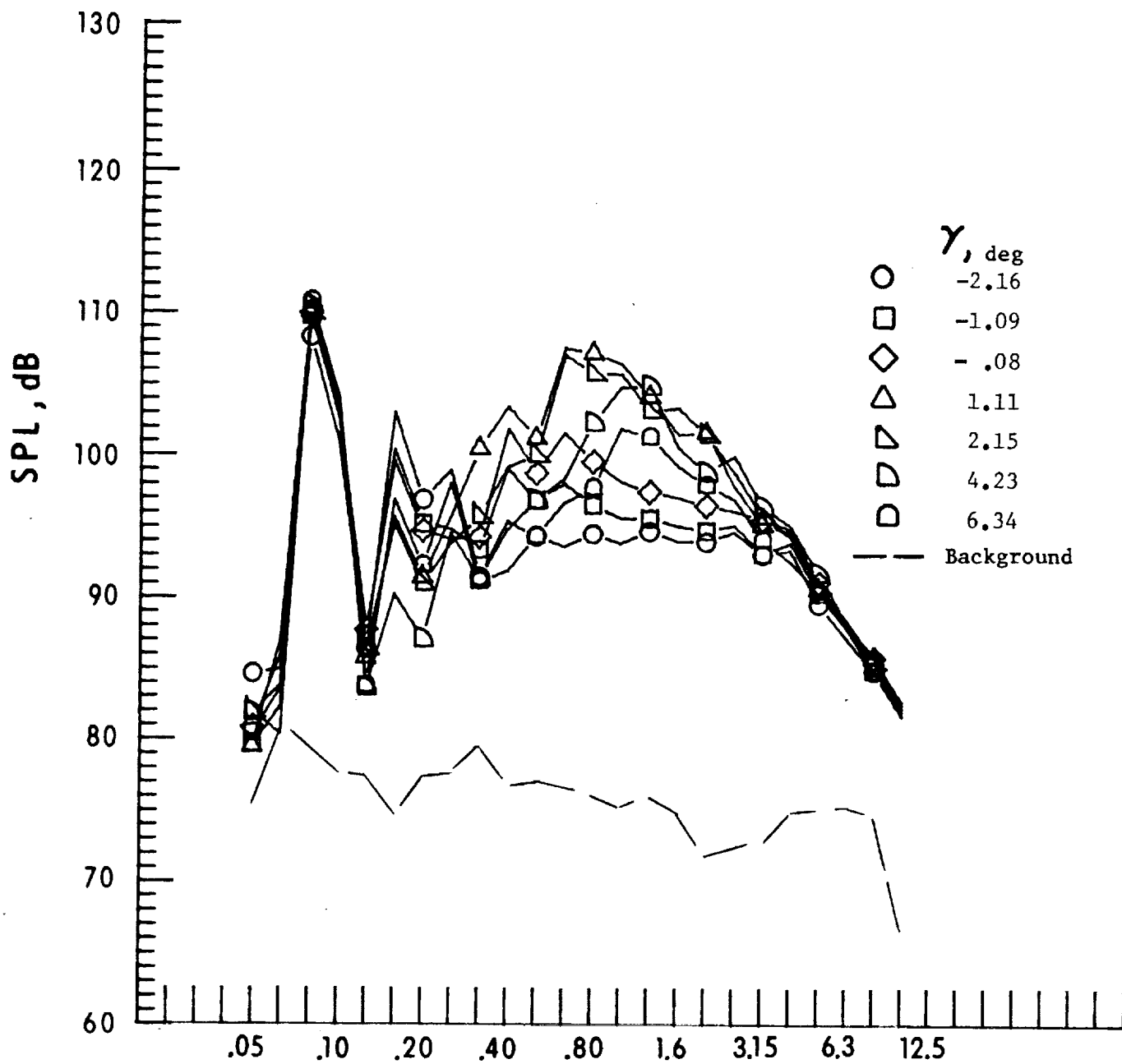
c. Narrow band analysis, Mic. no. 1, $\gamma = -2.16^0$.

Figure 12. - Continued.



d. Narrow band analysis, Mic. no. 1, $\gamma = 2.15^0$.

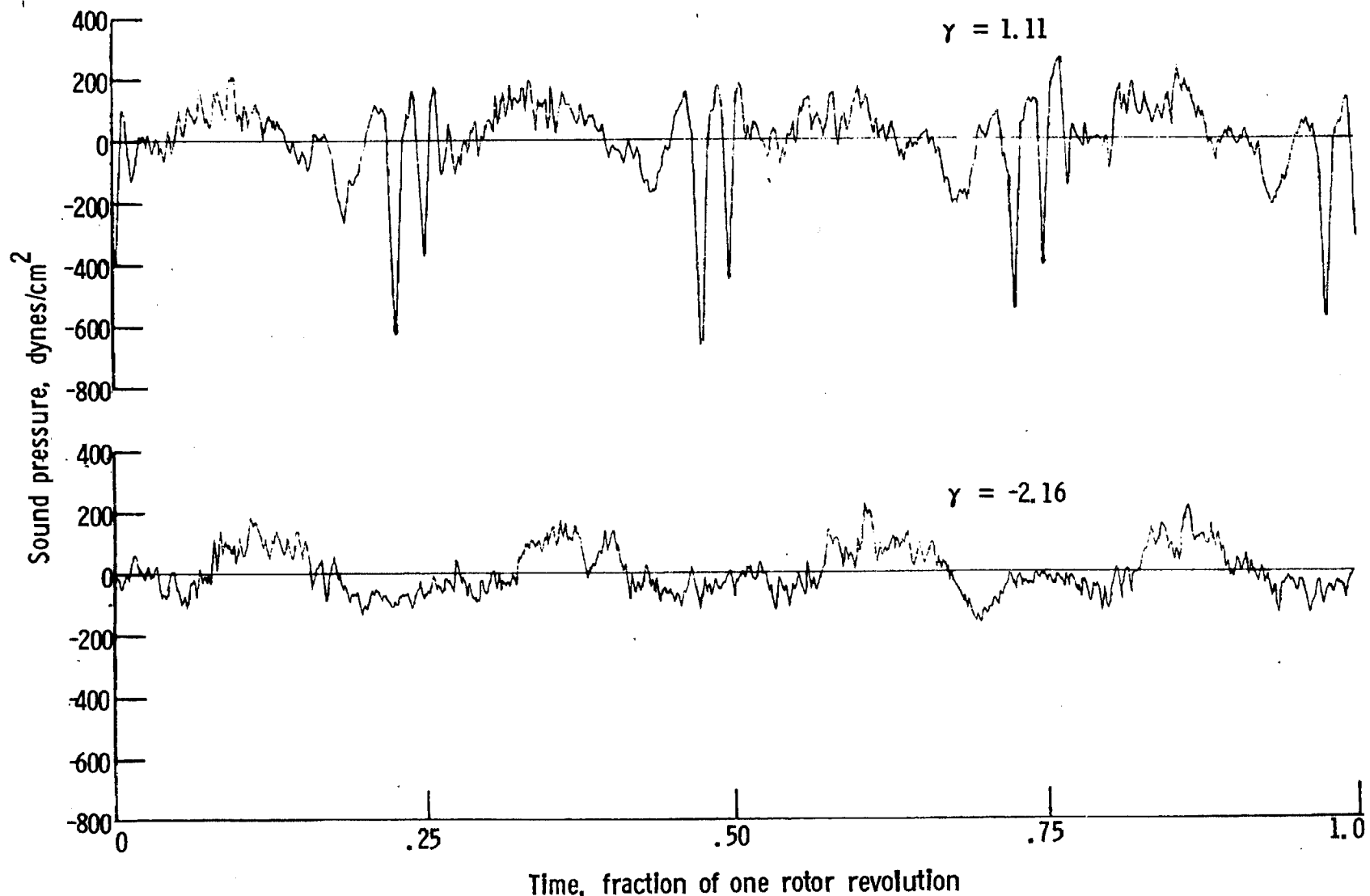
Figure 12. - Continued.



One-third-octave-band center frequency, kHz

e. Mic. no. 3.

Figure 12. - Continued.

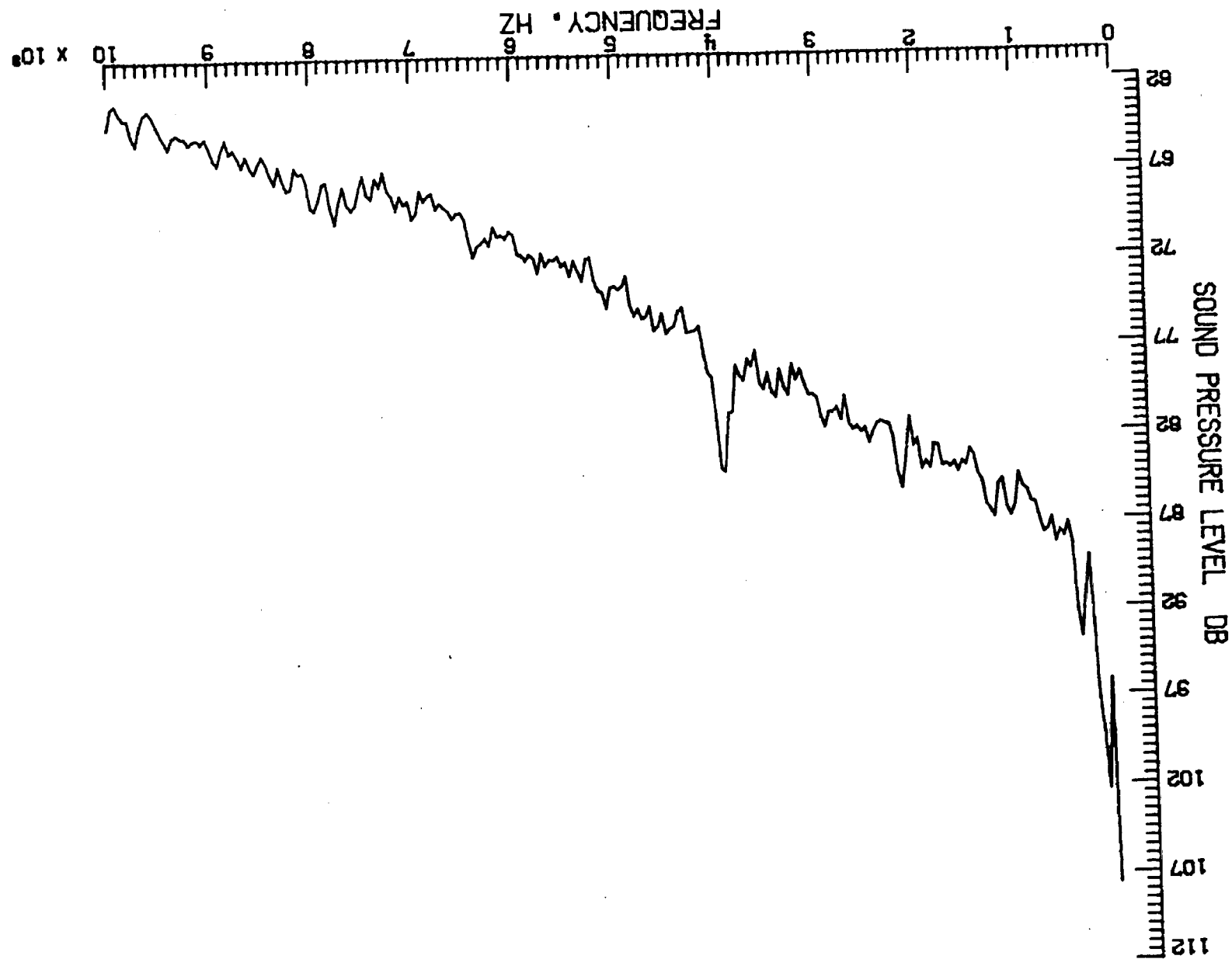


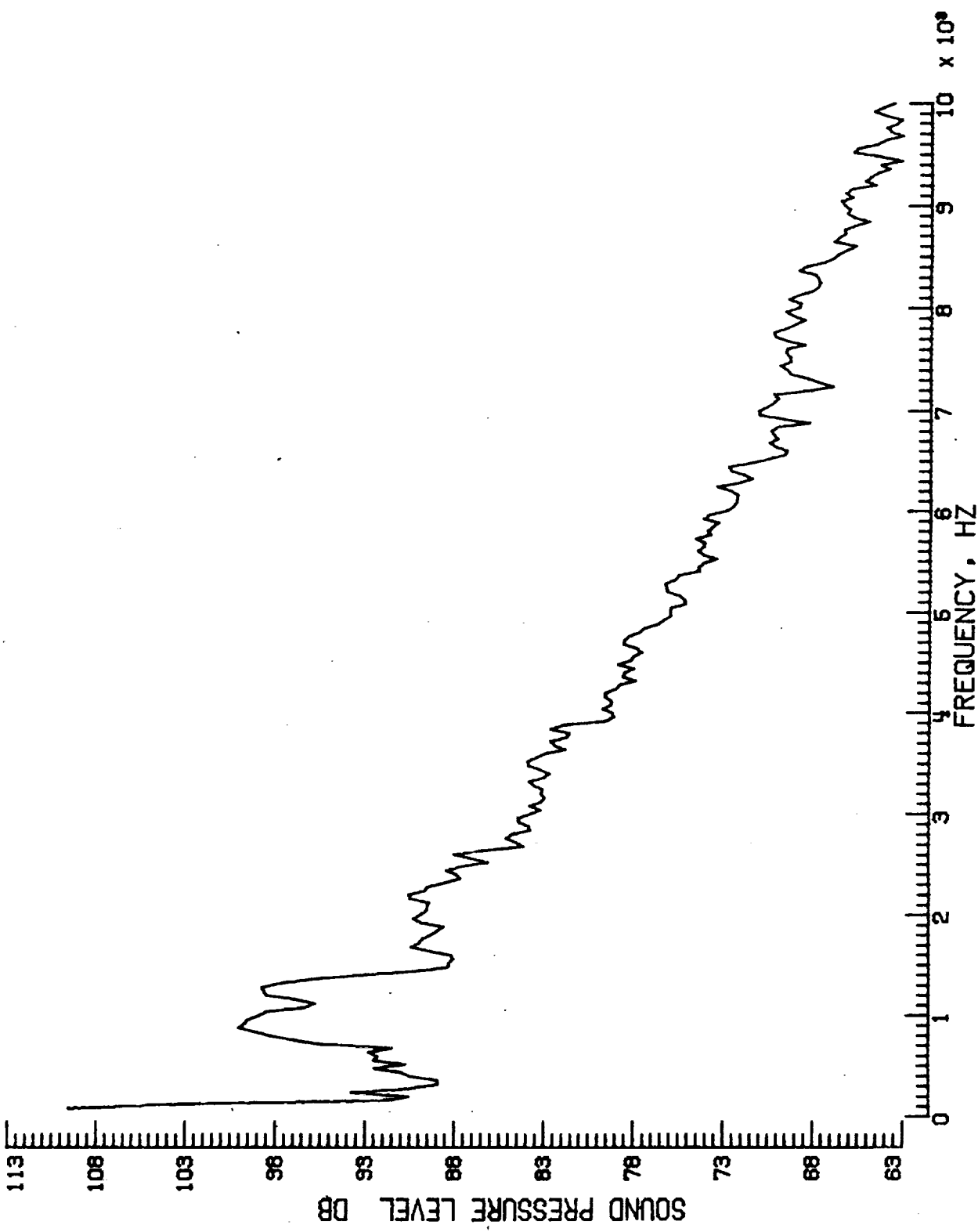
f. Pressure-time histories, Mic. no. 3.

Figure 12. - Continued.

Figure 12. - Continued.

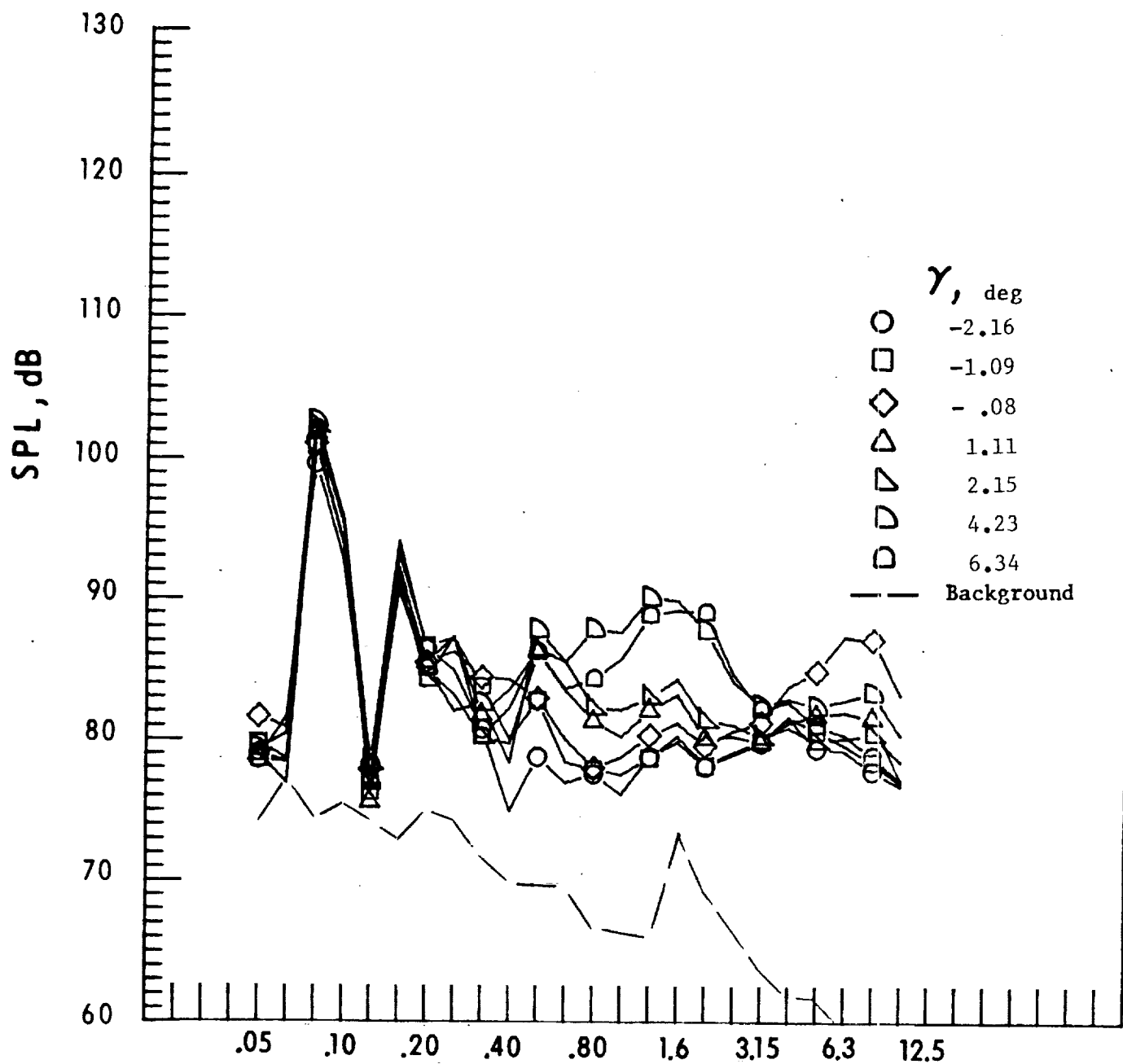
g. Narrow band analysis, Mic. no. 3, $y = -2.16^{\circ}$.





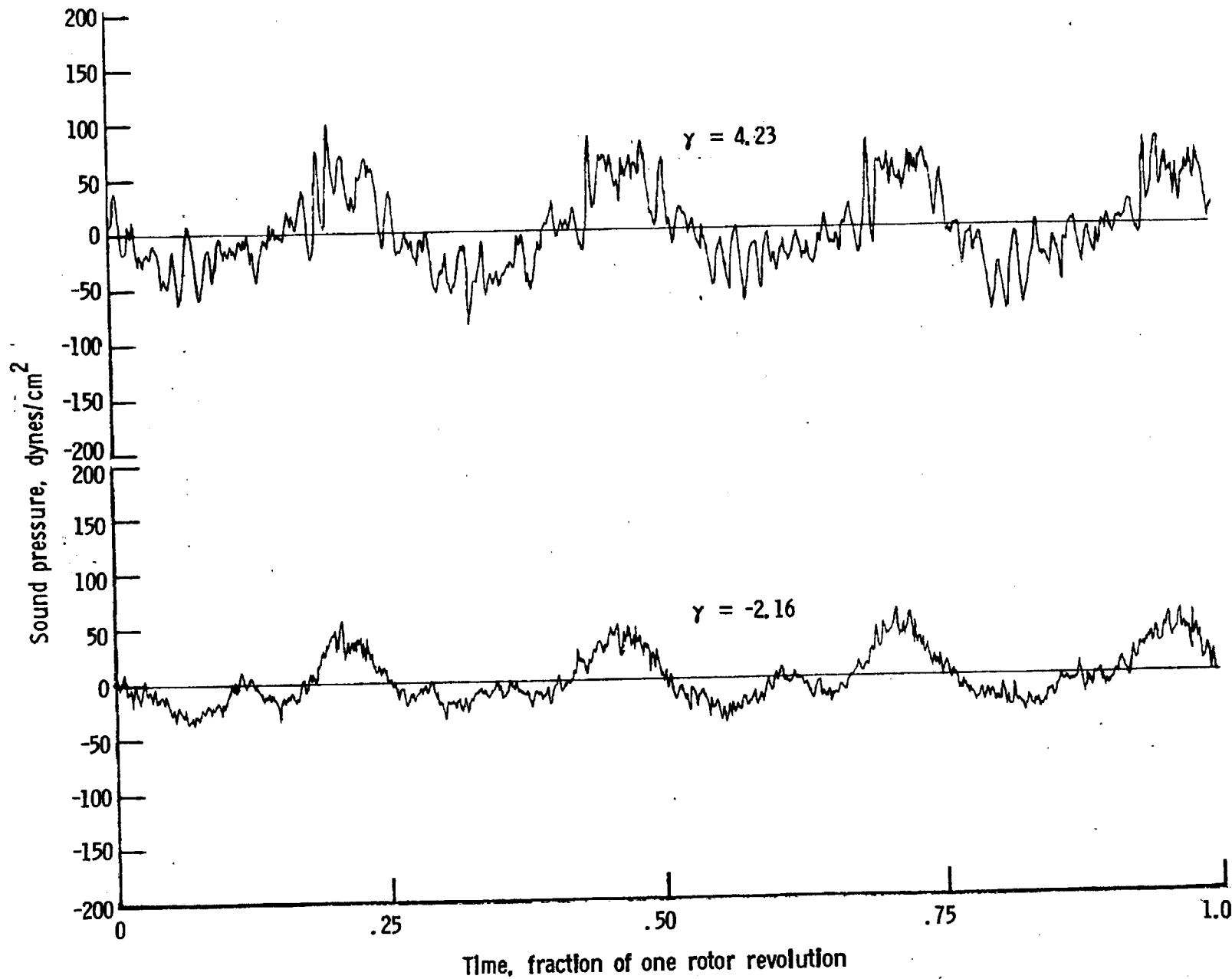
h. Narrow band analysis, Mic. no. 3, $\gamma = 1.11^0$.

Figure 12. - Continued.



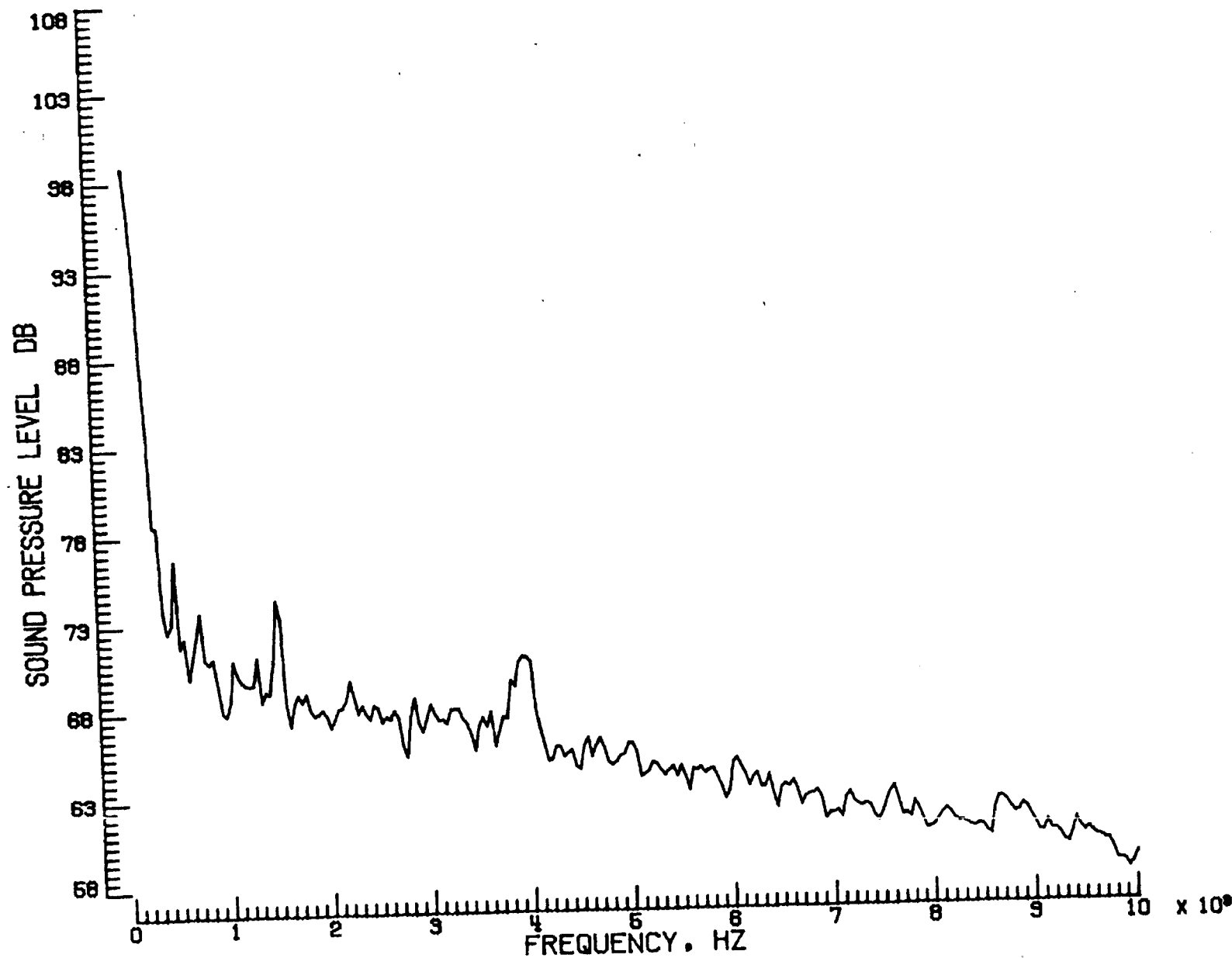
One-third-octave-band center frequency, kHz
 i. Mic. no. 4.

Figure 12. - Continued.



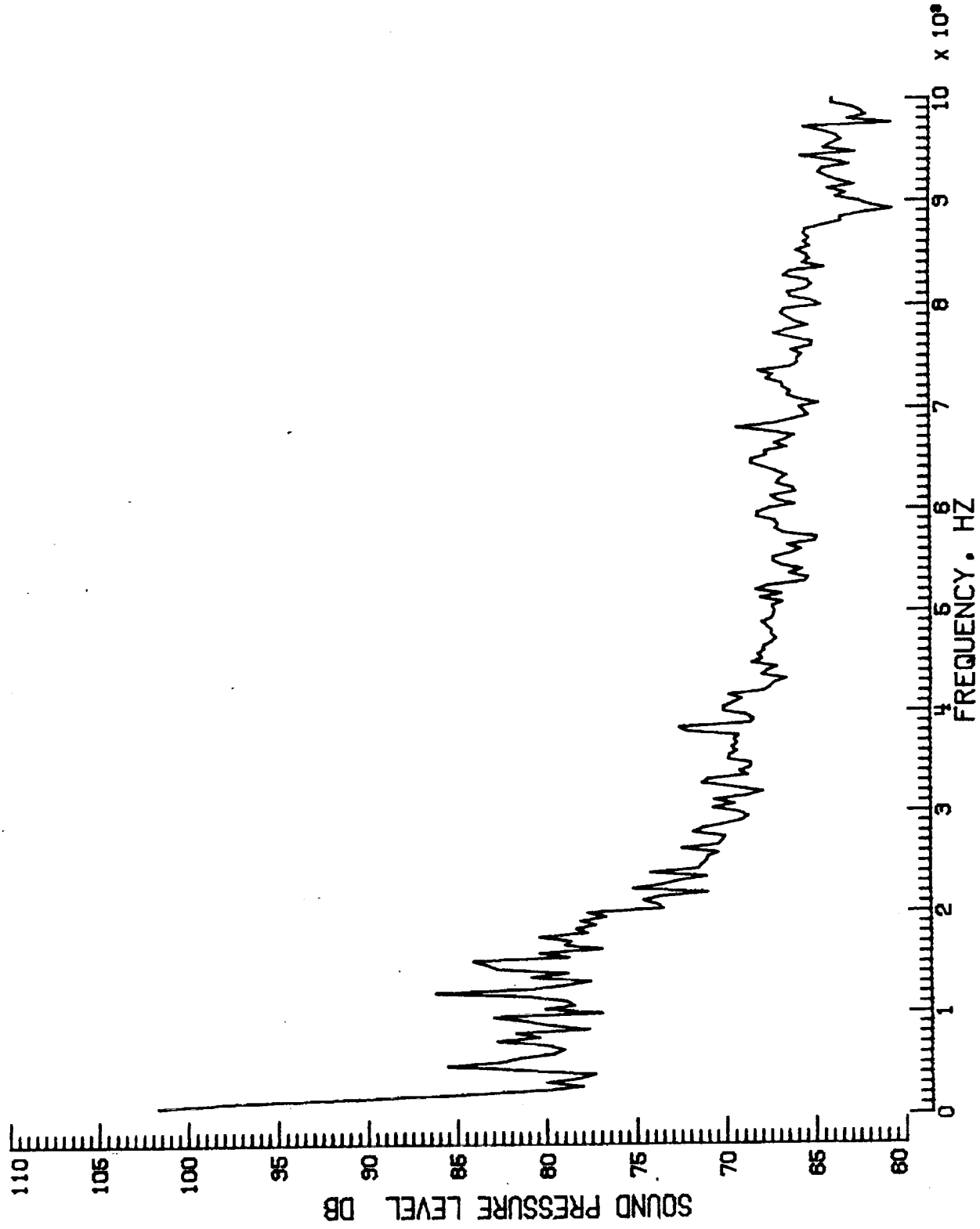
j. Pressure-time histories, Mic. no. 4.

Figure 12. - Continued.



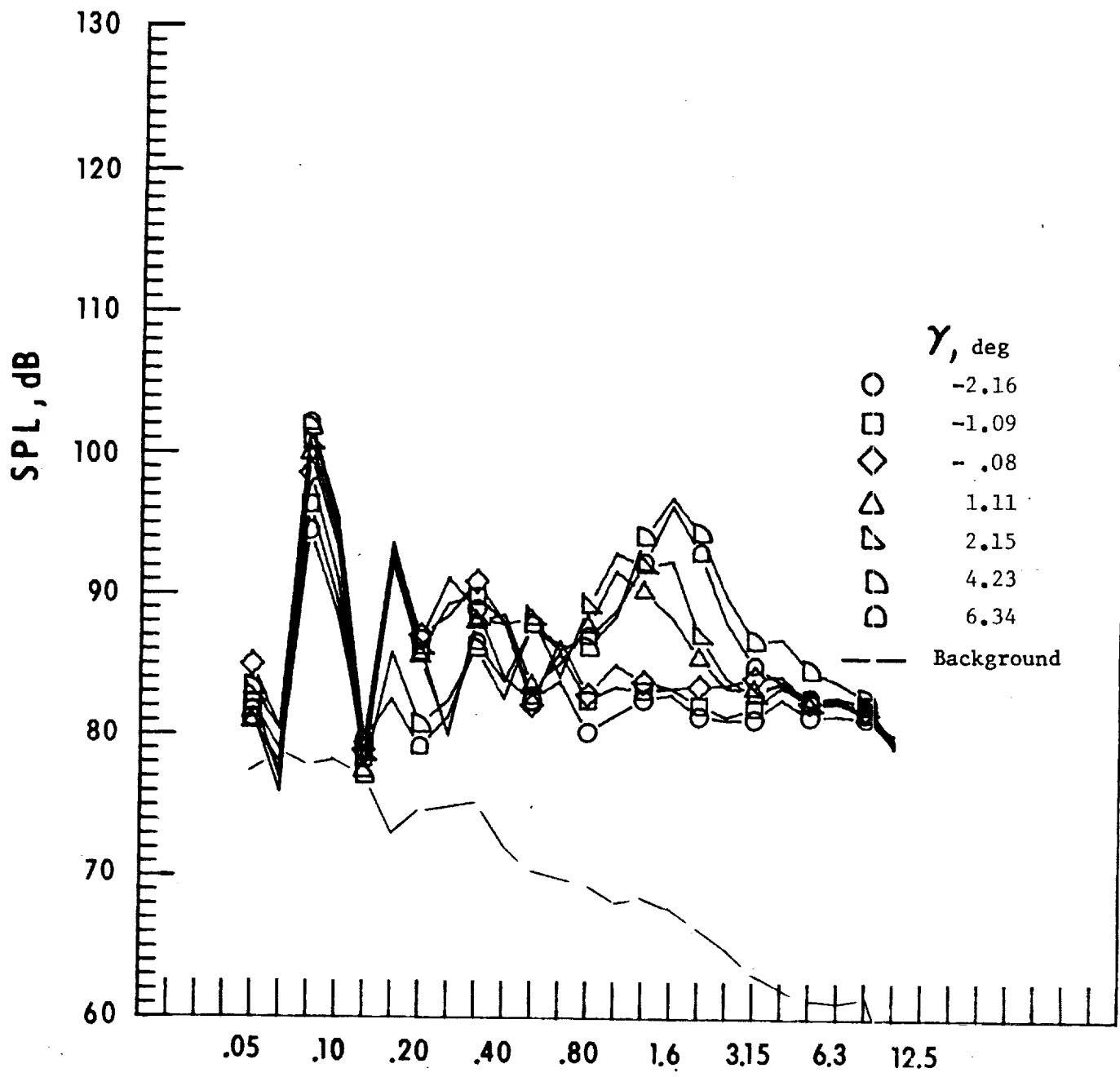
k. Narrow band analysis, Mic. no. 4, $\gamma = -2.16^0$.

Figure 12. - Continued.



I. Narrow band analysis, Mic. no. 4, $\gamma = 4.23^0$.

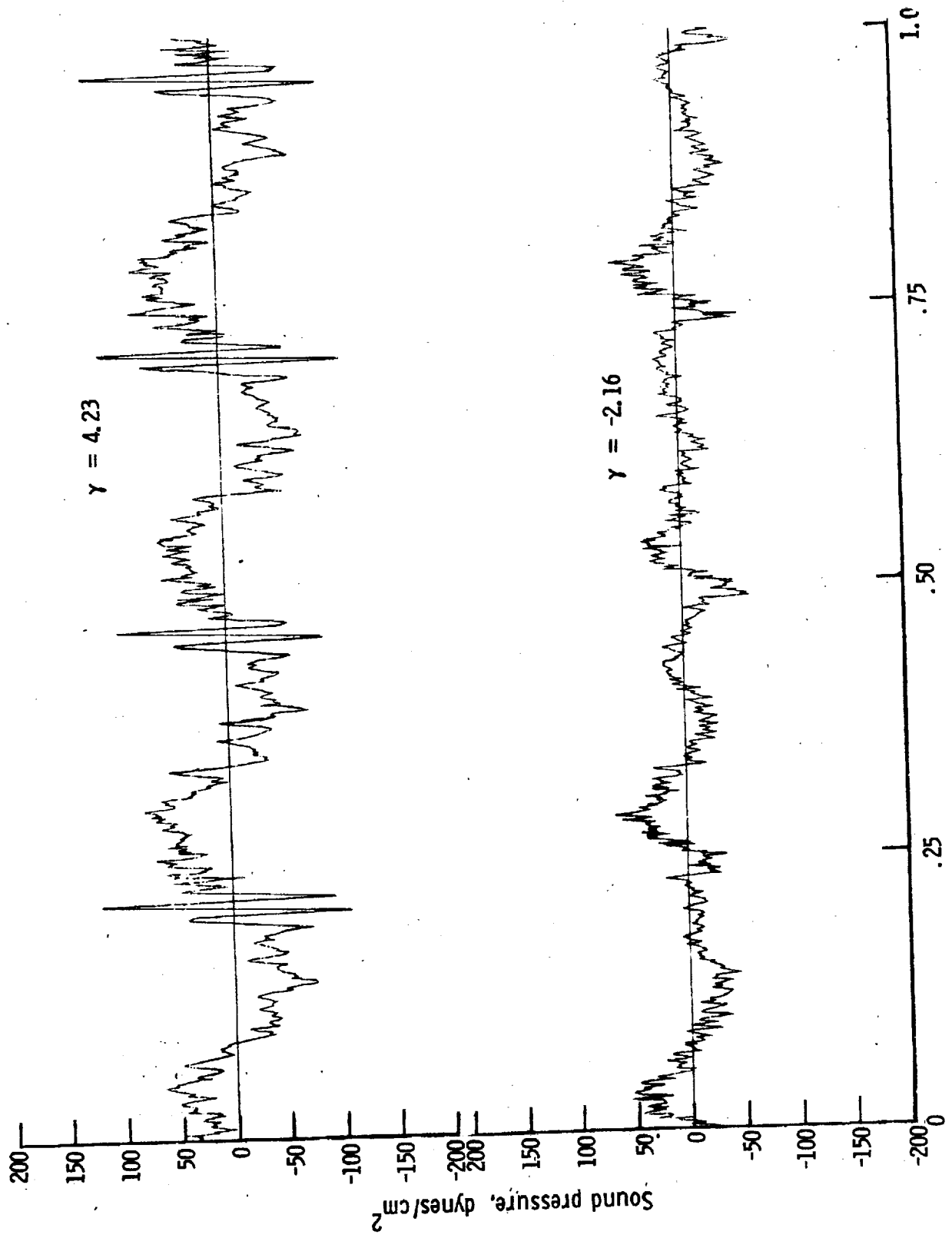
Figure 12. - Continued.



One-third-octave-band center frequency, kHz

m. Mic. no. 5.

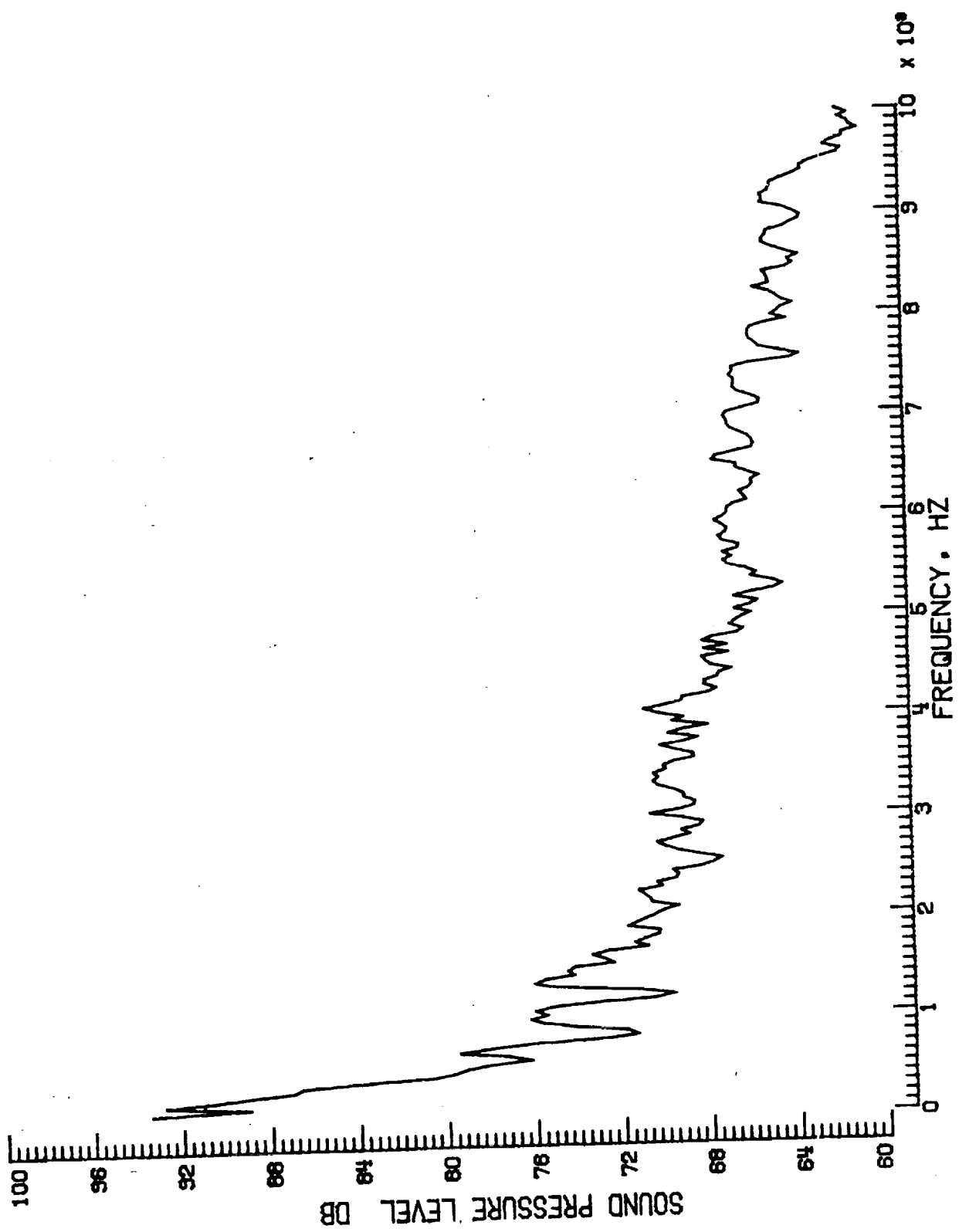
Figure 12. - Continued.



Time, fraction of one rotor revolution

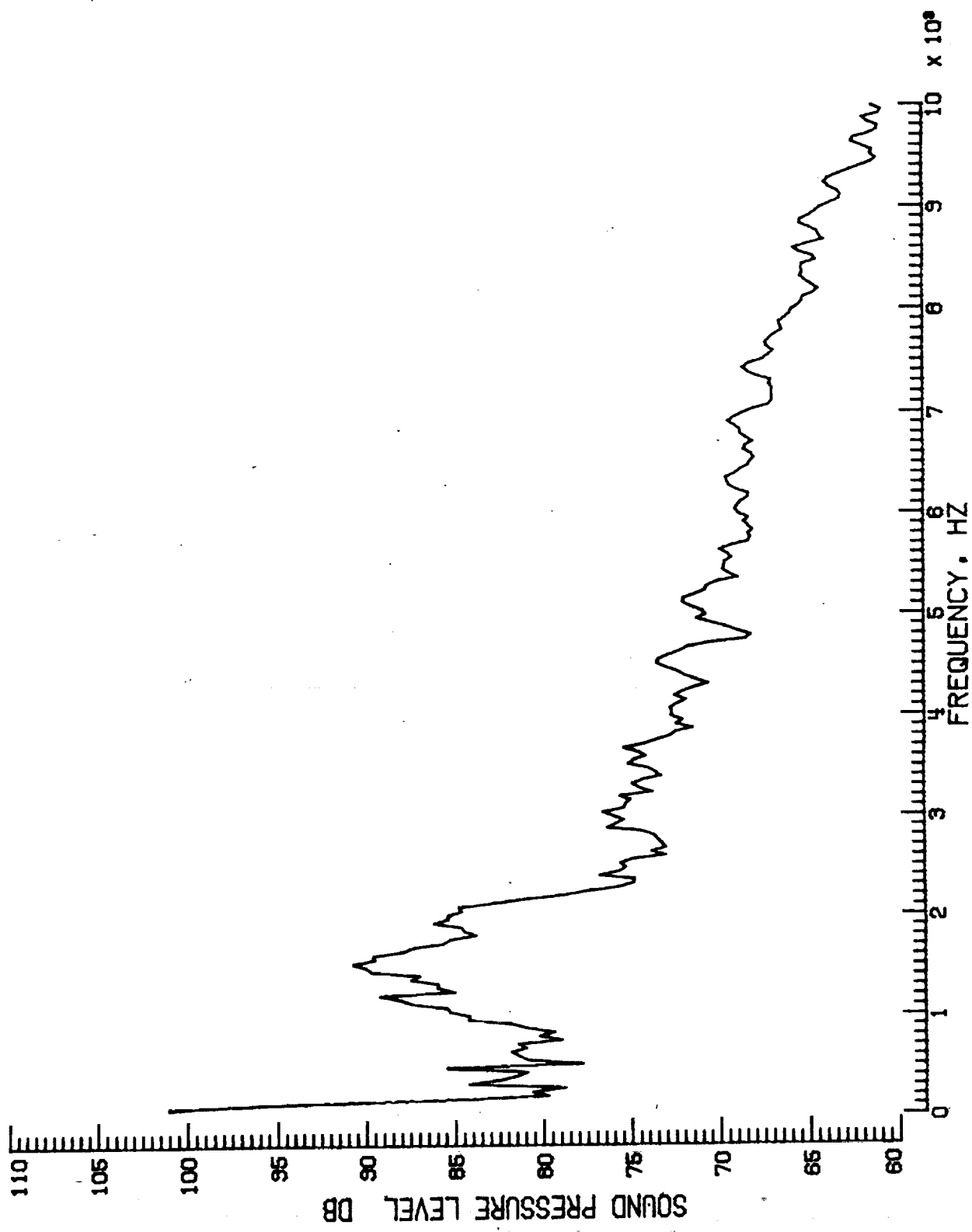
n. Pressure-time histories, Mic. no. 5.

Figure 12. - Continued.

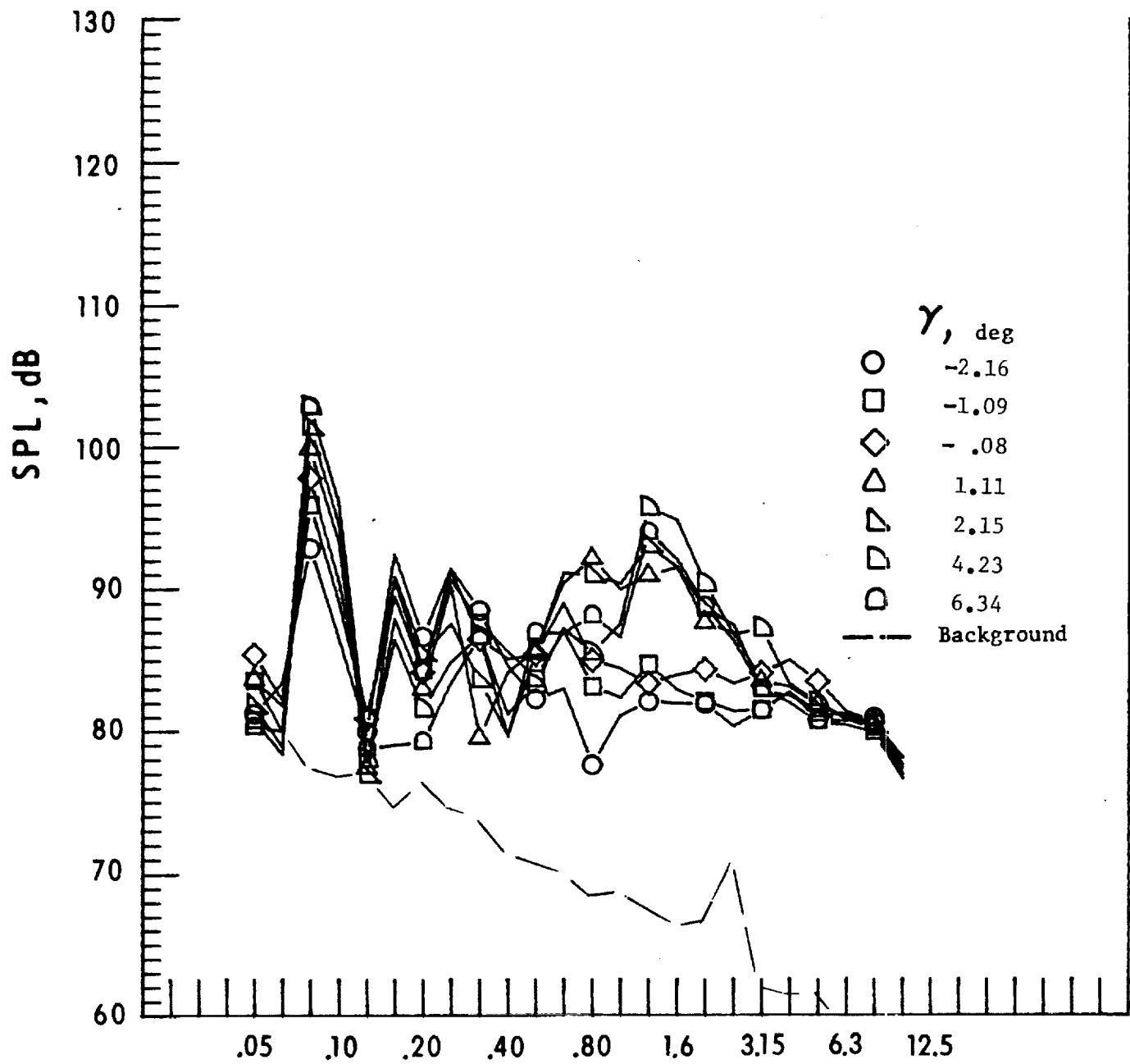


o. Narrow band analysis, Mic. no. 5, $\gamma = -2.16^0$.

Figure 12. - Continued.



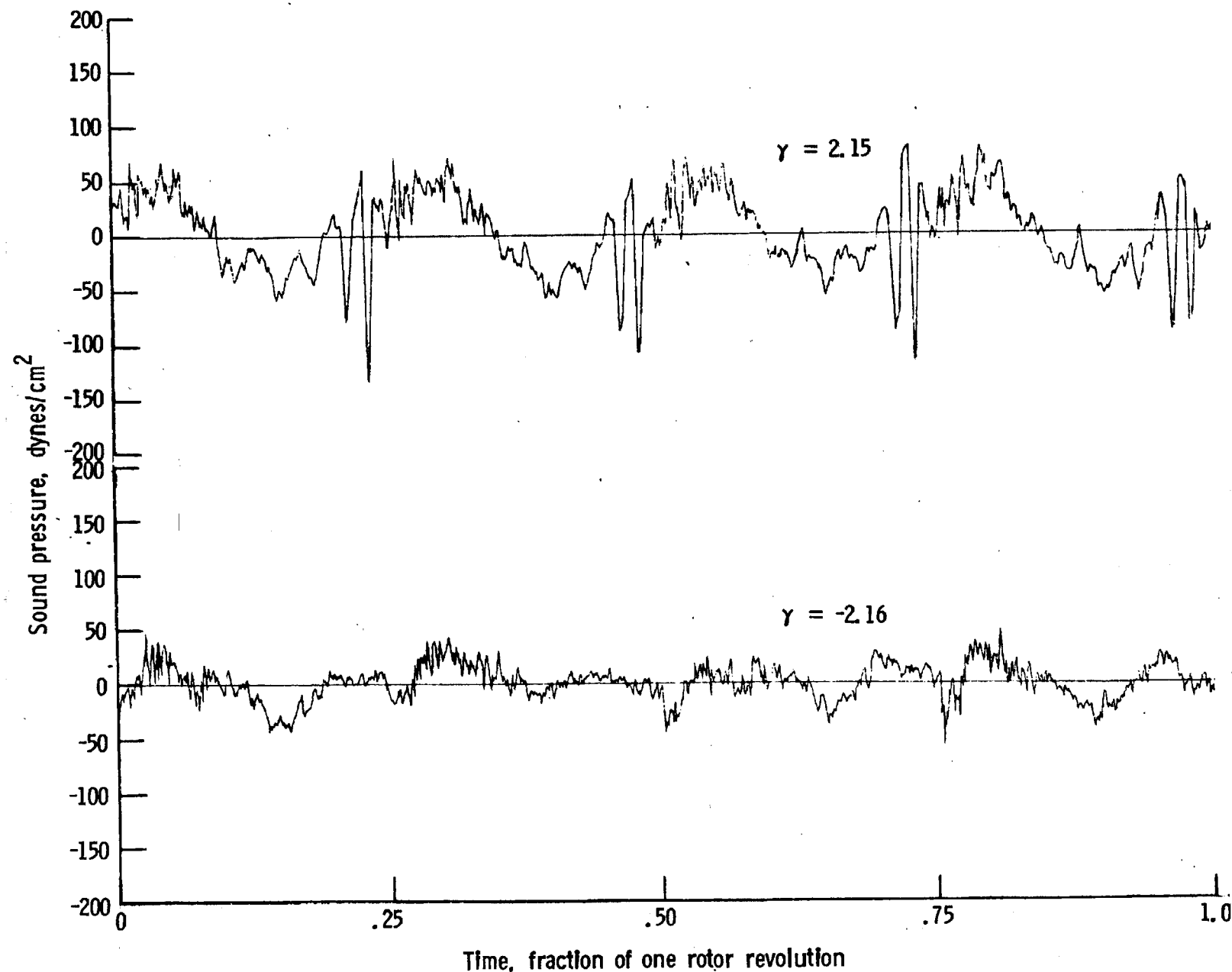
p. Narrow band analysis, Mic. no. 5, $\gamma = 4.23^0$.



One-third-octave-band center frequency, kHz

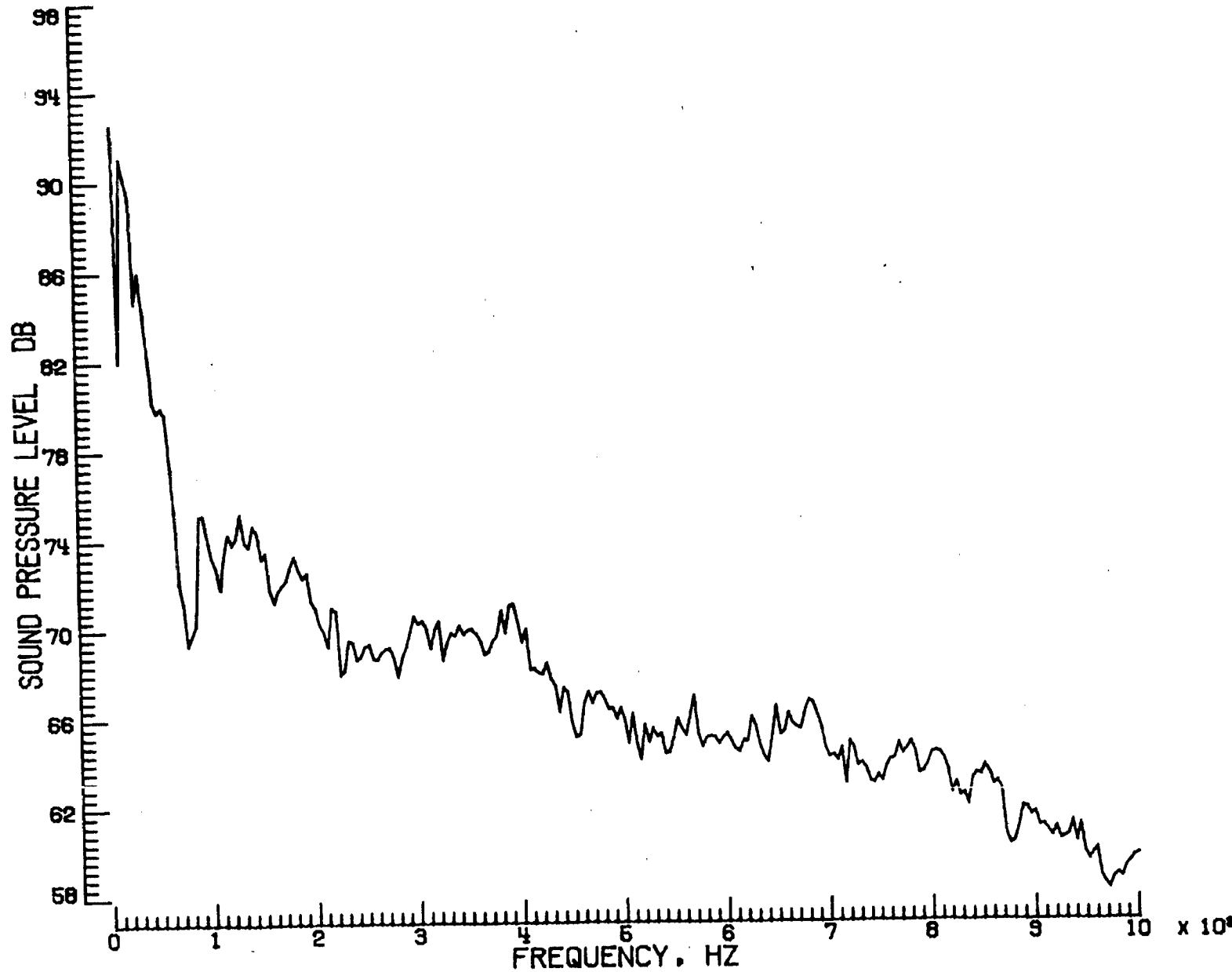
q. Mic. no. 6.

Figure 12. - Continued.



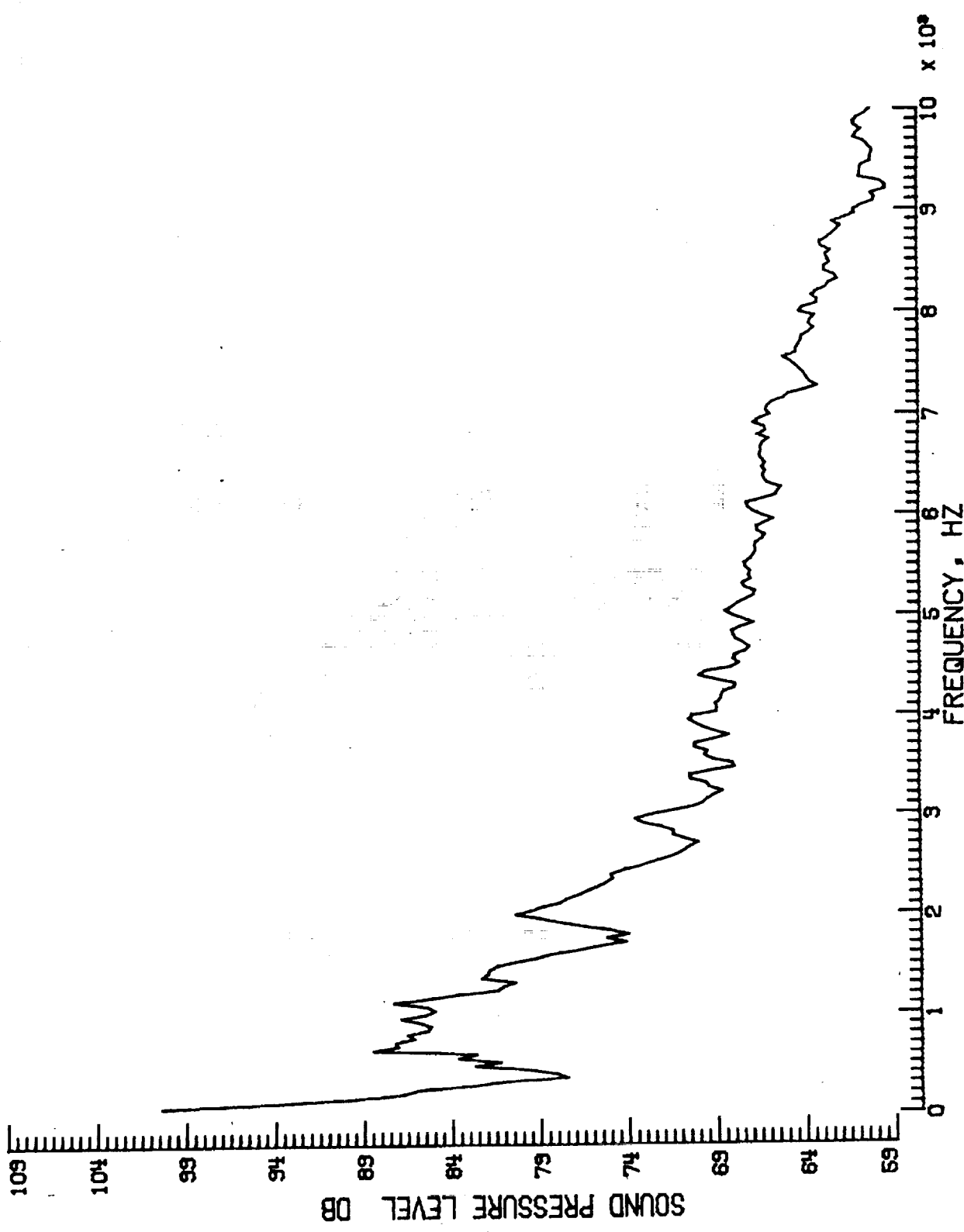
r. Pressure-time histories, Mic. no. 6.

Figure 12. - Continued.

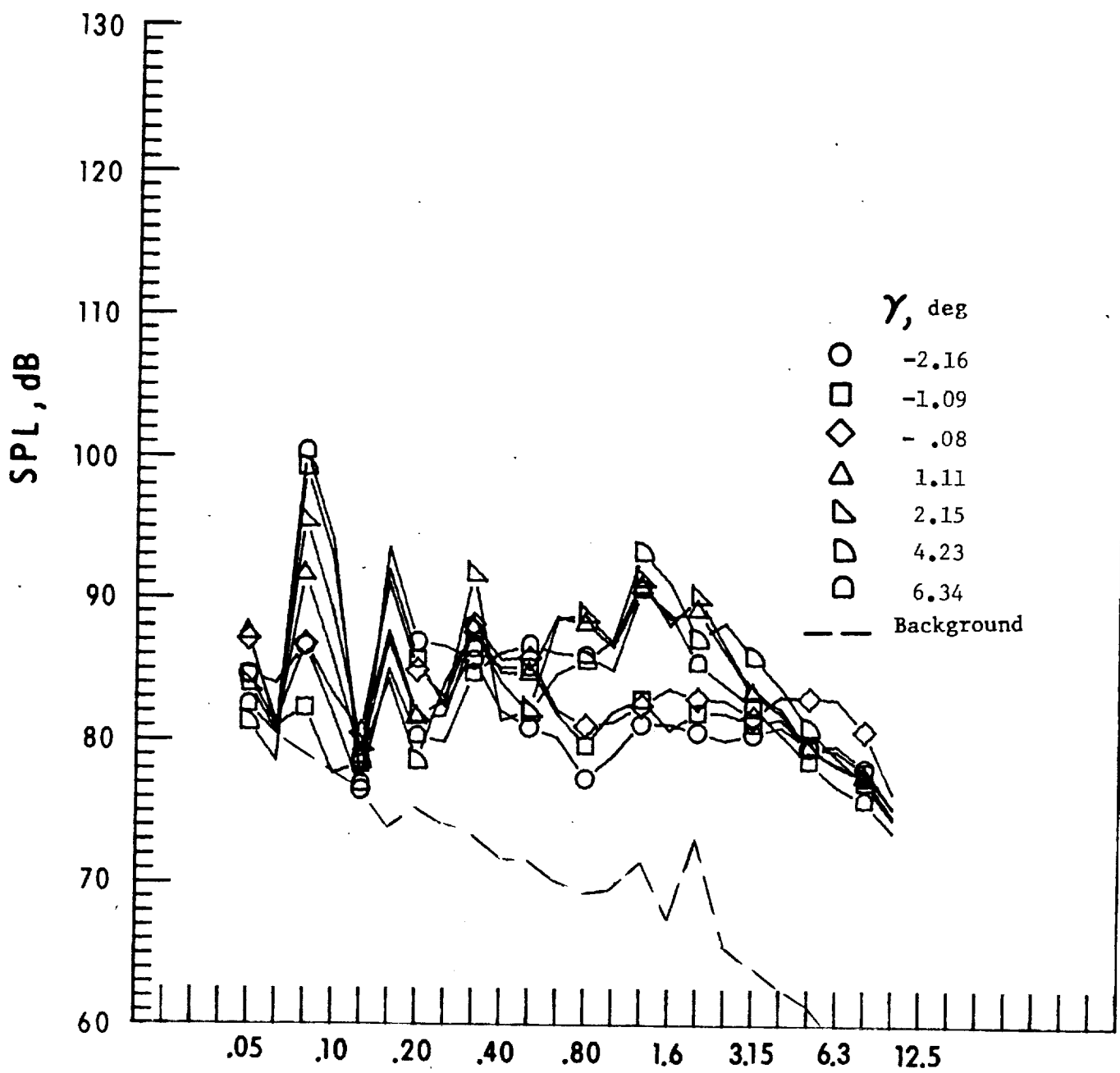


s. Narrow band analysis, Mic. no. 6, $\gamma = -2.16^0$.

Figure 12. - Continued.



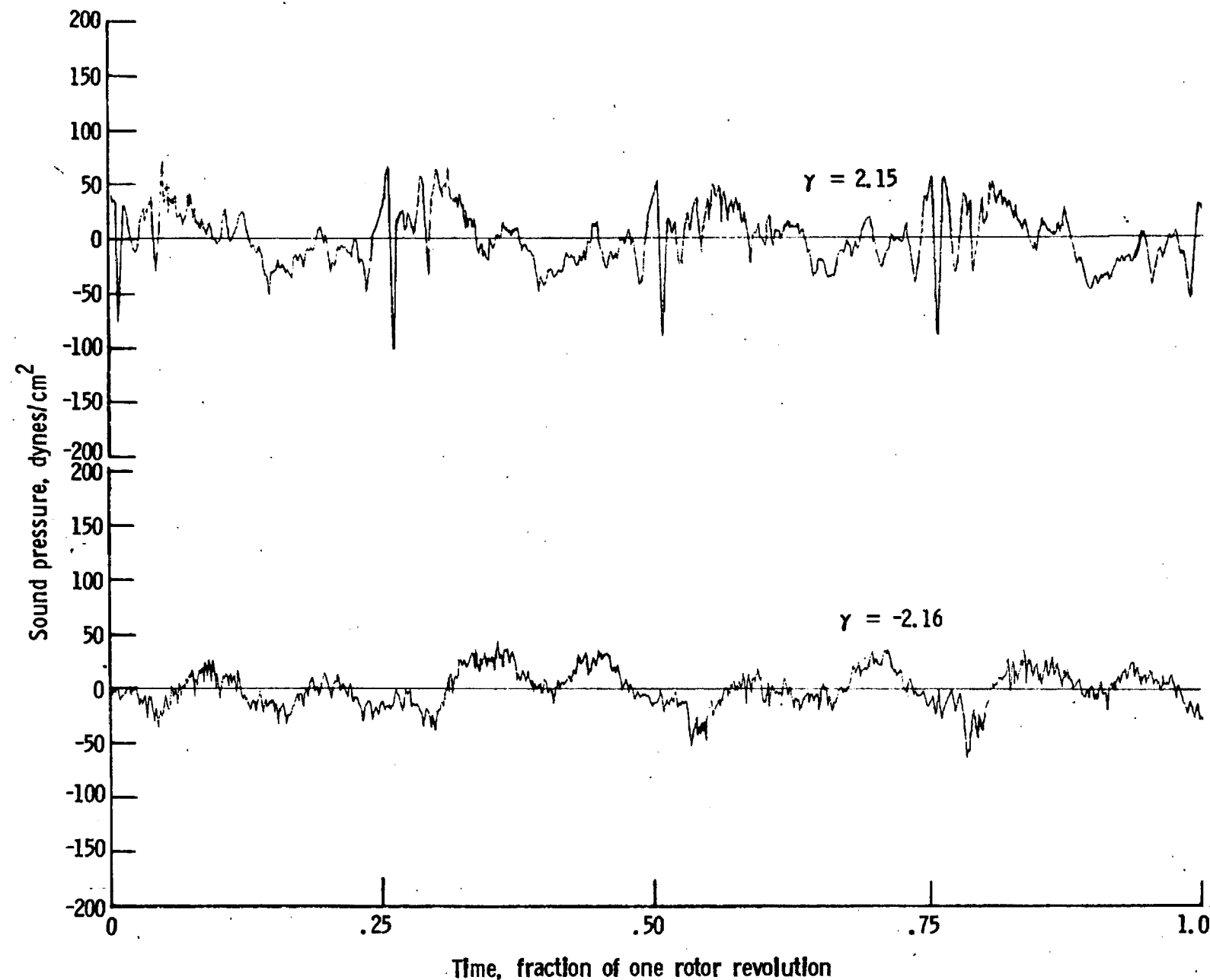
t. Narrow band analysis, Mic. no. 6, $\gamma = 2.15^\circ$.



One-third-octave-band center frequency, kHz

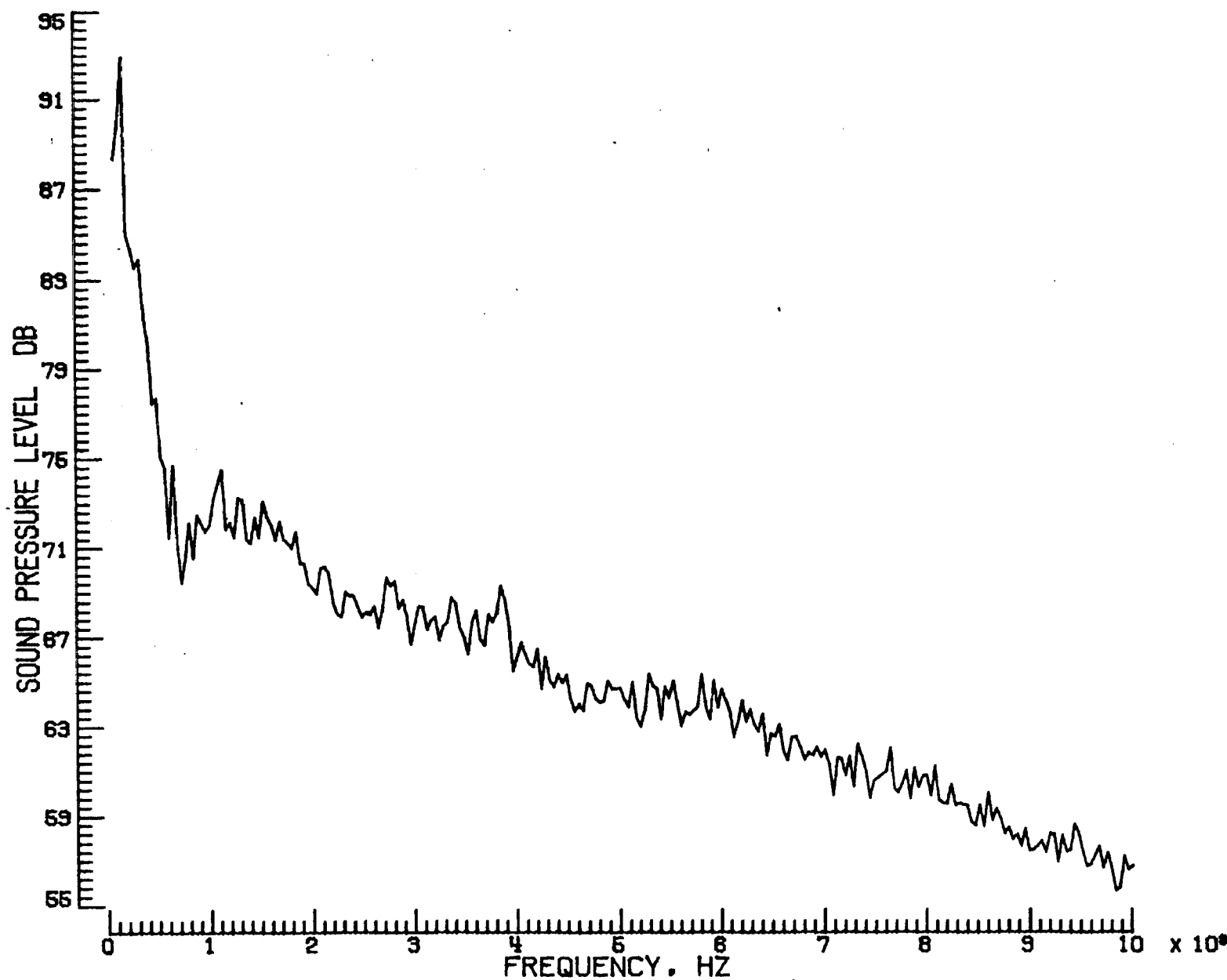
u. Mic. no. 7.

Figure 12. - Continued.



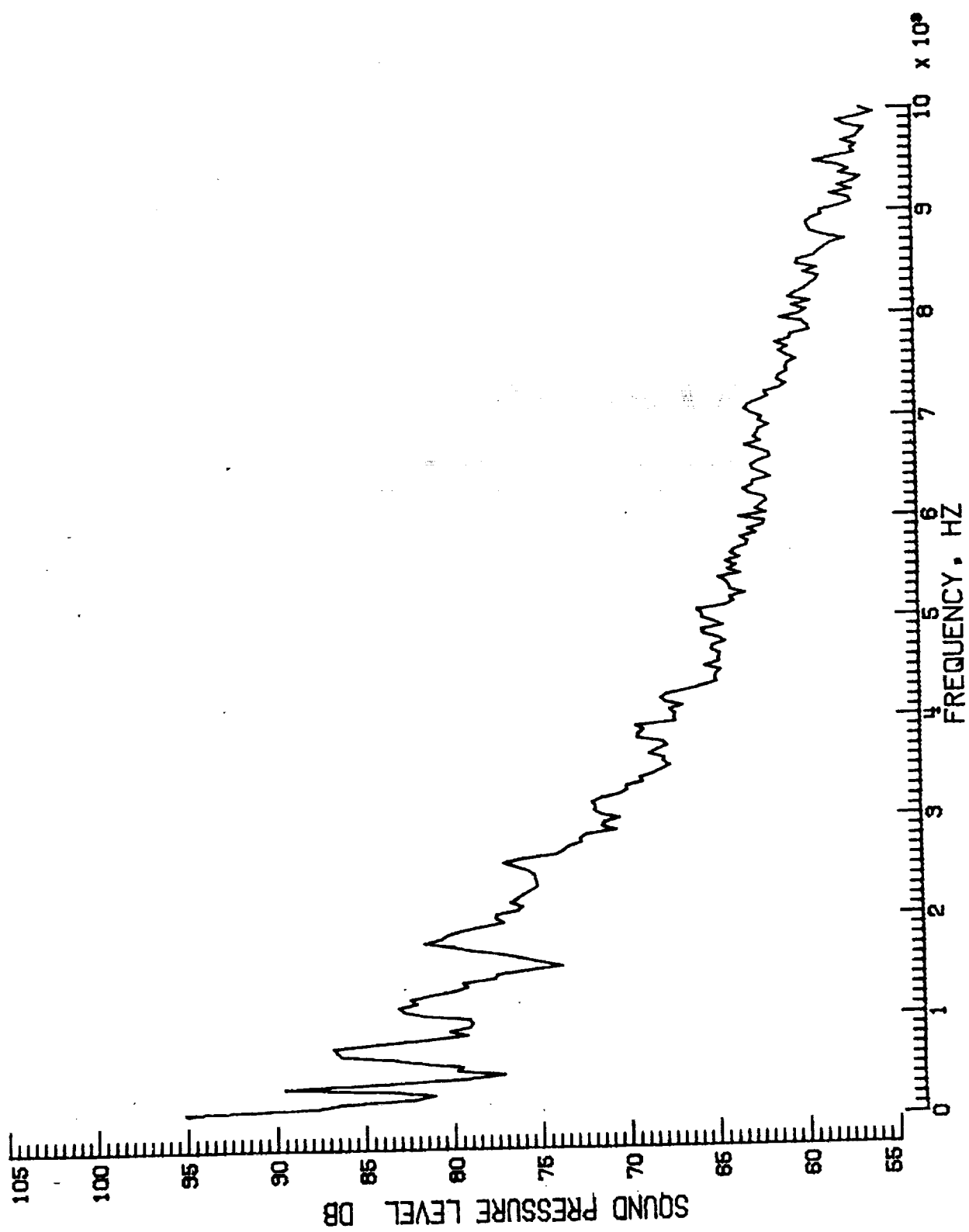
v. Pressure-time histories, Mic. no. 7.

Figure 12. - Continued.



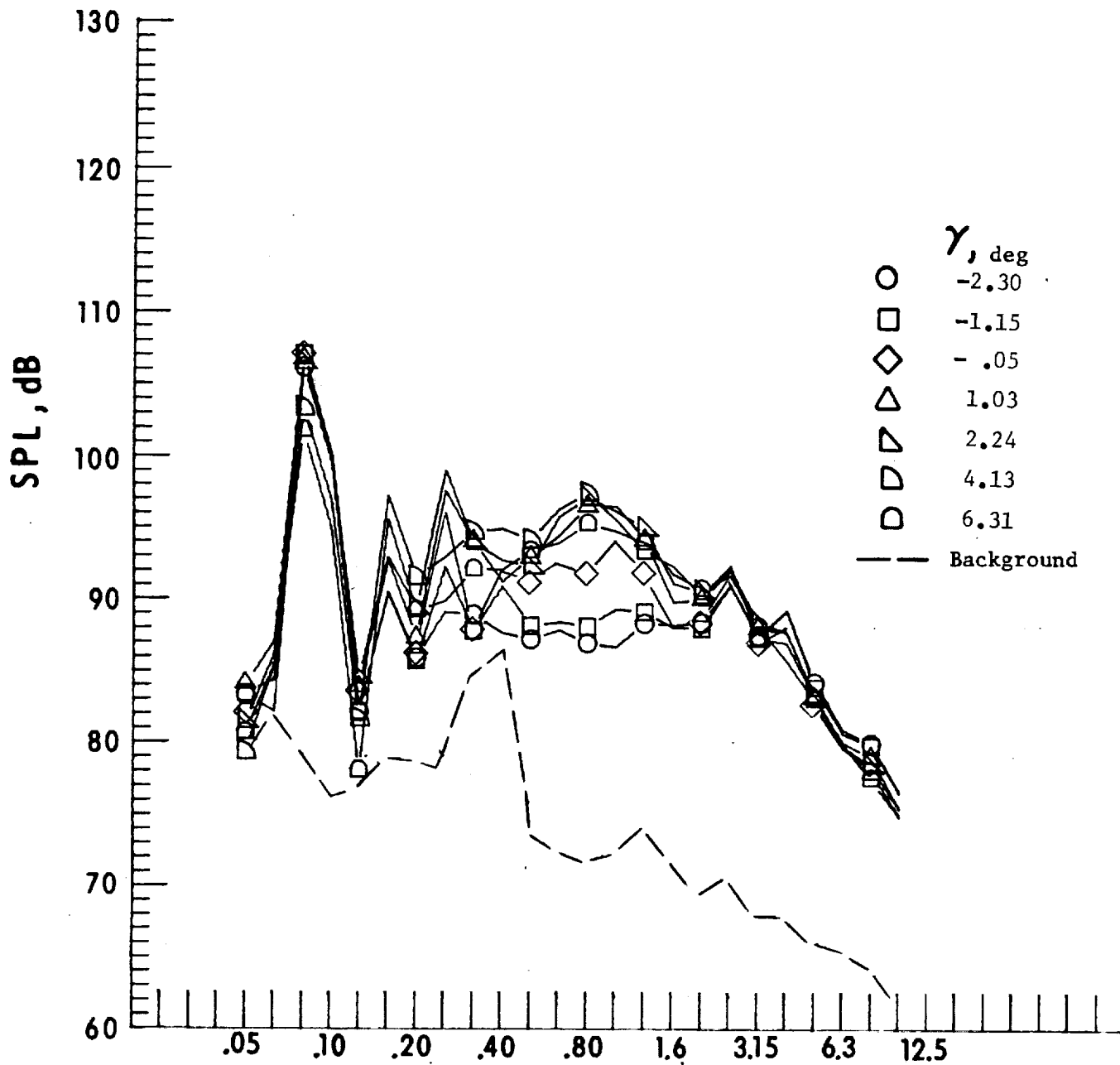
w. Narrow band analysis, Mic. no. 7, $\gamma = -2.16^0$.

Figure 12. - Continued.



x. Narrow band analysis, Mic. no. 7, $\gamma = 2.15^0$.

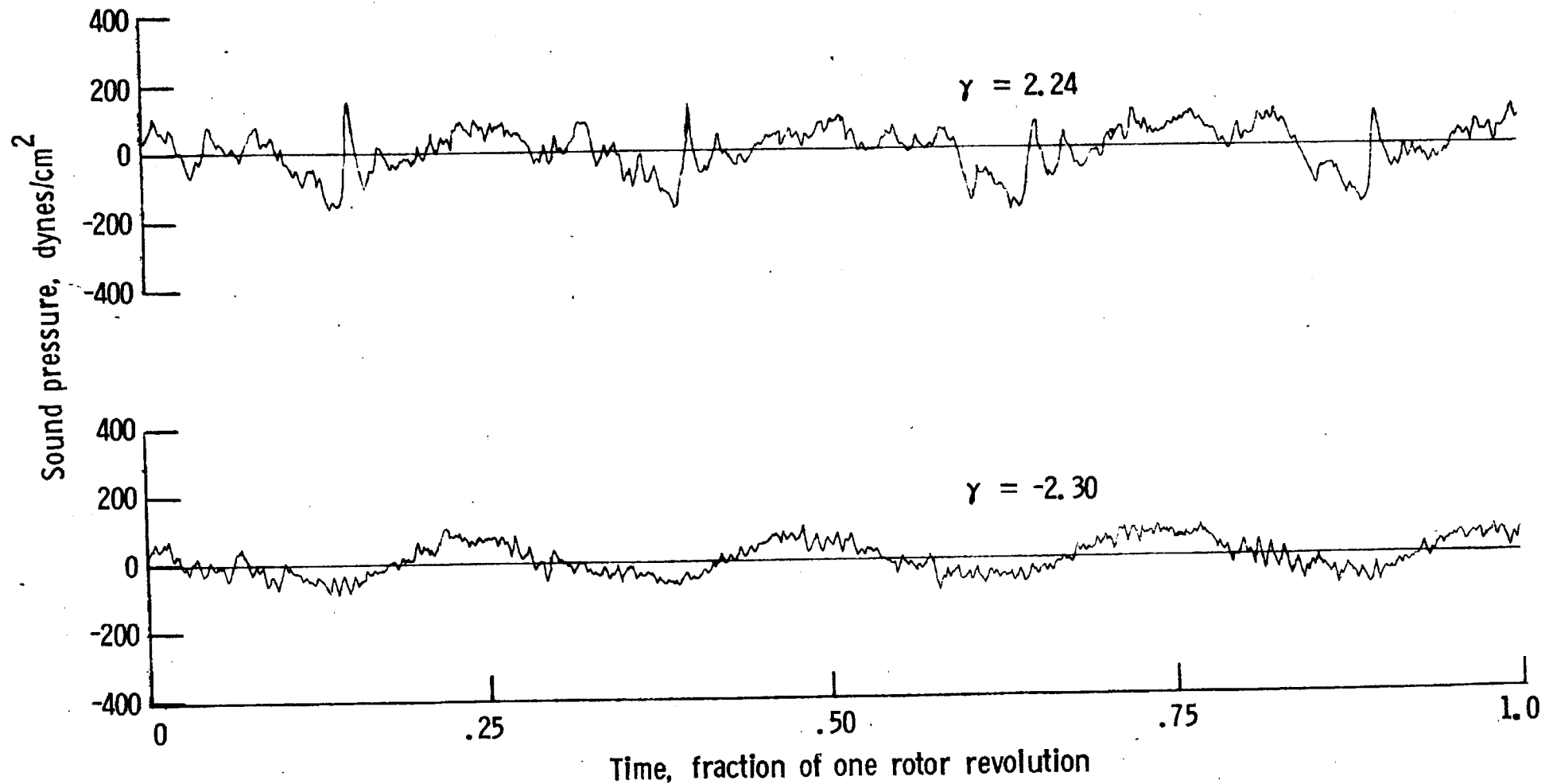
Figure 12. - Concluded.



One-third-octave-band center frequency, kHz

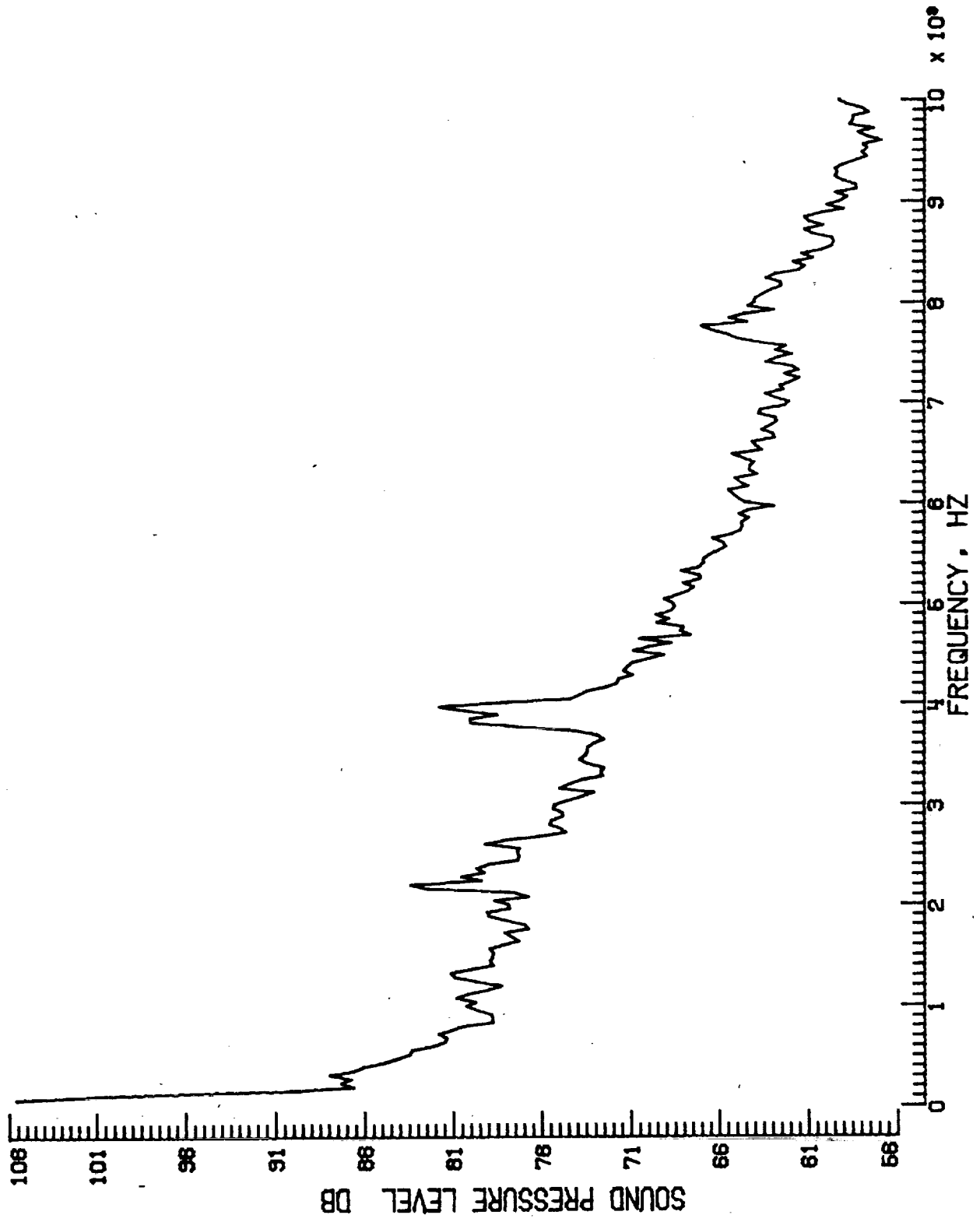
a. Mic. no. 1.

Figure 13. - Effect of descent angle variation on noise generated by helicopter model with swept-tapered tips installed. $V_{\infty} = 50.6$ knots.



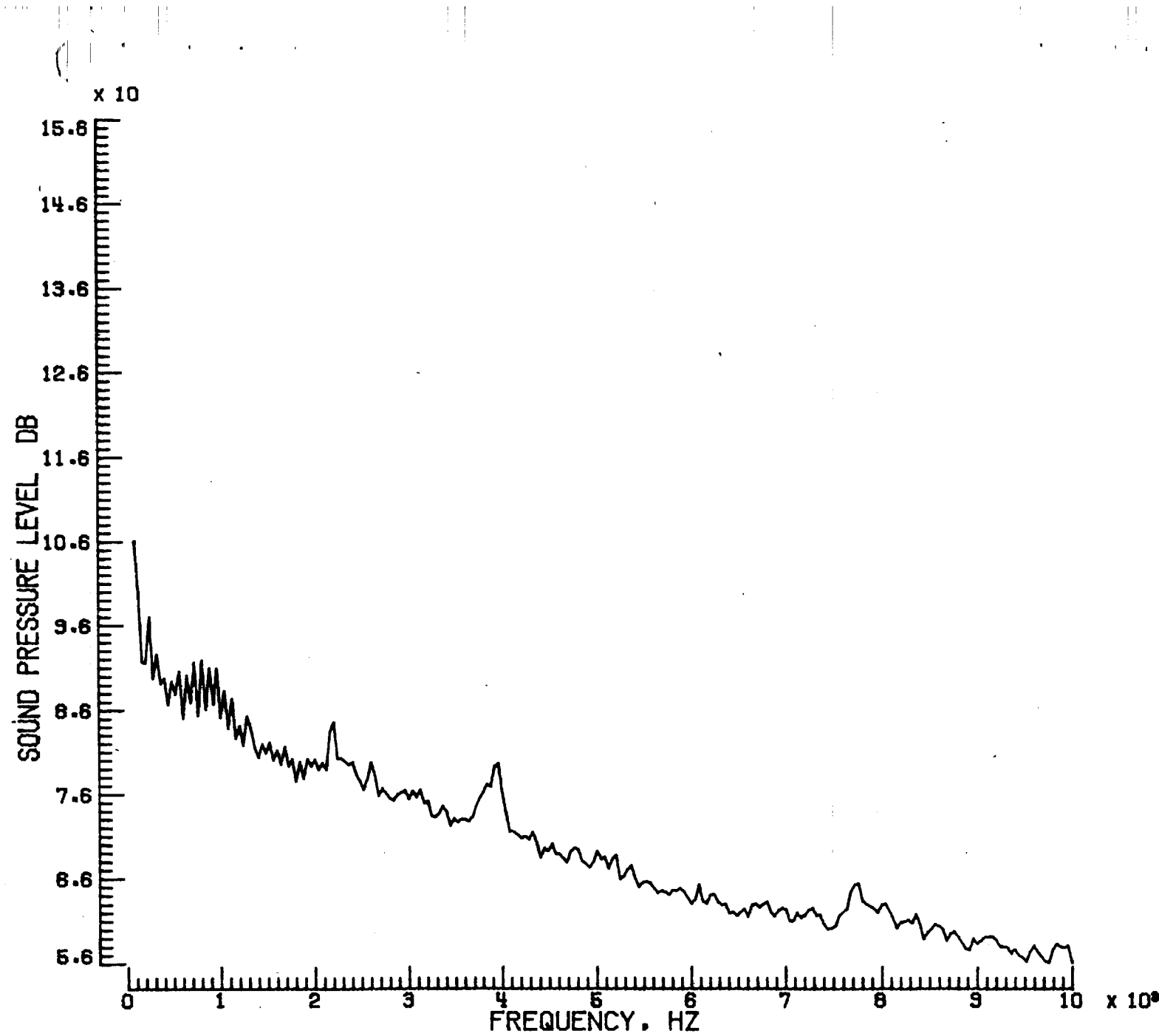
b. Pressure-time histories, Mic. no. 1.

Figure 13. - Continued.

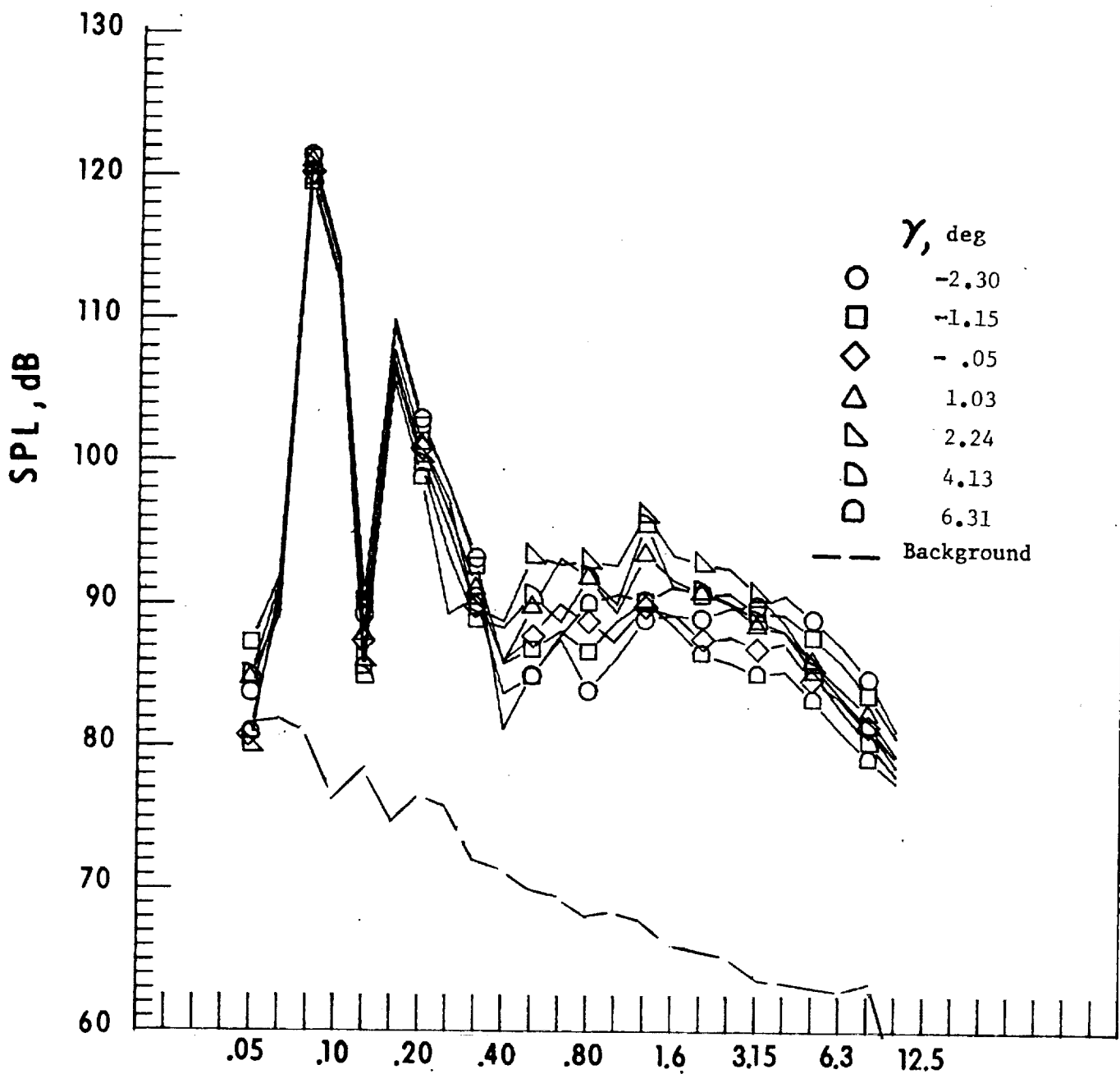


c. Narrow band analysis, Mic. no. 1, $\gamma = -2.30^0$.

Figure 13. - Continued.



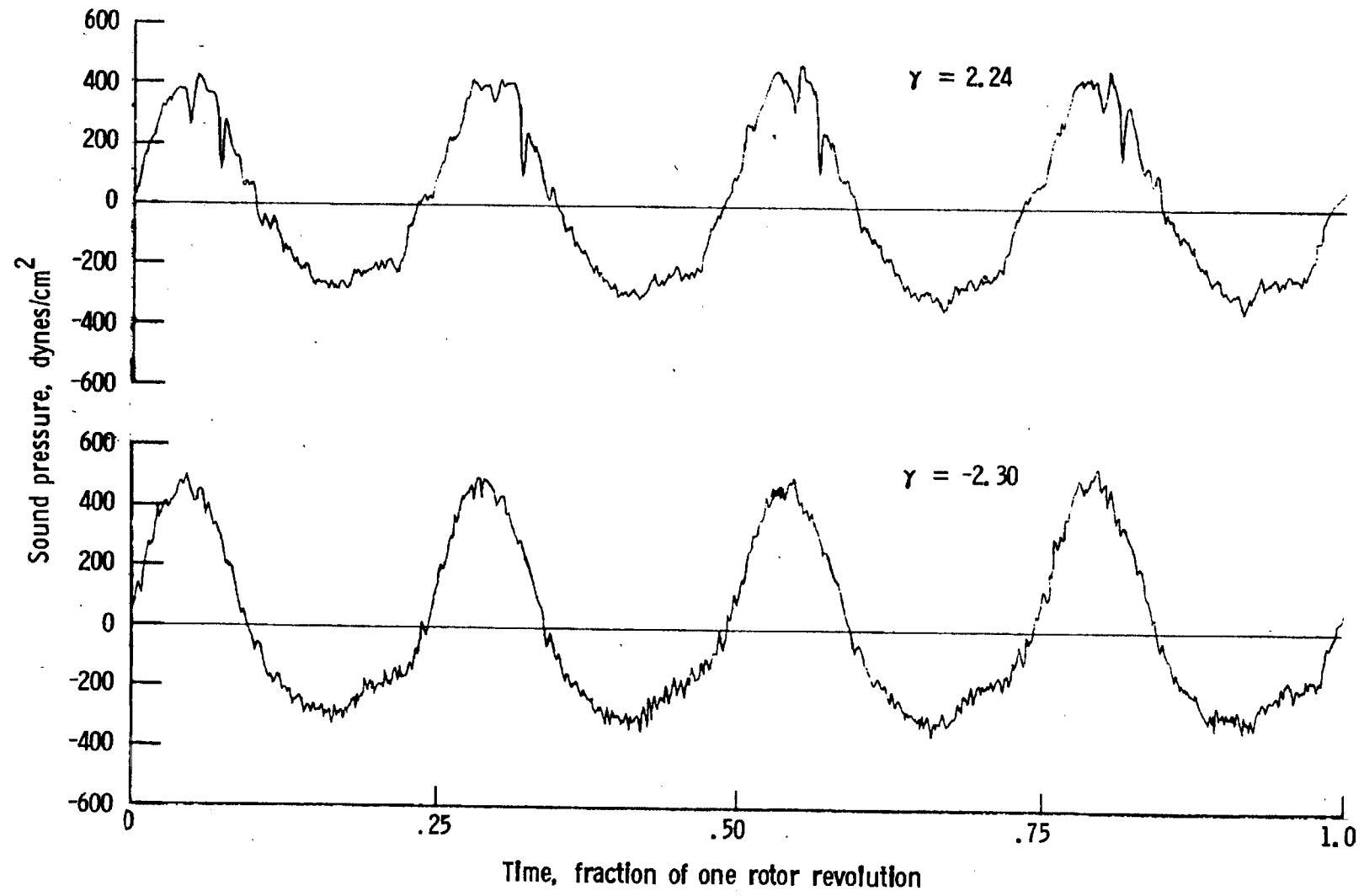
d. Narrow band analysis, Mic. no. 1, $\gamma = 2.24^0$



One-third-octave-band center frequency, kHz

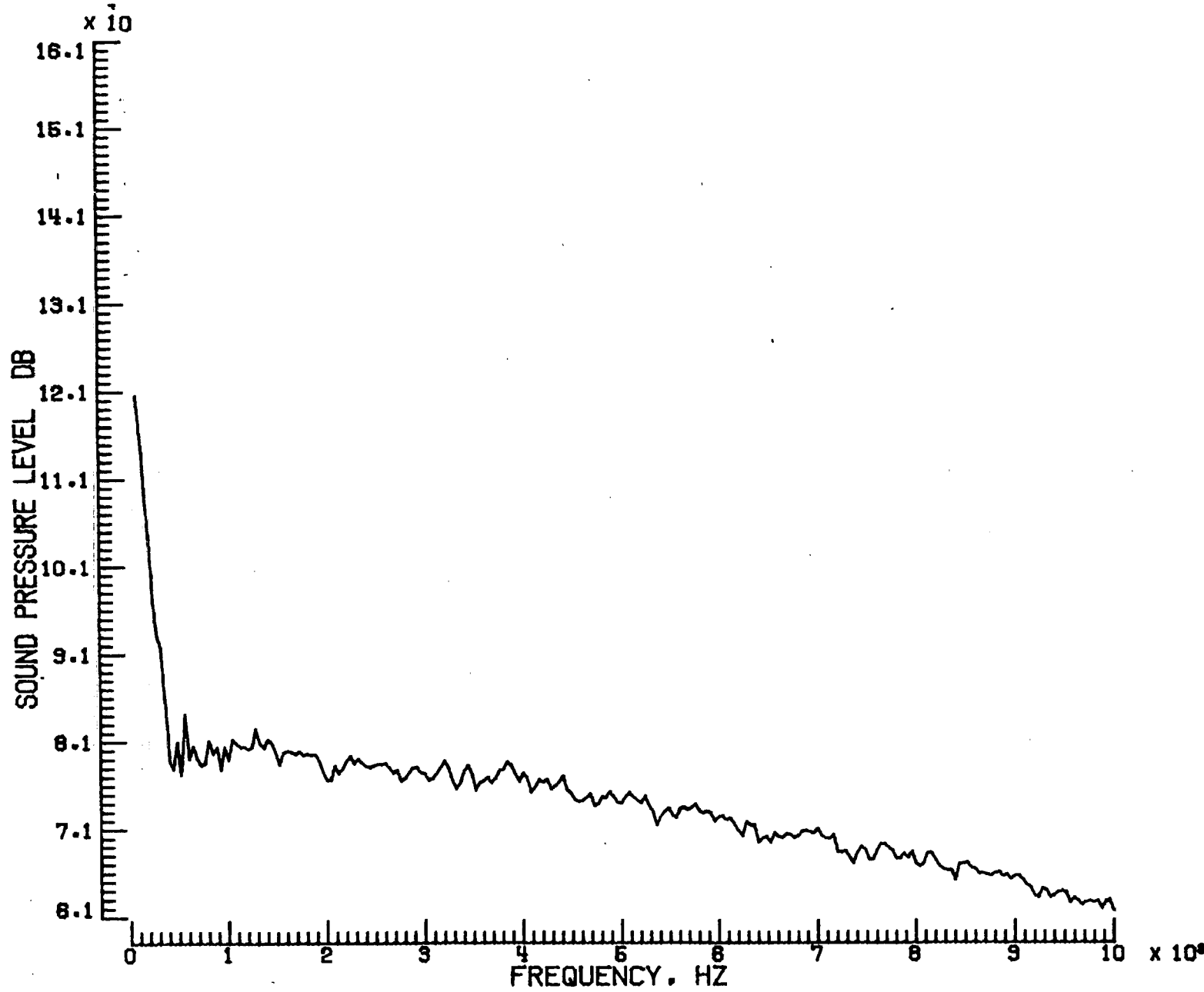
e. Mic. no. 2.

Figure 13. - Continued.



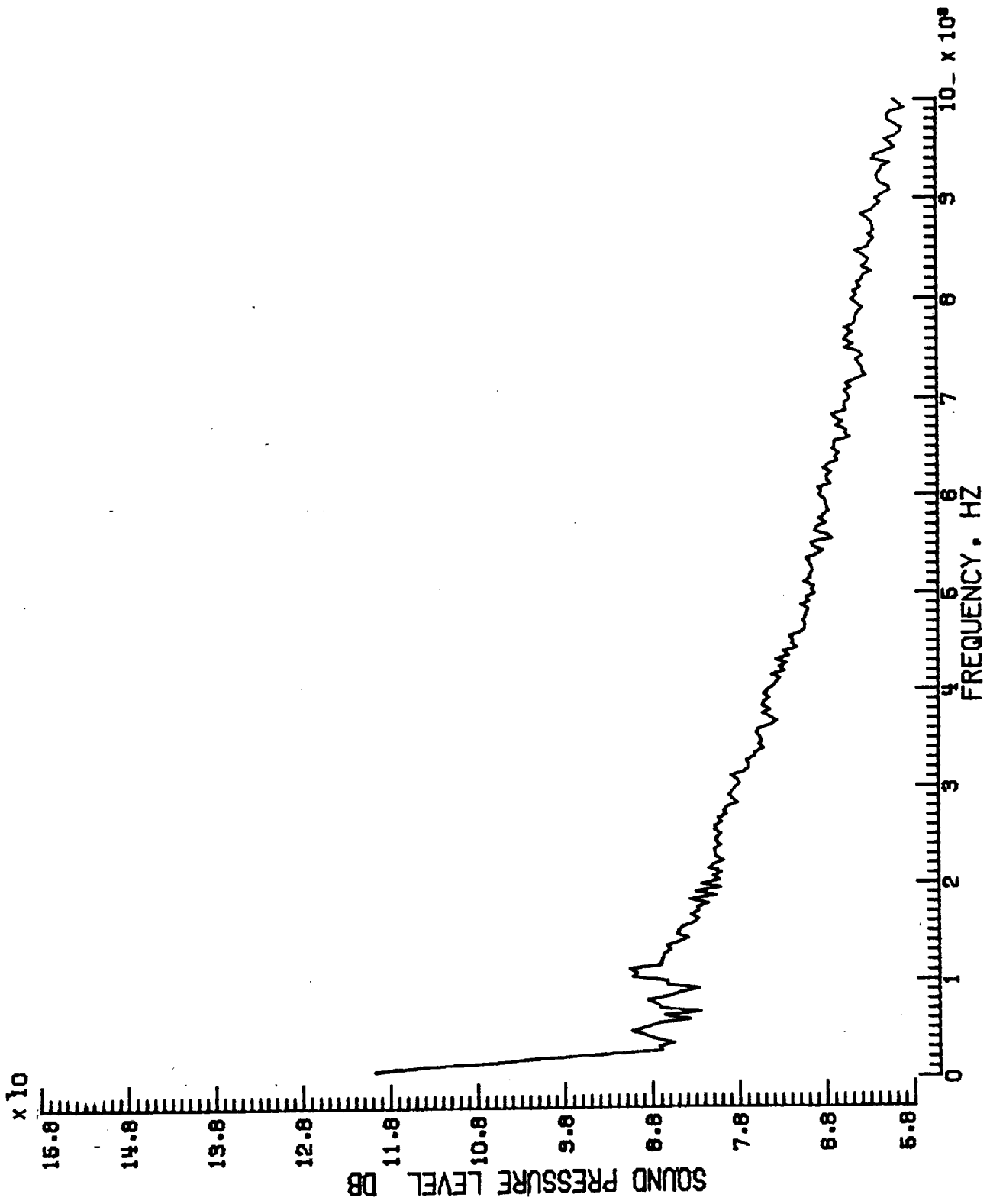
f. Pressure-time histories, Mic. no. 2.

Figure 13. - Continued.

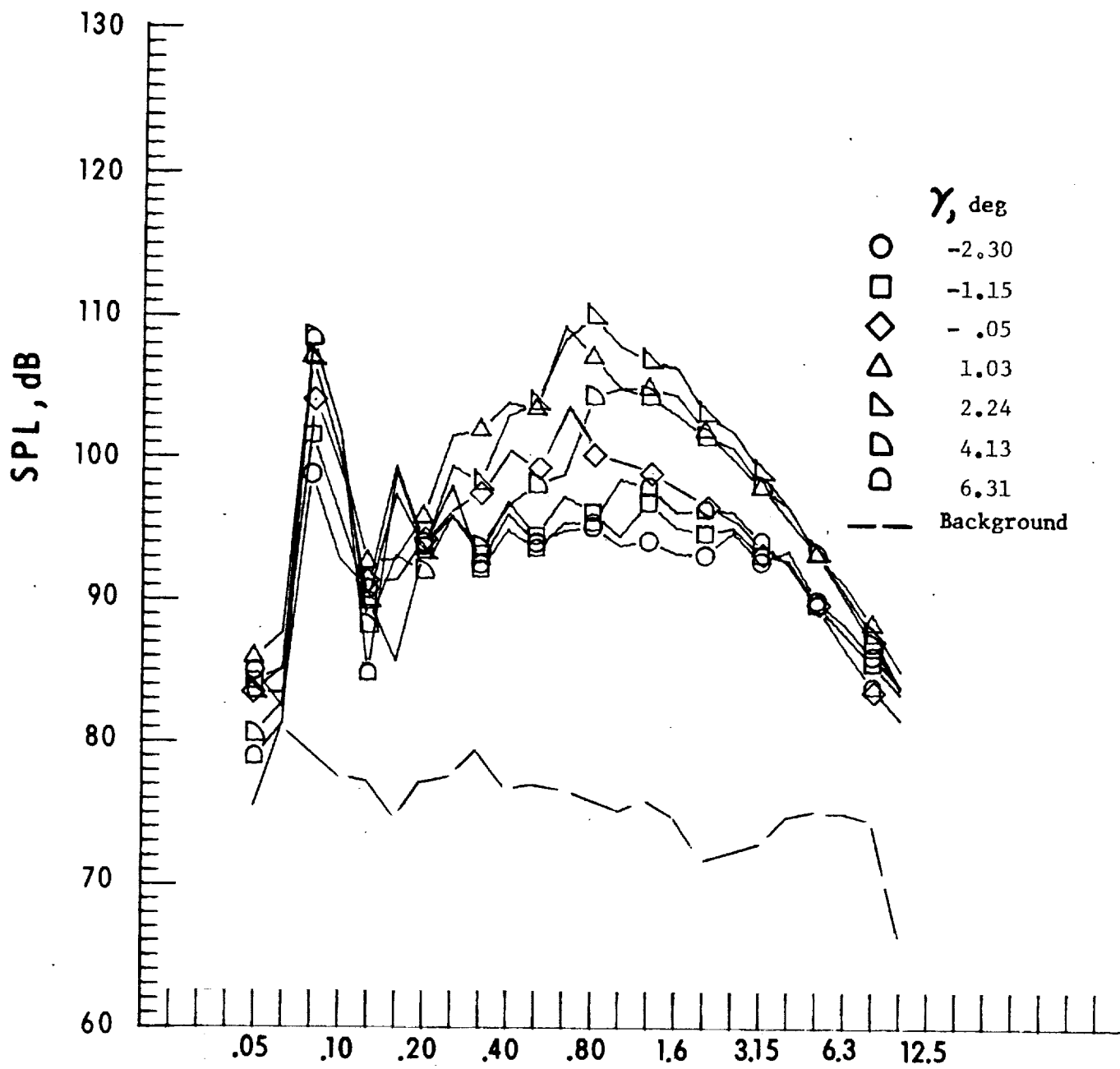


g. Narrow band analysis, Mic. no. 2, $\gamma = -2.30^\circ$.

Figure 13. - Continued.

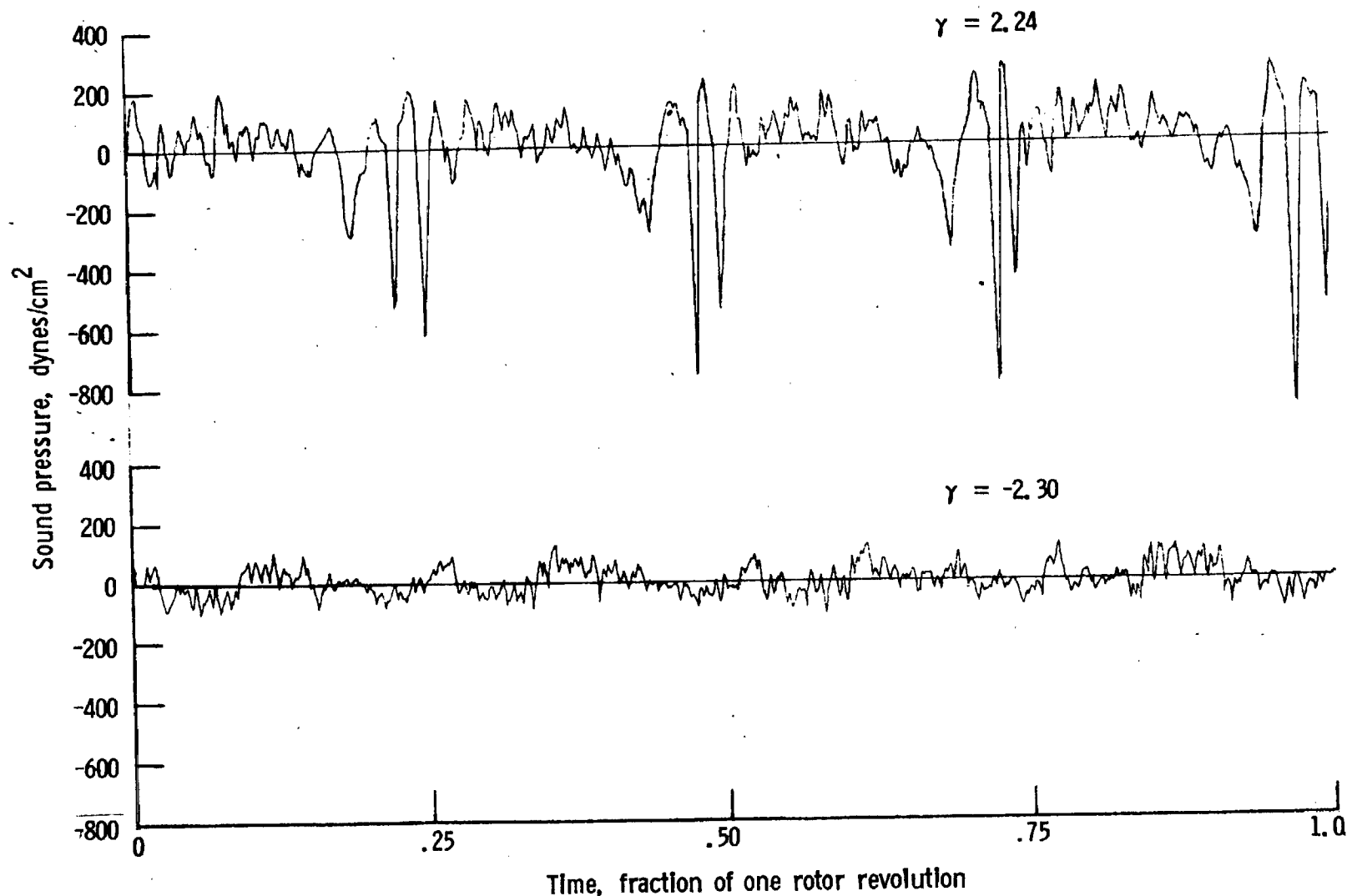


h. Narrow band analysis, Mic. no. 2, $\gamma = 2.24^0$.



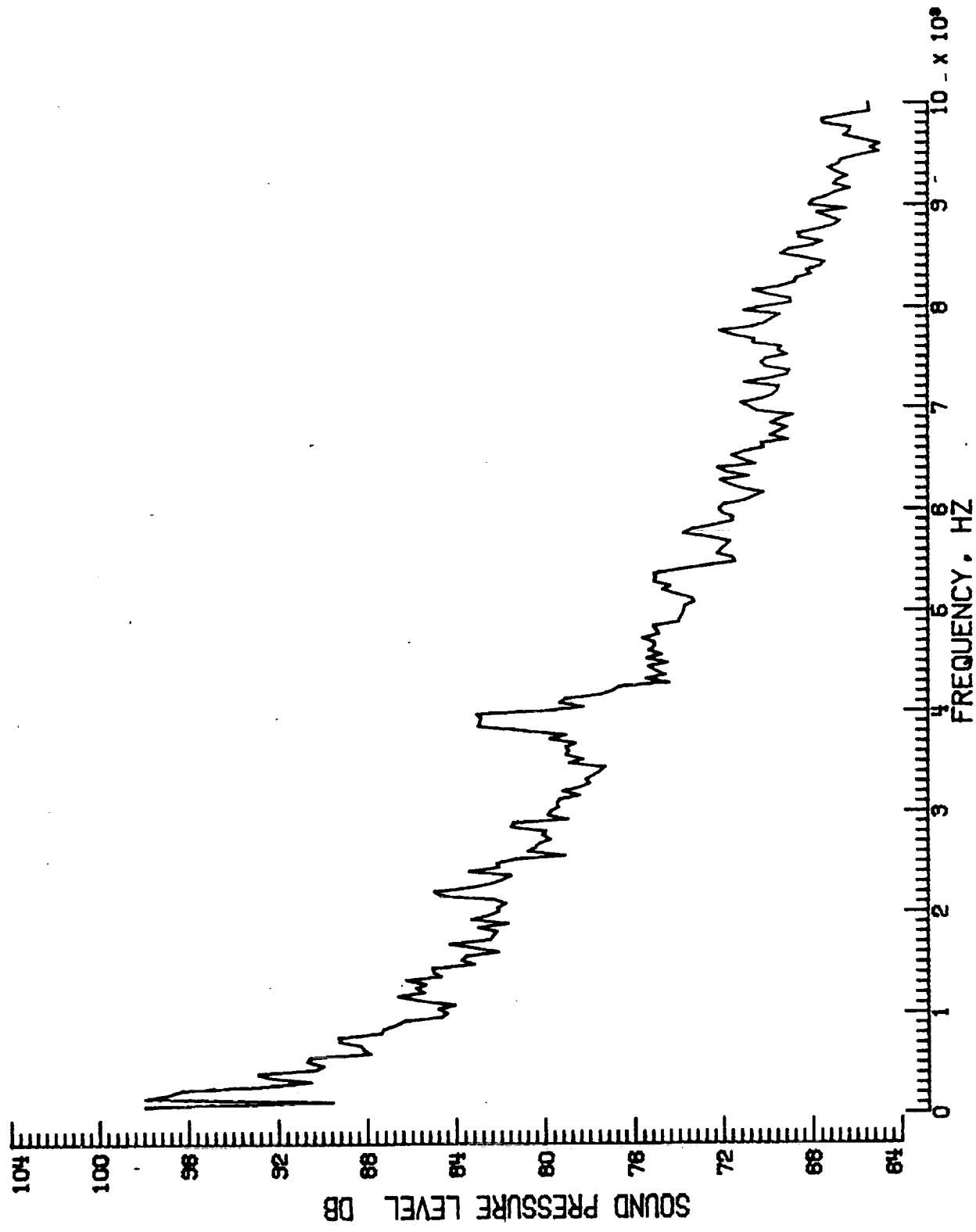
One-third-octave-band center frequency, kHz
 i. Mic. no. 3.

Figure 13. - Continued.



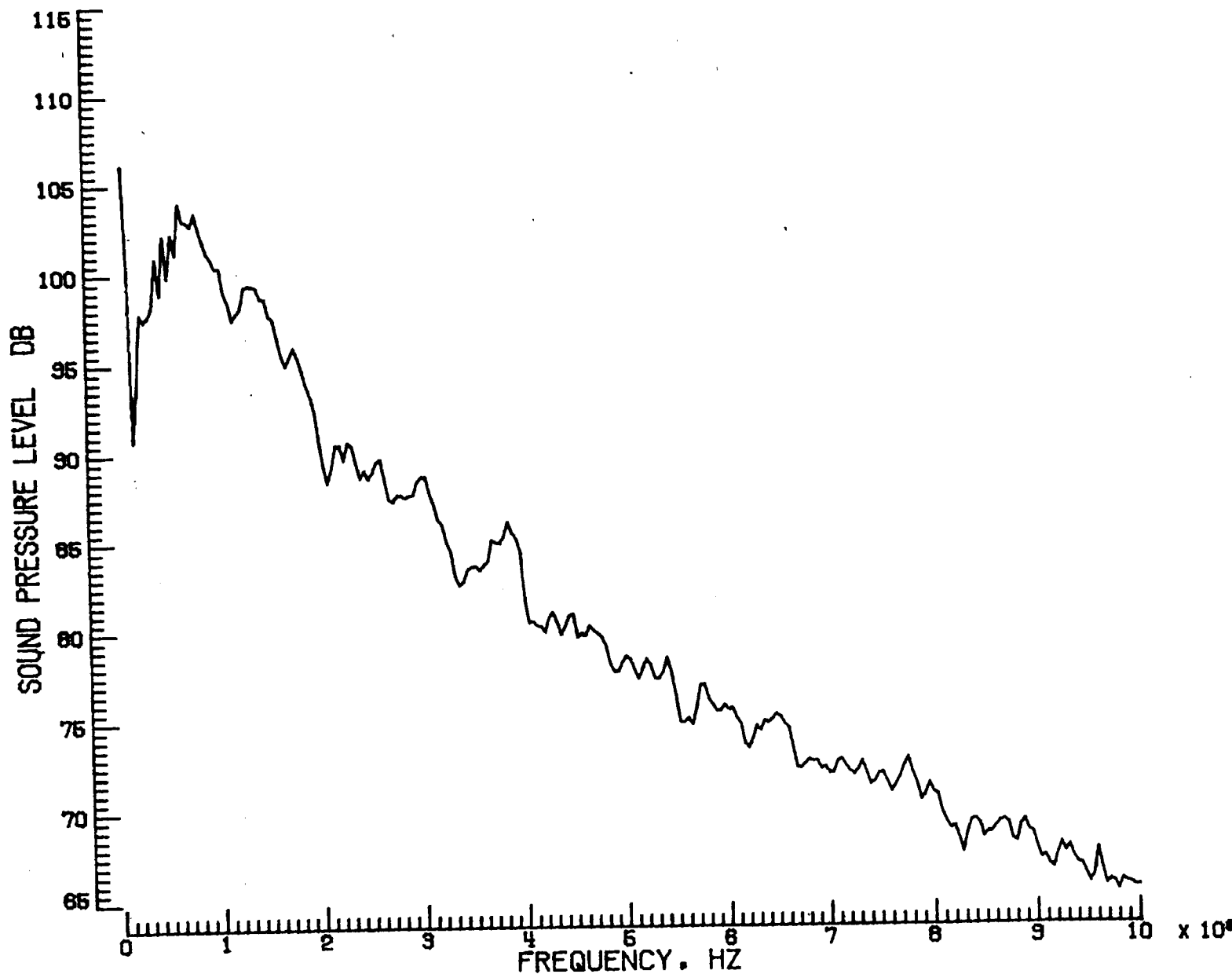
j. Pressure-time histories, Mic. no. 3.

Figure 13. - Continued.



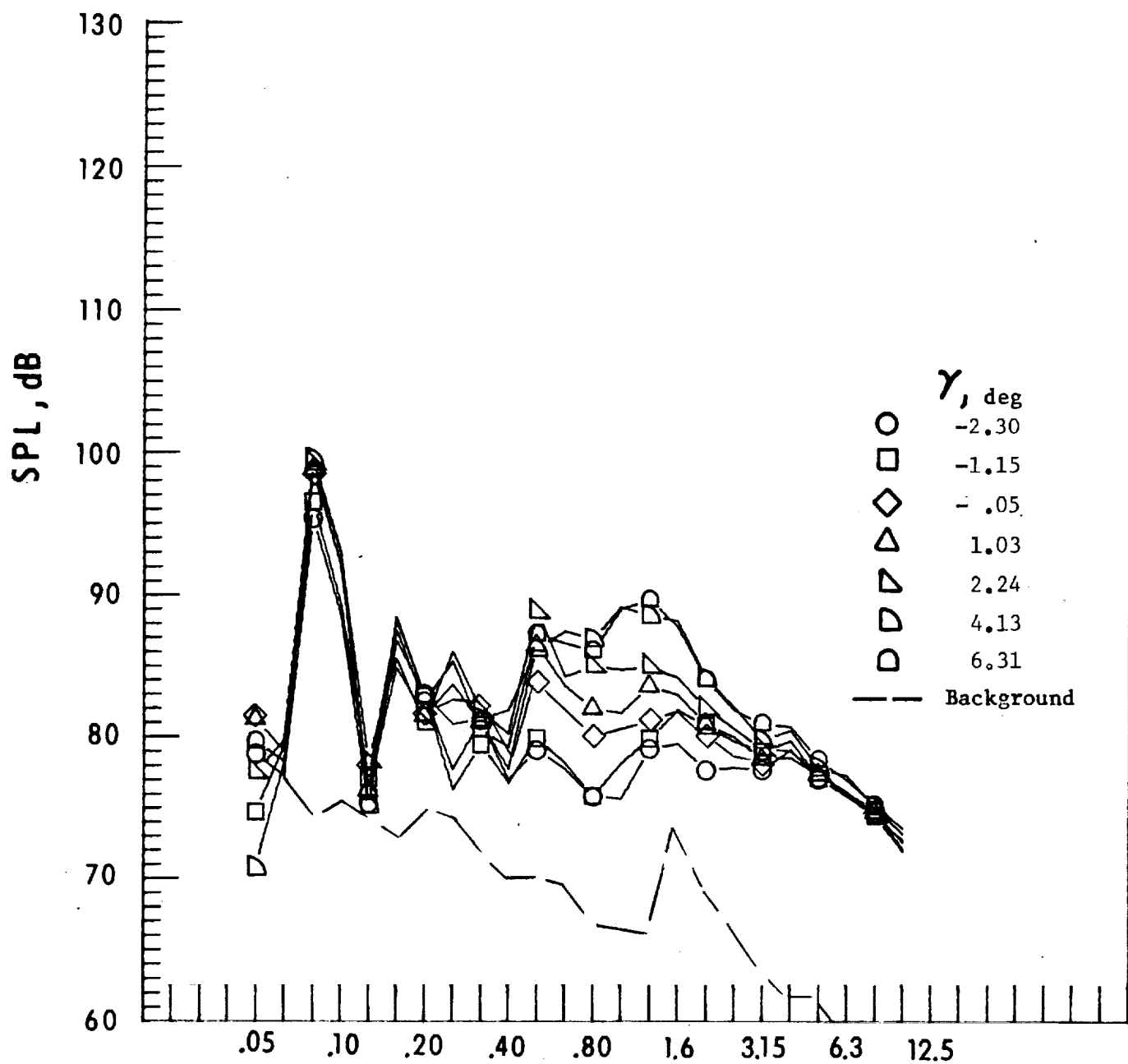
k. Narrow band analysis, Mic. no. 3, $\gamma = -2.30^\circ$.

Figure 13. - Continued.



I. Narrow band analysis, Mic. no. 3, $\gamma = 2.24^0$.

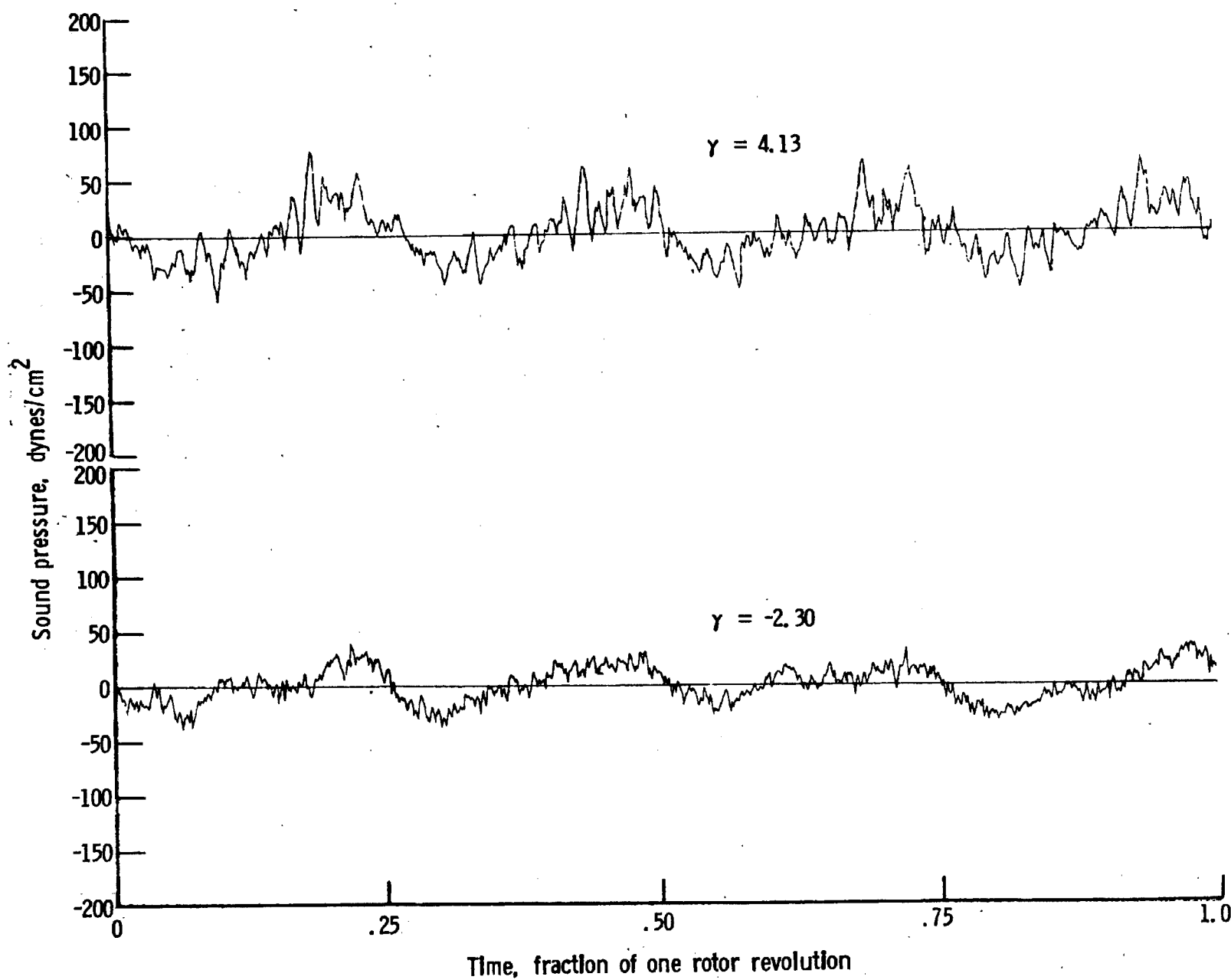
Figure 13 - Continued



One-third-octave-band center frequency, kHz

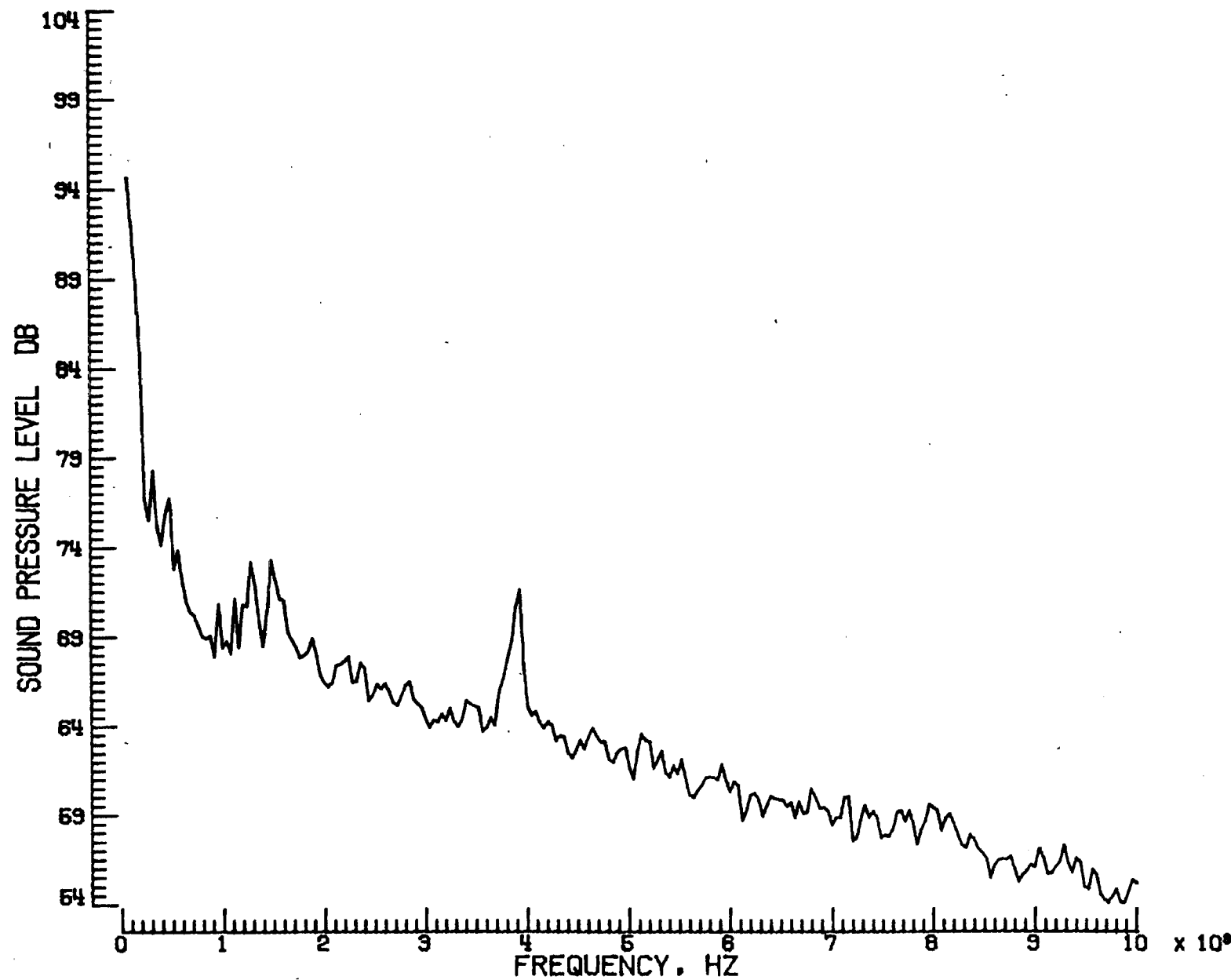
m. Mic. no. 4.

Figure 13. - Continued.



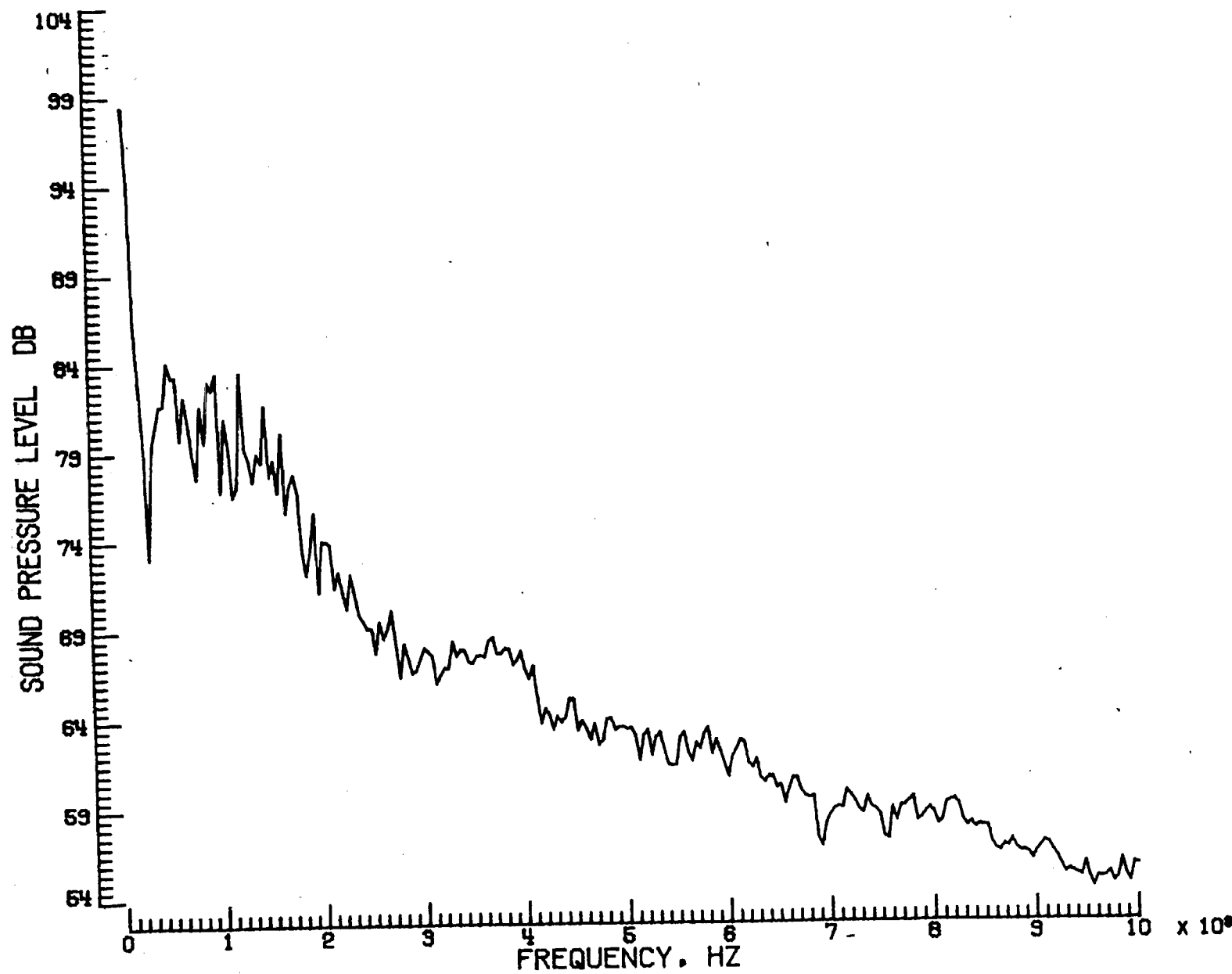
n. Pressure-time histories, Mic. no. 4.

Figure 13. - Continued.



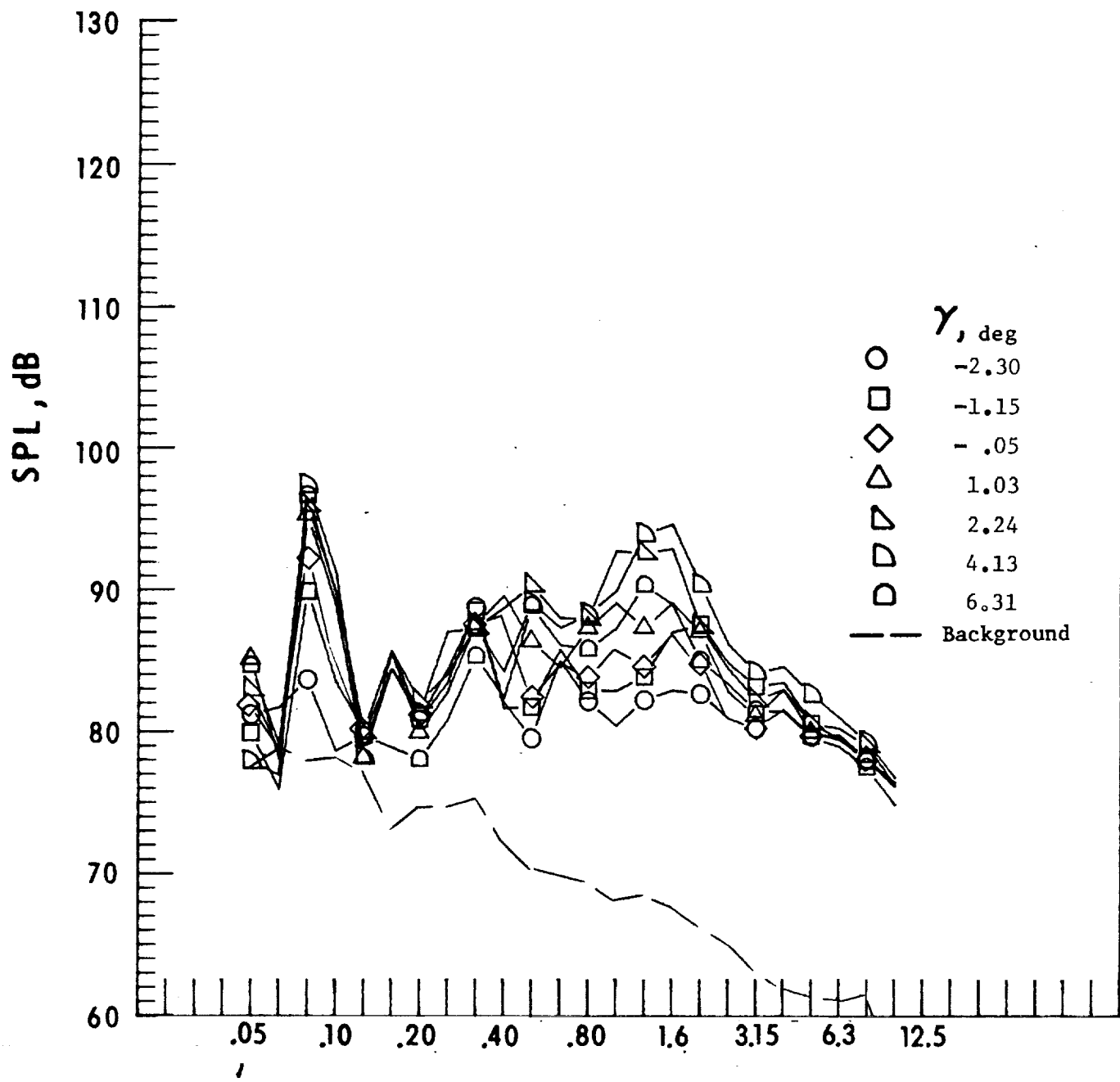
o. Narrow band analysis, Mic. no. 4, $\gamma = -2.30^0$.

Figure 13. - Continued.



p. Narrow band analysis, Mic. no. 4, $\gamma = 4.13^\circ$.

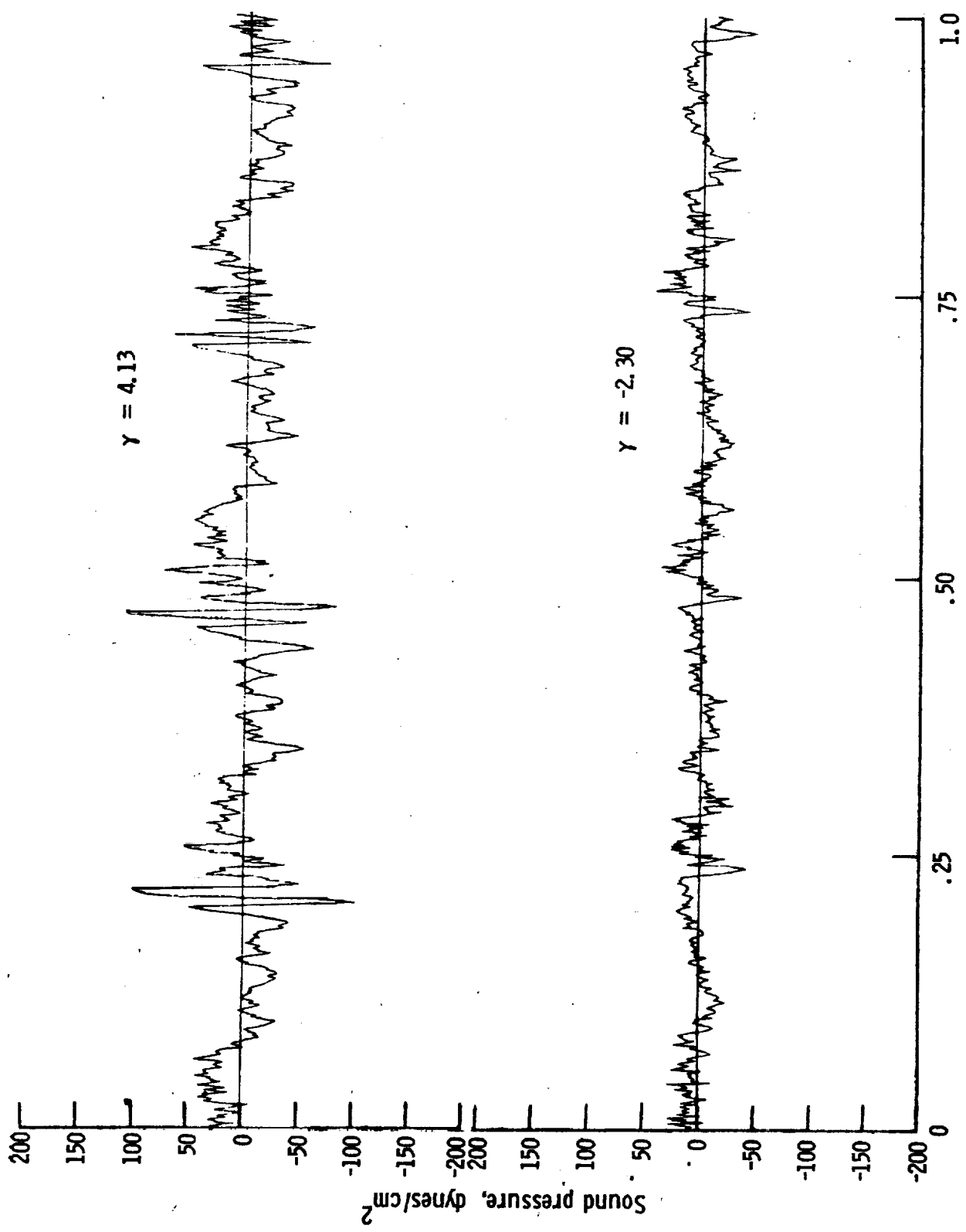
Figure 13. - Continued.



One-third-octave-band center frequency, kHz

q. Mic. no. 5.

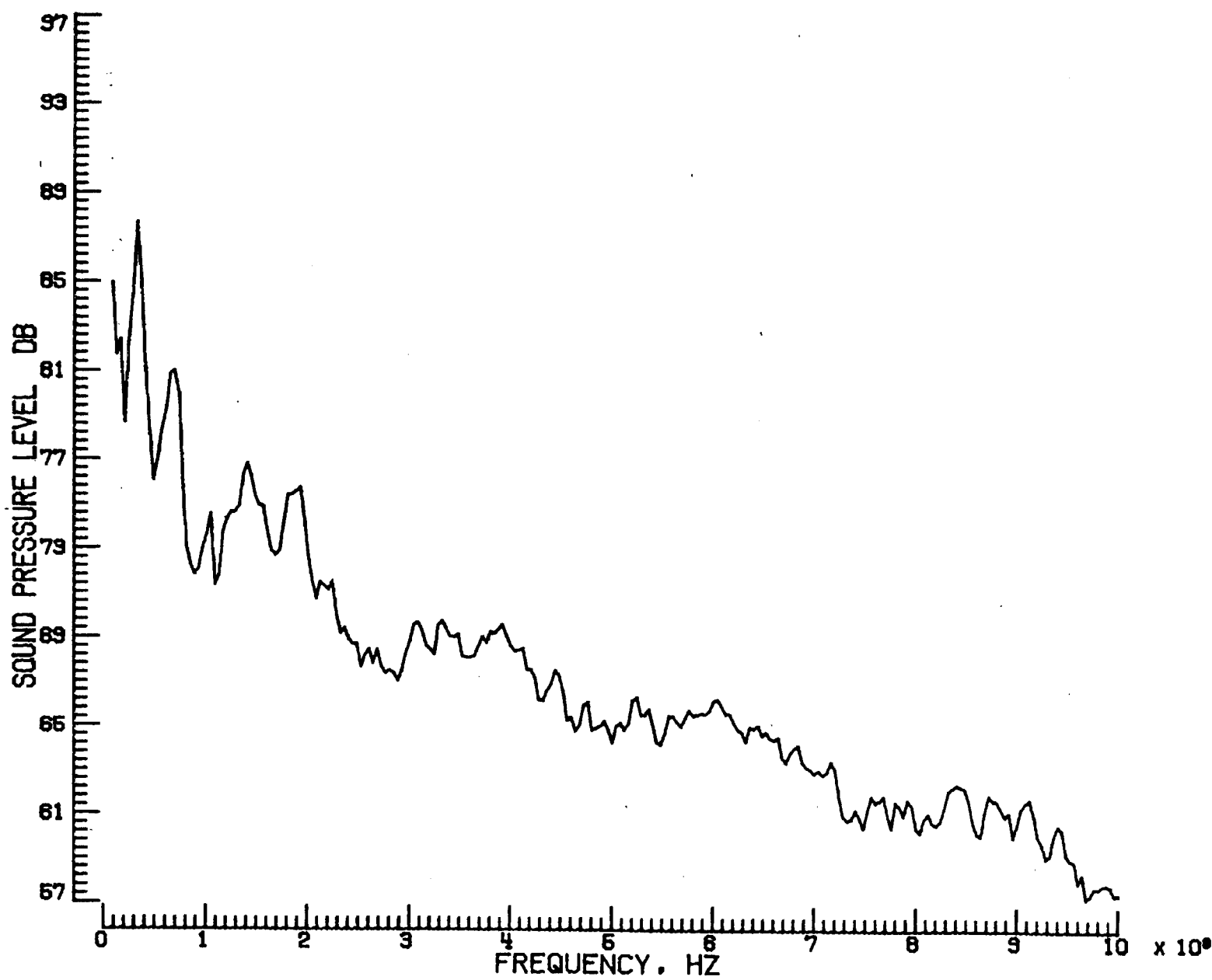
Figure 13. - Continued.



Time, fraction of one rotor revolution

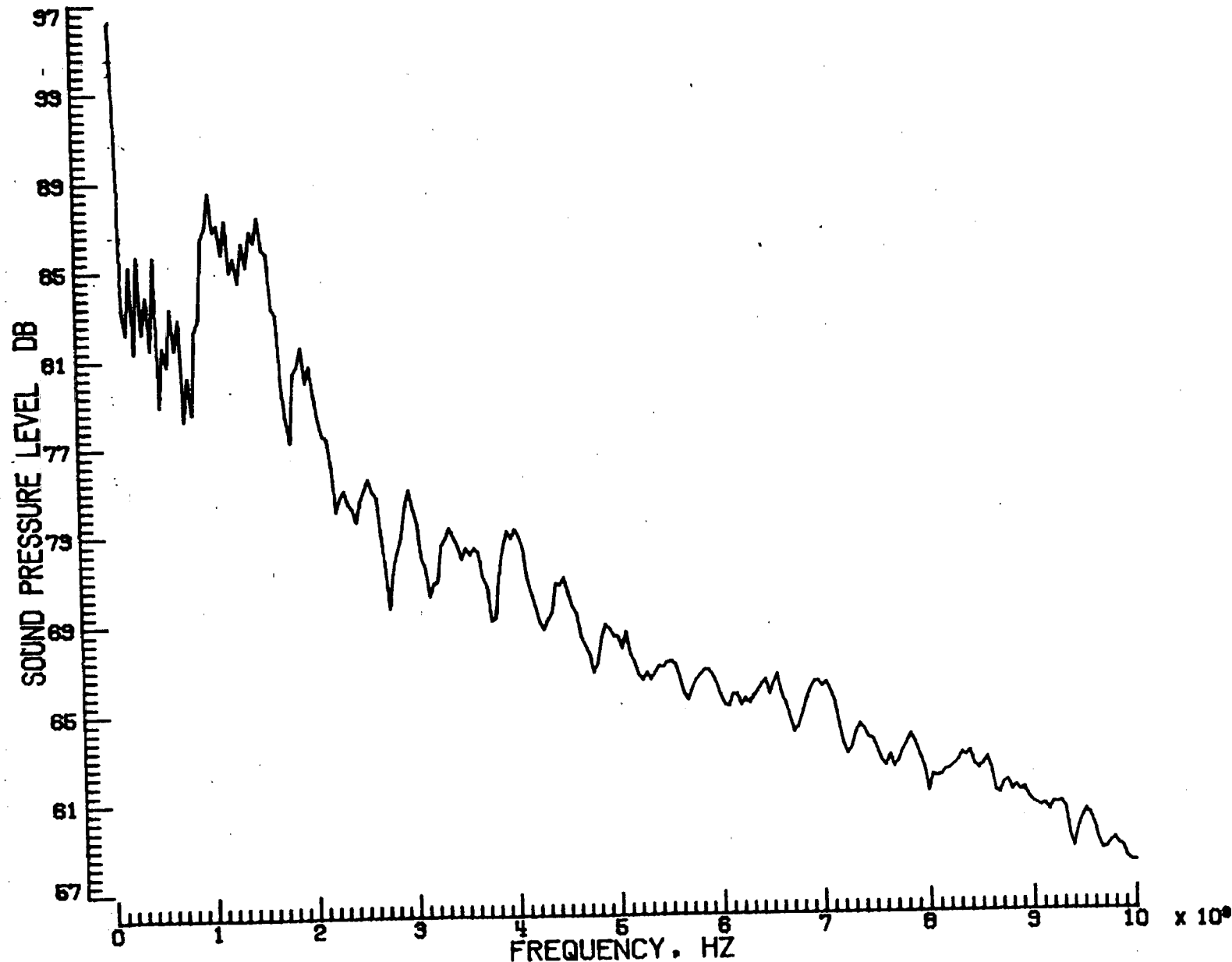
r. Narrow band analysis, Mlc. no. 5.

Figure 13. - Continued.



s. Narrow band analysis, Mic. no. 5, $\gamma = -2.30^\circ$.

Figure 13. - Continued.



t. Narrow band analysis, Mic. no. 5, $\gamma = 4.13^0$.

Figure 13. - Continued.

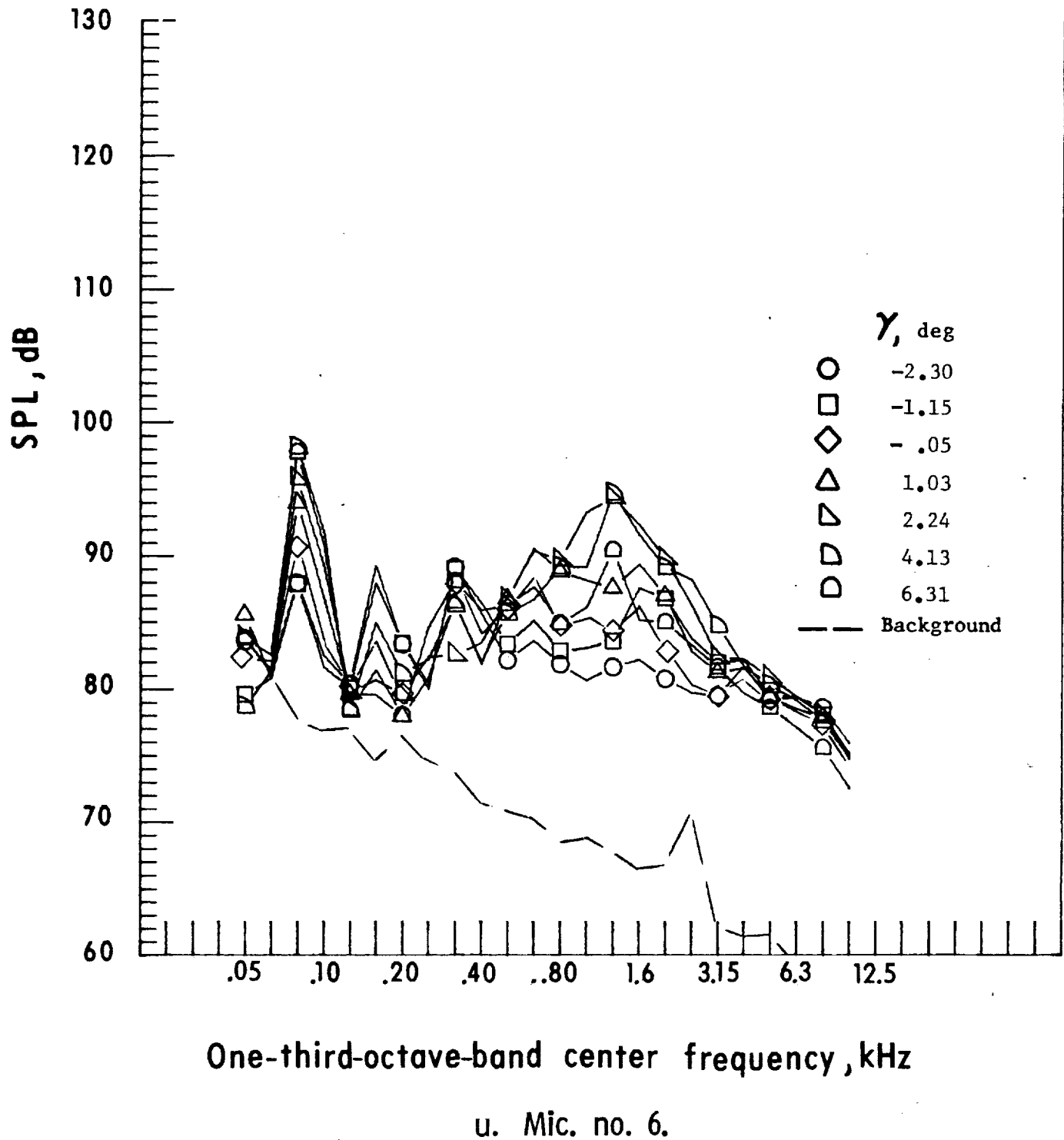
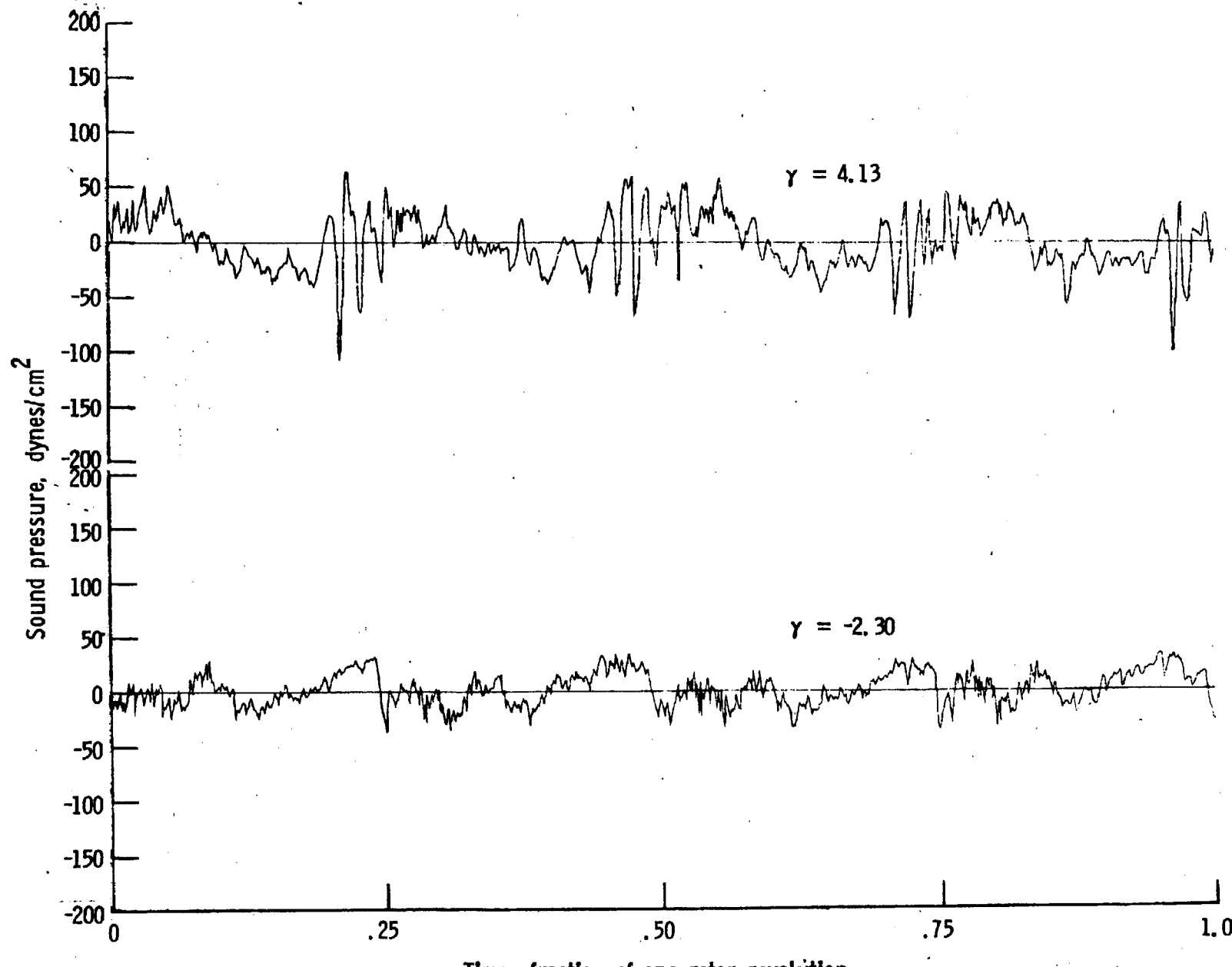
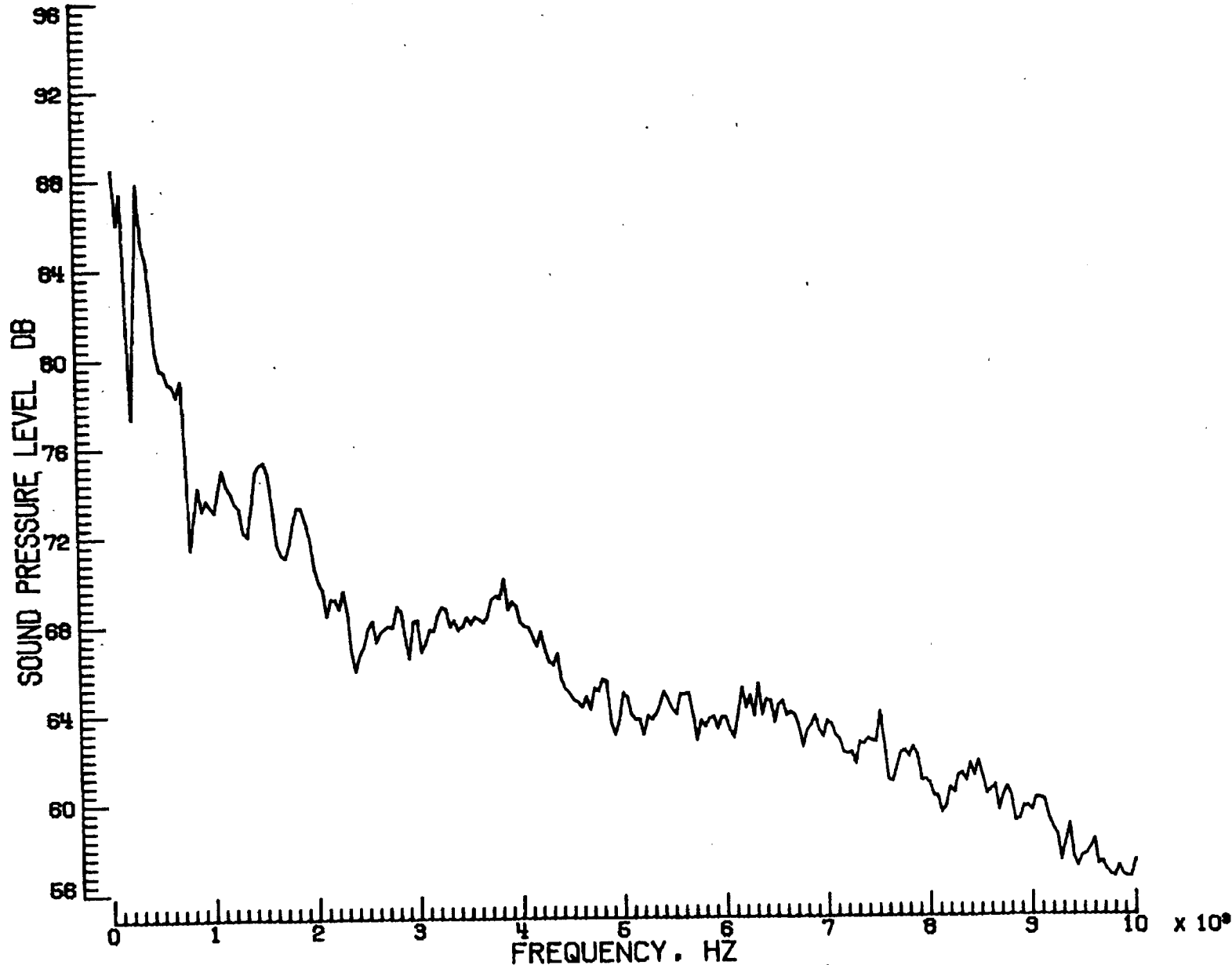


Figure 13. - Continued.



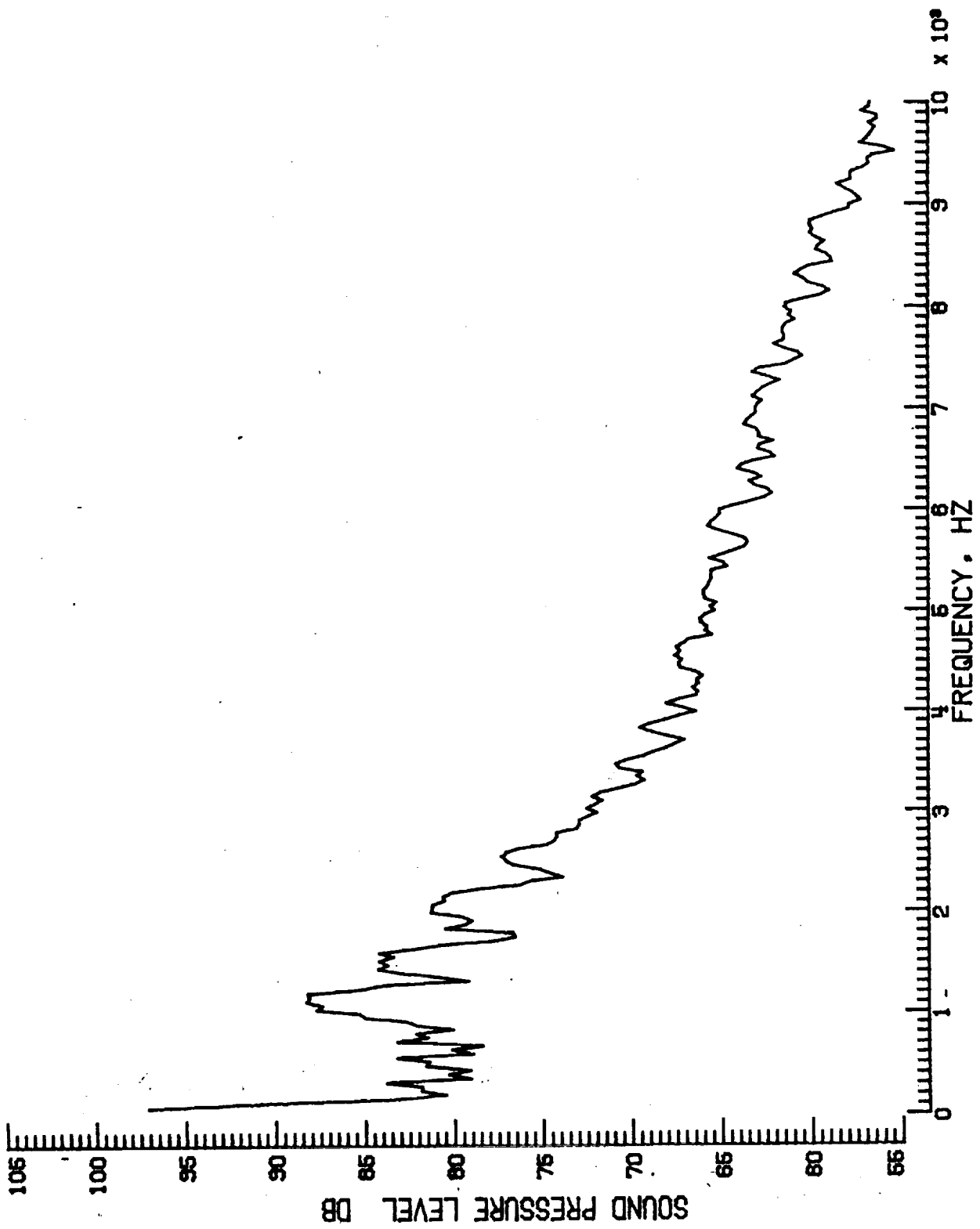
v. Pressure-time histories, Mic. no. 6.

Figure 13. - Continued.



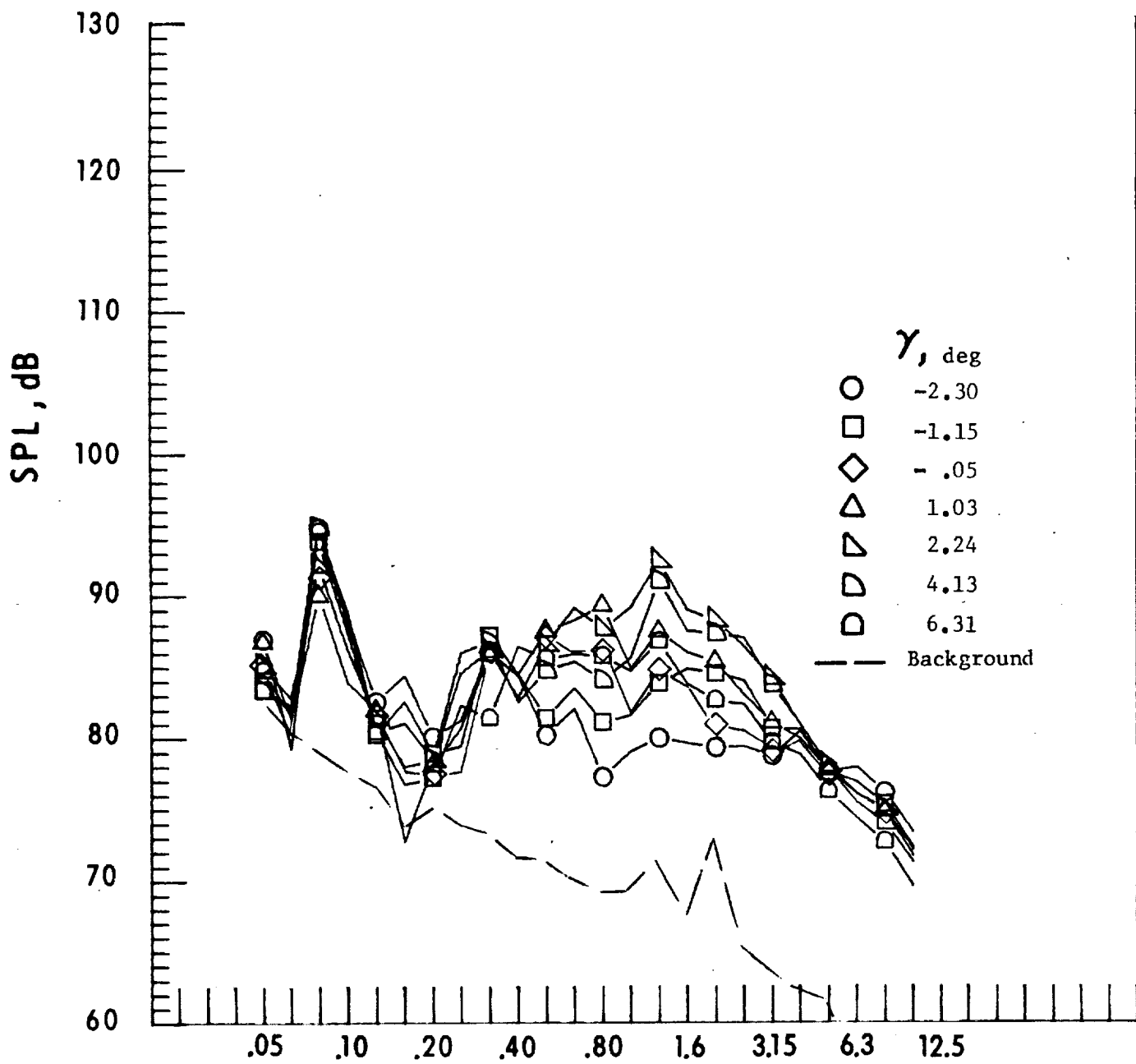
w. Narrow band analysis, Mic. no. 6, $\gamma = -2.30^\circ$.

Figure 13. - Continued.



x. Narrow band analysis, Mic. no. 6, $\gamma = 4.13^0$.

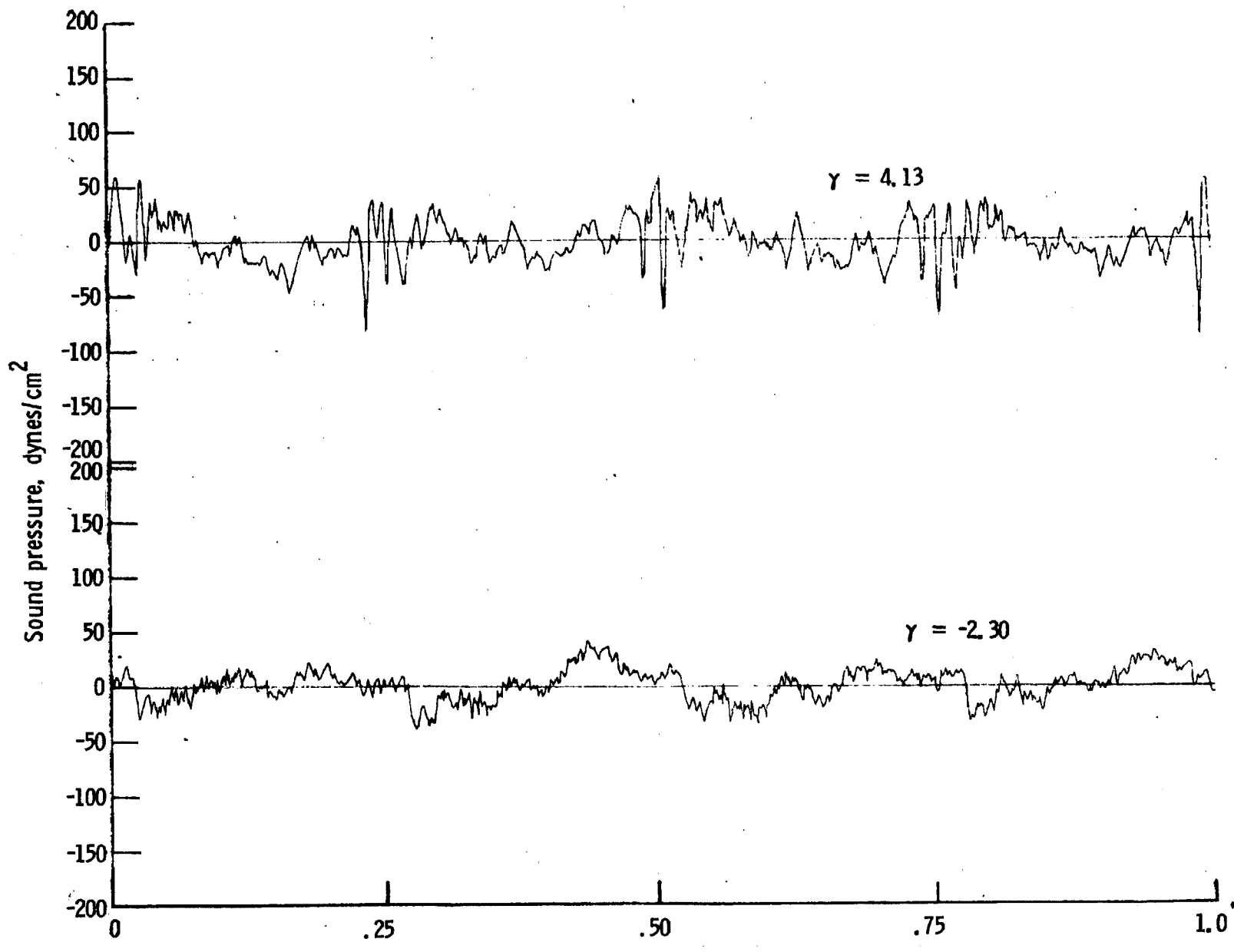
Figure 13. - Continued.



One-third-octave-band center frequency, kHz

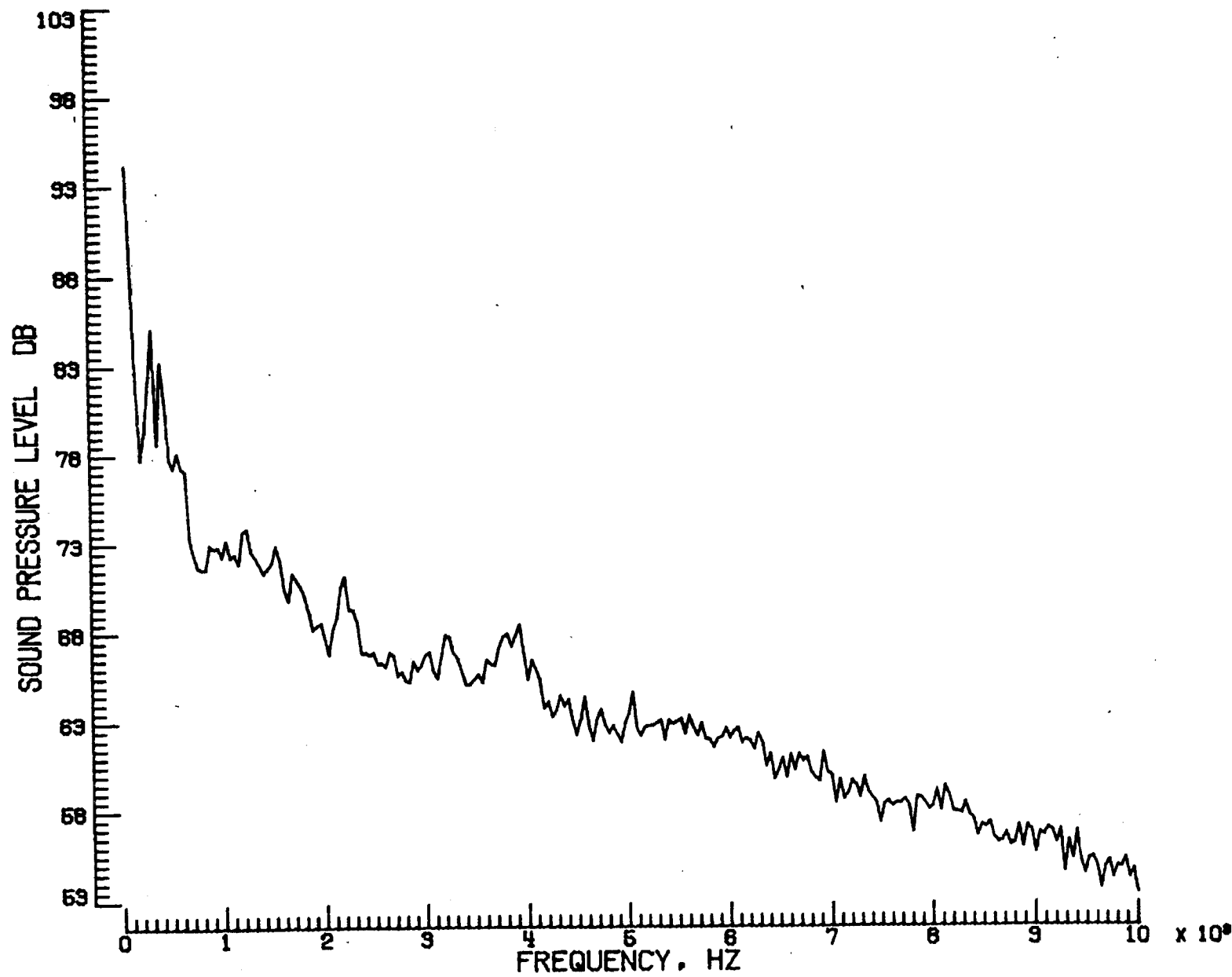
y. Mic. no. 7.

Figure 13. - Continued.



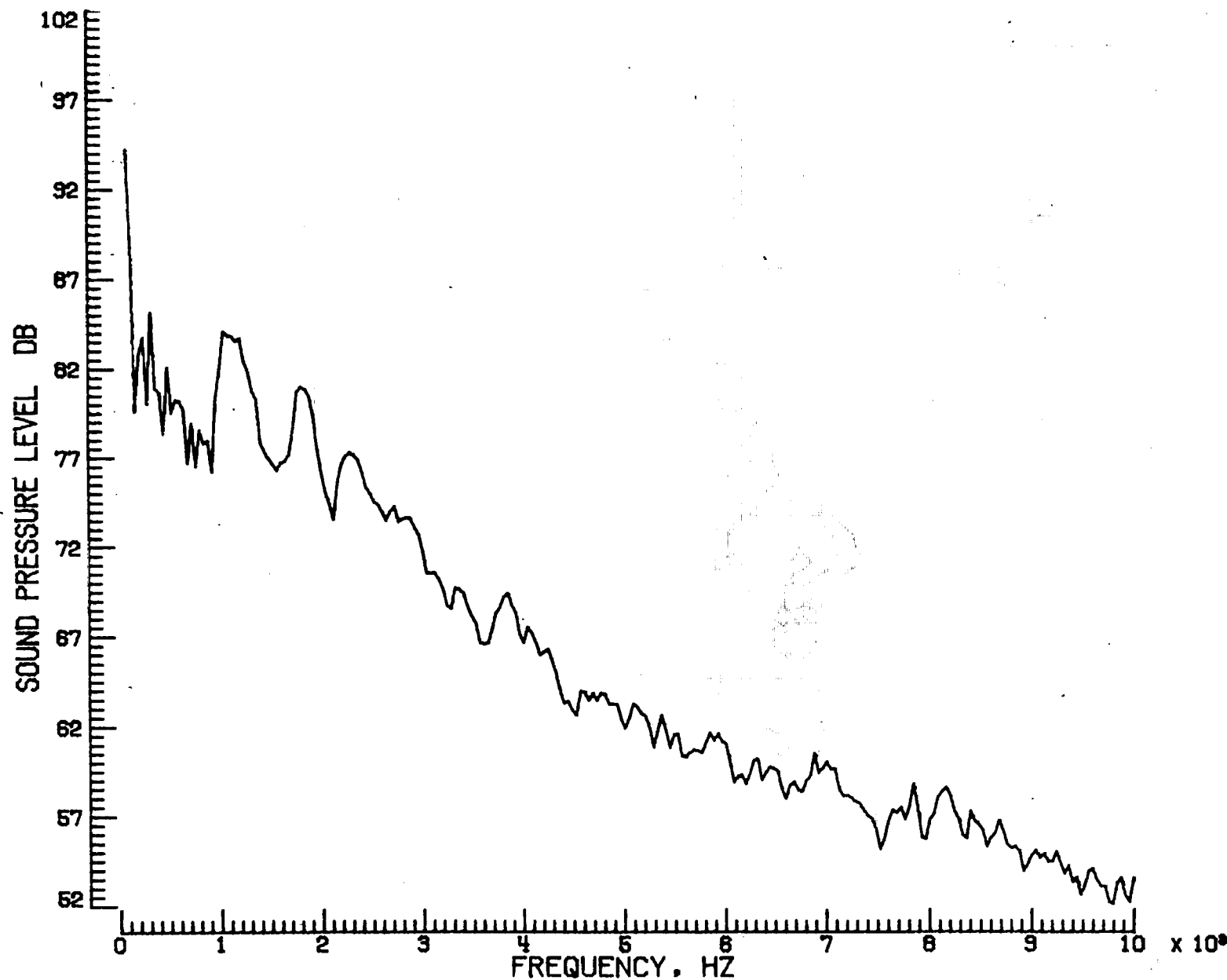
z. Pressure-time histories, Mic. no. 7.

Figure 13. - Continued.

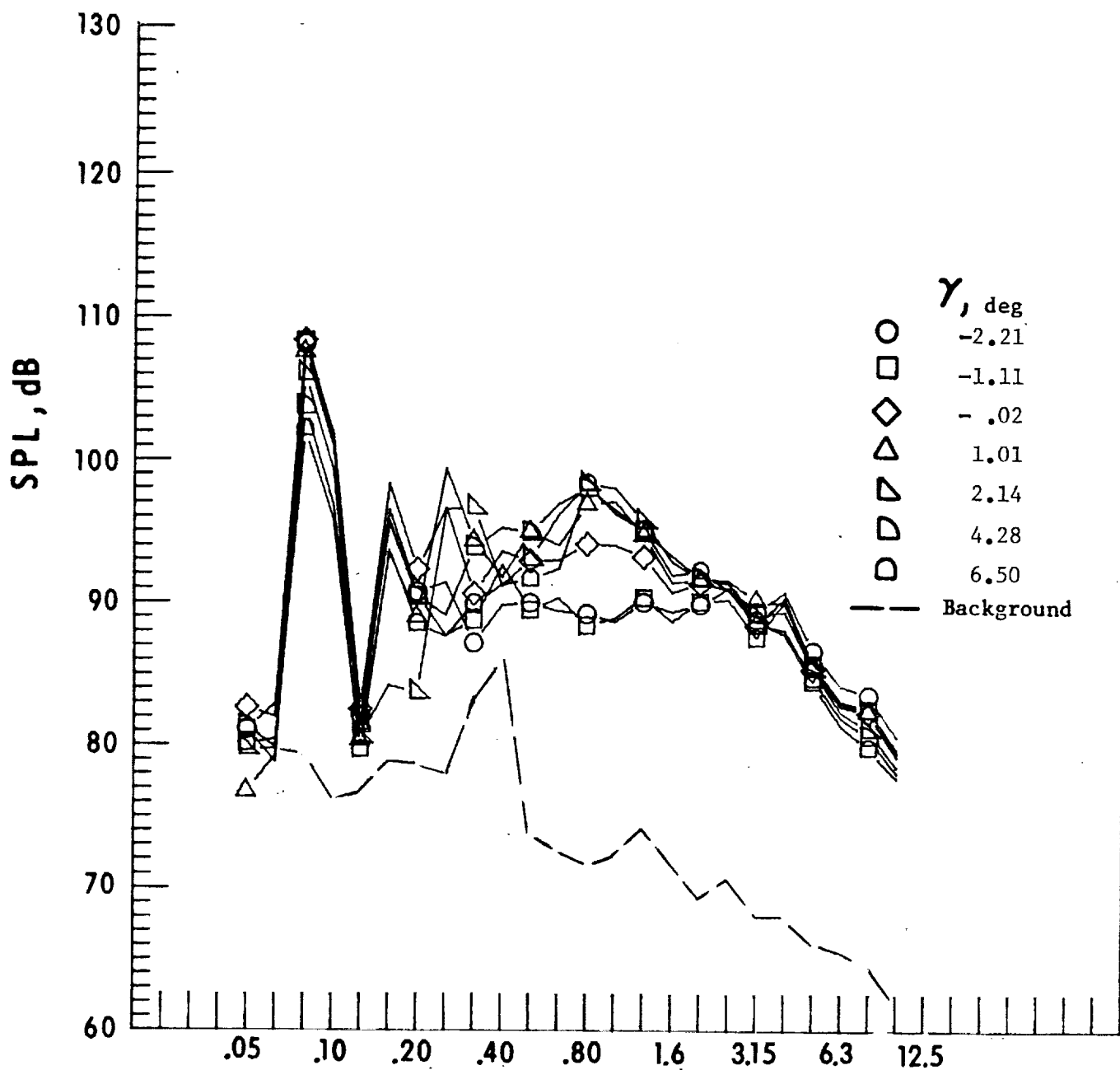


aa. Narrow band analysis, Mic. no. 7, $\gamma = -2.30^\circ$.

Figure 13. - Continued.



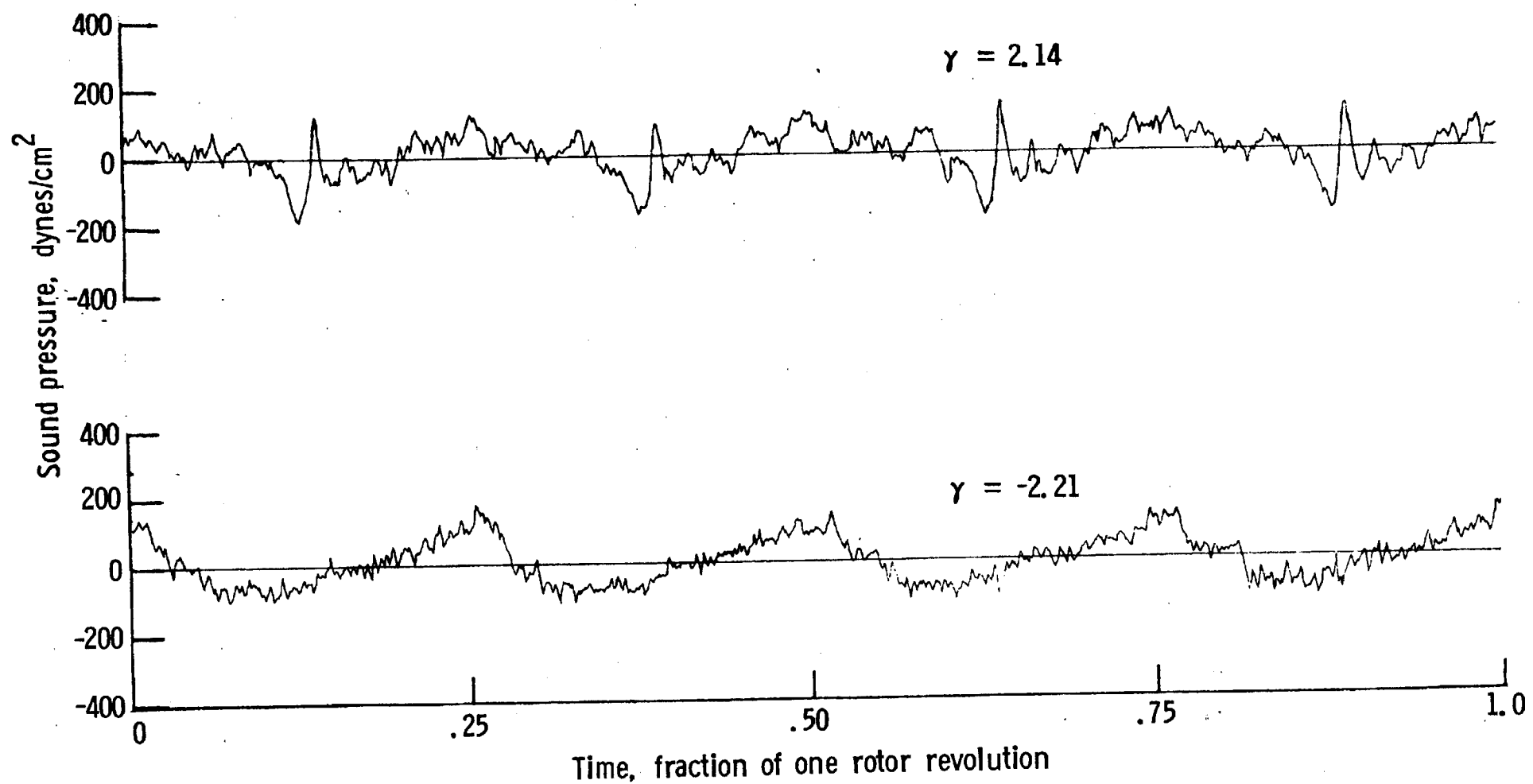
bb. Narrow band analysis, Mic. no. 7, $\gamma = 4.13^0$.



One-third-octave-band center frequency, kHz

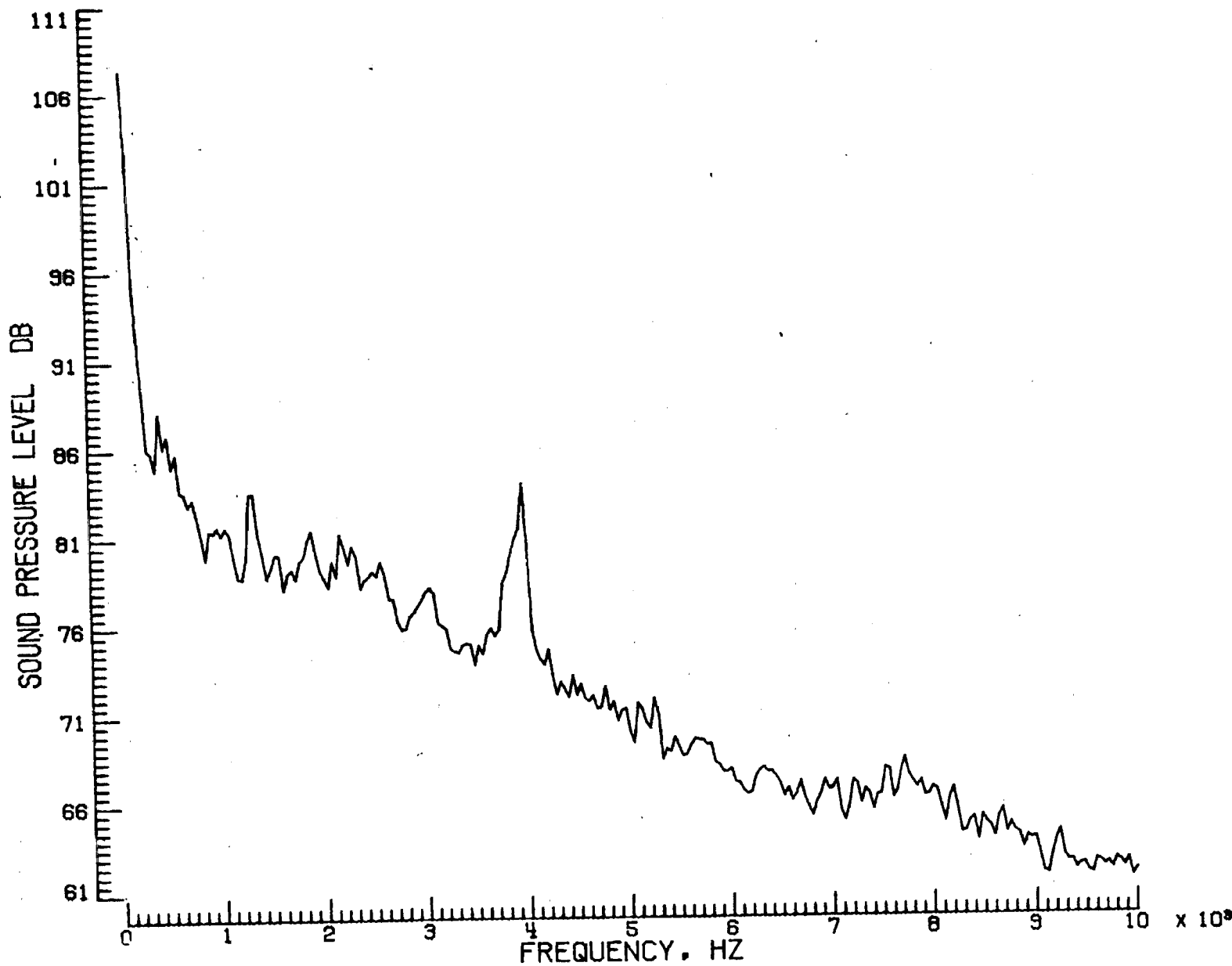
a. Mic. no. 1.

Figure 14. - Effect of descent angle variation on noise generated by helicopter model with end-plate tips installed. $V_{\infty} = 50.4$ knots.



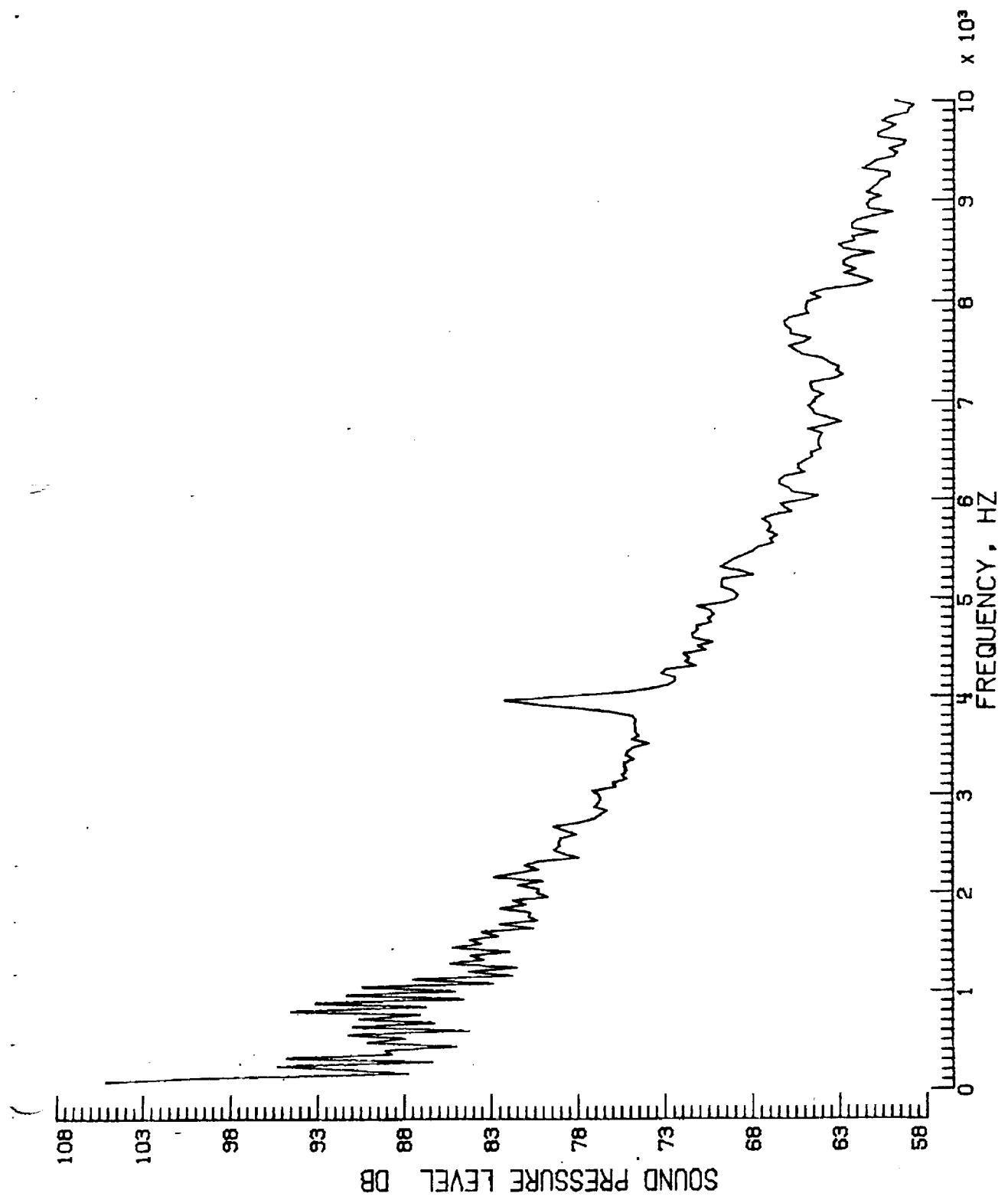
b. Pressure-time histories, Mic. no. 1.

Figure 14. - Continued.



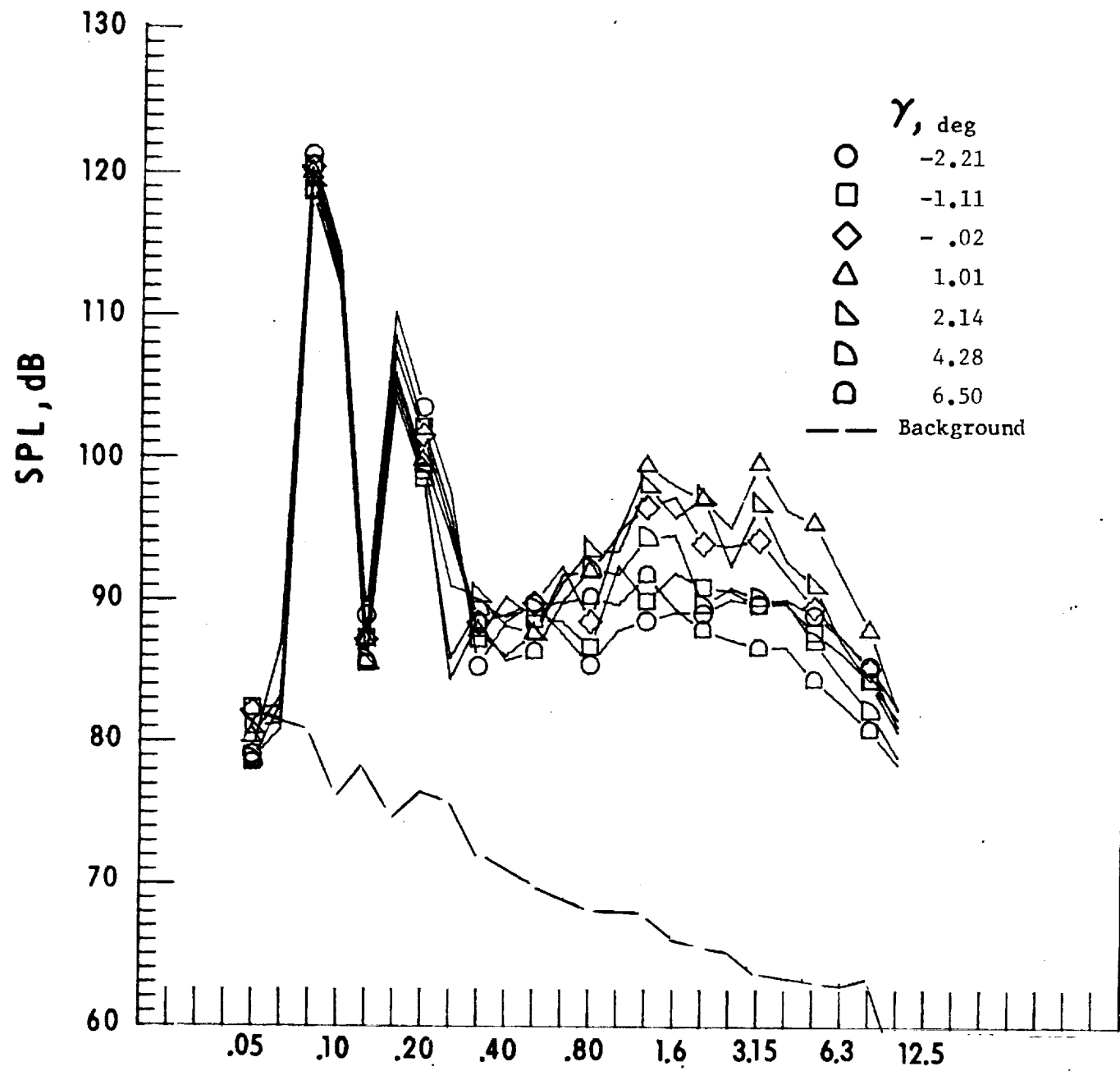
c. Narrow band analysis, Mic. no. 1, $\gamma = -2.21^0$.

Figure 14. - Continued.



d. Narrow band analysis, Mic. no. 1, $\gamma = 2.14^0$.

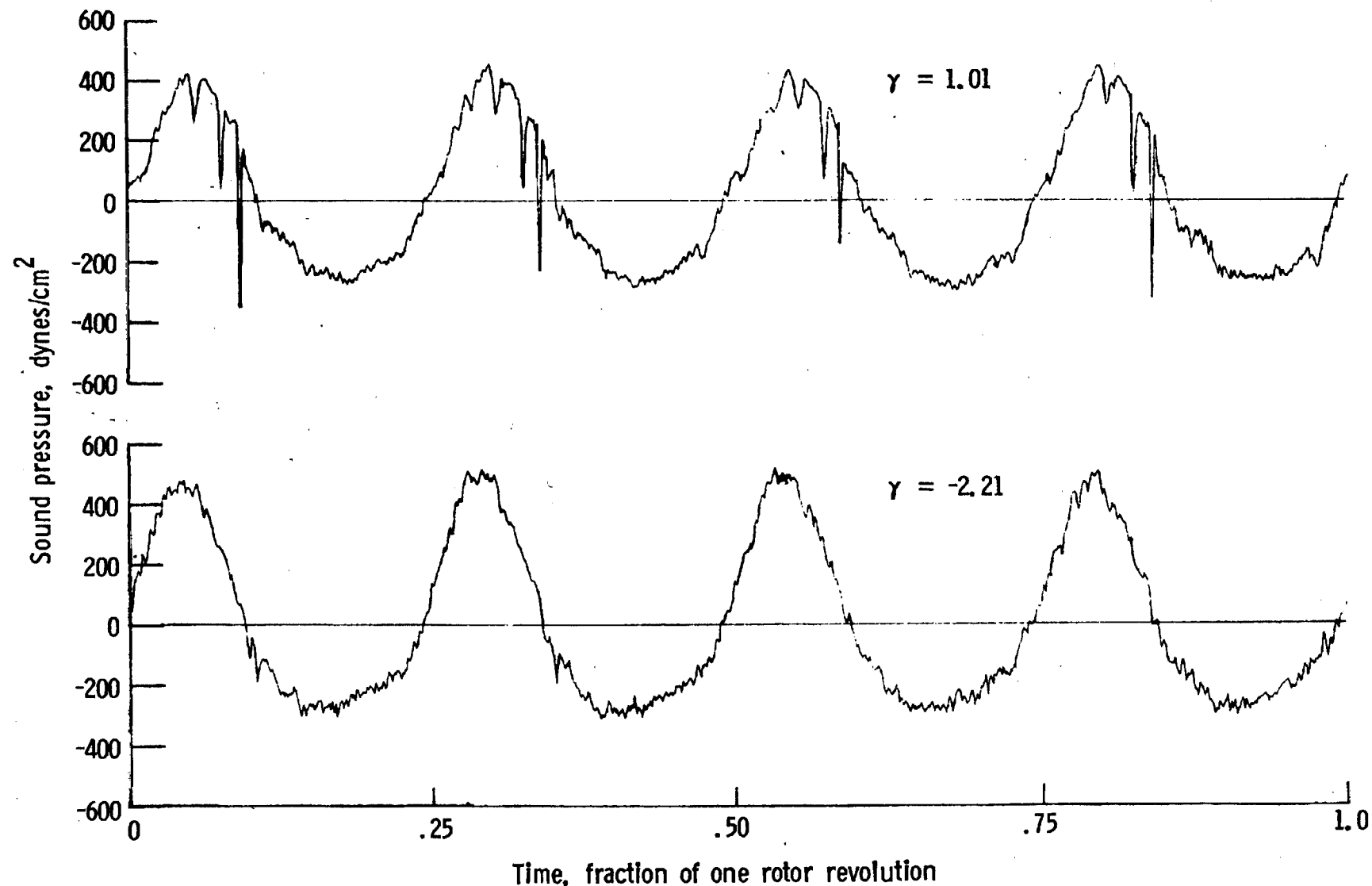
Figure 14. - Continued.



One-third-octave-band center frequency, kHz

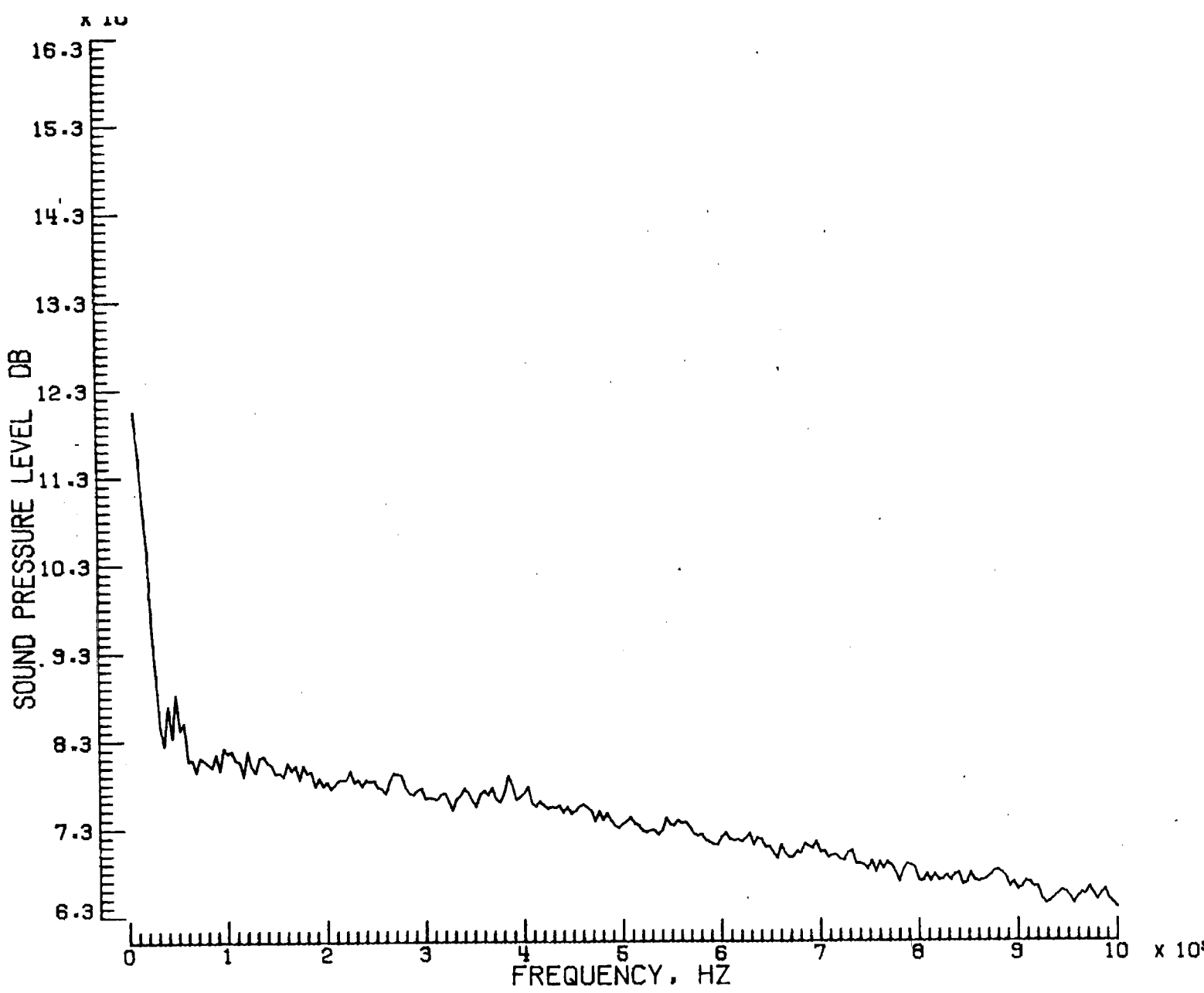
e. Mic. no. 2.

Figure 14. - Continued.



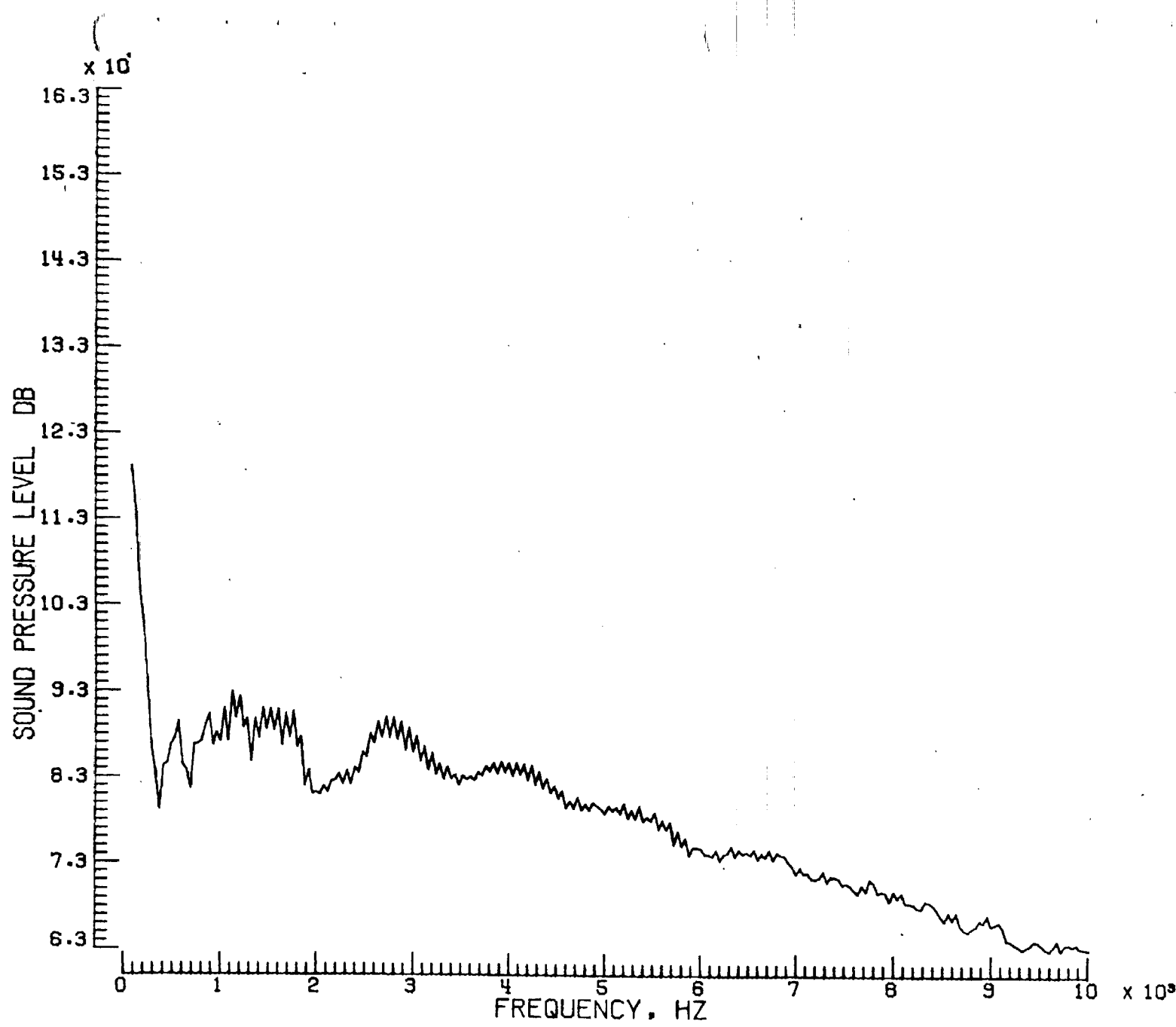
f. Pressure-time histories, Mic. no. 2.

Figure 14. - Continued.



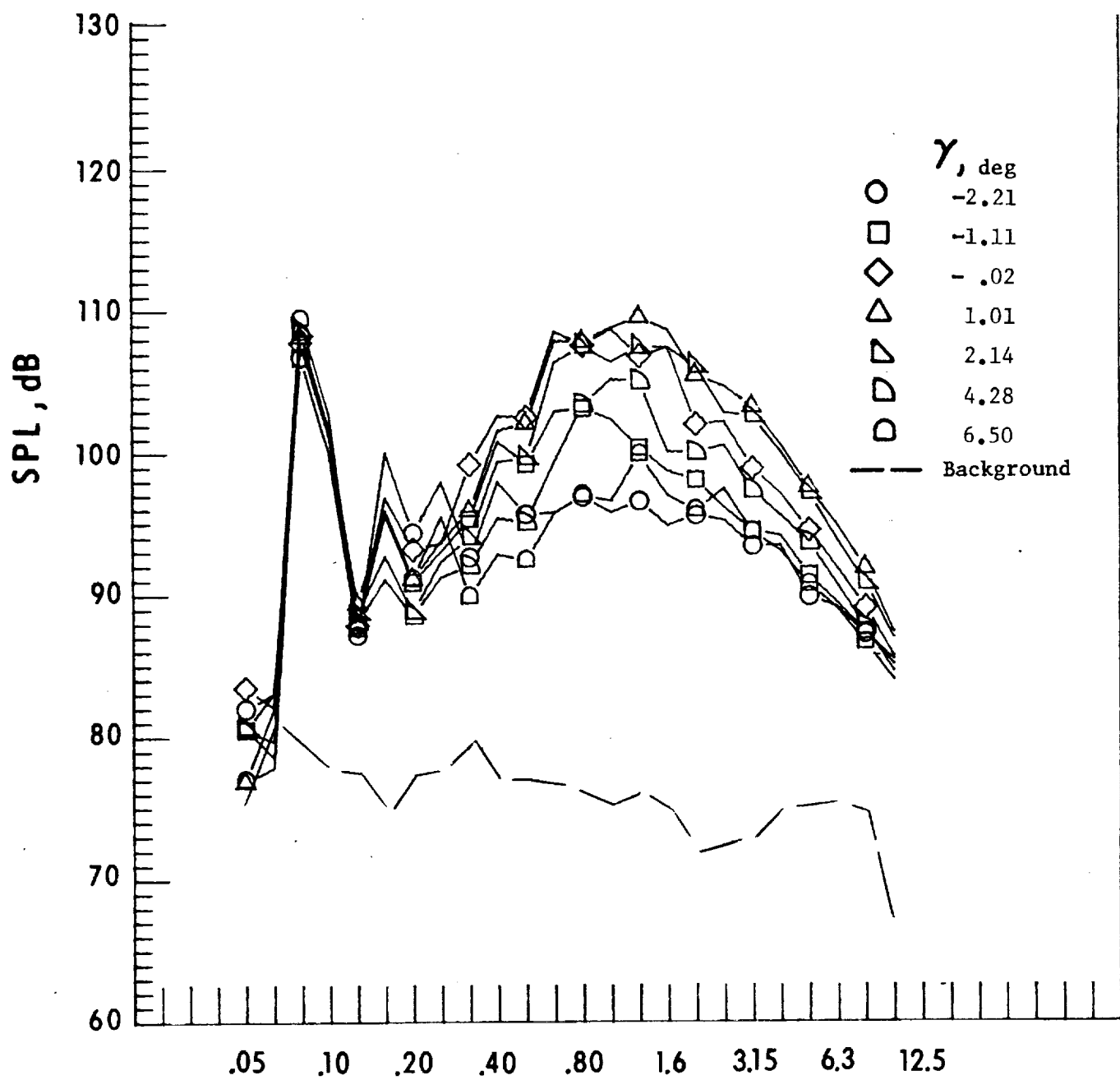
g. Narrow band analysis, Mic. no. 2, $\gamma = -2.21^\circ$.

Figure 14. - Continued.



h. Narrow band analysis, Mic. no. 2, $\gamma = 1.01^0$.

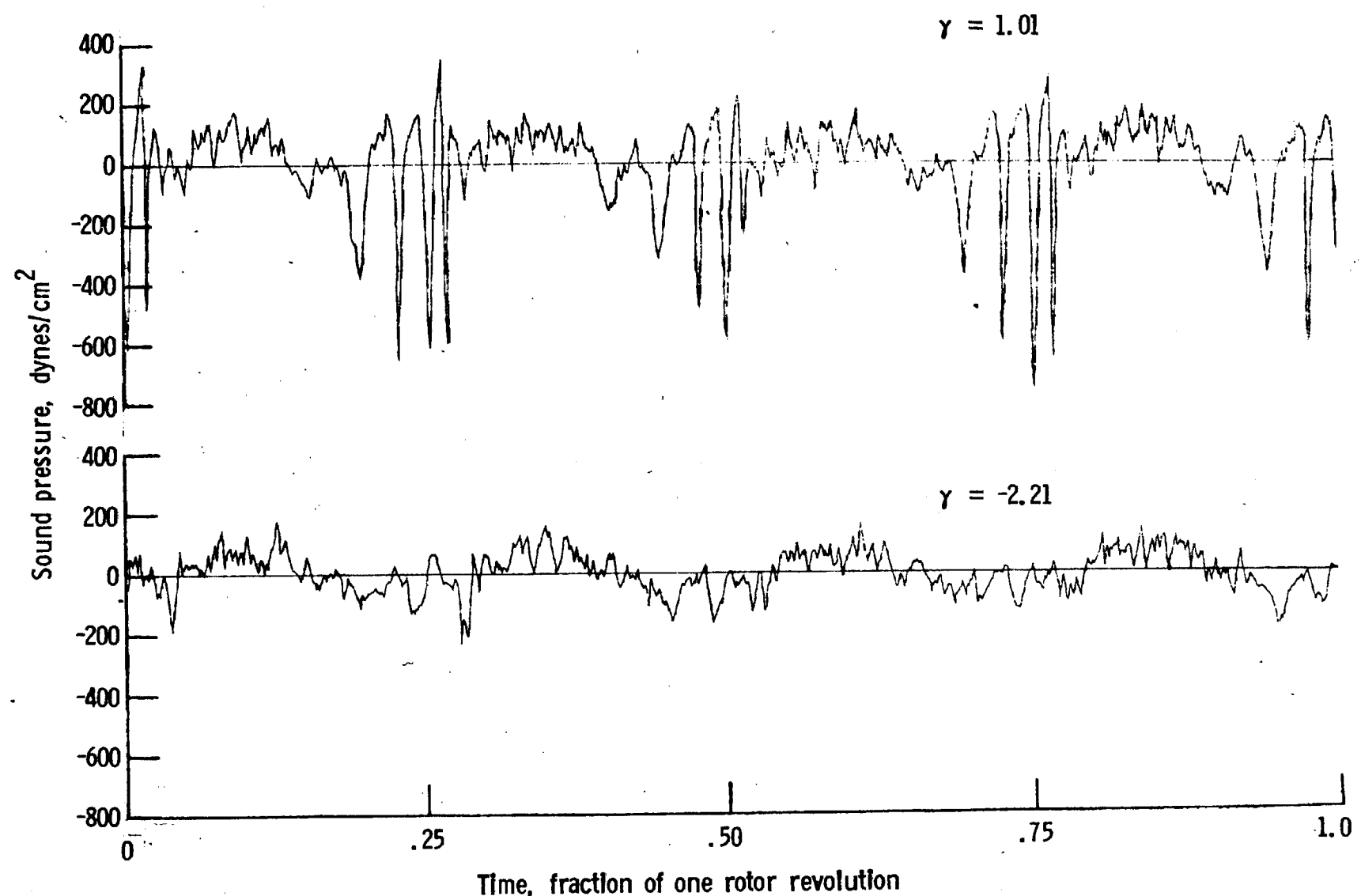
Figure 14. - Continued.



One-third-octave-band center frequency, kHz

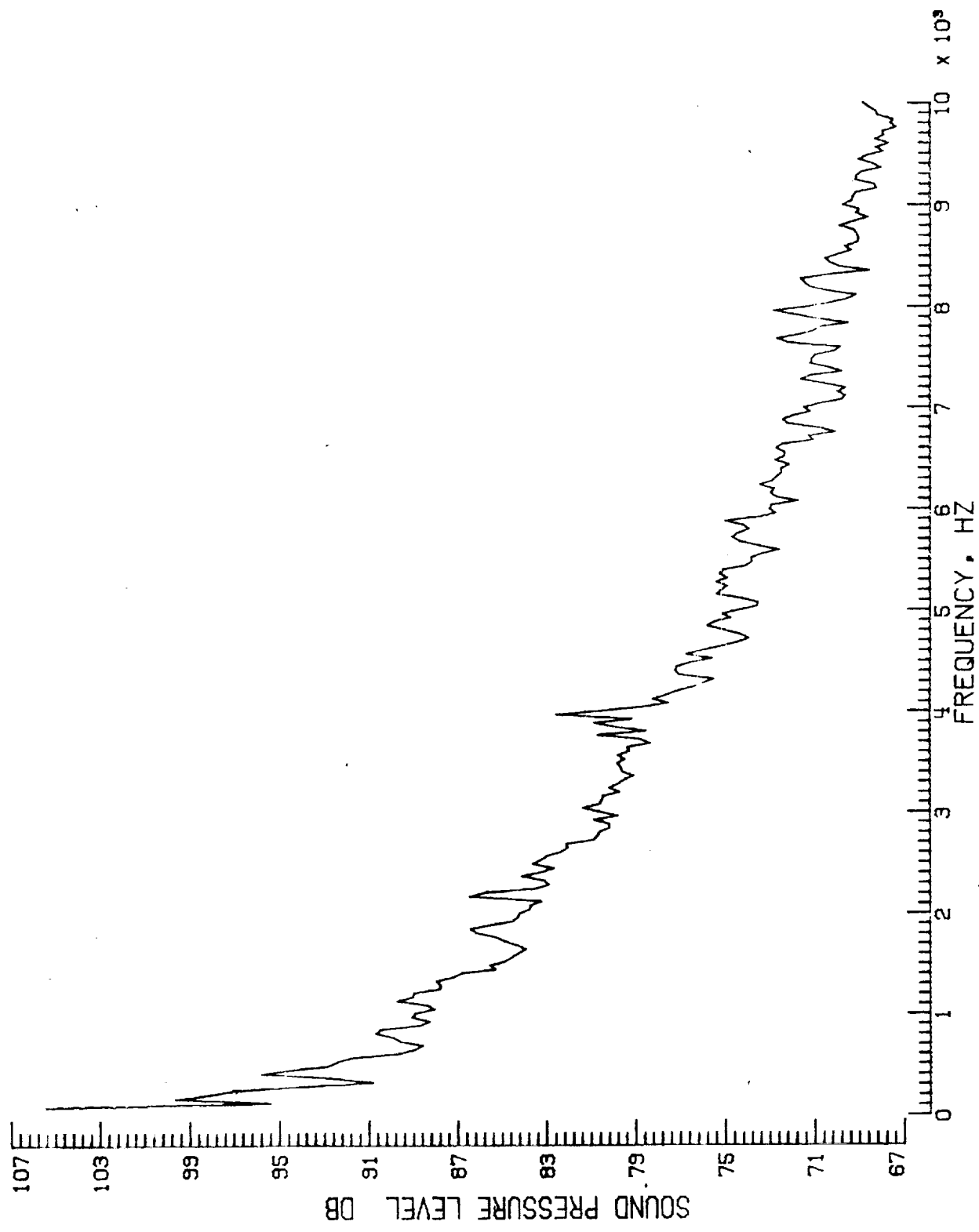
i. Mic. no. 3.

Figure 14. - Continued.



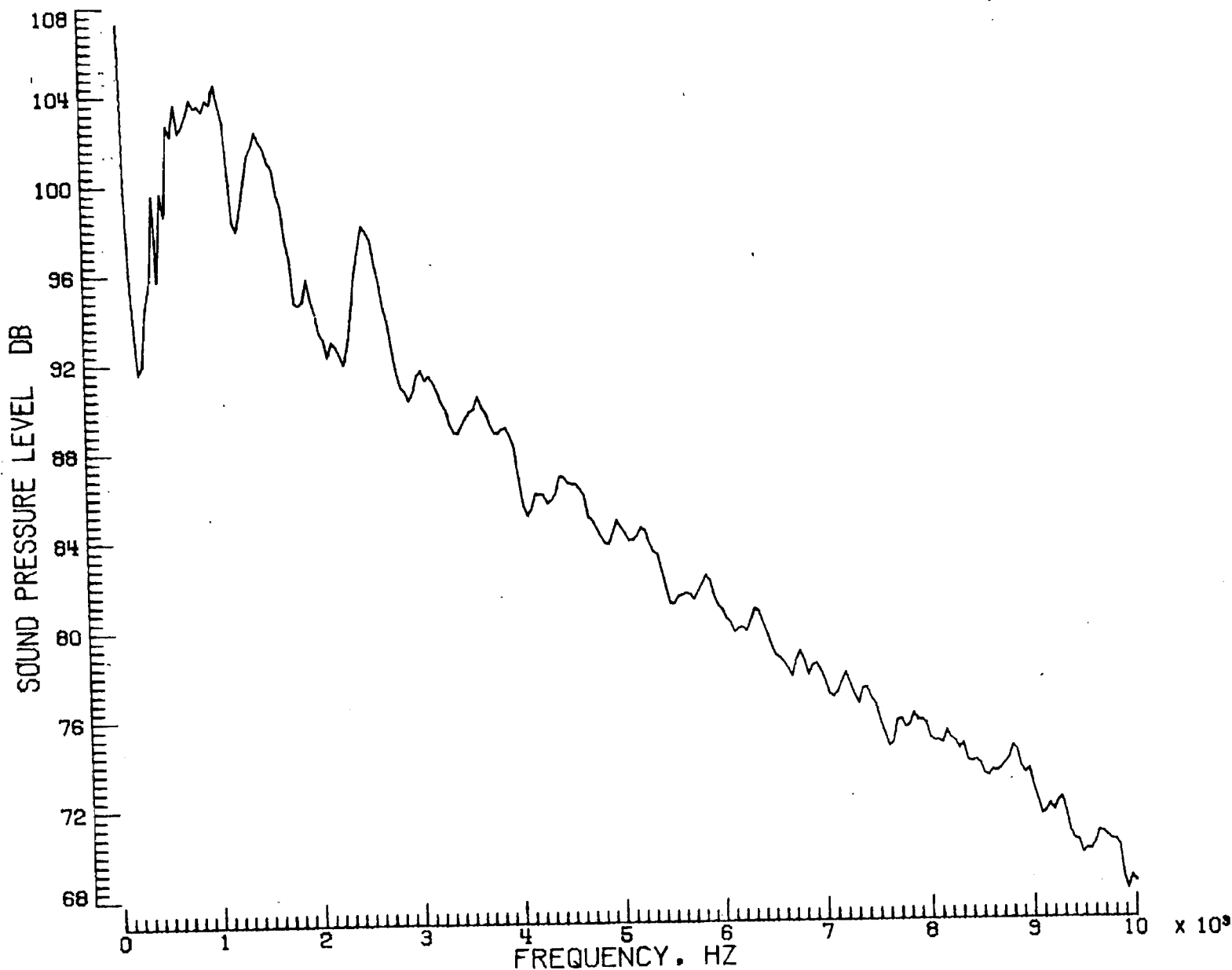
j. Pressure-time histories, Mic. no. 3.

Figure 14. - Continued.



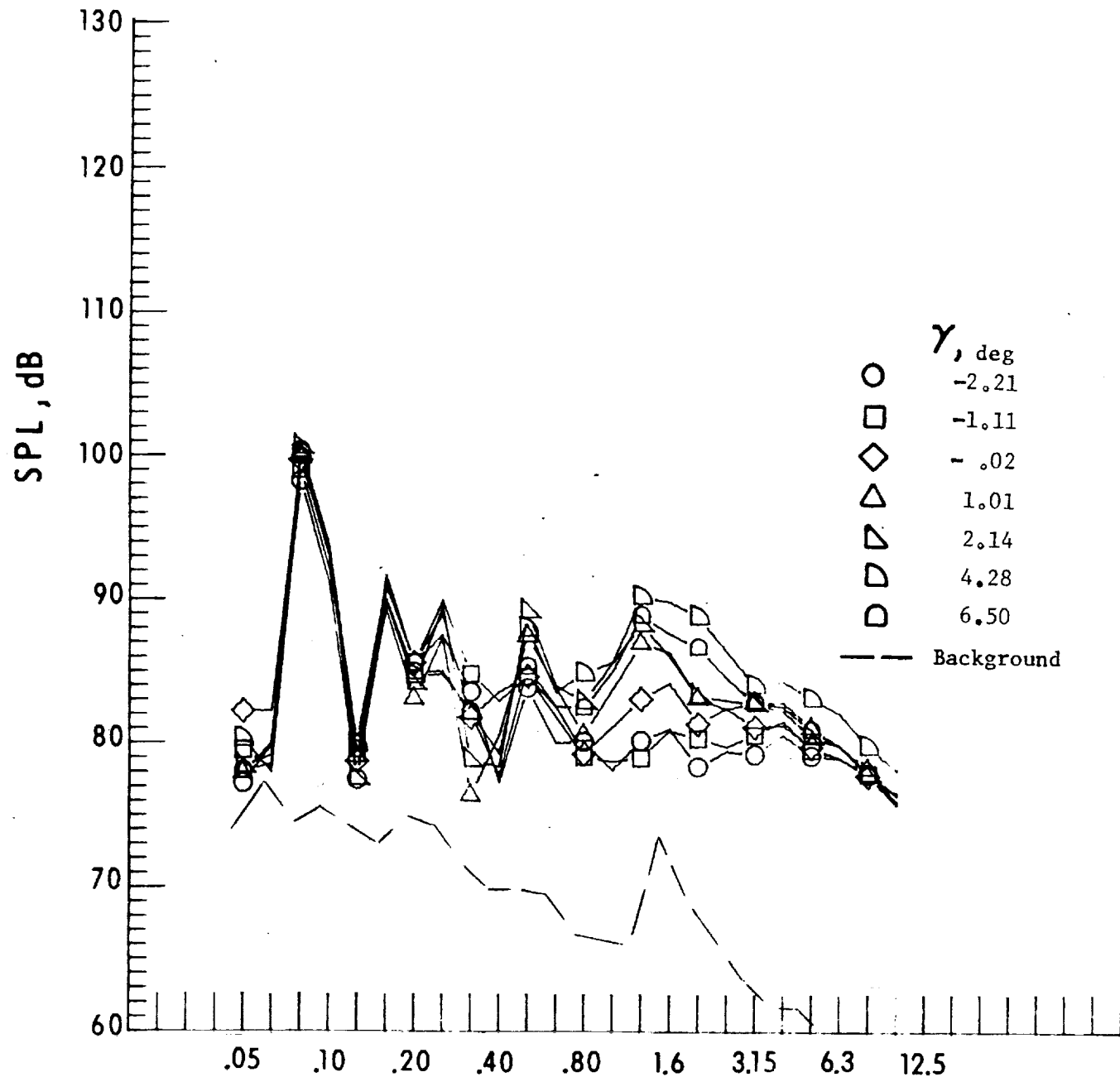
k. Narrow band analysis, Mic. no. 3, $\gamma = -2.21^{\circ}$.

Figure 14.- Continued.



I. Narrow band analysis, Mic. no. 3, $\gamma = 1.01^0$.

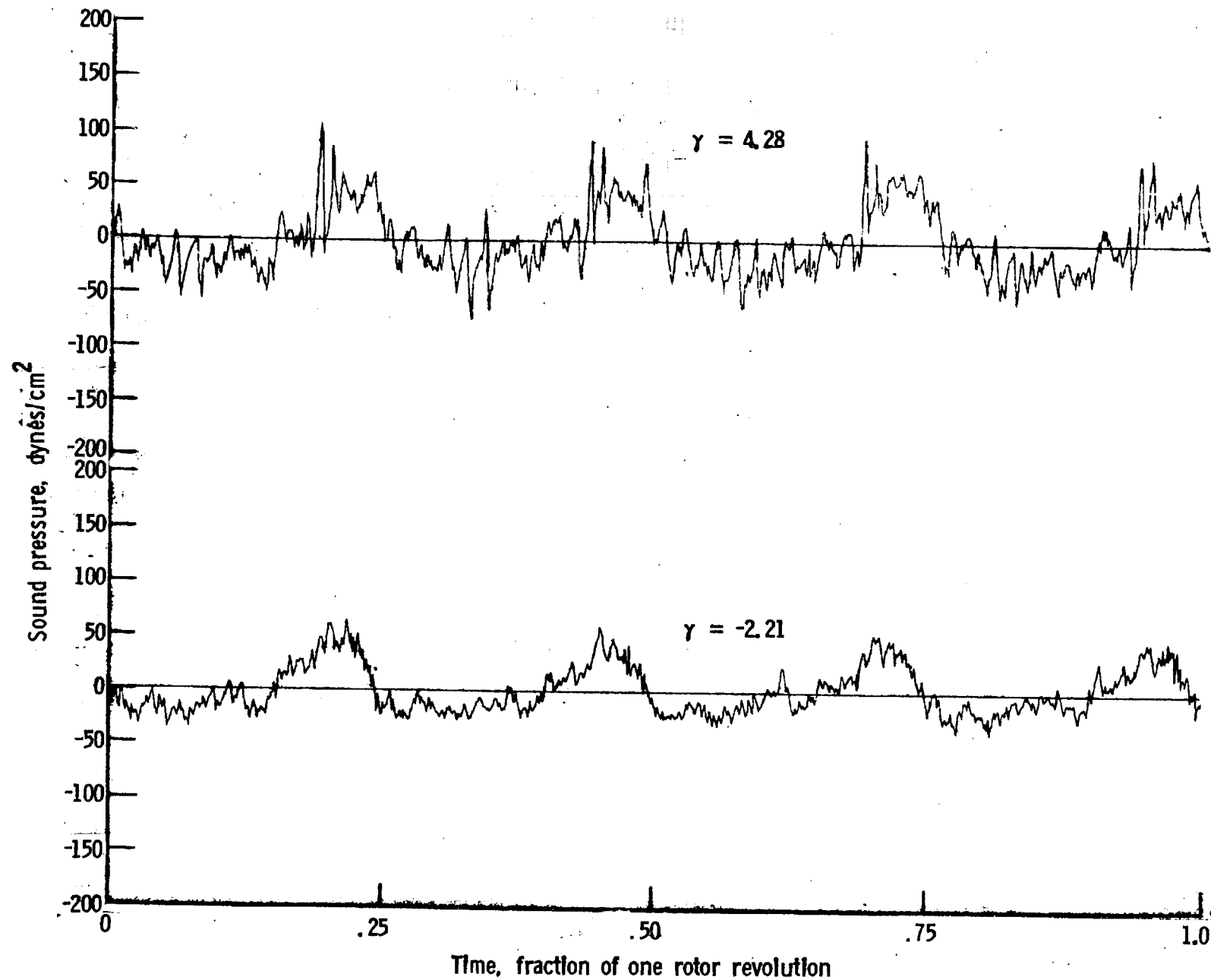
Figure 14. - Continued.



One-third-octave-band center frequency, kHz

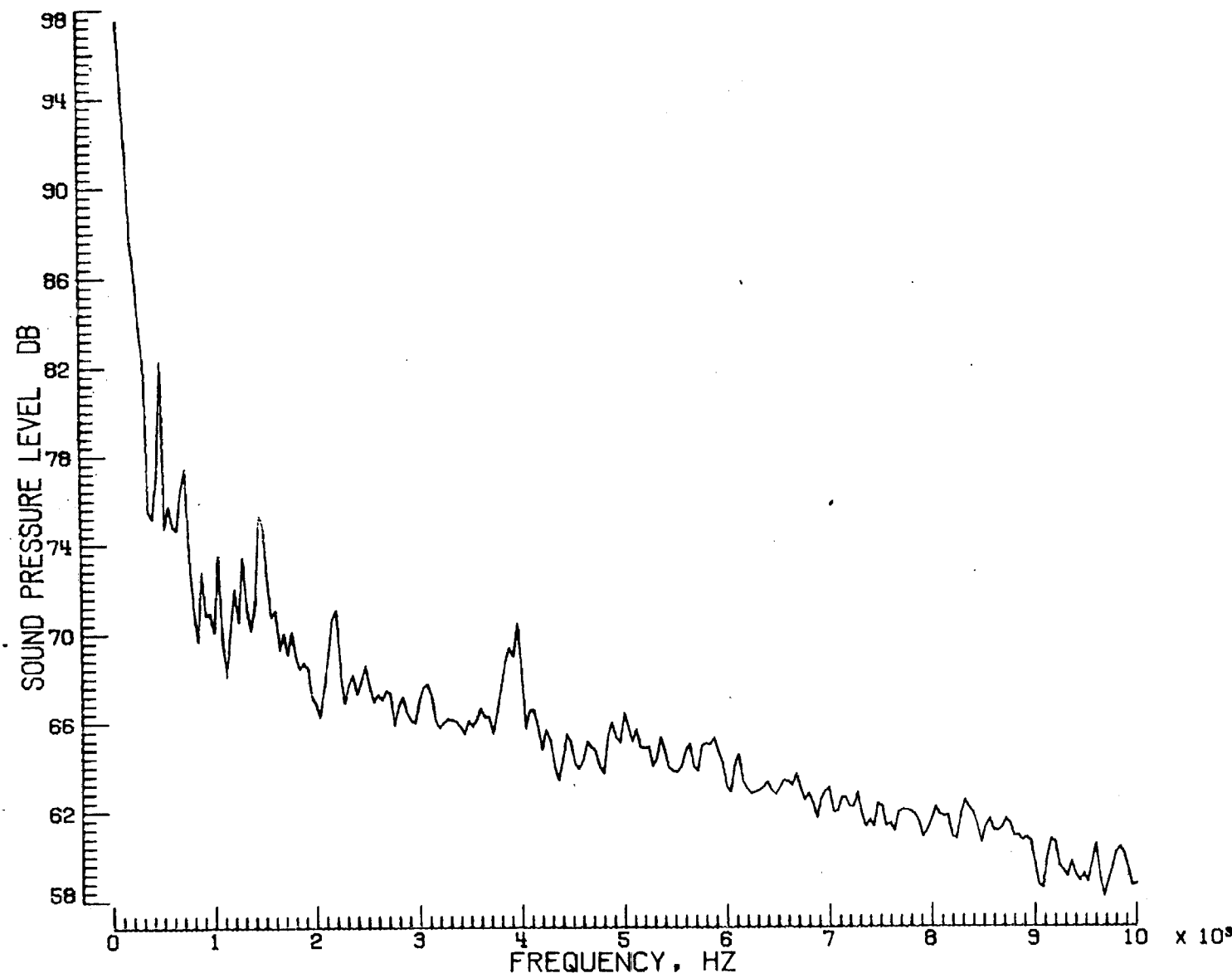
m. Mic. no. 4.

Figure 14. - Continued.



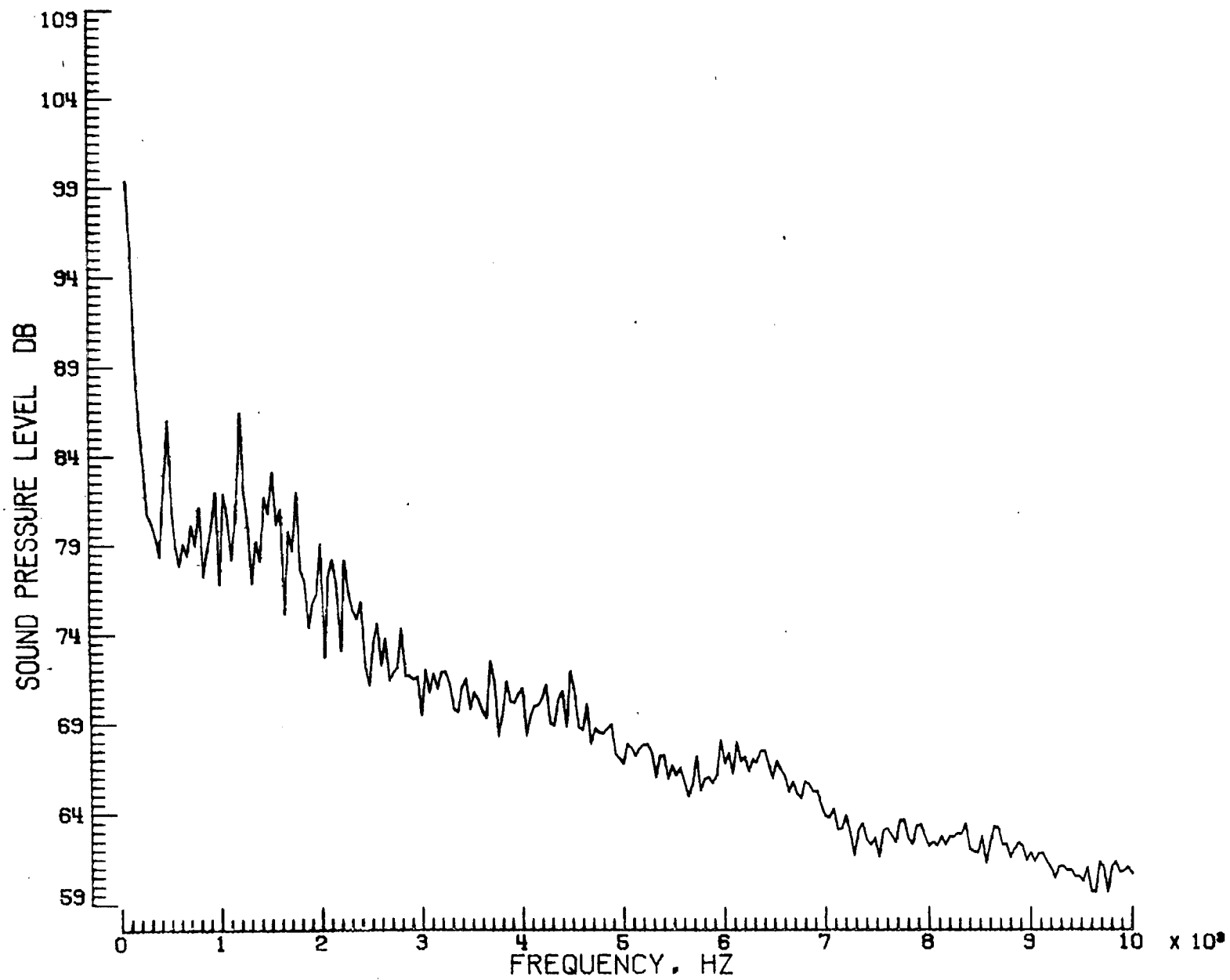
n. Pressure-time histories, Mic. no. 4.

Figure 14. - Continued.



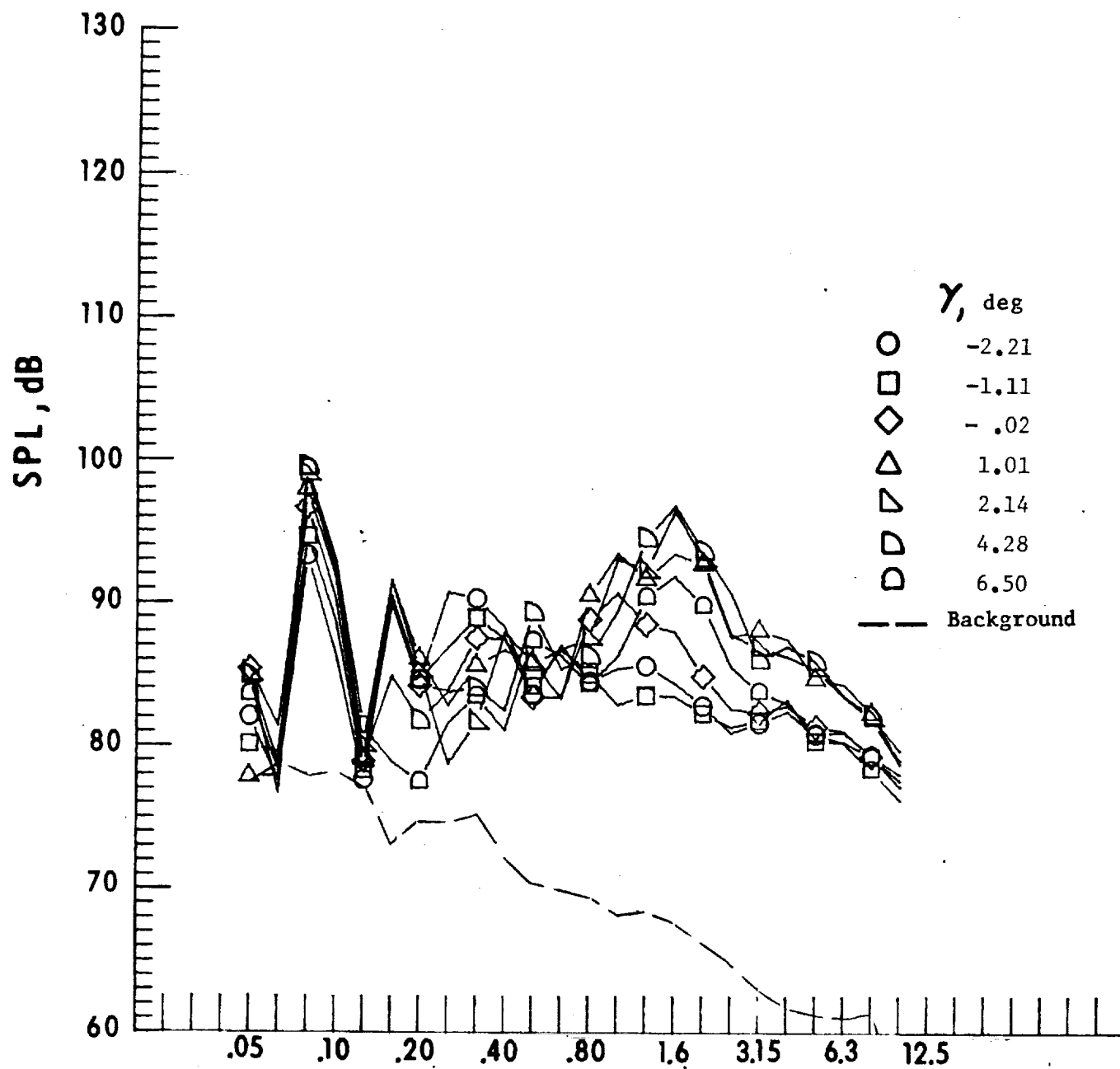
o. Narrow band analysis, Mic. no. 4, $\gamma = -2.21^0$.

Figure 14. - Continued.



p. Narrow band analysis, Mic. no. 4, $\gamma = 4.28^0$.

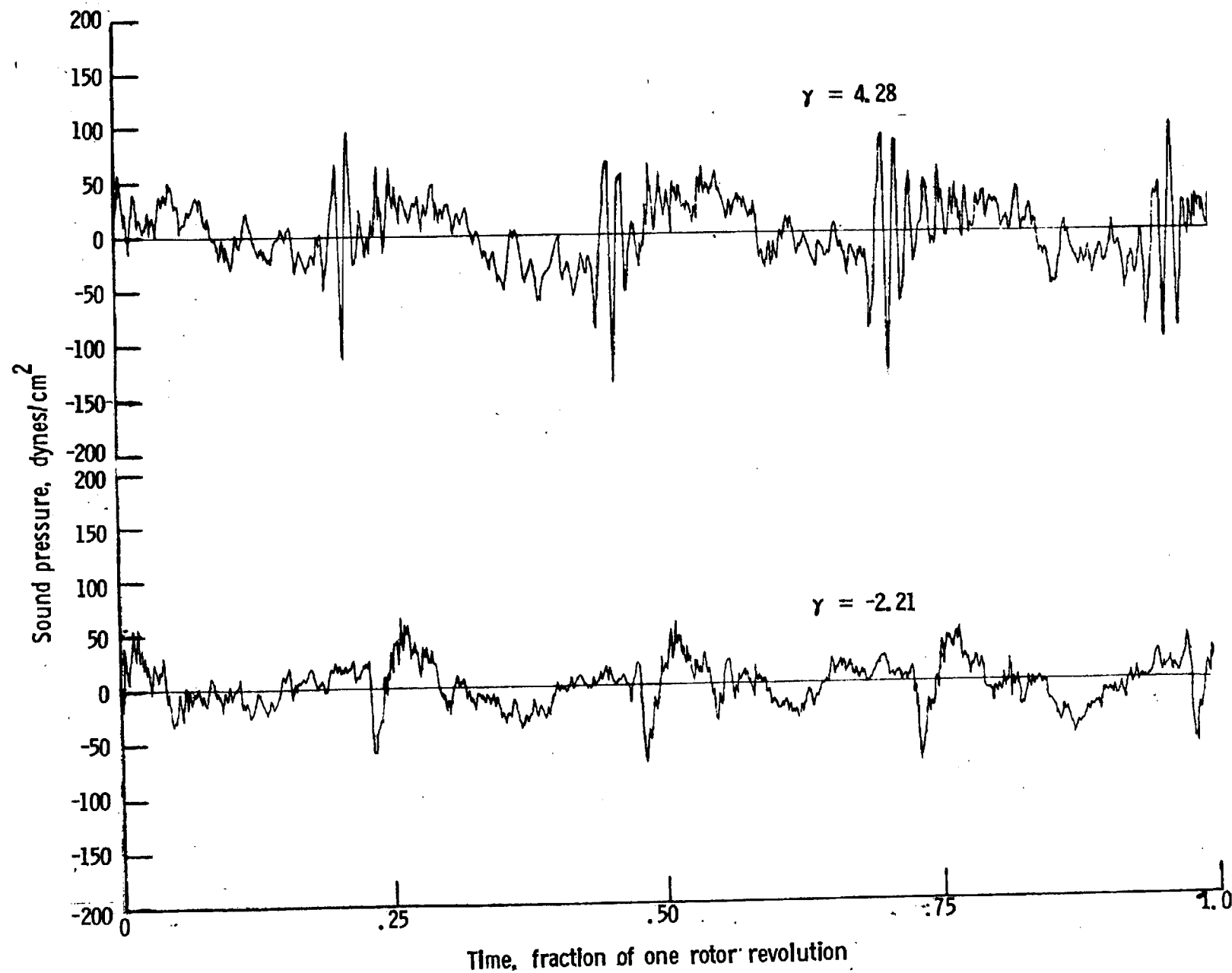
Figure 14 - Continued



One-third-octave-band center frequency, kHz

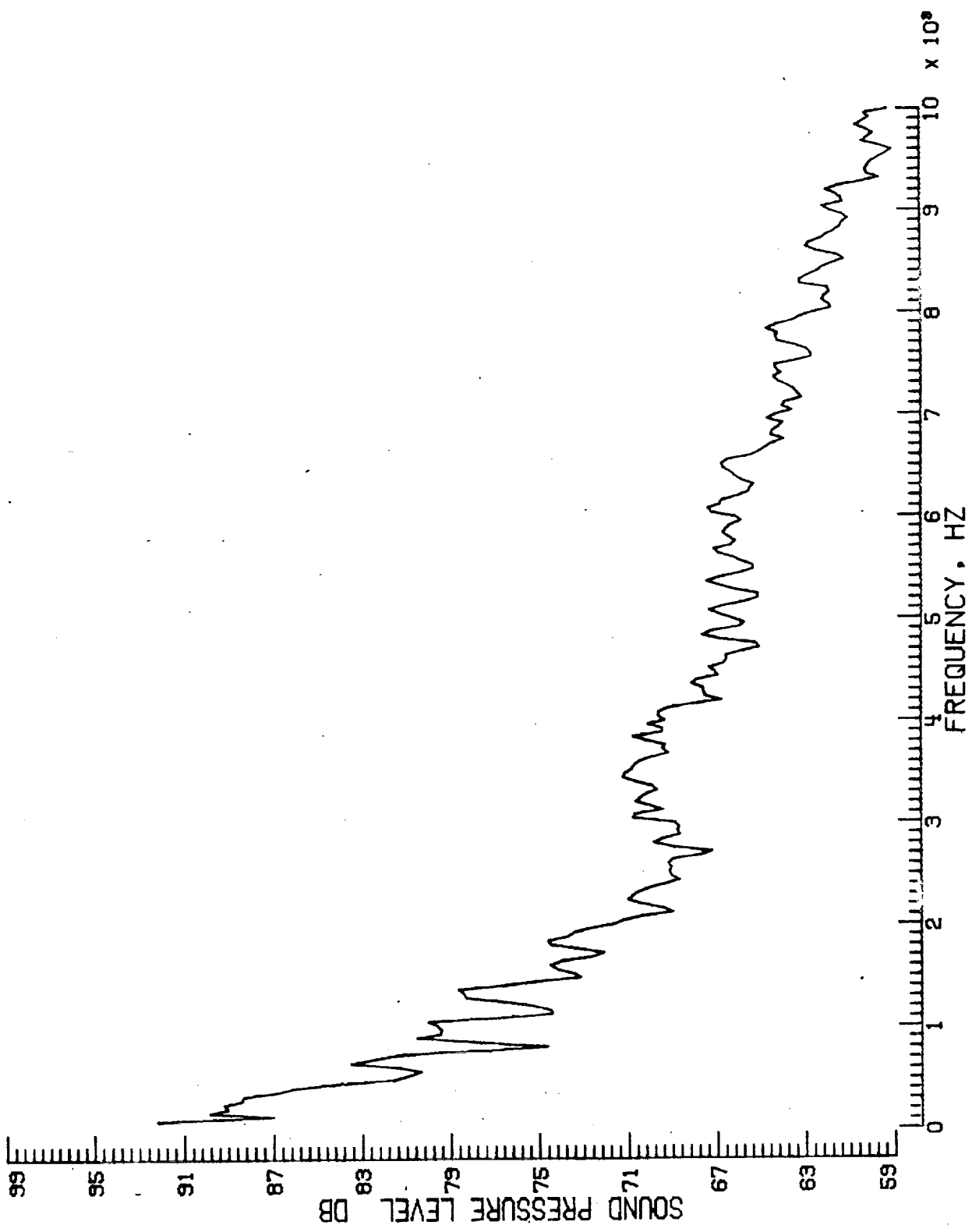
q. Mic. no. 5.

Figure 14. - Continued.



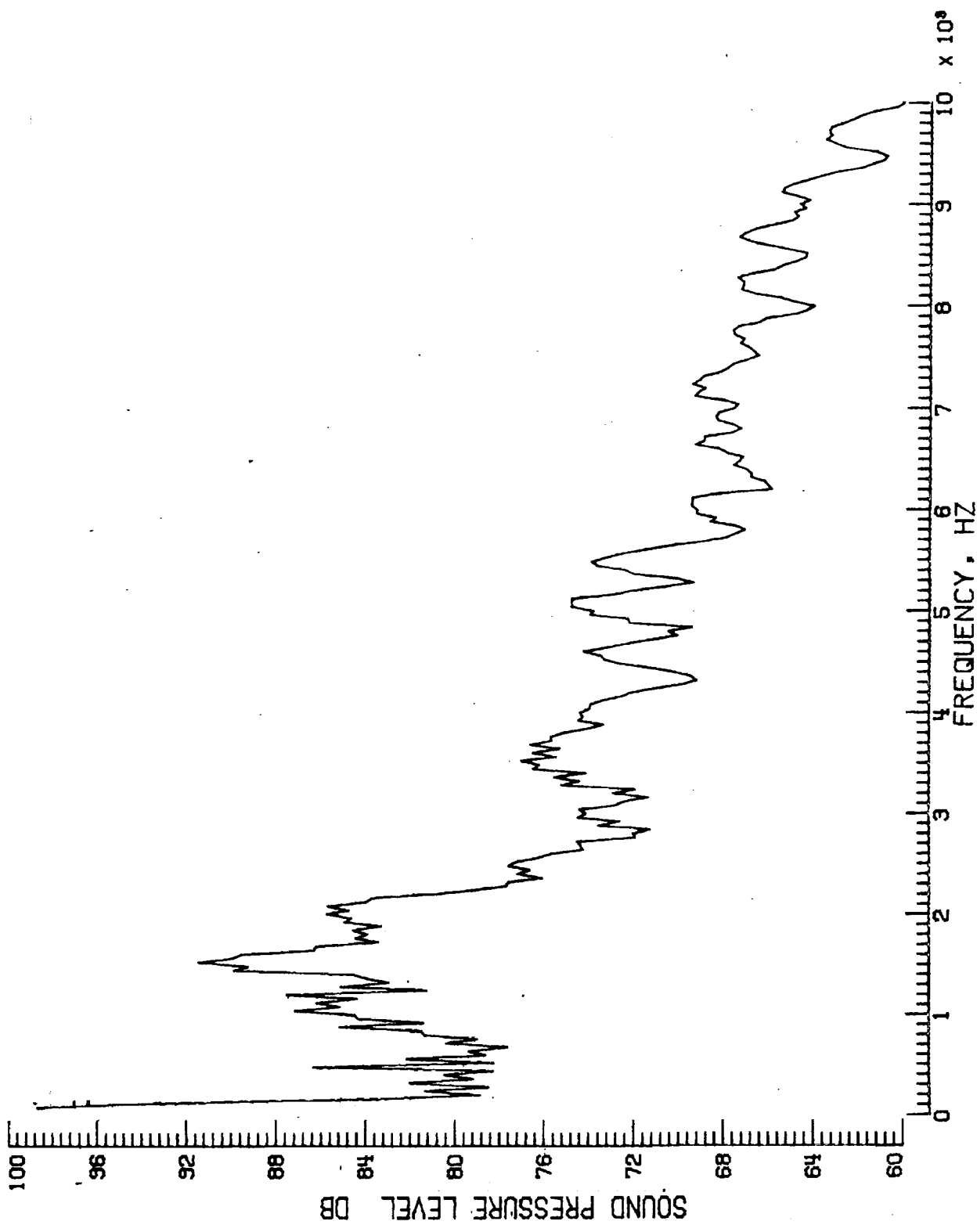
r. Pressure-time histories, Mic. no. 5.

Figure 14. - Continued.



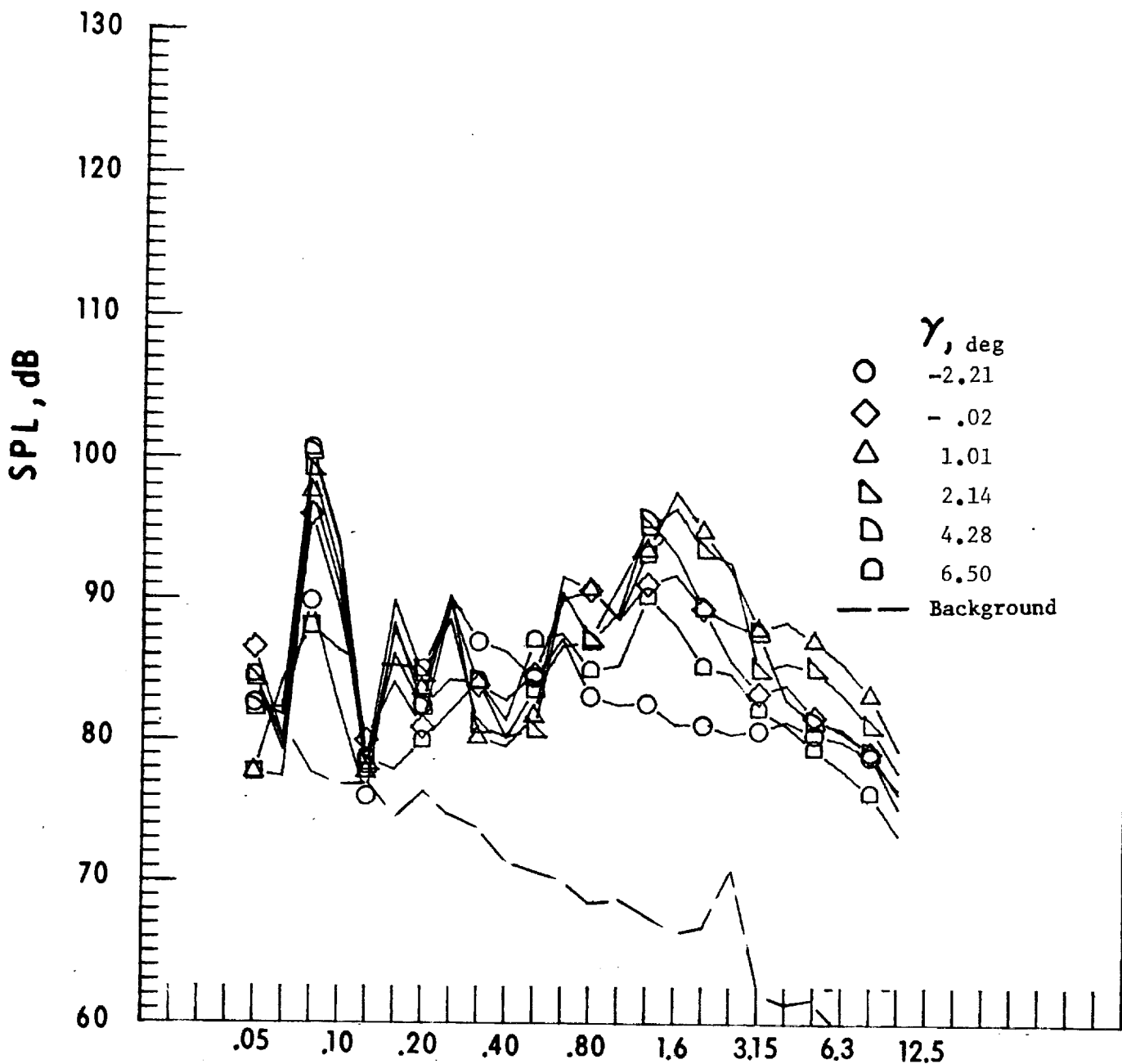
S. Narrow band analysis, Mic. no. 5, $\gamma = -2.21^\circ$.

Figure 14. - Continued.



t. Narrow band analysis, Mic. no. 5, $\gamma = 4.280$.

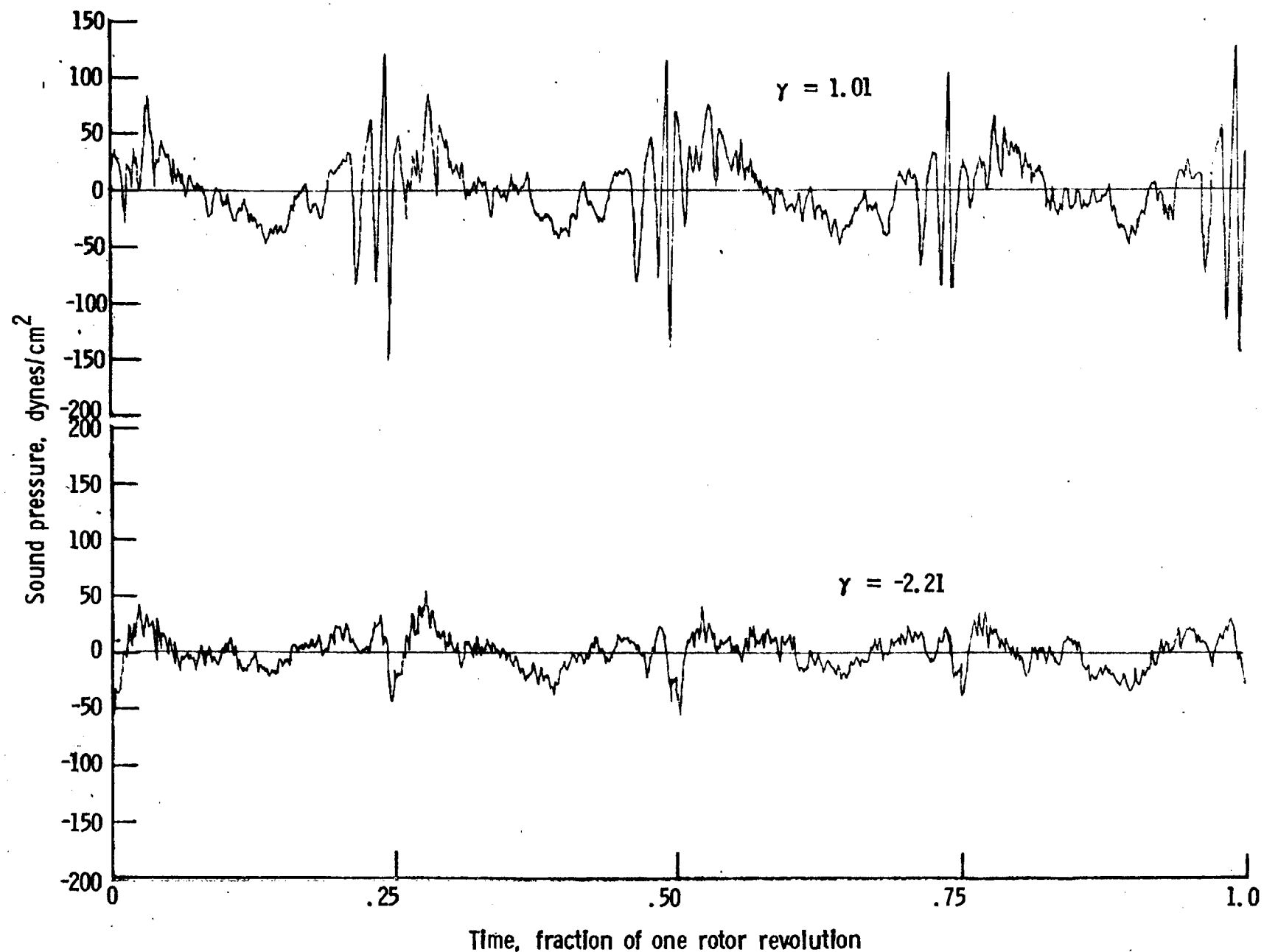
Figure 14. - Continued.



One-third-octave-band center frequency, kHz

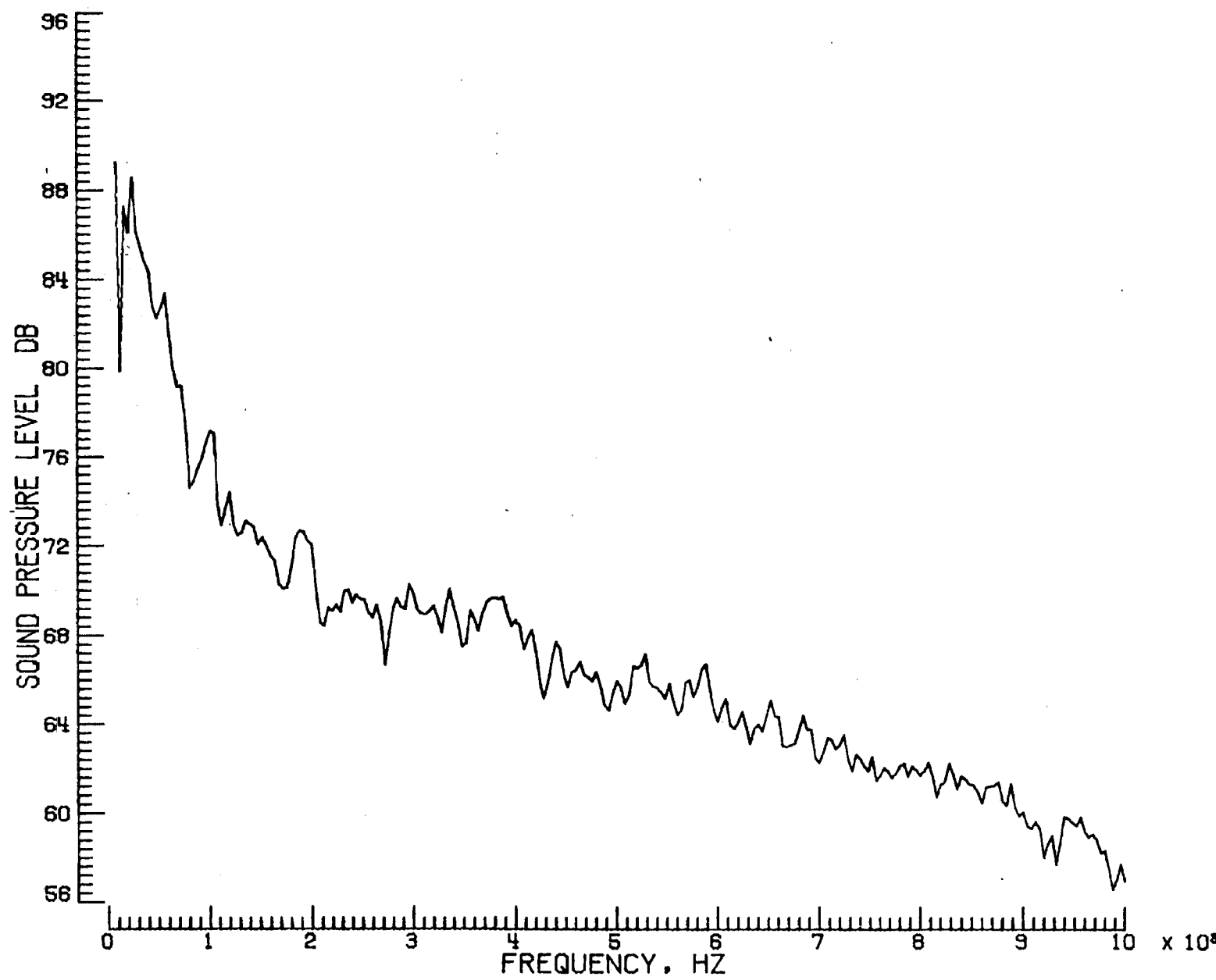
u. Mic. no. 6.

Figure 14. - Continued.



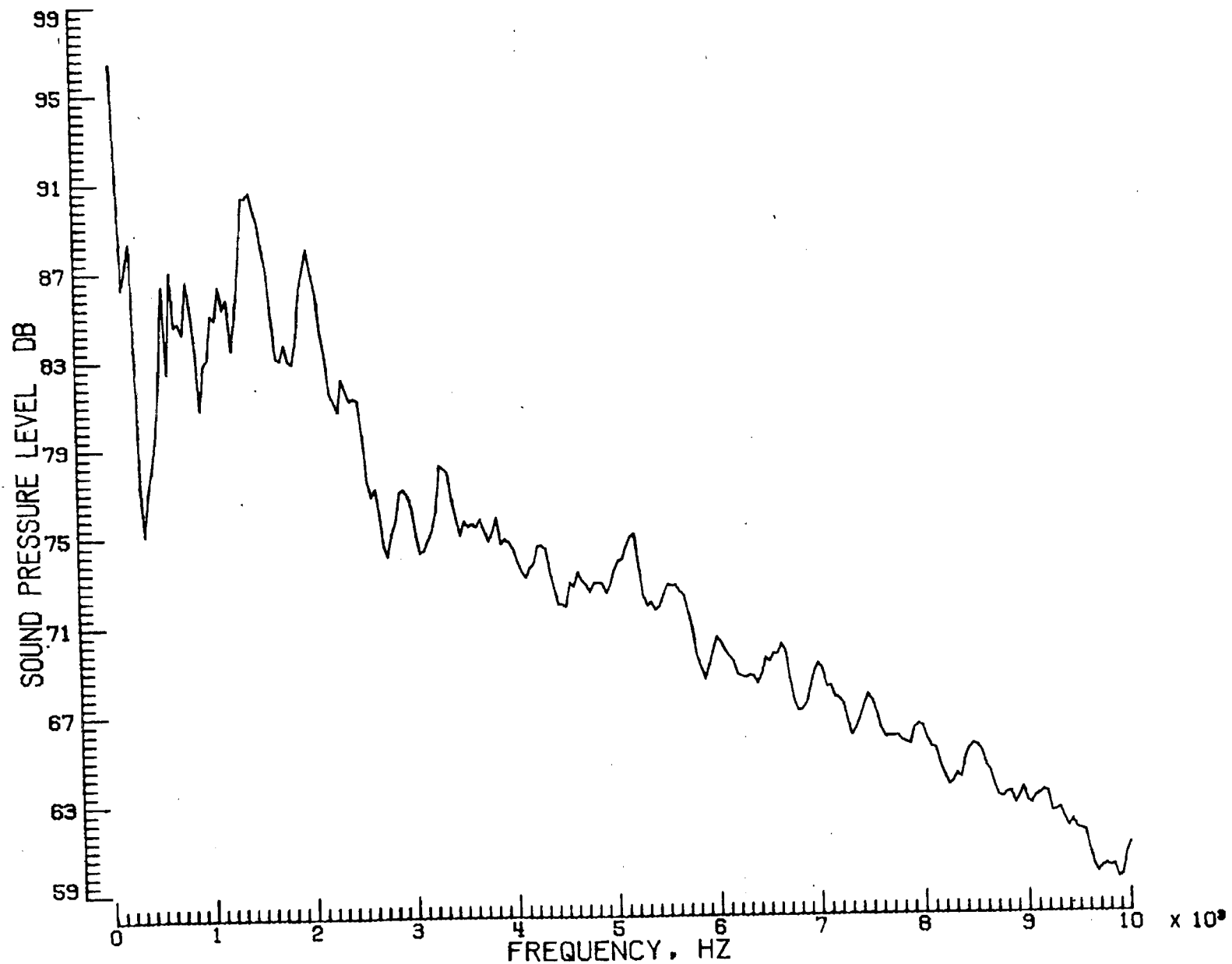
v. Pressure-time histories, Mic. no. 6.

Figure 14. - Continued



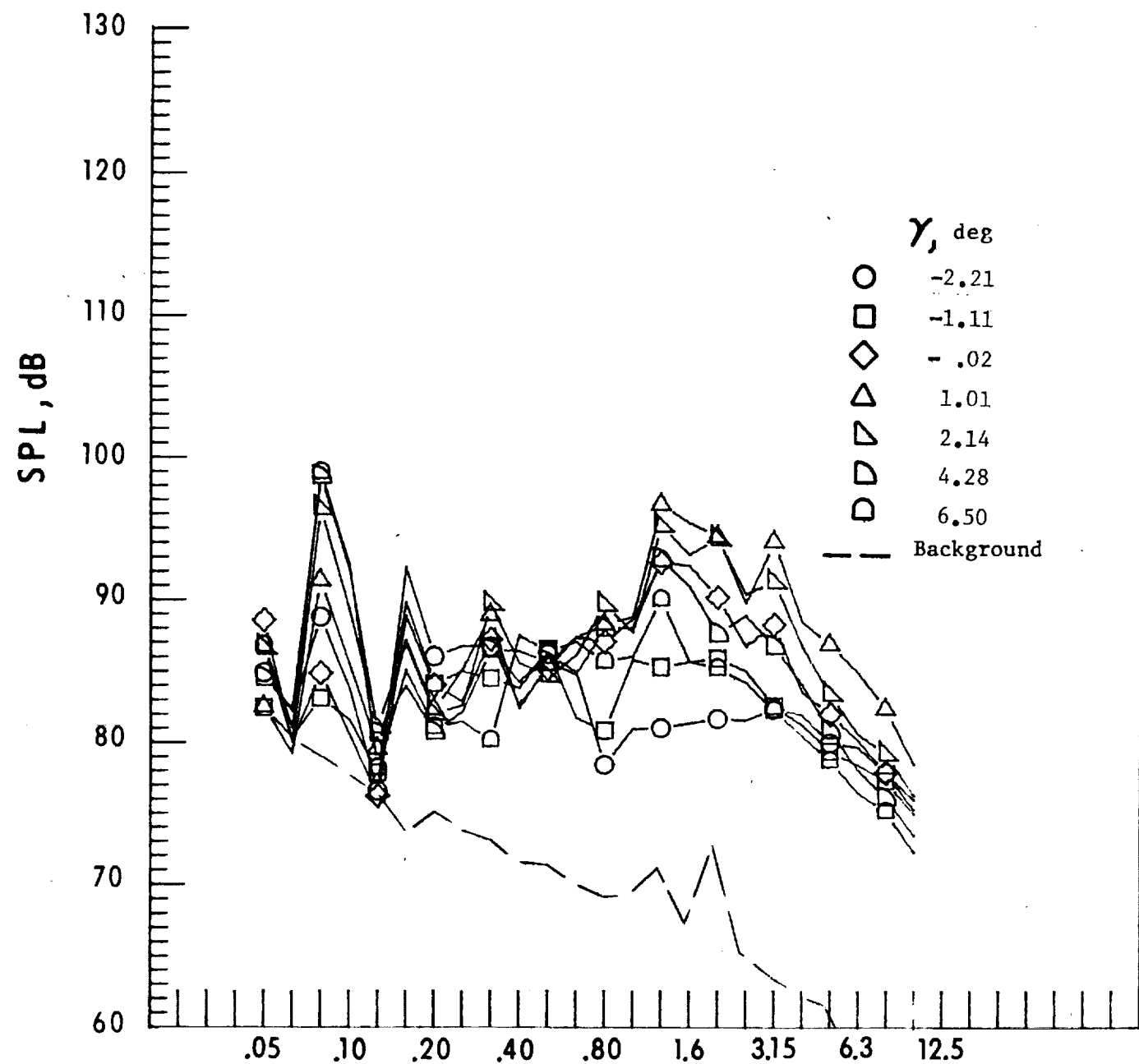
w. Narrow band analysis, Mic. no. 6, $\gamma = -2.21^\circ$.

Figure 14. - Continued.



x. Narrow band analysis, Mic. no. 7, $\gamma = 1.01^0$.

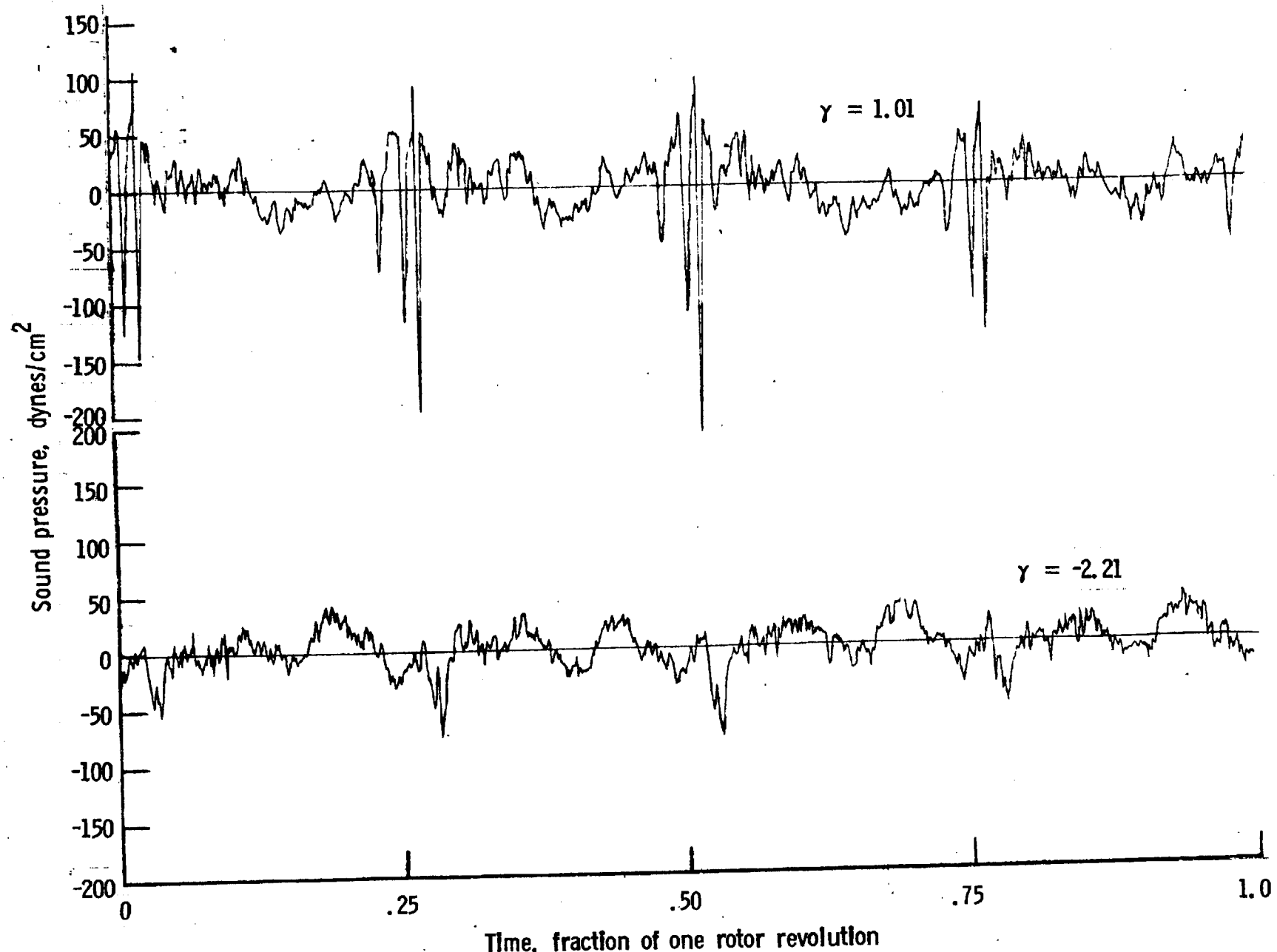
Figure 14 - Continued.



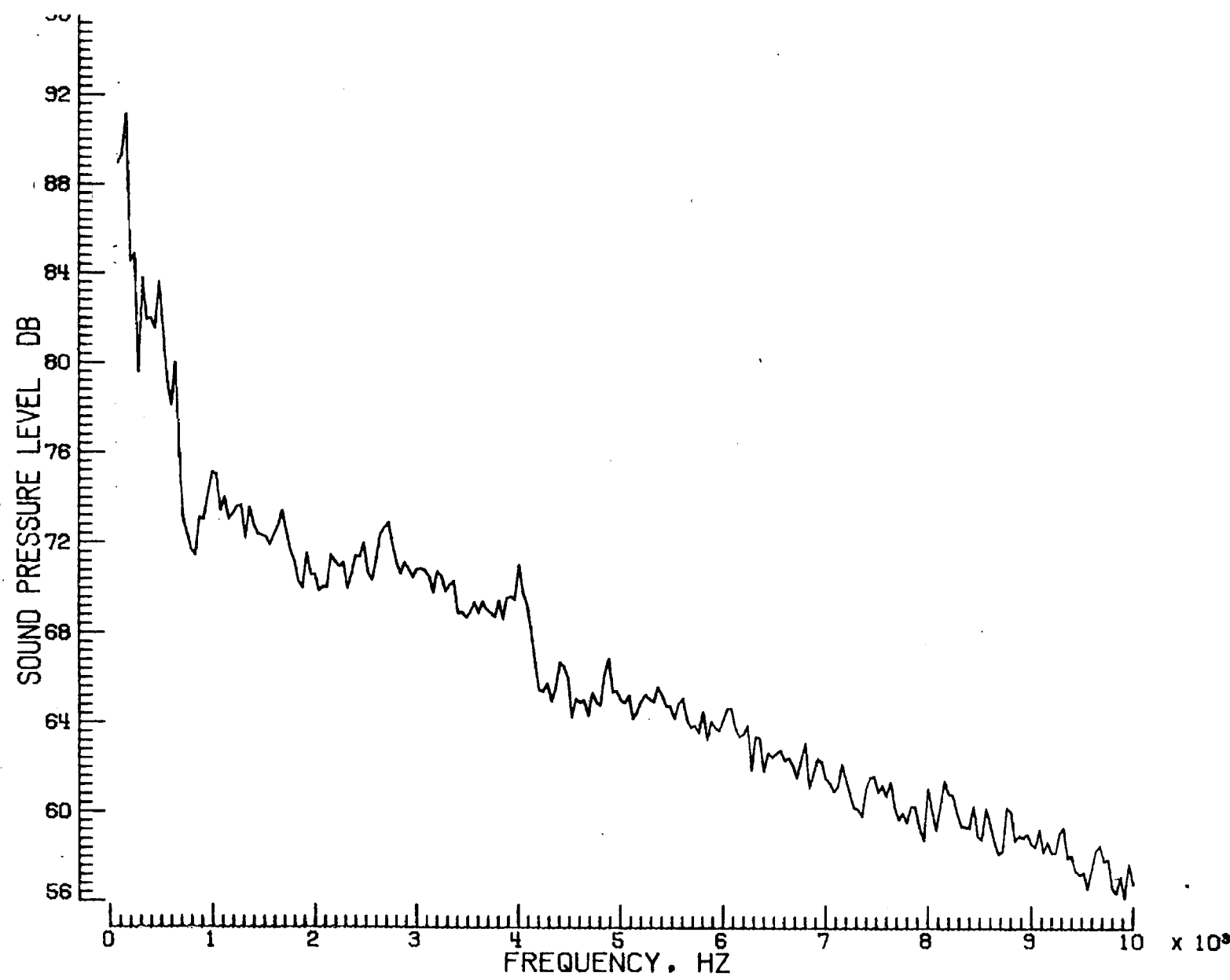
One-third-octave-band center frequency, kHz

y. Mic. no. 7.

Figure 14. - Continued.

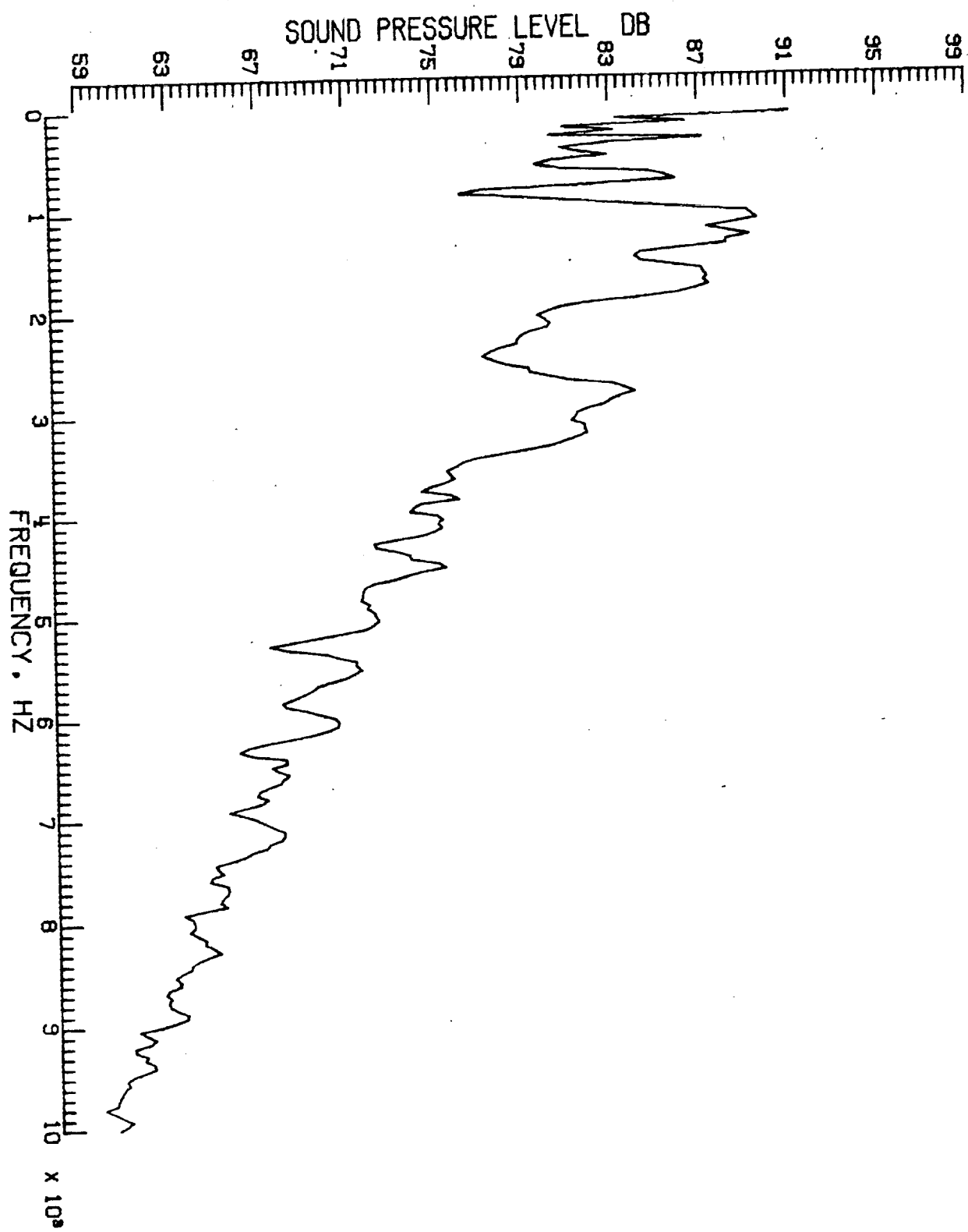


z. Pressure-time histories, Mic. no. 7.



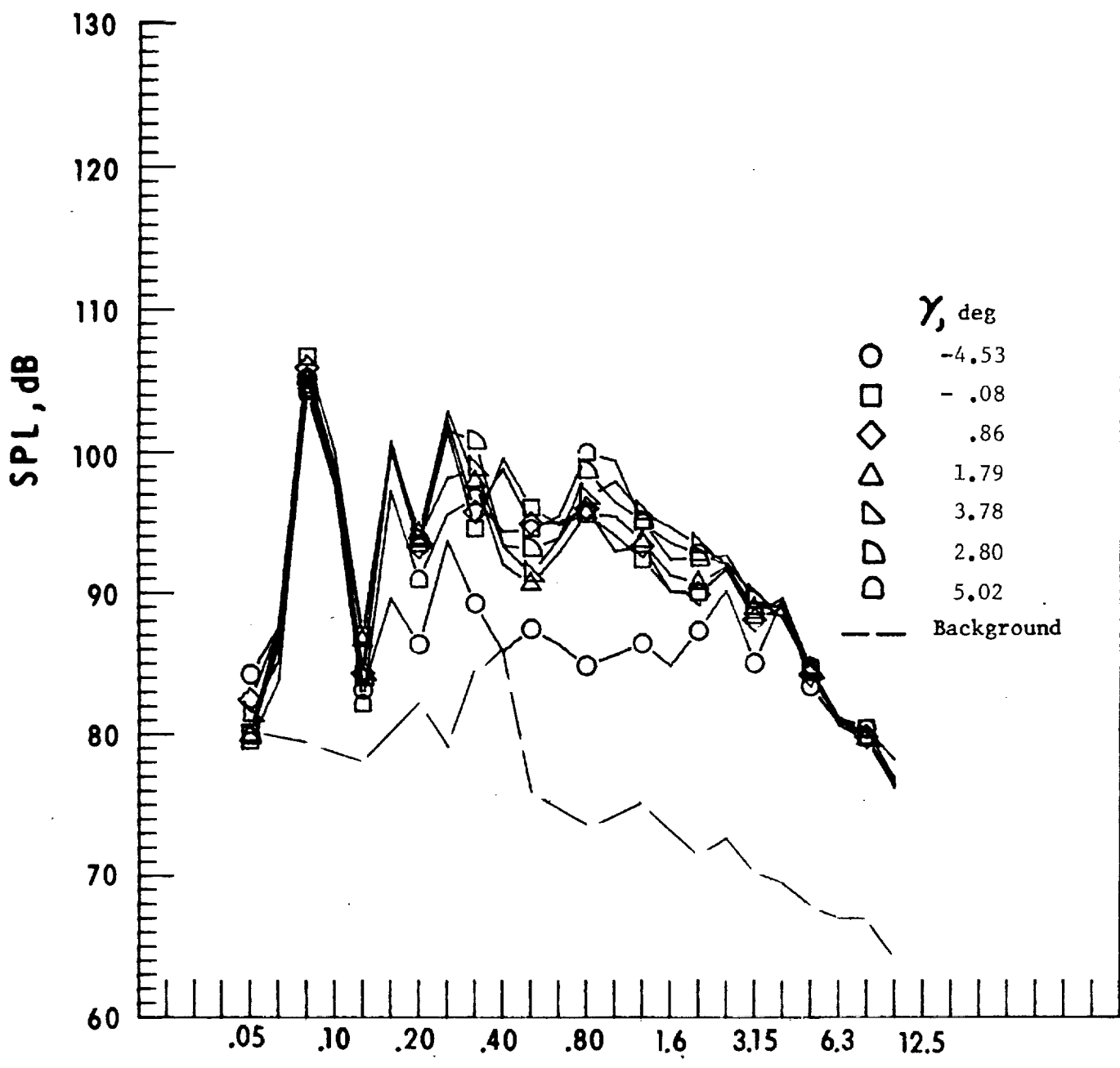
aa. Narrow band analysis, Mic. no. 7, $\gamma = -2.21^\circ$.

Figure 14. - Continued.



bb. Narrow band analysis, Mic. no. 7, $\gamma = 1.01^0$.

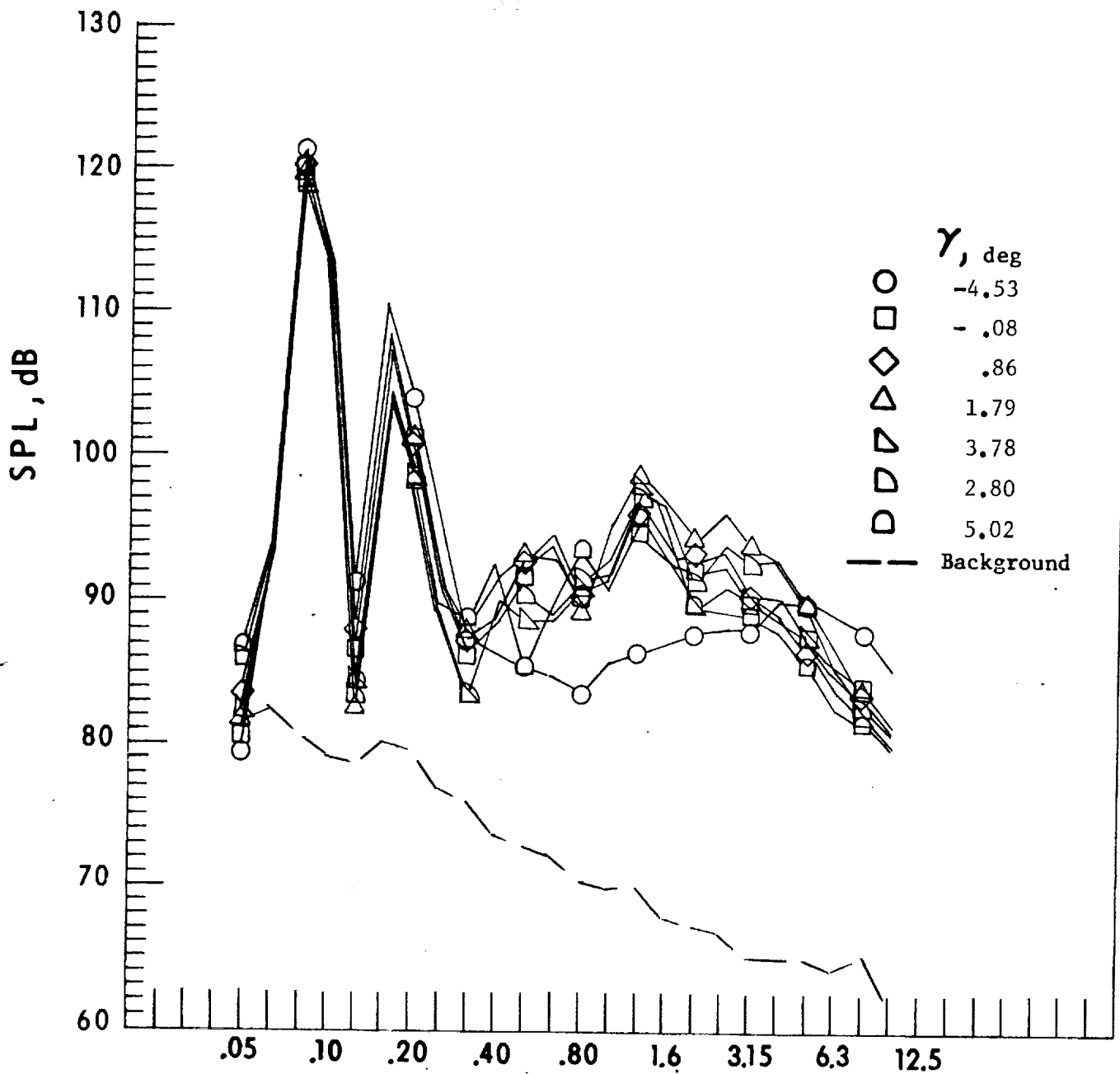
Figure 14. - Concluded.



One-third-octave-band center frequency, kHz

a. Mic. no. 1.

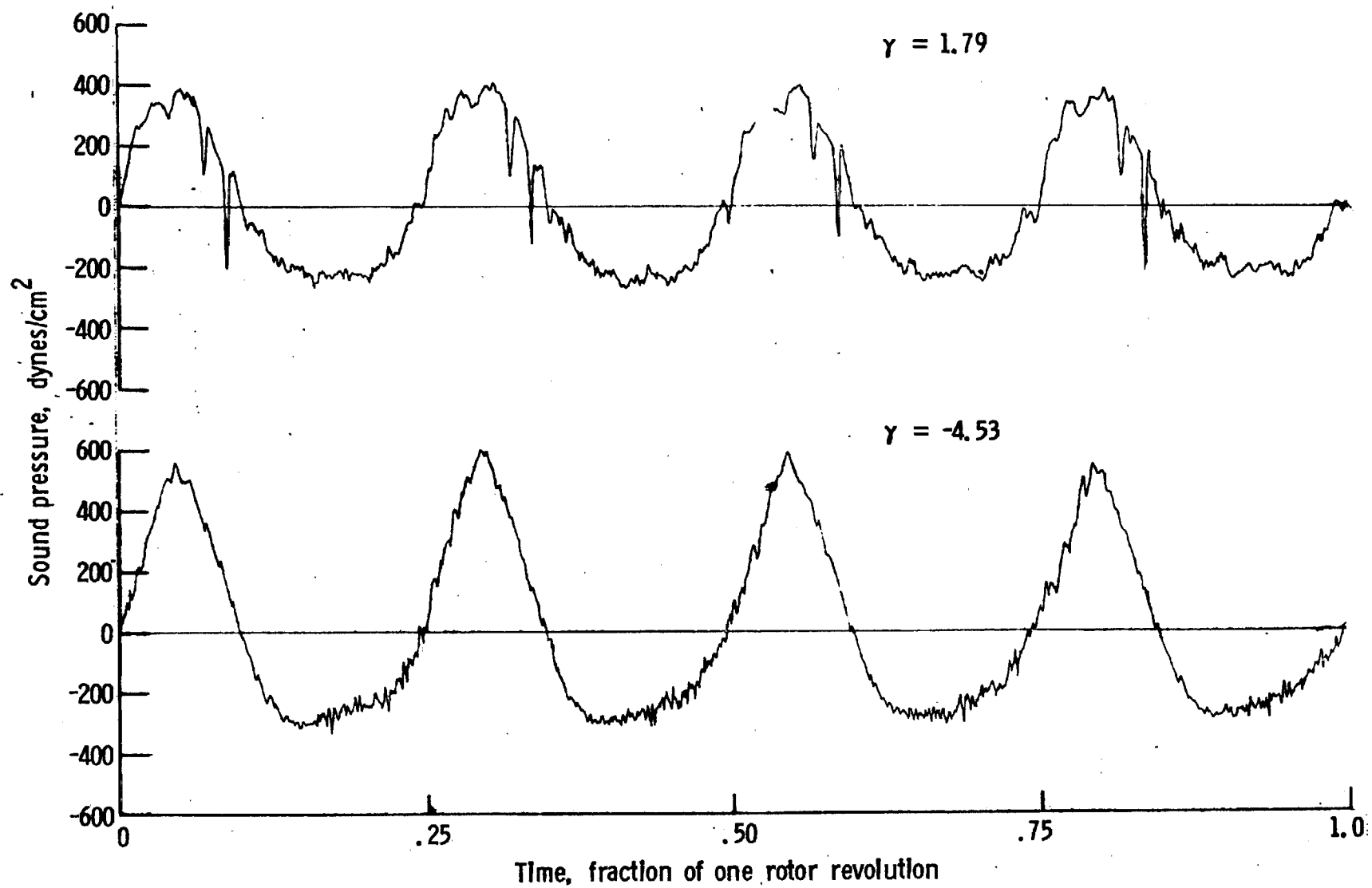
Figure 15. - Effect of descent angle variation on noise generation by helicopter model with square tips installed. $V_{\infty} = 56.2$ knots.



One-third-octave-band center frequency, kHz

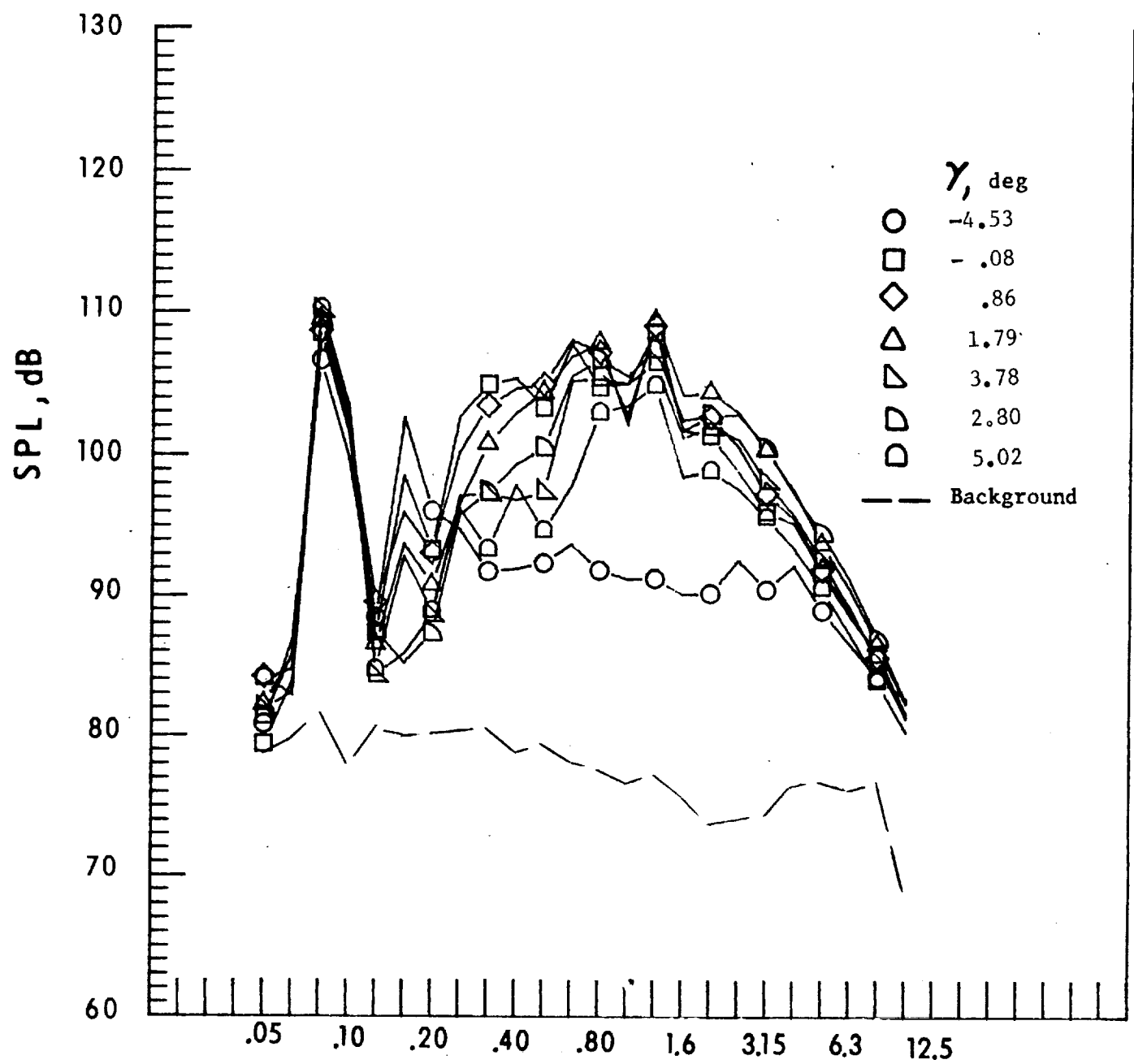
b. V_∞ = Mic. no. 2.

Figure 15. - Continued.



c. Pressure-time histories, Mic. no. 2.

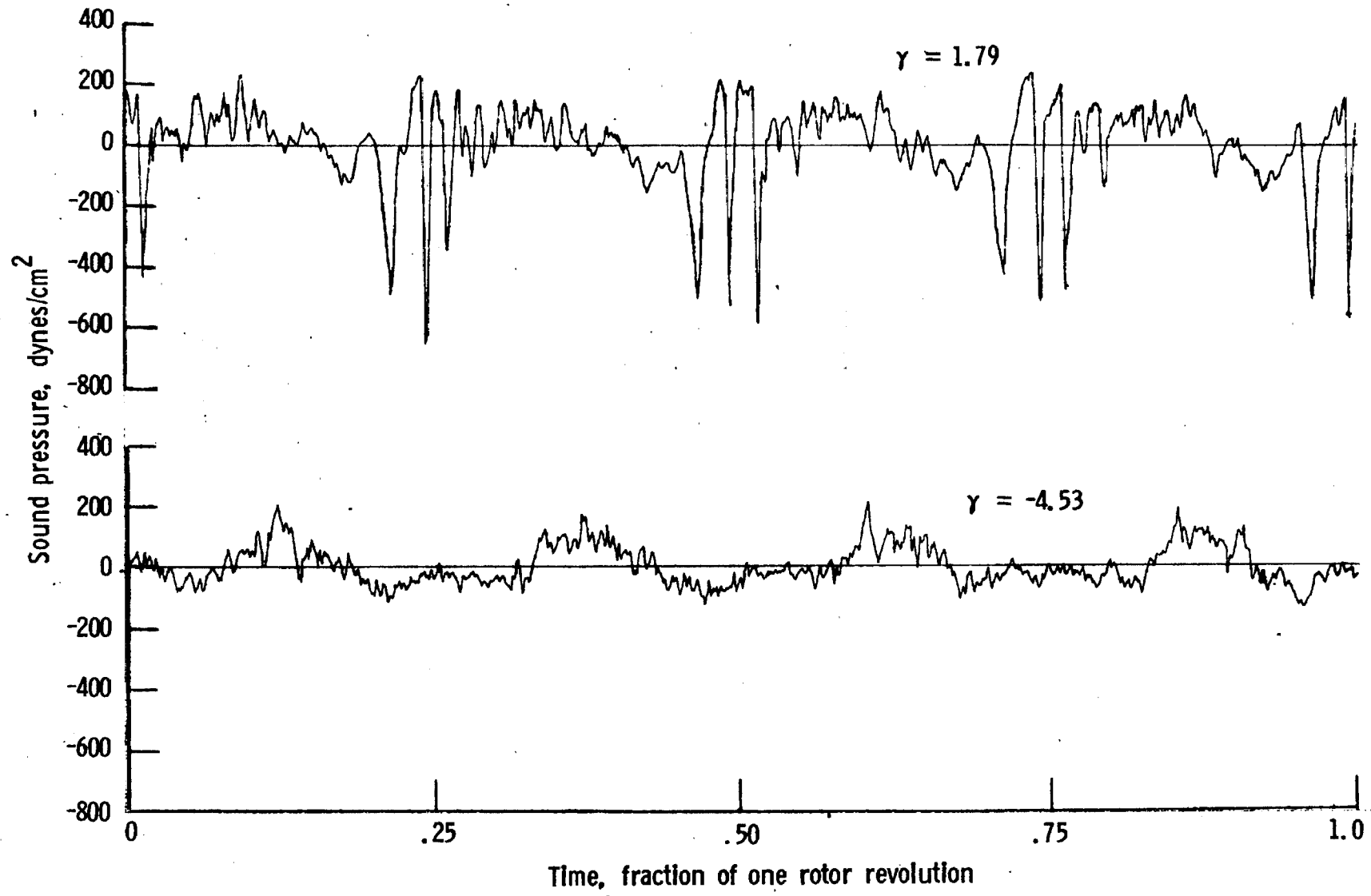
Figure 15. - Continued.



One-third-octave-band center frequency, kHz

d. Mic. no. 3.

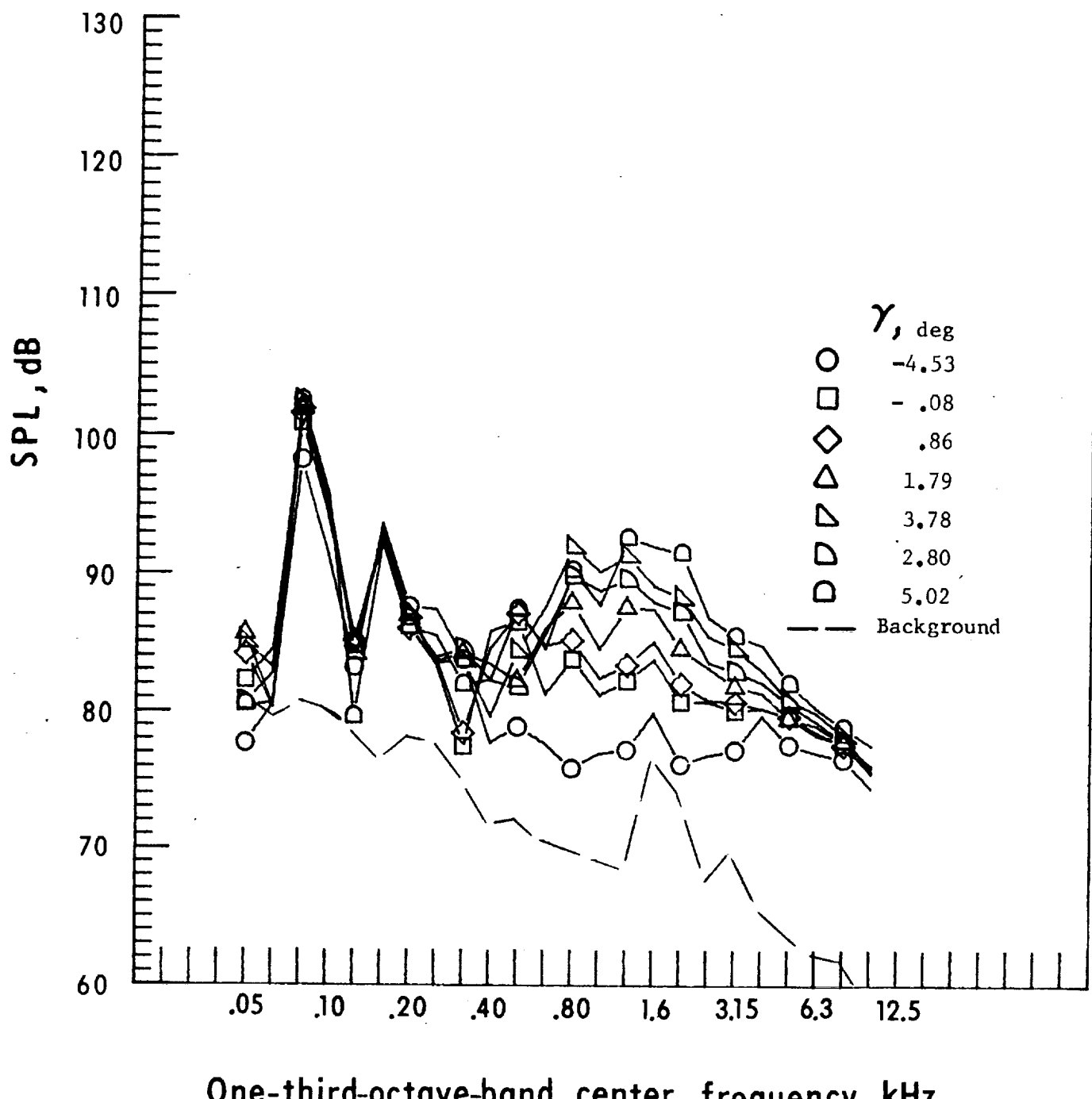
Figure 15. - Continued.



e. Pressure-time histories, Mic. no. 3.

Figure 15. - Continued.

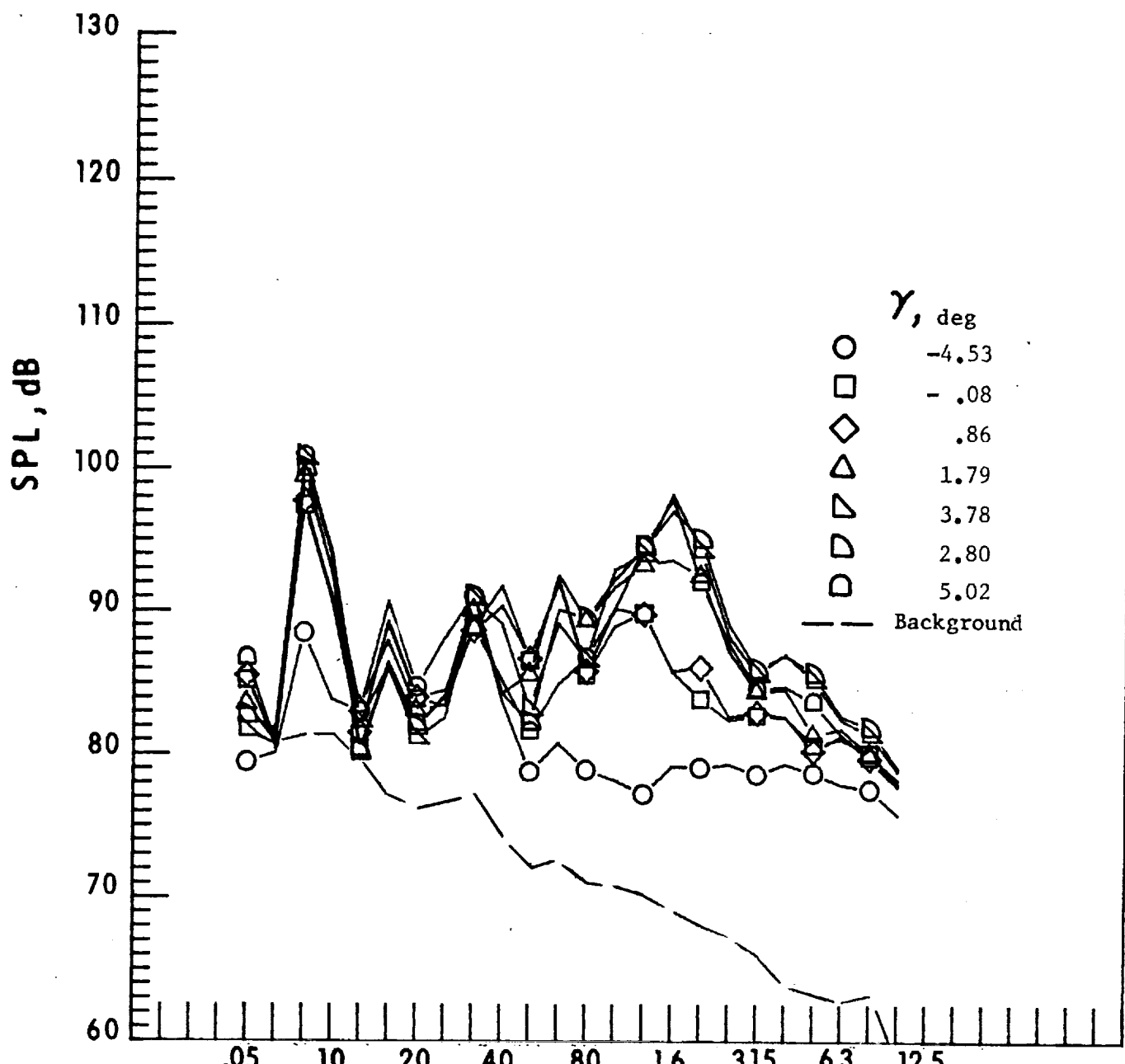
E-D



One-third-octave-band center frequency, kHz

f. Mic. no. 4.

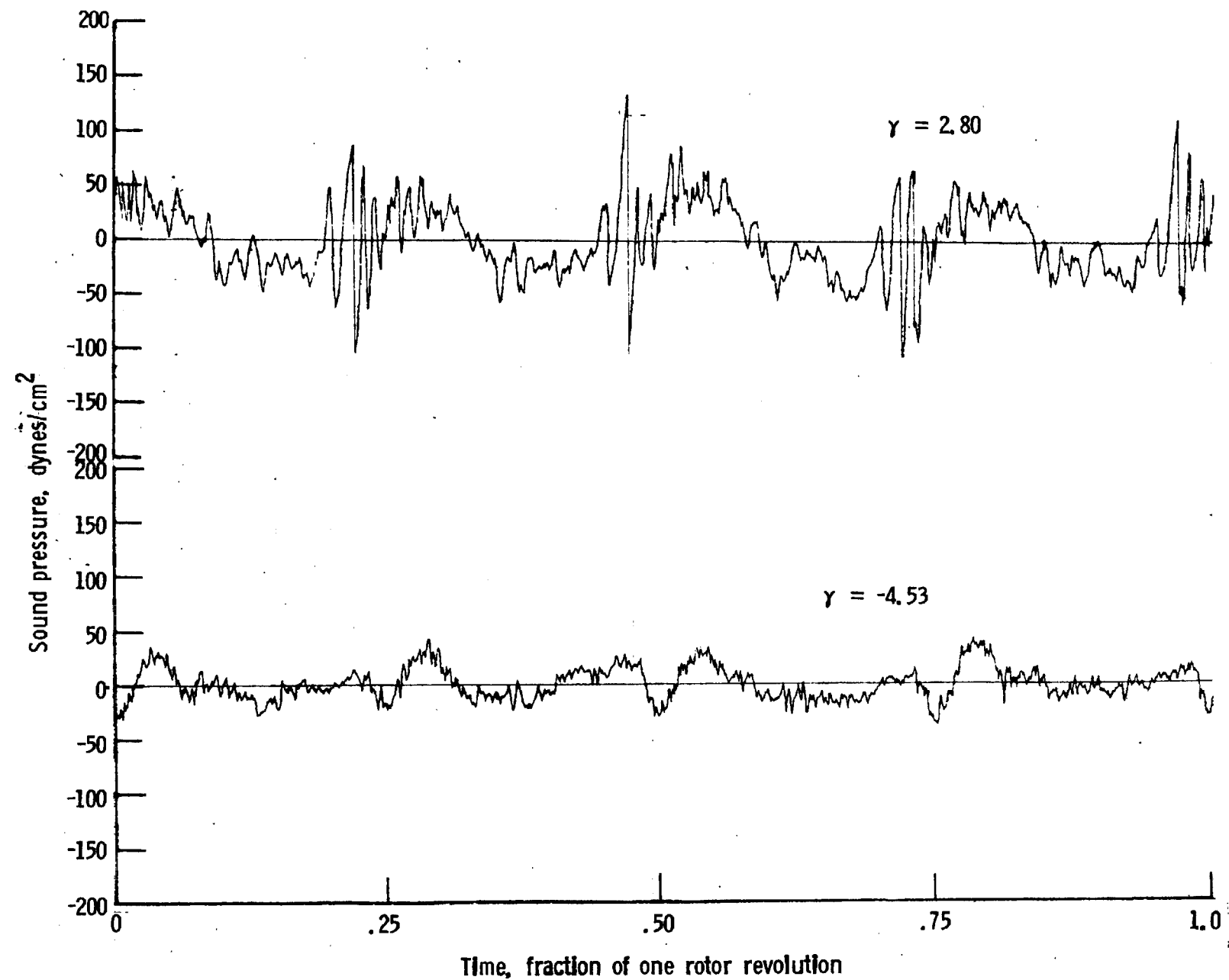
Figure 15. - Continued.



One-third-octave-band center frequency, kHz

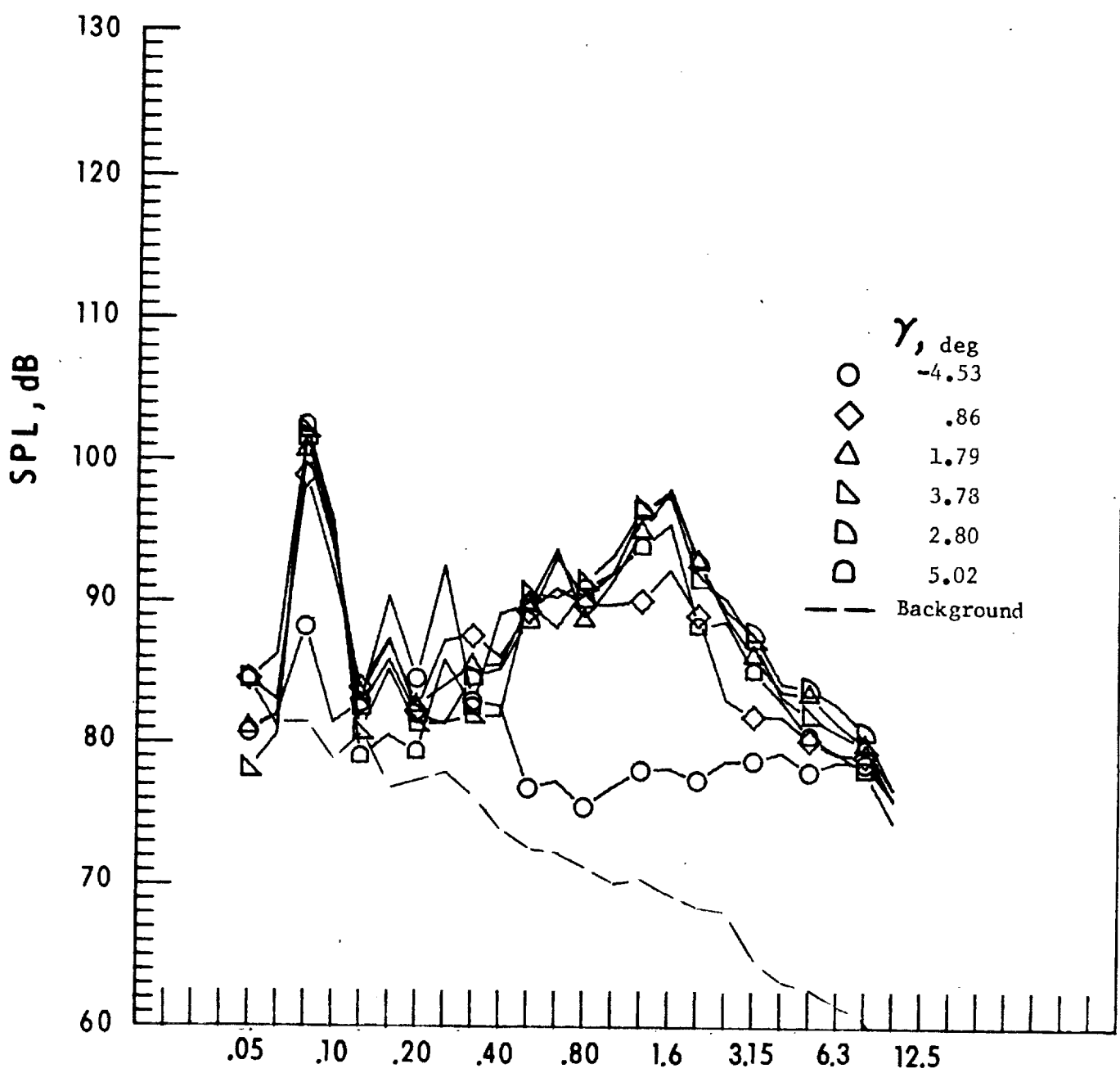
g. Mic. no. 5.

Figure 15. - Continued.



h. Pressure-time histories, Mic. no. 5.

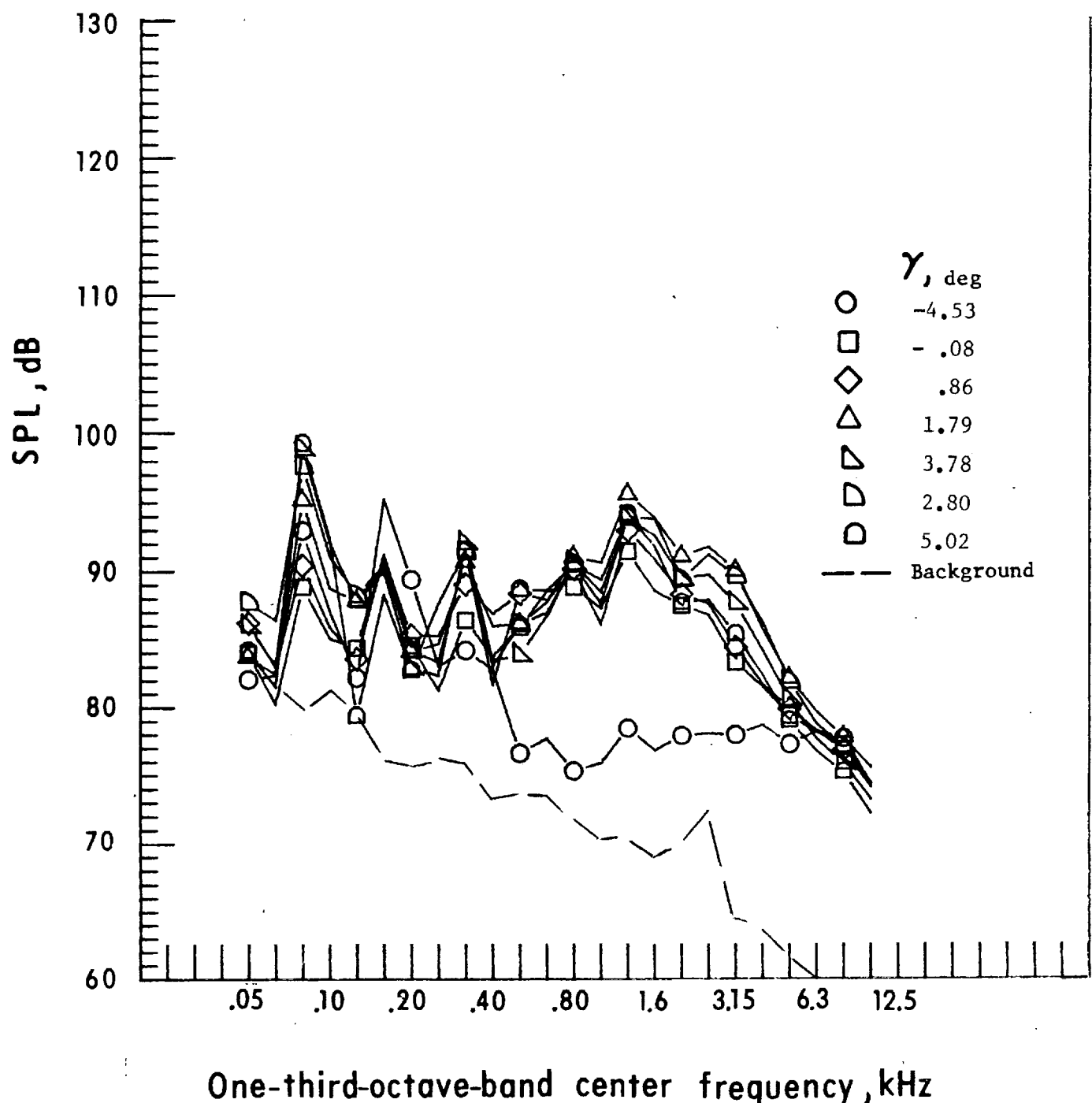
Figure 15. - Continued.



One-third-octave-band center frequency, kHz

I. Mic. no. 6.

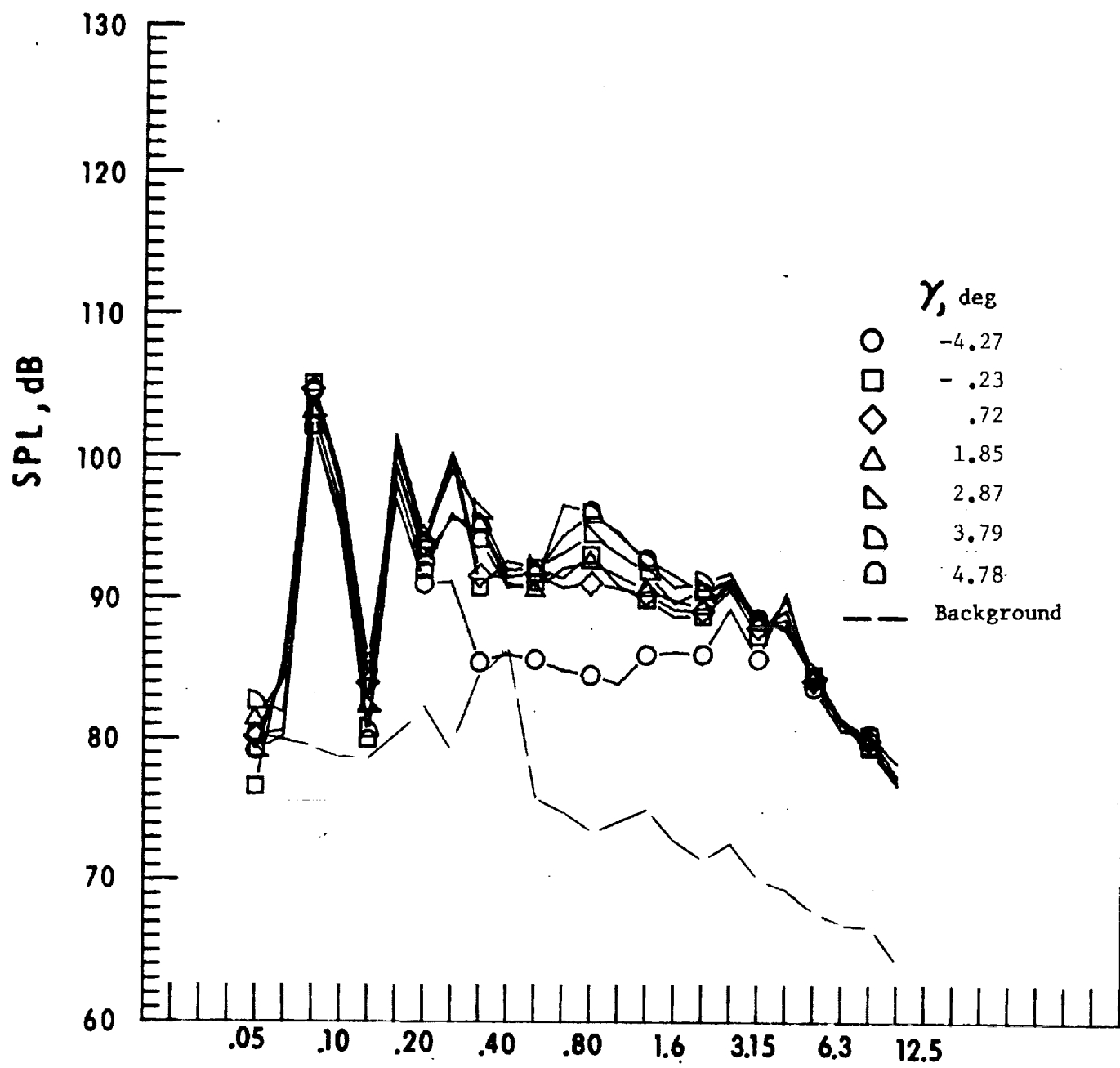
Figure 15. - Continued.



One-third-octave-band center frequency, kHz

j. Mic. no. 7.

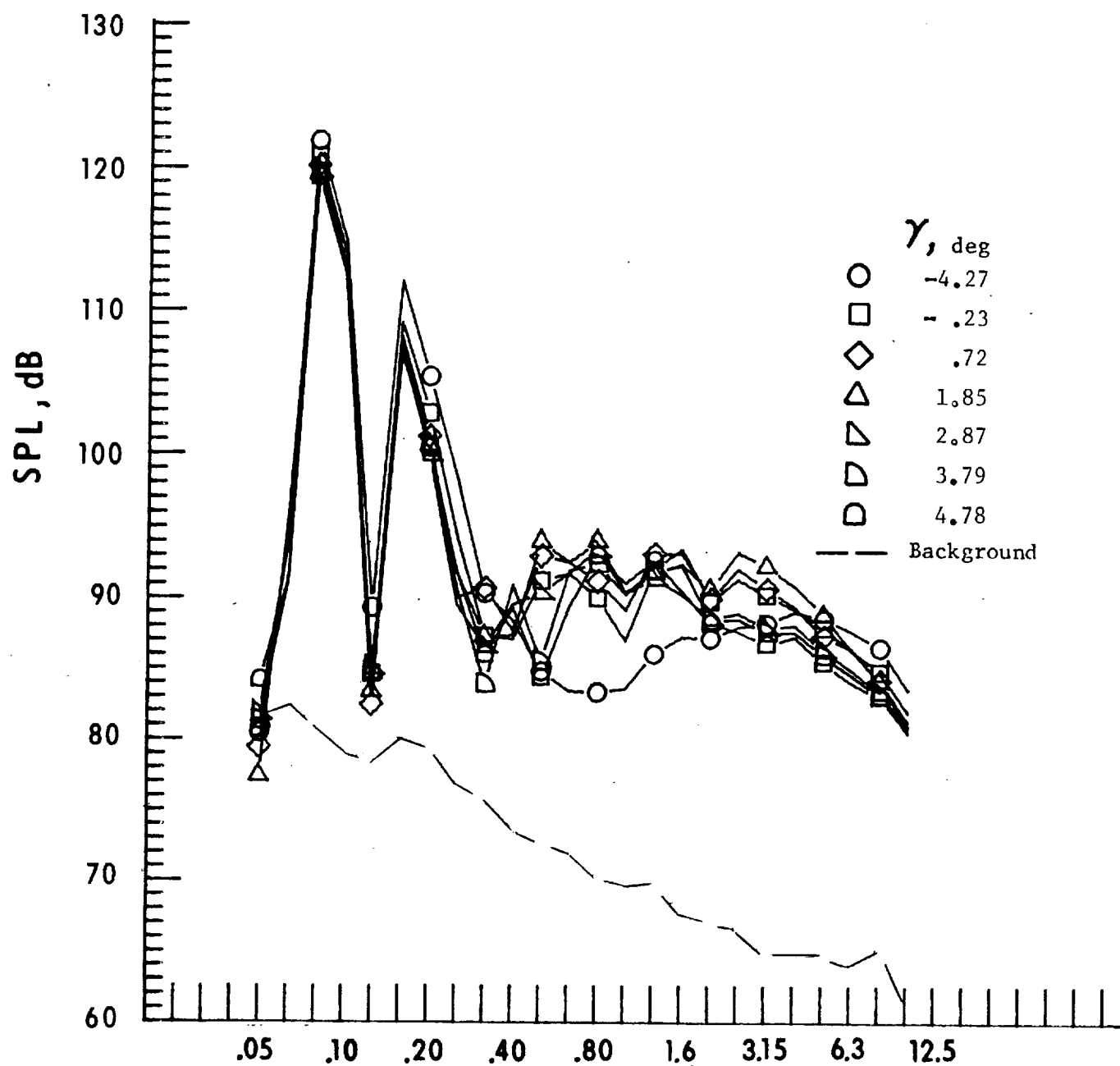
Figure 15. - Concluded.



One-third-octave-band center frequency, kHz

a. Mic. no. 1.

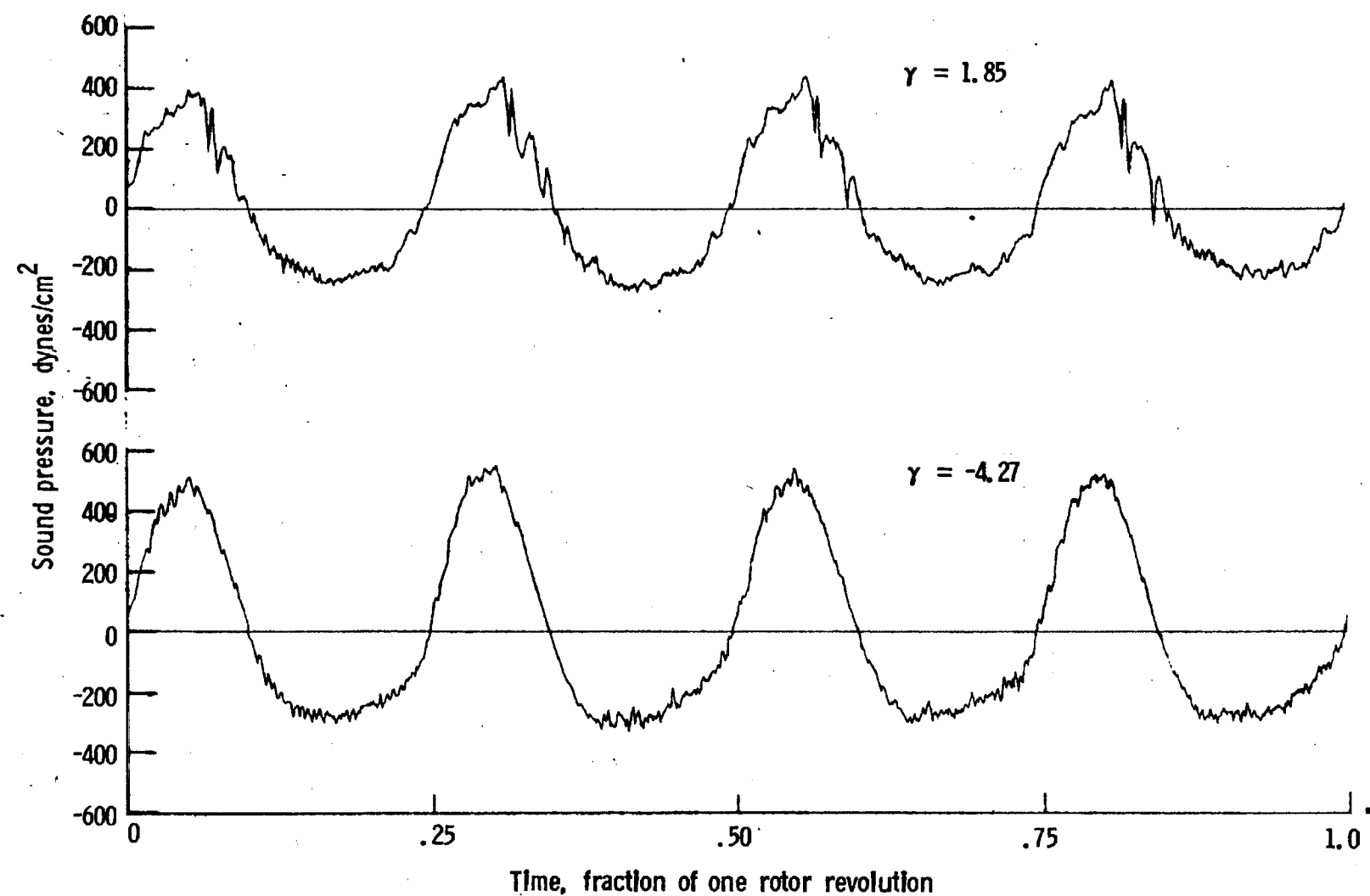
Figure 16. - Effect of descent angle variation on noise generation by helicopter model with ogee tips installed. $V_\infty = 55.9$ knots.



One-third-octave-band center frequency, kHz

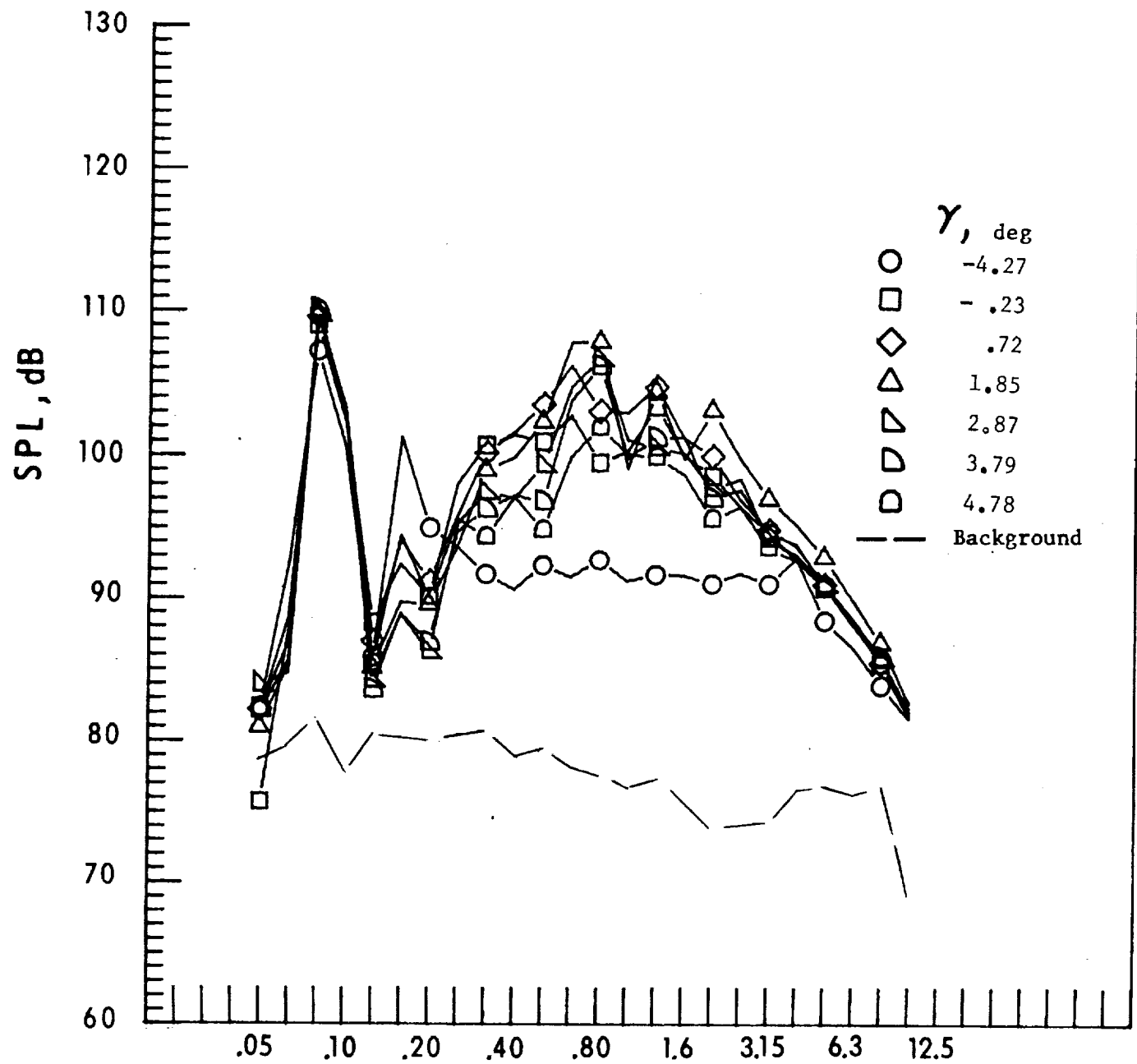
b. Mic. no. 2.

Figure 16. - Continued.



c. Pressure-time histories, Mic. no. 2.

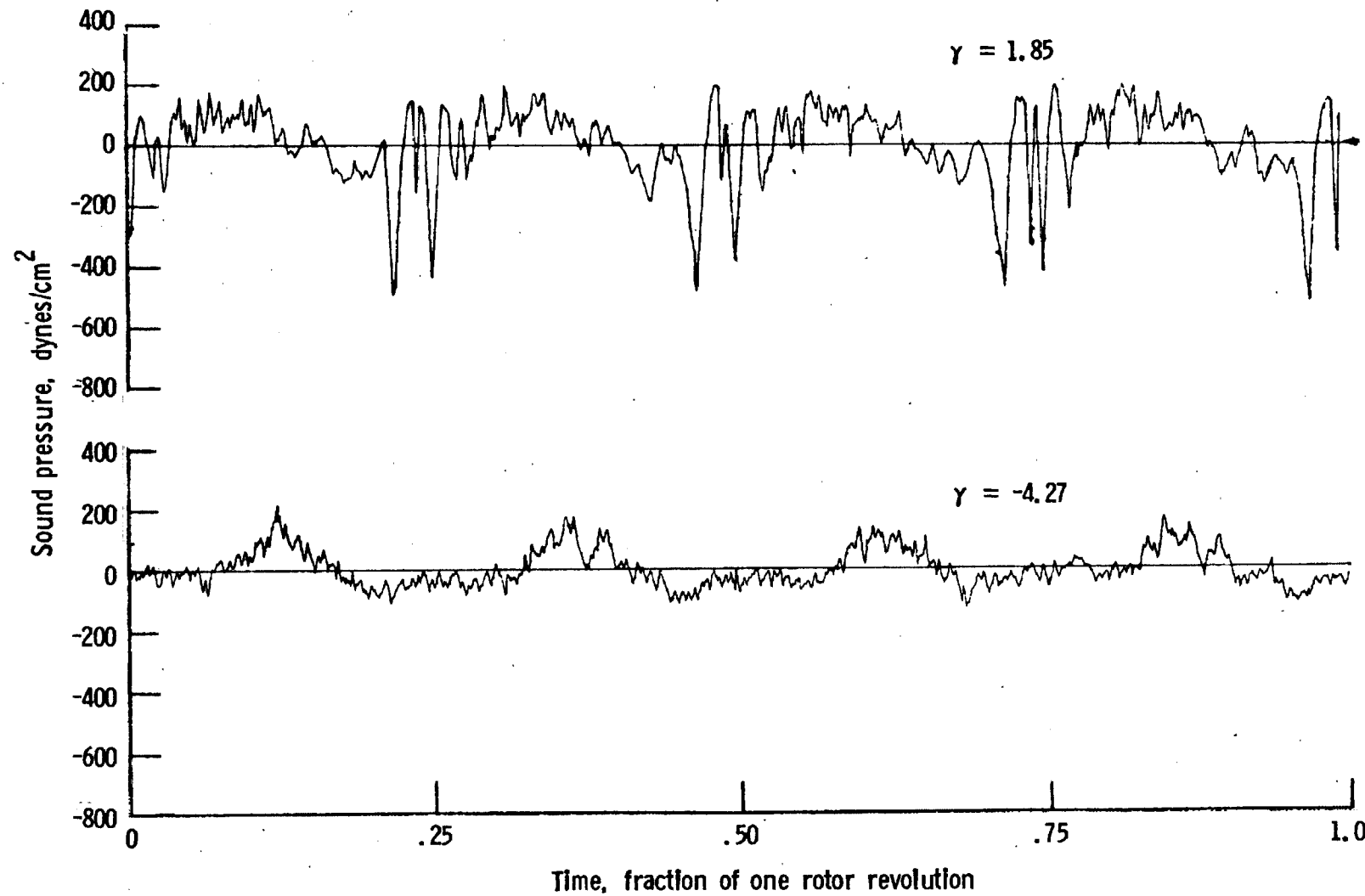
Figure 16. - Continued.



One-third-octave-band center frequency, kHz

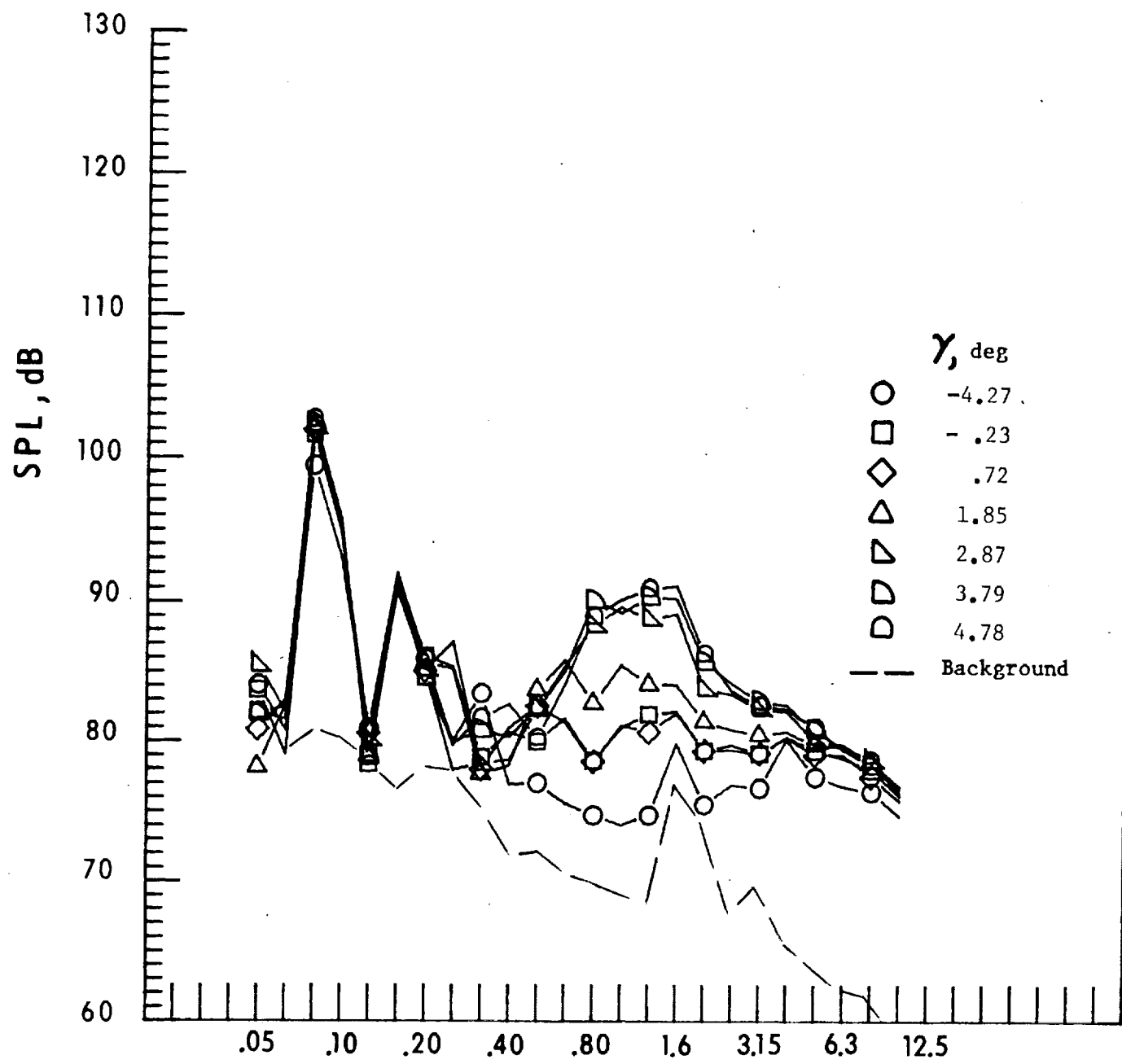
d. Mic. no. 3.

Figure 16. - Continued.



e. Pressure-time histories, Mic. no. 3.

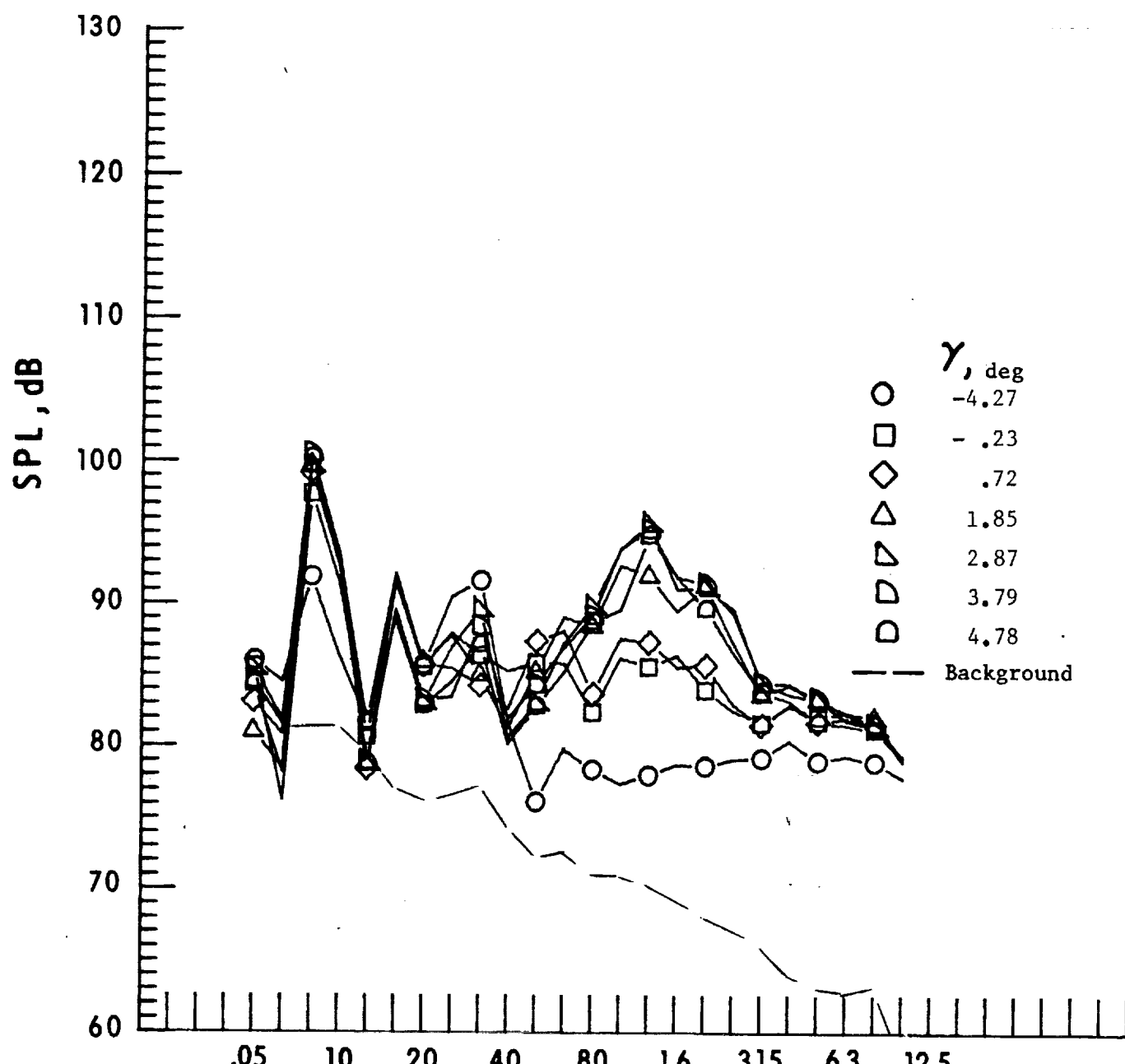
Figure 16. - Continued.



One-third-octave-band center frequency, kHz

f. Mic. no. 4.

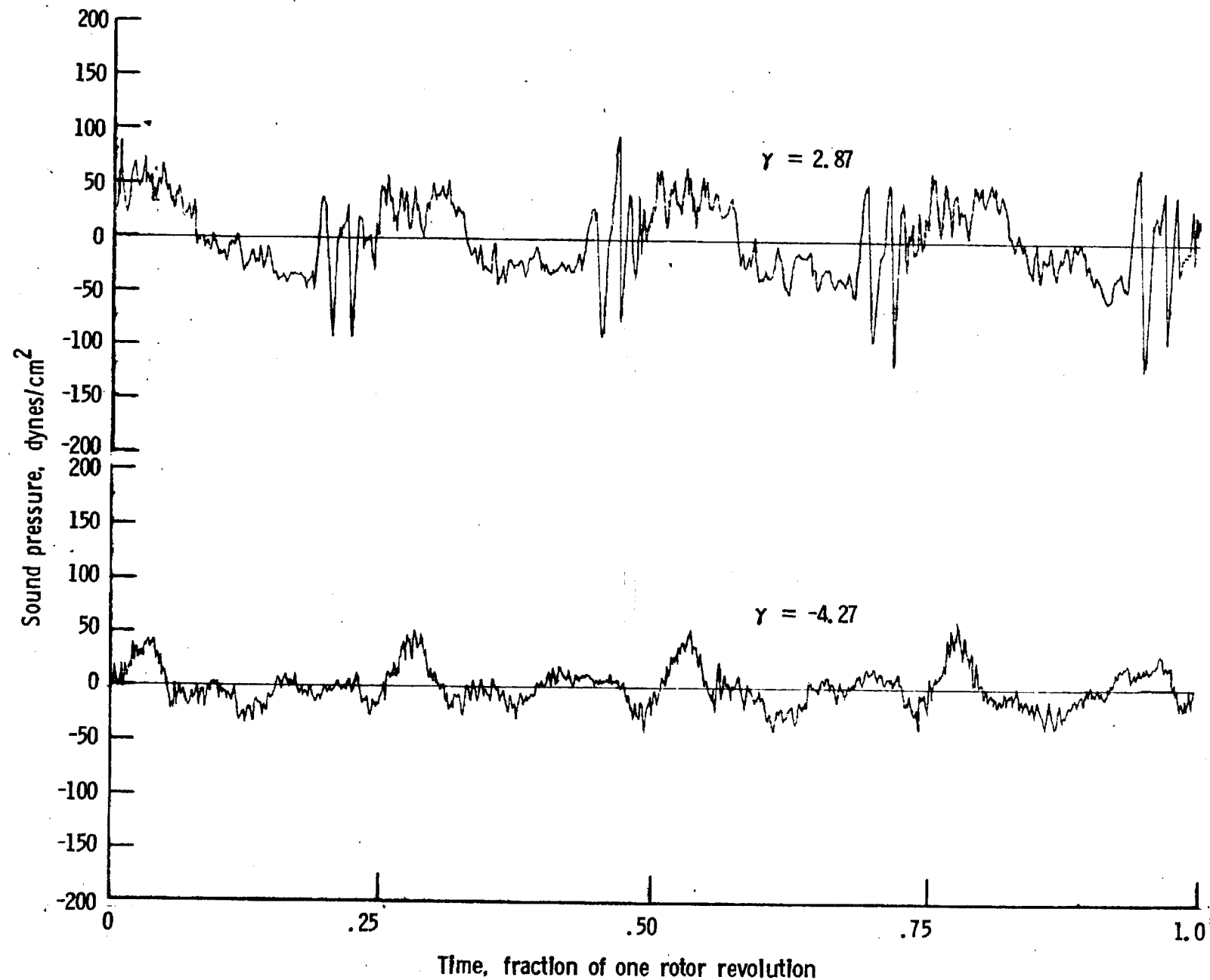
Figure 16. - Continued.



One-third-octave-band center frequency, kHz

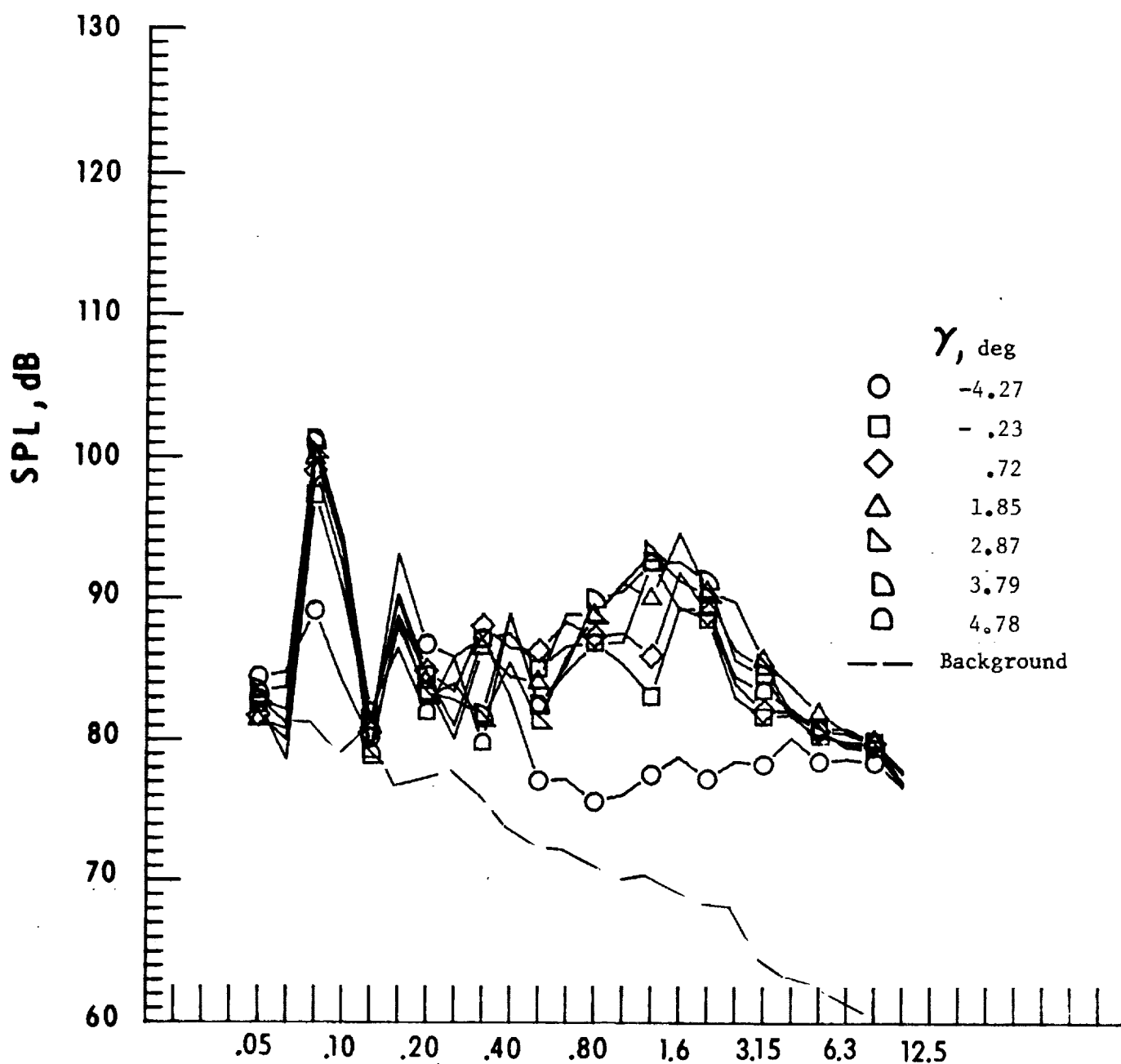
g. Mic. no. 5.

Figure 16. - Continued.



h. Pressure-time histories, Mic. no. 5.

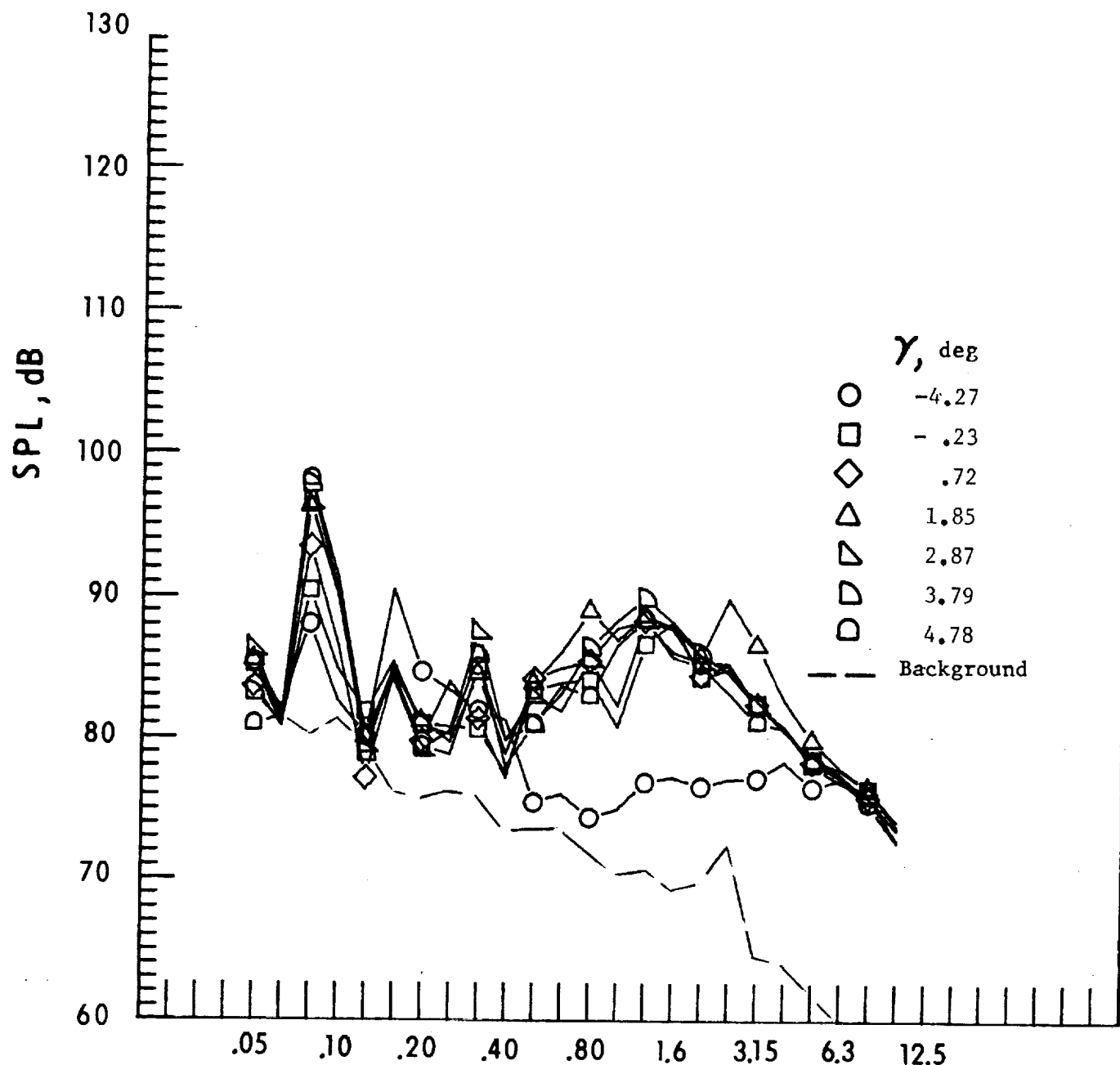
Figure 16. - Continued.



One-third-octave-band center frequency, kHz

i. Mic. no. 6.

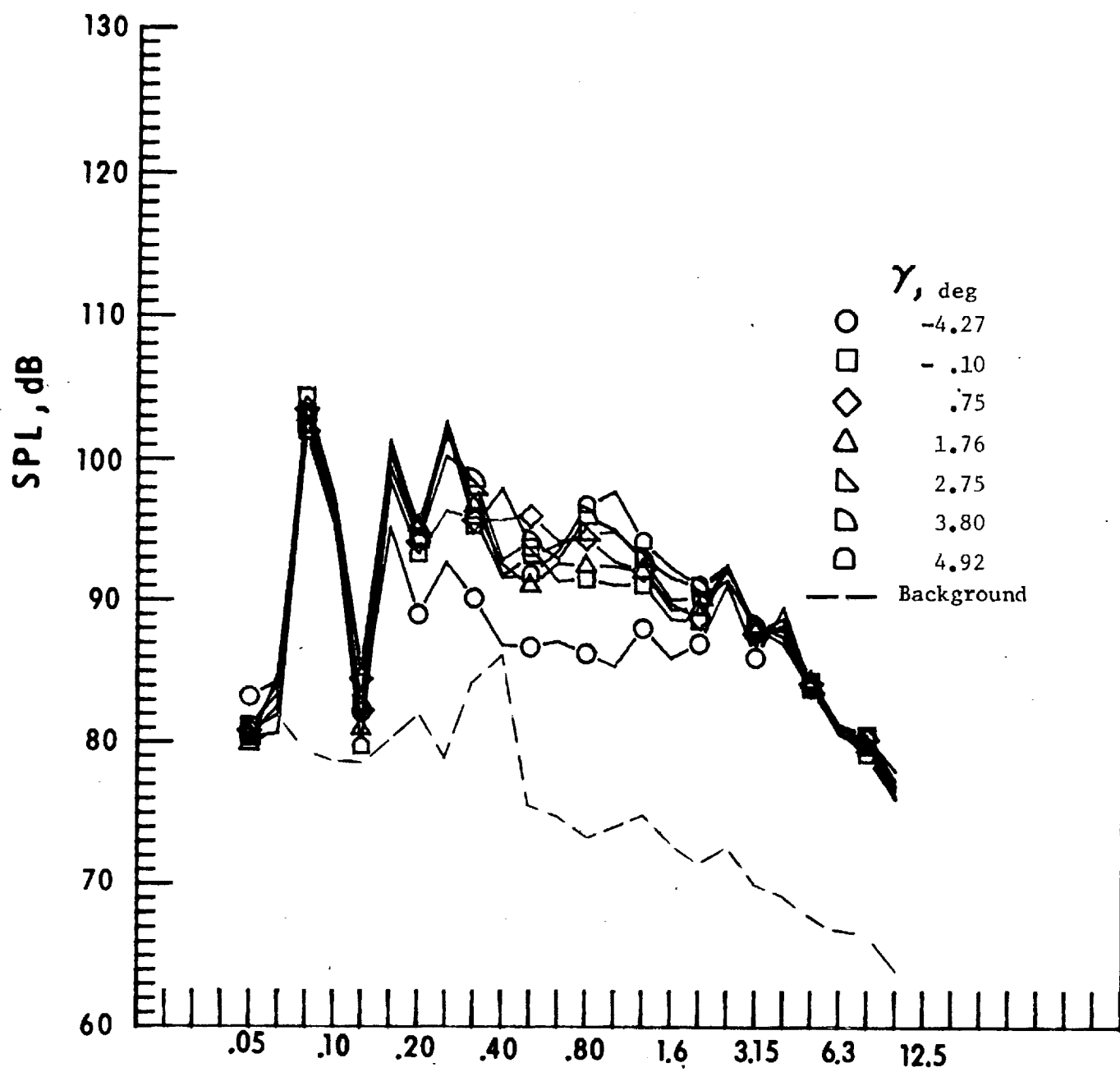
Figure 16. - Continued.



One-third-octave-band center frequency, kHz

j. Mic. no. 7.

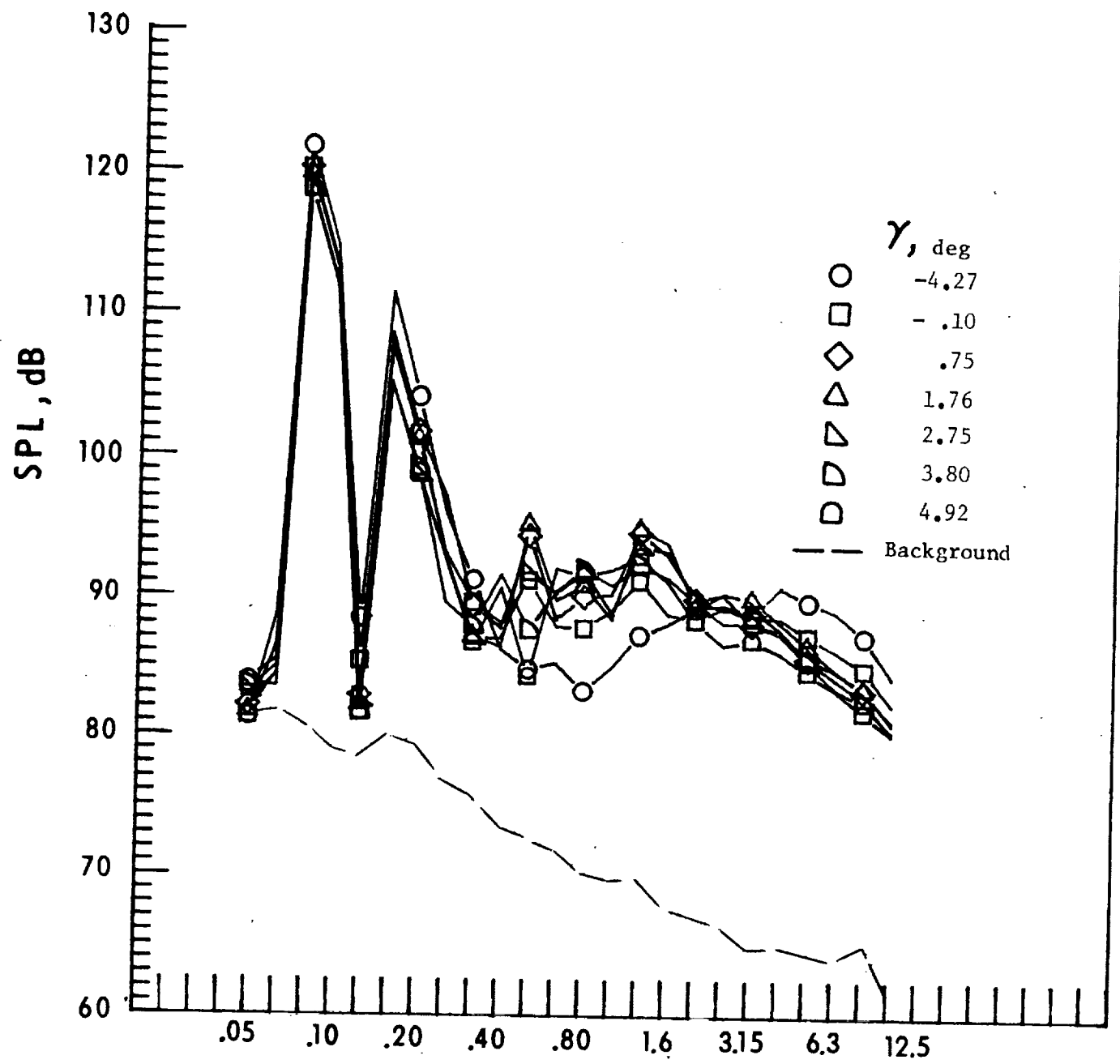
Figure 16. - Concluded.



One-third-octave-band center frequency, kHz

a. Mic. no. 1.

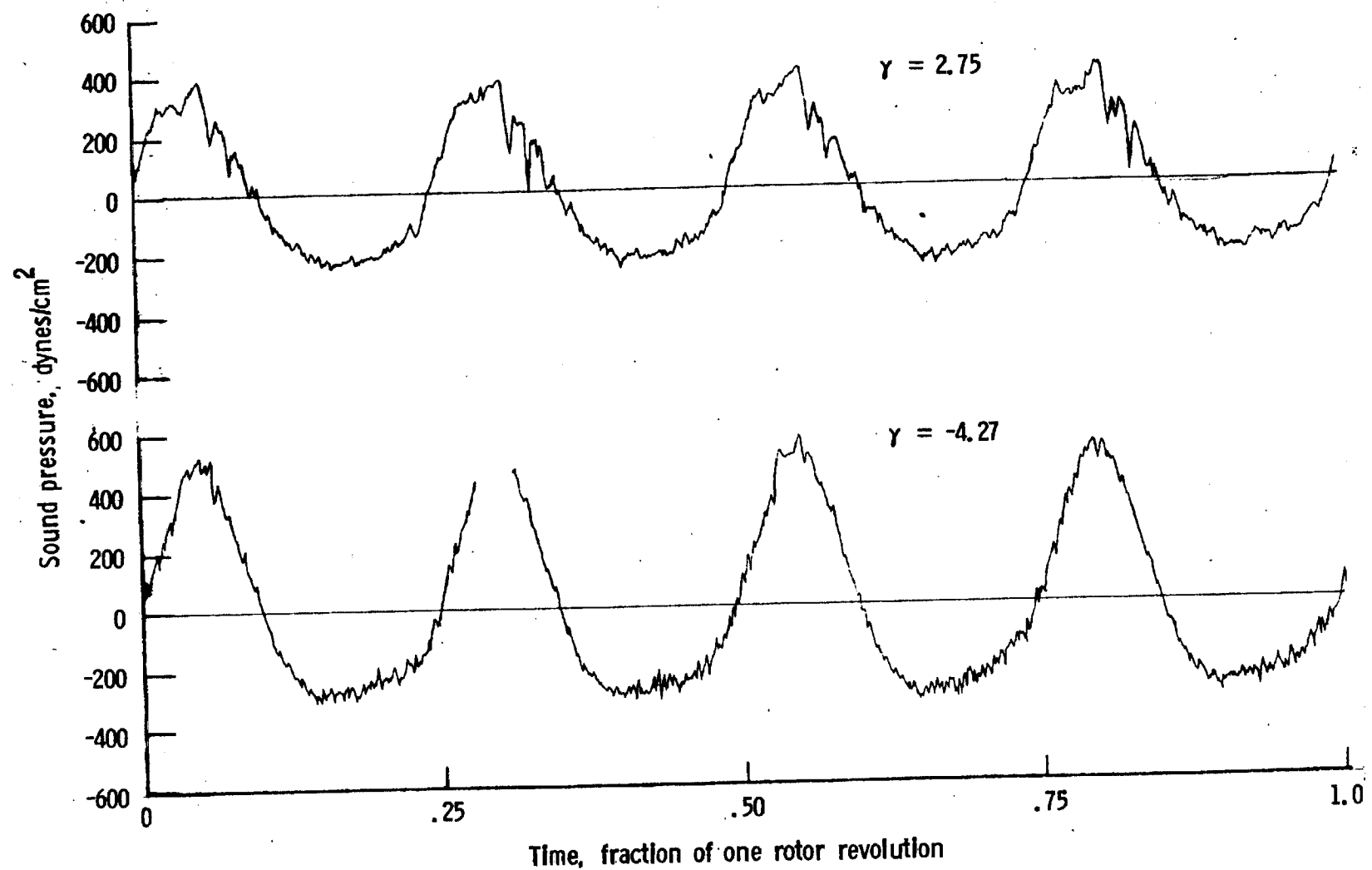
Figure 17. - Effect of descent angle variation on noise generation by helicopter model with sub-wing tips installed. $V_{\infty} = 55.8$ knots.



One-third-octave-band center frequency, kHz

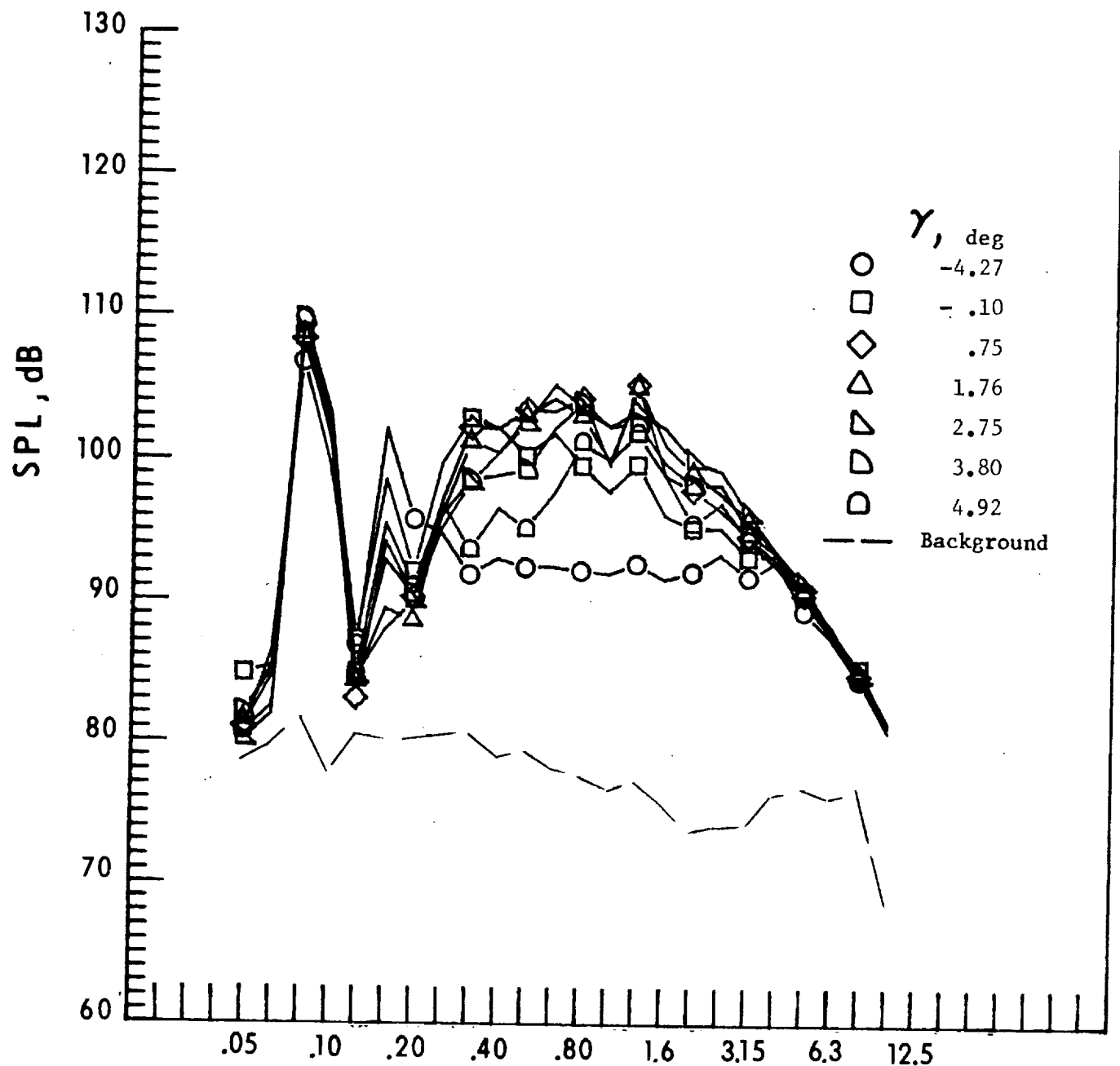
b. Mic. no. 2.

Figure 17. - Continued.



c. Pressure-time histories, Mic. no. 2.

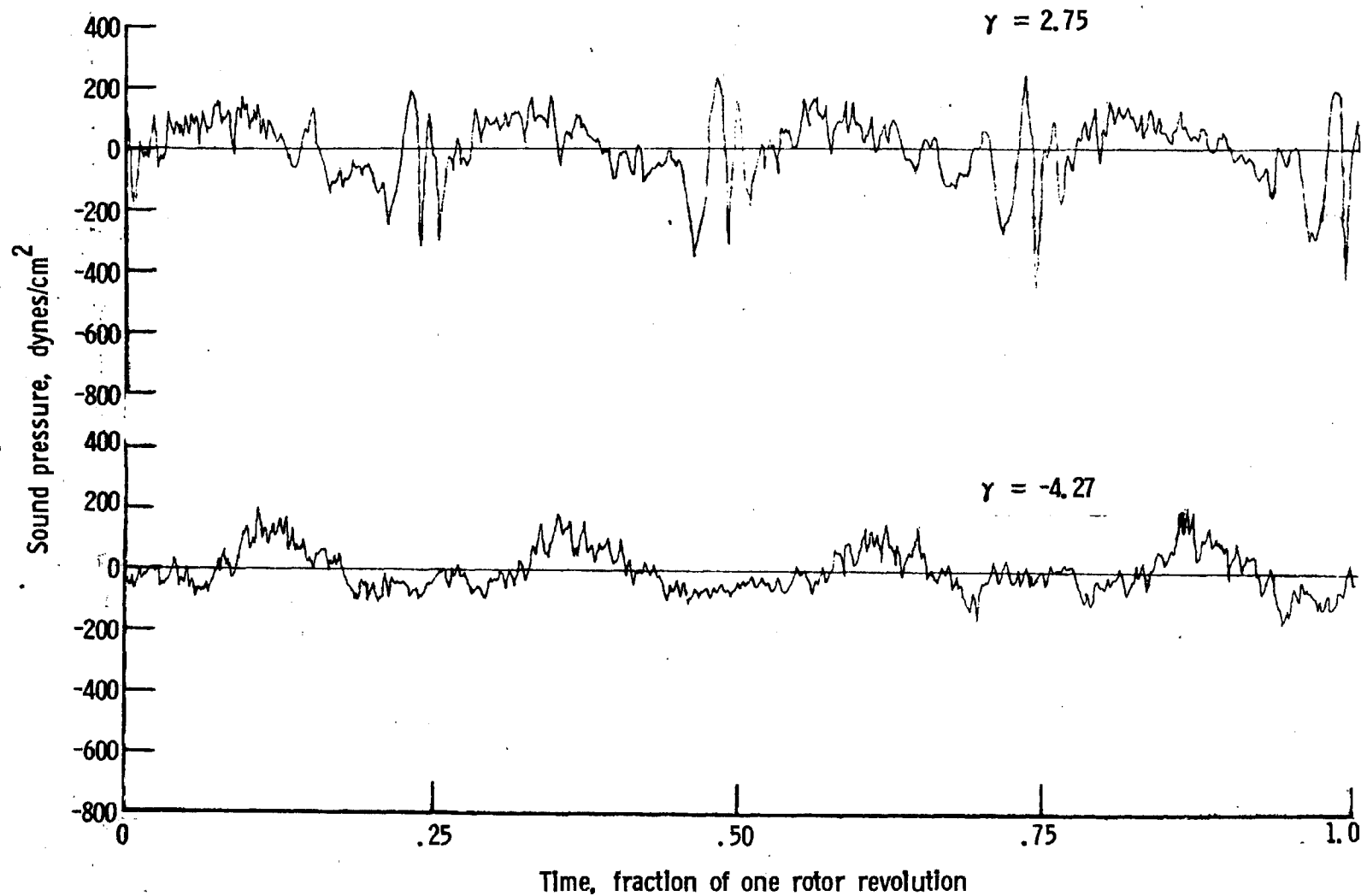
Figure 17. - Continued.



One-third-octave-band center frequency, kHz

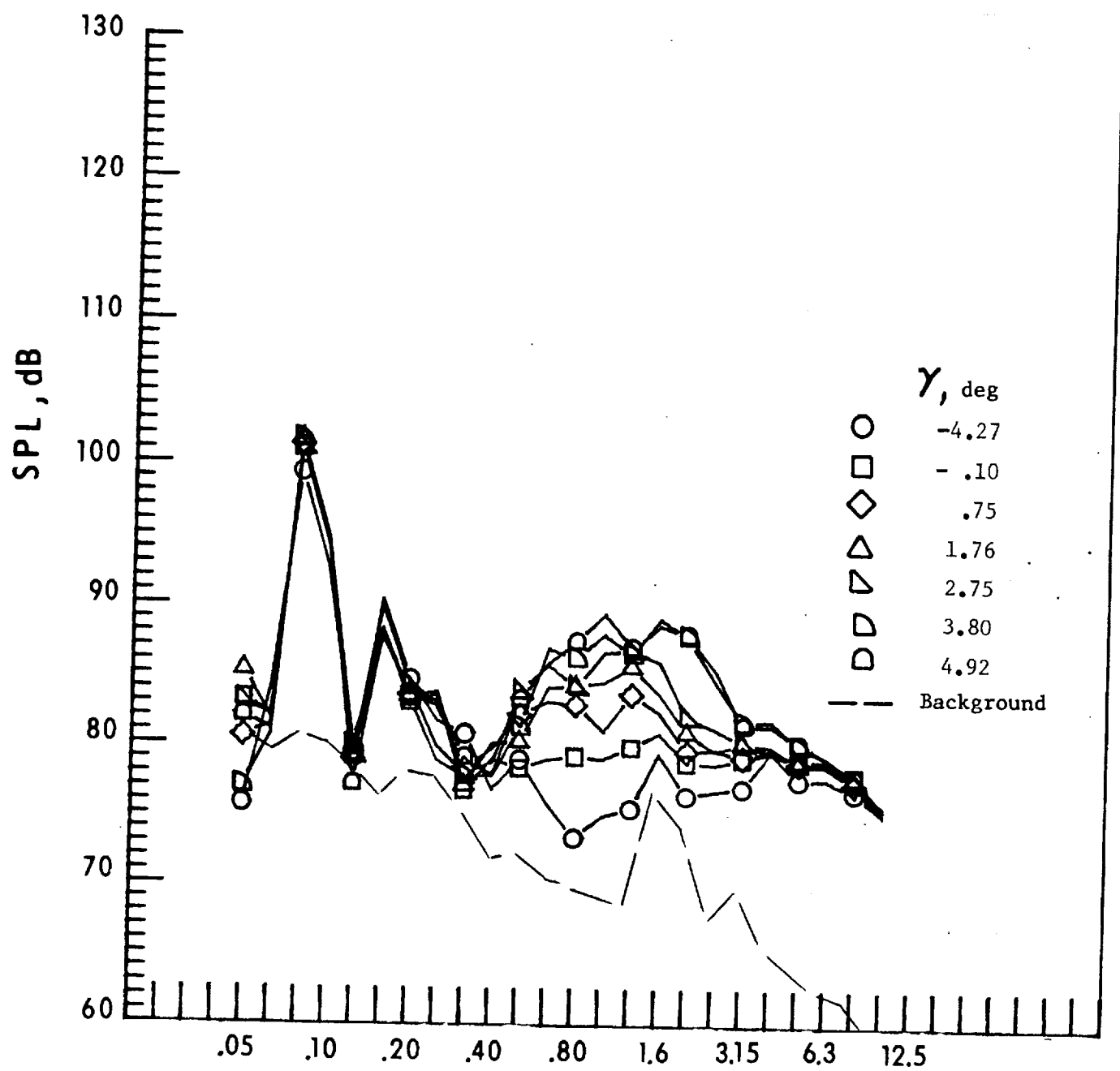
d. Mic. no. 3.

Figure 17. - Continued.



e. Pressure-time histories, Mic. no. 3.

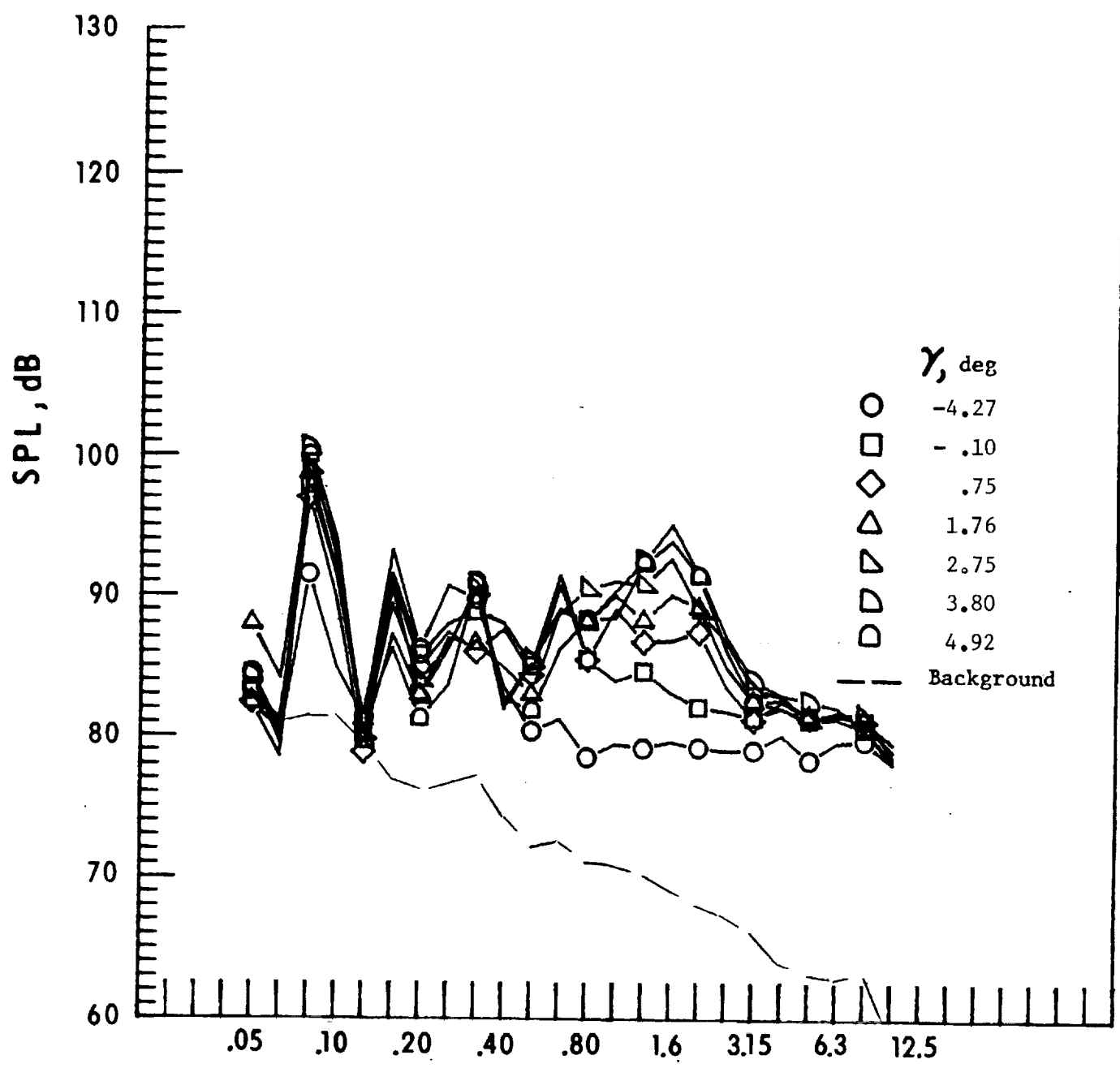
Figure 17. - Continued.



One-third-octave-band center frequency, kHz

f. Mic. no. 4.

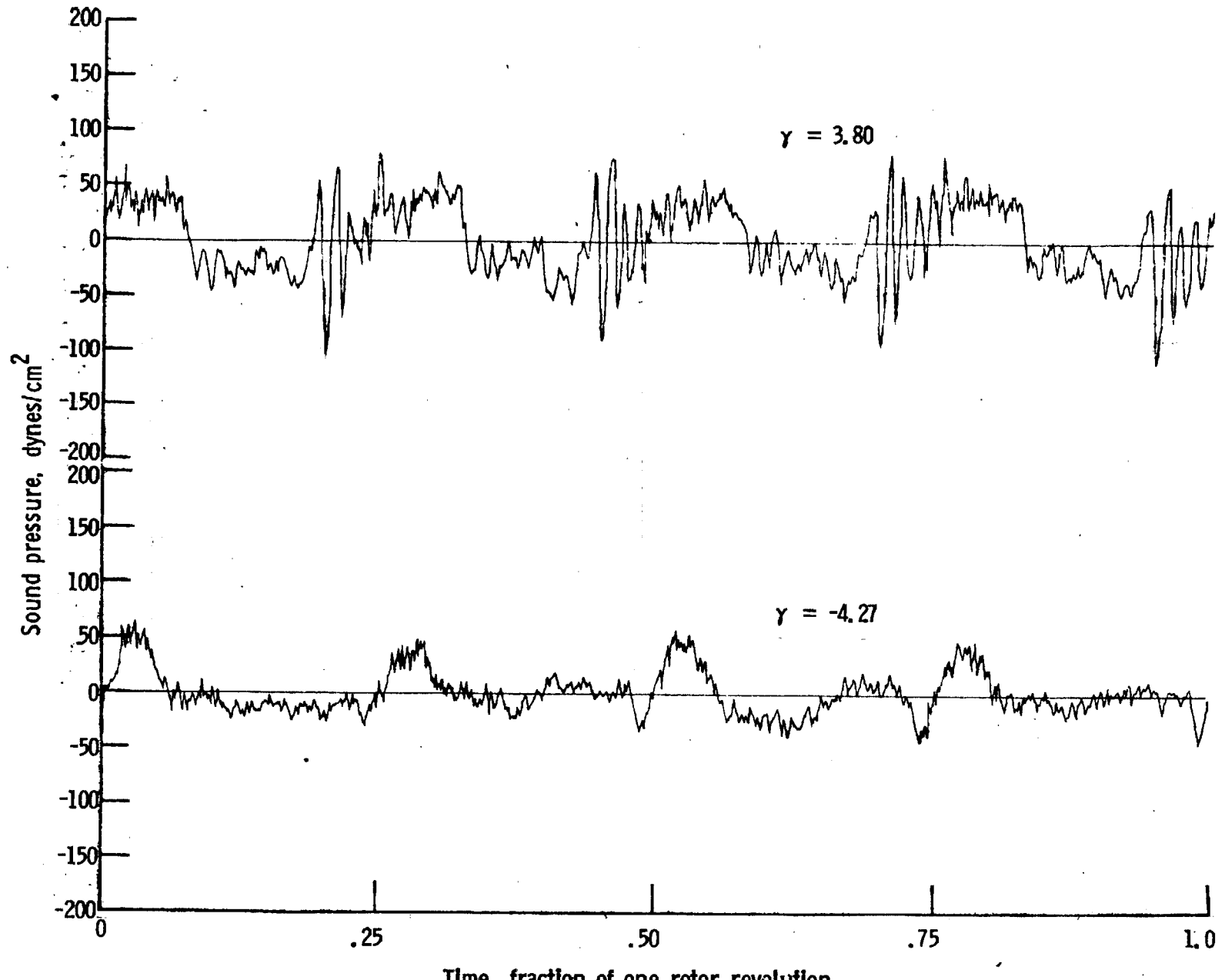
Figure 17. - Continued.



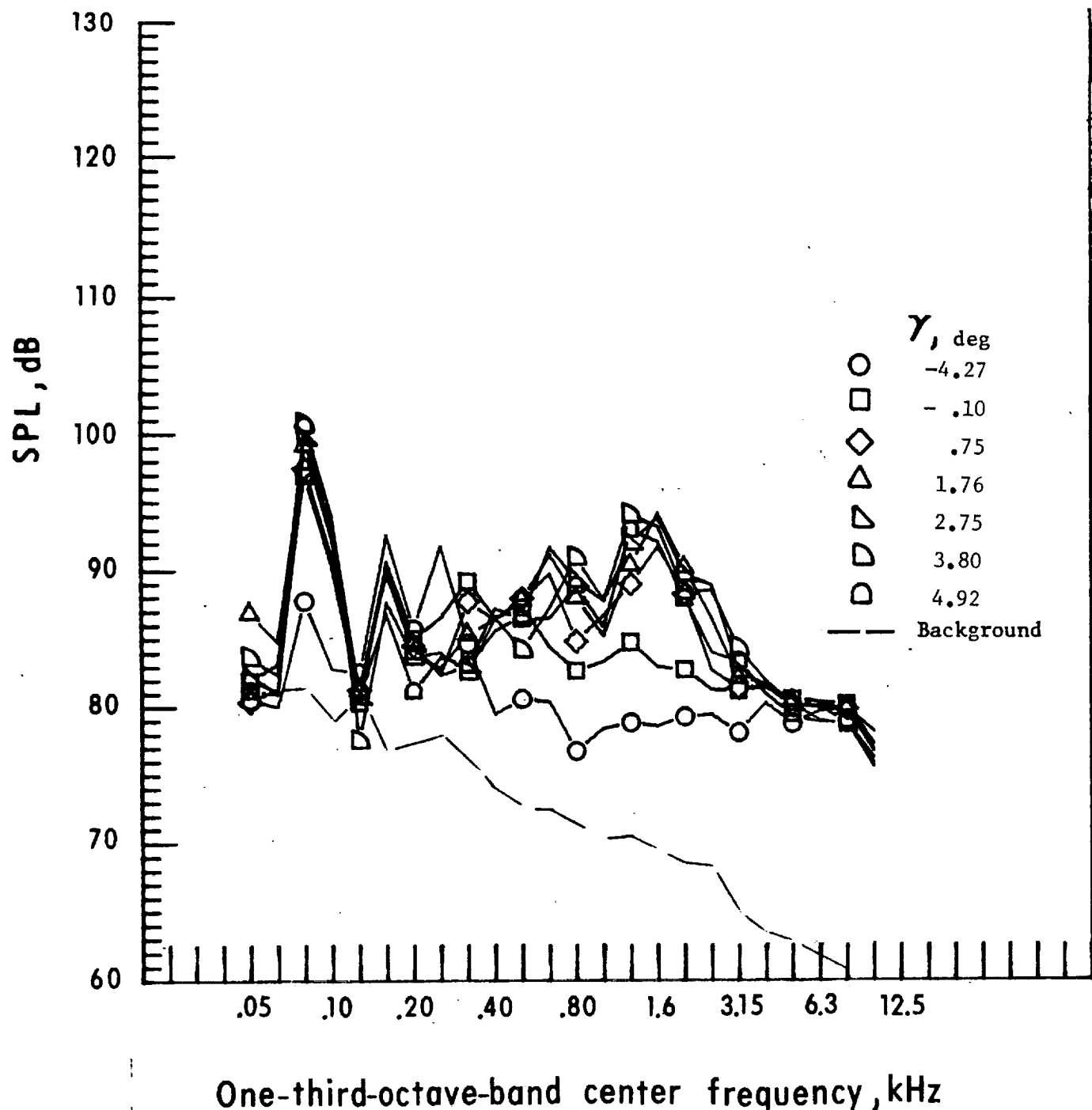
One-third-octave-band center frequency, kHz

g. Mic. no. 5.

Figure 17. - Continued.



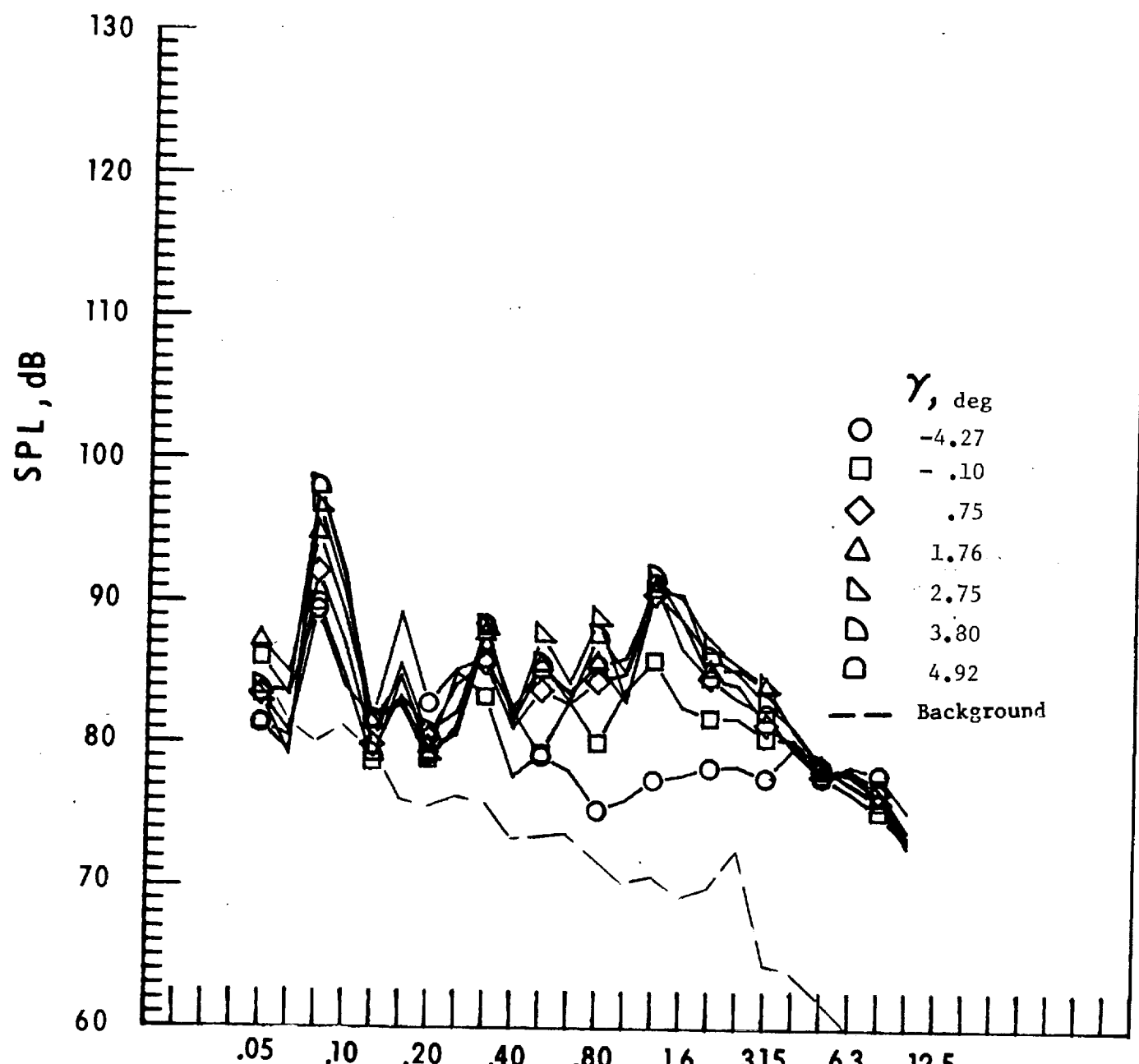
h. Pressure-time histories, Mic. no. 5.



One-third-octave-band center frequency, kHz

i. Mic. no. 6.

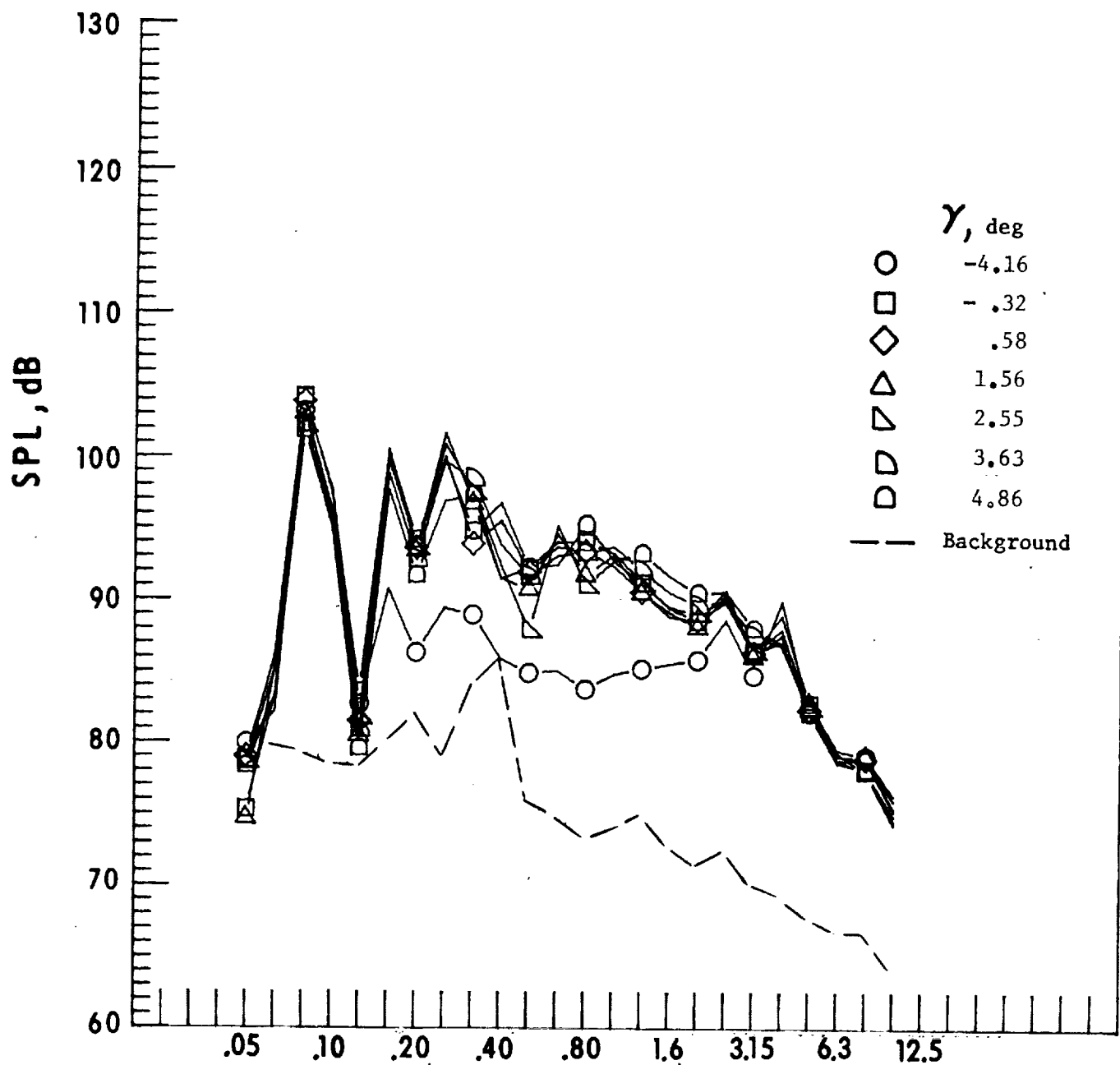
Figure 17. - Continued.



One-third-octave-band center frequency, kHz

j. Mic. no. 7.

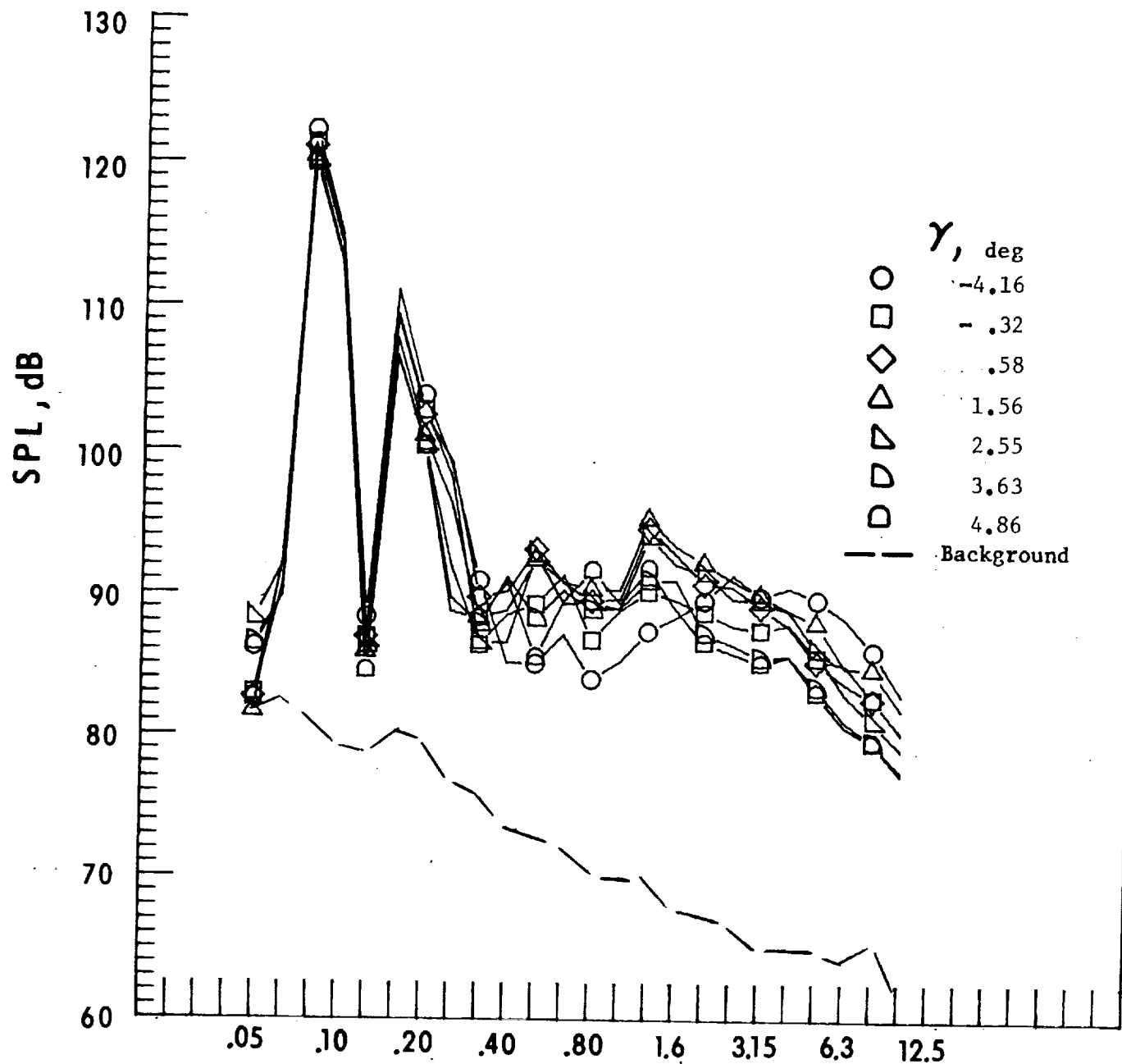
Figure 17. - Concluded.



One-third-octave-band center frequency, kHz

a. Mic. no. 1.

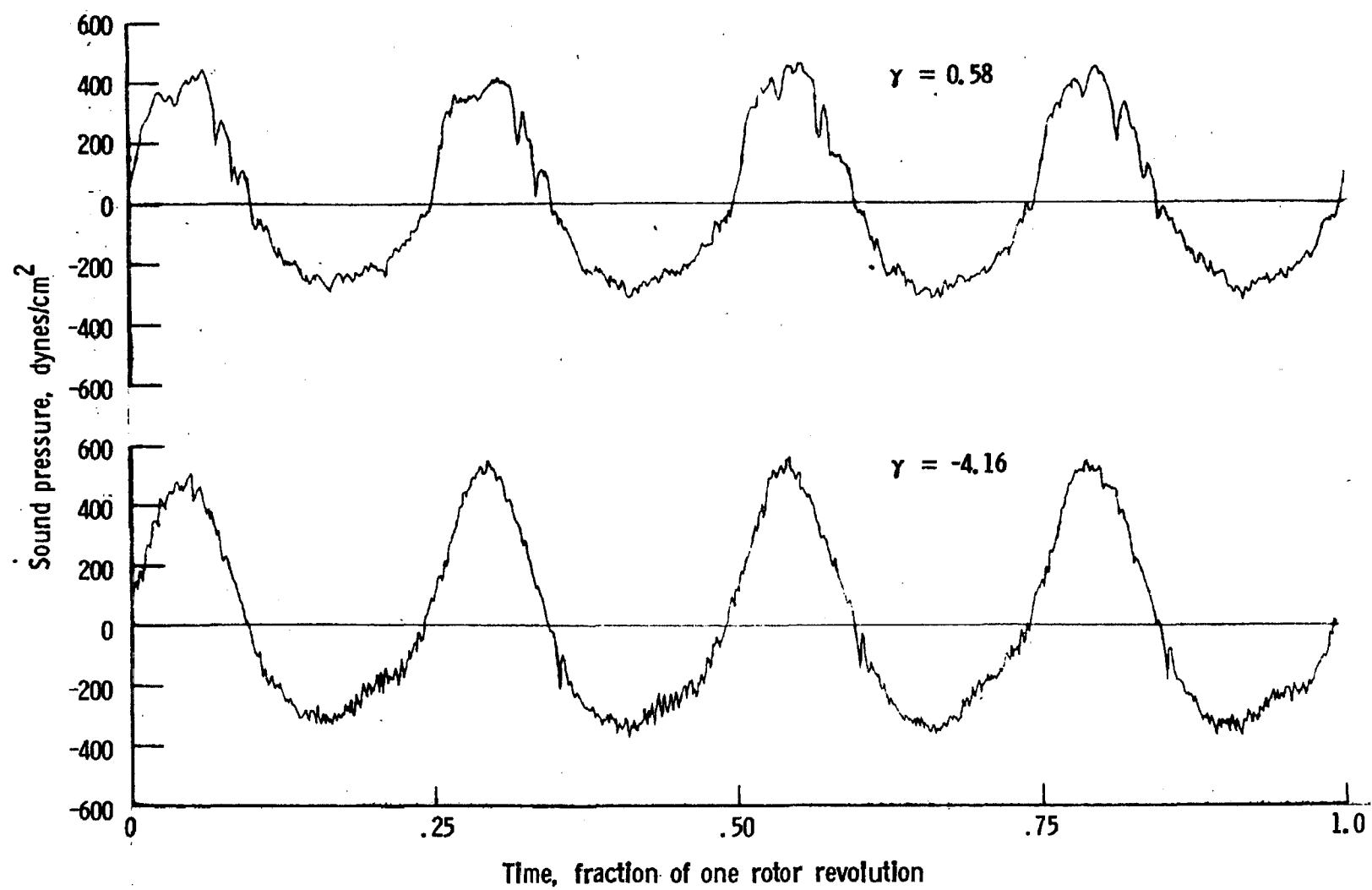
Figure 18. - Effect of descent angle variation on noise generation by helicopter model with swept-tapered tips installed. $V_\infty = 55.8$ knots.



One-third-octave-band center frequency, kHz

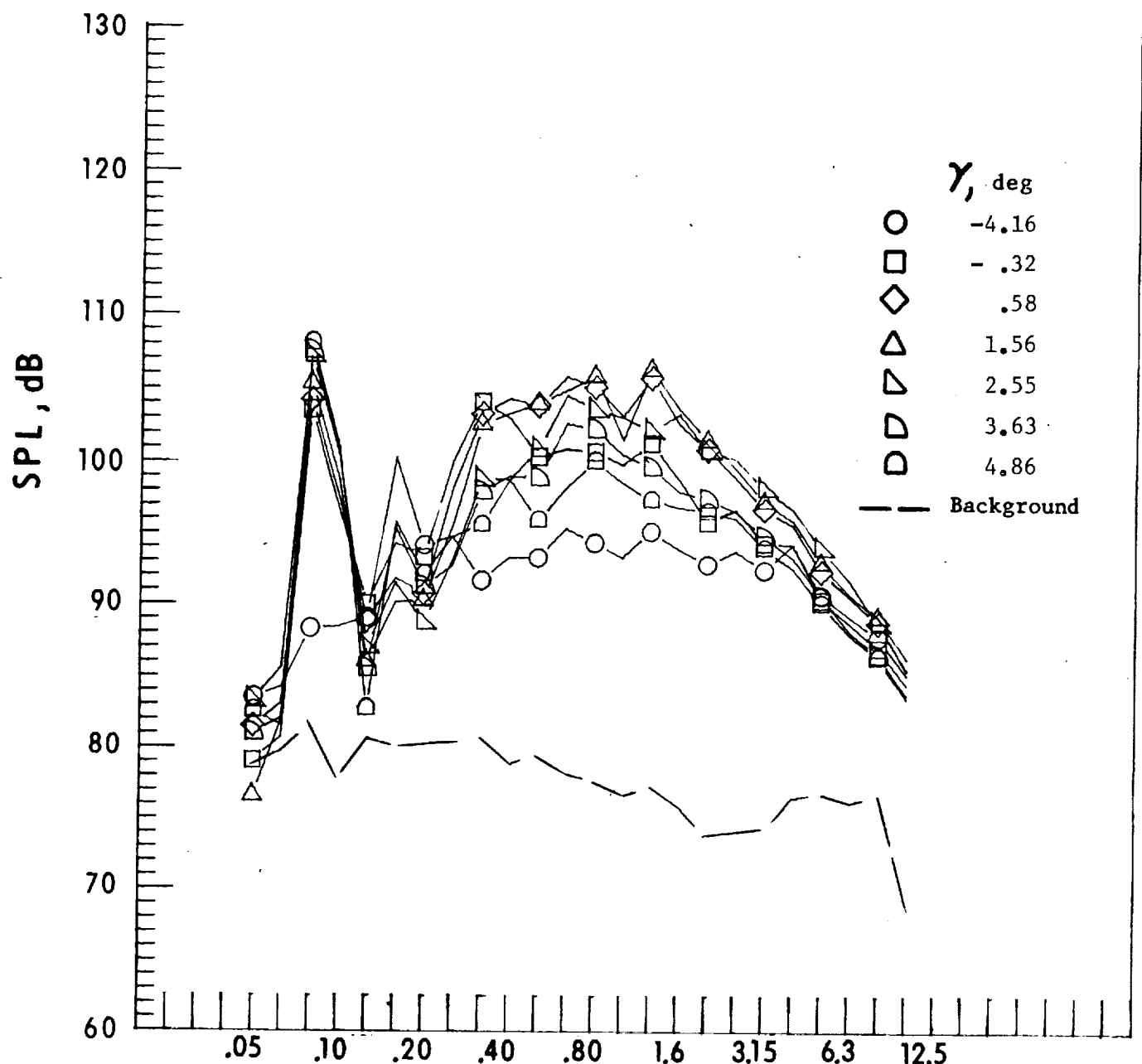
b. Mic. no. 2.

Figure 18. - Continued.



c. Pressure-time histories, Mic. no. 2.

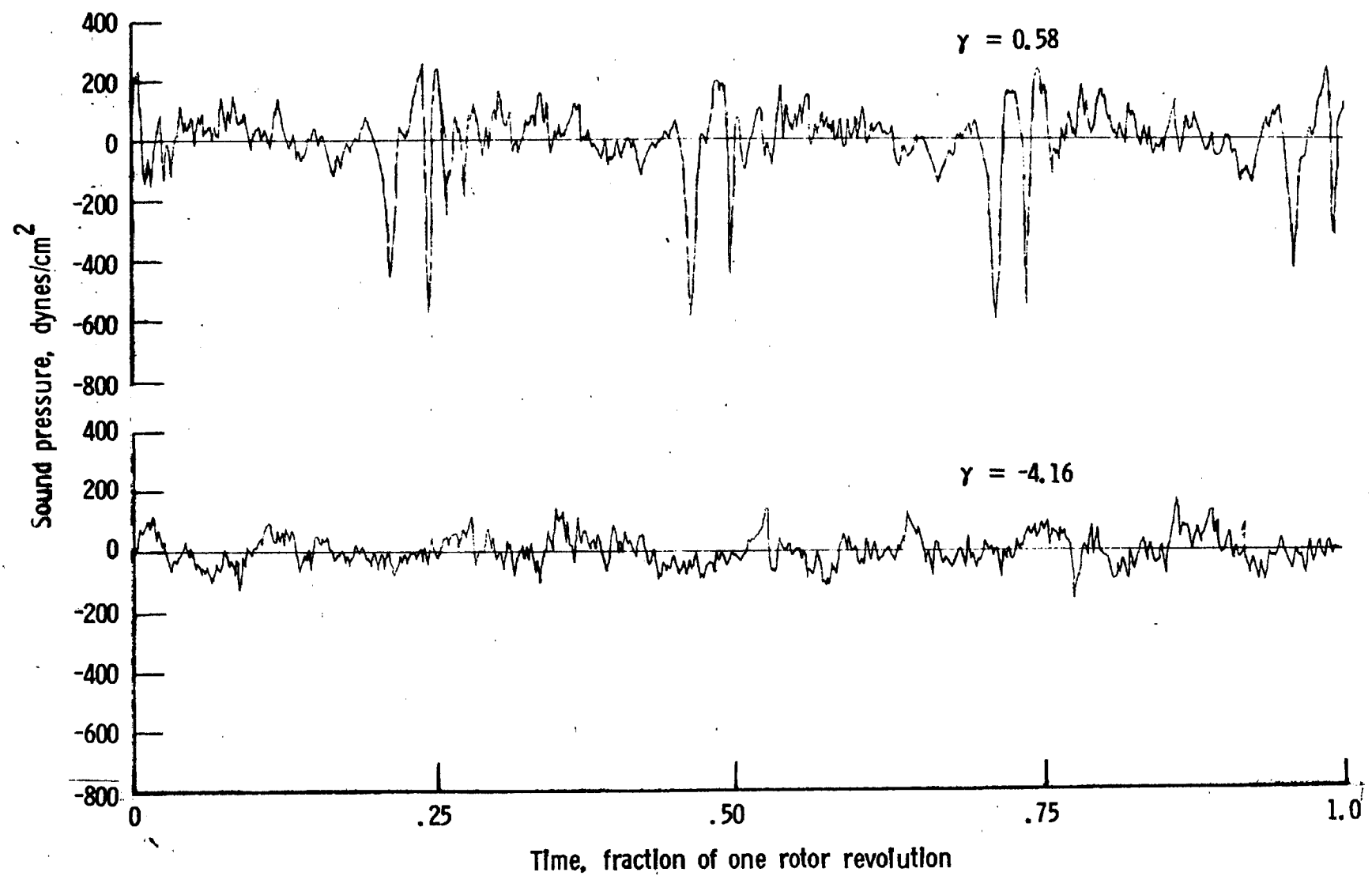
Figure 18. - Continued.



One-third-octave-band center frequency, kHz

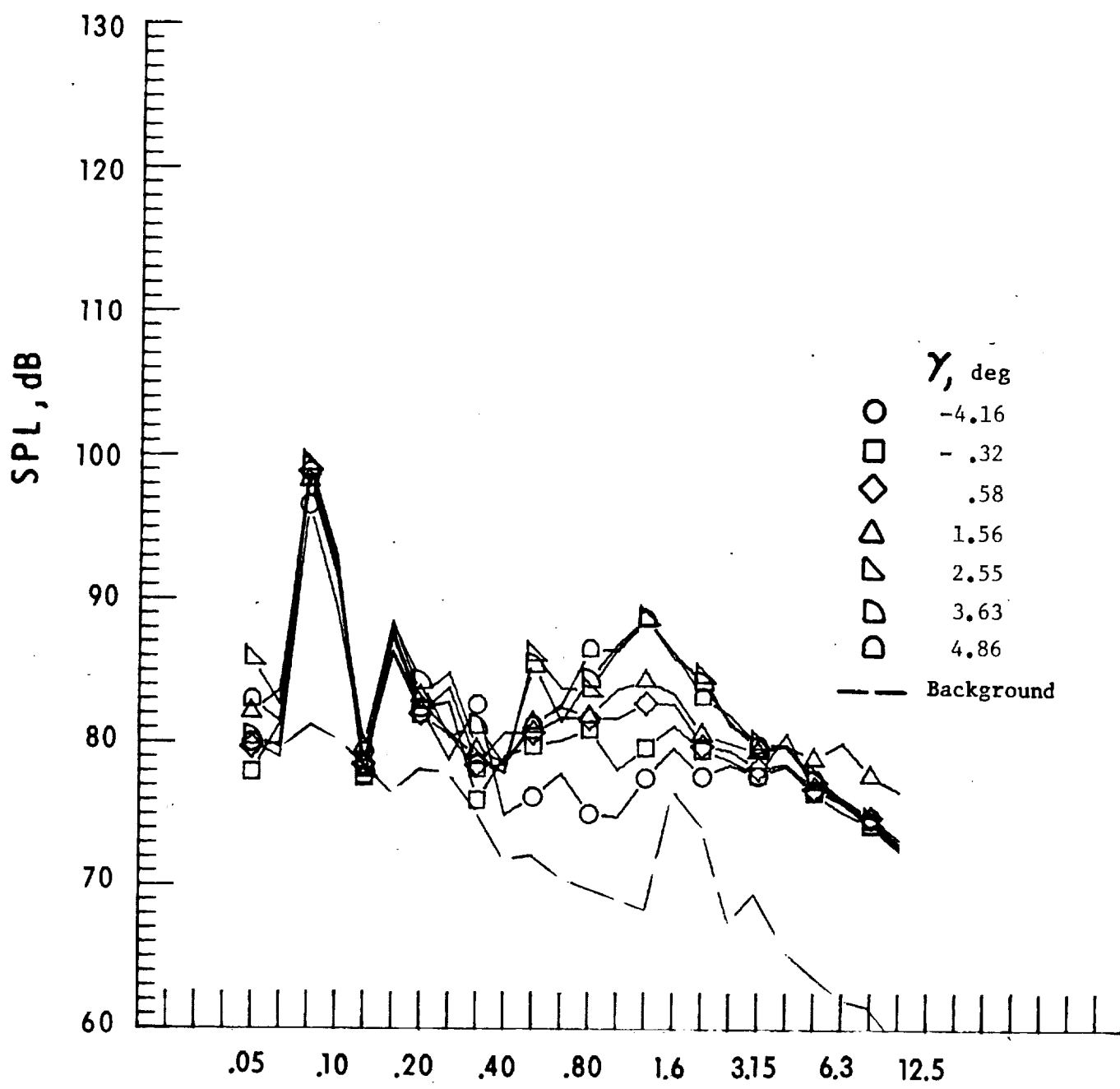
d. Mic. no. 3.

Figure 18. - Continued.



e. Pressure-time histories, Mic. no. 3.

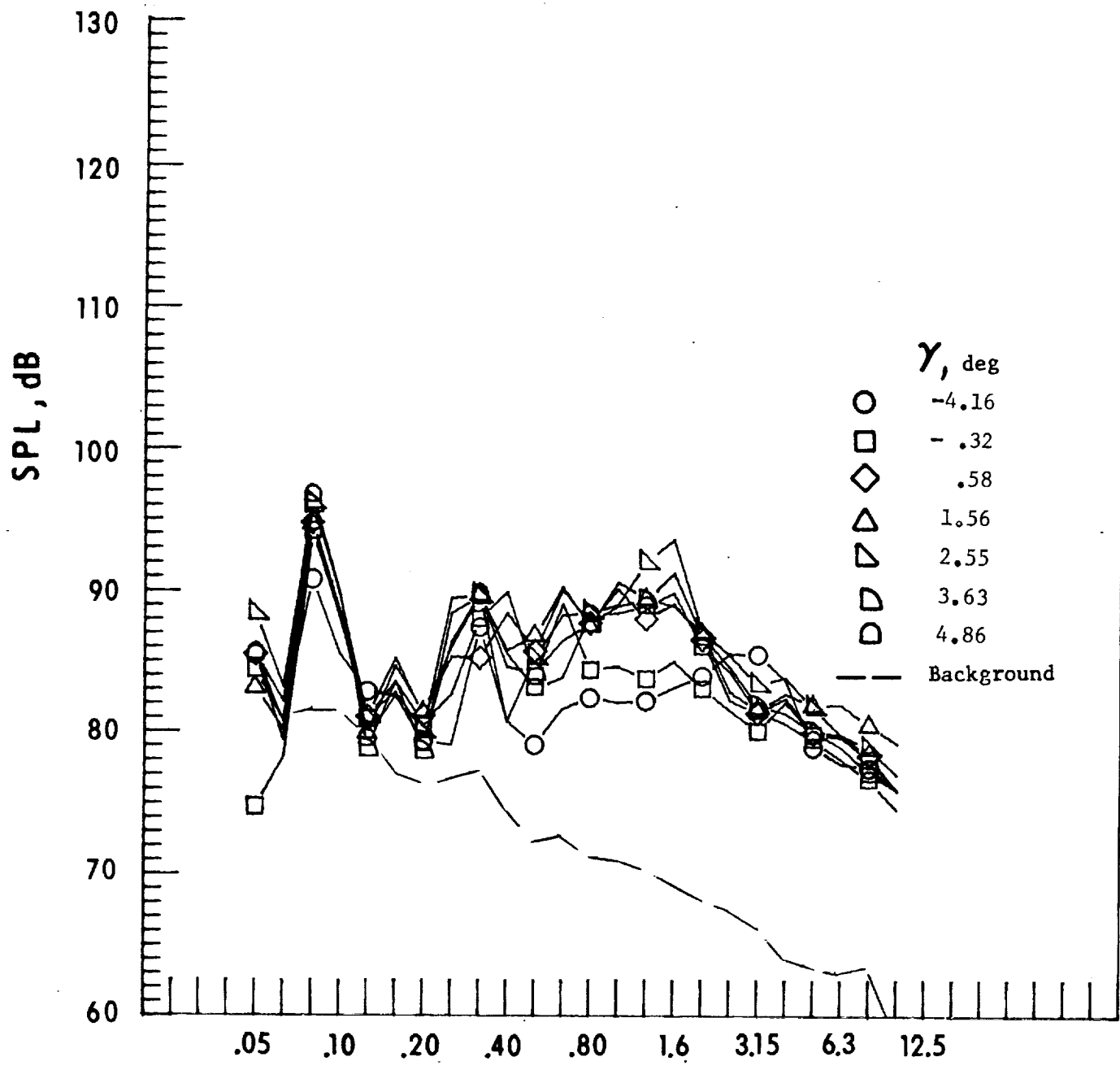
Figure 18. - Continued.



One-third-octave-band center frequency, kHz

f. Mic. no. 4.

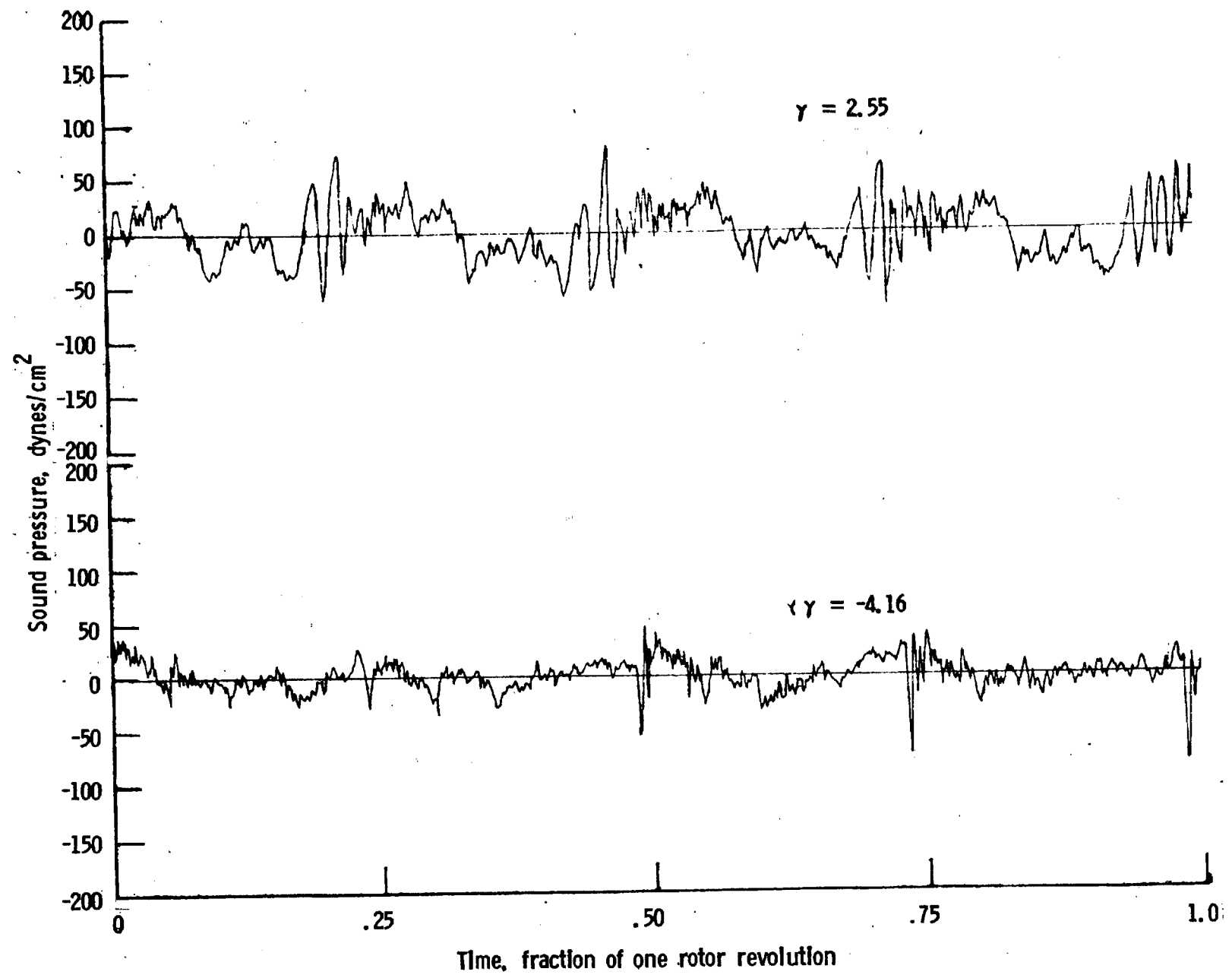
Figure 18. - Continued.



One-third-octave-band center frequency, kHz

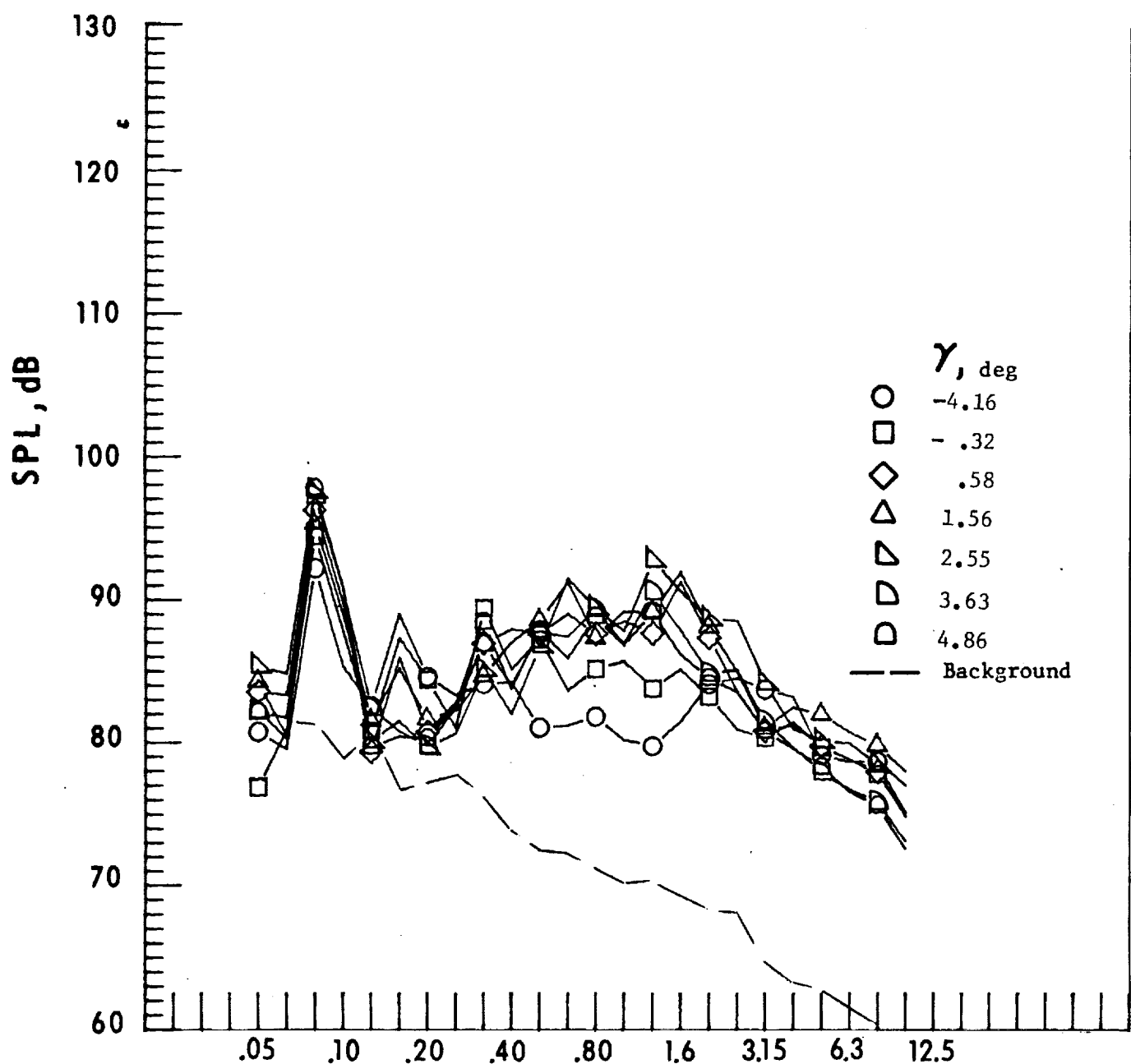
g. Mic. no. 5.

Figure 18. - Continued.



h. Pressure-time histories, Mic. no. 5.

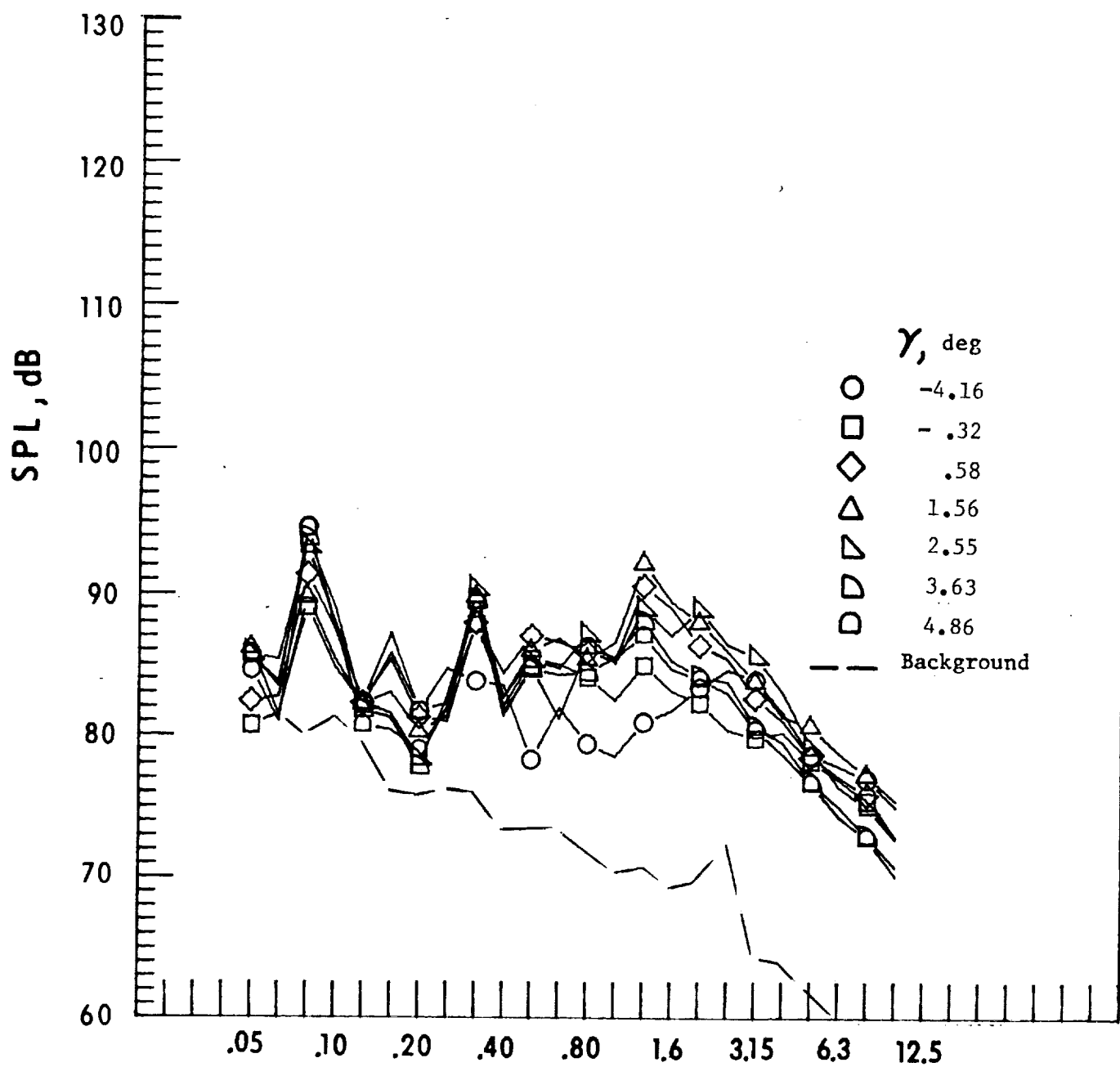
Figure 18. - Continued.



One-third-octave-band center frequency, kHz

i. Mic. no. 6.

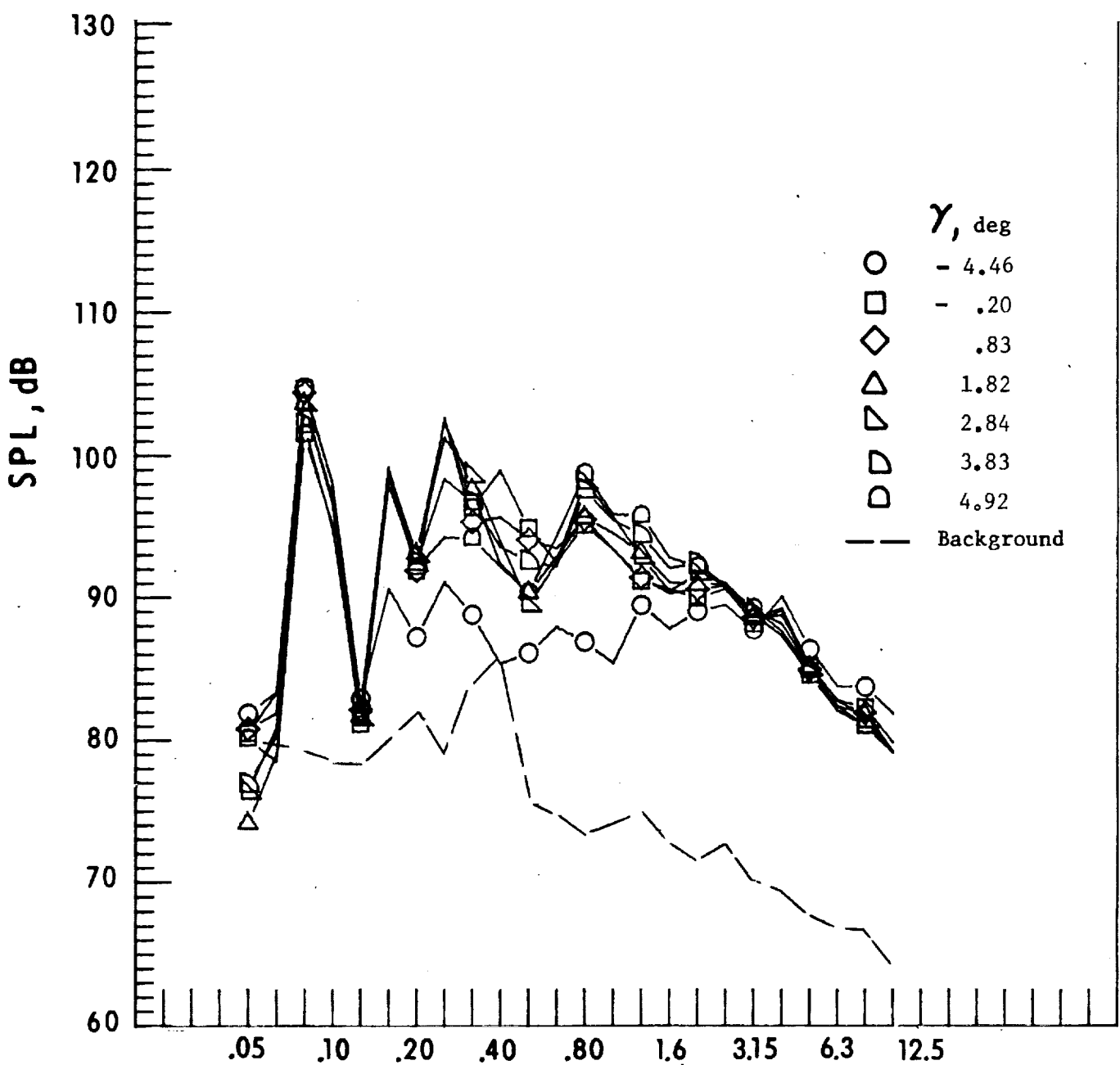
Figure 18. - Continued.



One-third-octave-band center frequency, kHz

j. Mic. no. 7.

Figure 18. - Concluded.



One-third-octave-band center frequency, kHz

a. Mic. no. 1.

Figure 19. - Effect of descent angle variation on noise generation by helicopter model with end-plate tips installed. $V_{\infty} = 55.3$ knots.

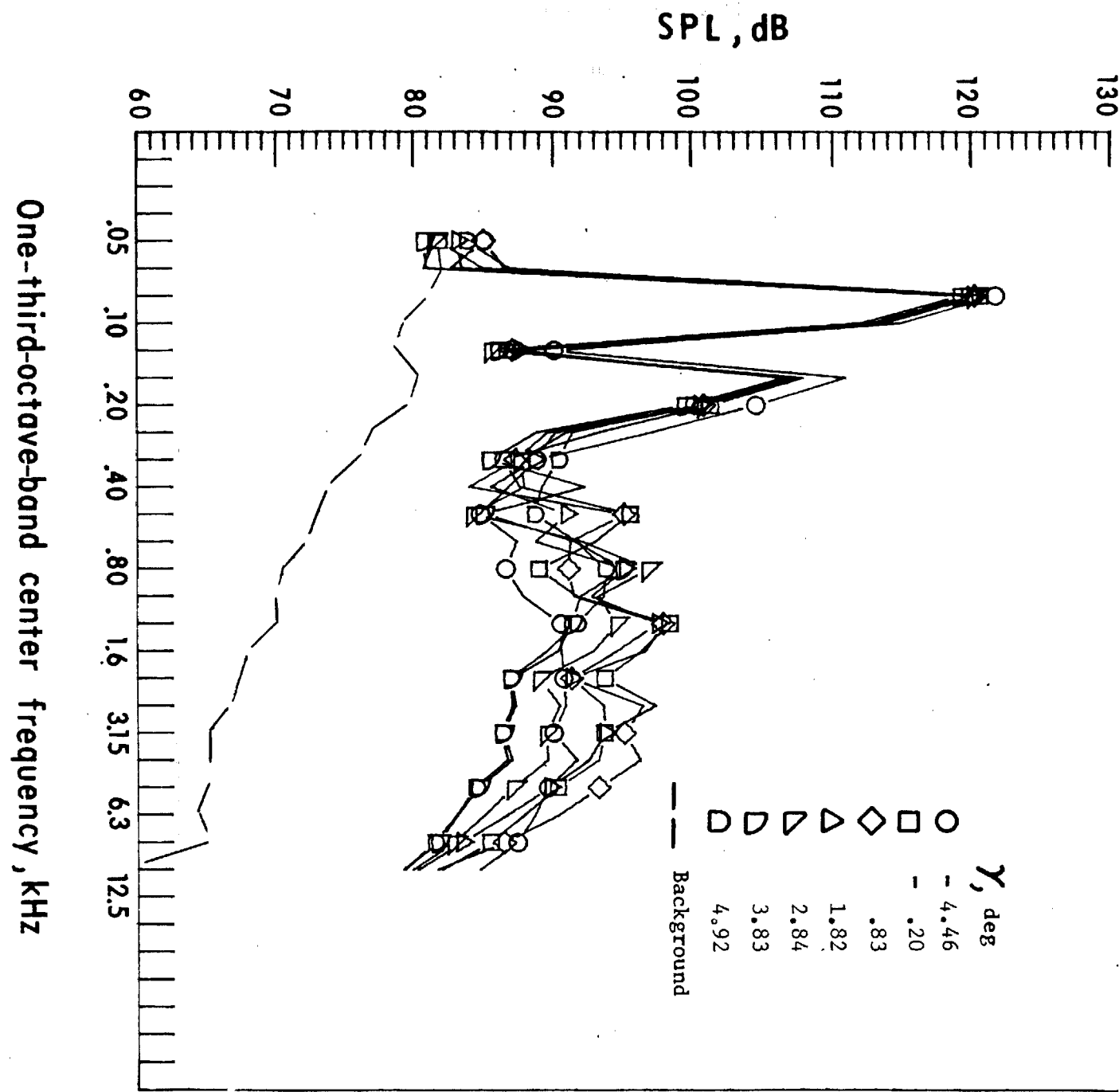
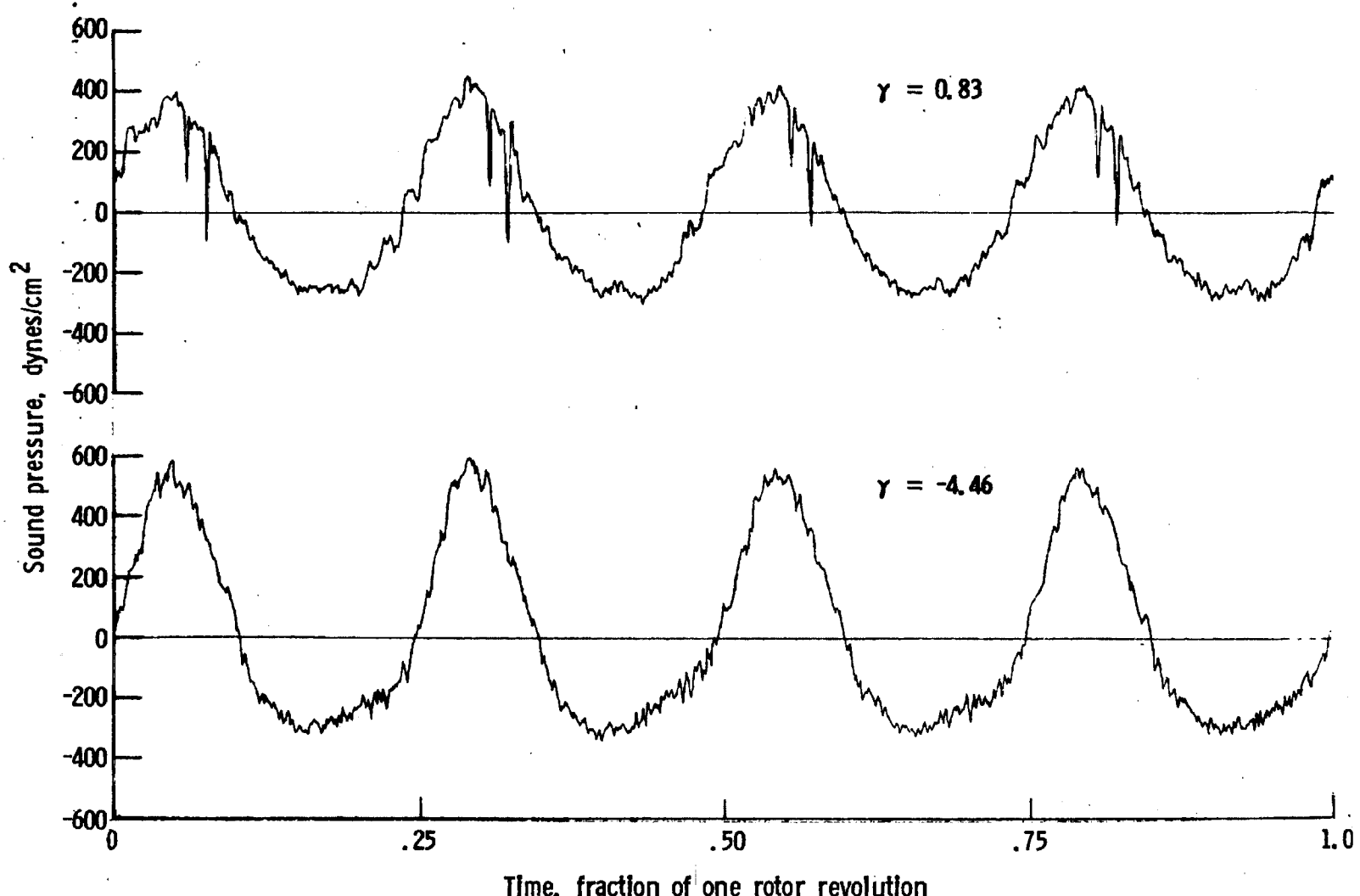


Figure 19. - Continued.

b. Mic. no. 2.



c. Pressure-time histories, Mic. no. 2.

Figure 19. - Continued.

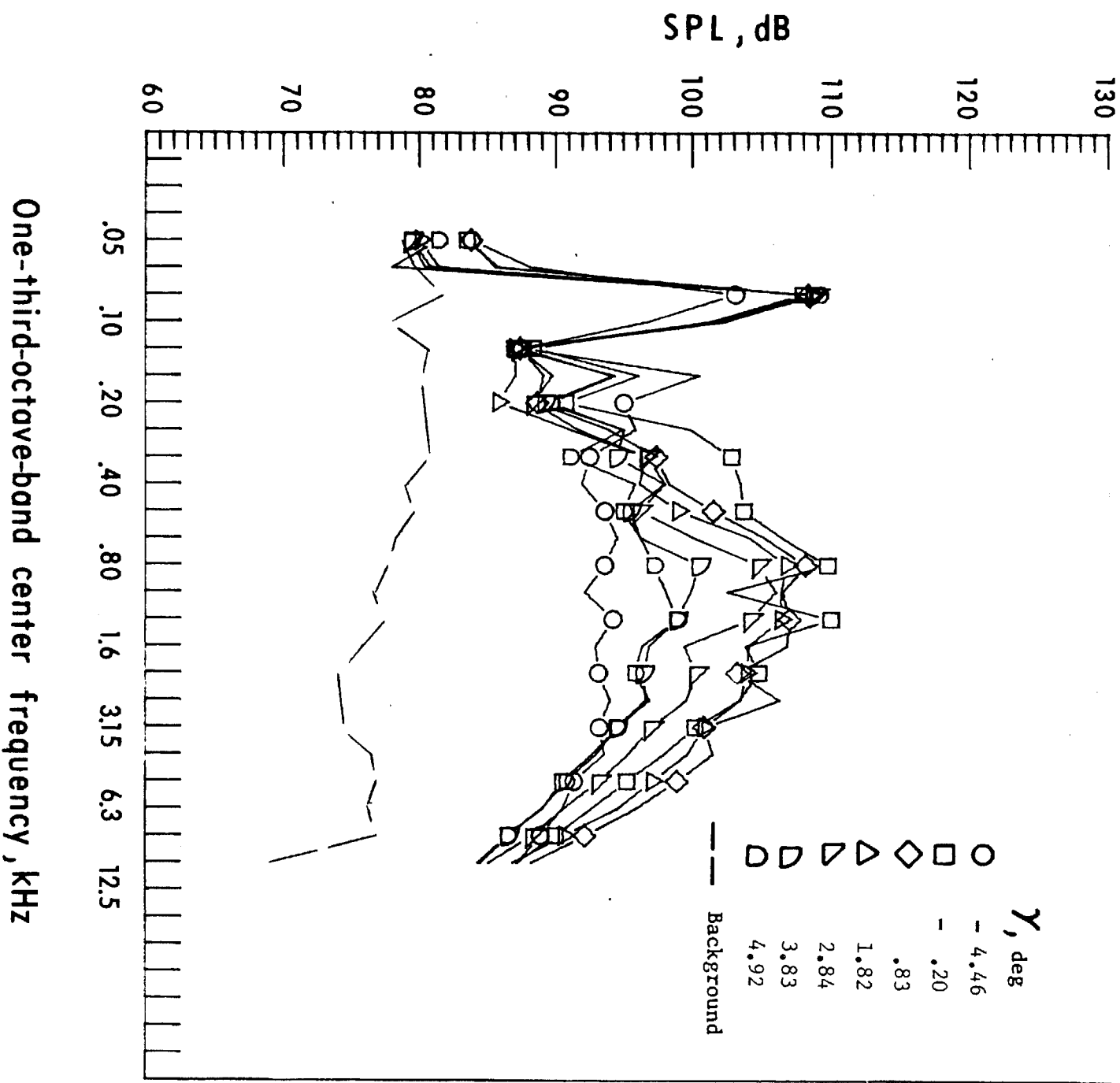
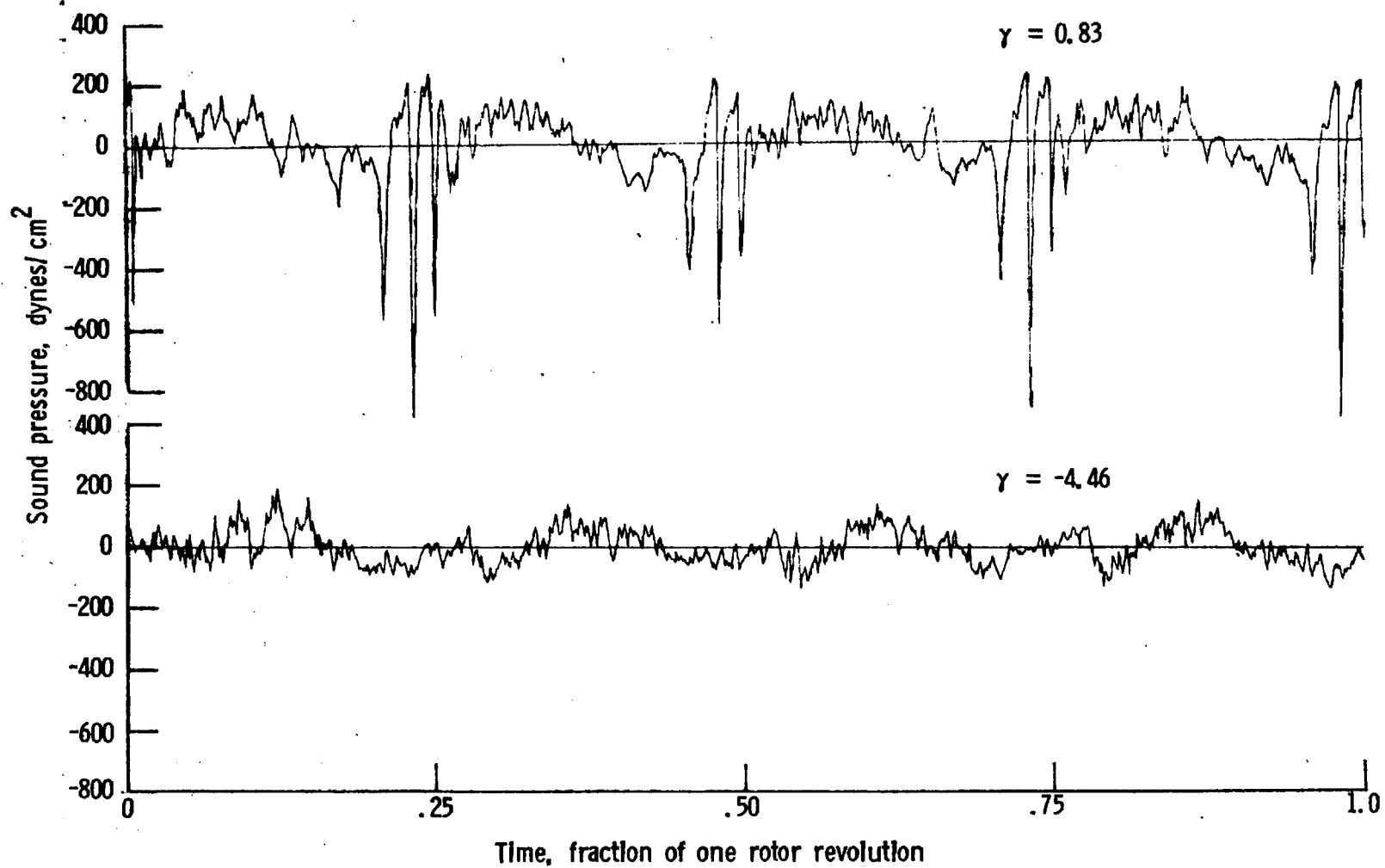


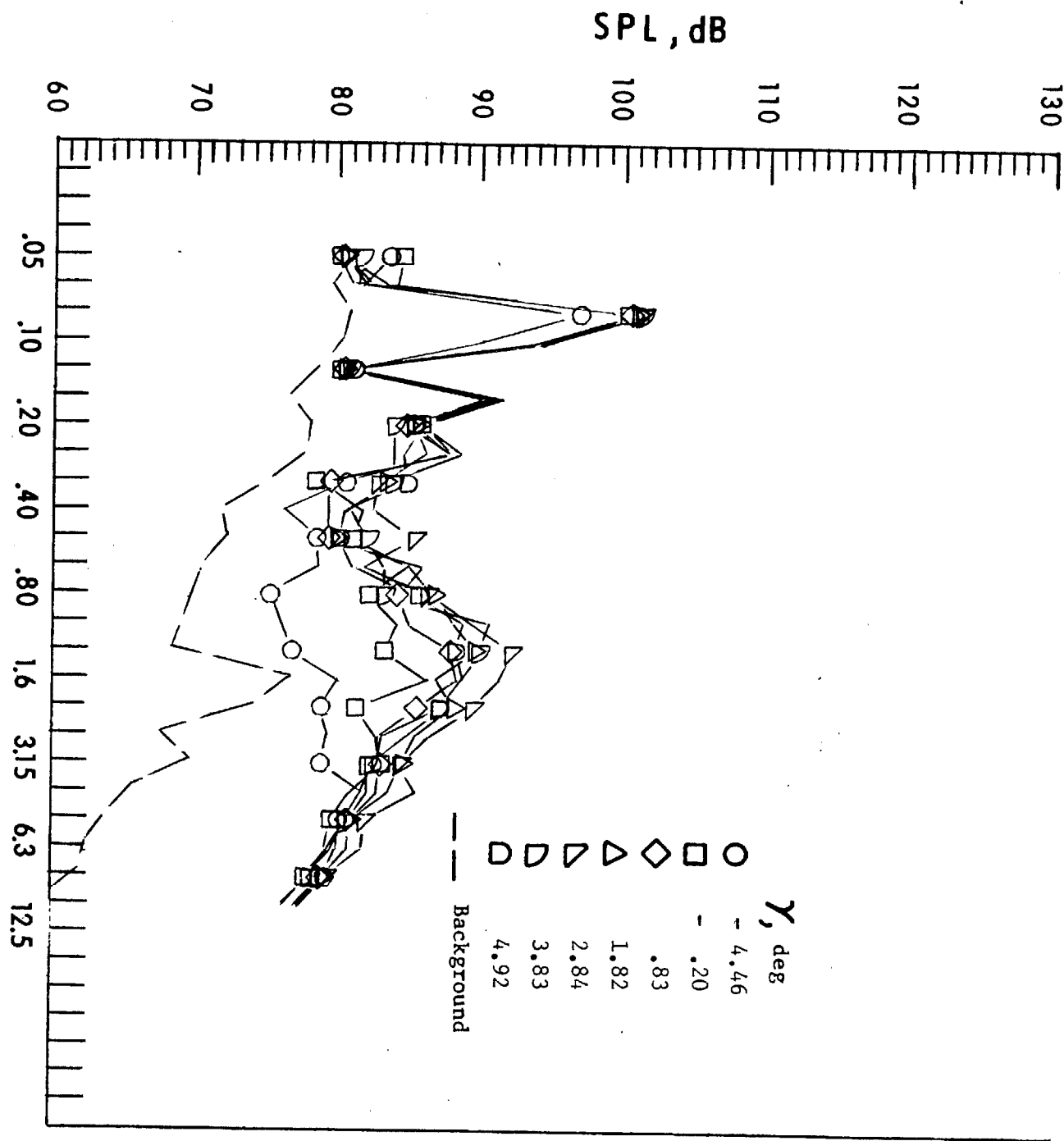
Figure 19. - Continued.

d. Mic. no. 3.



e. Pressure-time histories, Mic. no. 3.

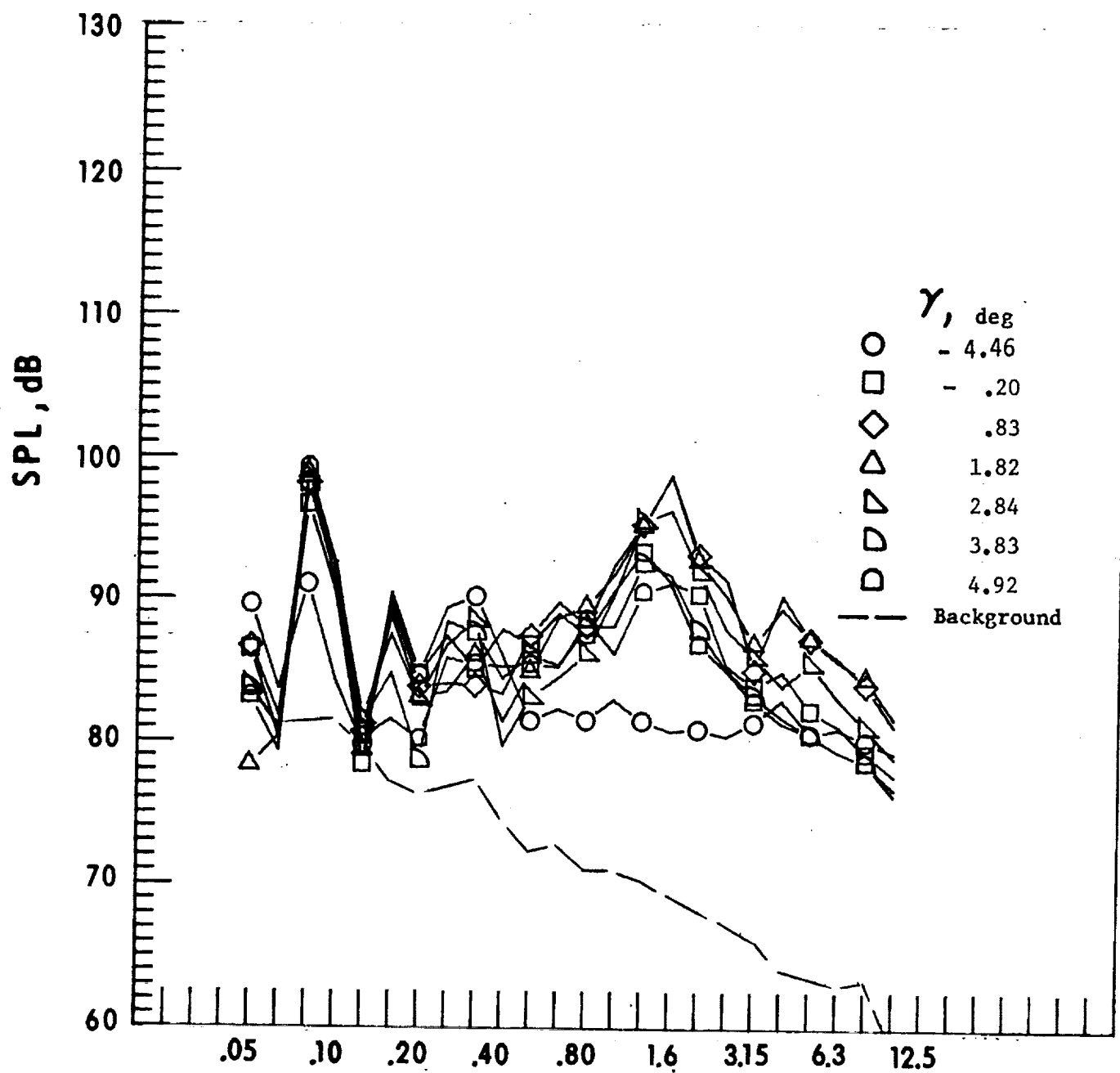
Figure 19. - Continued.



One-third-octave-band center frequency, kHz

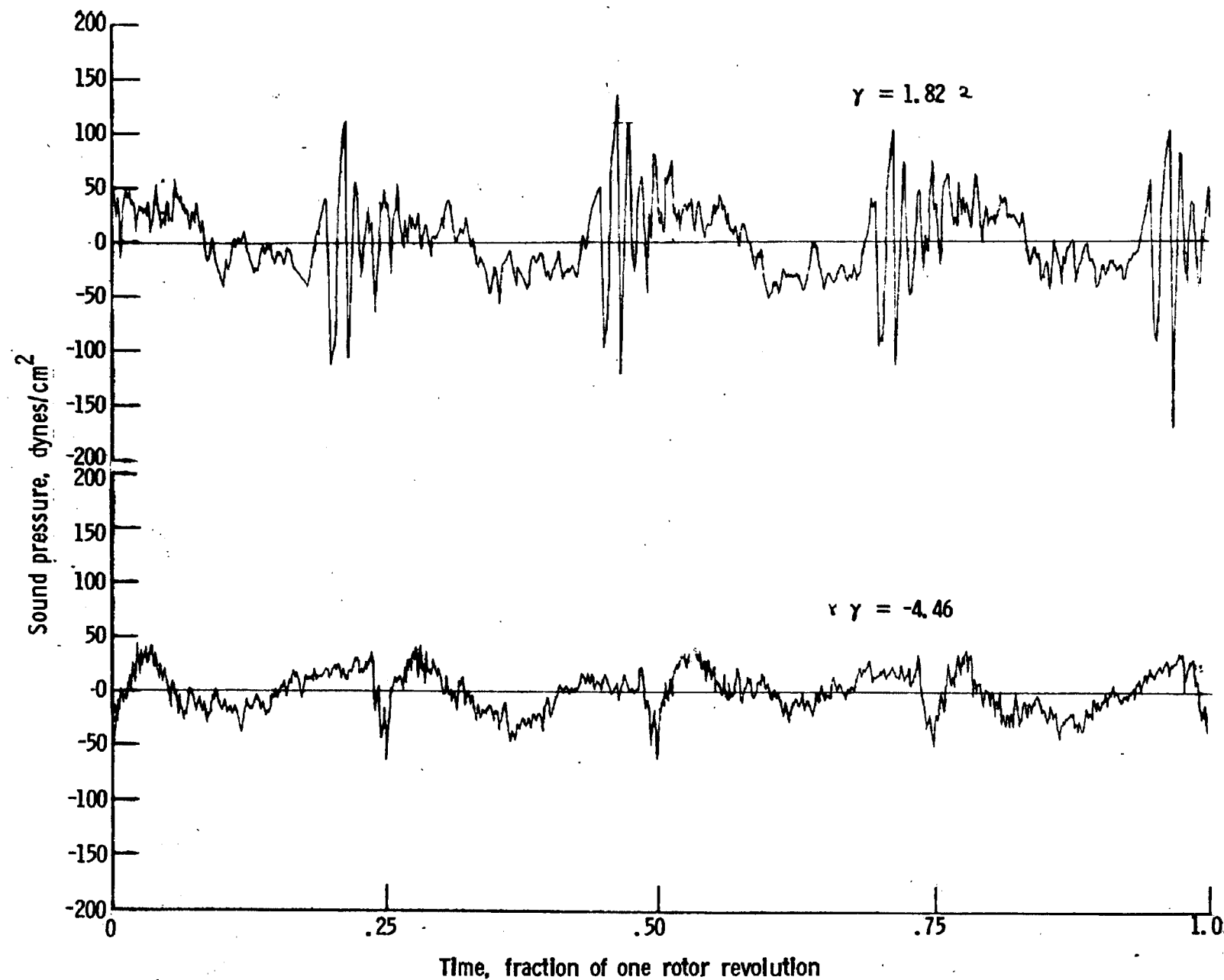
f. Mic. no. 4.

Figure 19. - Continued.

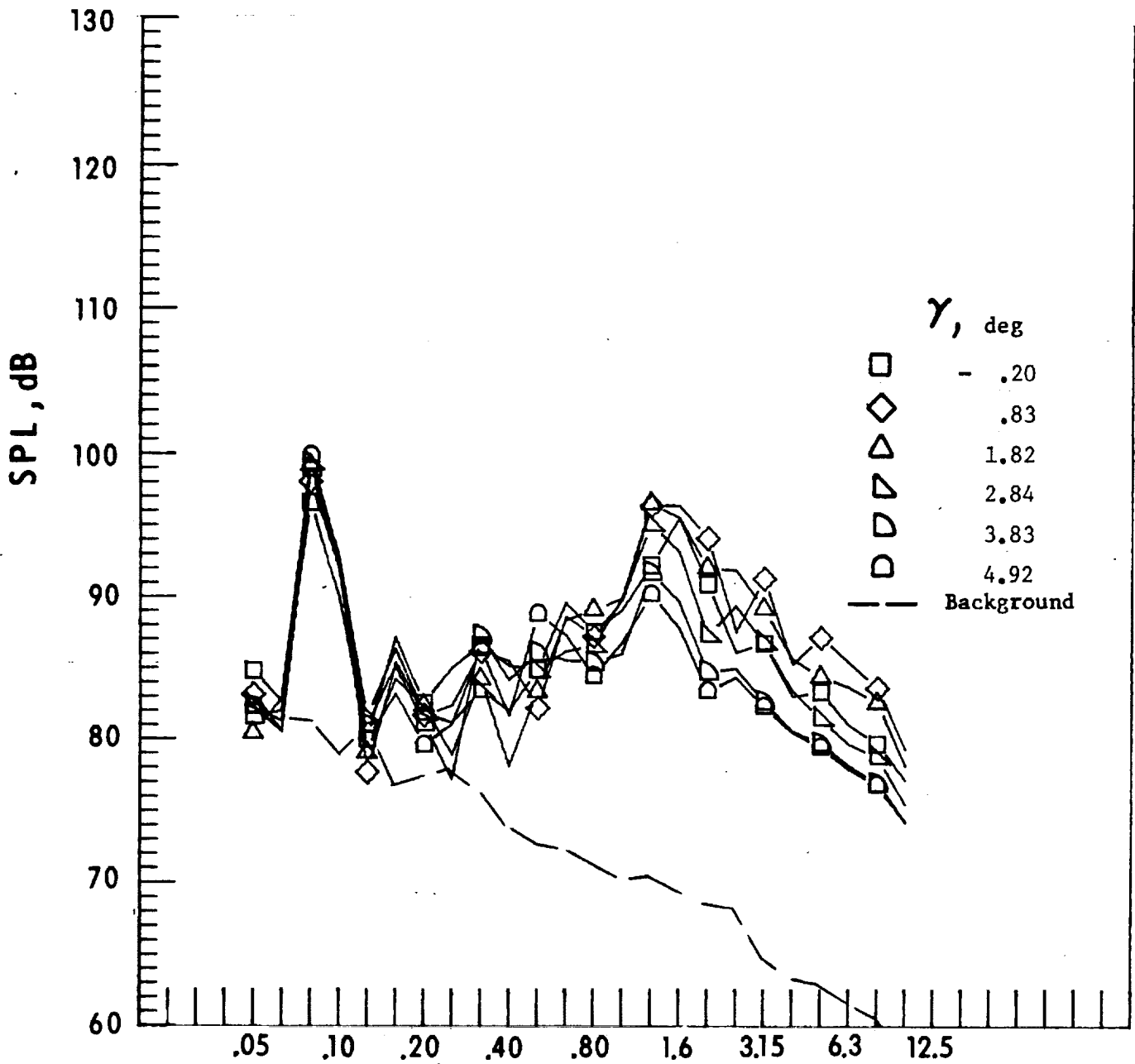


g. Mic. no. 5.

Figure 19. - Continued.



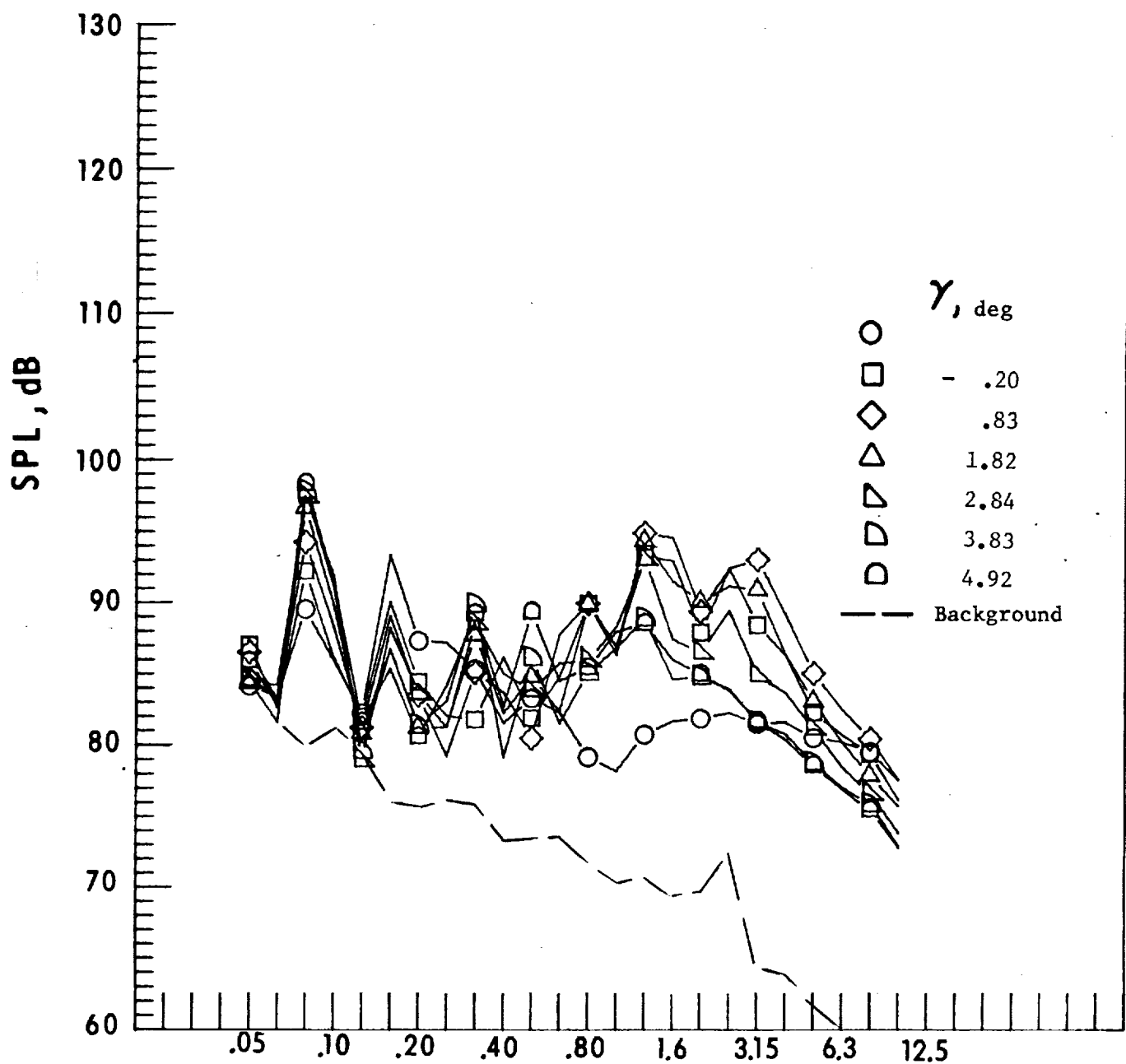
h. Pressure-time histories, Mic. no. 5.



One-third-octave-band center frequency, kHz

i. Mic. no. 6.

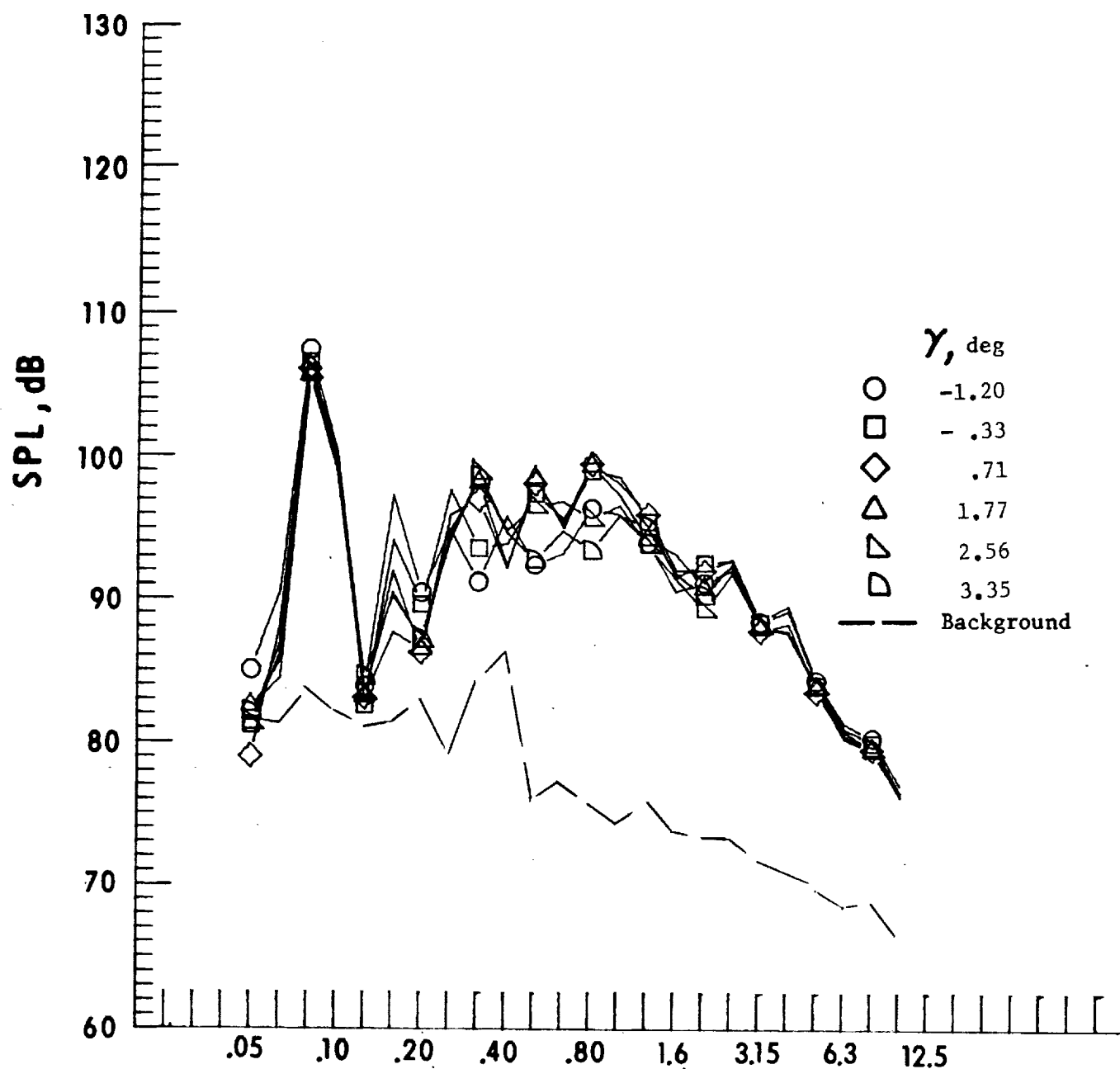
Figure 19. - Continued.



One-third-octave-band center frequency, kHz

j. Mic. no. 7.

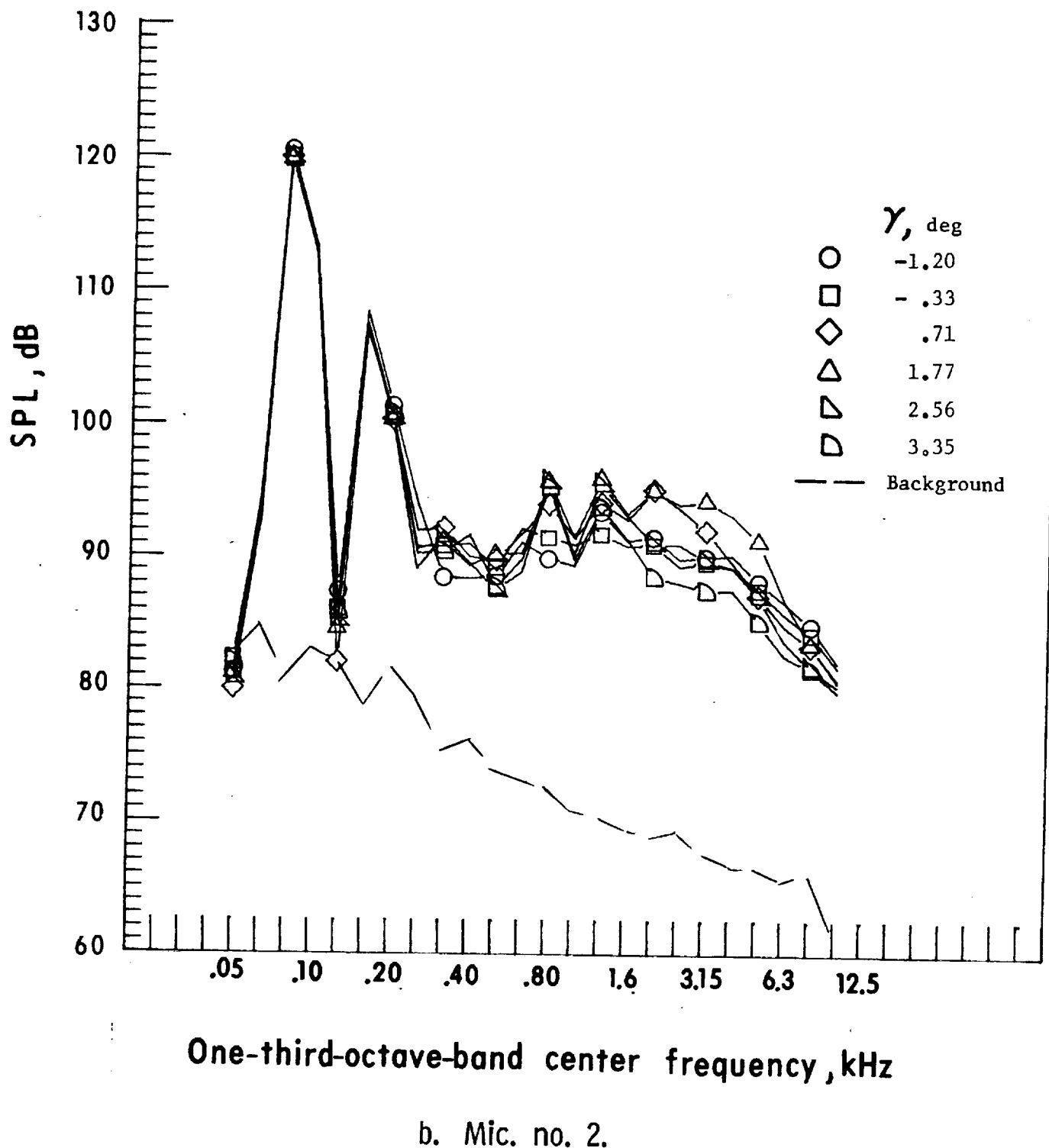
Figure 19. - Concluded.



One-third-octave-band center frequency, kHz

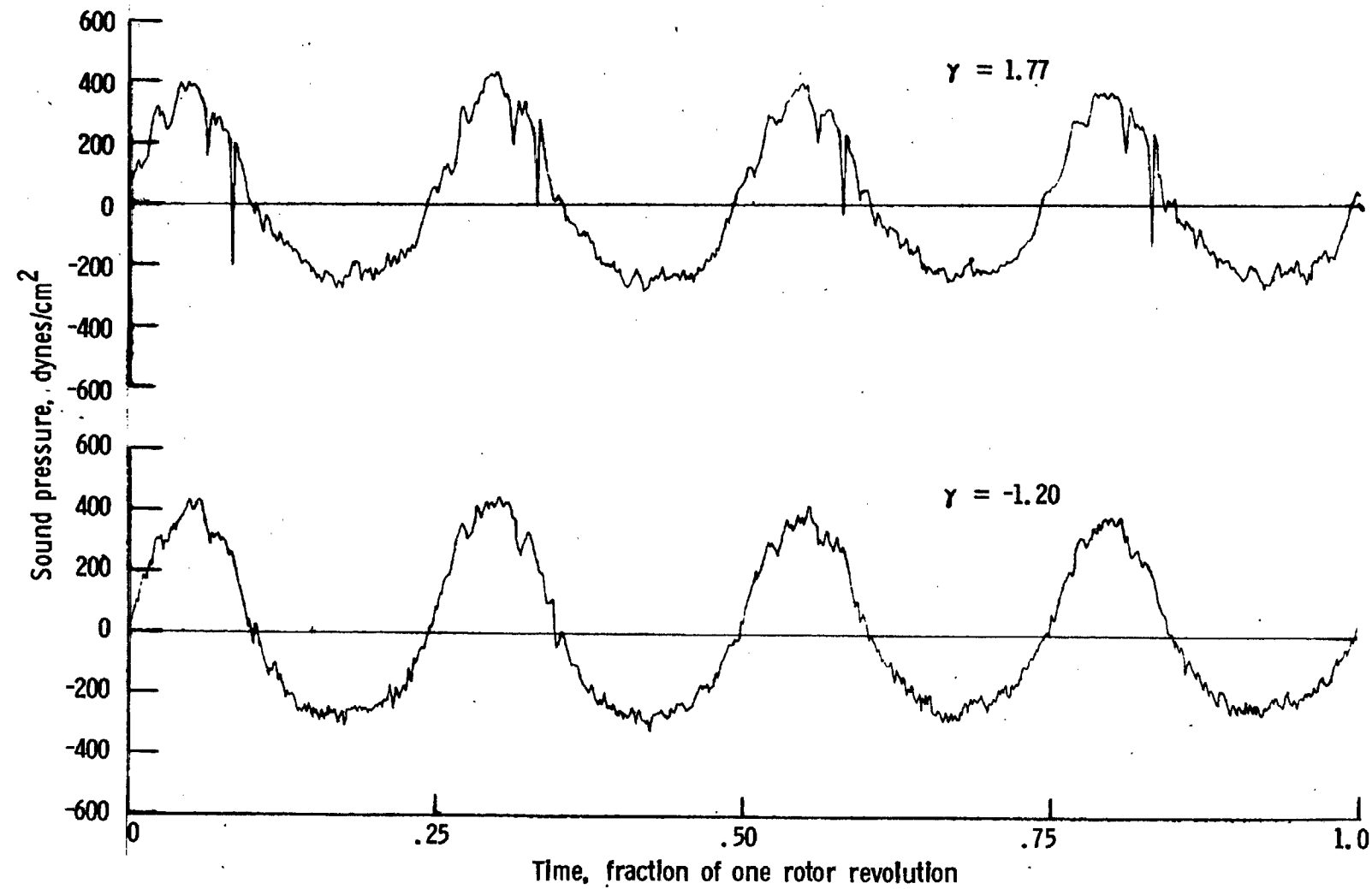
a. Mic. no. 1.

Figure 20. - Effect of descent angle variation on noise generation by helicopter model with square tips installed. $V_\infty = 61.3$ knots.



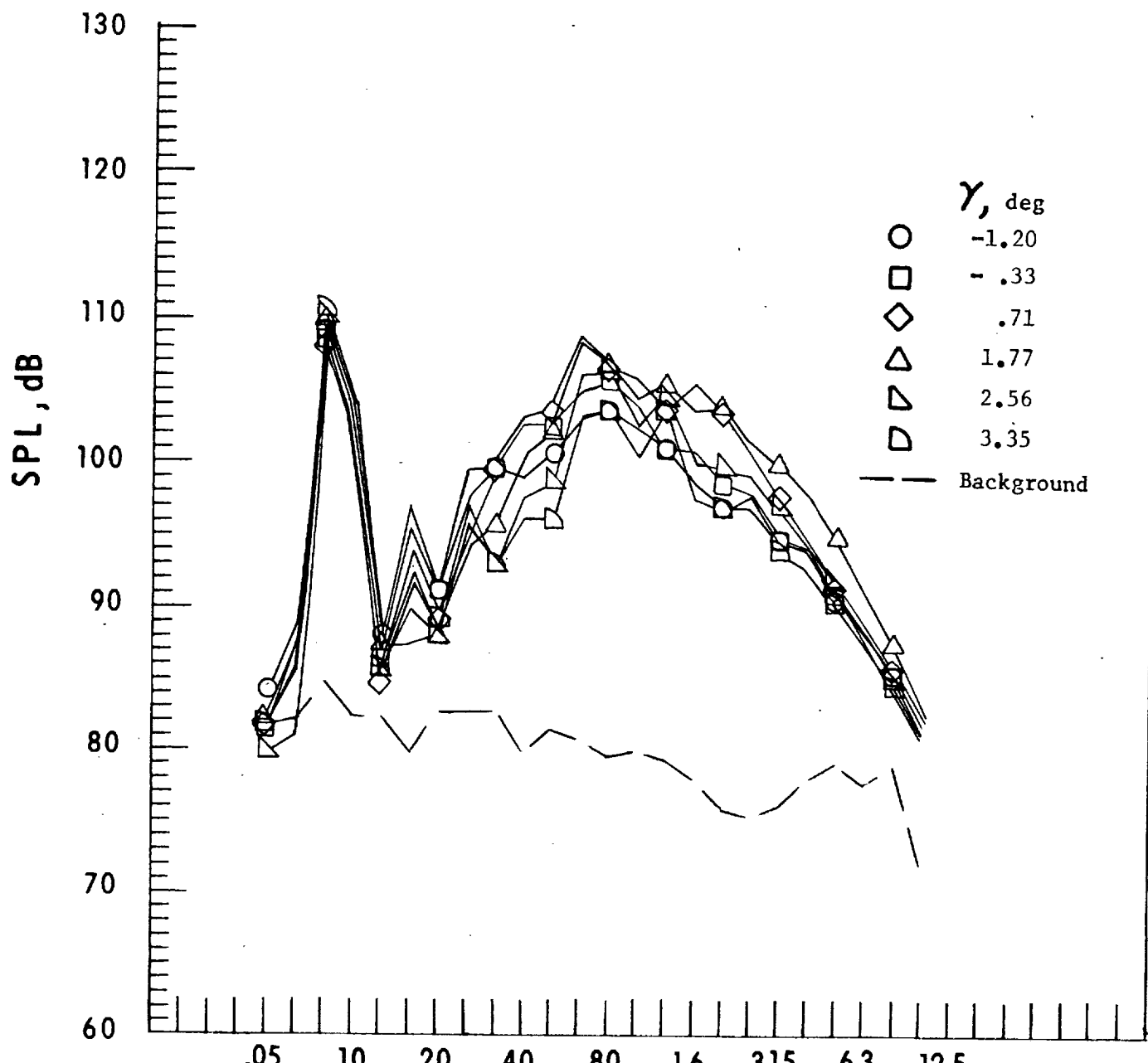
b. Mic. no. 2.

Figure 20. - Continued.



c. Pressure-time histories, Mic. no. 2.

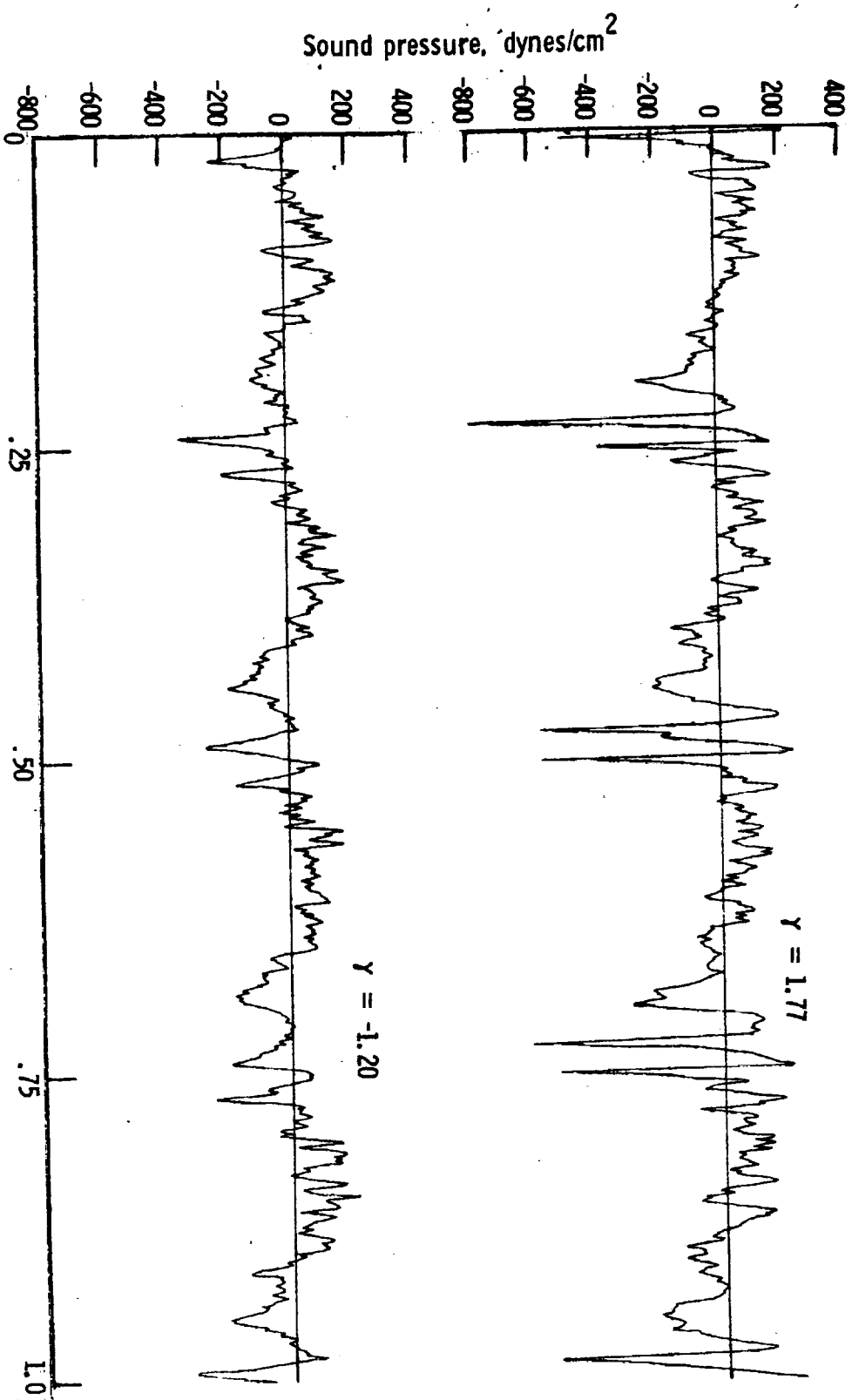
Figure 20. - Continued.



One-third-octave-band center frequency, kHz

d. Mic. no. 3.

Figure 20. - Continued.



e. Pressure-time histories, Mic. no. 3.

Figure 20. - Continued.

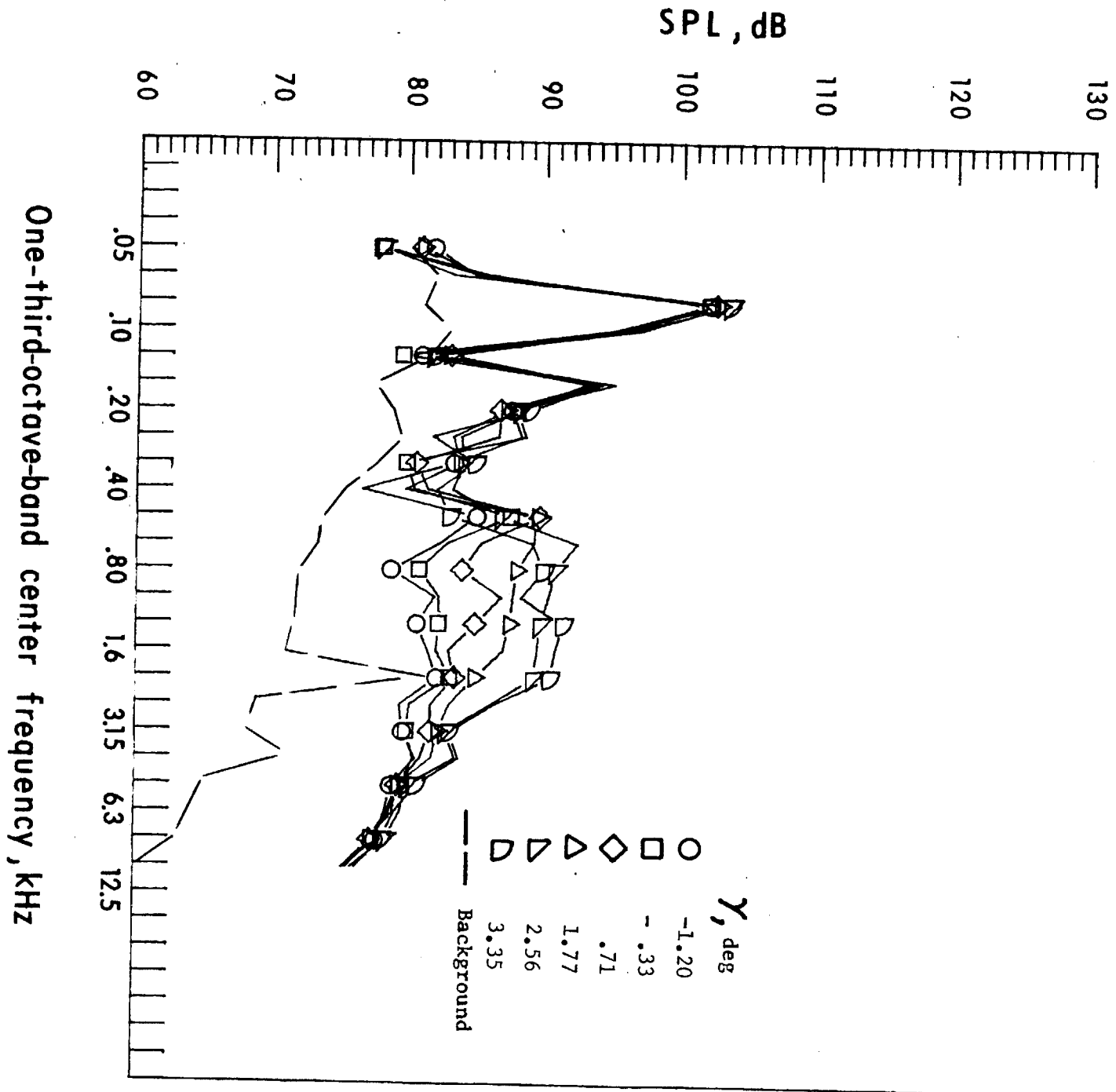
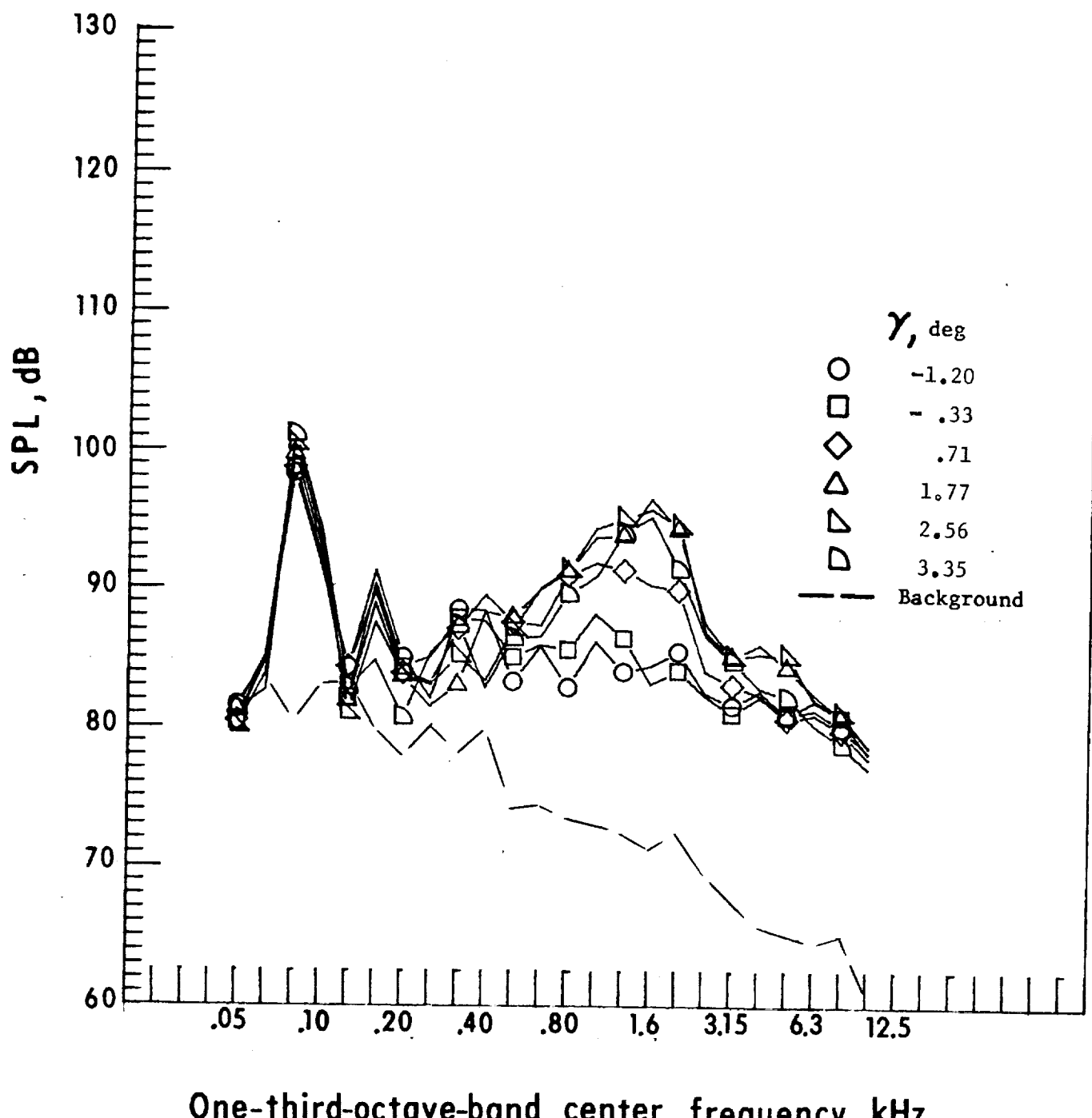


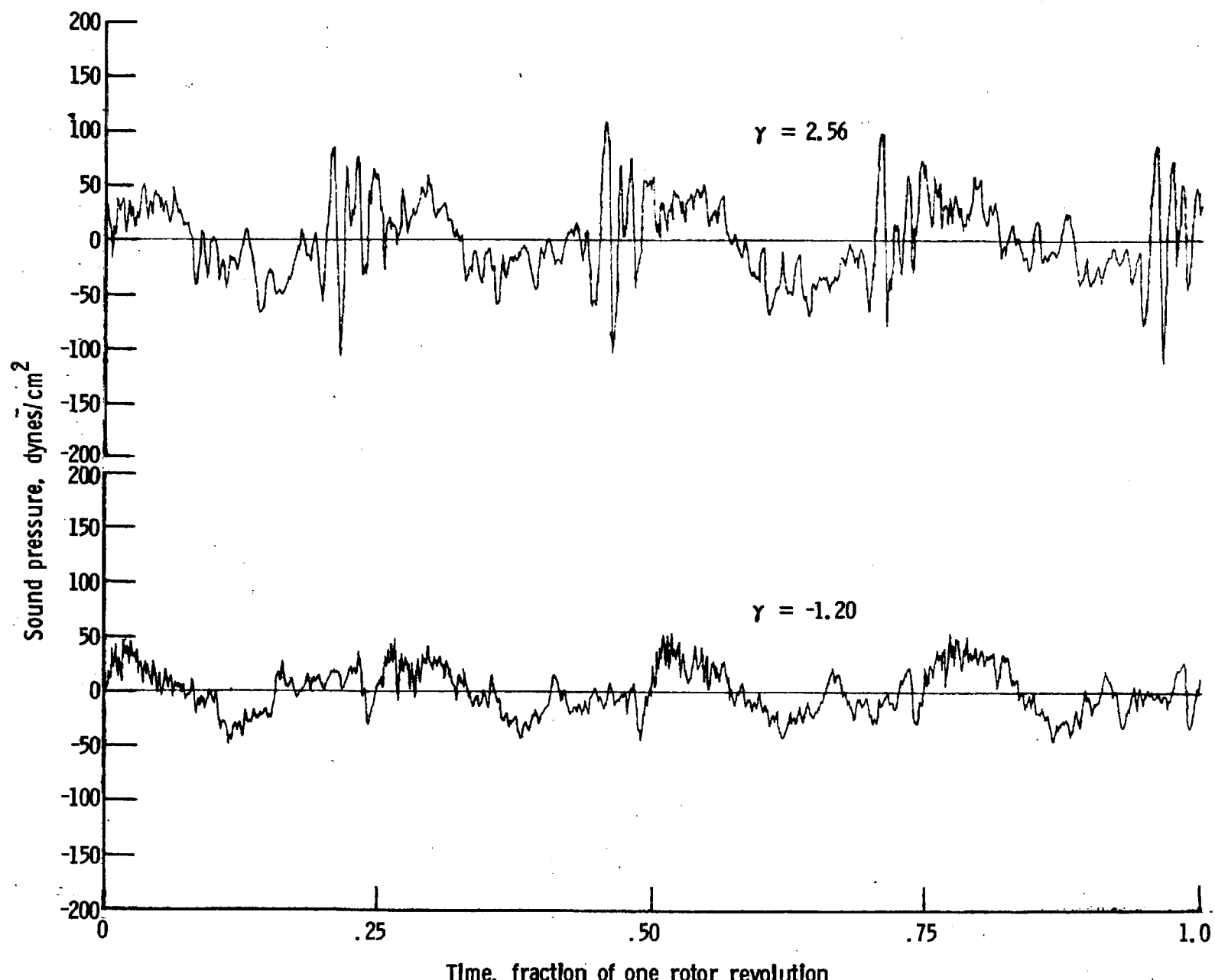
Figure 20. - Continued.



One-third-octave-band center frequency, kHz

g. Mic. no. 5.

Figure 20. - Continued.



h. Pressure-time histories, Mic. no. 5.

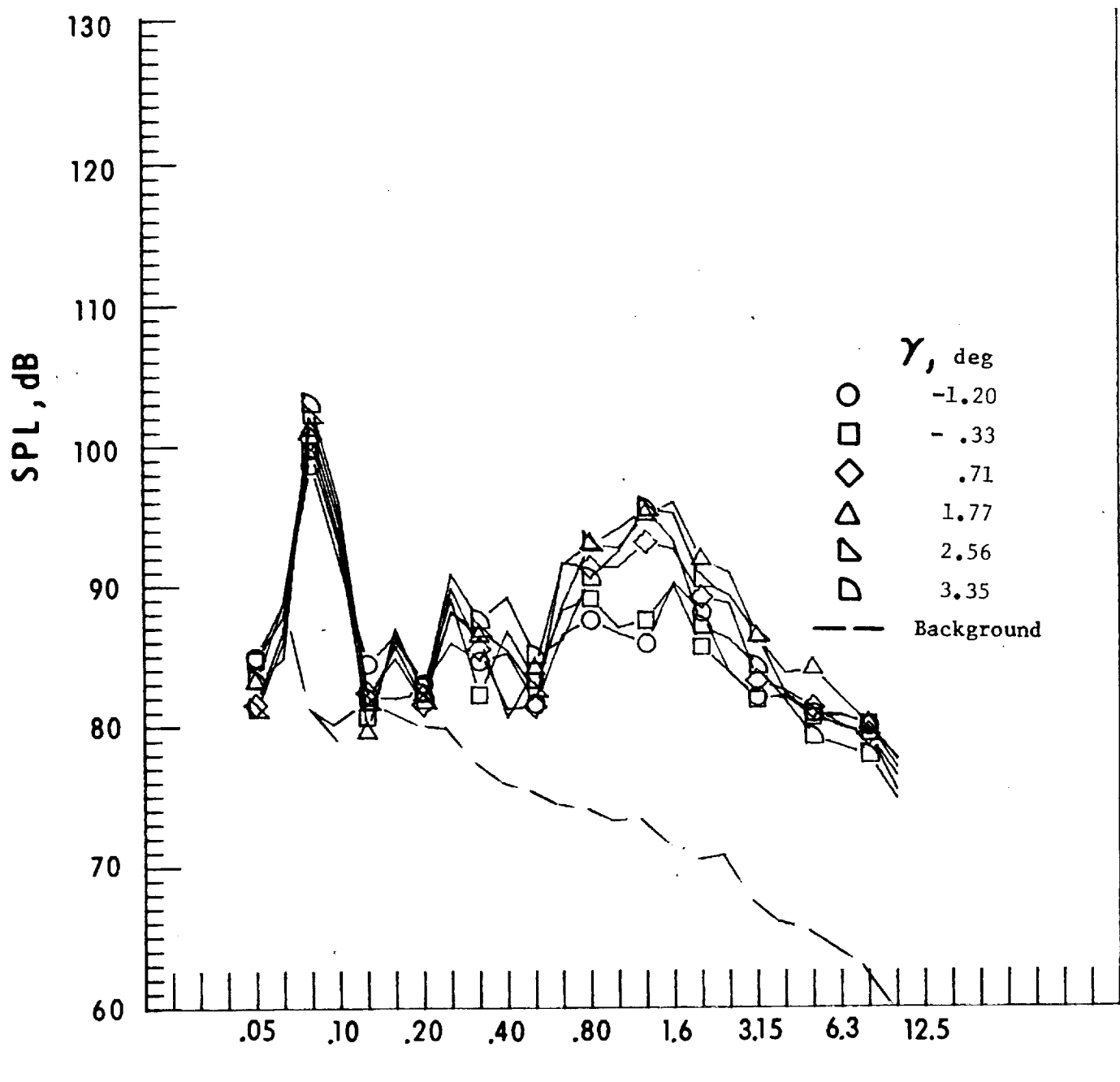
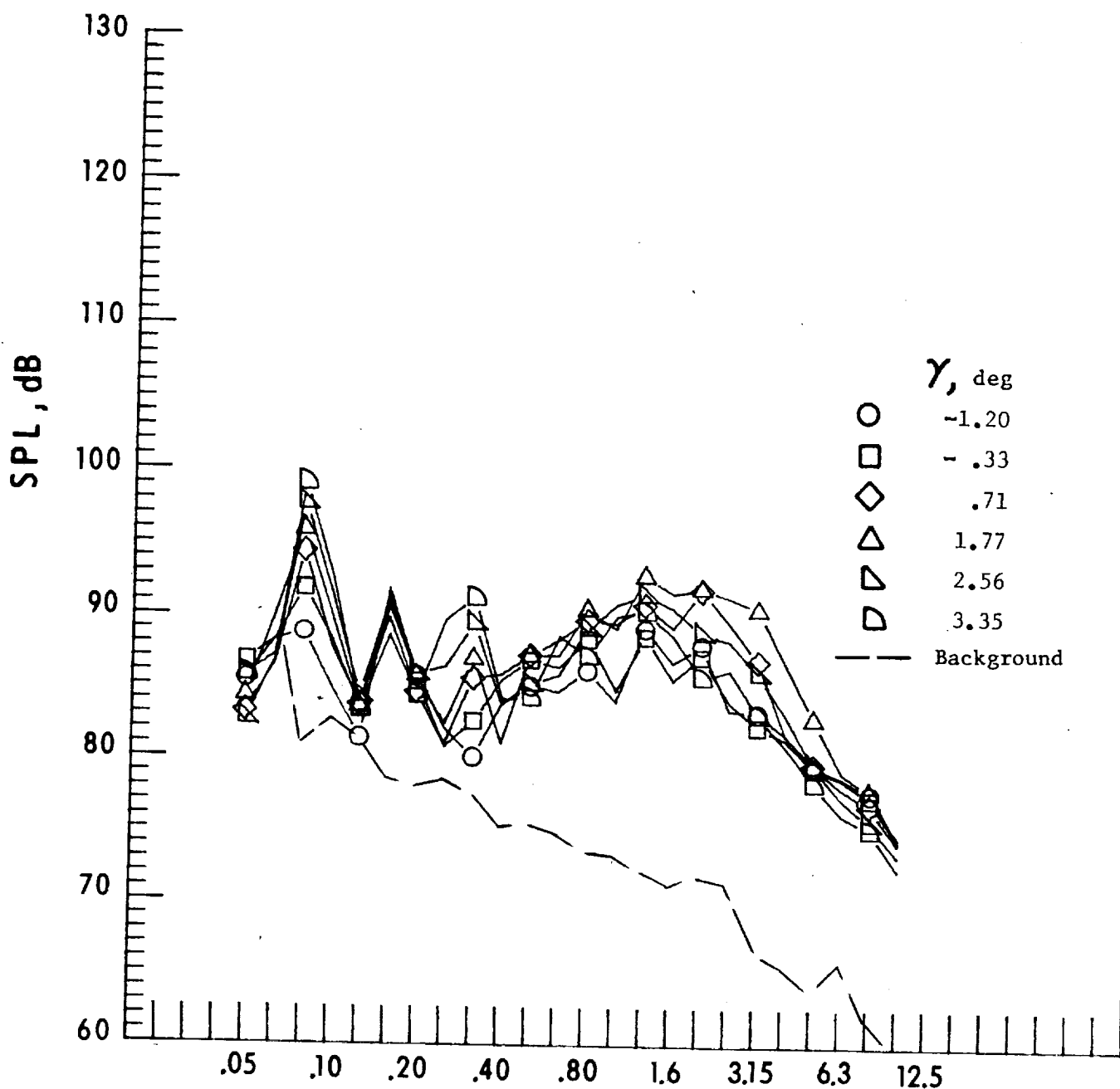


Figure 20. - Continued.

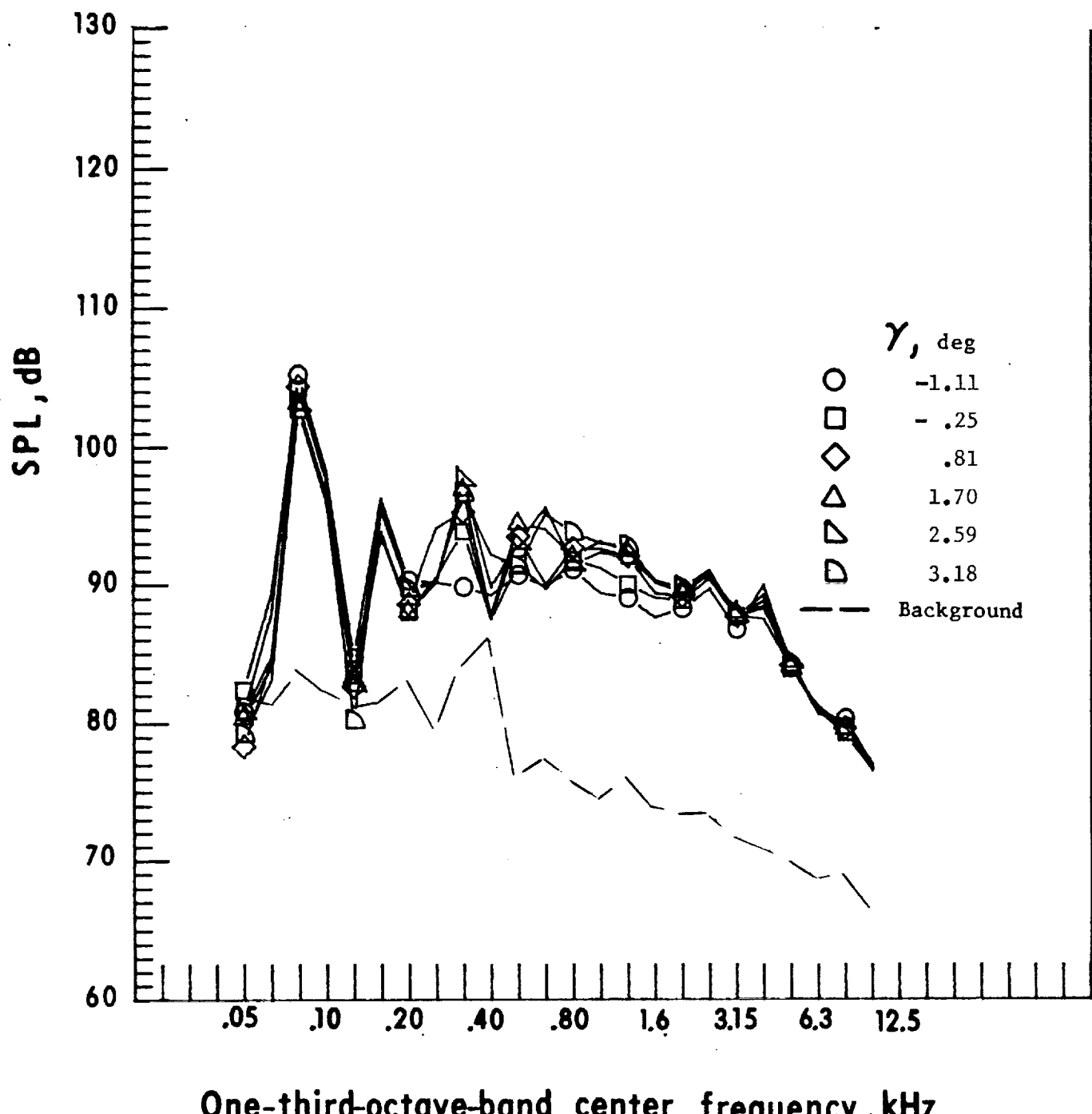
i. Mic. no. 6.



One-third-octave-band center frequency, kHz

j. Mic. no. 7.

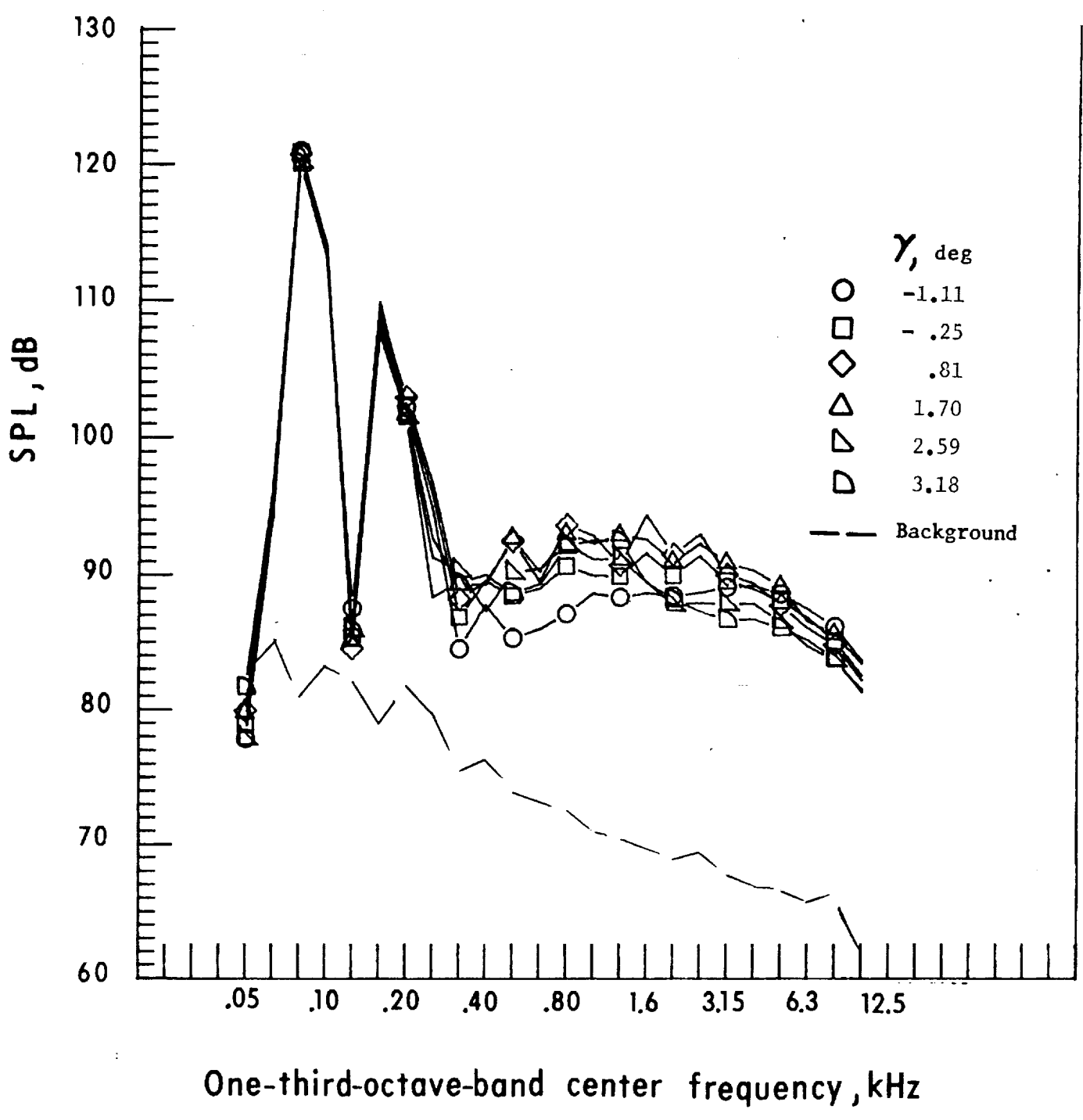
Figure 20. - Concluded.



One-third-octave-band center frequency, kHz

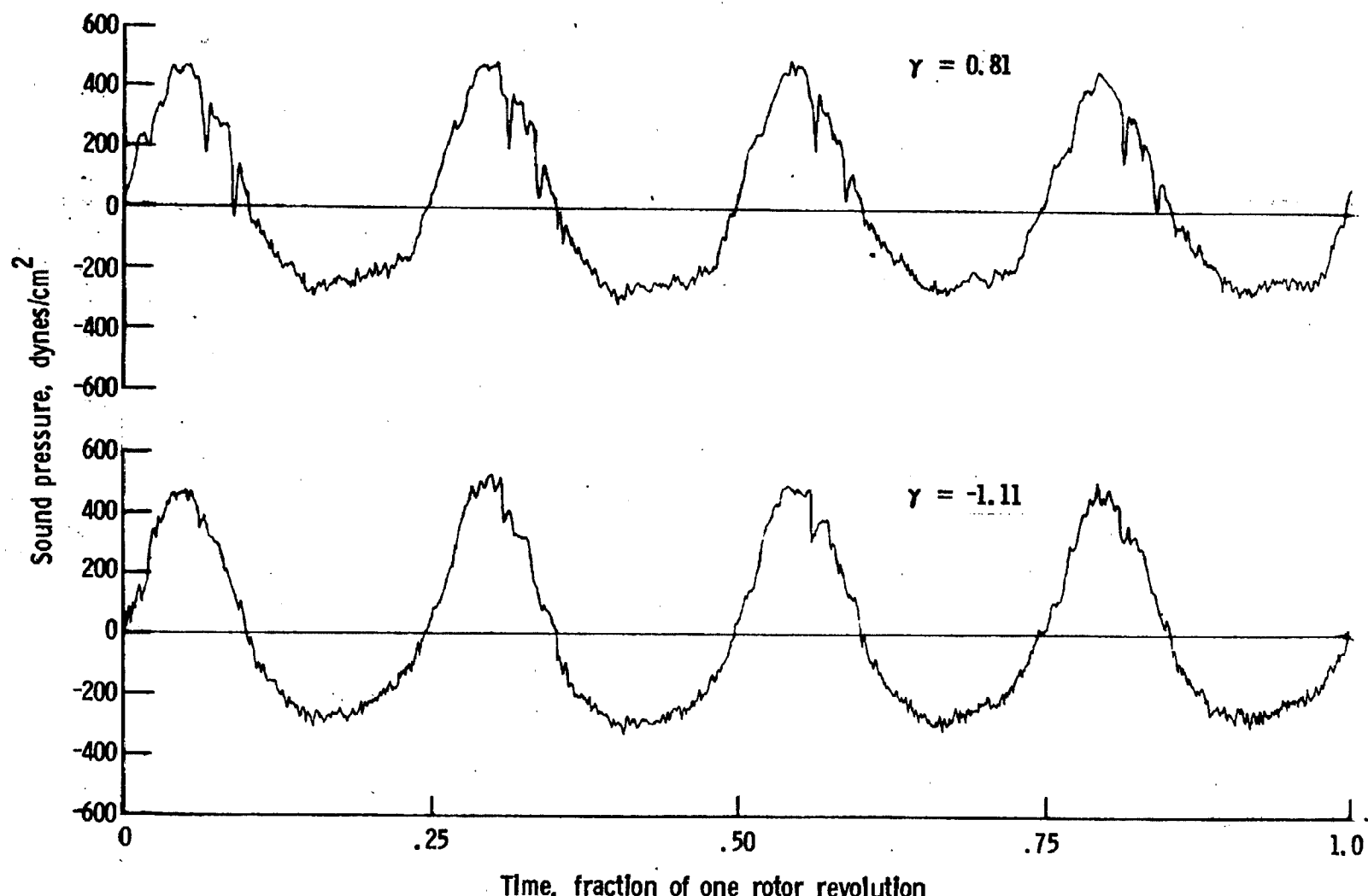
a. Mic. no. 1.

Figure 21. - Effect of descent angle variation on noise generated by helicopter model with ogee tips installed. $V_\infty = 61.2$ knots.



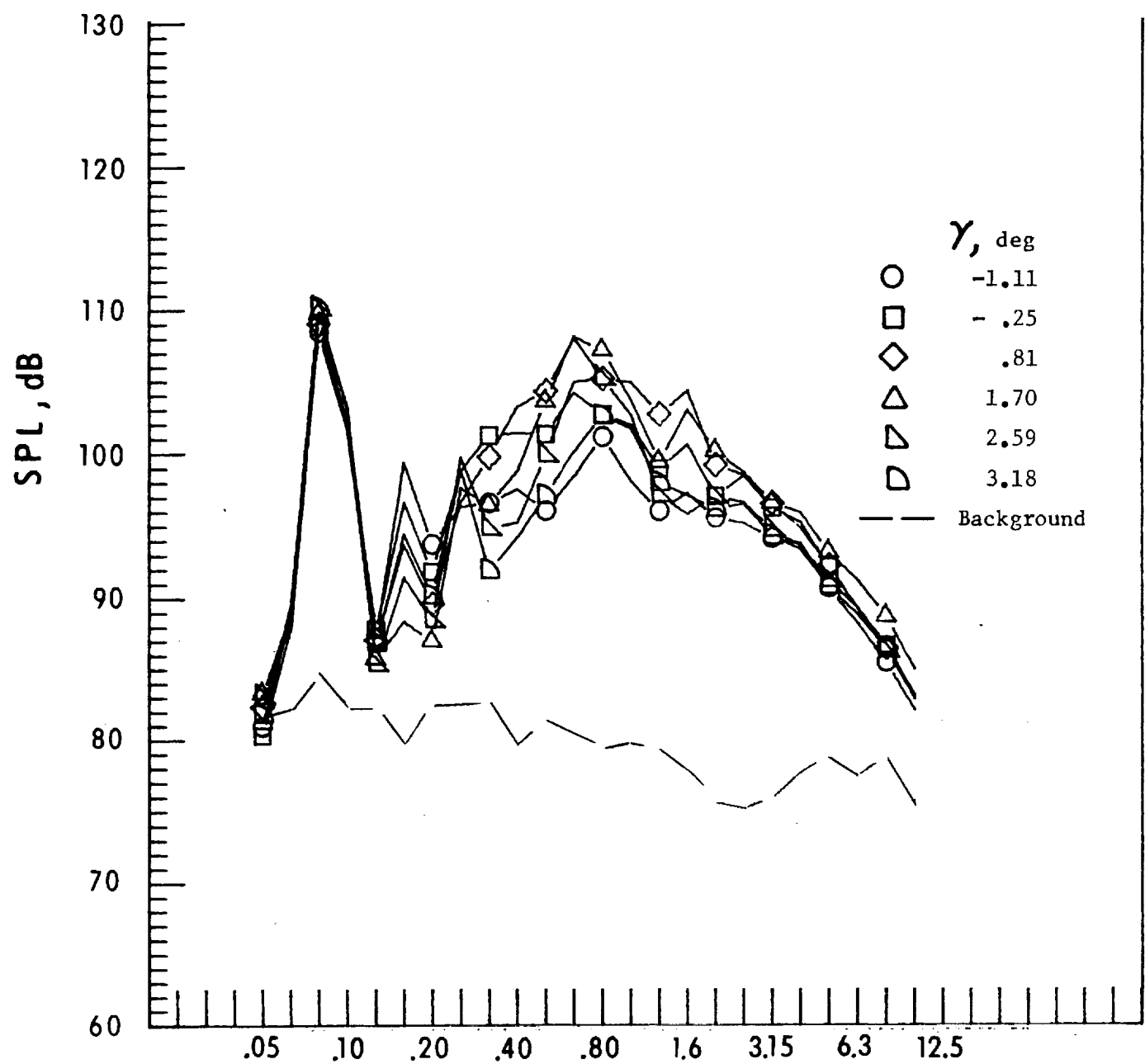
b. Mic. no. 2.

Figure 21. - Continued.



c. Pressure-time histories, Mic. no. 2.

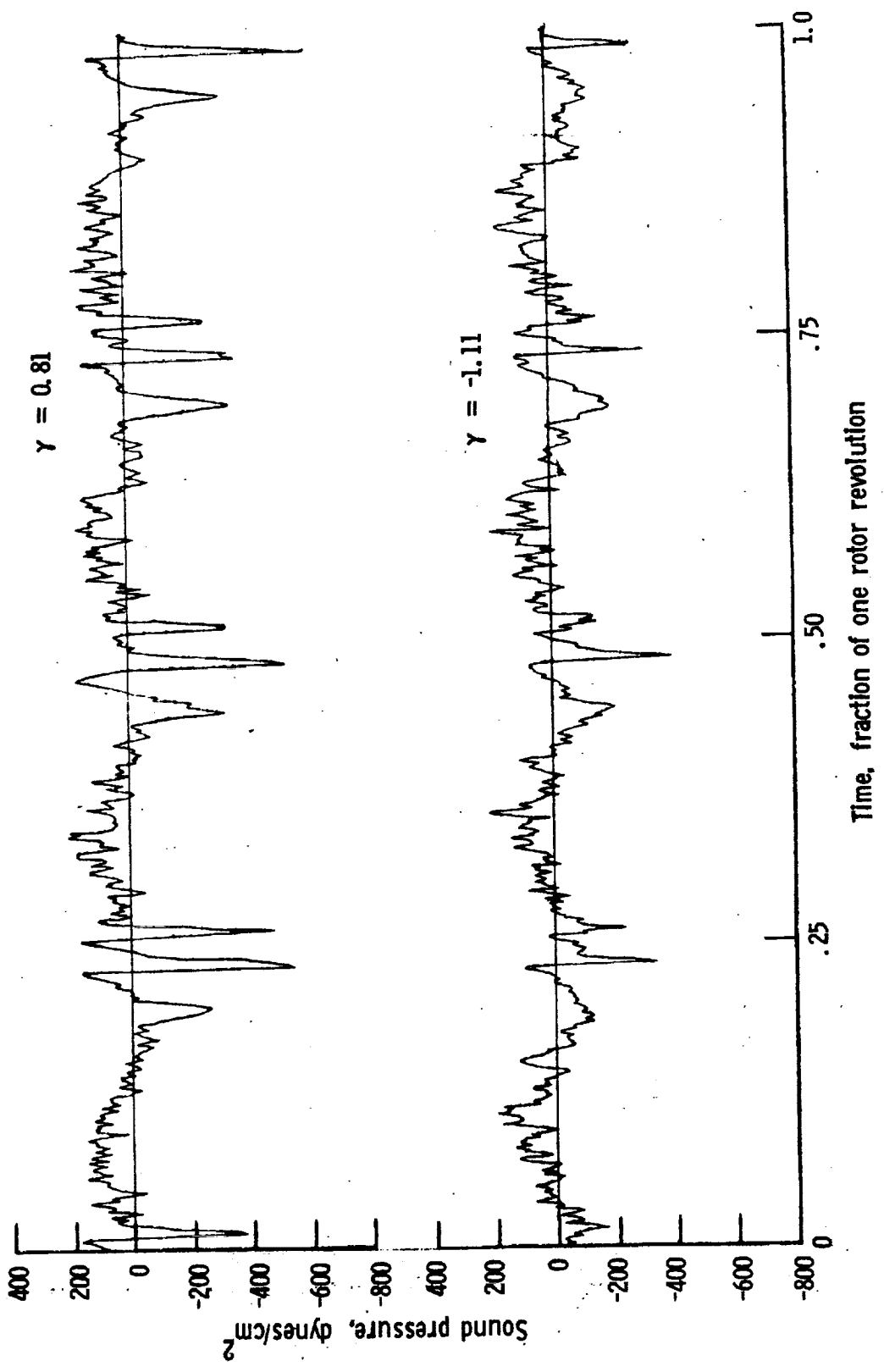
Figure 21. - Continued.



One-third-octave-band center frequency, kHz

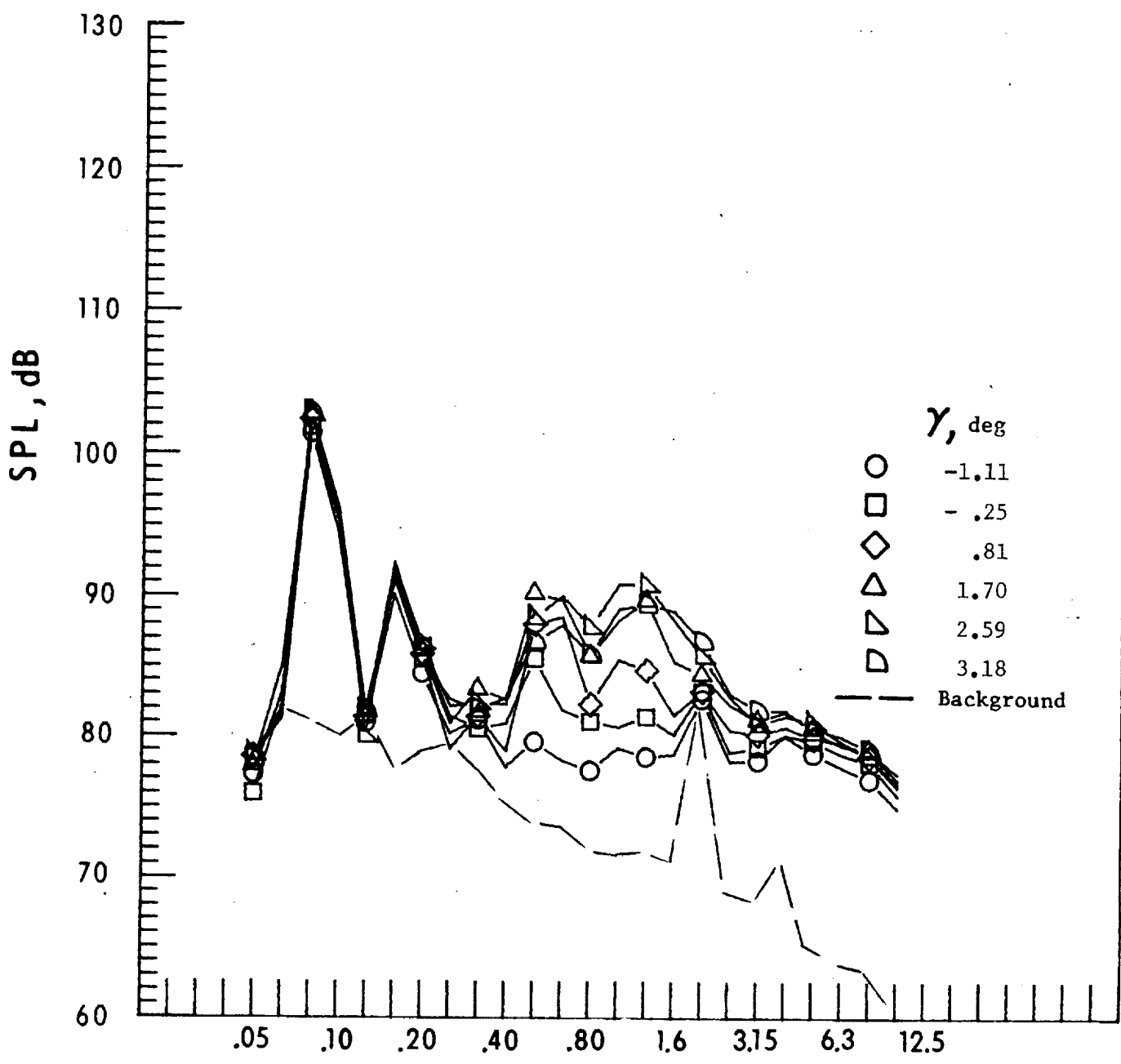
d. Mic. no. 3.

Figure 21. - Continued.



e. Pressure-time histories, Mic. no. 3.

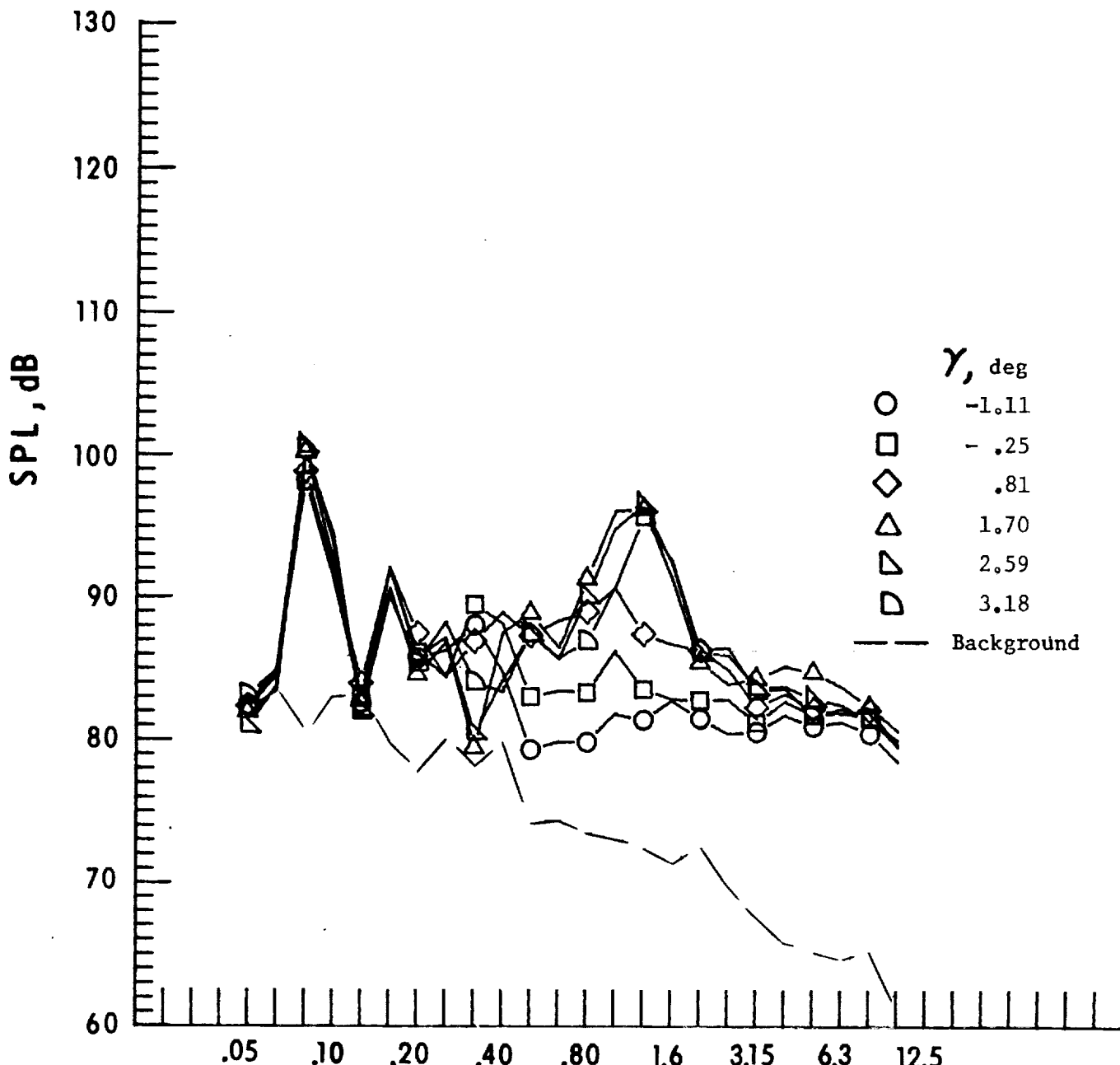
Figure 21. - Continued.



One-third-octave-band center frequency, kHz

f. Mic. no. 4.

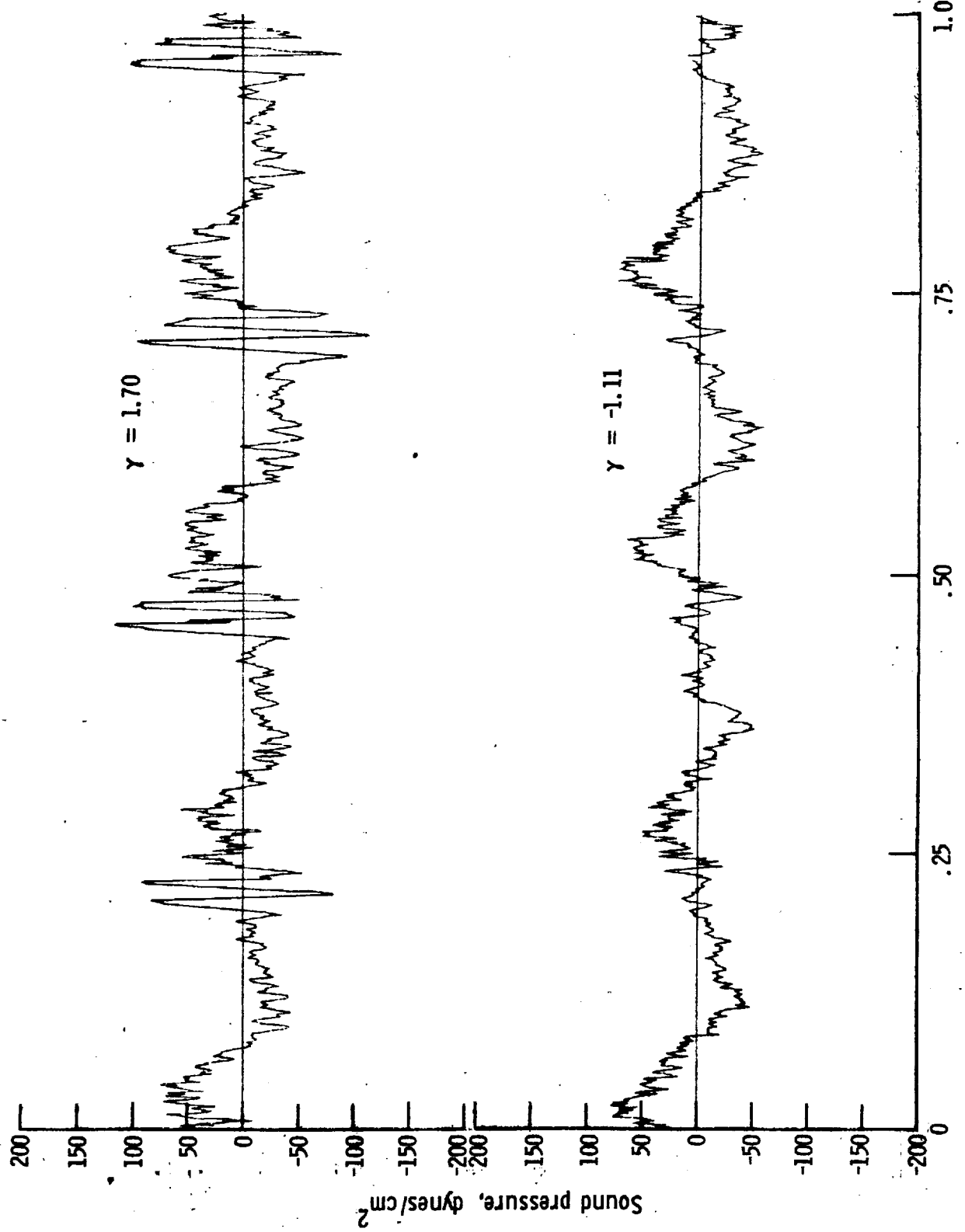
Figure 21. - Continued.



One-third-octave-band center frequency, kHz

g. Mic. no. 5.

Figure 21. - Continued.



h. Pressure-time histories, Mic. no. 5.

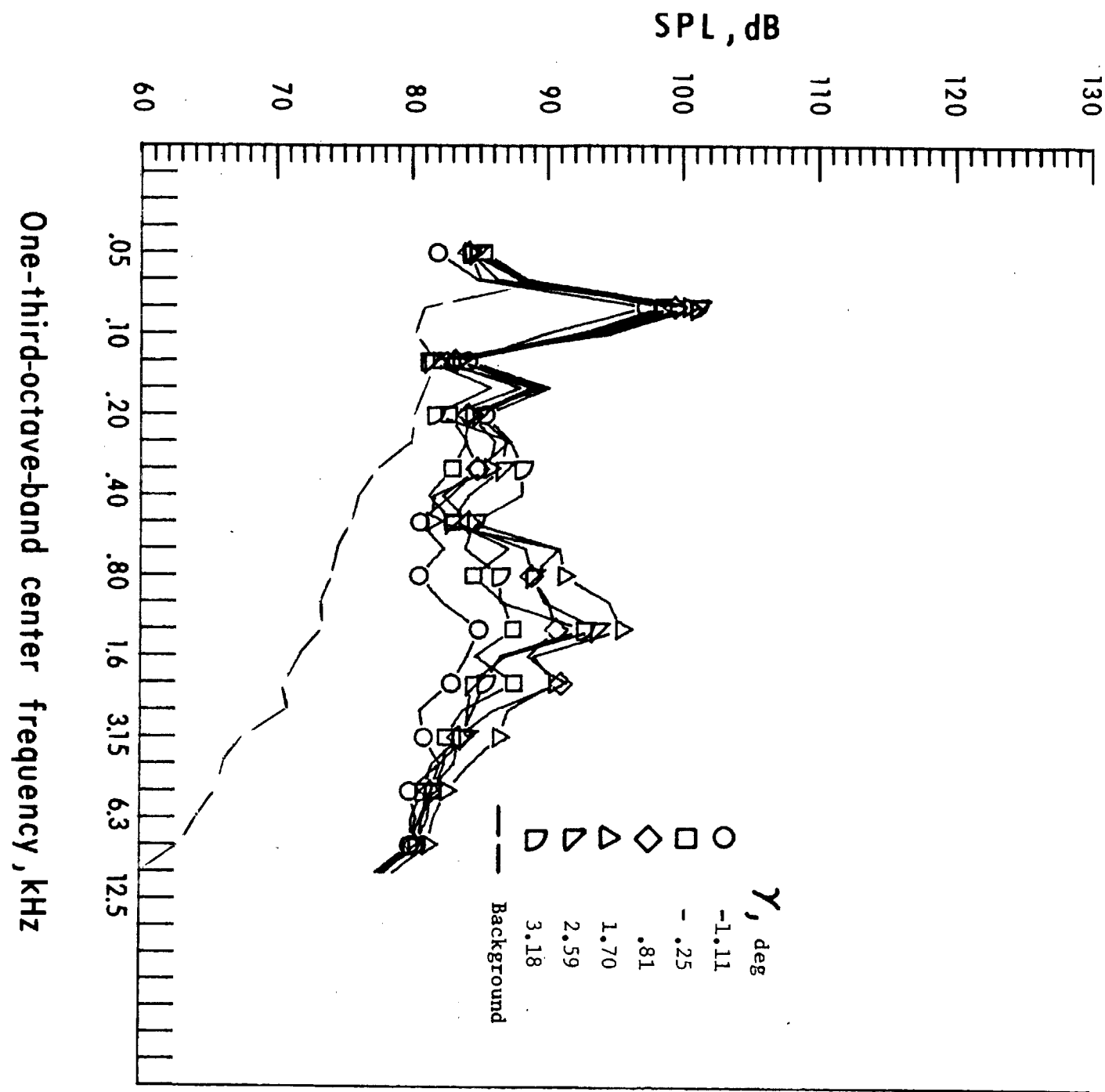
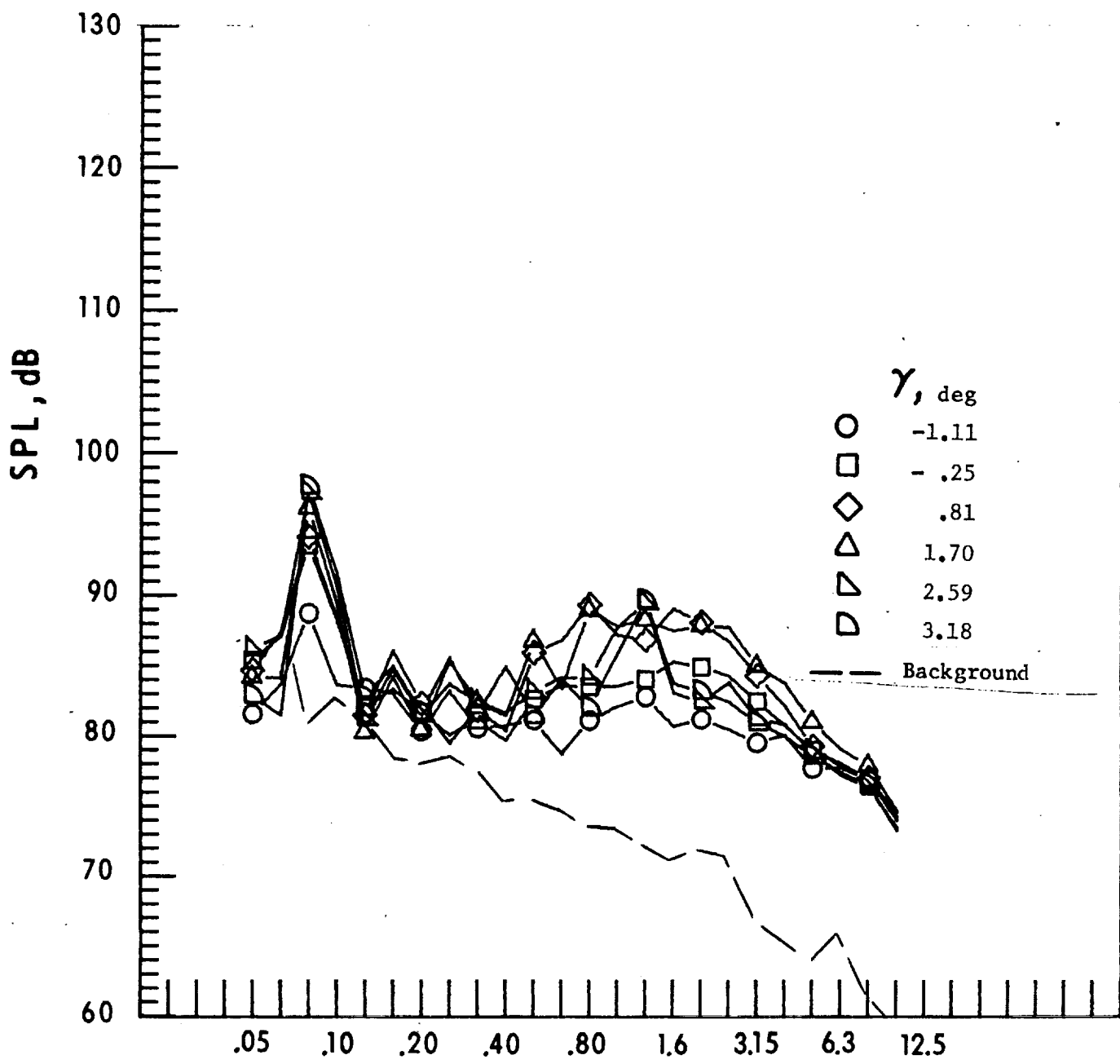


Figure 21. - Continued.

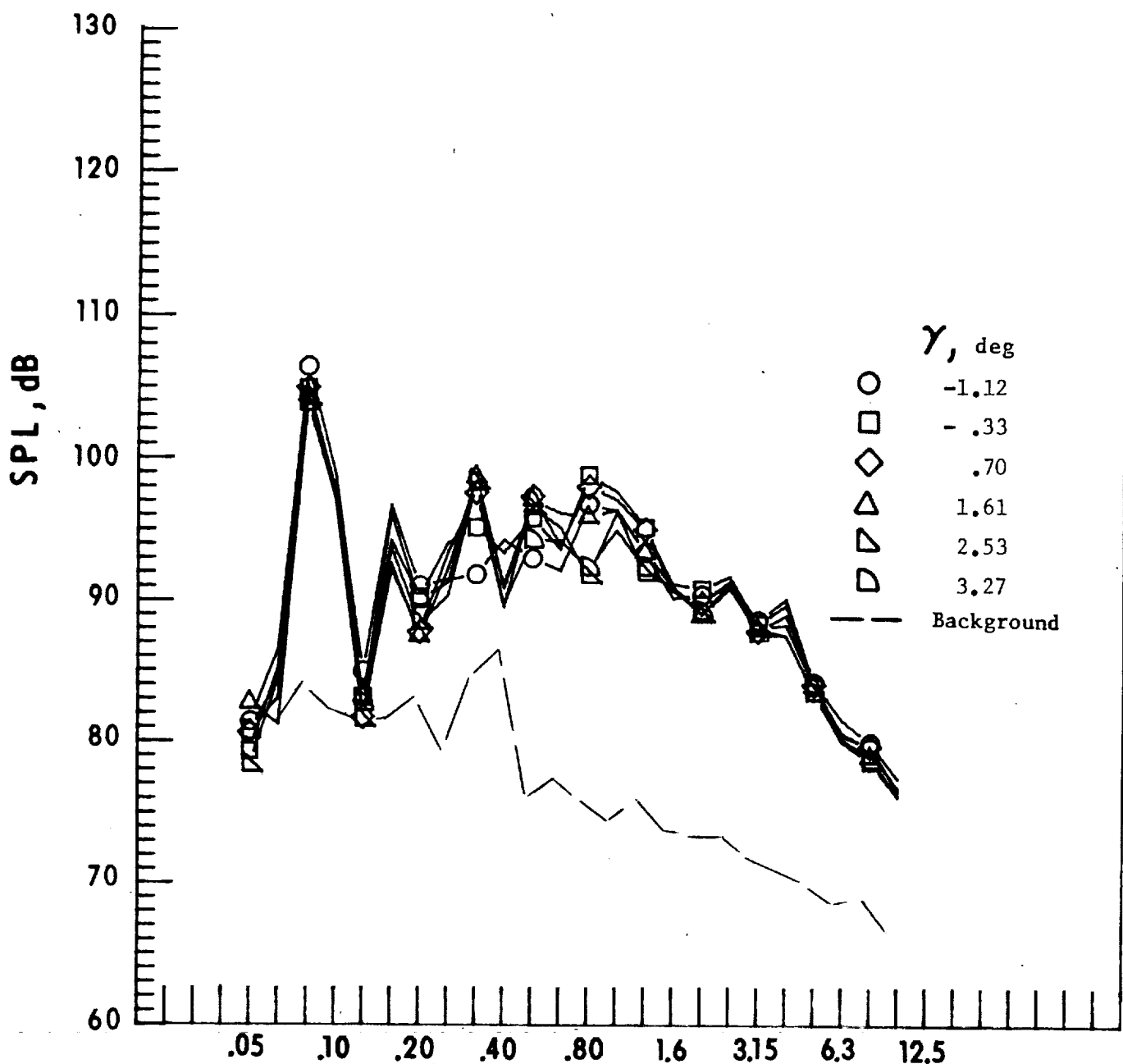
i. Mic. no. 6.



One-third-octave-band center frequency, kHz

j. Mic. no. 7.

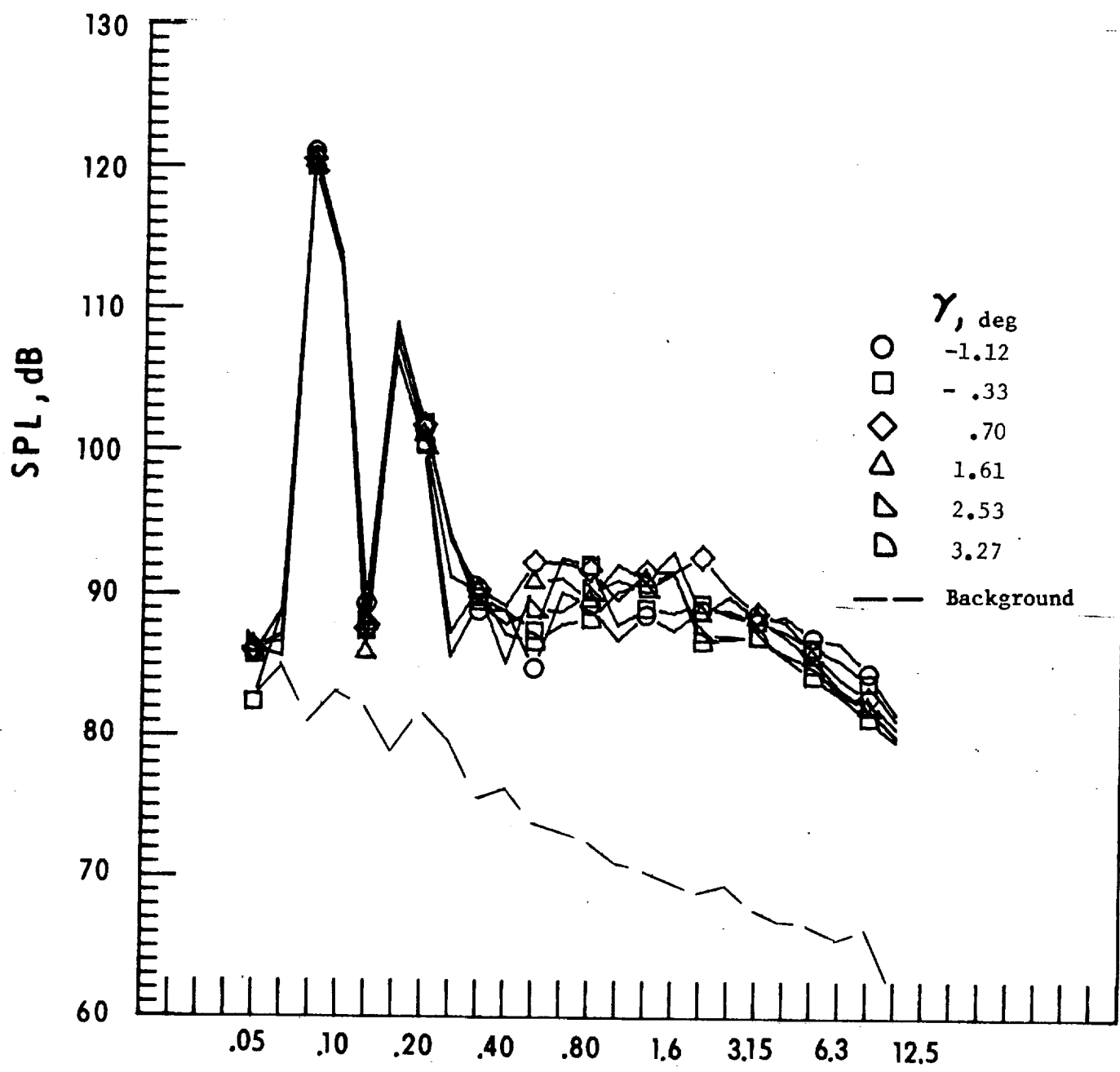
Figure 21. - Concluded.



One-third-octave-band center frequency, kHz

a. Mic. no. 1.

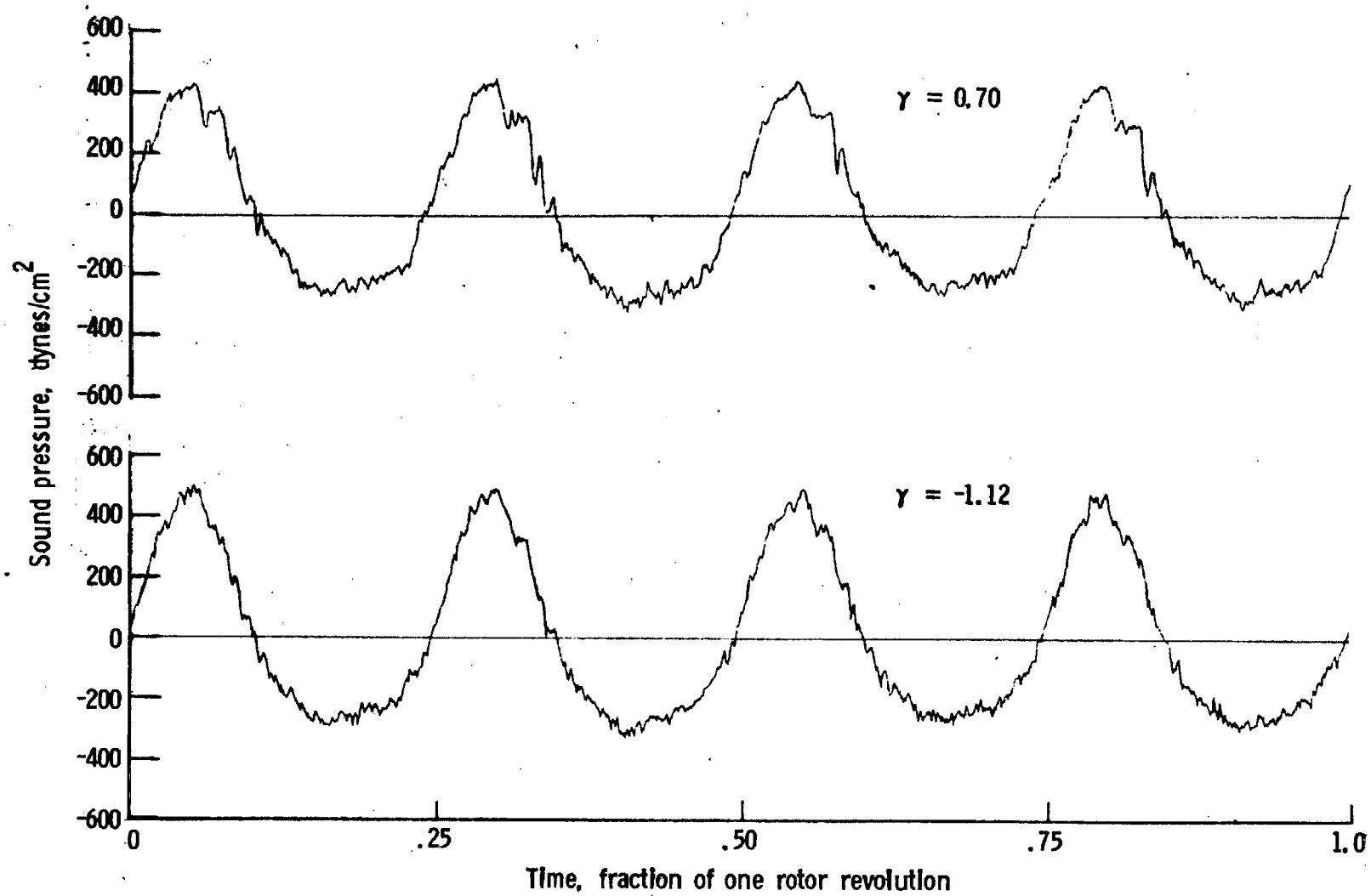
Figure 22. - Effect of descent angle variation on noise generated by helicopter model with sub-wing tips installed. $V_{\infty} = 60.9$ knots.



One-third-octave-band center frequency, kHz

b. Mic. no. 2.

Figure 22. - Continued.



c. Pressure-time histories, Mic. no. 2.

Figure 22. - Continued.

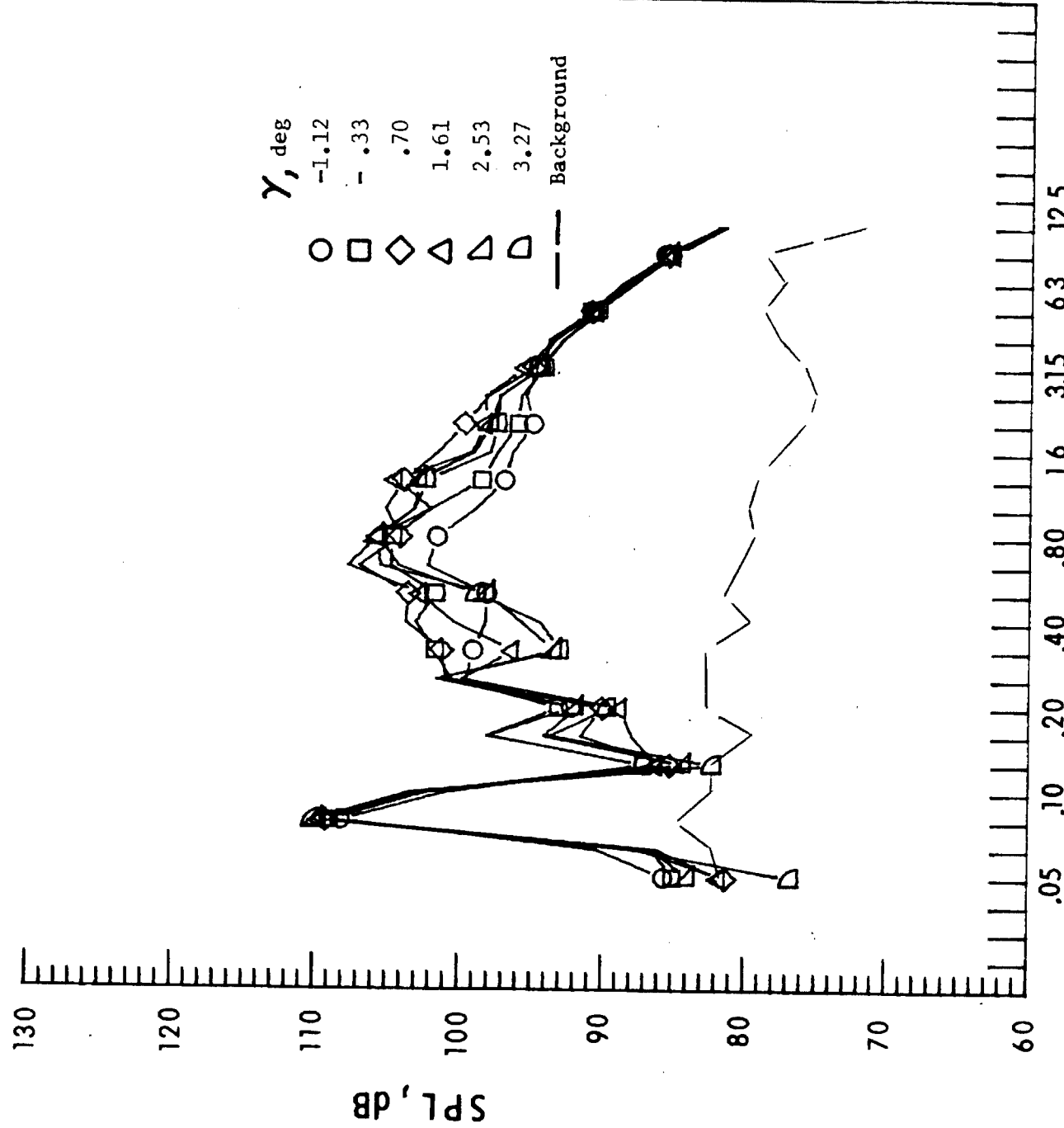
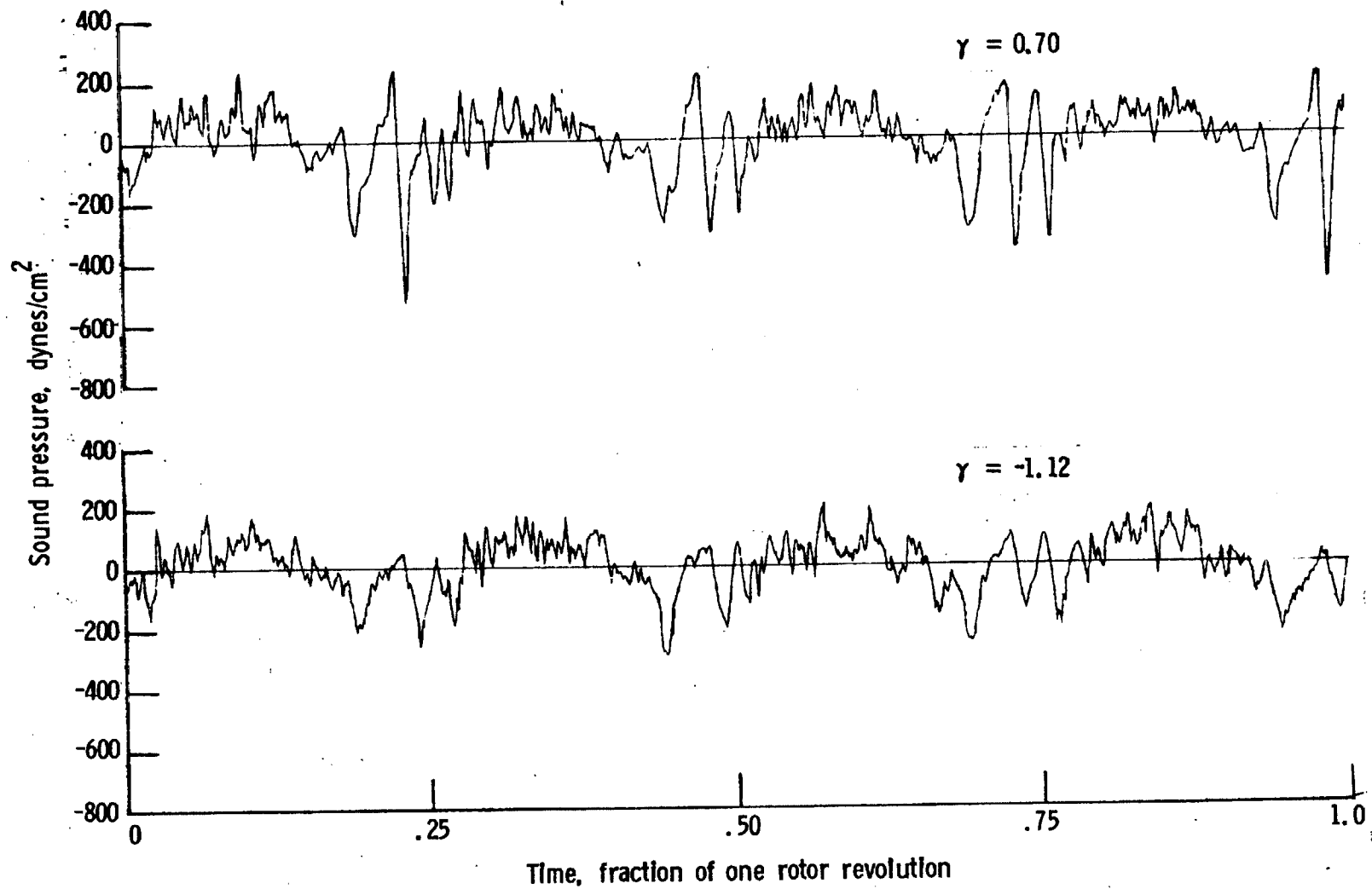


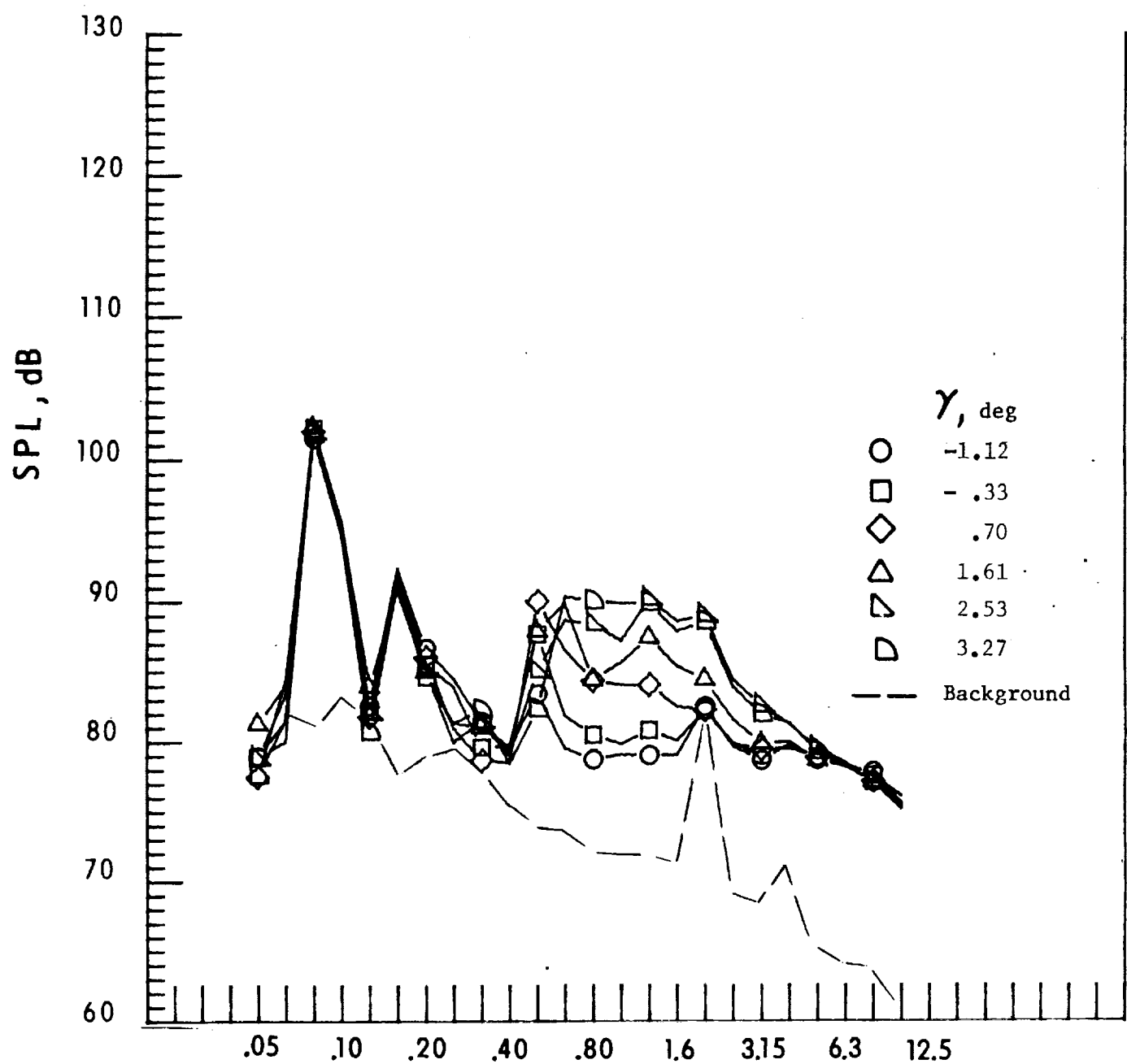
Figure 22. - Continued.

d. Mic. no. 3.



e. Pressure-time histories, Mic. no. 3.

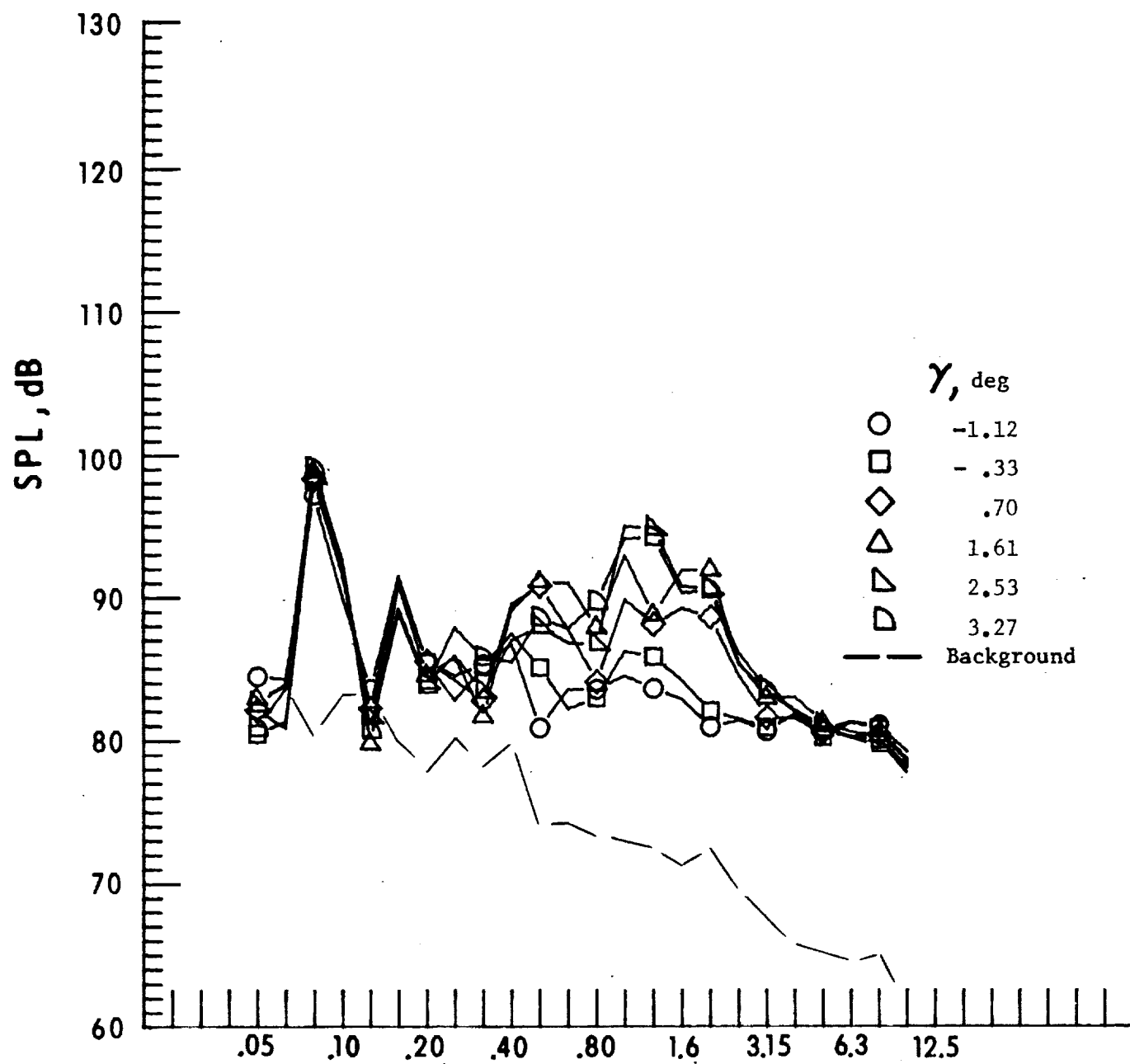
Figure 22. - Continued.



One-third-octave-band center frequency, kHz

f. Mic. no. 4.

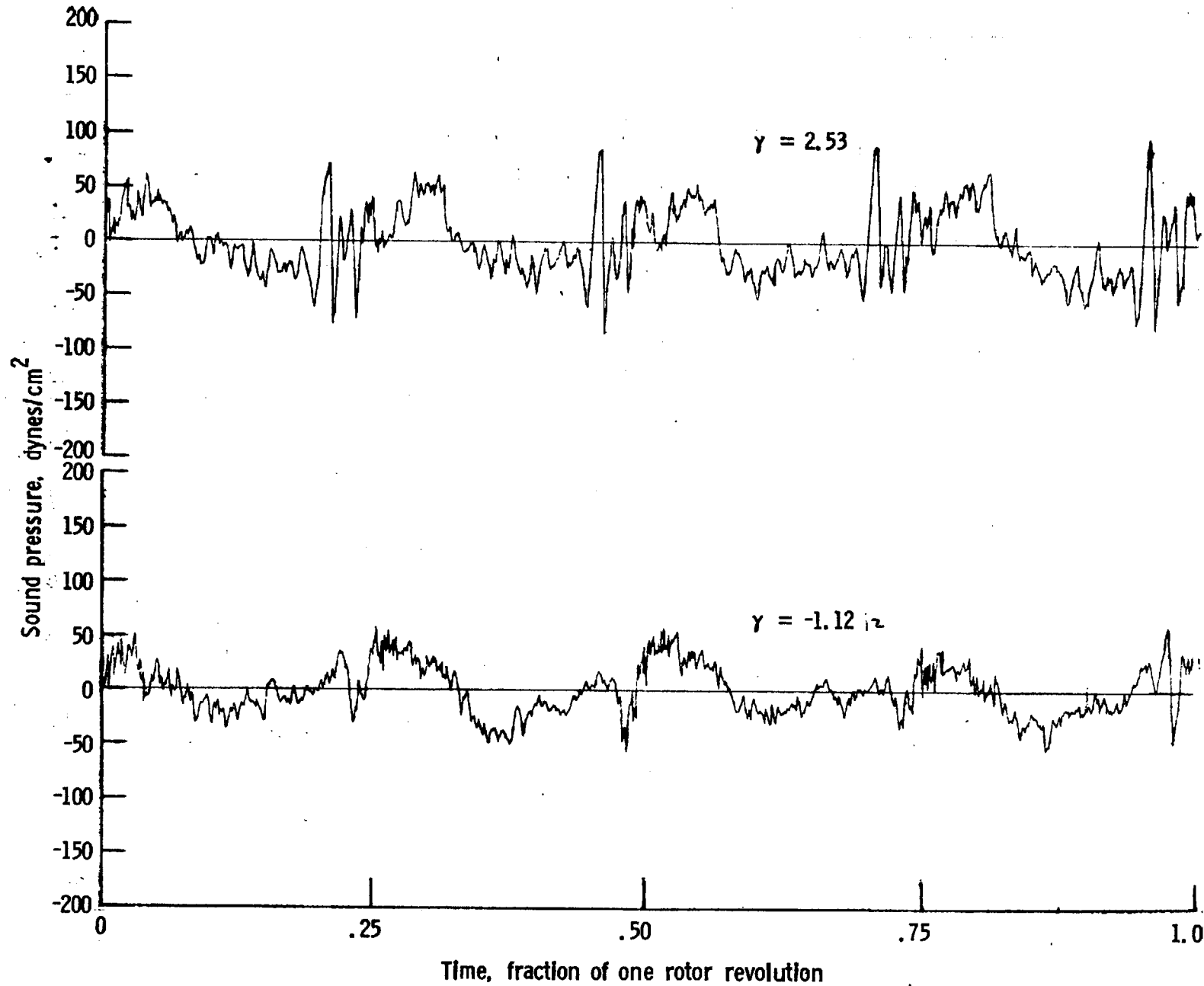
Figure 22. - Continued.



One-third-octave-band center frequency, kHz

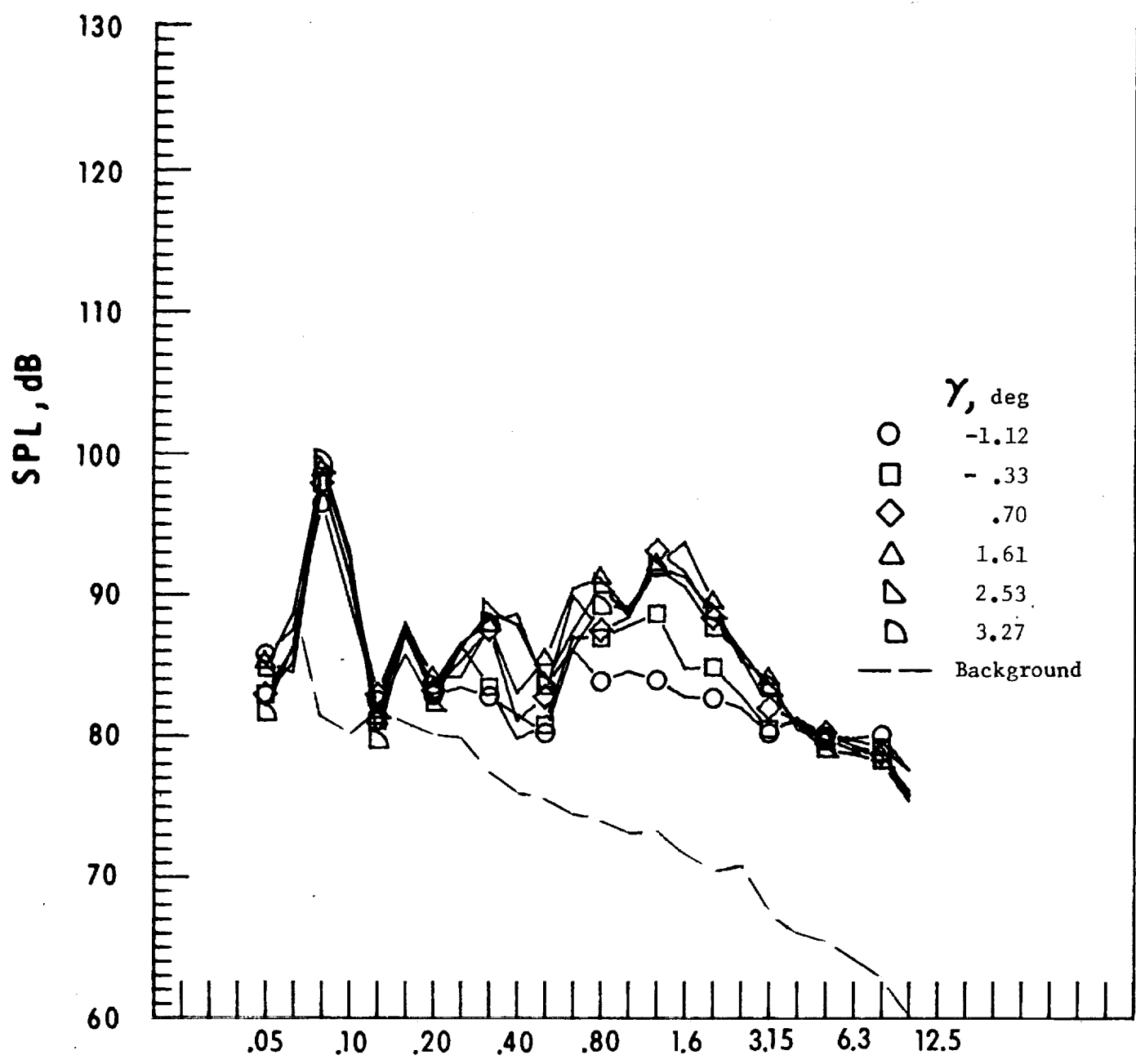
g. Mic. no. 5.

Figure 22. - Continued.



h. Pressure-time histories, Mic. no. 5.

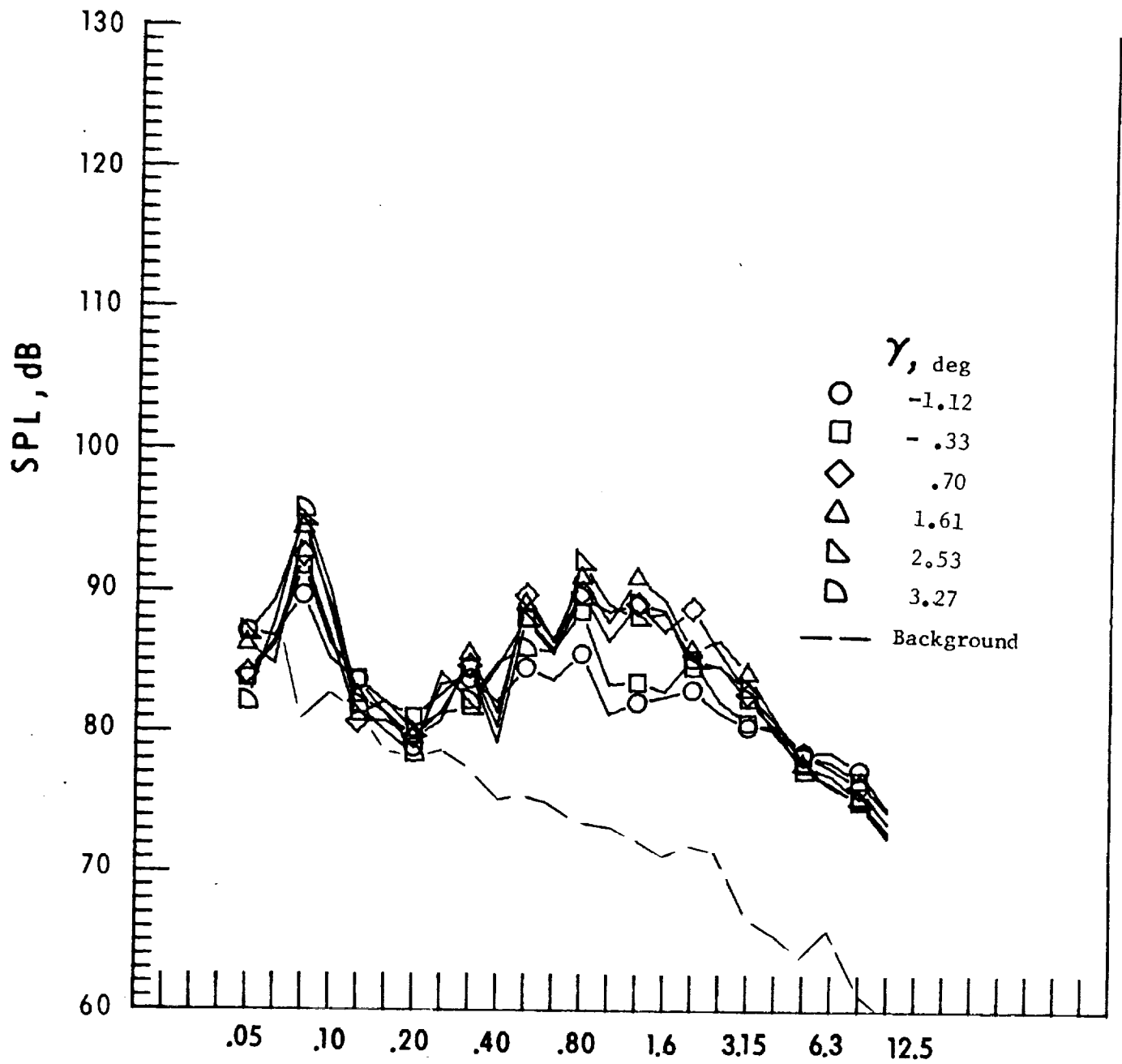
Figure 22. - Continued.



One-third-octave-band center frequency, kHz

i. Mic. no. 6.

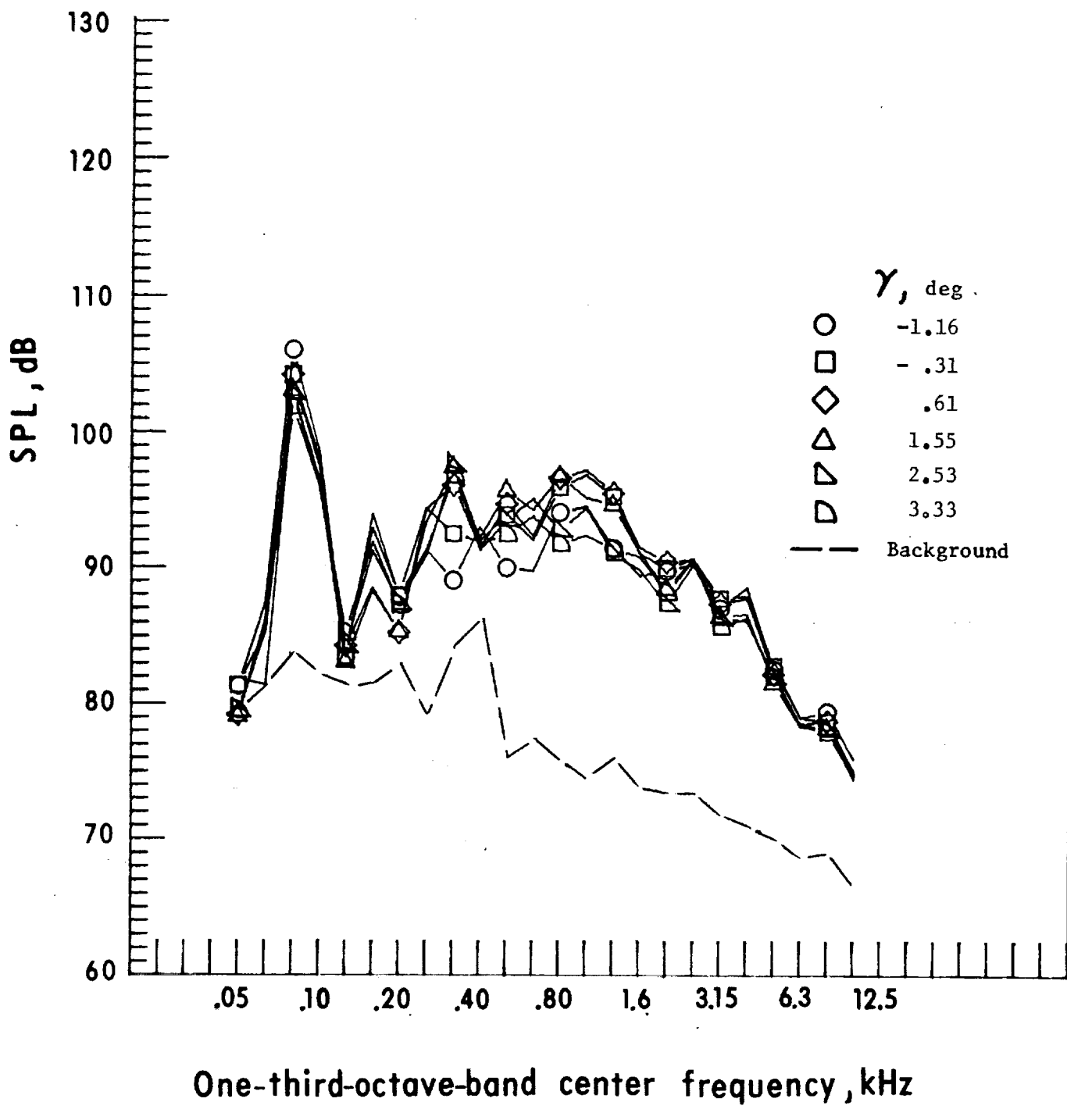
Figure 22. - Continued.



One-third-octave-band center frequency, kHz

j. Mic. no. 7.

Figure 22. - Concluded.



One-third-octave-band center frequency, kHz

a. Mic. no. 1.

Figure 23. - Effect of descent angle variation on noise generated by helicopter model with swept-tapered tips installed. $V_\infty = 60.6$ knots.

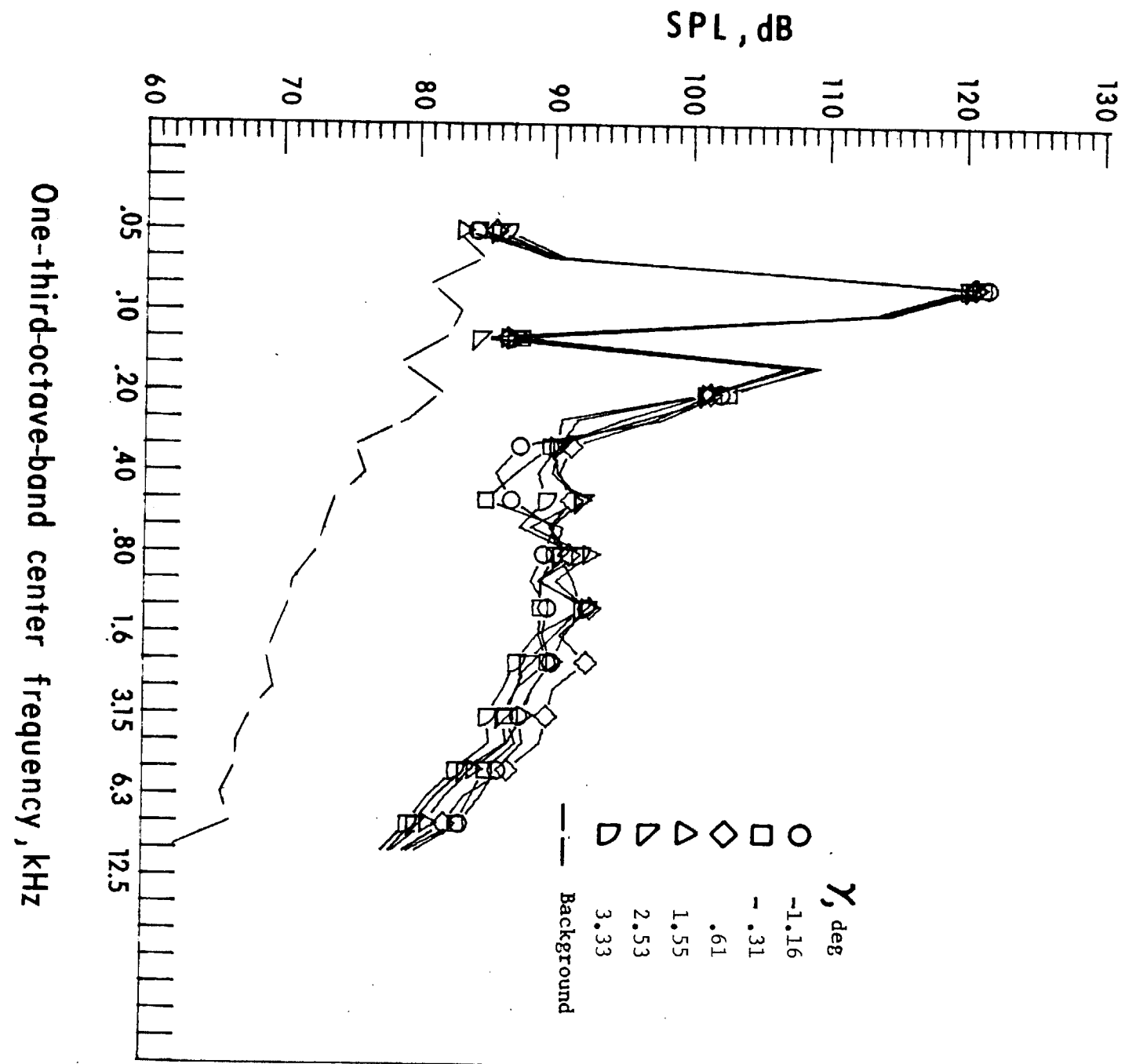
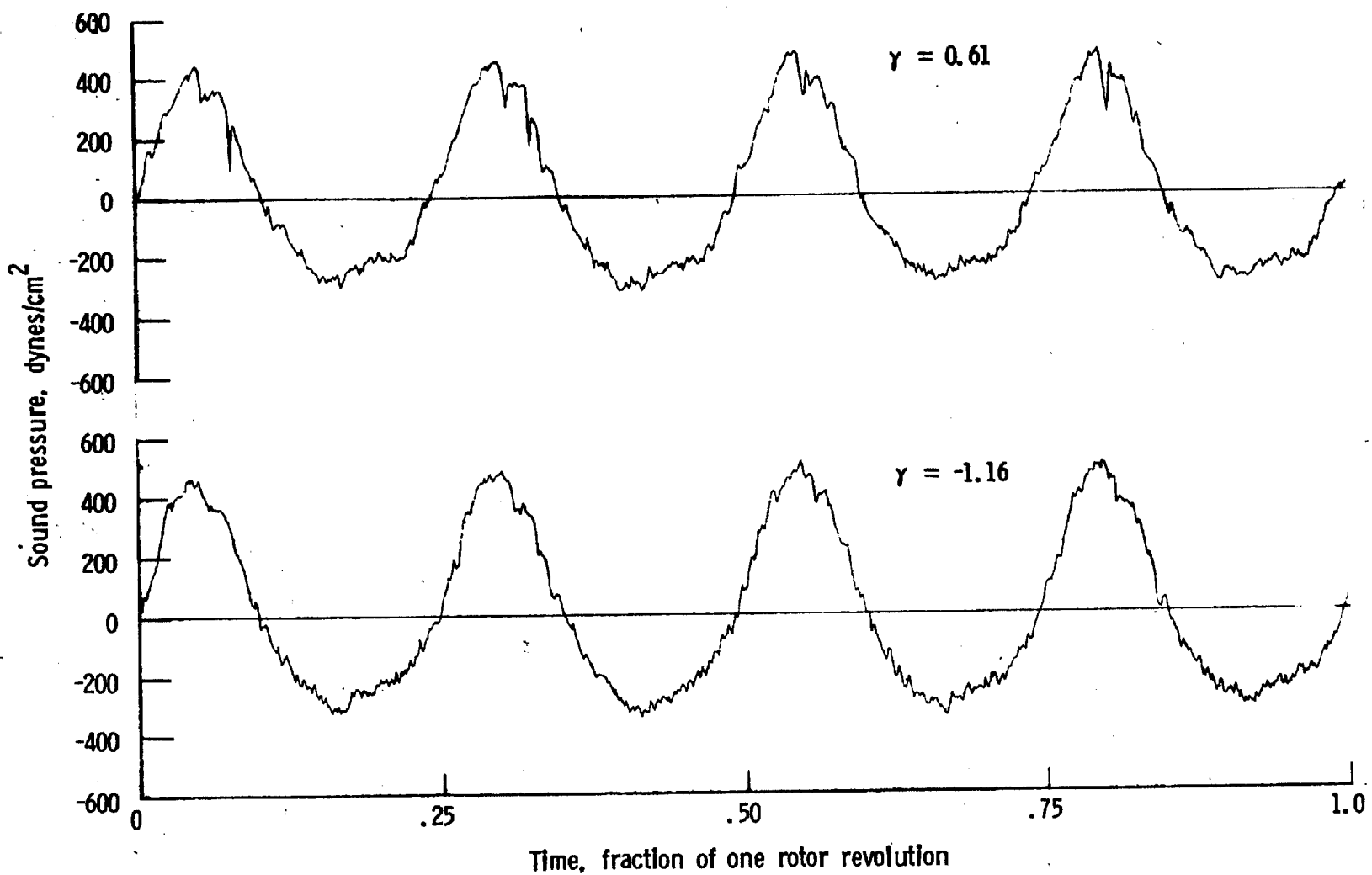


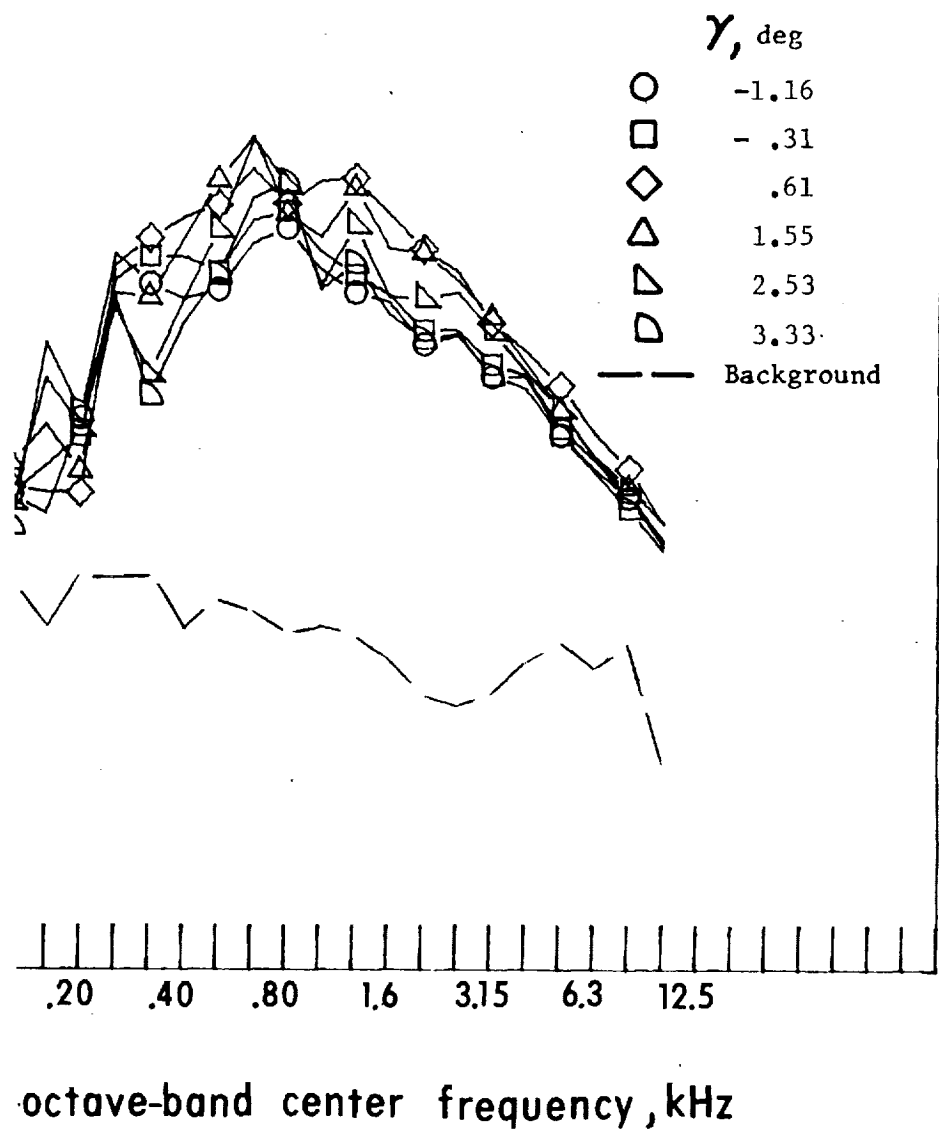
Figure 23. - Continued.

b. Mic. no. 2.



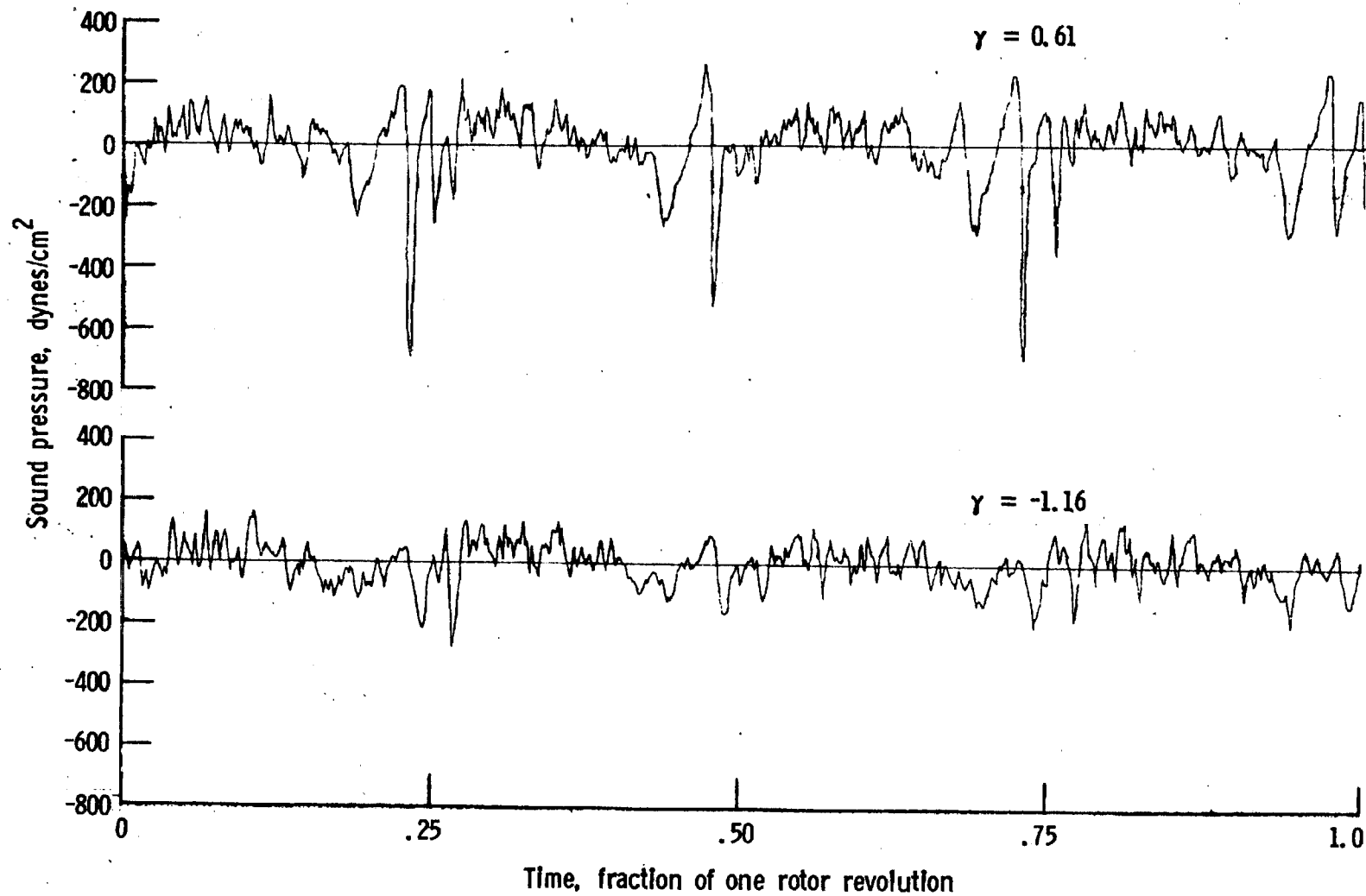
c. Pressure-time histories, Mic. no. 2.

Figure 23. - Continued.



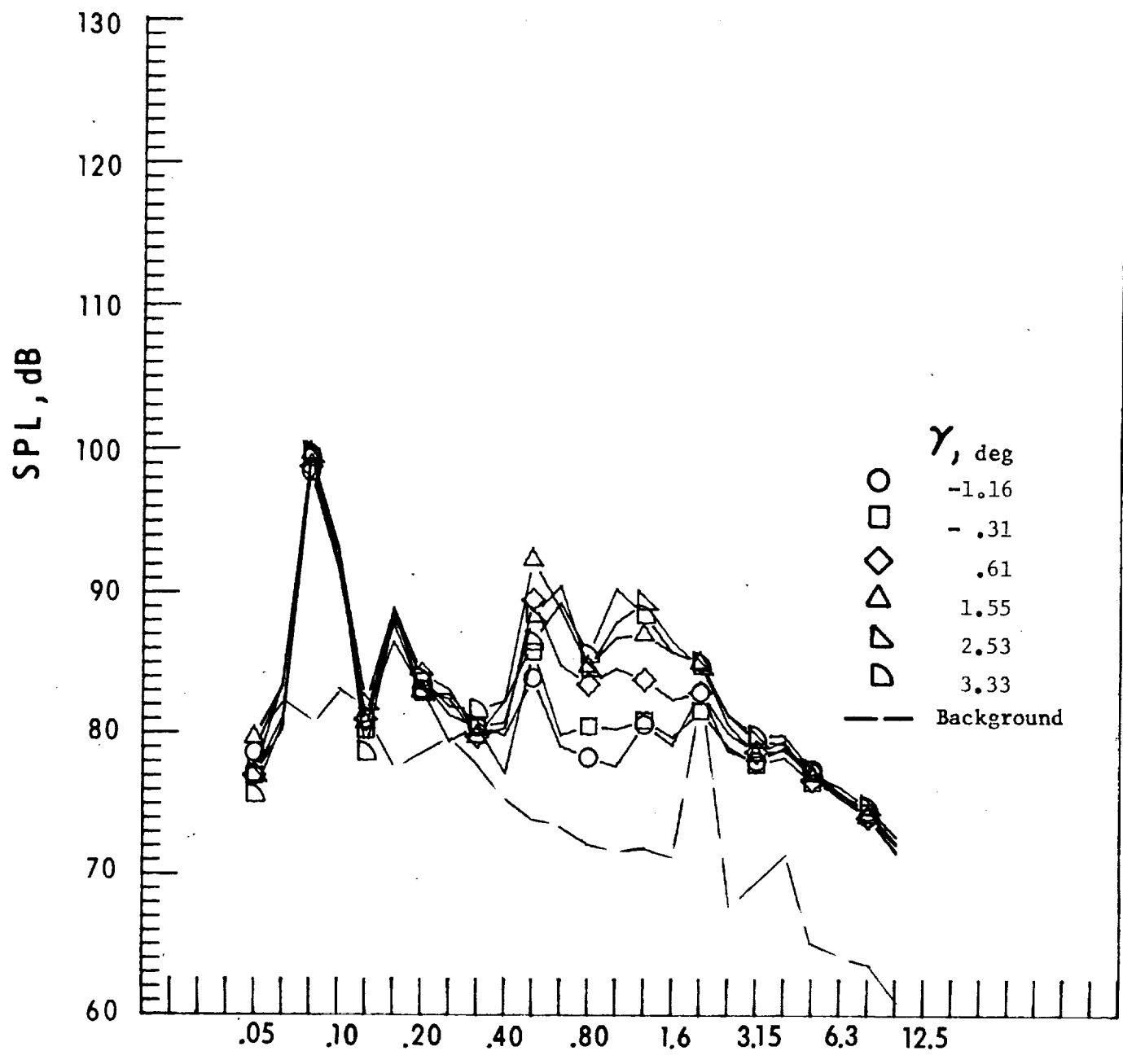
d. Mic. no. 3.

Figure 23. - Continued.



e. Pressure-time histories, Mic. no. 3.

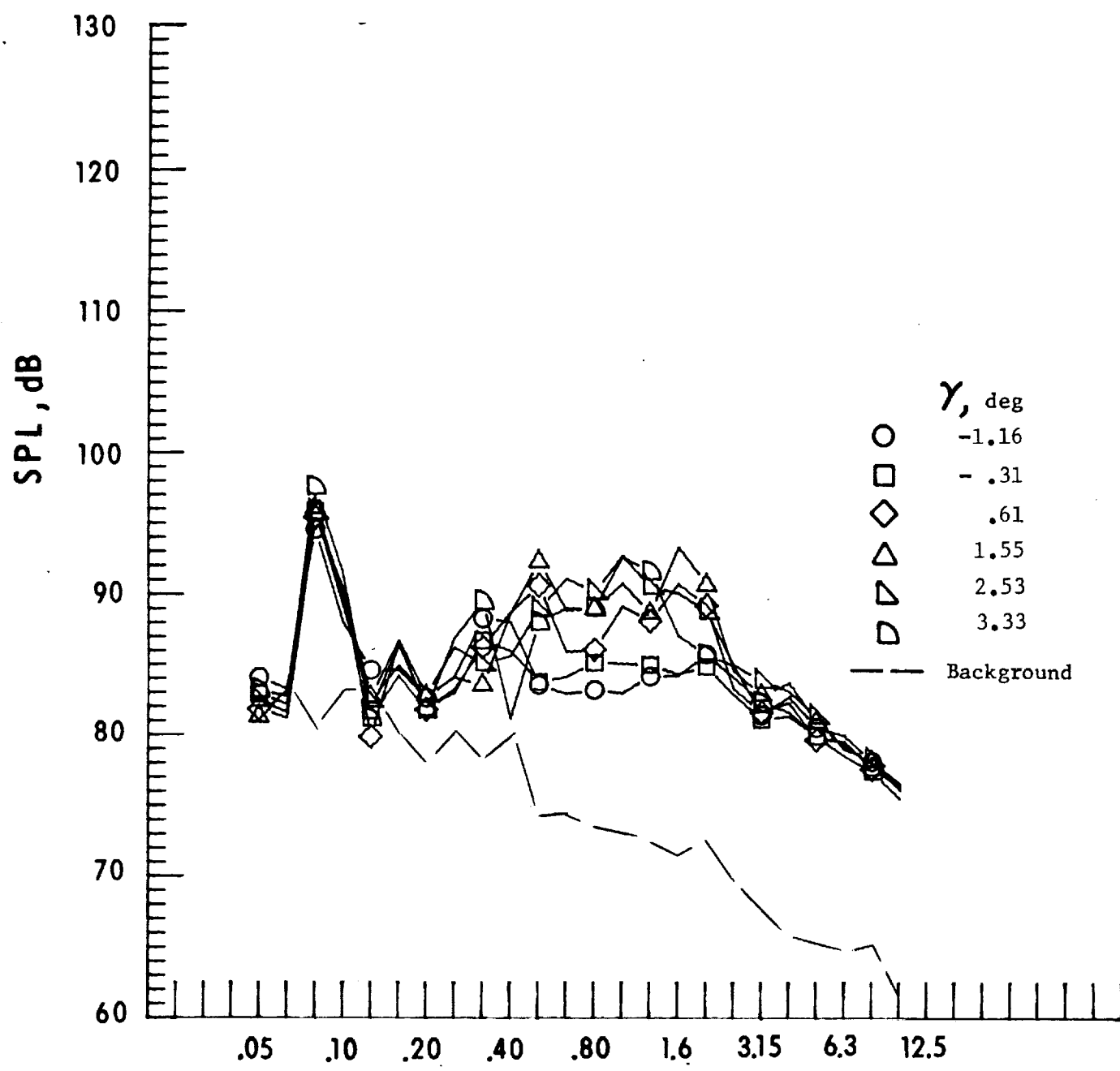
Figure 23. - Continued.



One-third-octave-band center frequency, kHz

f. Mic. no. 4.

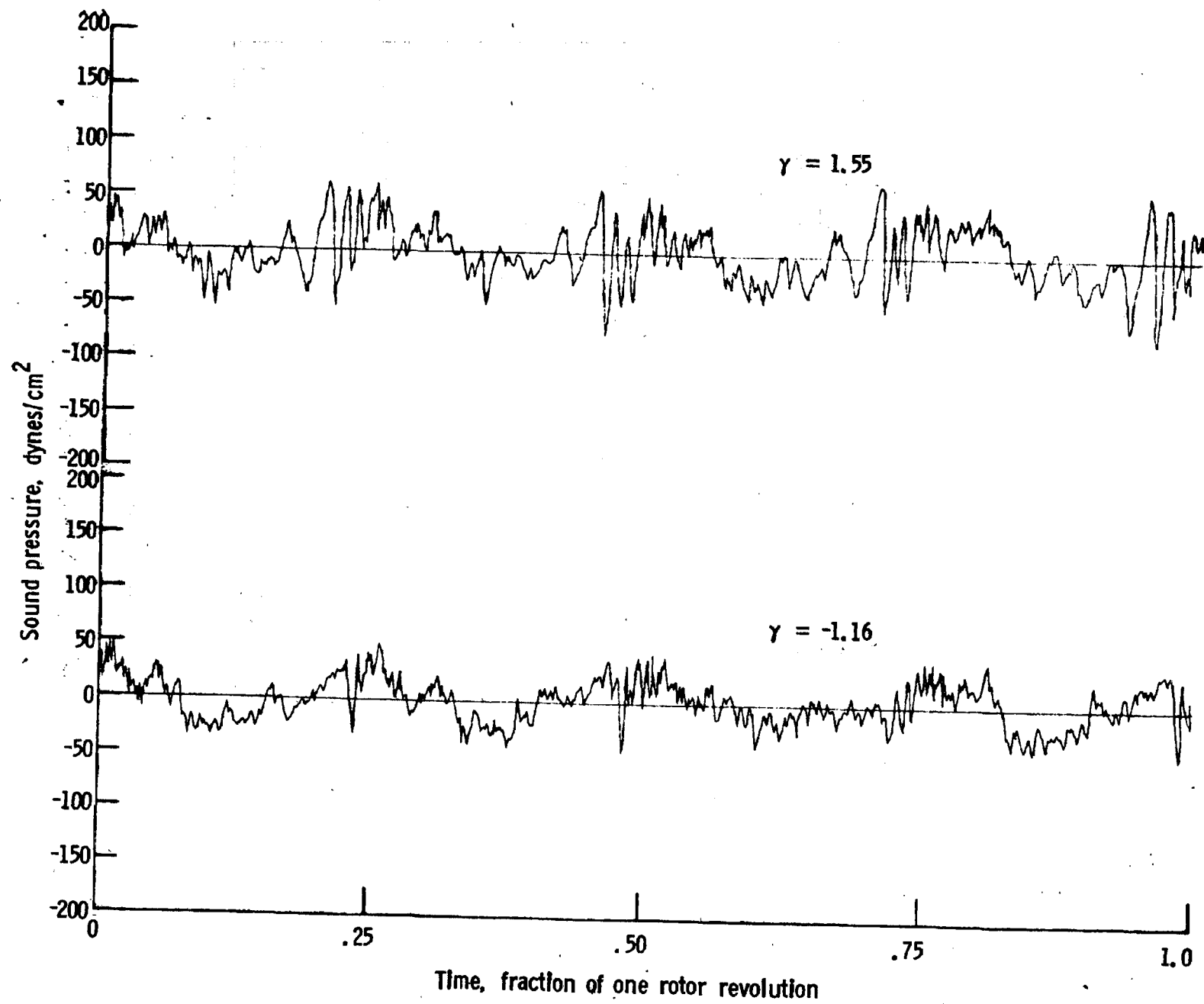
Figure 23. - Continued.



One-third-octave-band center frequency, kHz

g. Mic. no. 5.

Figure 23. - Continued.



h. Pressure-time histories, Mic. no. 5.

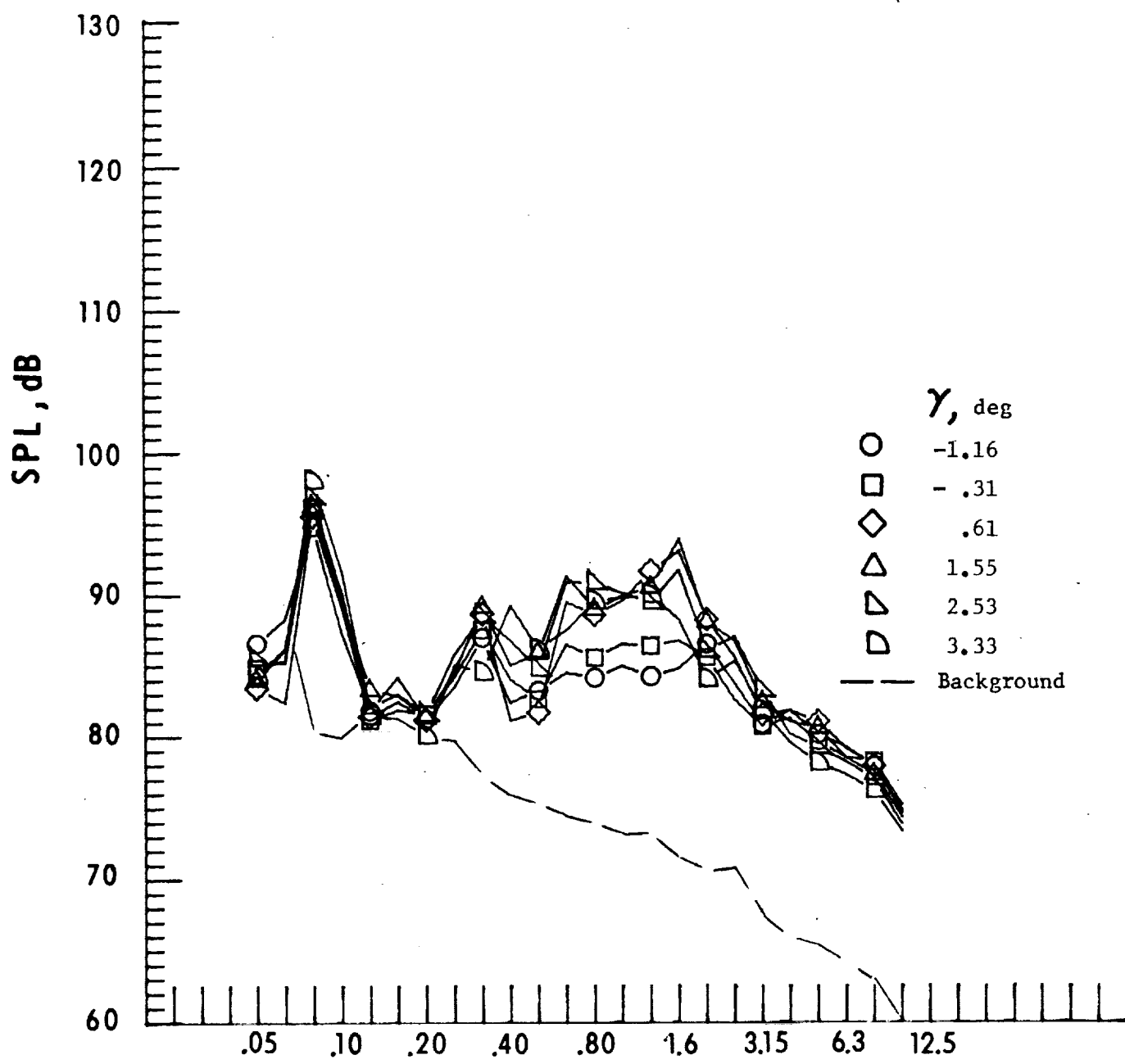
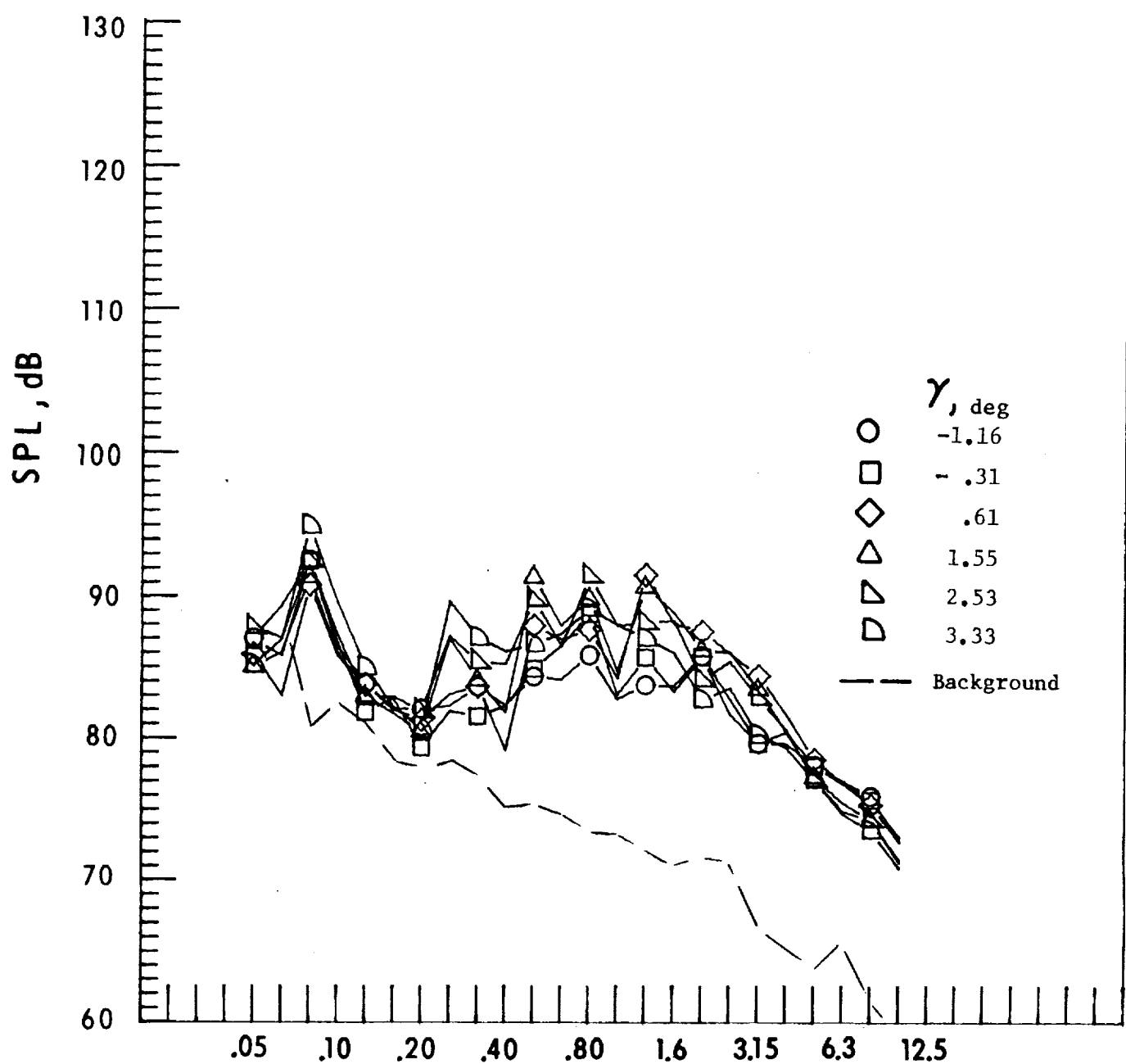


Figure 23. - Continued.

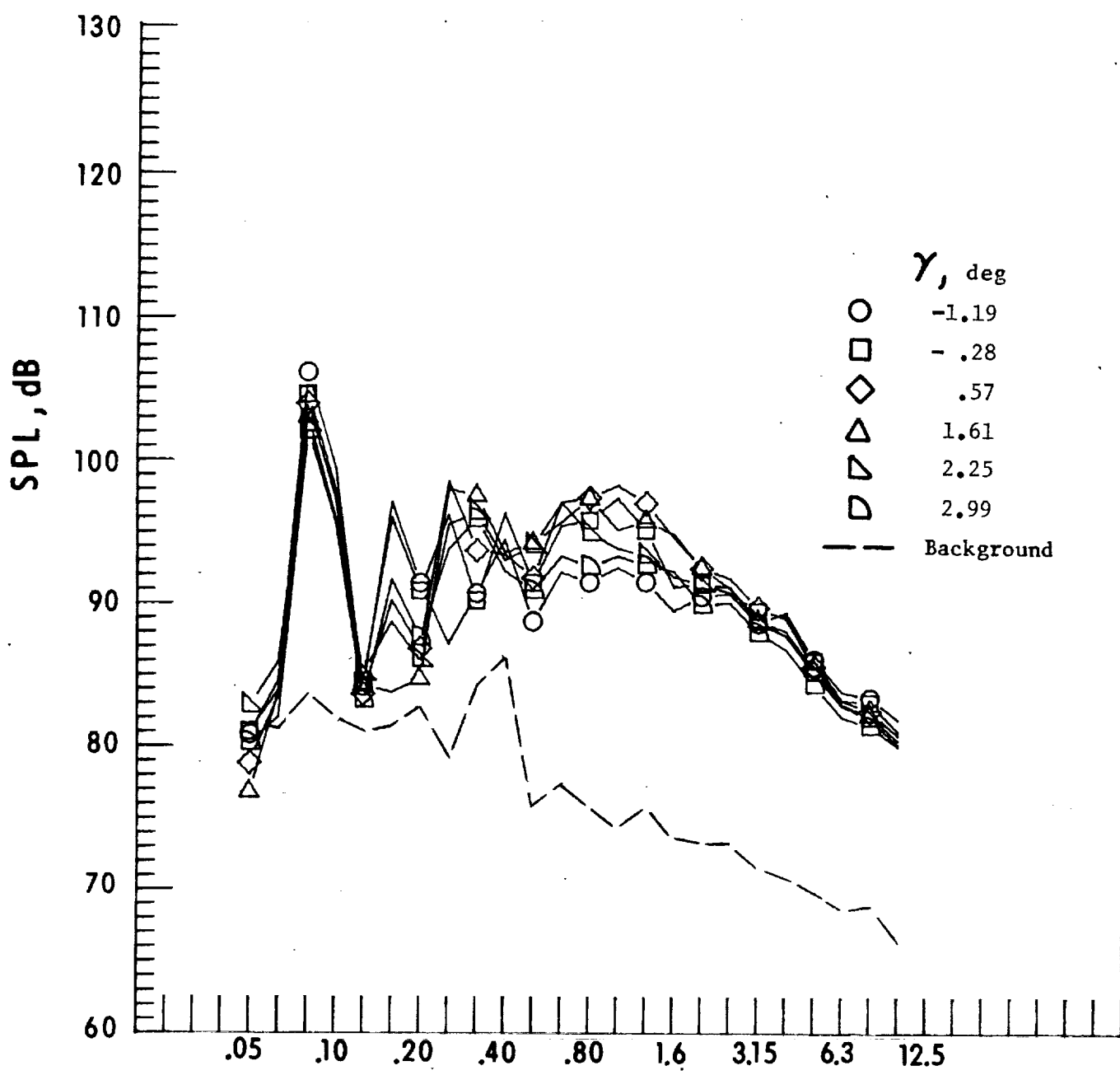
i. Mic. no. 6.



One-third-octave-band center frequency, kHz

j. Mic. no. 7.

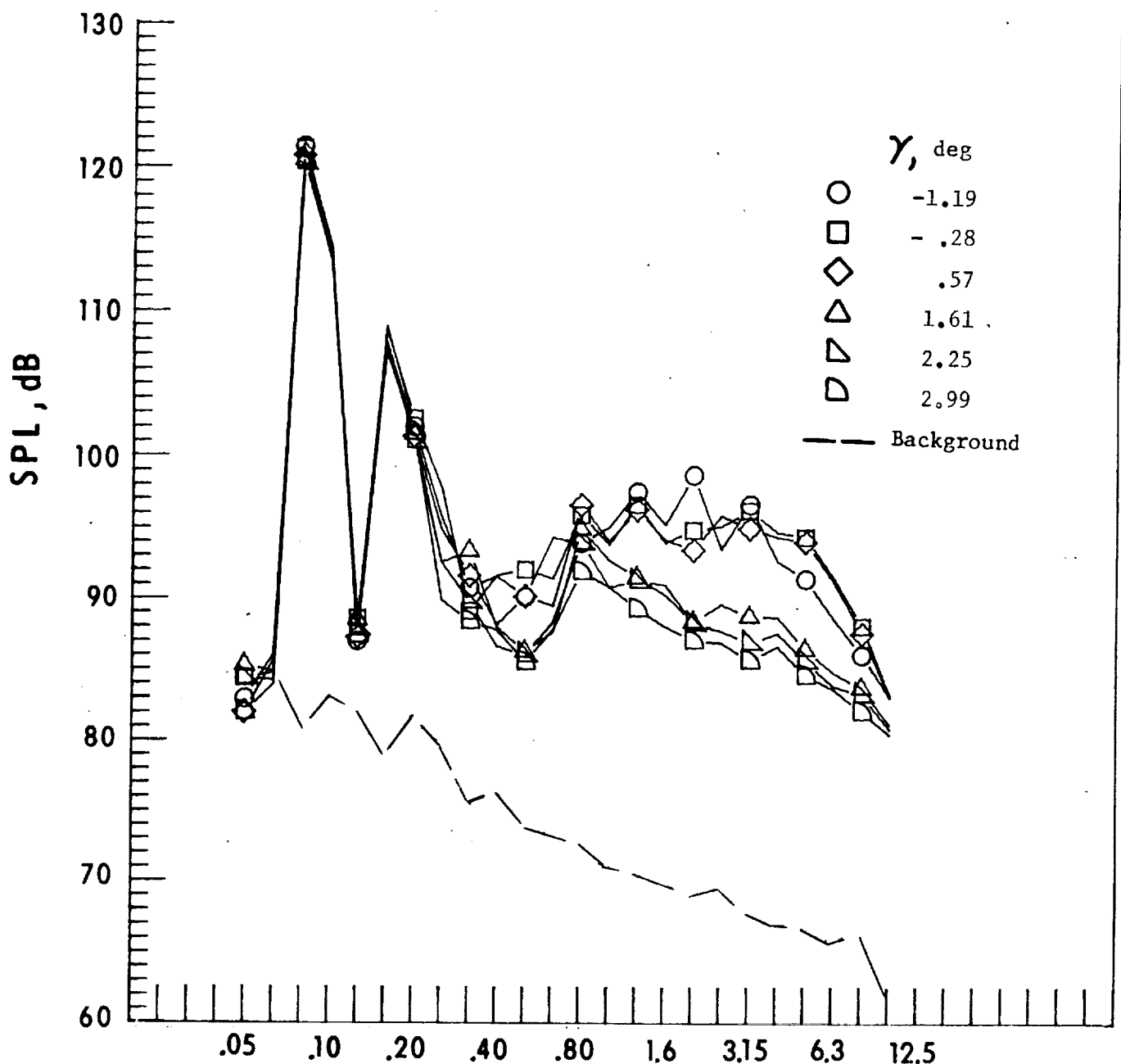
Figure 23. - Concluded.



One-third-octave-band center frequency, kHz

a. Mic. no. 1.

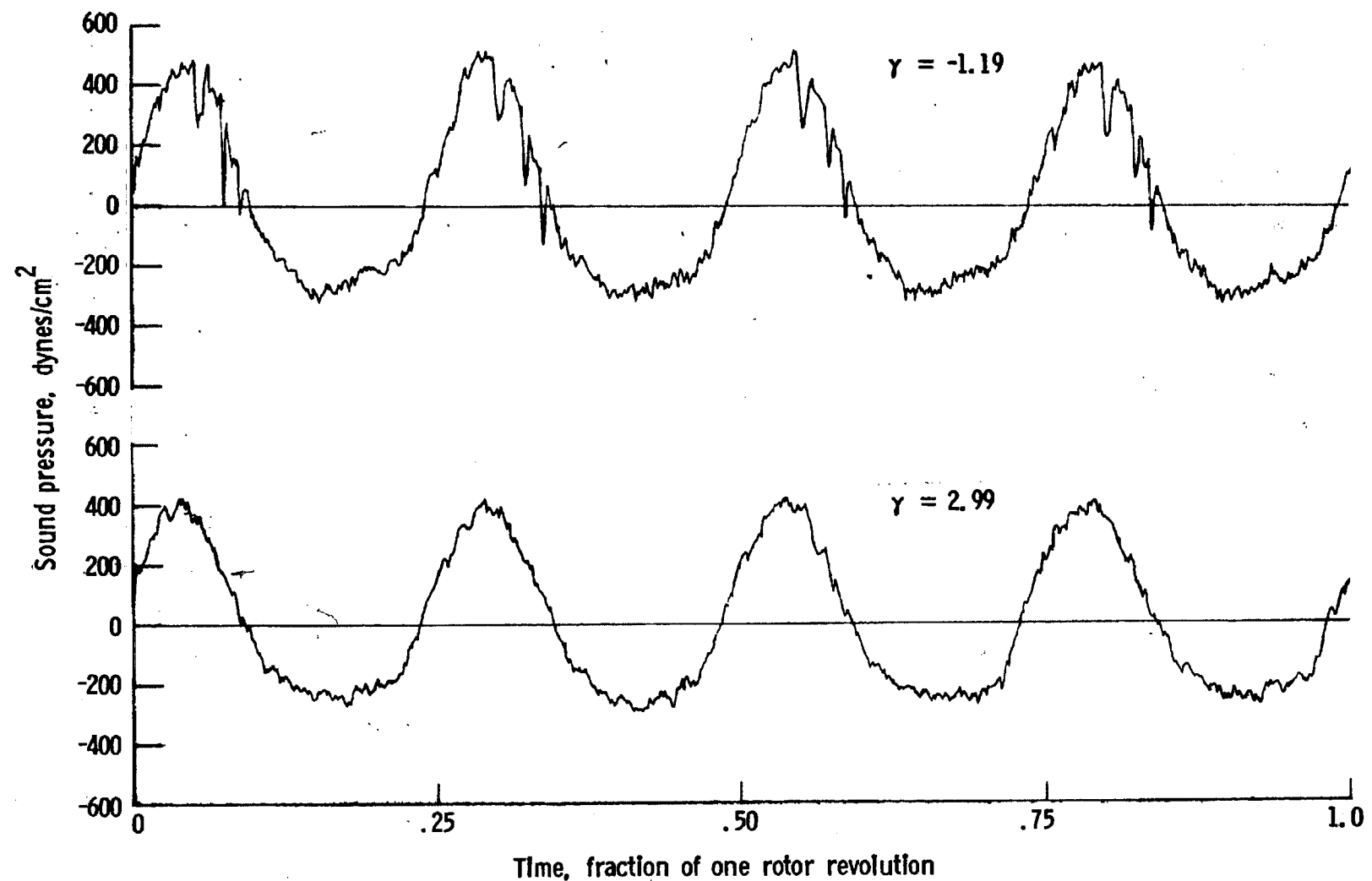
Figure 24. - Effect of descent angle variation on noise generated by helicopter model with end-plate tips installed. $V_{\infty} = 62.3$ knots.



One-third-octave-band center frequency, kHz

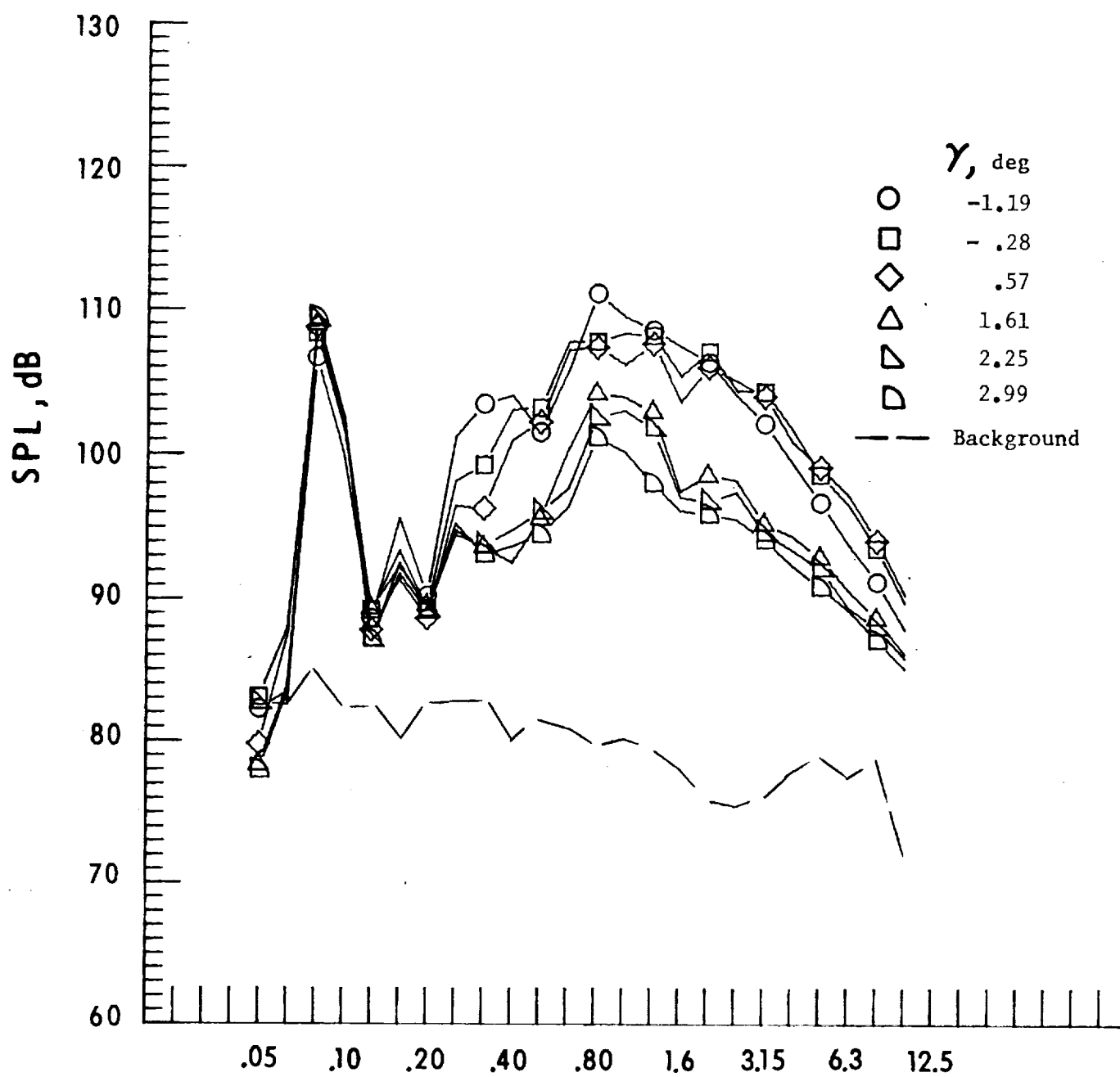
b. Mic. no. 2.

Figure 24. - Continued.



c. Pressure-time histories, Mic. no. 2.

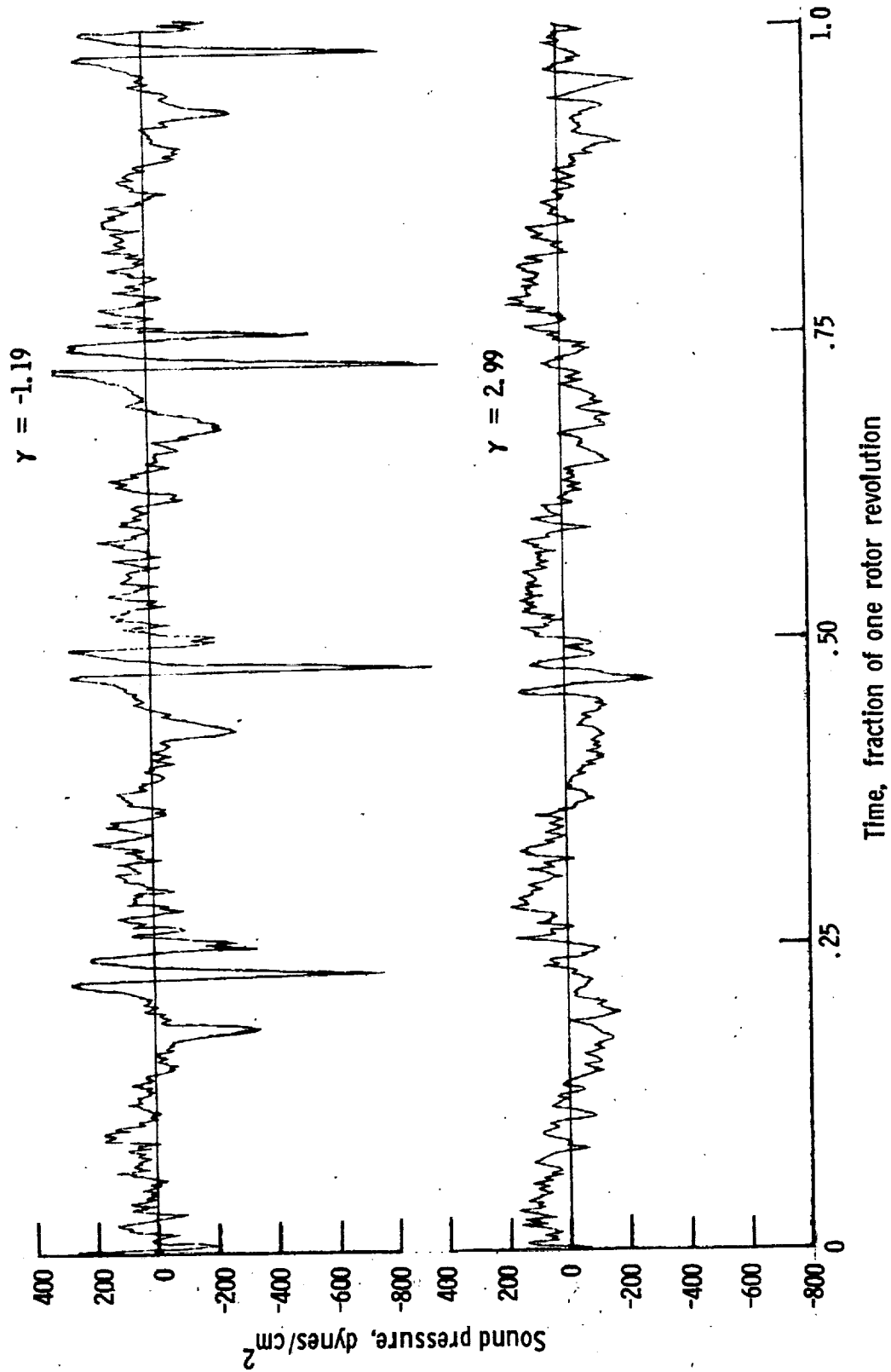
Figure 24. - Continued.



One-third-octave-band center frequency, kHz

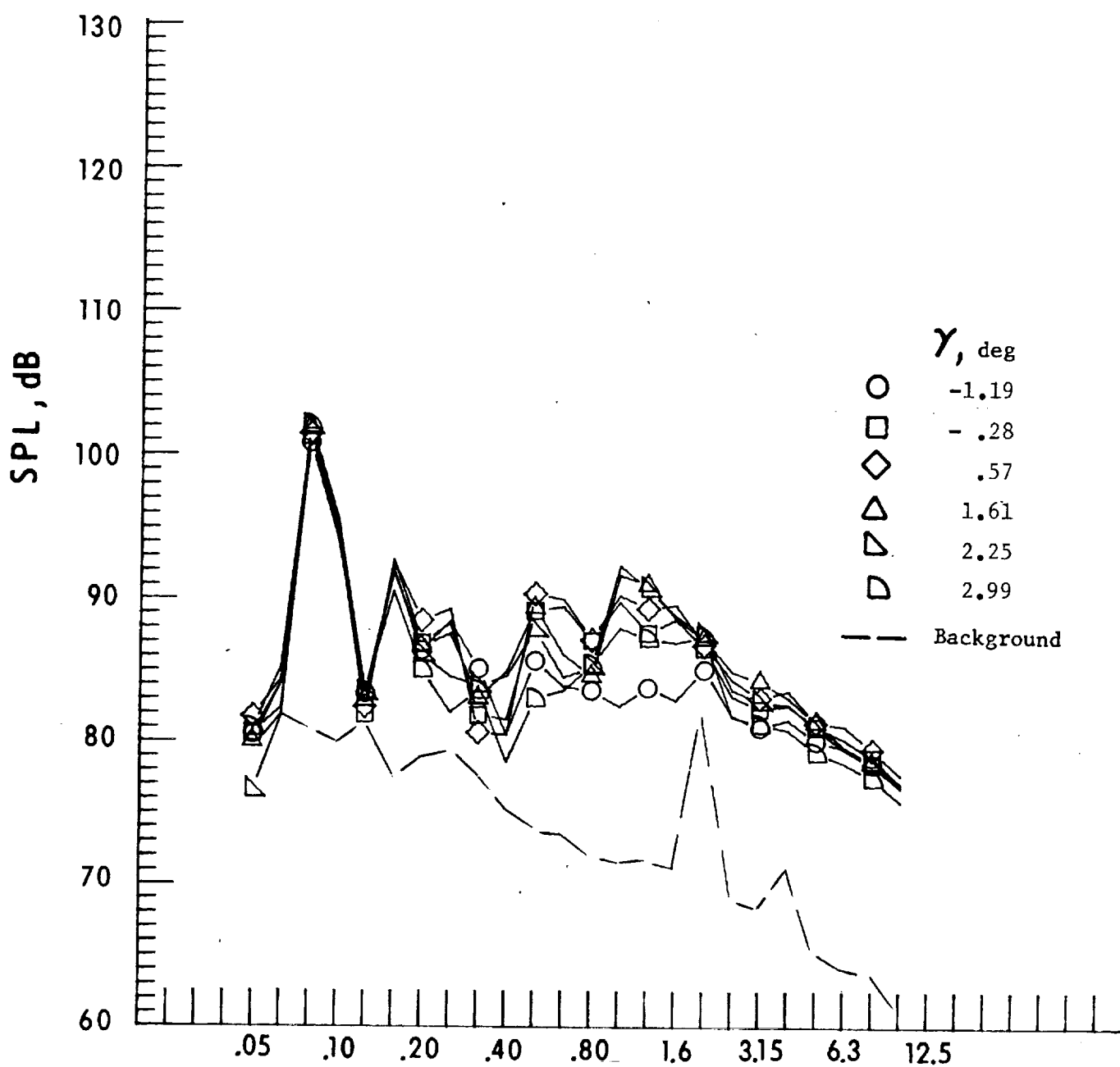
d. Mic. no. 3.

Figure 24. - Continued.



e. Pressure-time histories, Mic. no. 3.

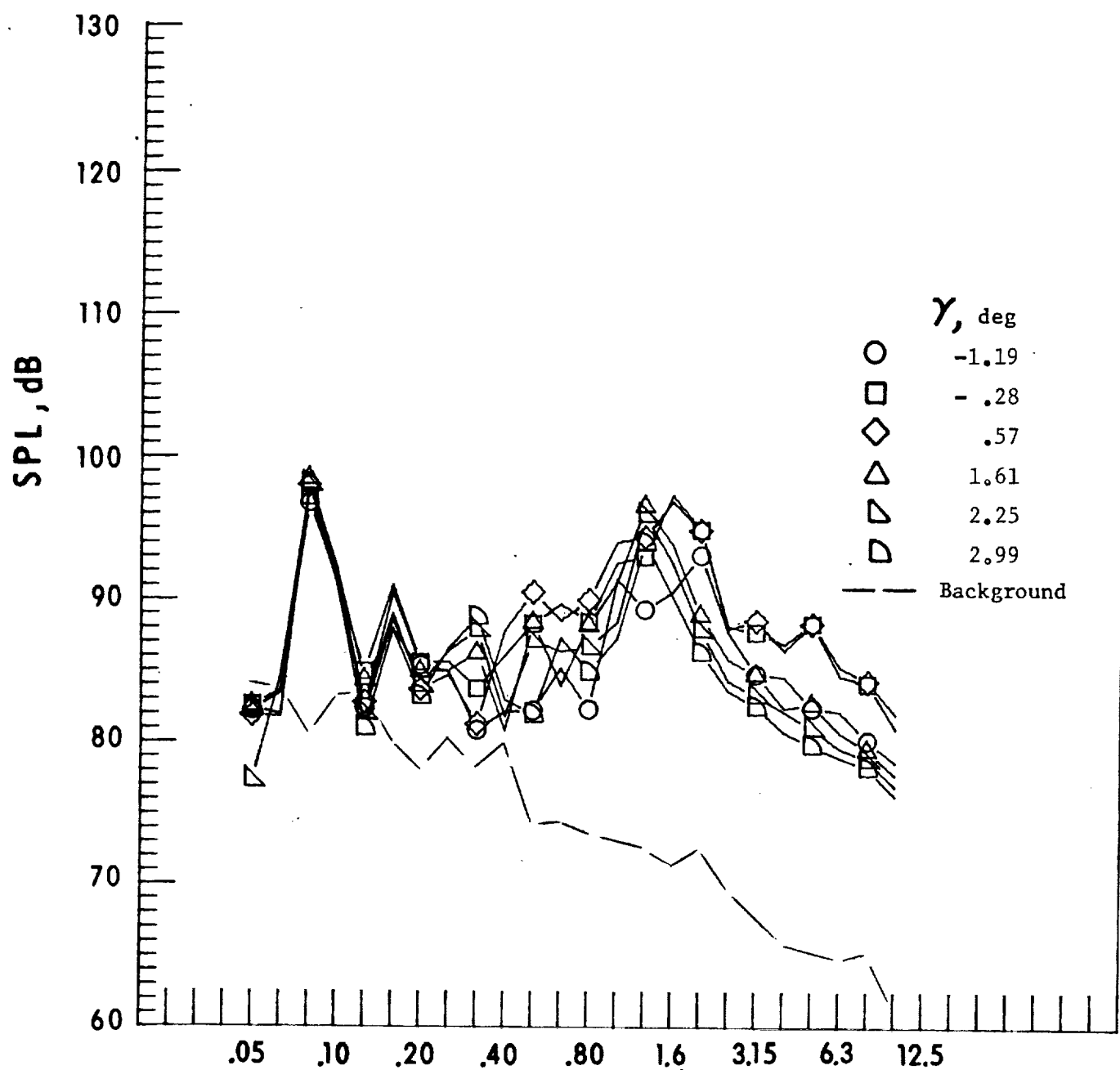
Figure 24. - Continued.



One-third-octave-band center frequency, kHz

f. Mic. no. 4.

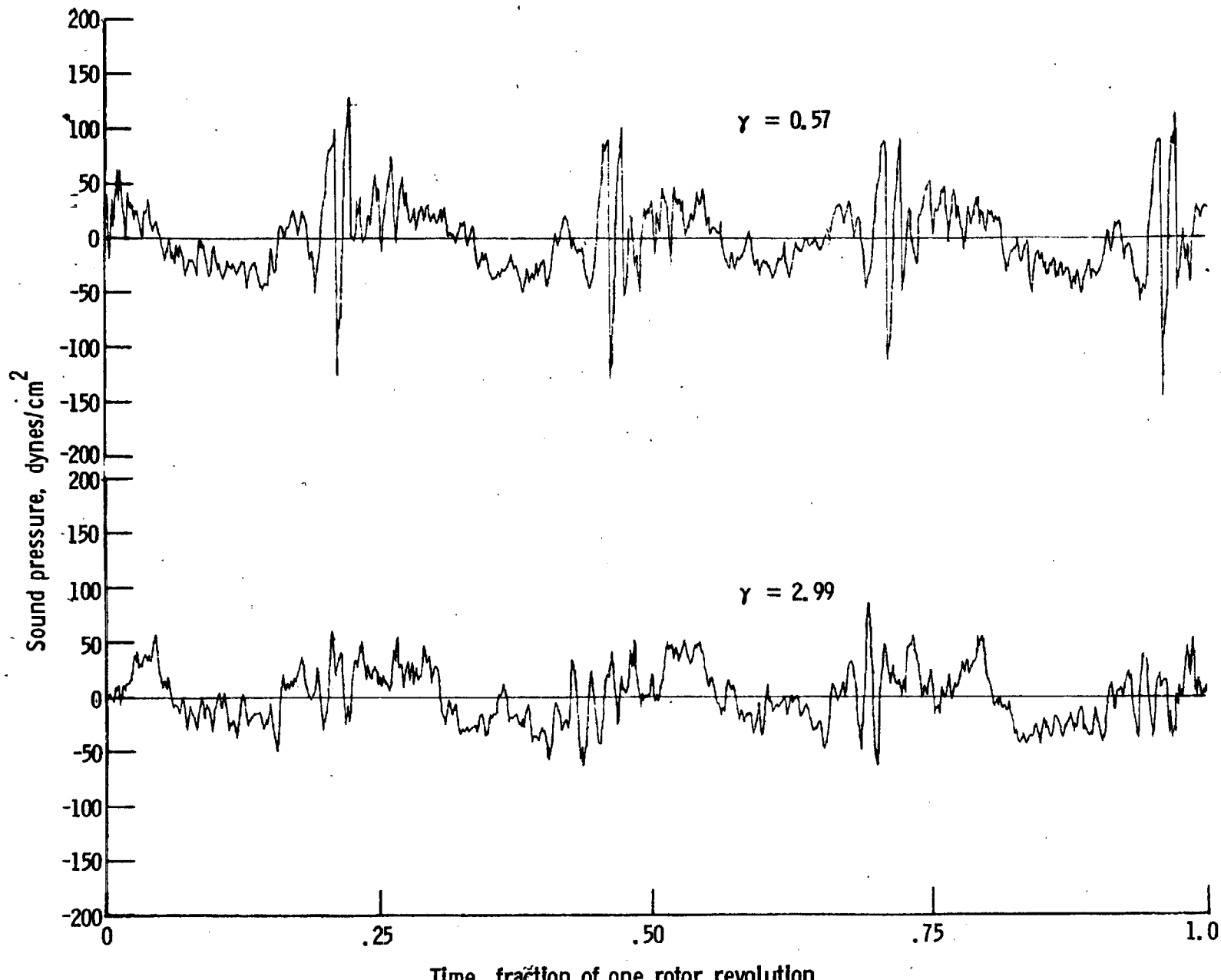
Figure 24. - Continued.



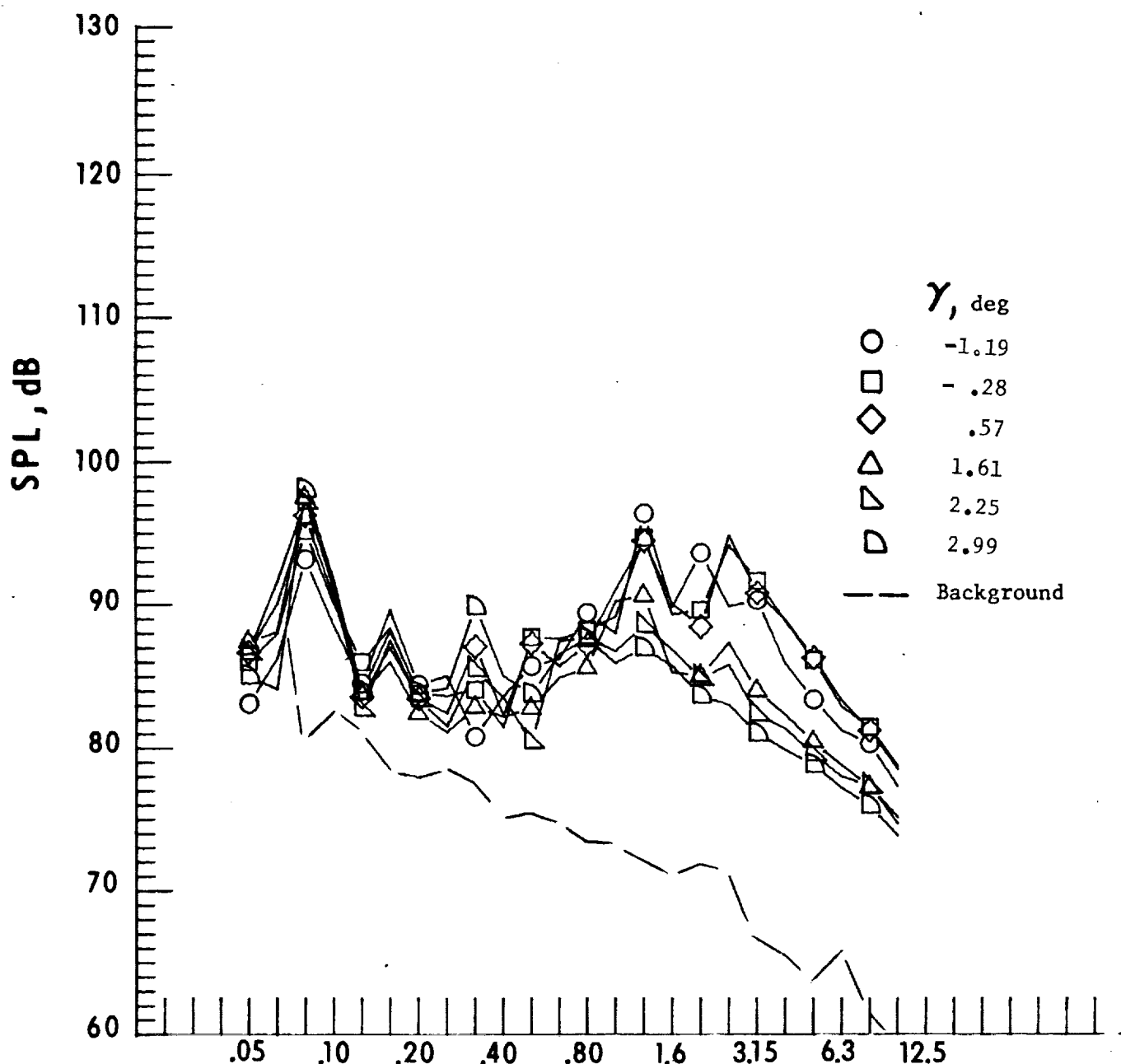
One-third-octave-band center frequency, kHz

g. Mic. no. 5.

Figure 24. - Continued.



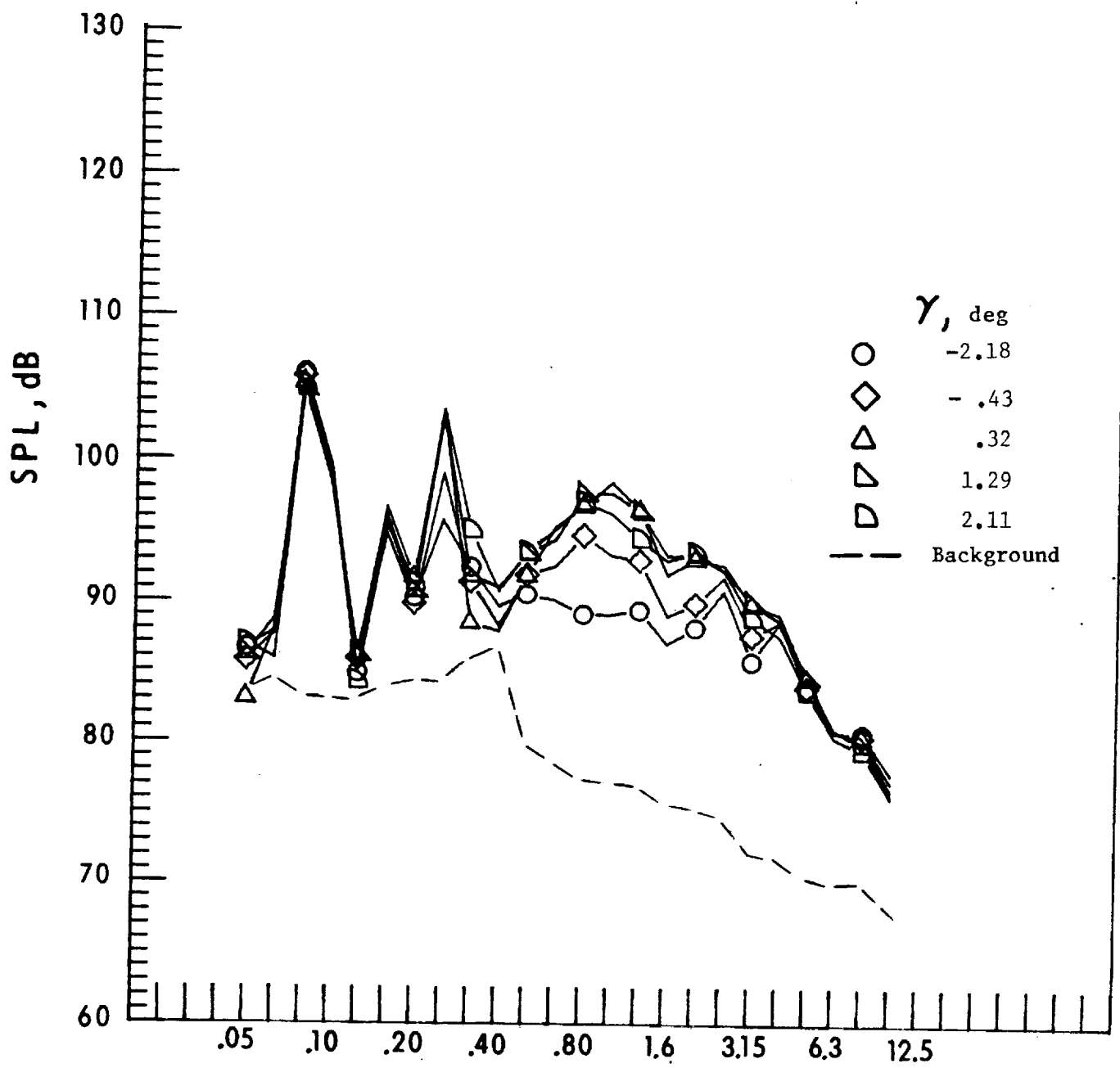
h. Pressure-time histories, Mic. no. 5.



One-third-octave-band center frequency, kHz

i. Mic. no. 7.

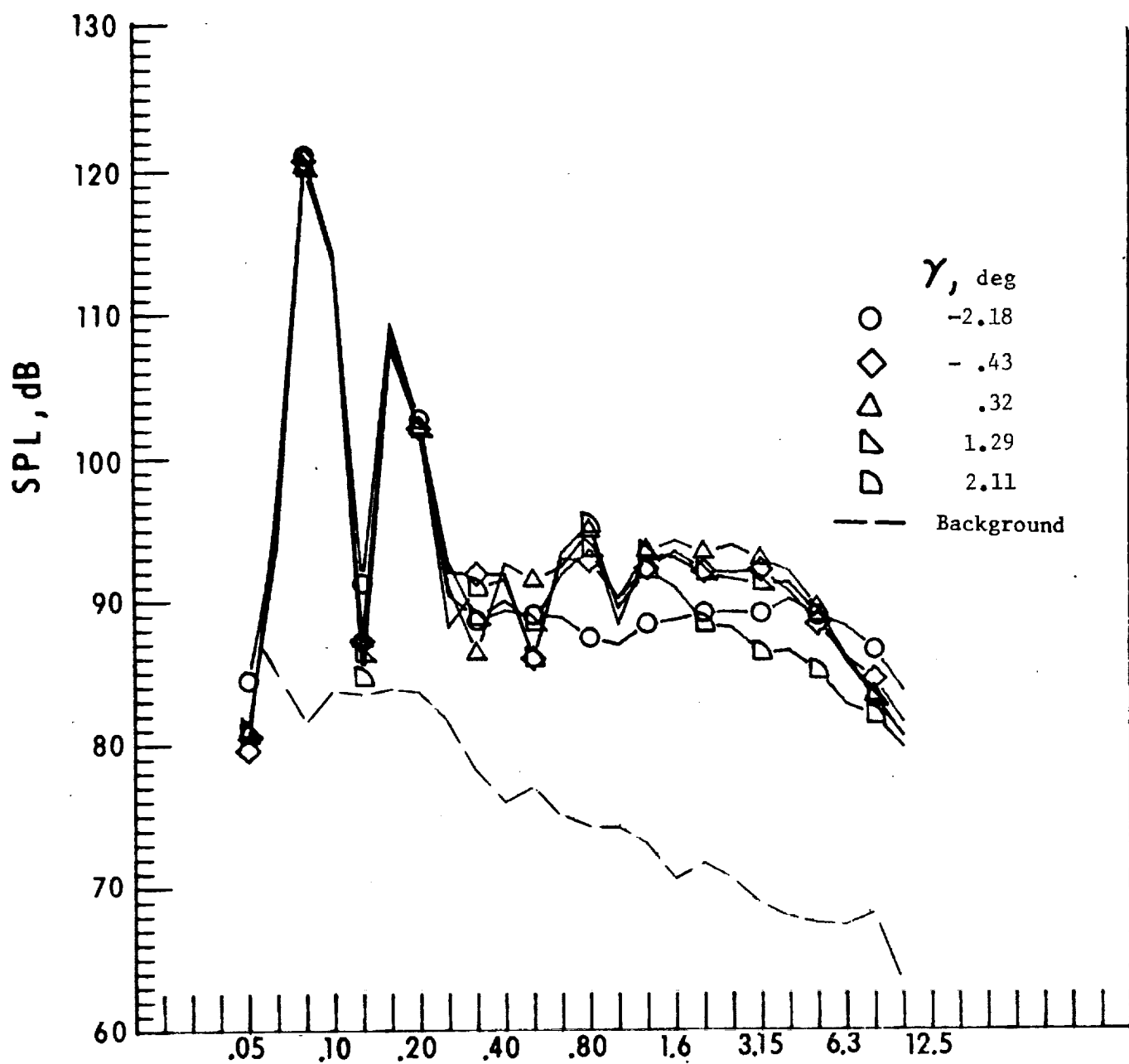
Figure 24. - Concluded.



One-third-octave-band center frequency, kHz

a. Mic. no. 1.

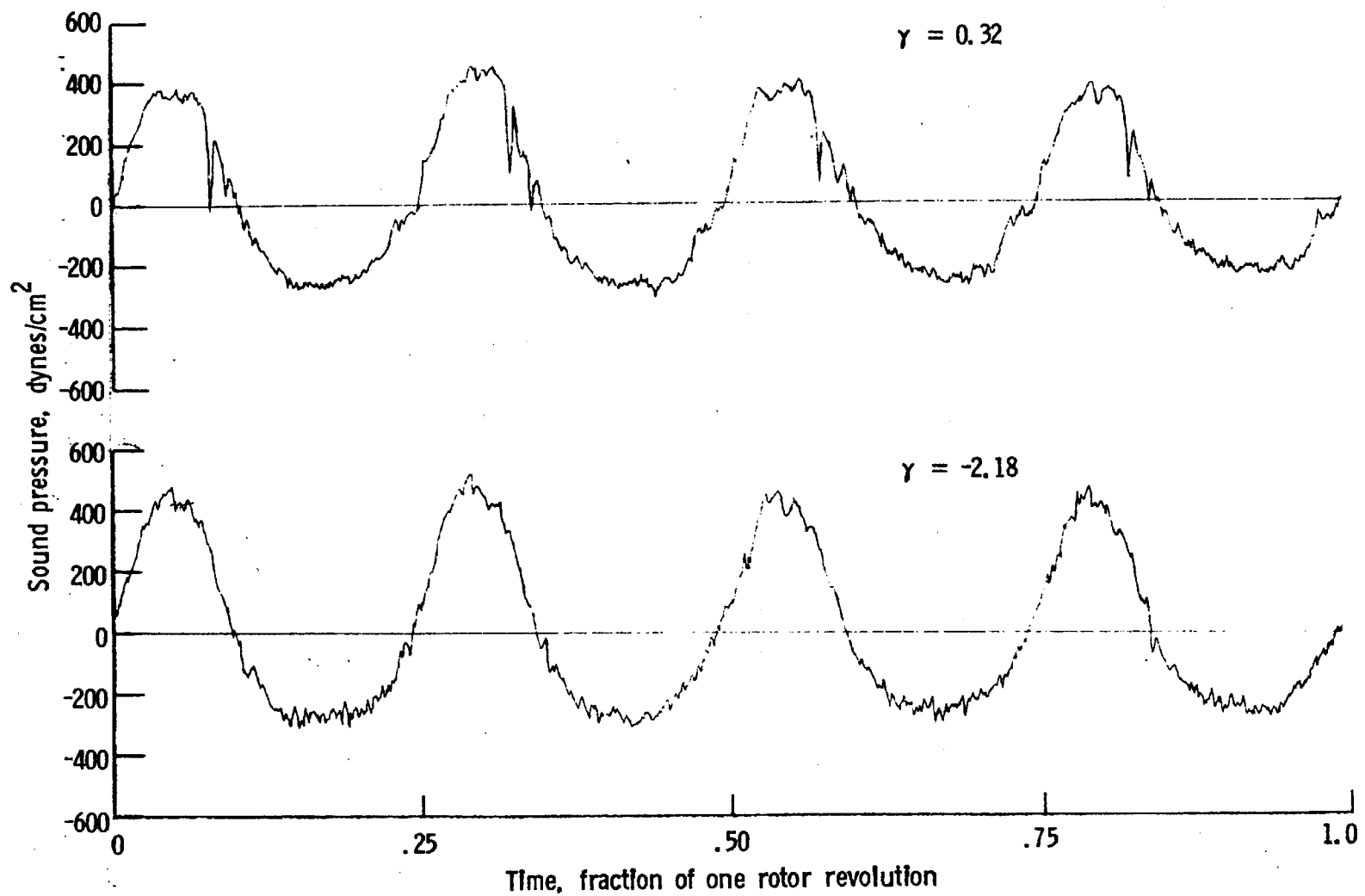
Figure 25. - Effect of descent angle variation on noise generated by helicopter model with square tips installed. $V_\infty = 65.7$ knots.



One-third-octave-band center frequency, kHz

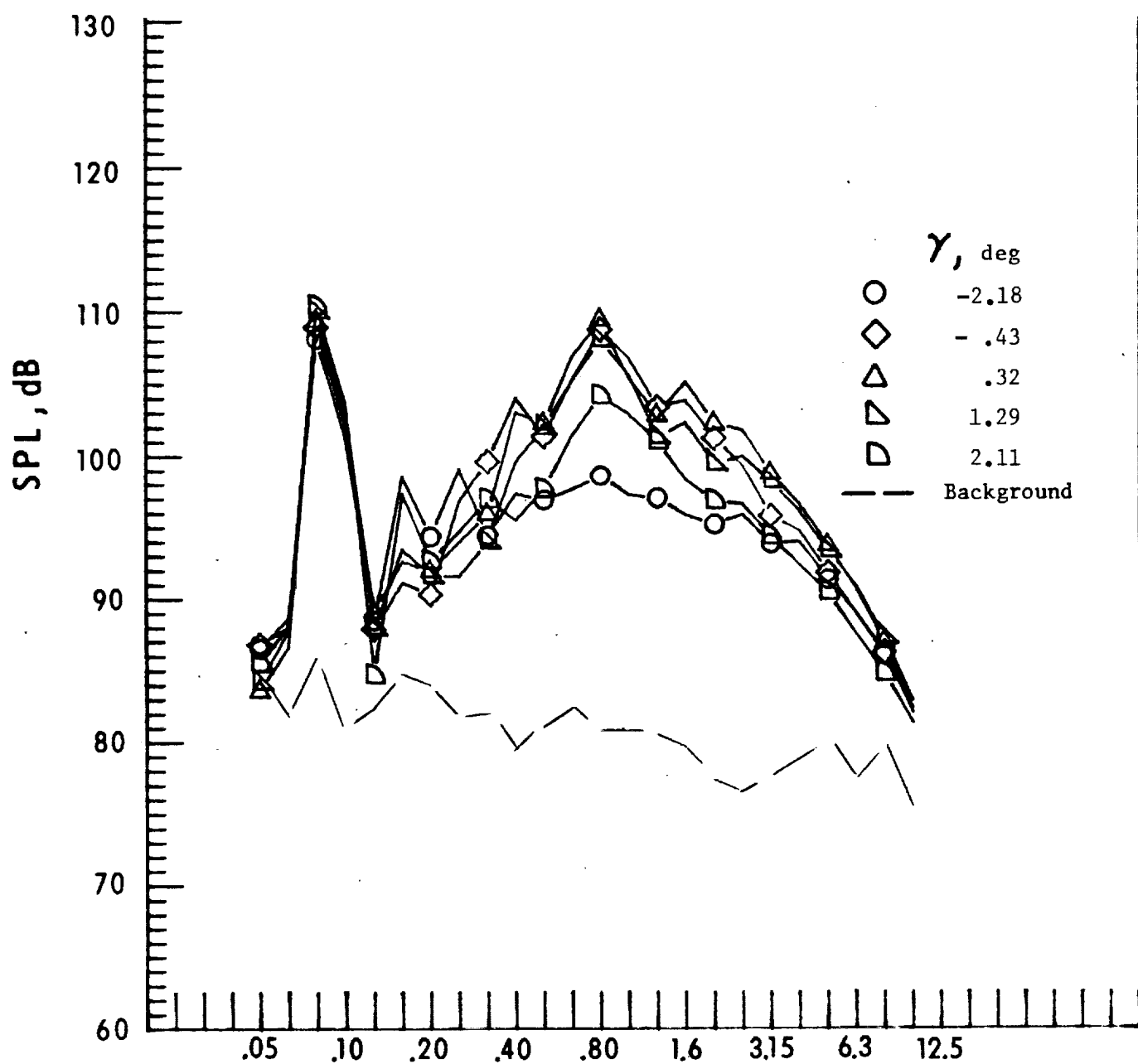
b. Mic. no. 2.

Figure 25. - Continued.



c. Pressure-time histories, Mic. no. 2.

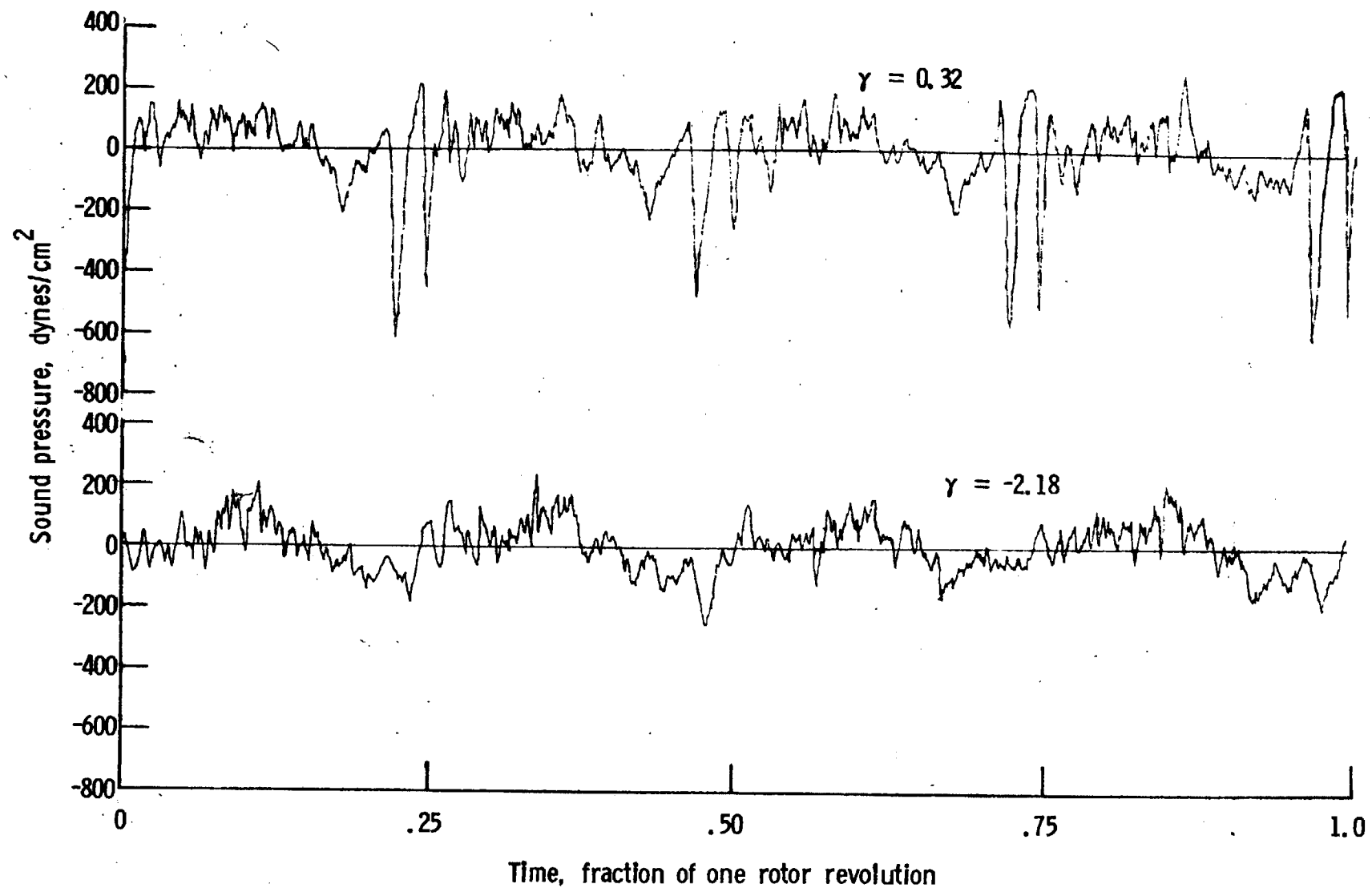
Figure 25. - Continued.



One-third-octave-band center frequency, kHz

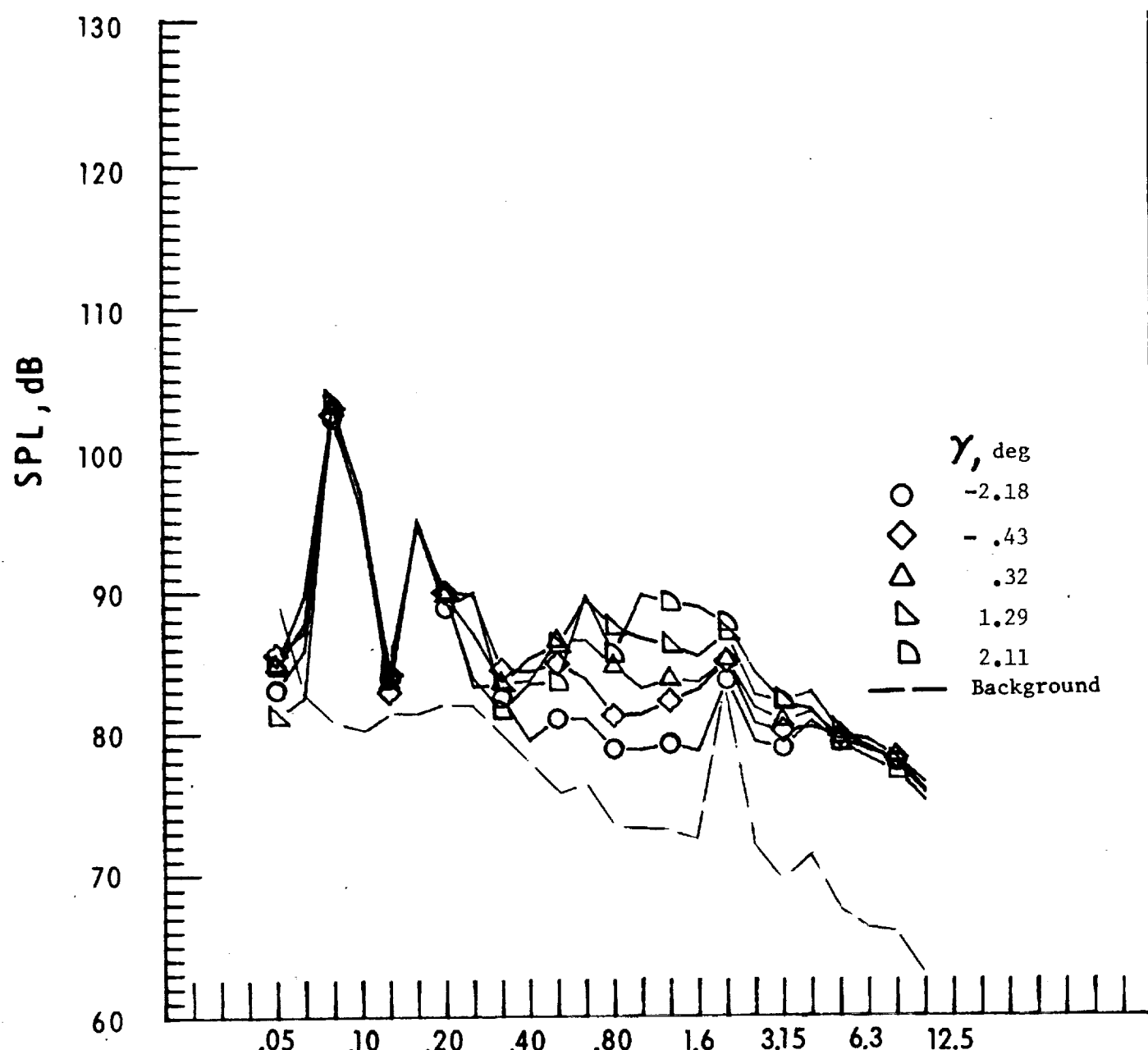
d. Mic. no. 3.

Figure 25. - Continued.



e. Pressure-time histories, Mic. no. 3.

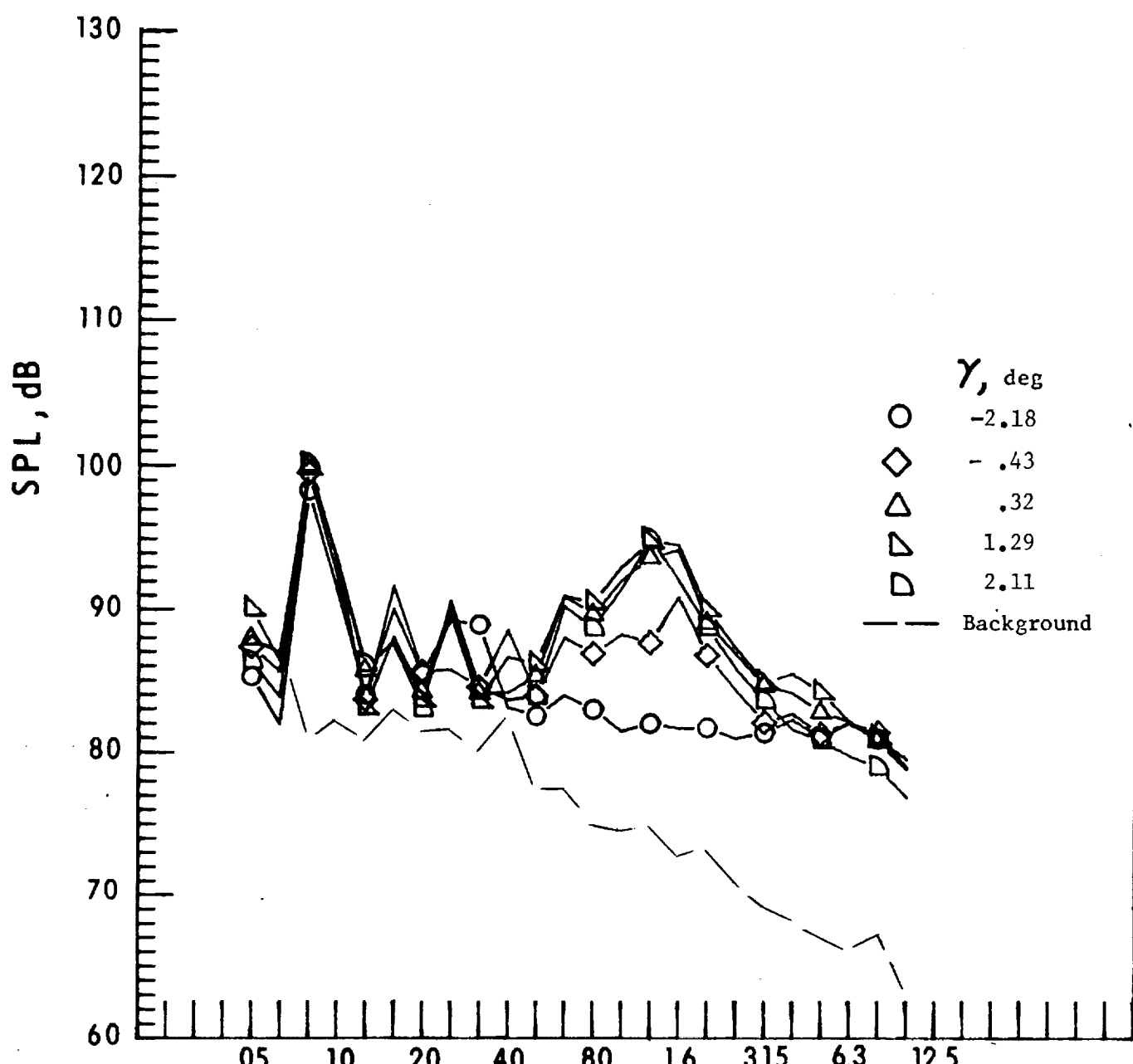
Figure 25. - Continued.



One-third-octave-band center frequency, kHz

f. Mic. no. 4.

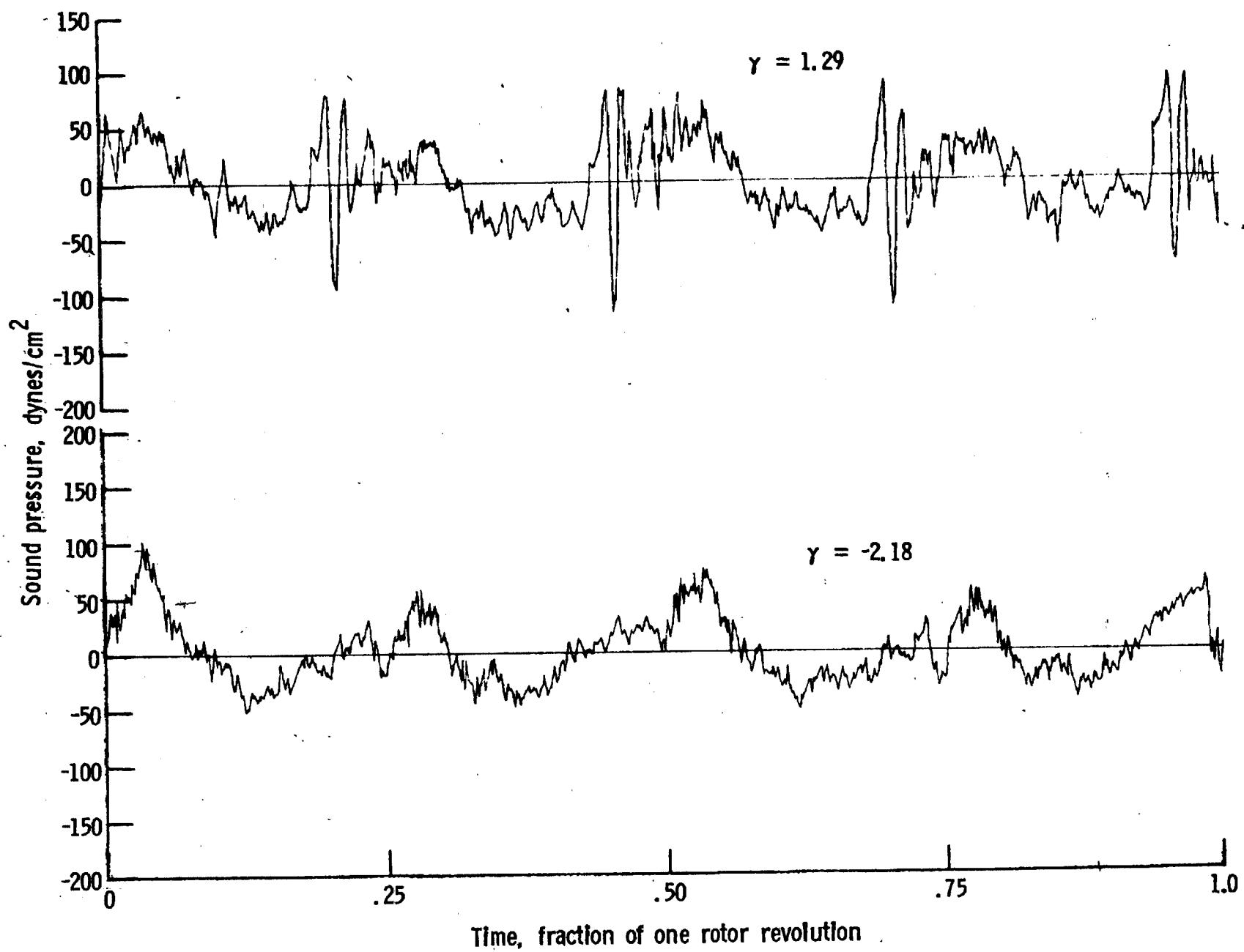
Figure 25. - Continued



One-third-octave-band center frequency, kHz

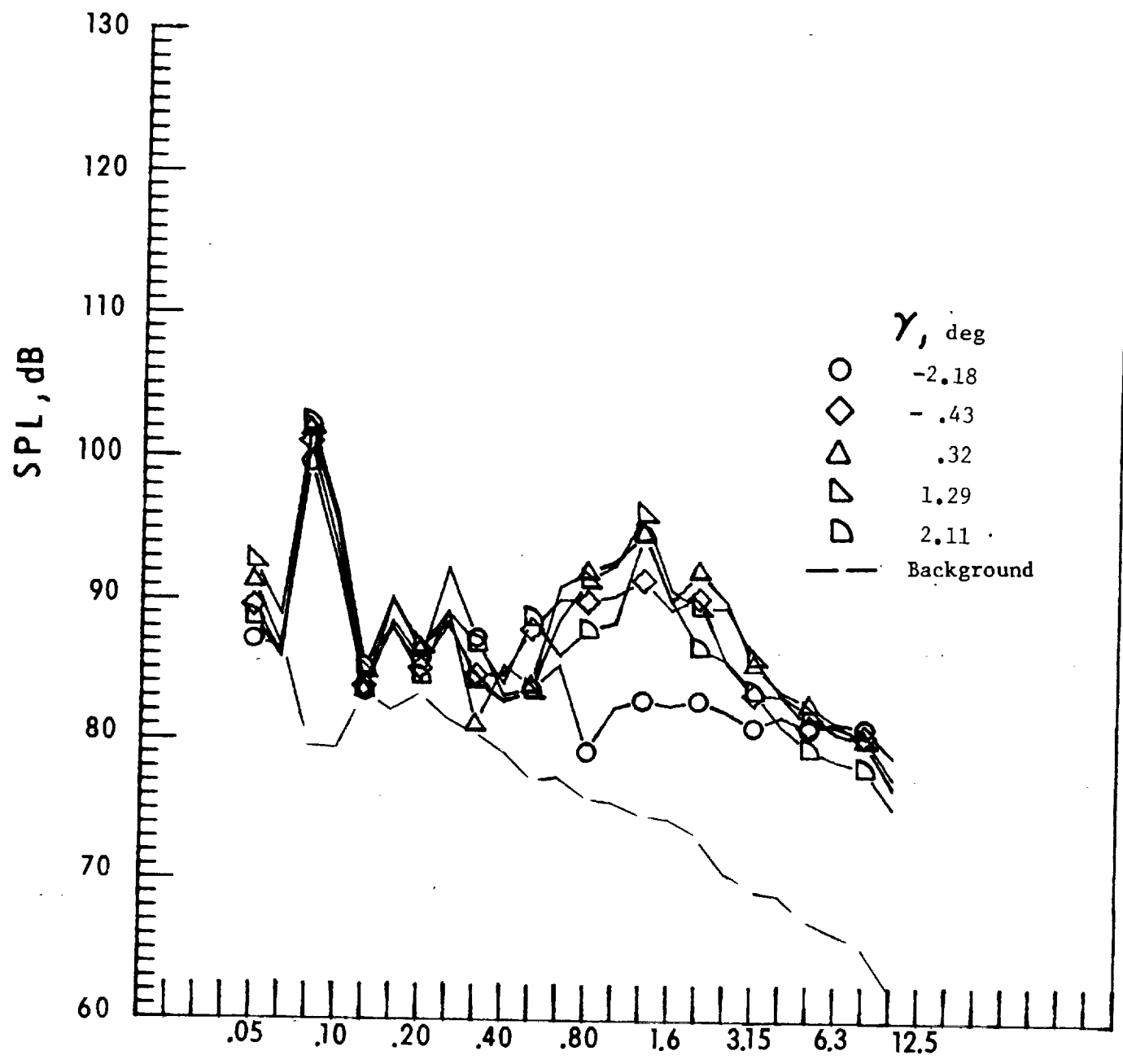
g. Mic. no. 5.

Figure 25. - Continued.



h. Pressure-time histories, Mic. no. 5

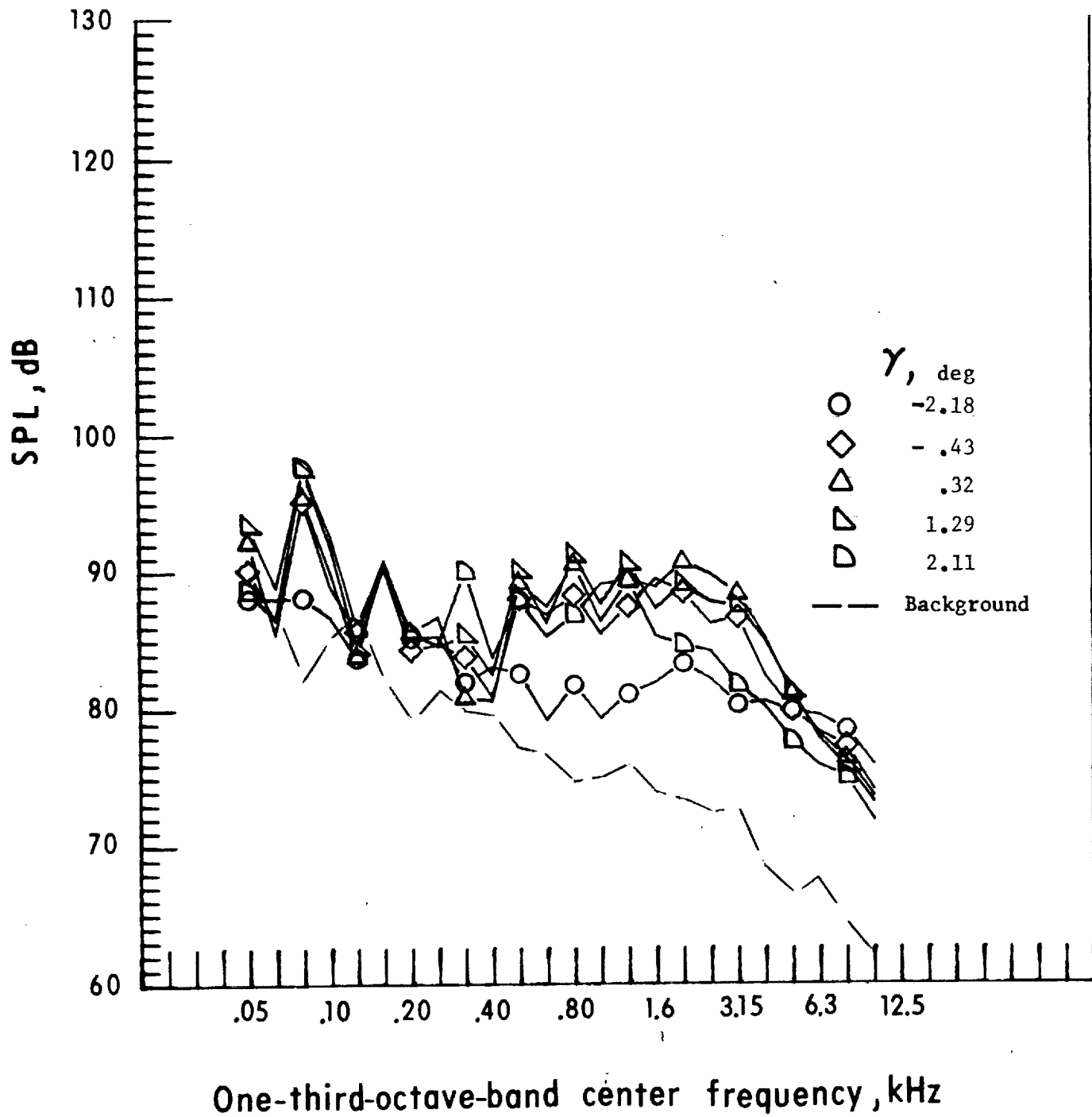
Figure 25. - Continued.



One-third-octave-band center frequency, kHz

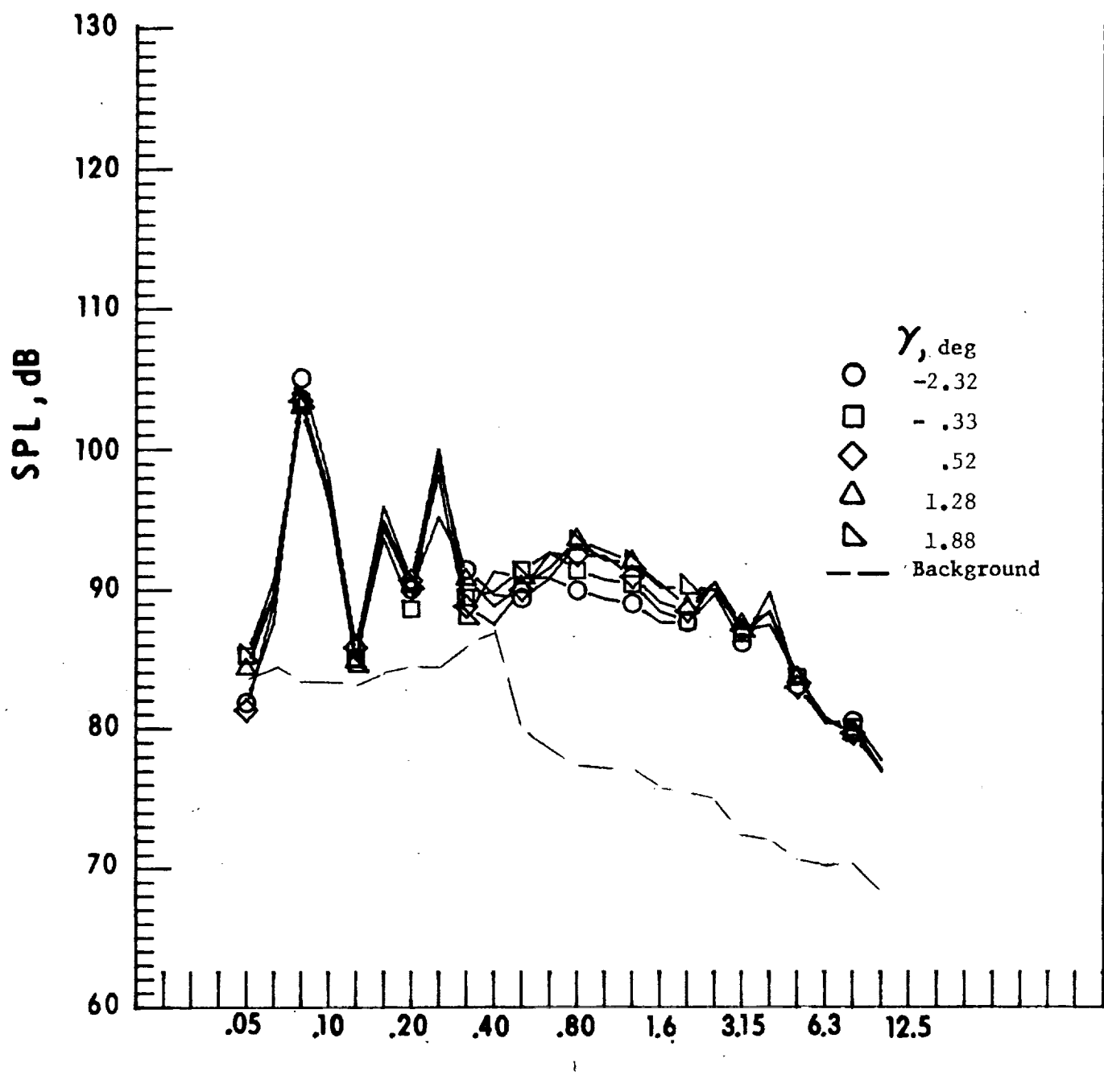
i. Mic. no. 6.

Figure 25. - Continued



j. Mic. no. 7.

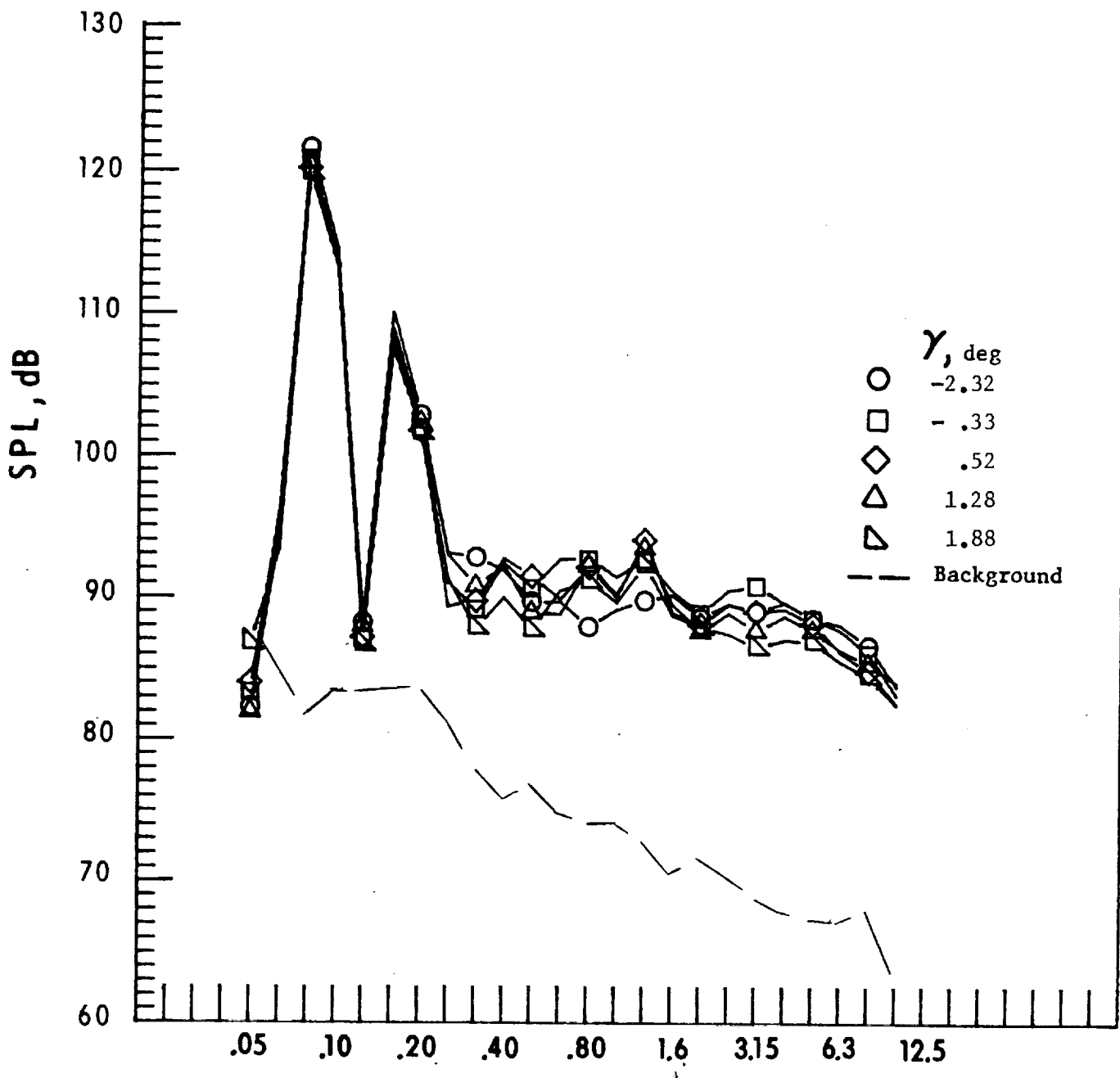
Figure 25. - Concluded



One-third-octave-band center frequency, kHz

a. Mic. no. 1.

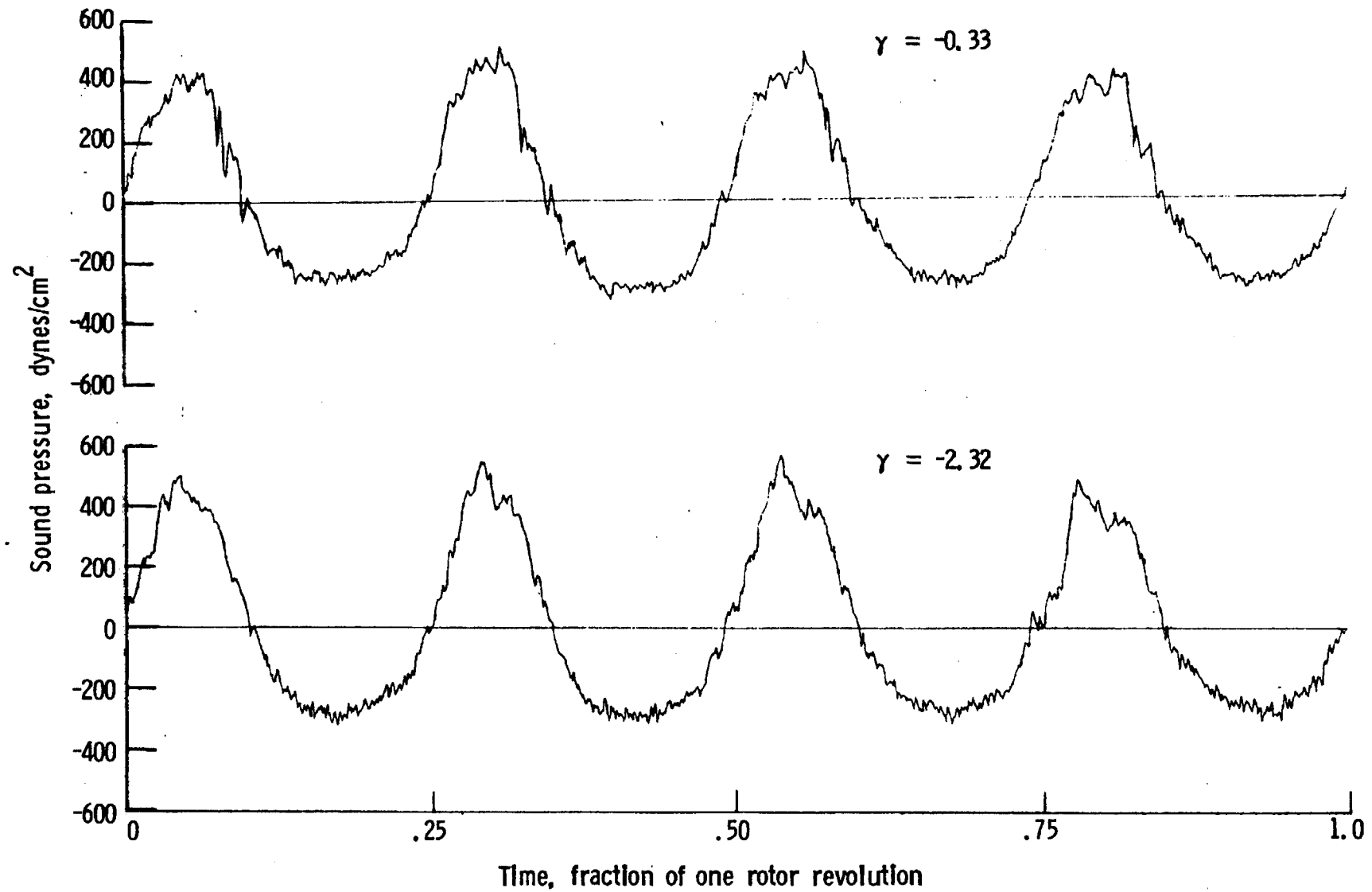
Figure 26. - Effect of descent angle variation on noise generated by helicopter model with ogee tips installed. $V_\infty = 66.7$ knots.



One-third-octave-band center frequency, kHz

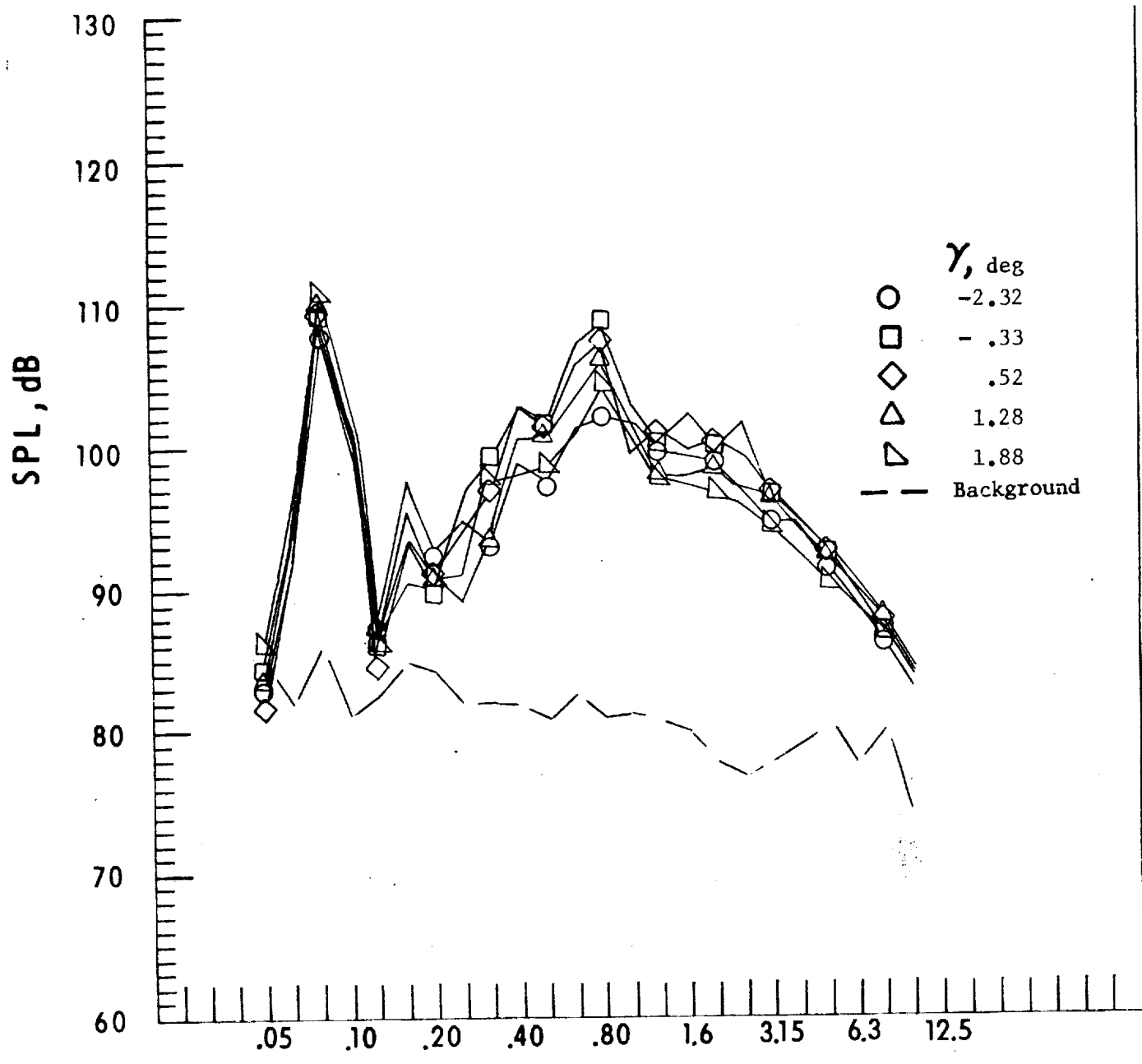
b. Mic. no. 2.

Figure 26. - Continued.



c. Pressure-time histories, Mic. no. 2.

Figure 26. - Continued.



One-third-octave-band center frequency, kHz

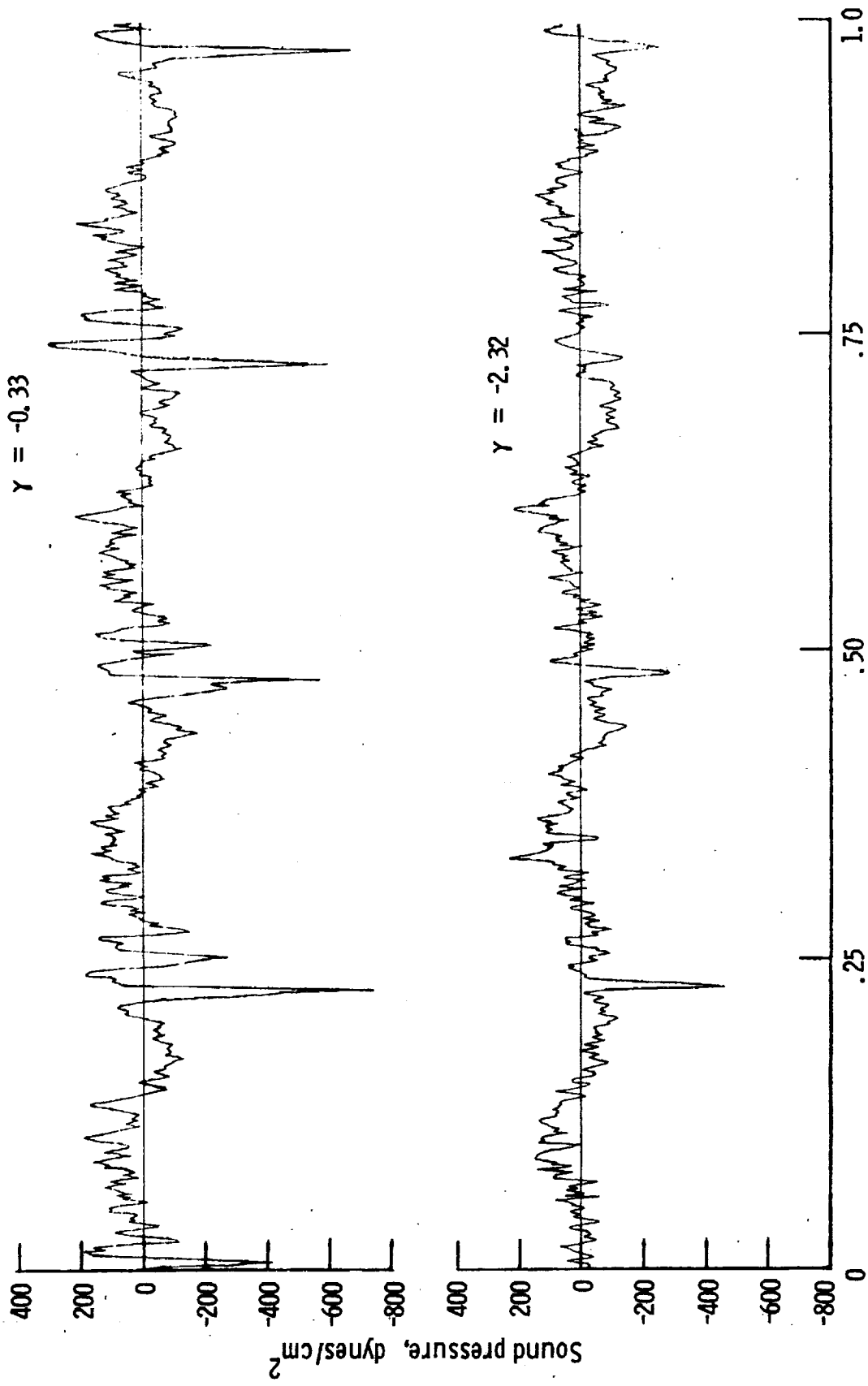
d. Mic. no. 3.

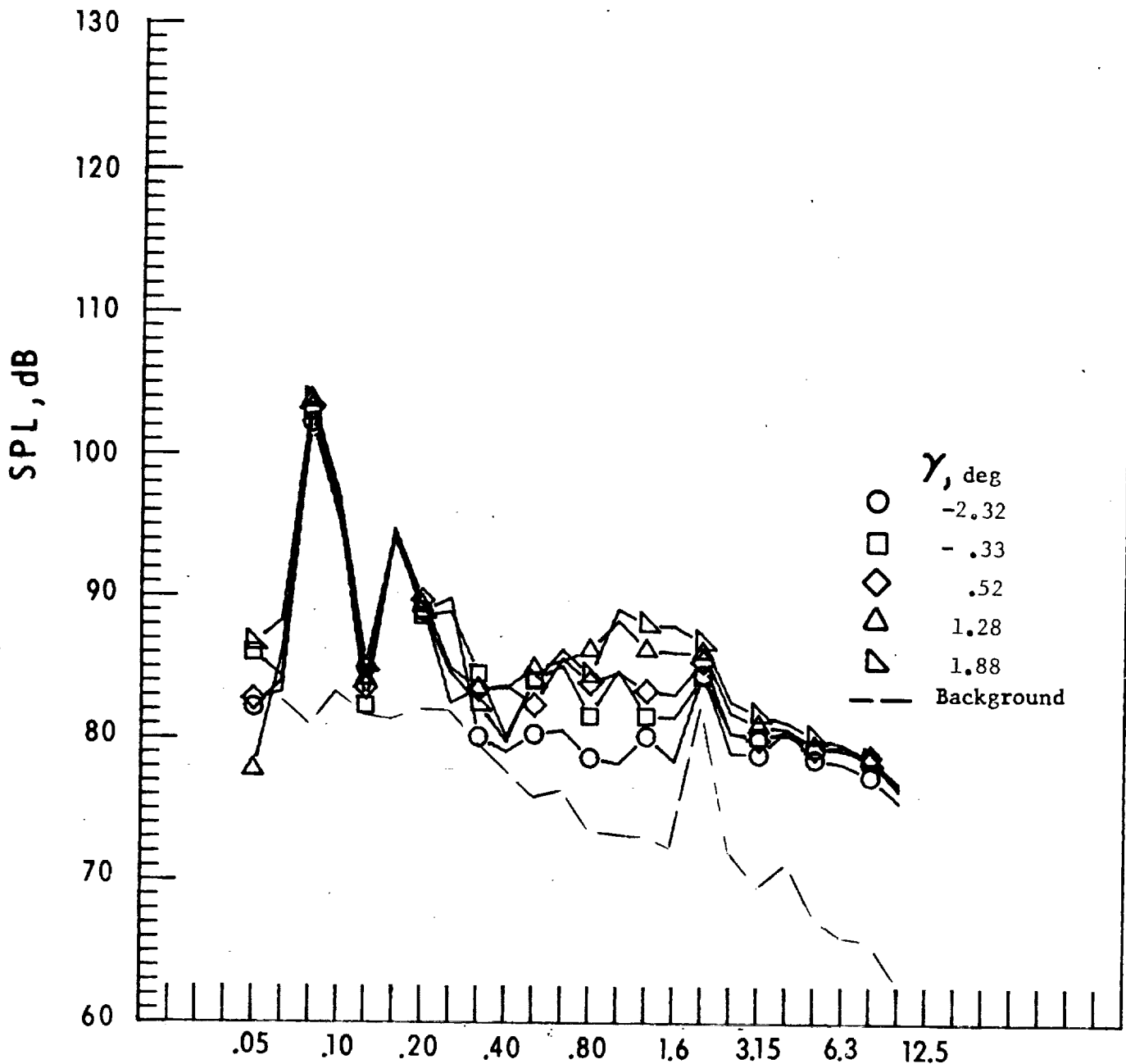
Figure 26. - Continued.

Figure 26 - Continued.

e. Pressure-time histories. Mic. no. 3.

Time, fraction of one rotor revolution





One-third-octave-band center frequency, kHz

f. Mic. no. 4.

Figure 26. - Continued.

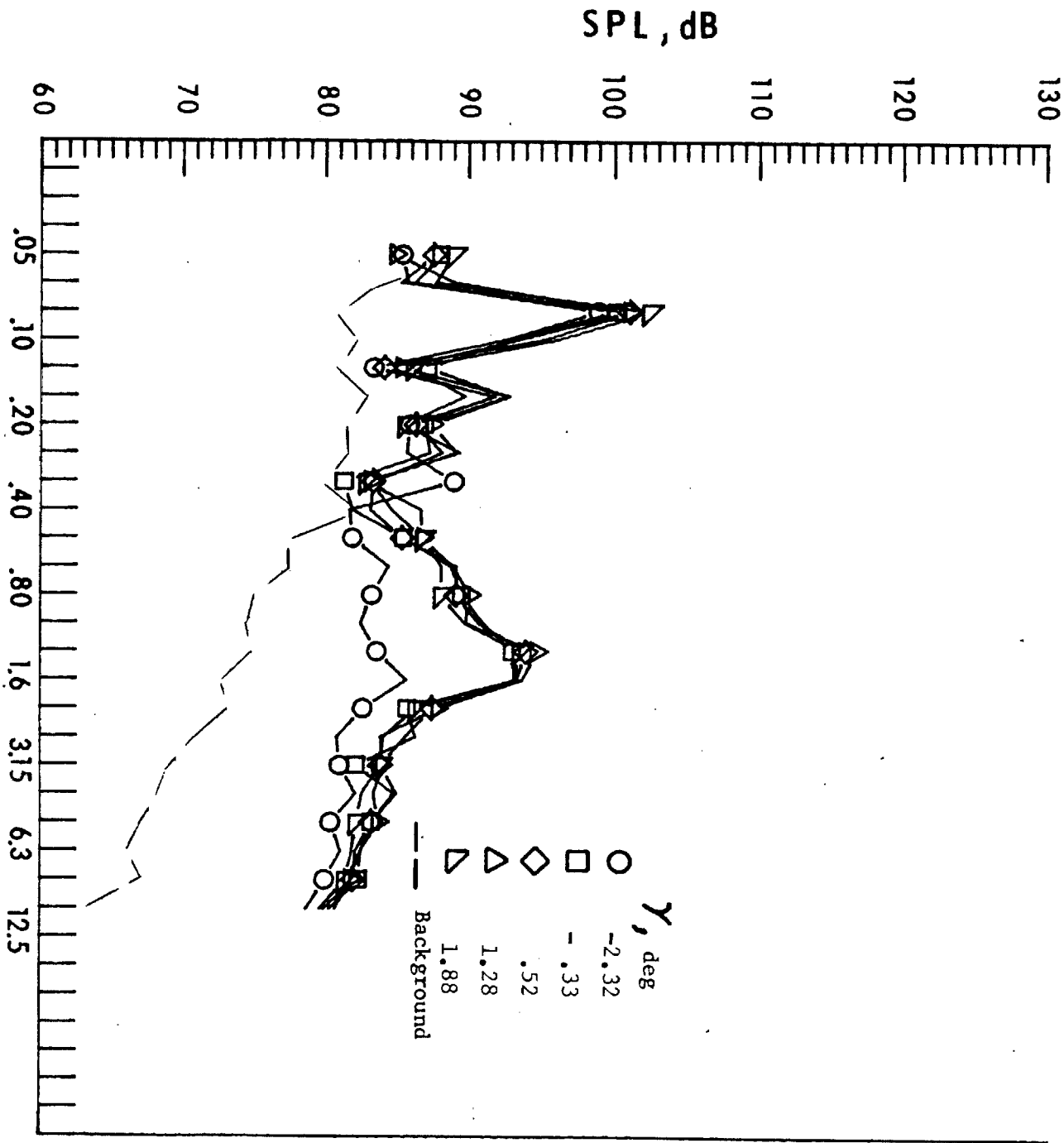
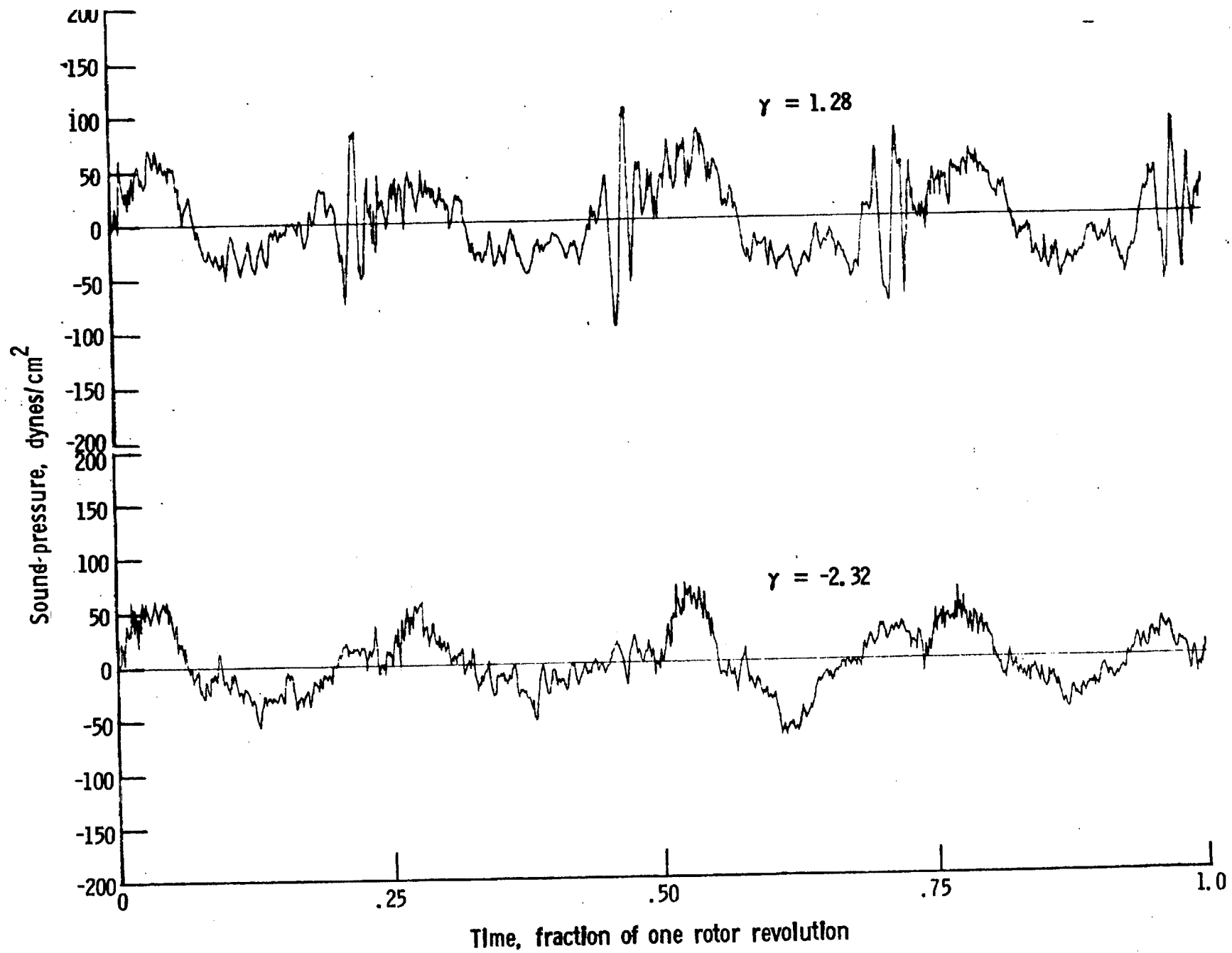


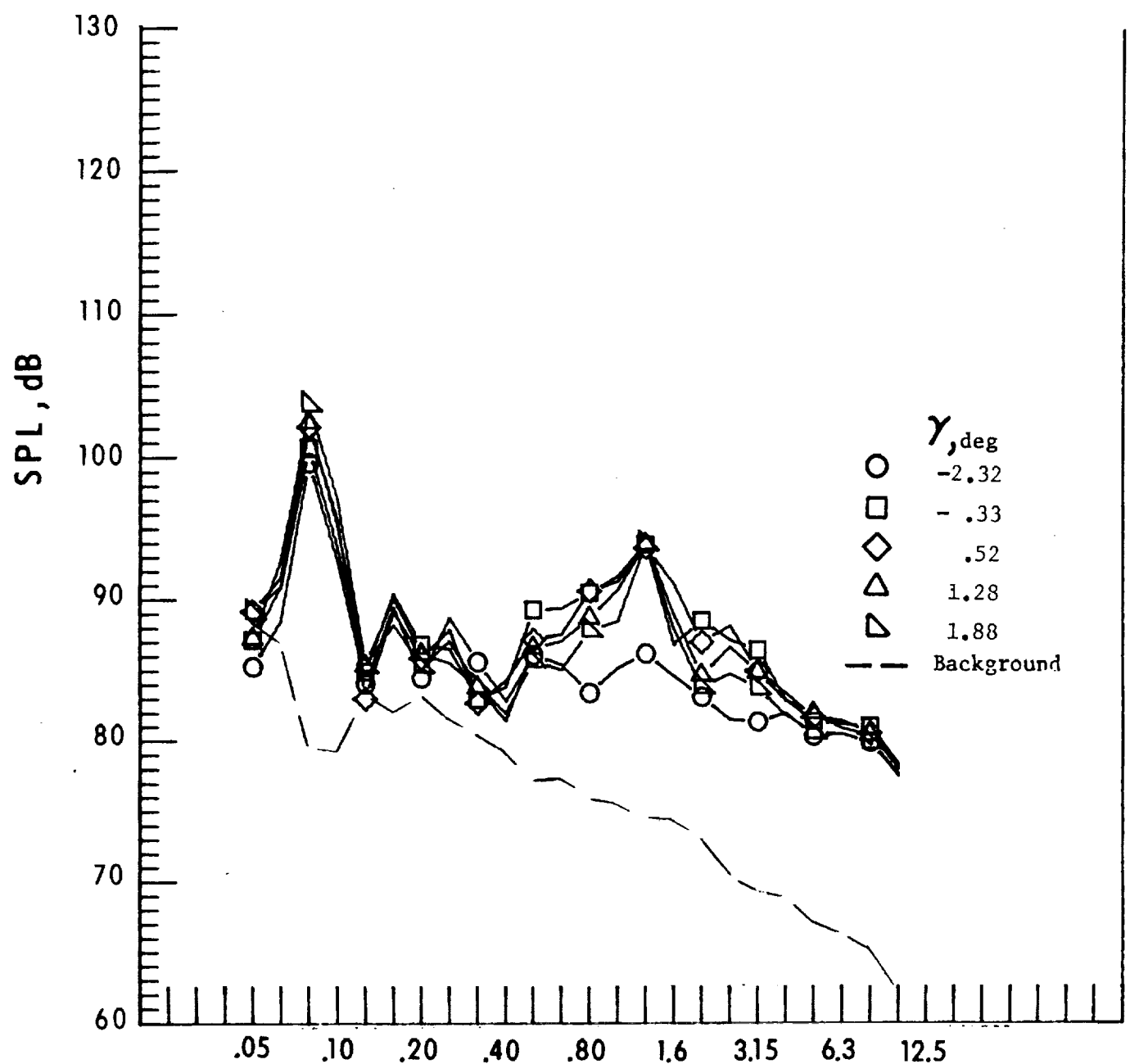
Figure 26. - Continued.

g. Mic. no. 5.



h. Pressure-time histories, Mic. no. 5.

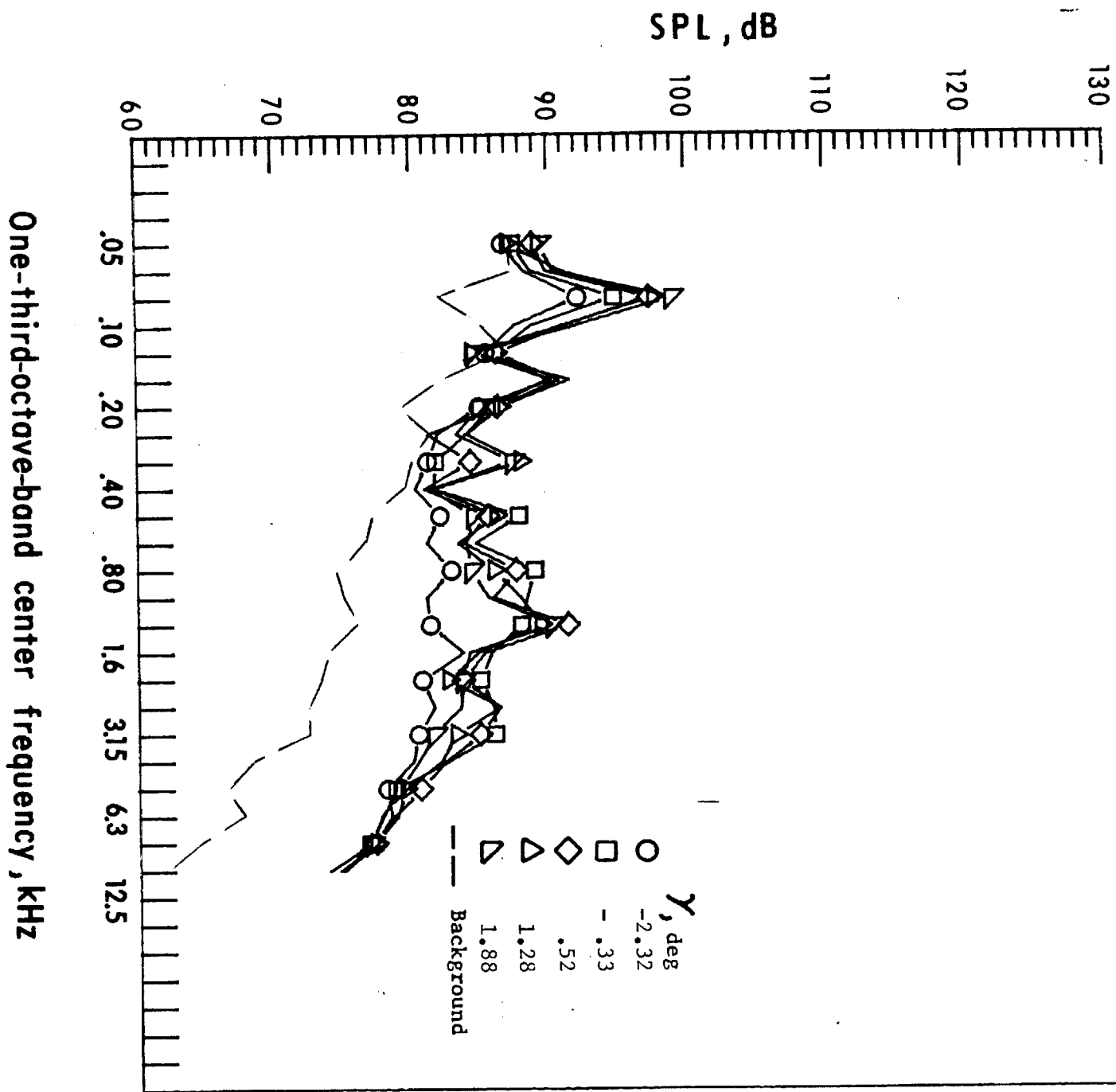
Figure 26. - Continued.



One-third-octave-band center frequency, kHz

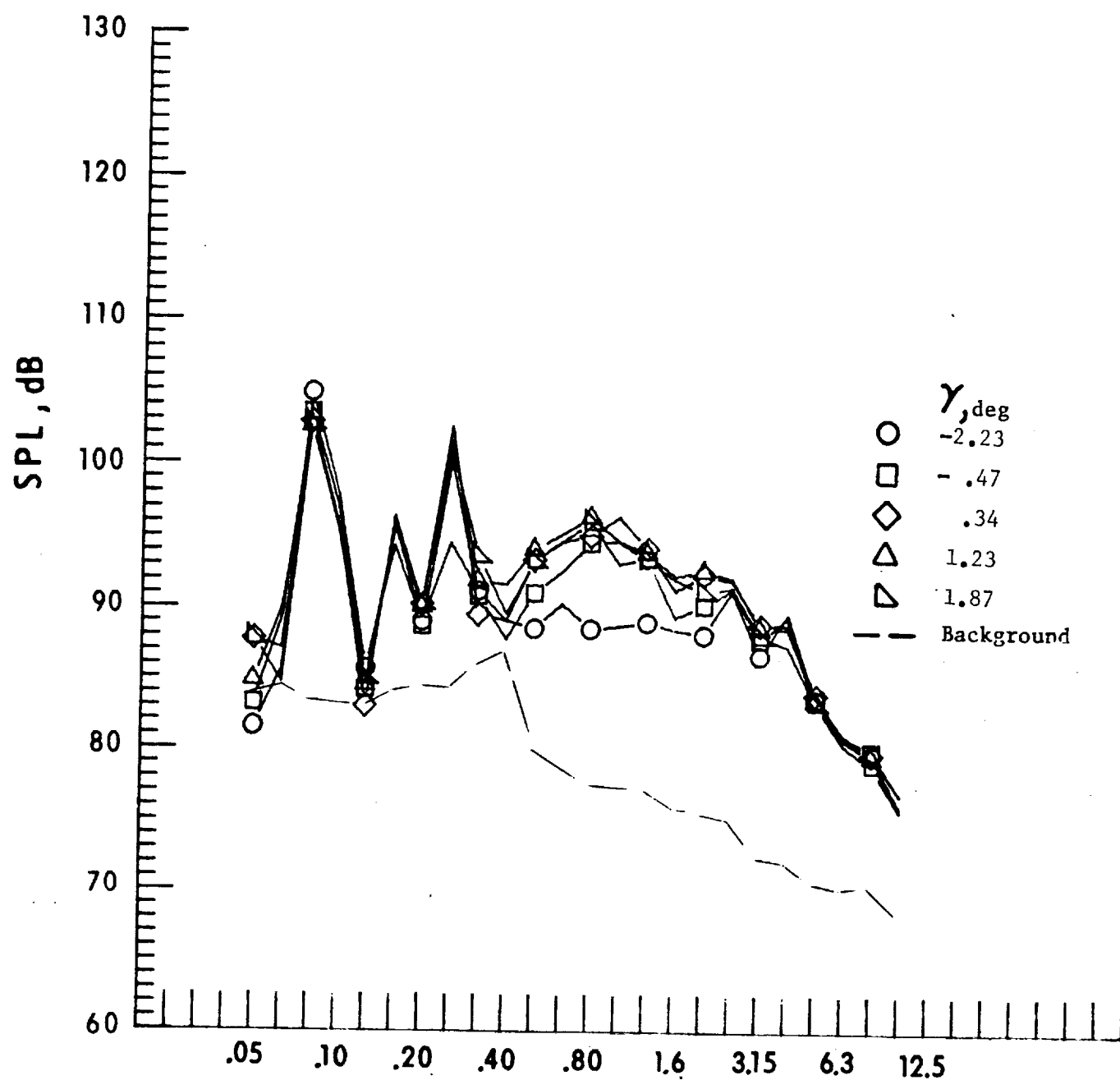
i. Mic. no. 6.

Figure 26. - Continued.



j. Mic. no. 7.

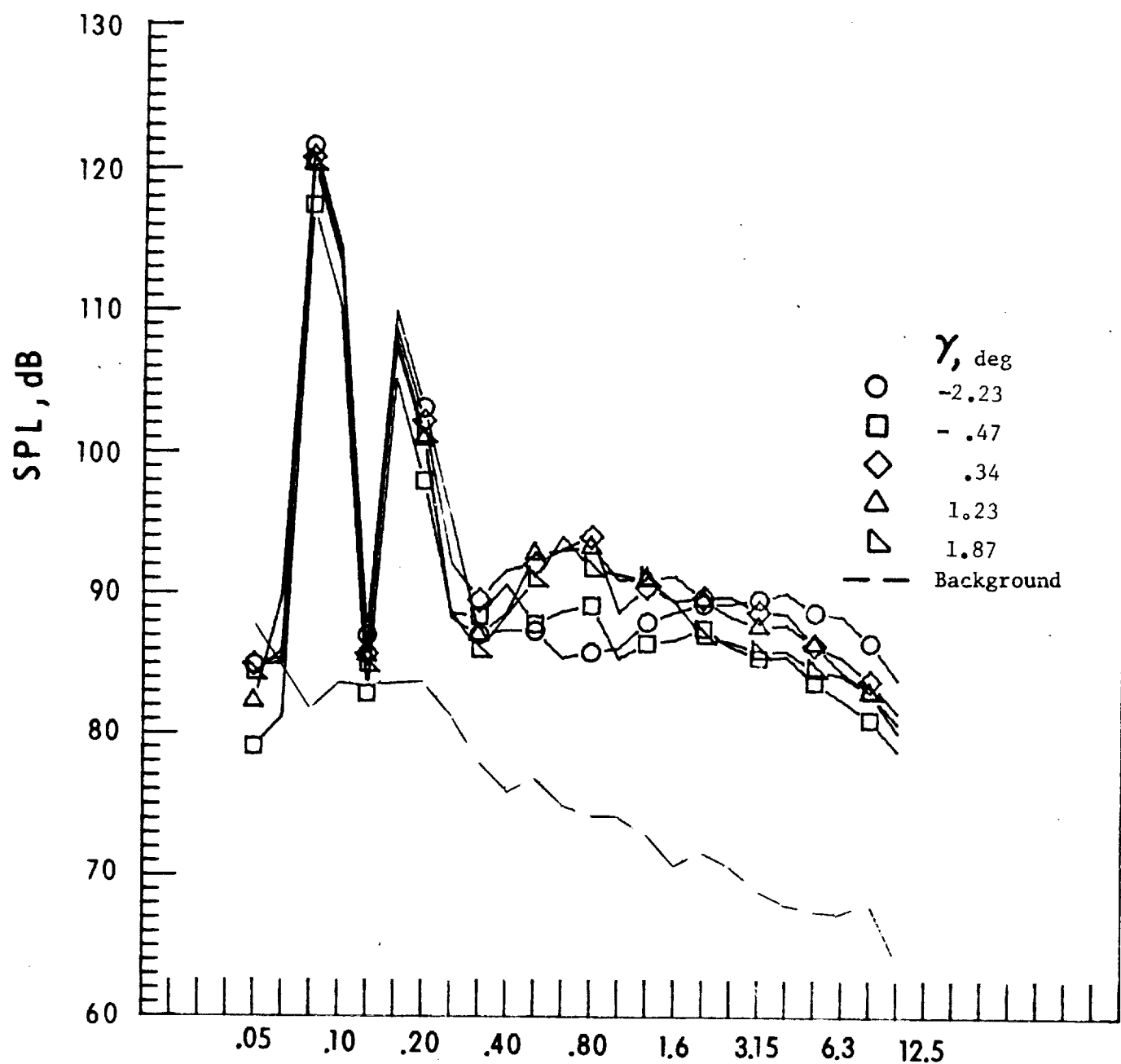
Figure 26. - Concluded.



One-third-octave-band center frequency, kHz

a. Mic. no. 1.

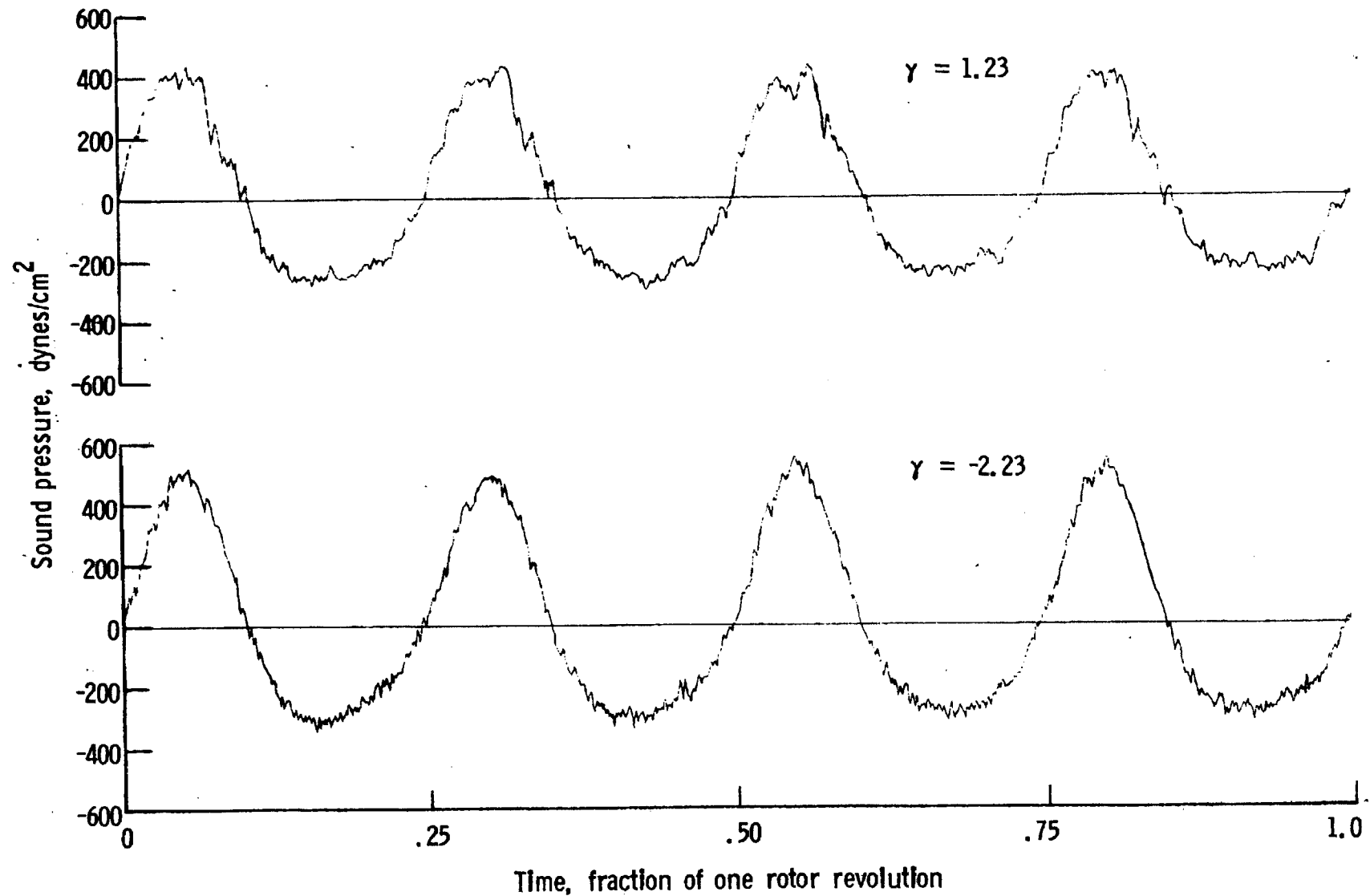
Figure 27. - Effect of descent angle variation on noise generated by helicopter model with sub-wing tips installed. $V_{\infty} = 66.2$ knots.



One-third-octave-band center frequency, kHz

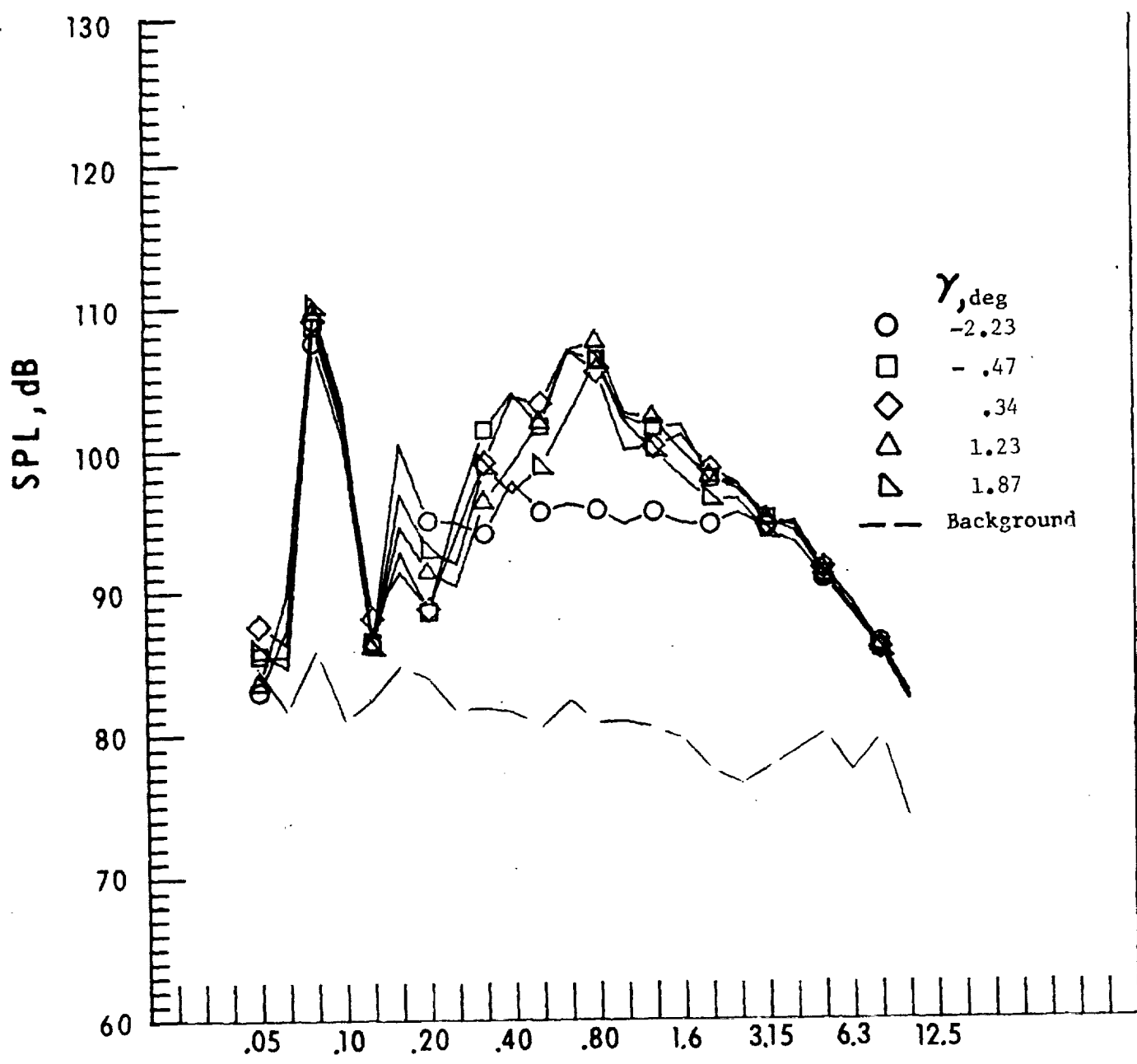
b. Mic. no. 2.

Figure 27. - Continued.



c. Pressure-time histories, Mic. no. 2.

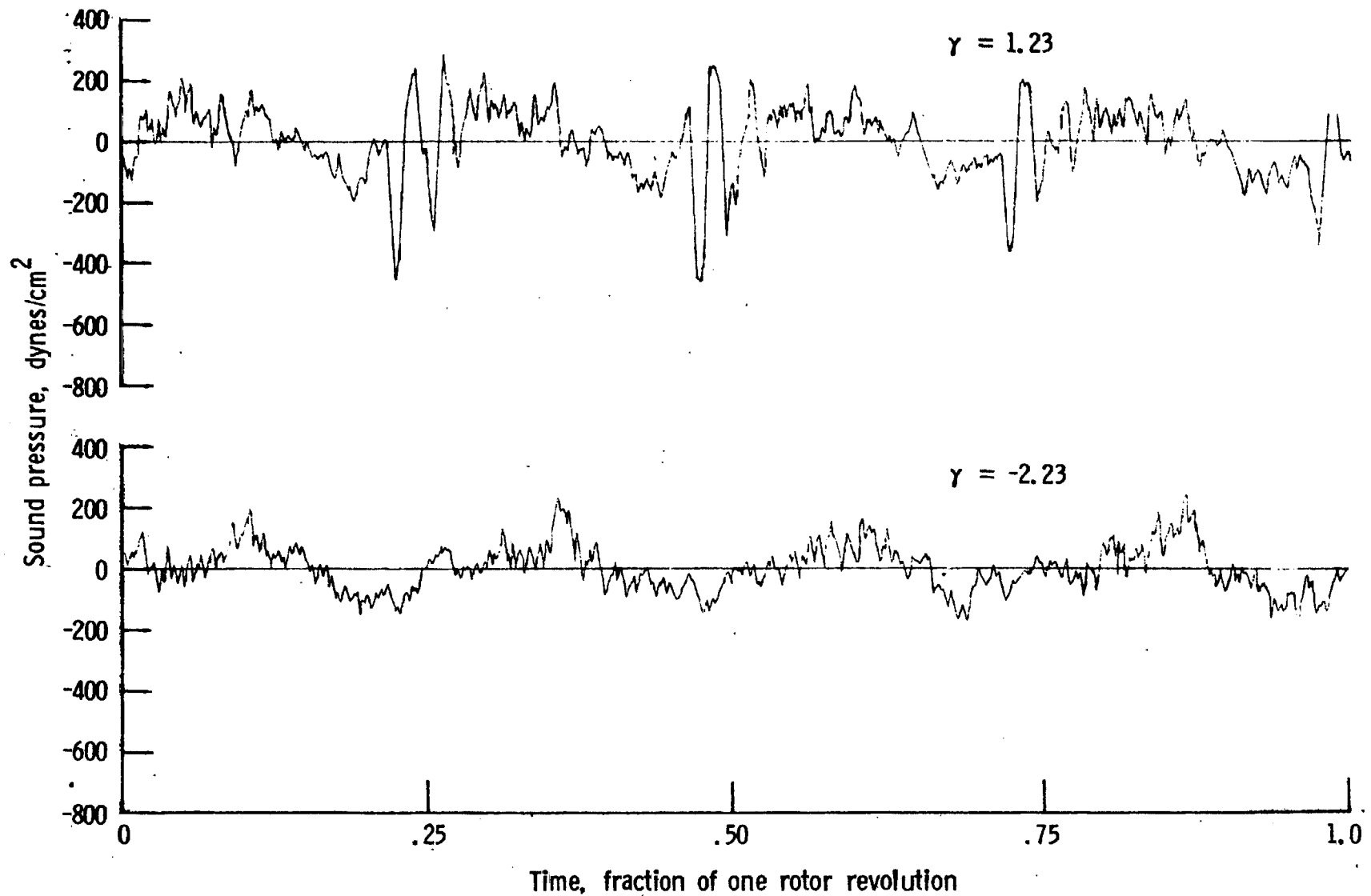
Figure 27. - Continued.



One-third-octave-band center frequency, kHz

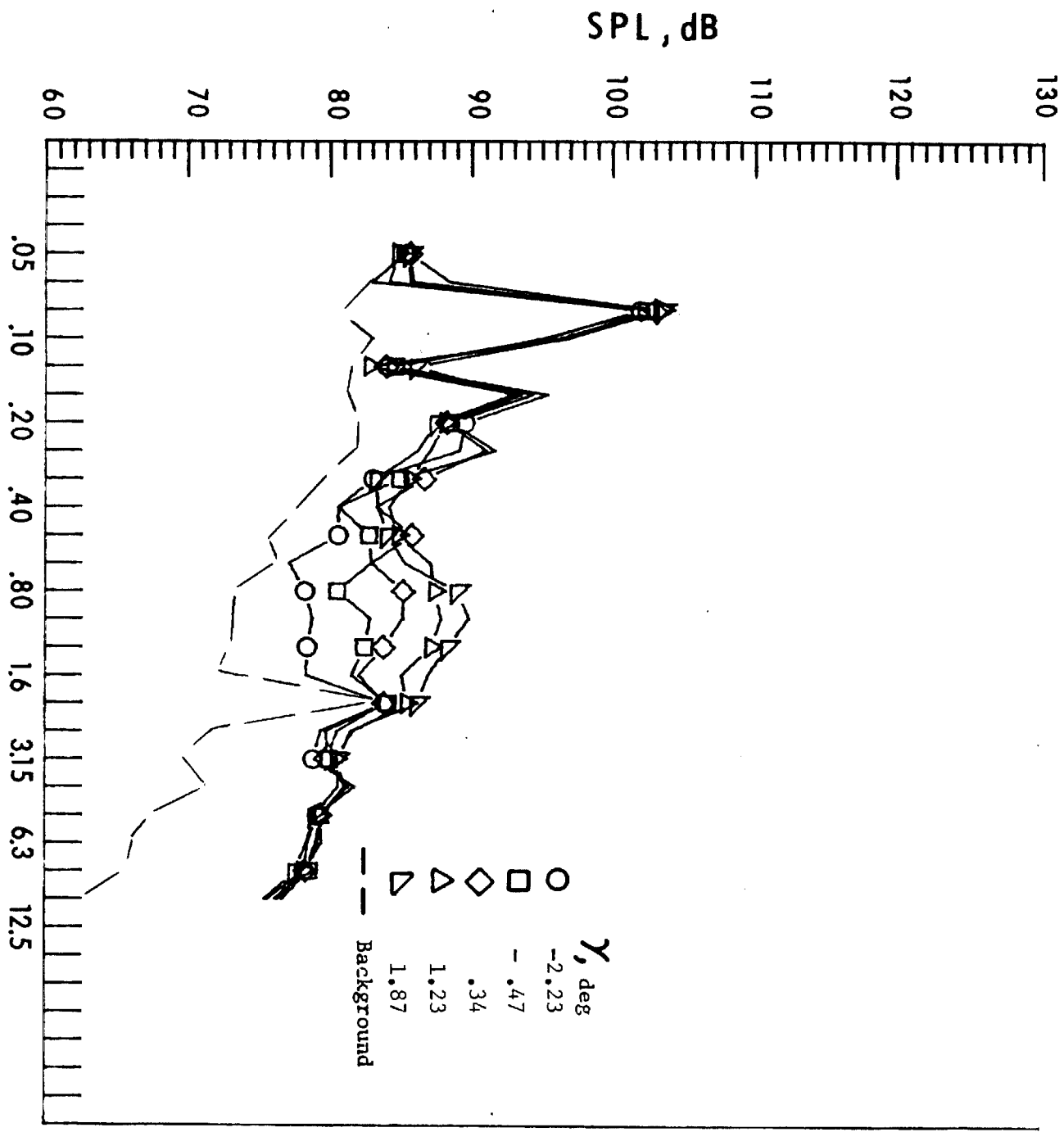
d. Mic. no. 3.

Figure 27. - Continued.



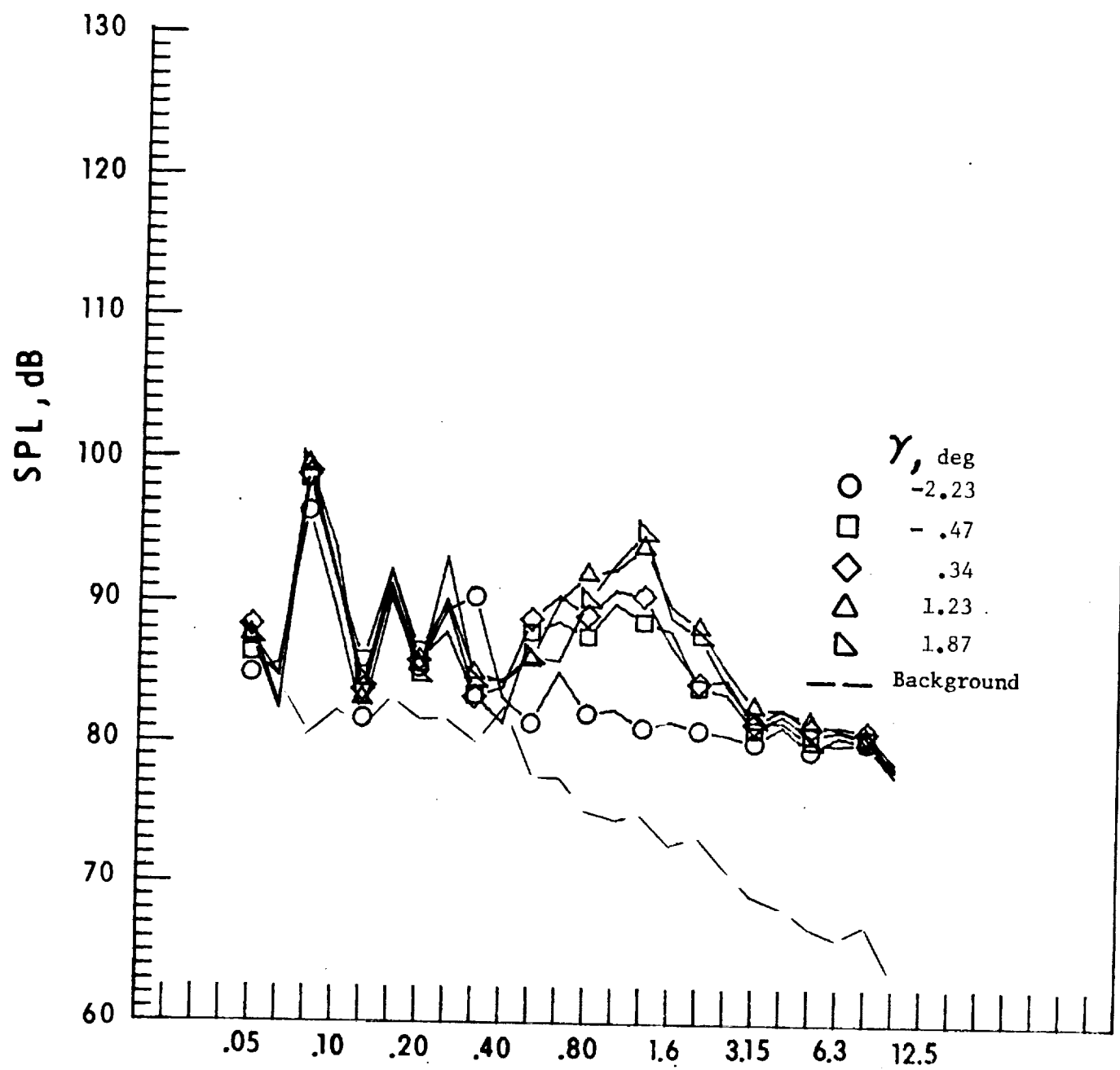
e. Pressure-time histories, Mic. no. 3.

Figure 27. - Continued.



f. Mic. no. 4.

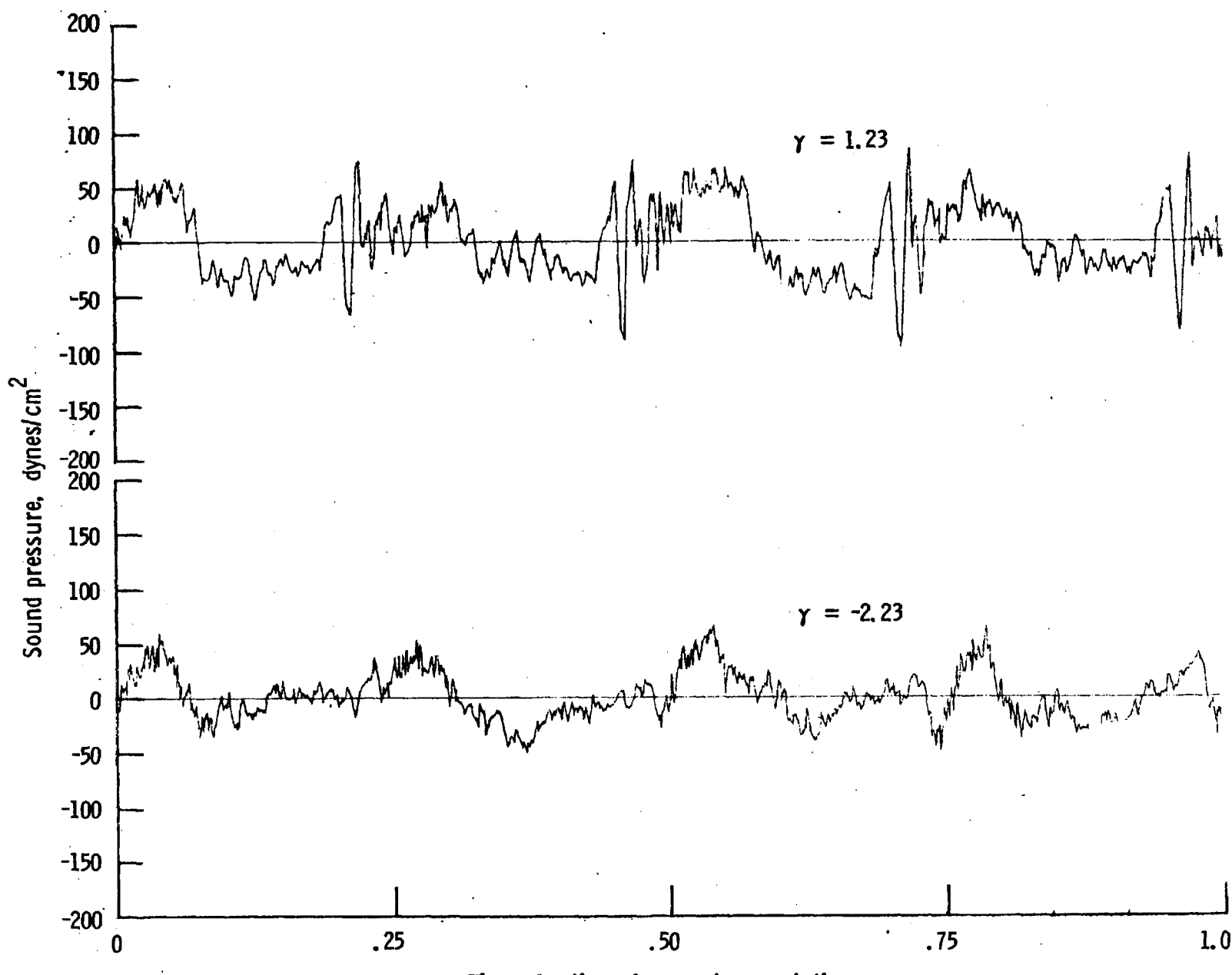
Figure 27. - Continued.



One-third-octave-band center frequency, kHz

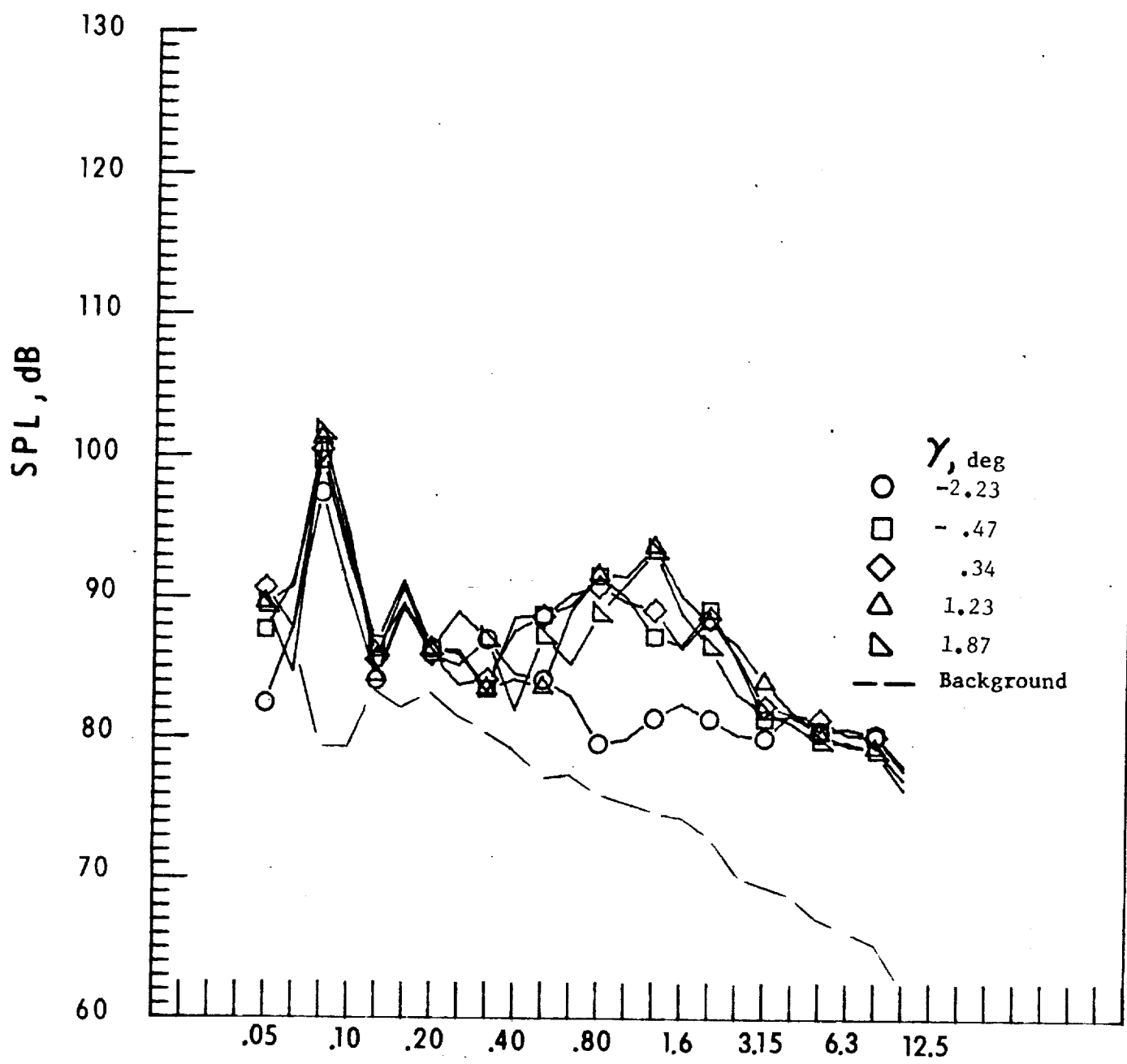
g. Mic. no. 5.

Figure 27. - Continued.



h. Pressure-time histories, Mic. no 5.

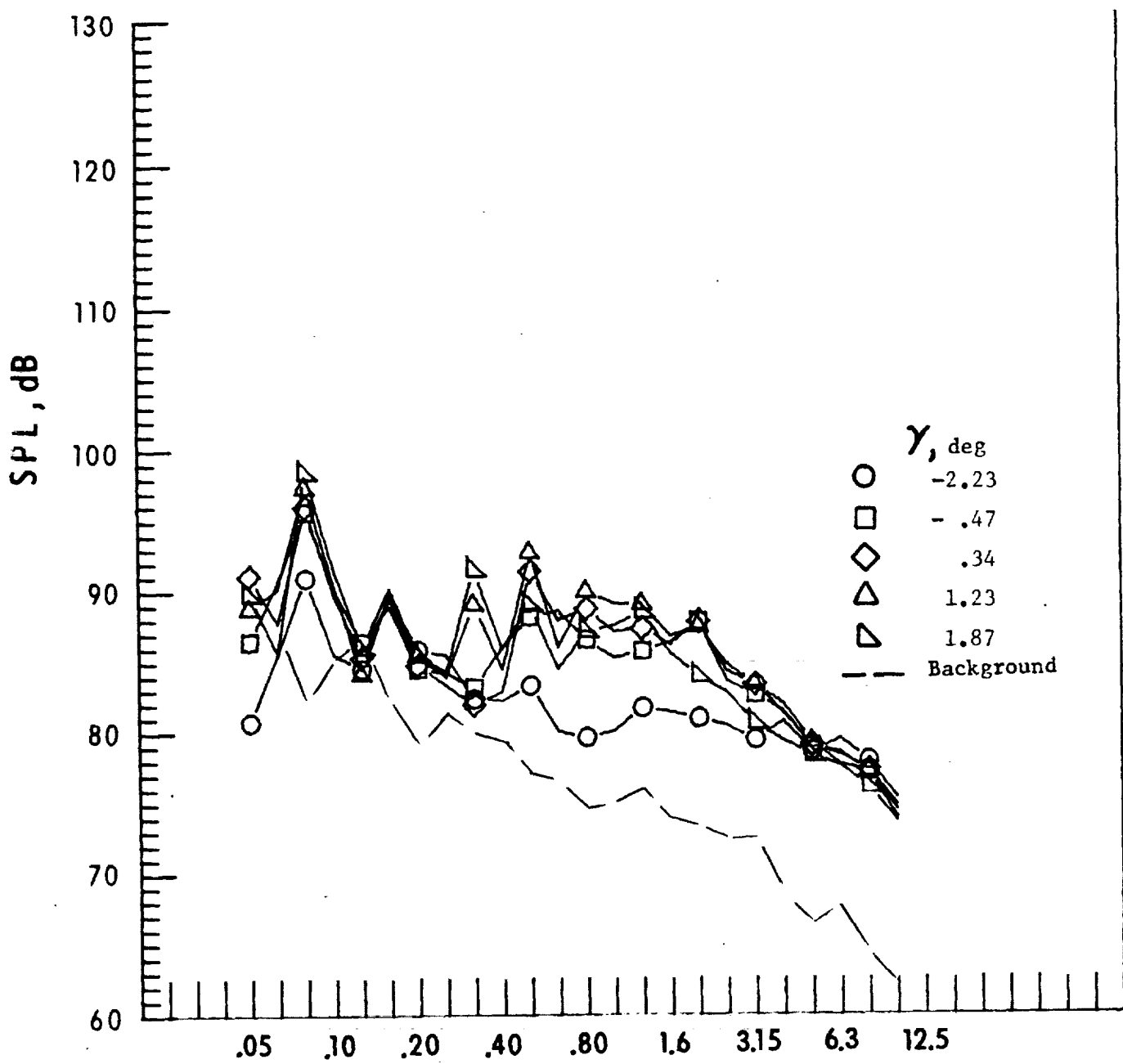
Figure 27. - Continued.



One-third-octave-band center frequency, kHz

i. Mic. no. 6.

Figure 27. - Continued.



One-third-octave-band center frequency, kHz

j. Mic. no. 7.

Figure 27. - Concluded.

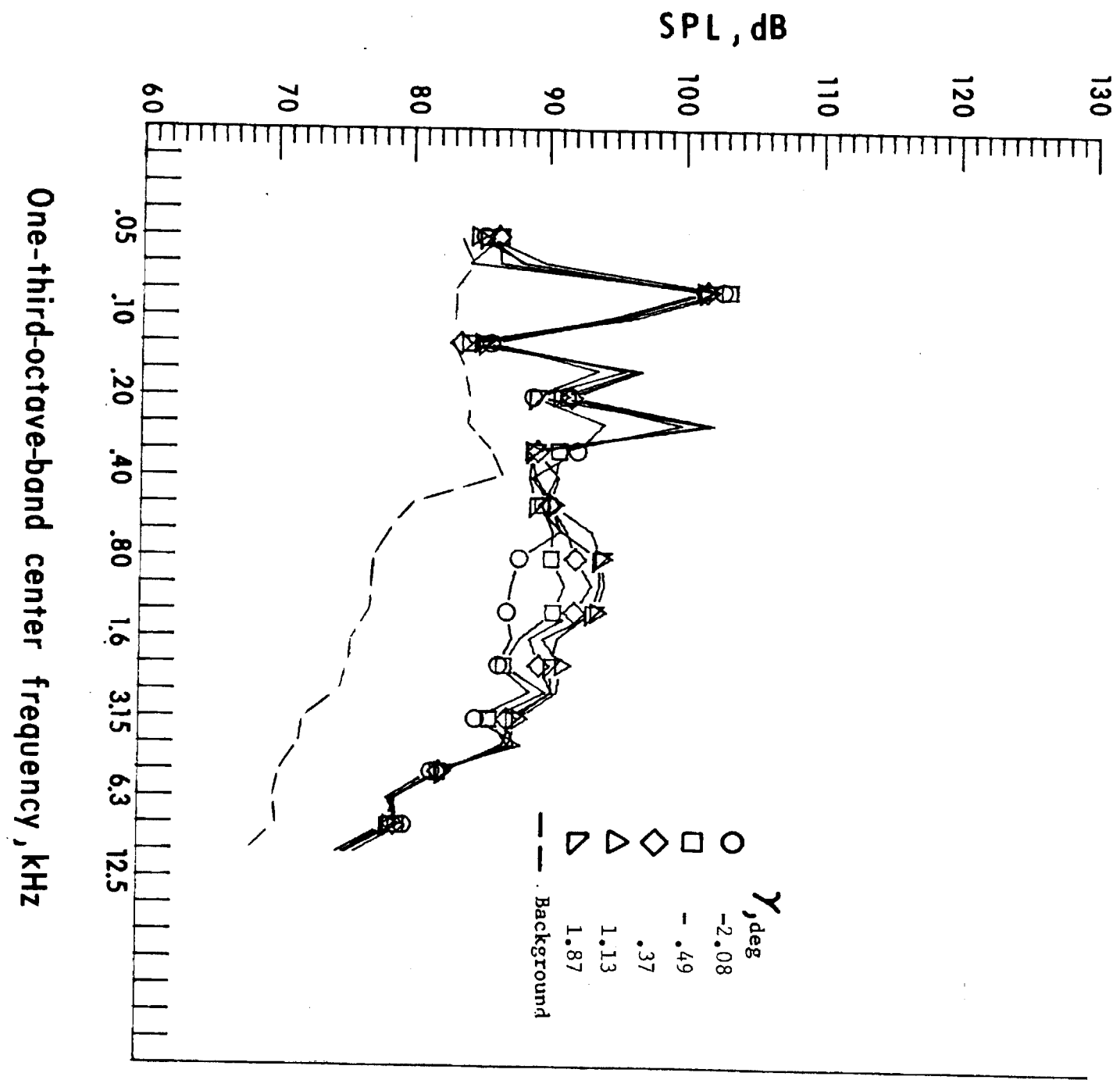
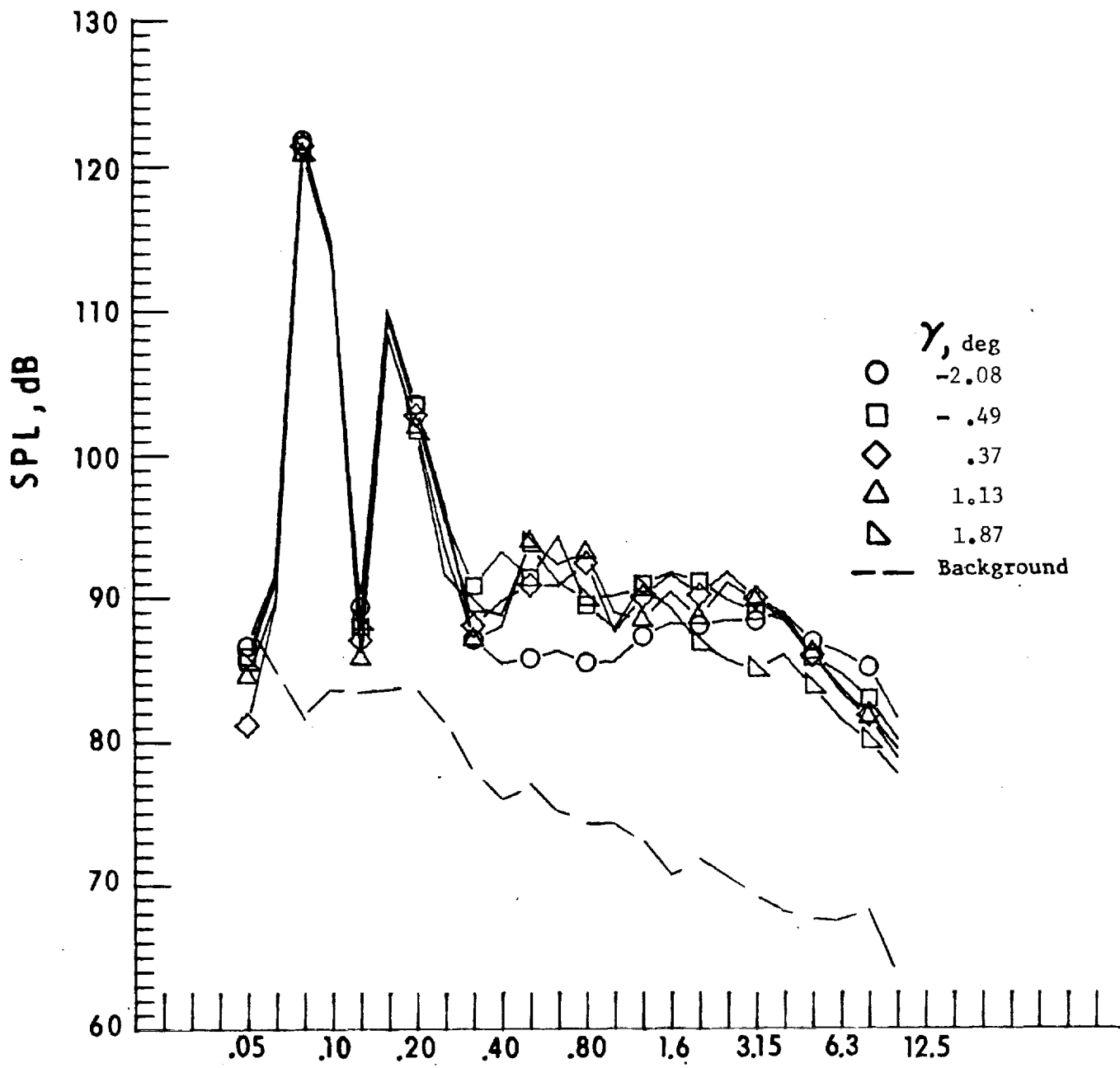


Figure 28. - Effect of descent angle variation on noise generated by helicopter model with swept-tapered tips installed. $V_\infty = 66.2$ knots.

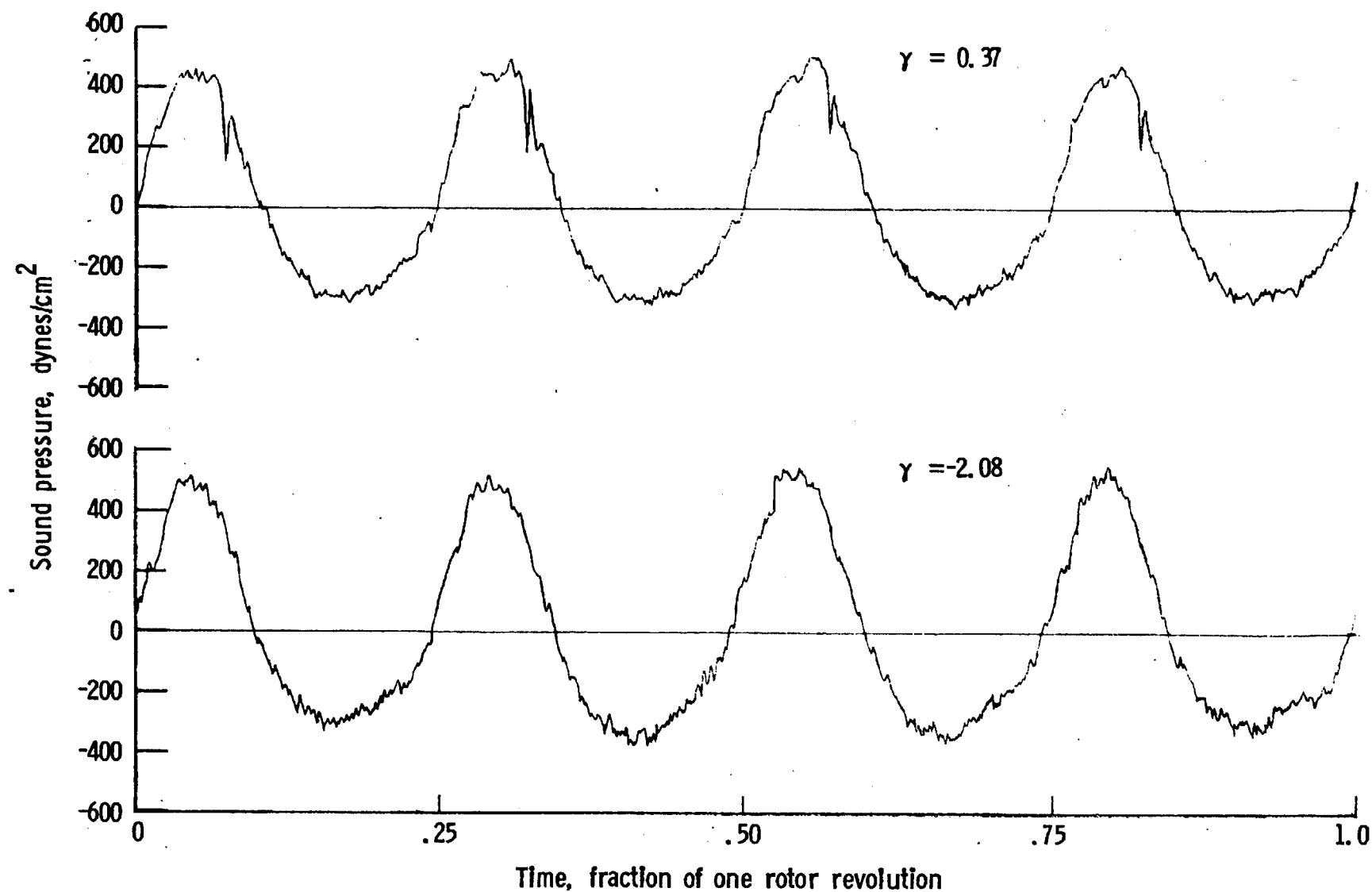
a. Mic. no. 1.



One-third-octave-band center frequency, kHz

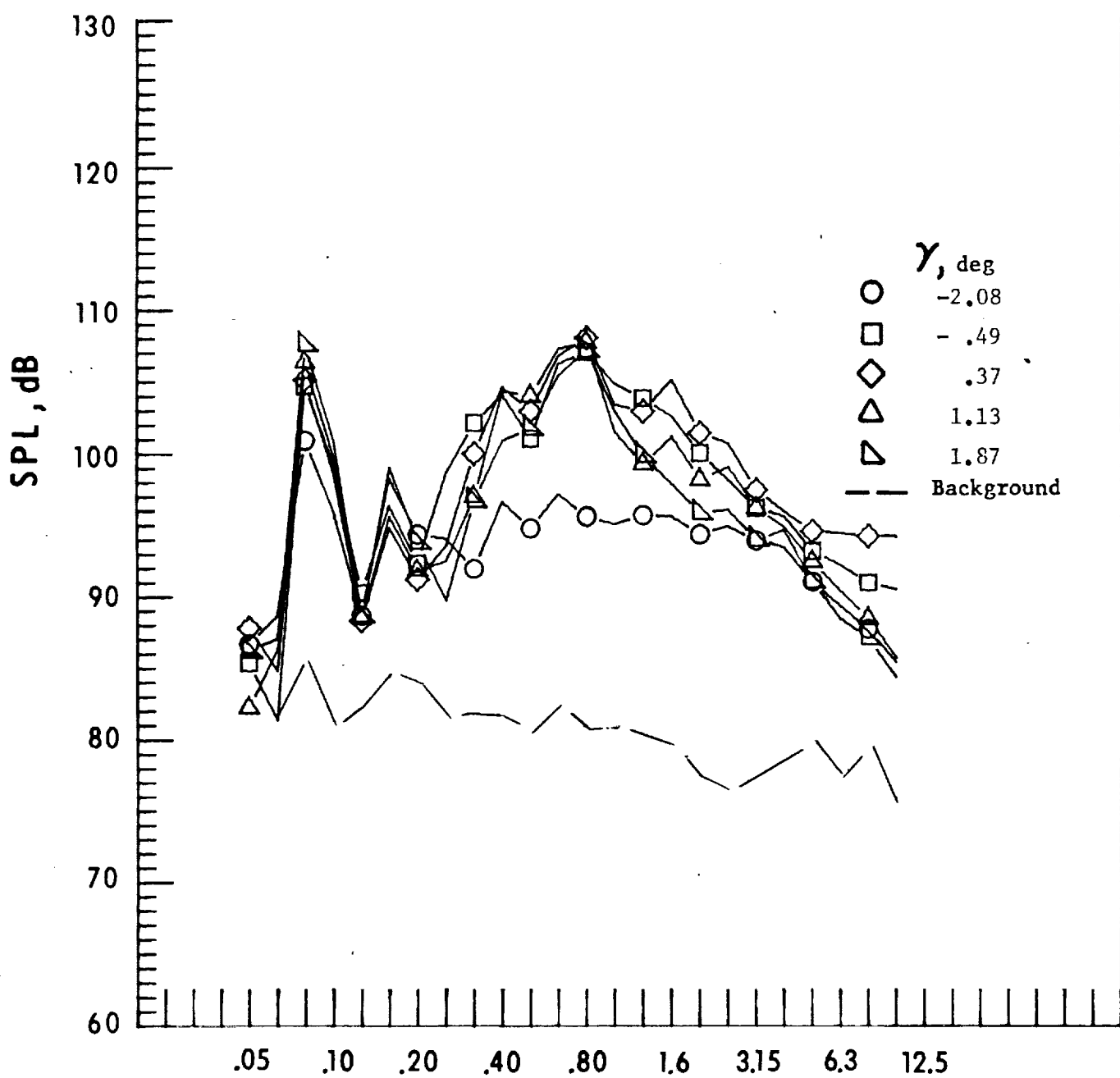
b. Mic. no. 2.

Figure 28. - Continued.



c. Pressure-time histories, Mic. no. 2.

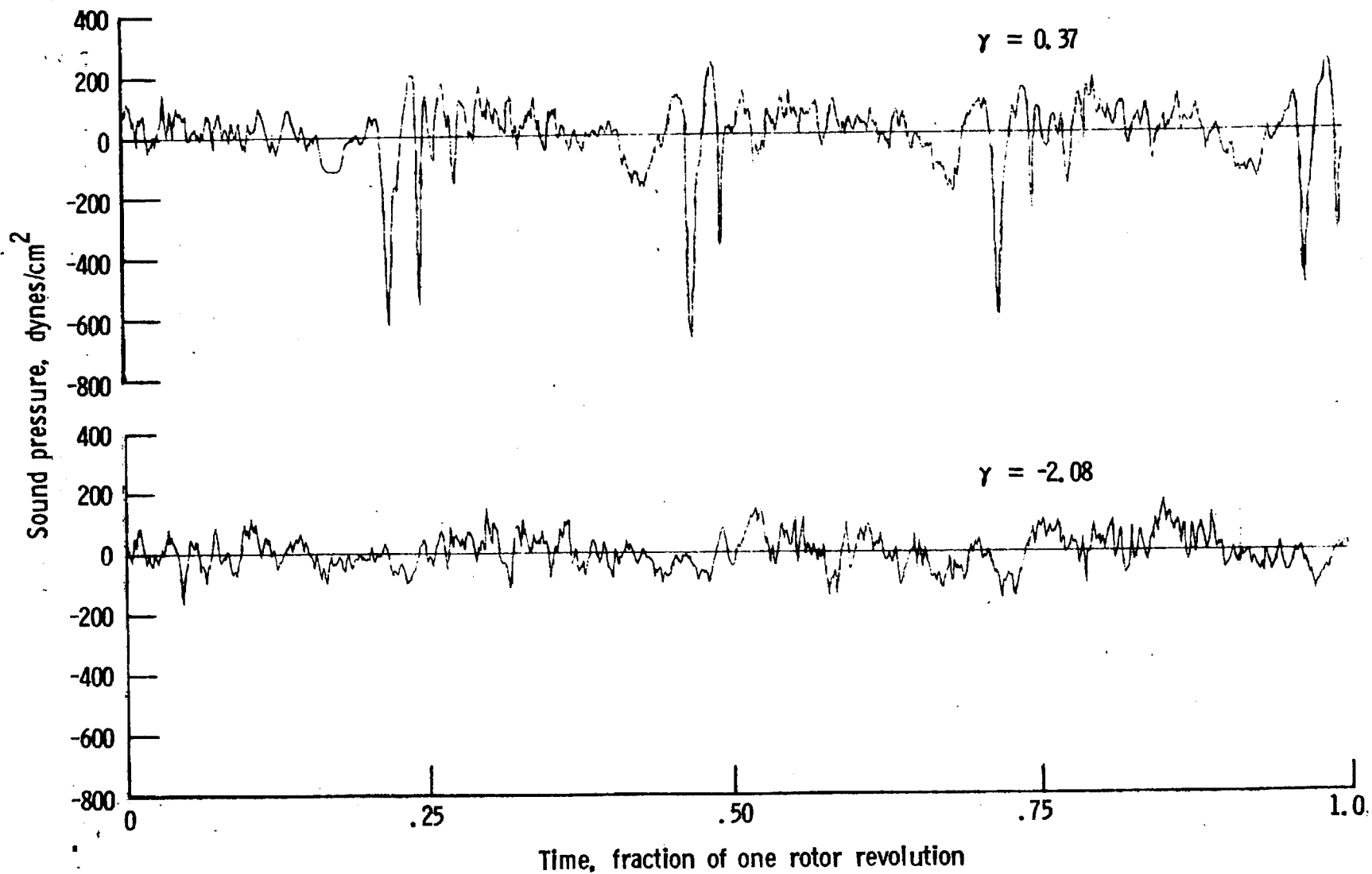
Figure 28. - Continued.



One-third-octave-band center frequency, kHz

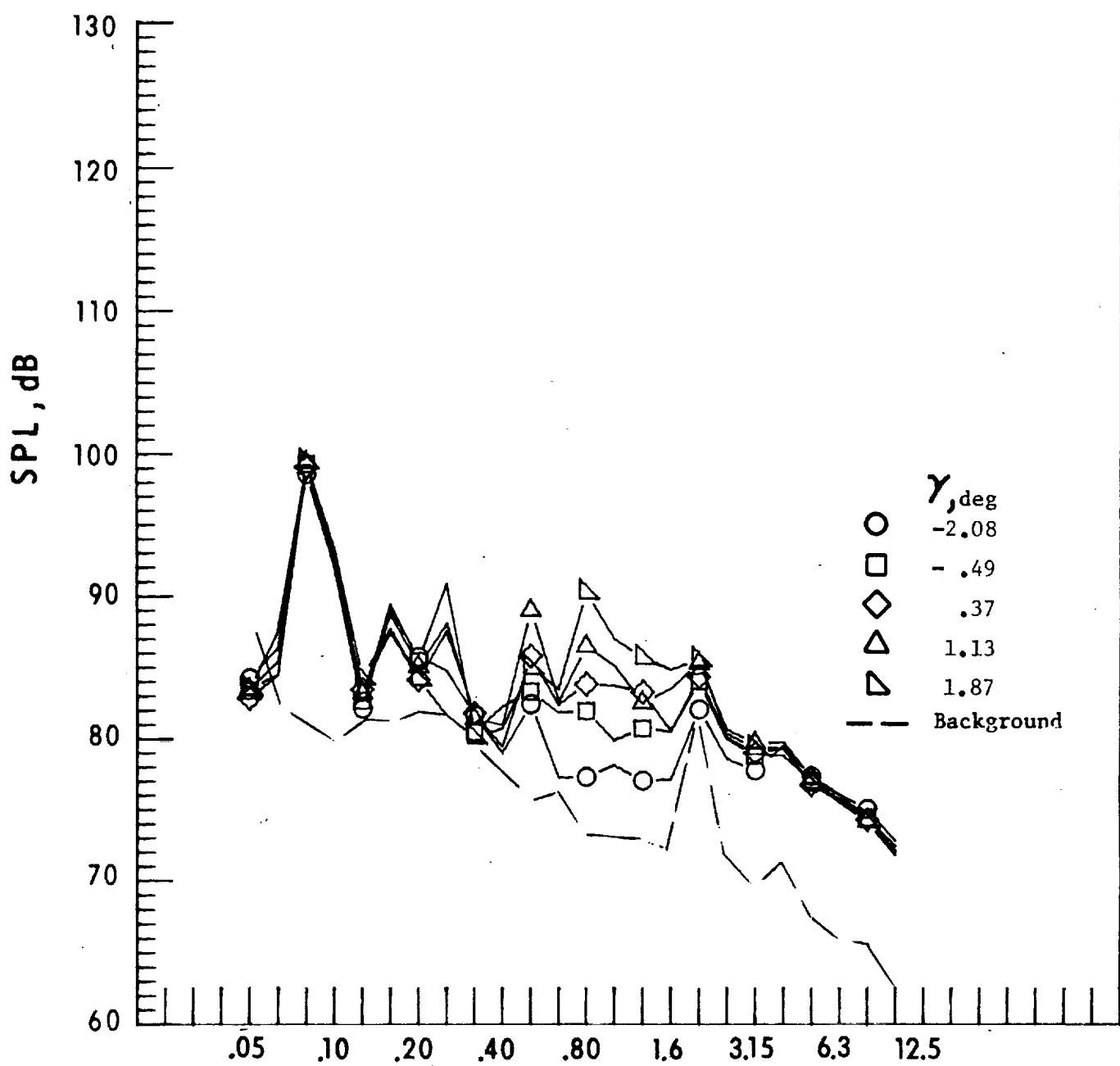
d. Mic. no. 3

Figure 28. - Continued.



e. Pressure-time histories, Mic. no. 3.

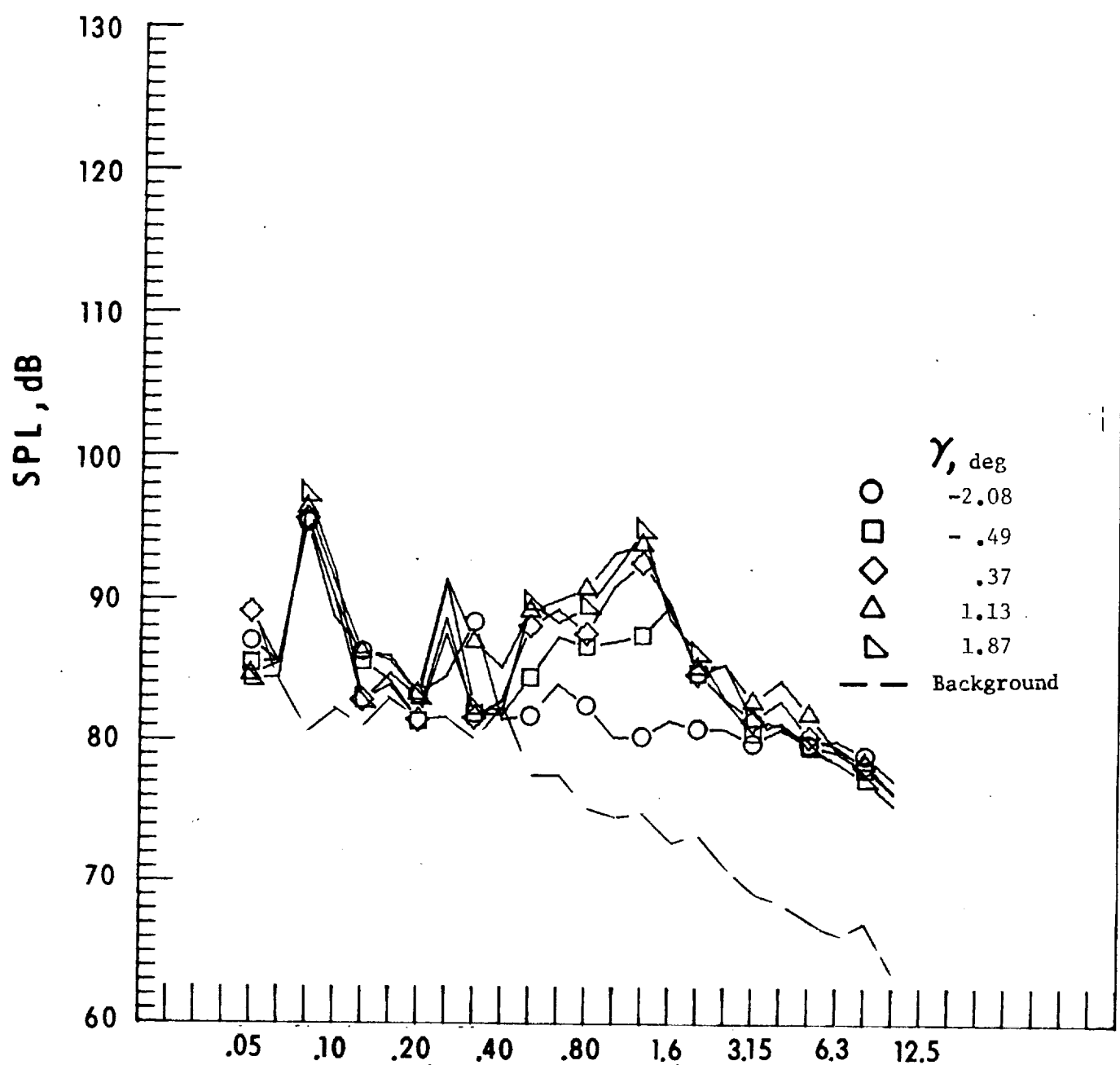
Figure 28. - Continued.



One-third-octave-band center frequency, kHz

f. Mic. no. 4.

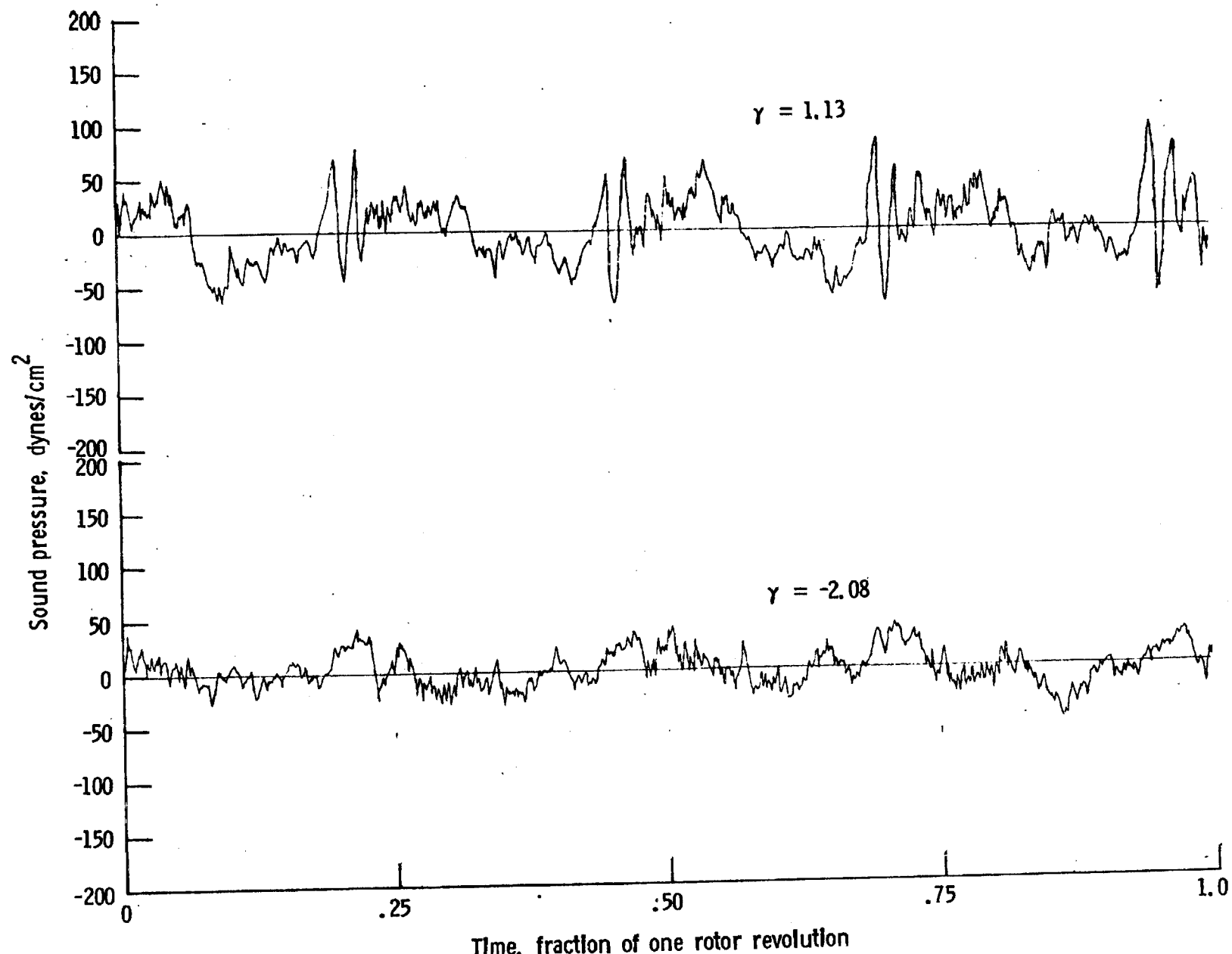
Figure 28. - Continued.



One-third-octave-band center frequency, kHz

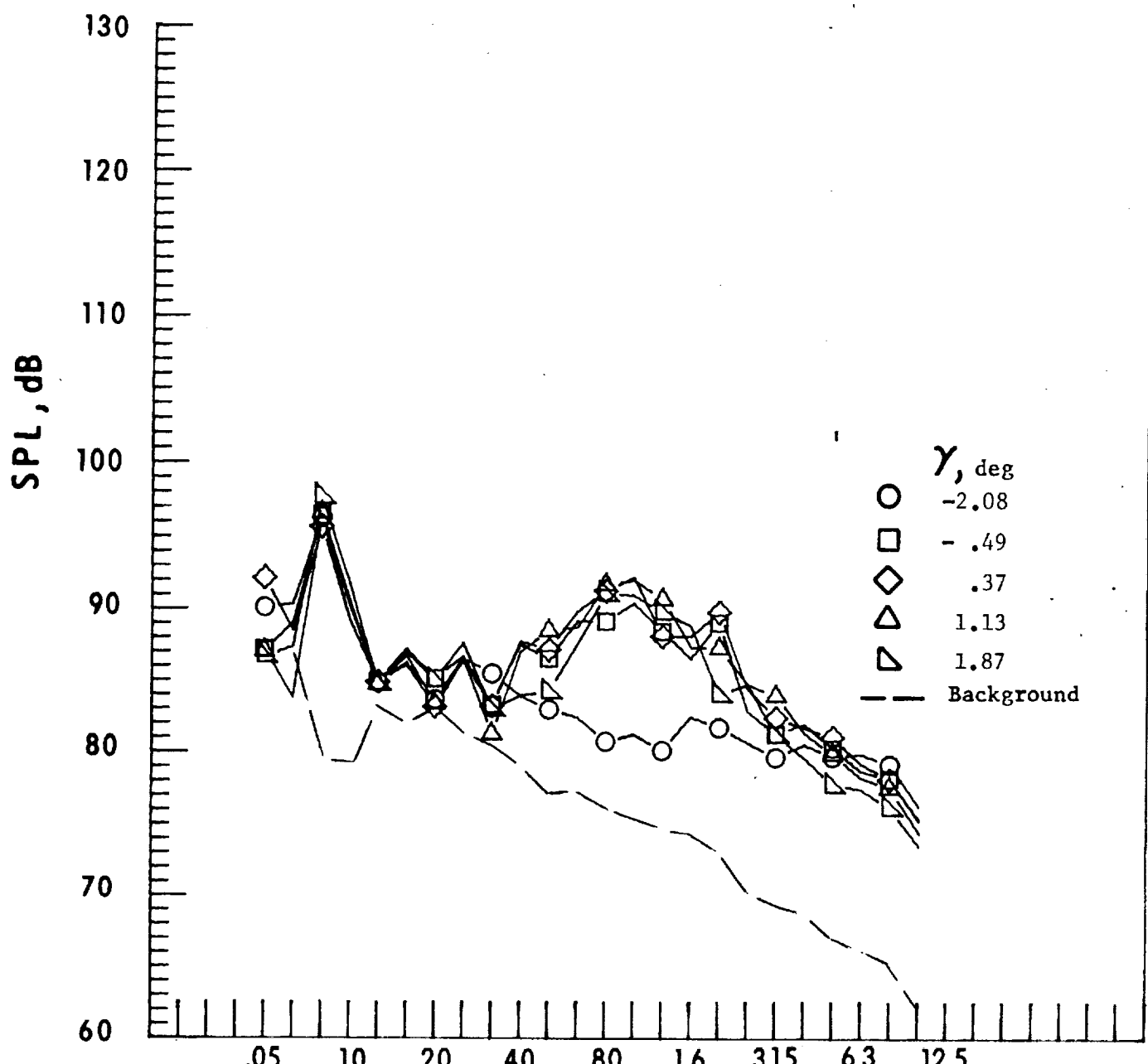
g. Mic. no. 5.

Figure 28. - Continued.



h. Pressure-time histories, Mic. no. 5.

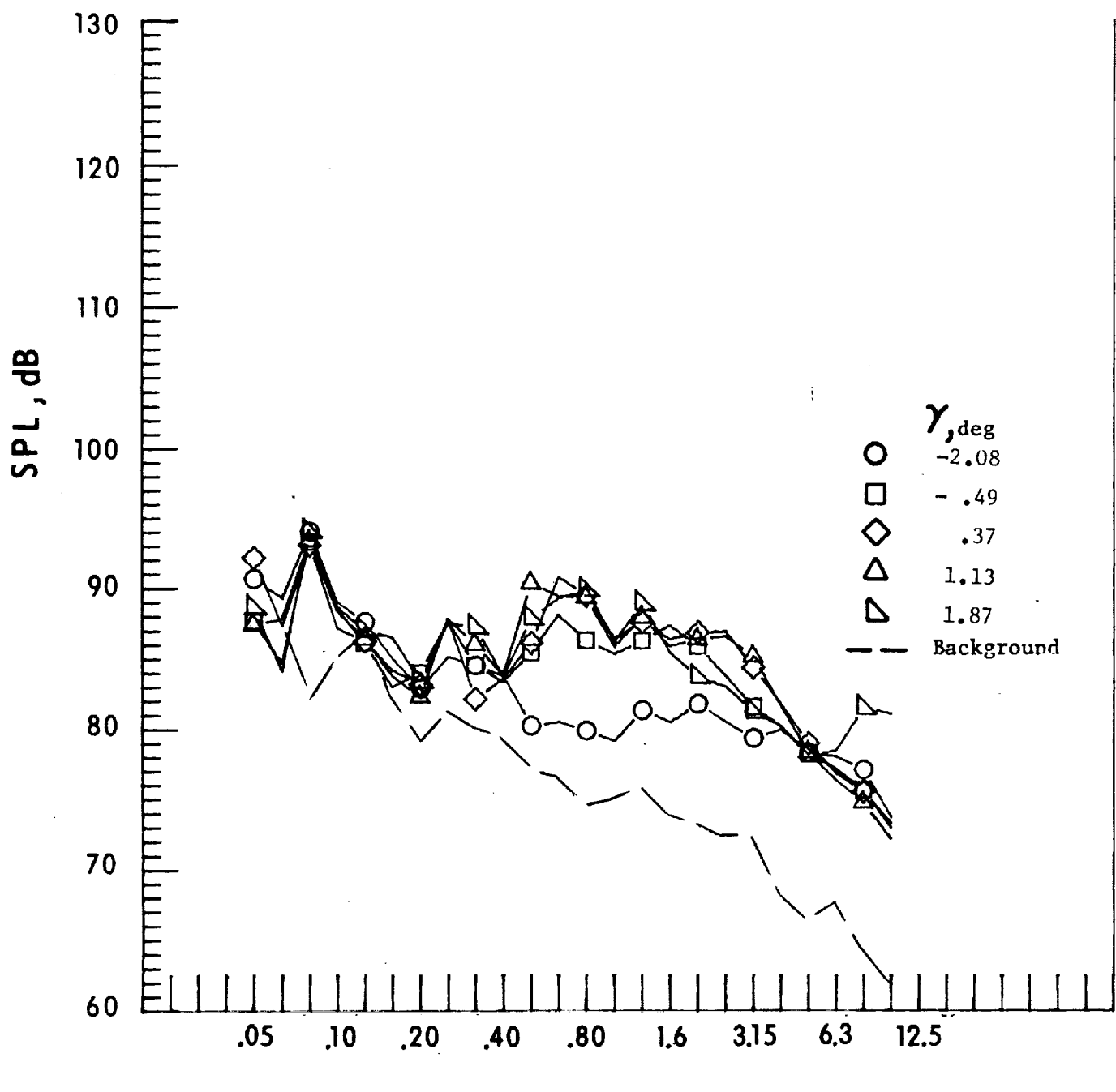
Figure 28.- Continued.



One-third-octave-band center frequency, kHz

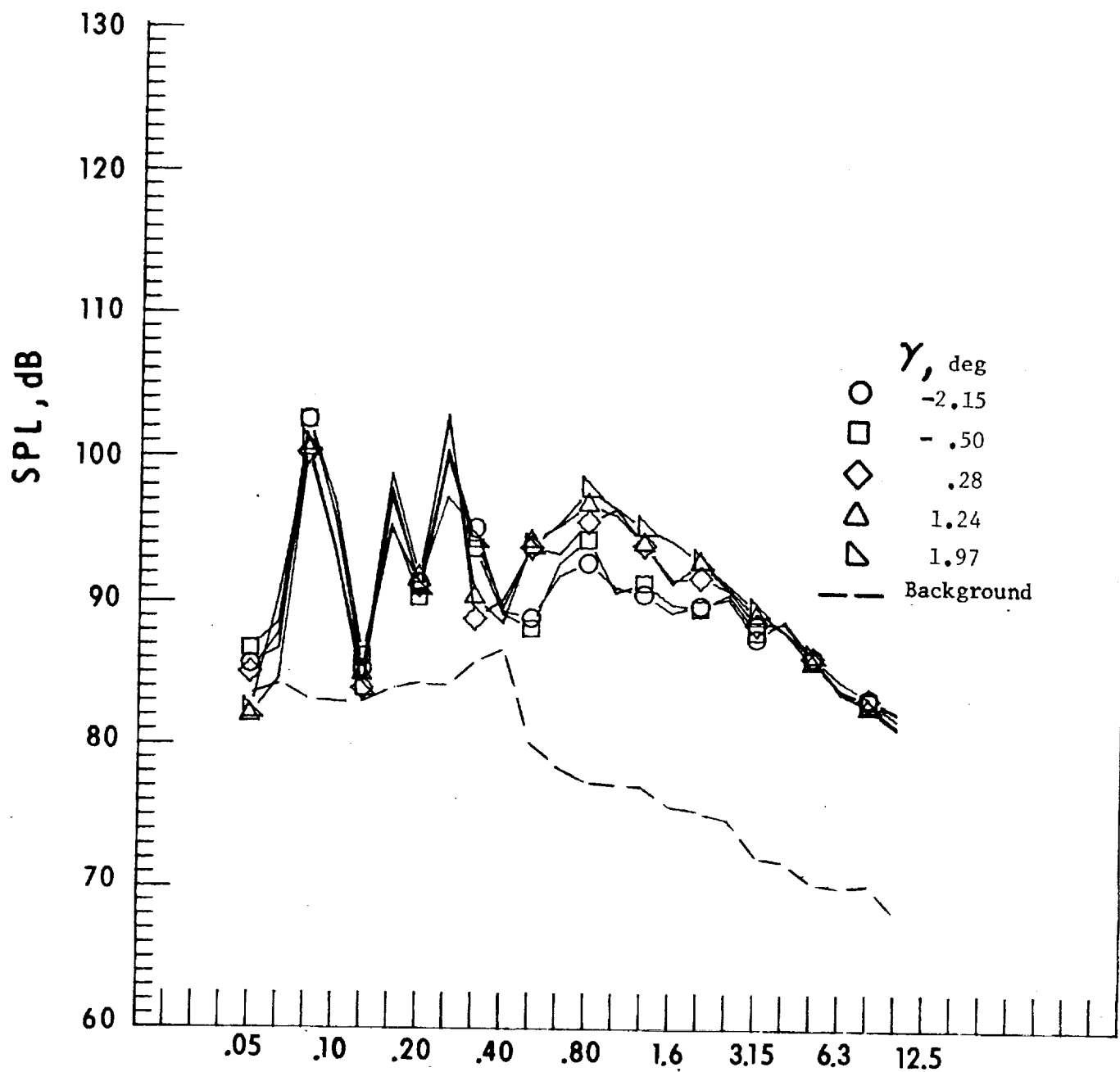
i. Mic. no. 6.

Figure 28. - Continued.



j. Mic. no. 7.

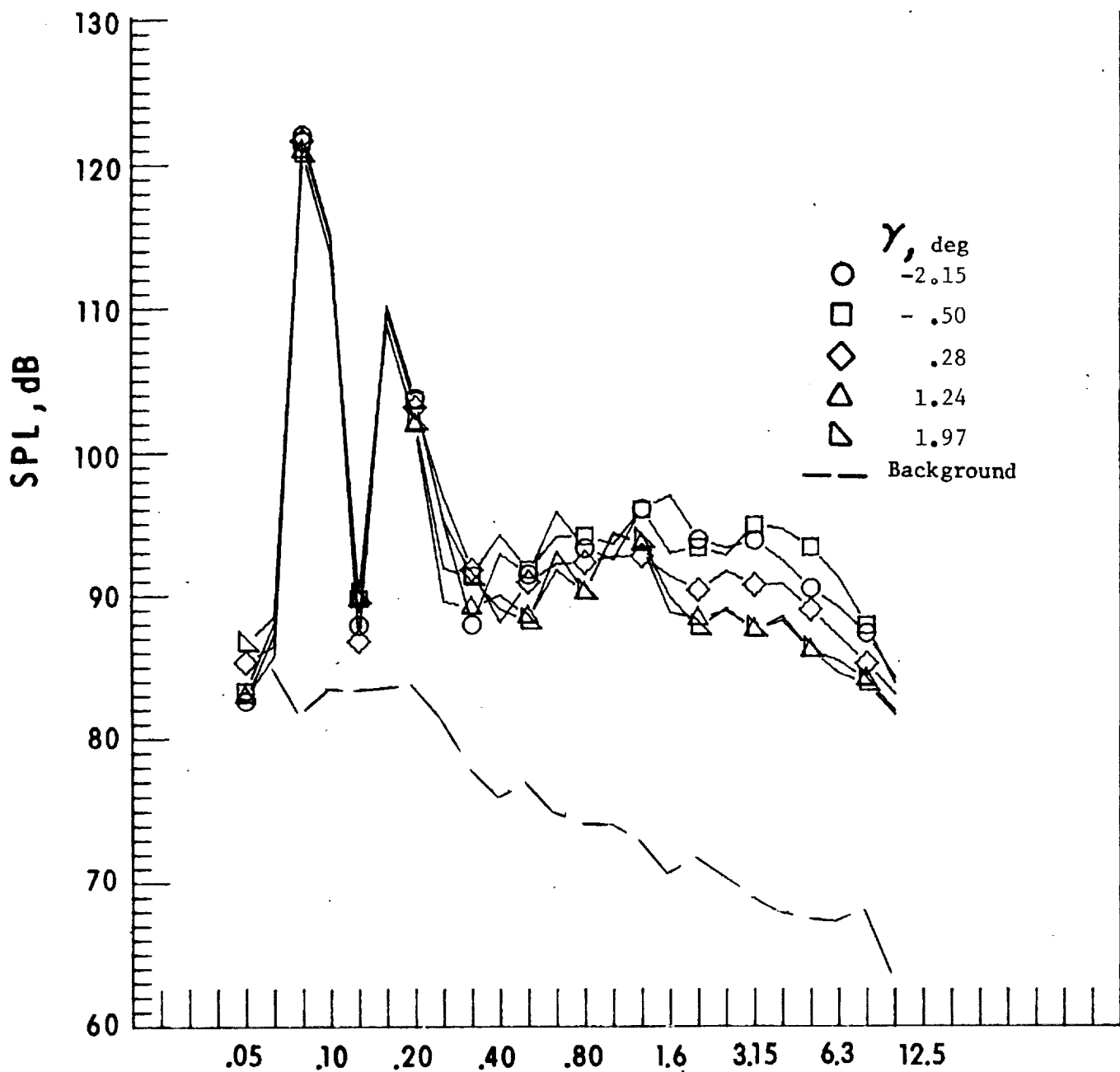
Figure 28. - Concluded.



One-third-octave-band center frequency, kHz

a. Mic. no. 1.

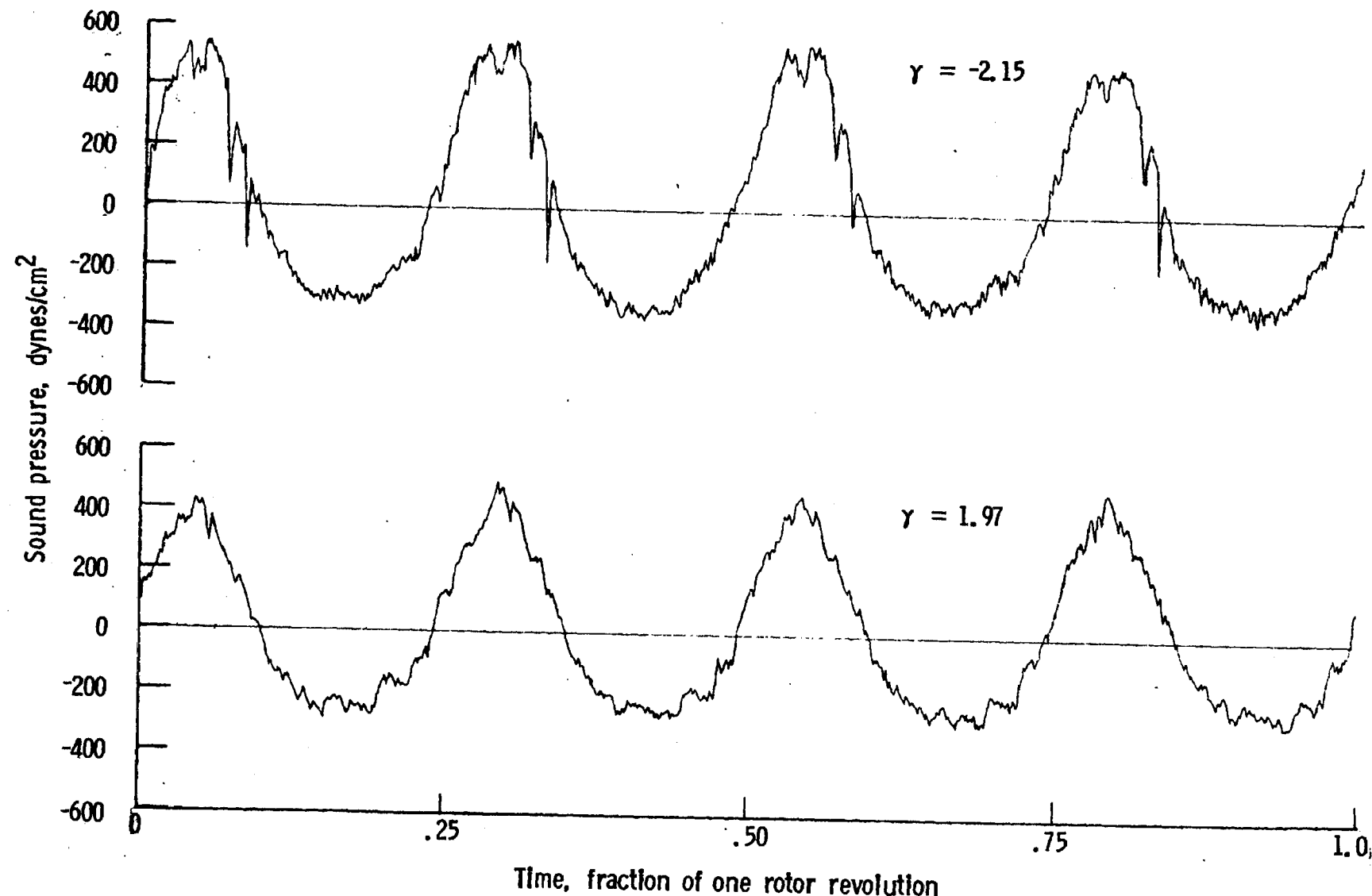
Figure 29. - Effect of descent angle variation on noise generated by helicopter model with end-plate tips installed. $V_{\infty} = 66.7$ knots.



One-third-octave-band center frequency, kHz

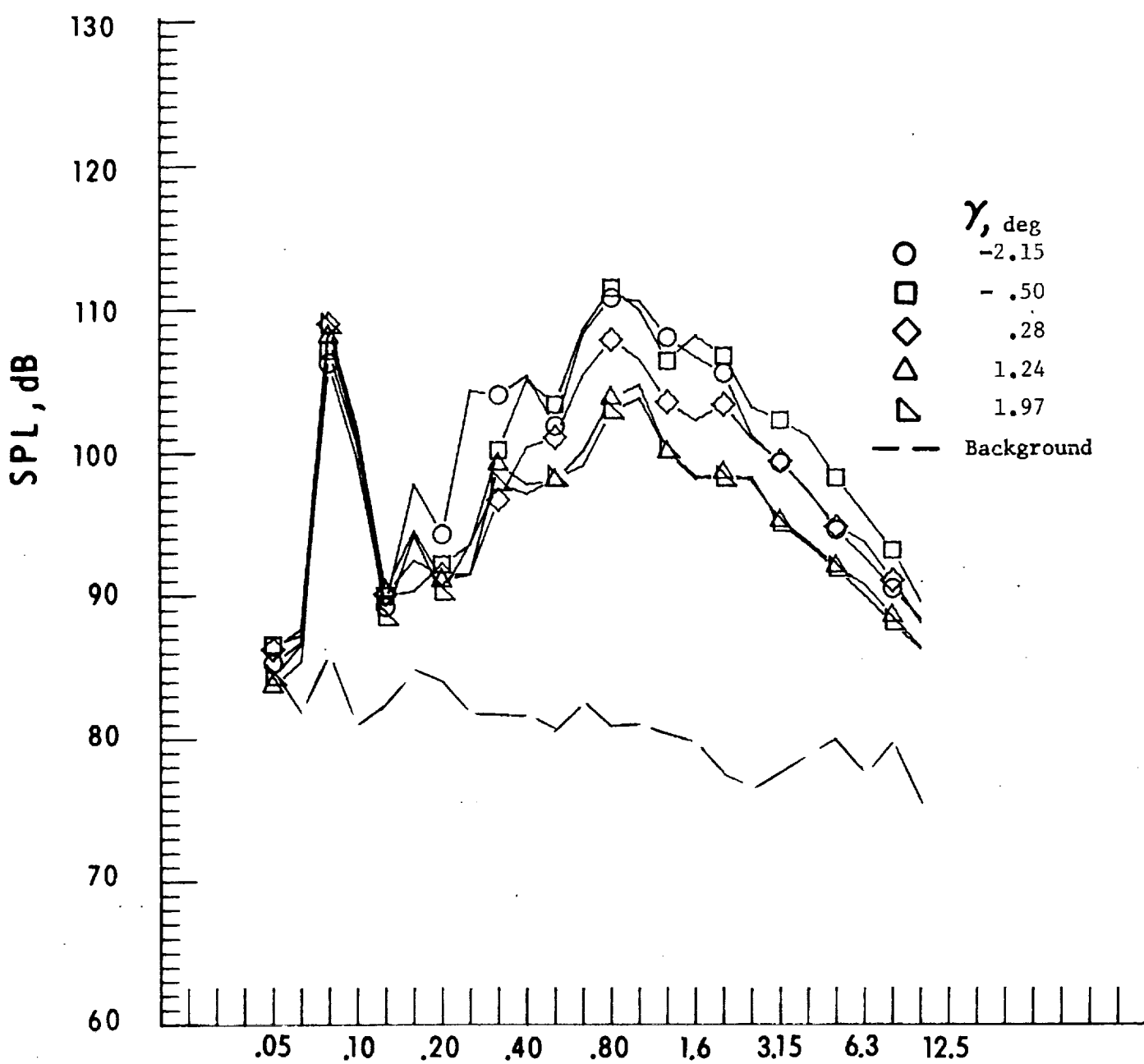
b. Mic. no. 2.

Figure 29. - Continued.



c. Pressure-time histories, Mic. no. 2.

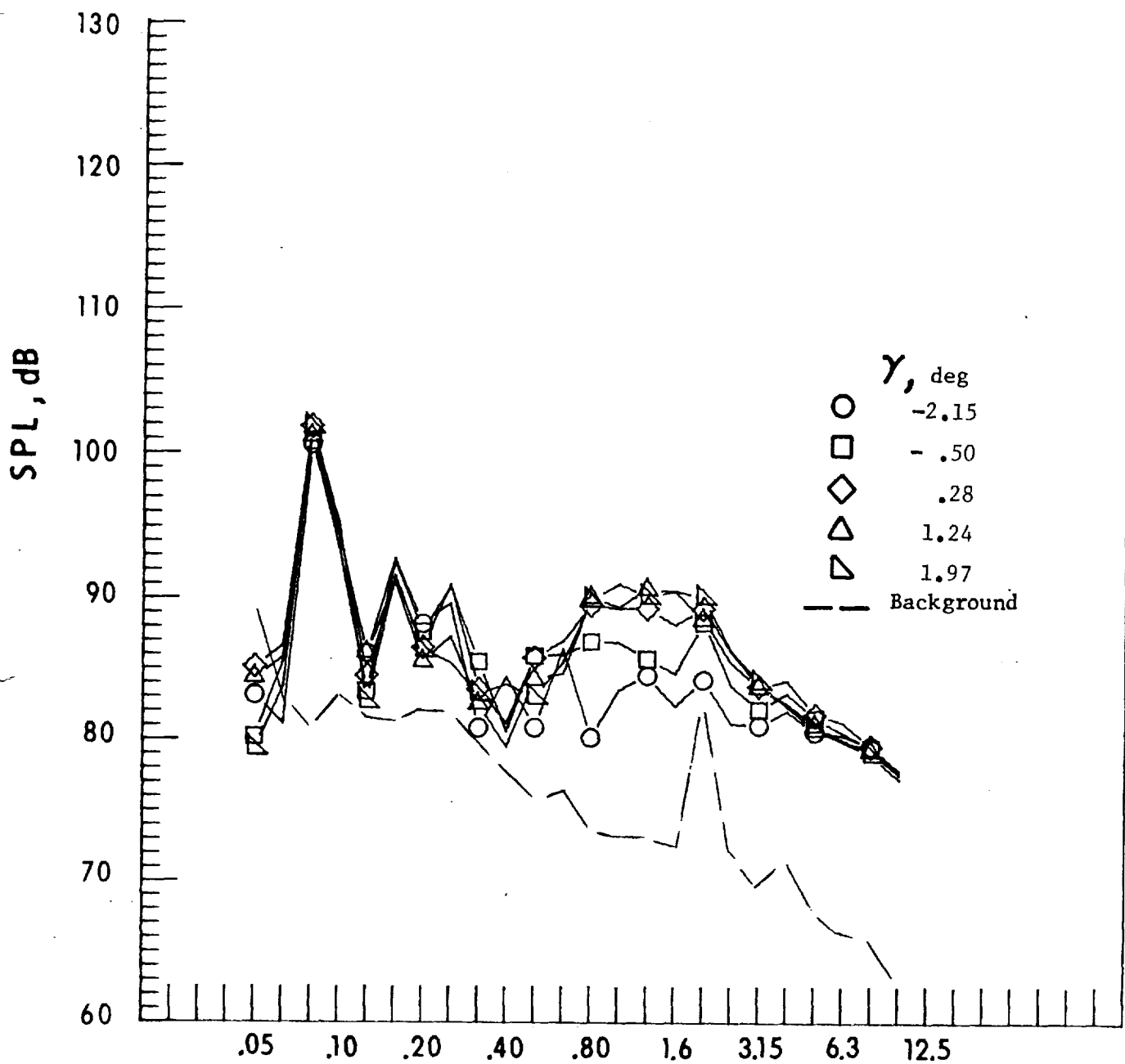
Figure 29. - Continued.



One-third-octave-band center frequency, kHz

d. Mic. no. 3.

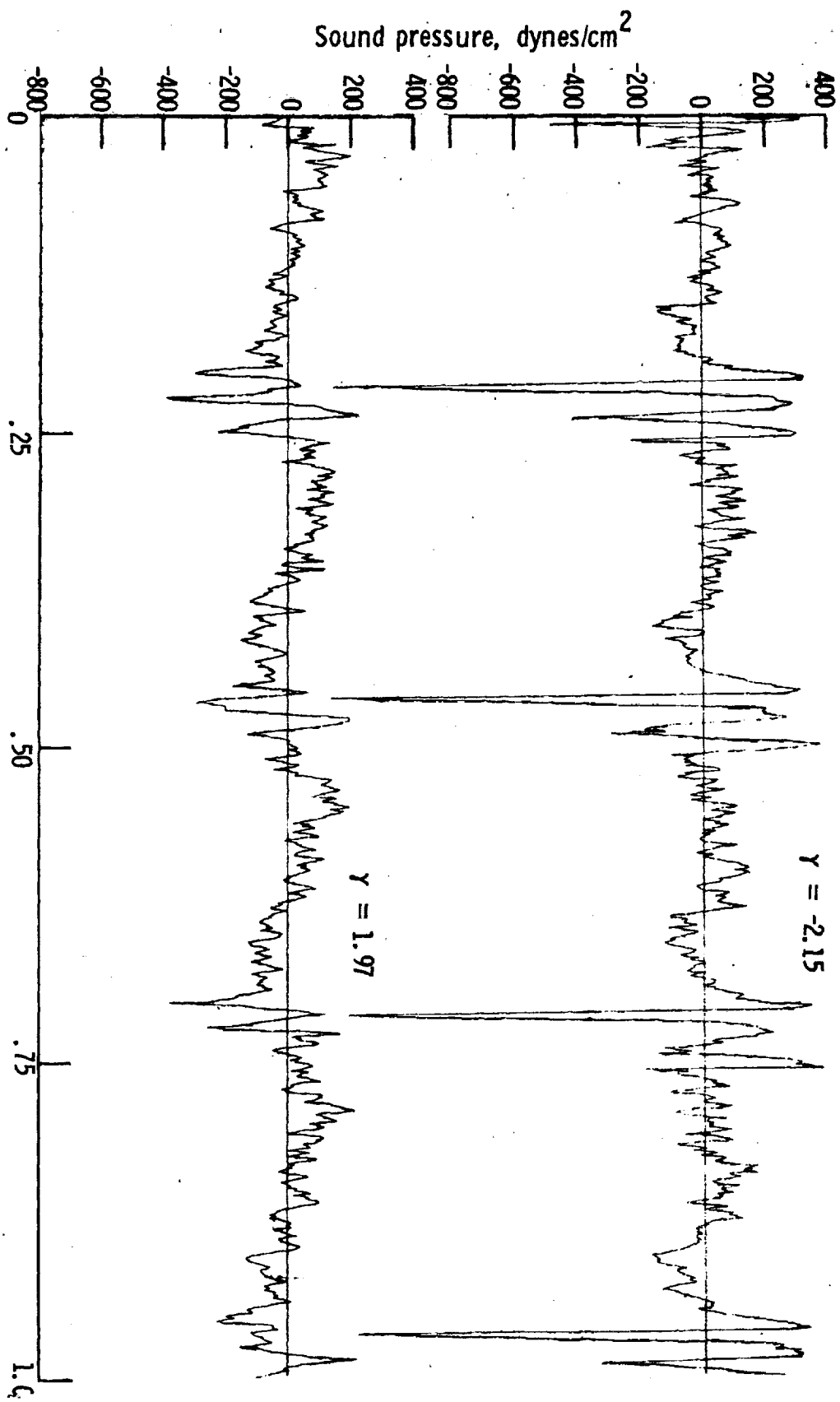
Figure 29. - Continued.



One-third-octave-band center frequency, kHz

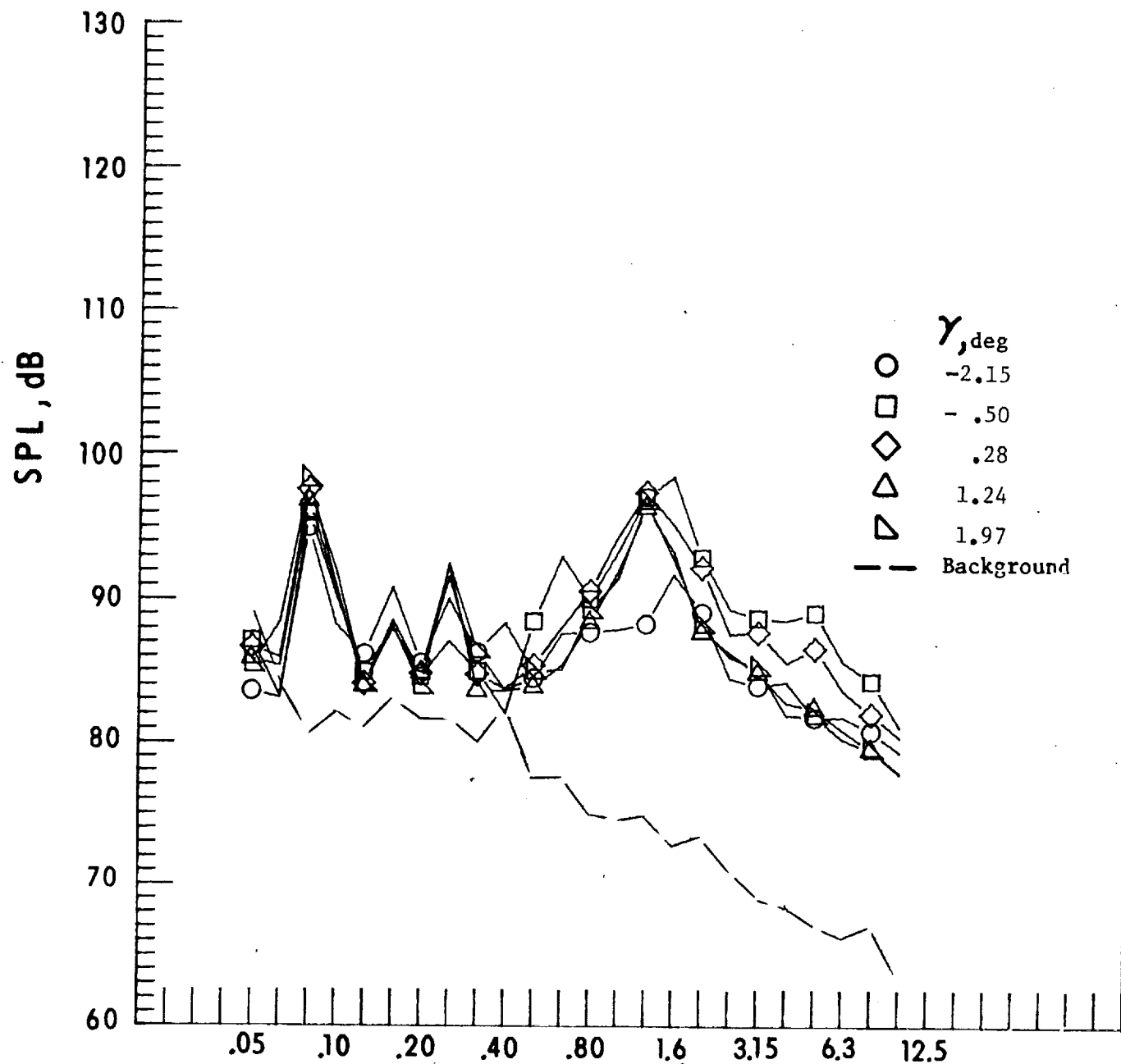
f. Mic. no. 4.

Figure 29. - Continued.



e. Pressure-time histories, Mc. no. 3.

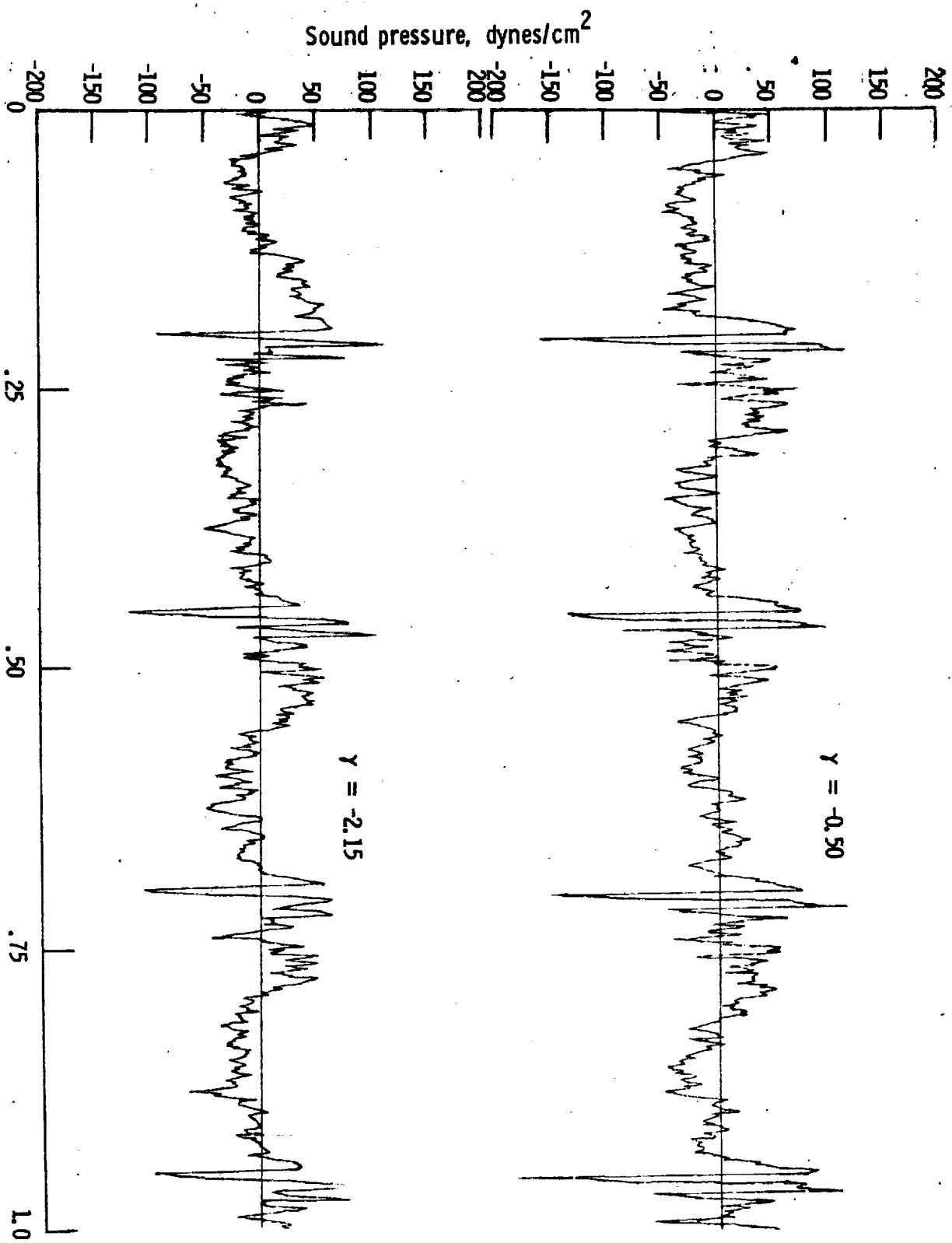
Figure 29. - Continued.



One-third-octave-band center frequency, kHz

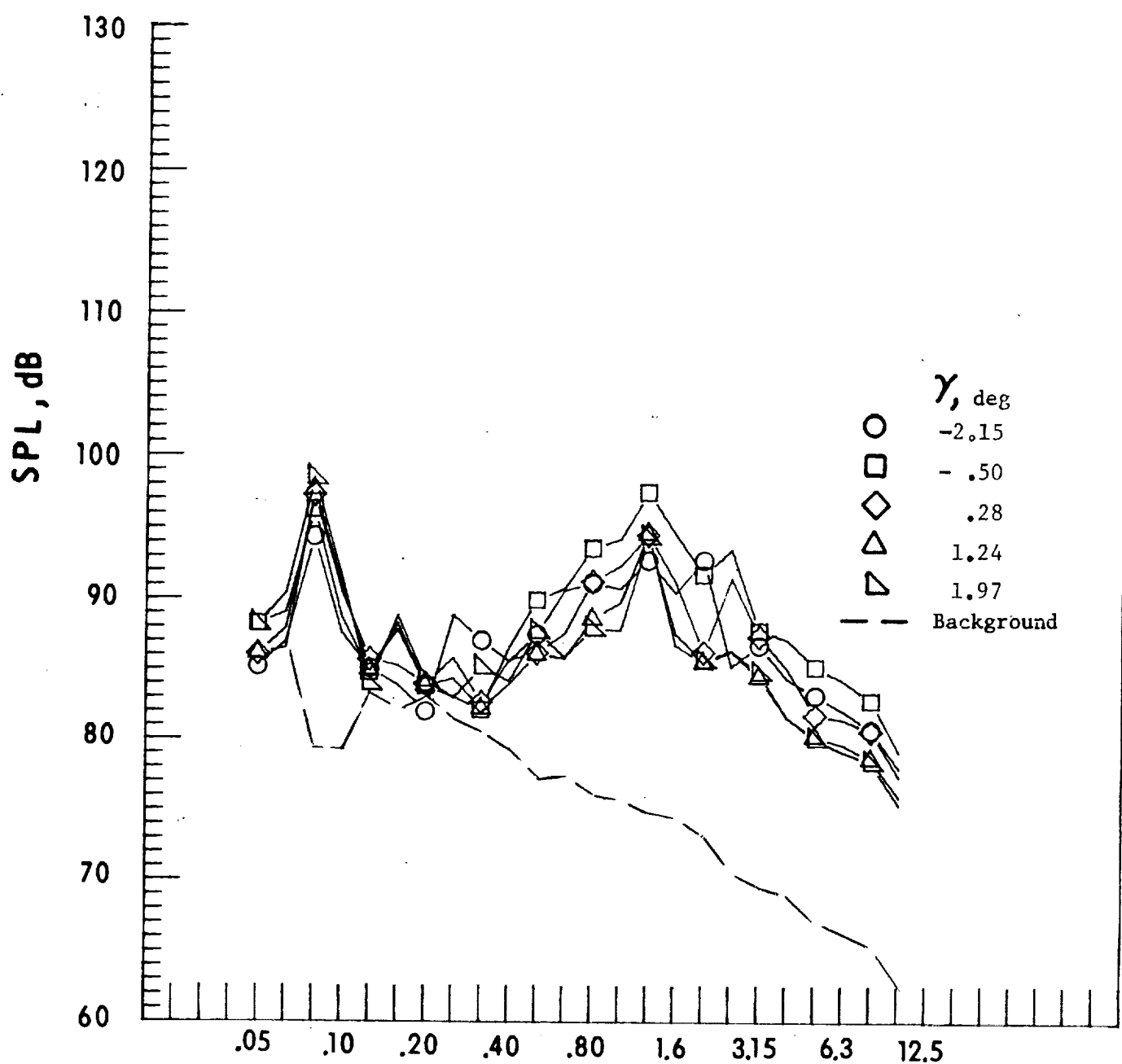
g. Mic. no. 5.

Figure 29. - Continued.



h. Pressure-time histories, Mic. no. 5.

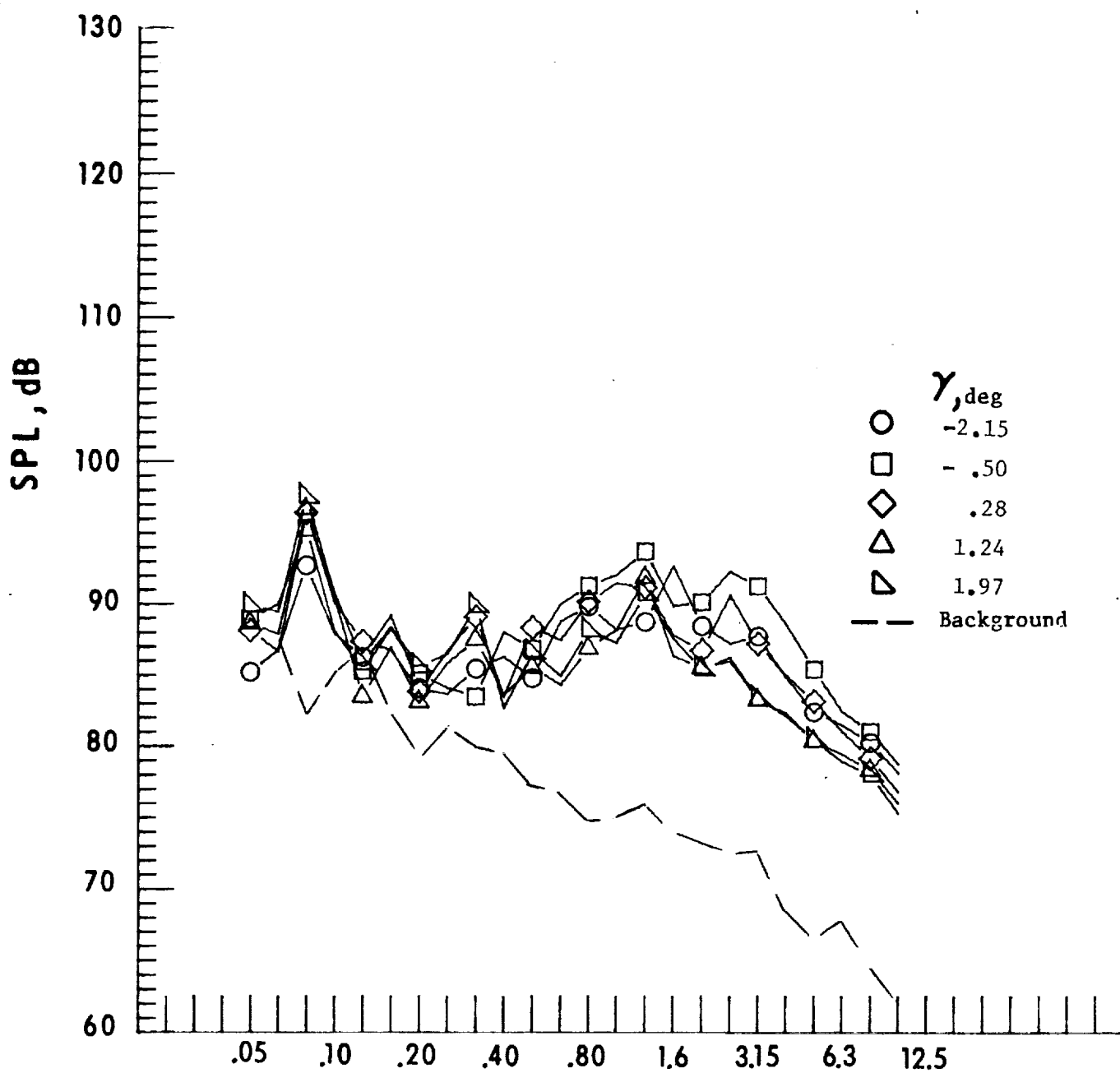
Figure 29. - Continued.



One-third-octave-band center frequency, kHz

i. Mic. no. 6.

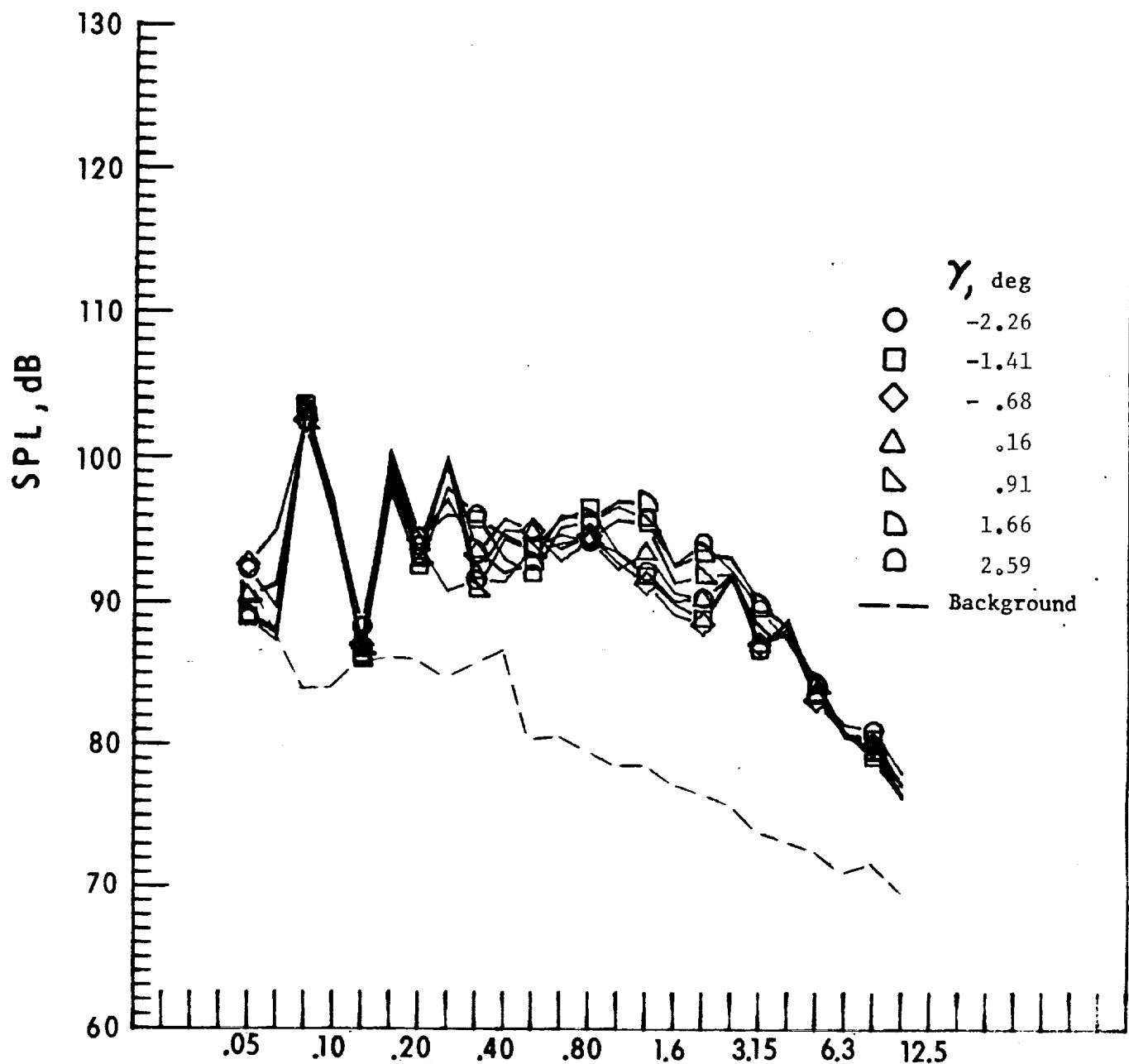
Figure 29. - Continued.



One-third-octave-band center frequency, kHz

j. Mic. no. 7.

Figure 29. - Concluded.



One-third-octave-band center frequency, kHz

a. Mic. no. 1.

Figure 30. - Effect of descent angle variation on noise generated by helicopter model with square tips installed. $V_{\infty} = 71.1$ knots.

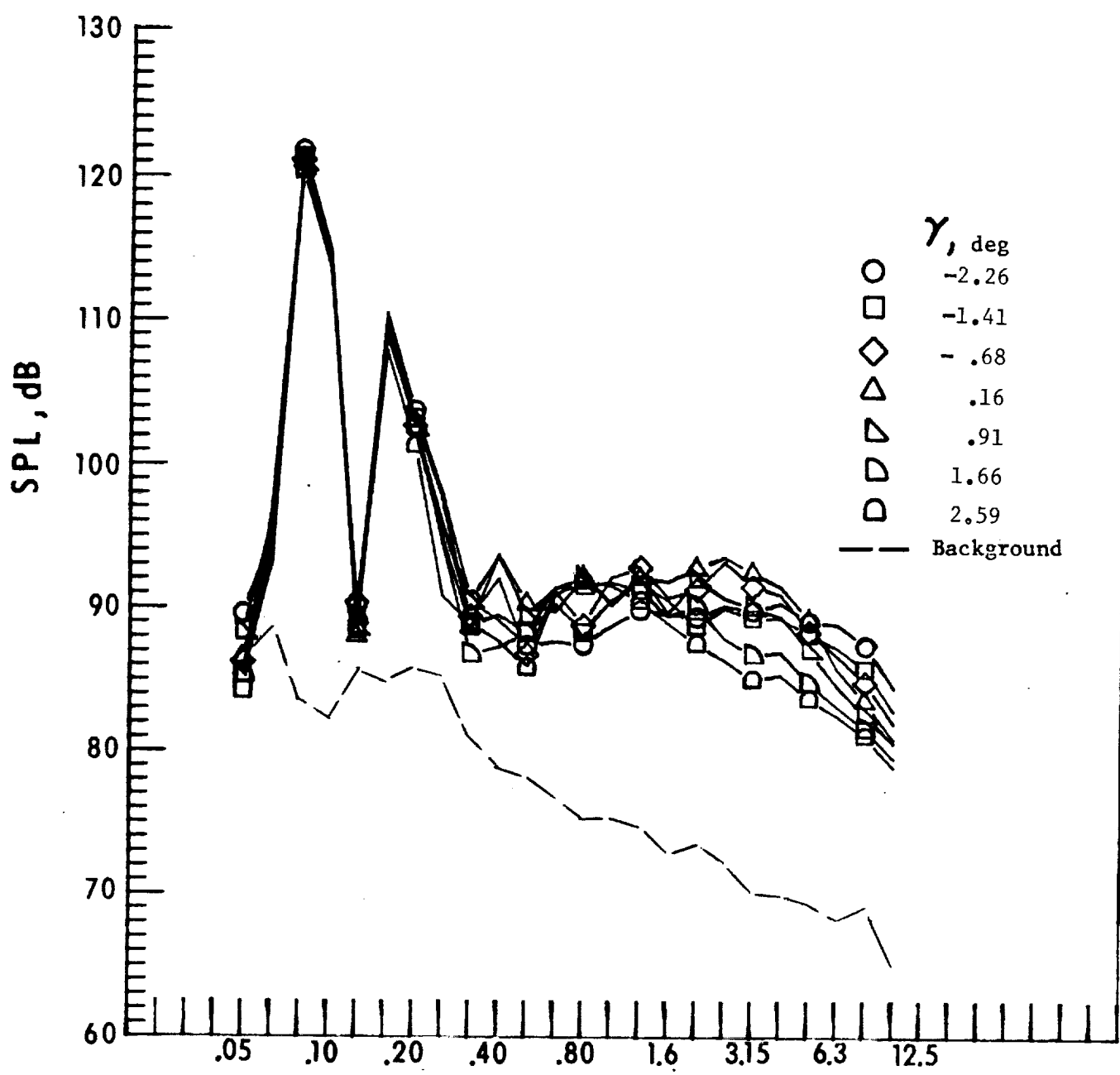
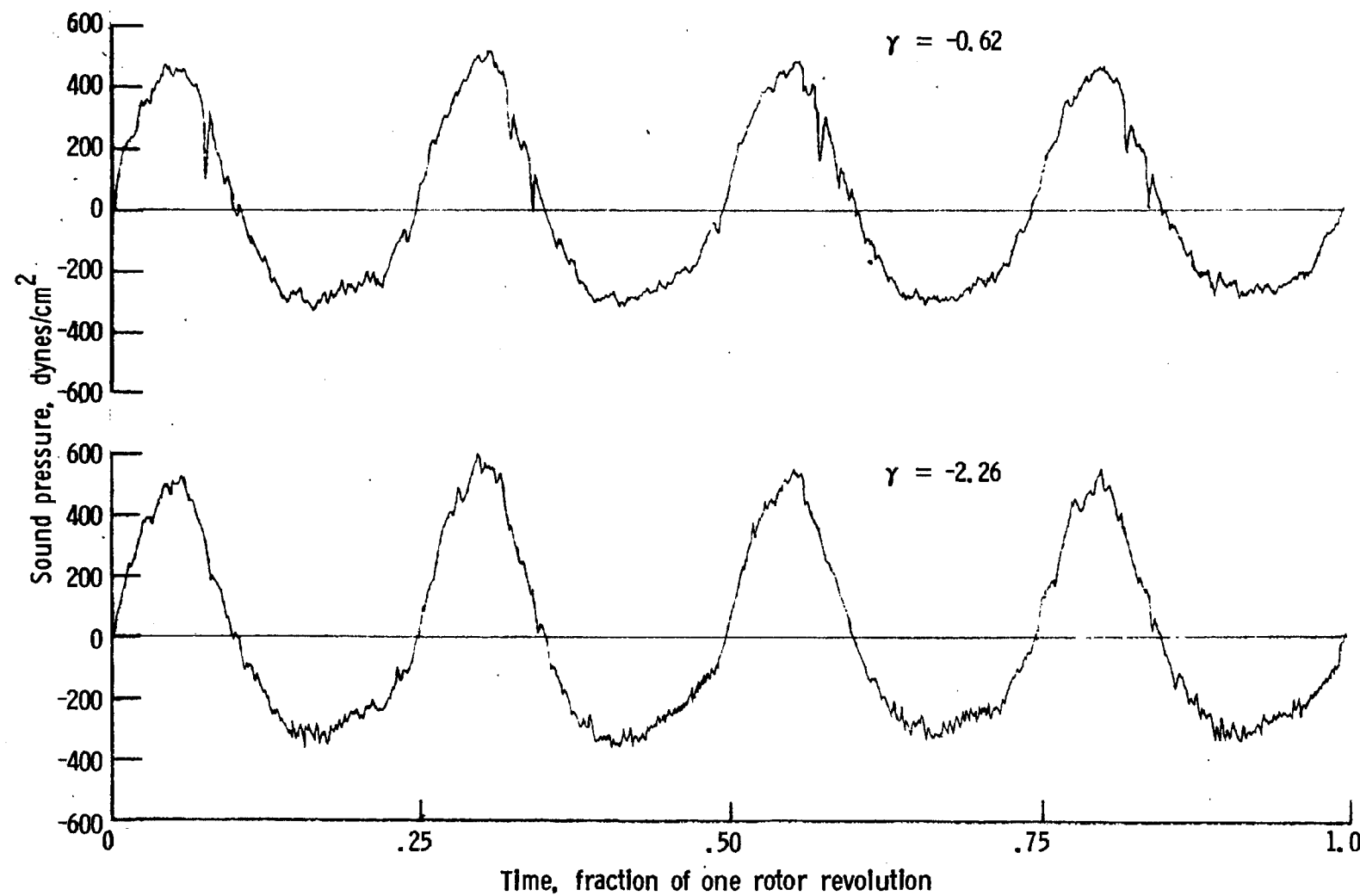


Figure 30. - Continued.

b. Mic. no. 2.



c. Pressure-time histories, Mic. no. 2.

Figure 30. - Continued.

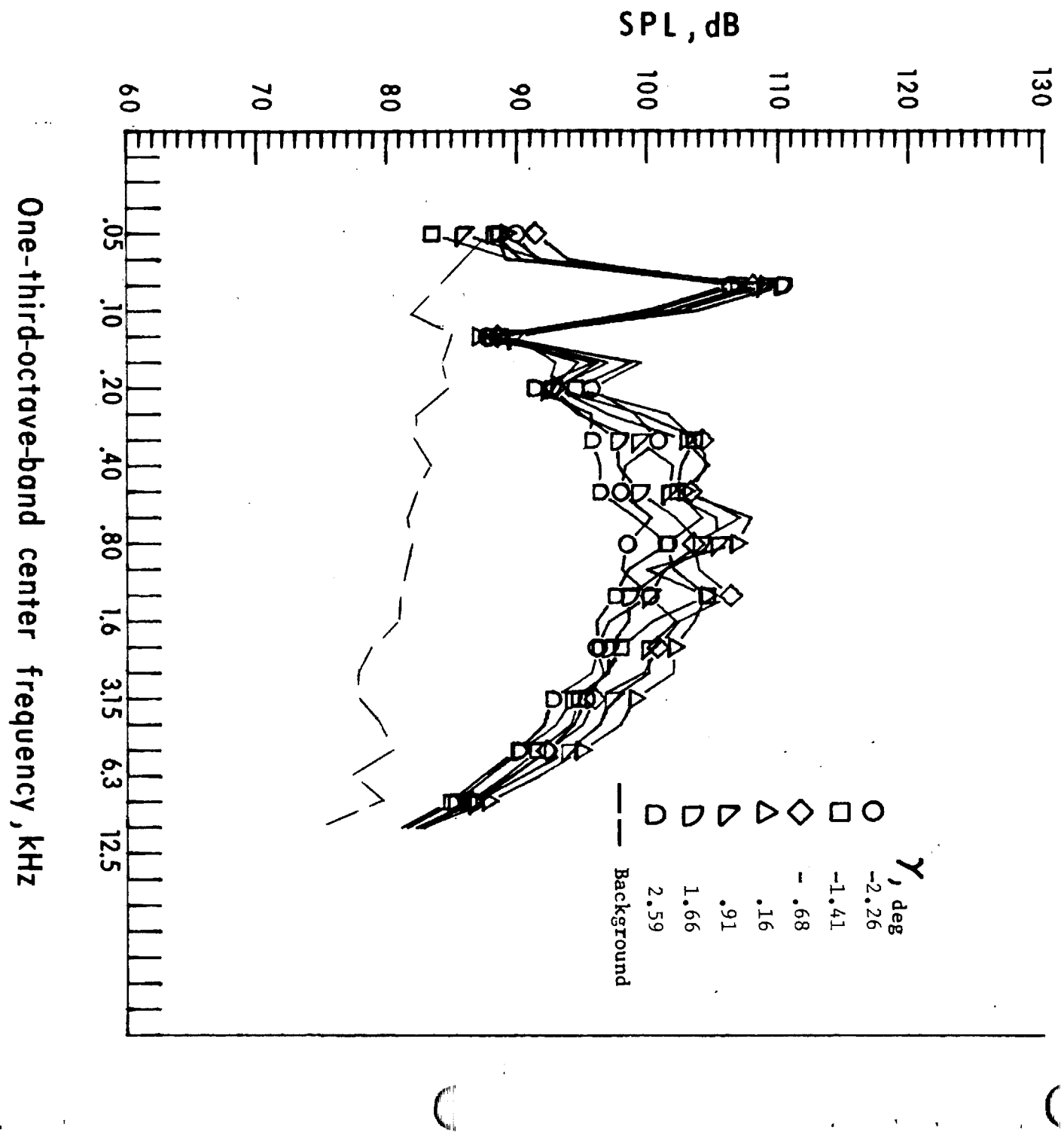
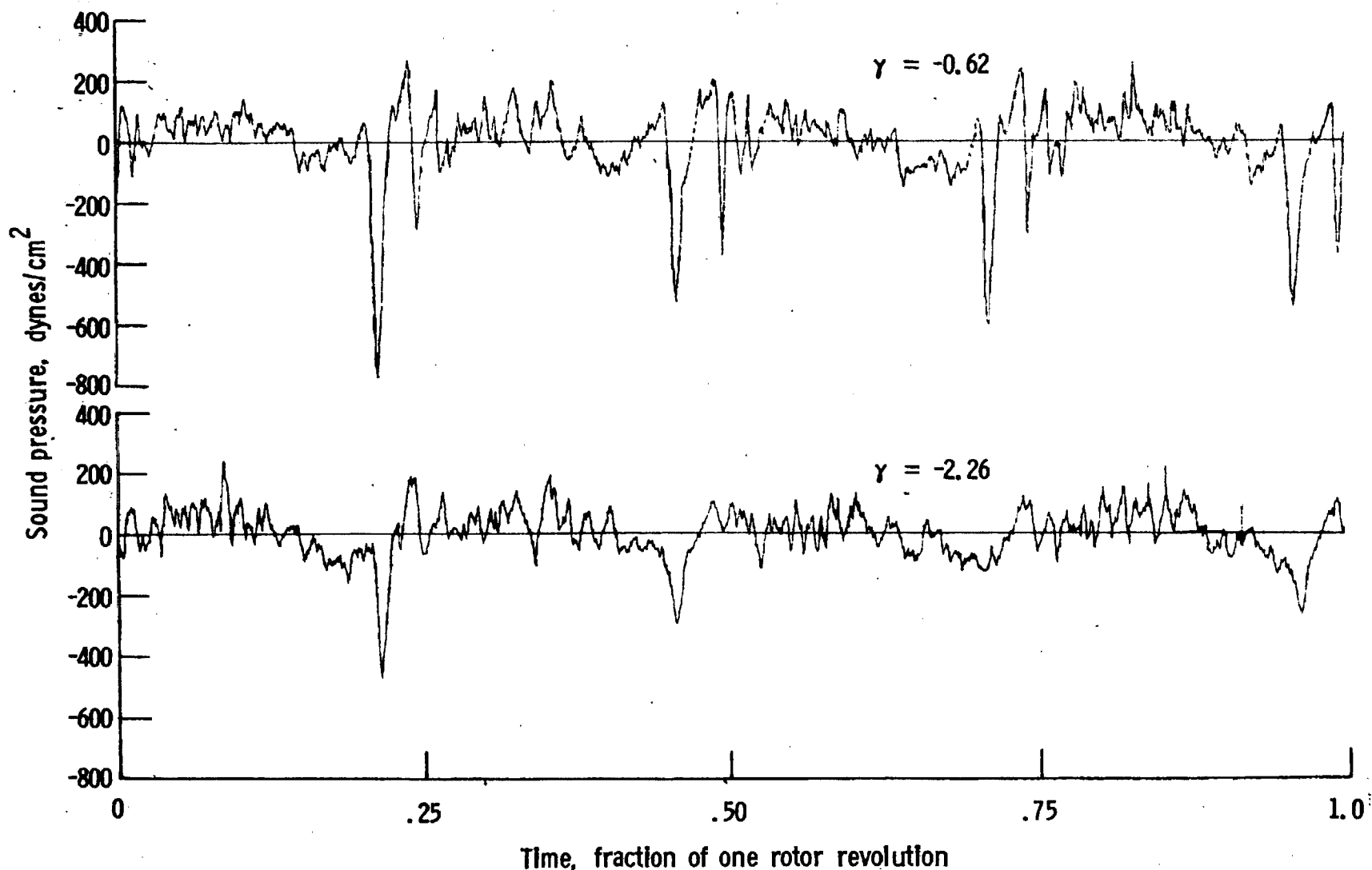


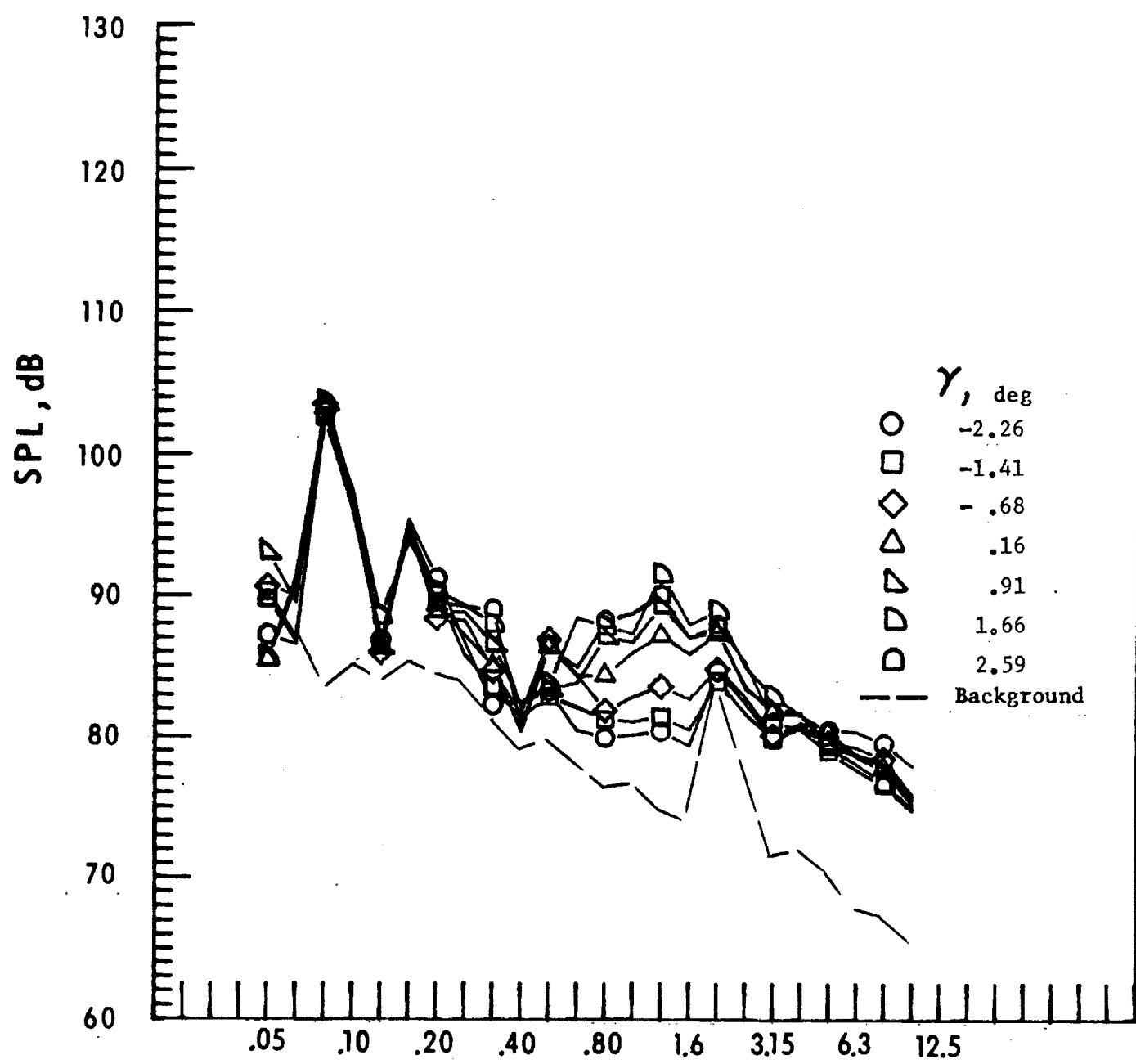
Figure 30. - Continued.

d. Mic. no. 3.



e. Pressure-time histories, Mic. no. 3.

Figure 30. - Continued.



f. Mic. no. 4.

Figure 30. - Continued.

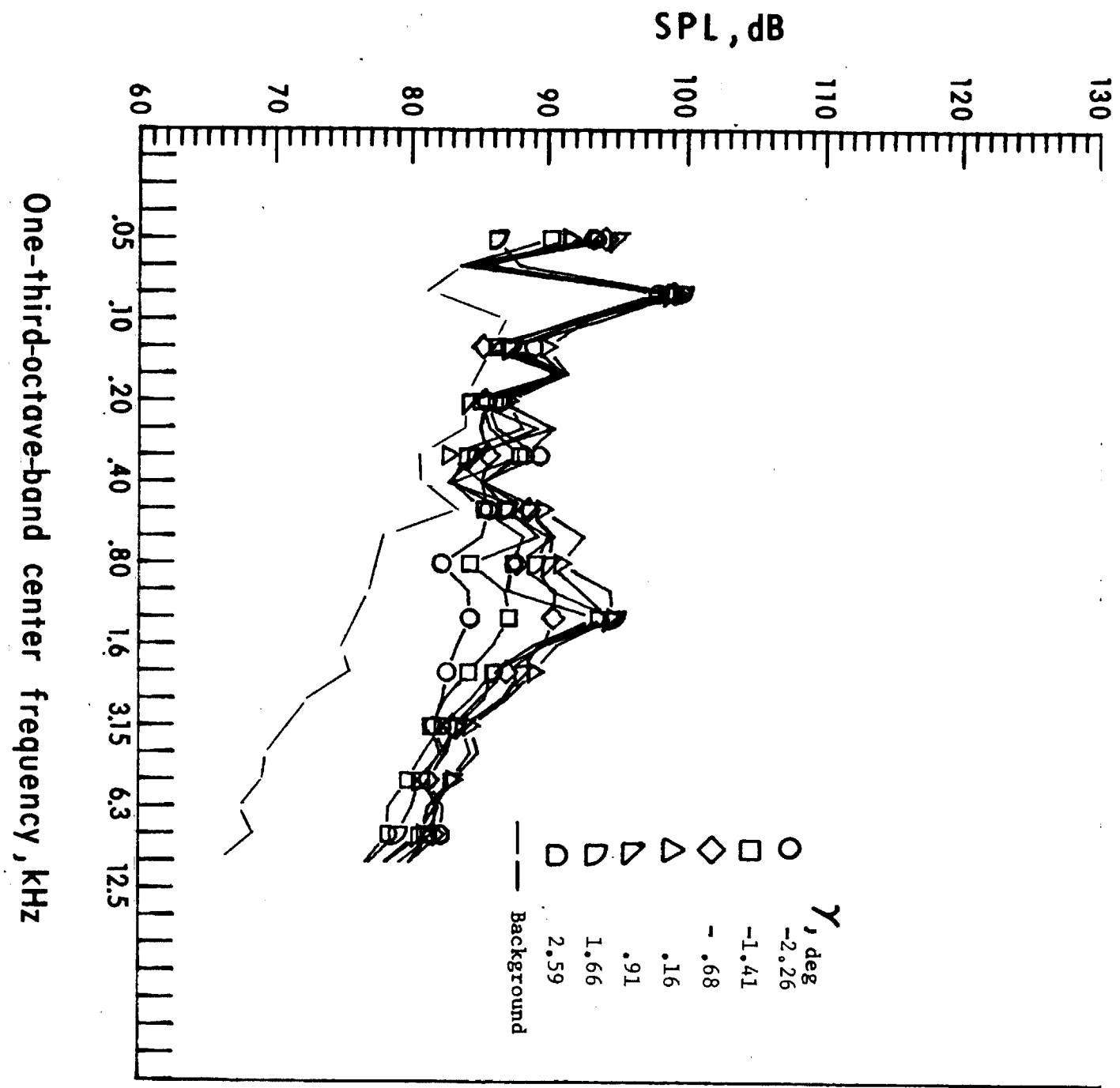
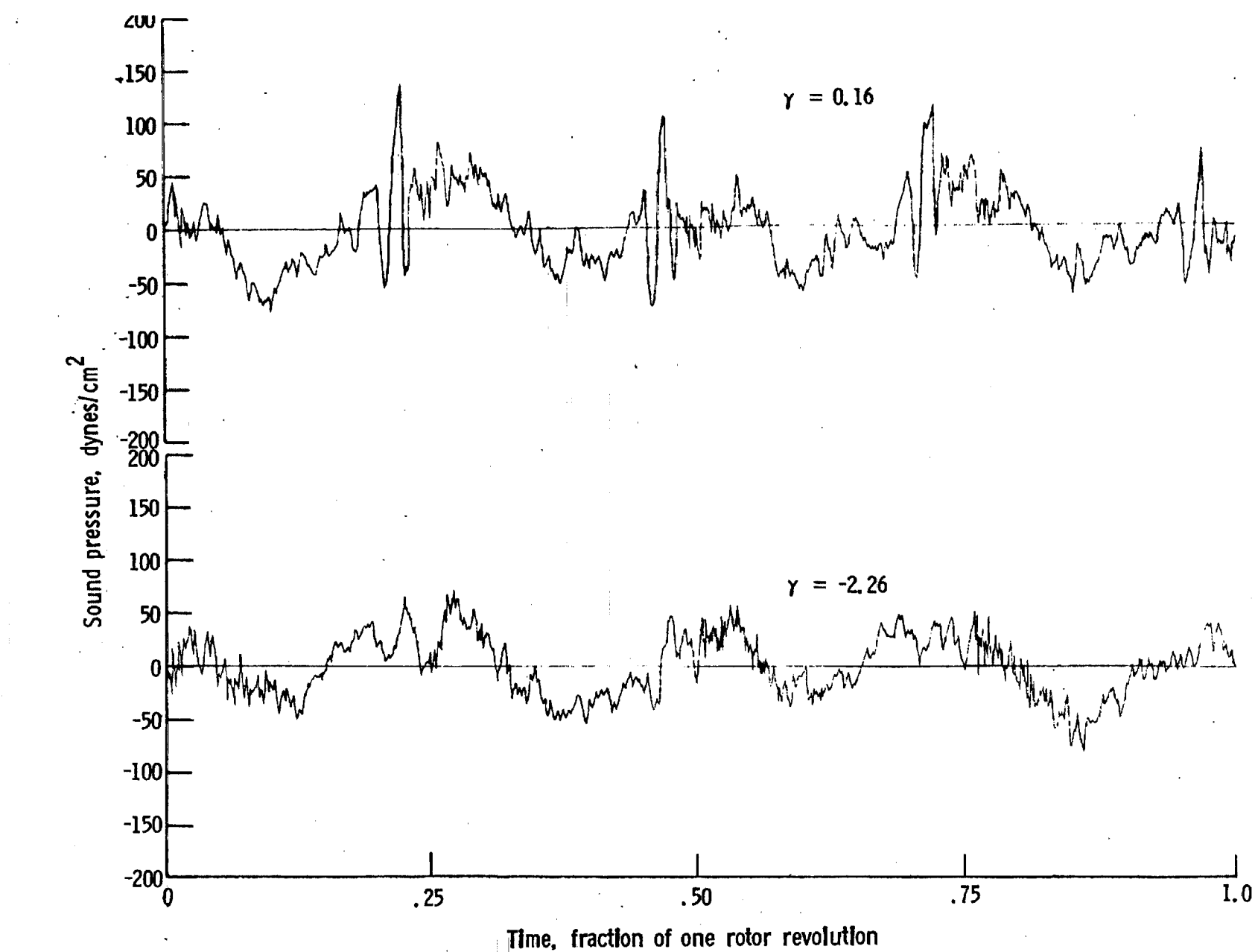


Figure 30. - Continued.

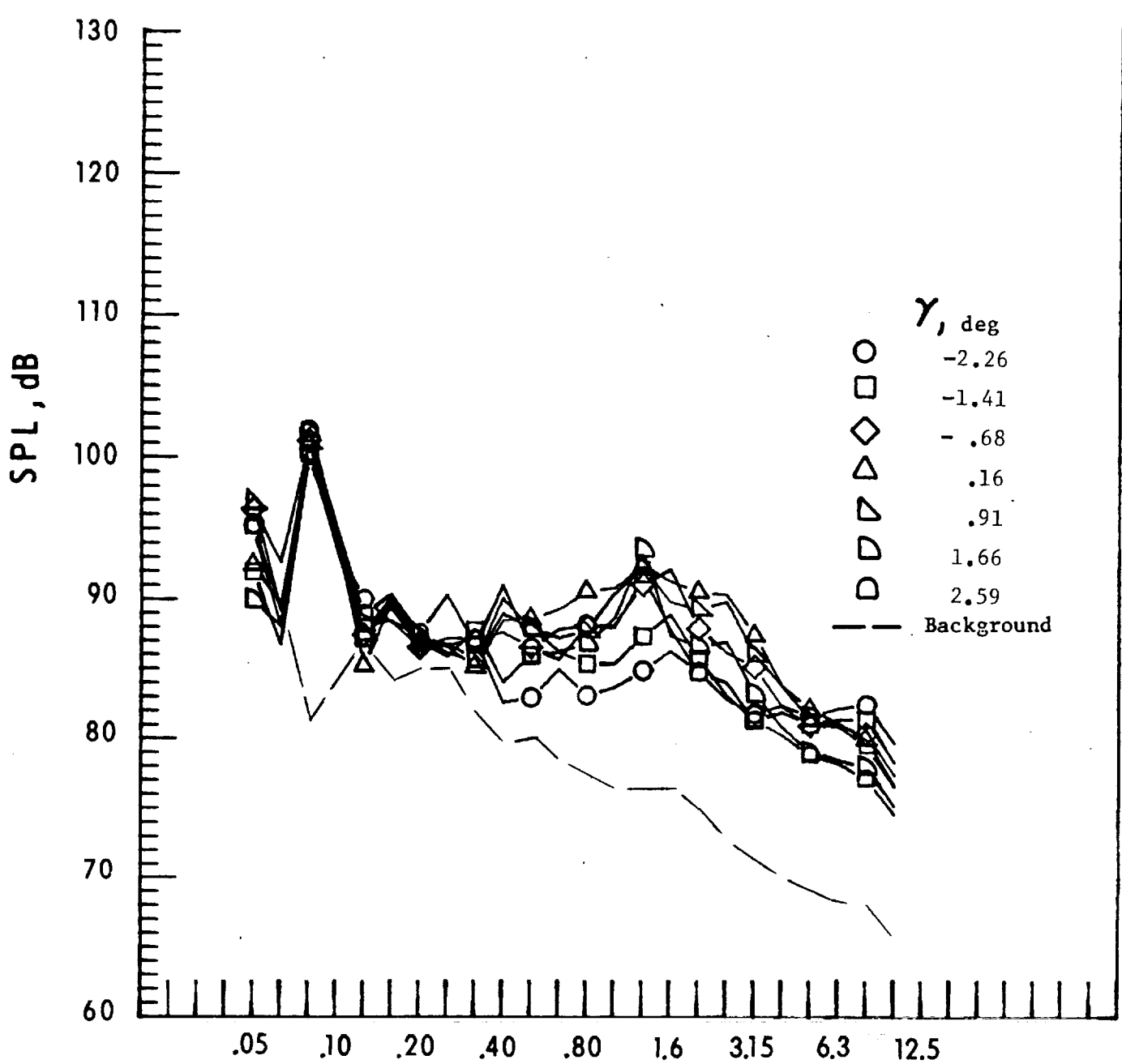
g. Mic. no. 5.



Time, fraction of one rotor revolution

h. Pressure-time histories, Mic. no. 5.

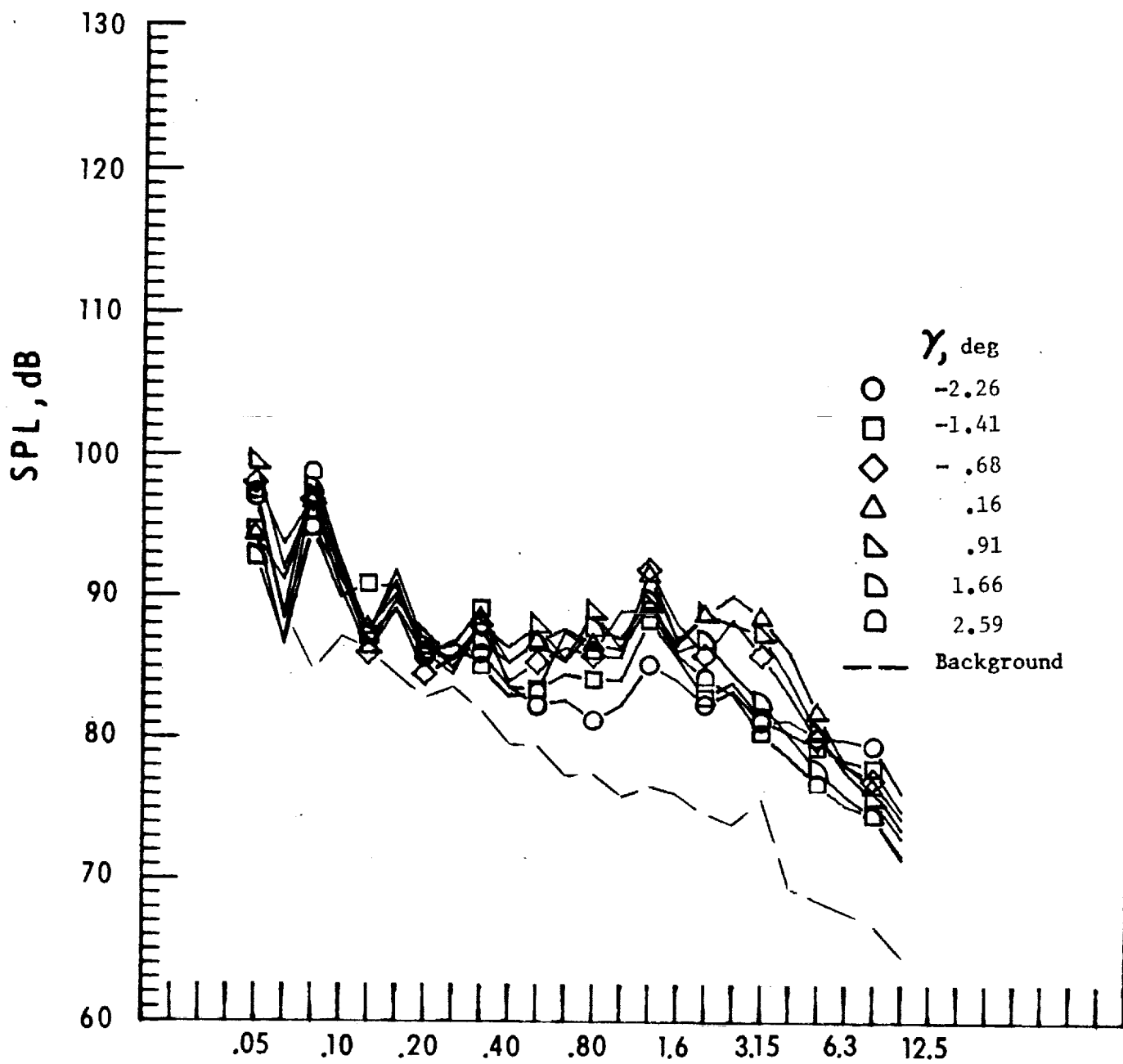
Figure 30. - Continued.



One-third-octave-band center frequency, kHz

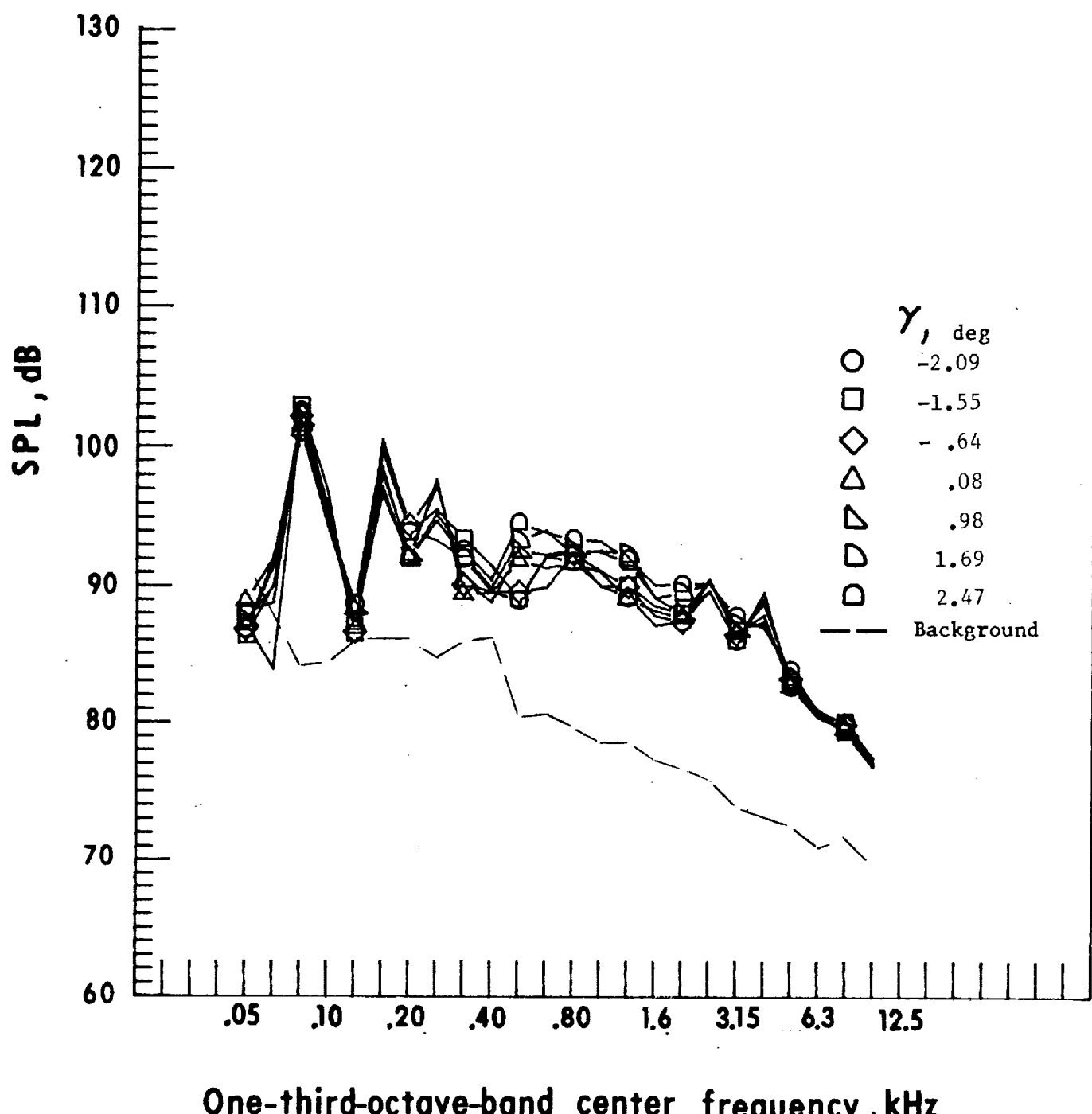
i. Mic. no. 6.

Figure 30. - Continued.



j. Mic. no. 7.

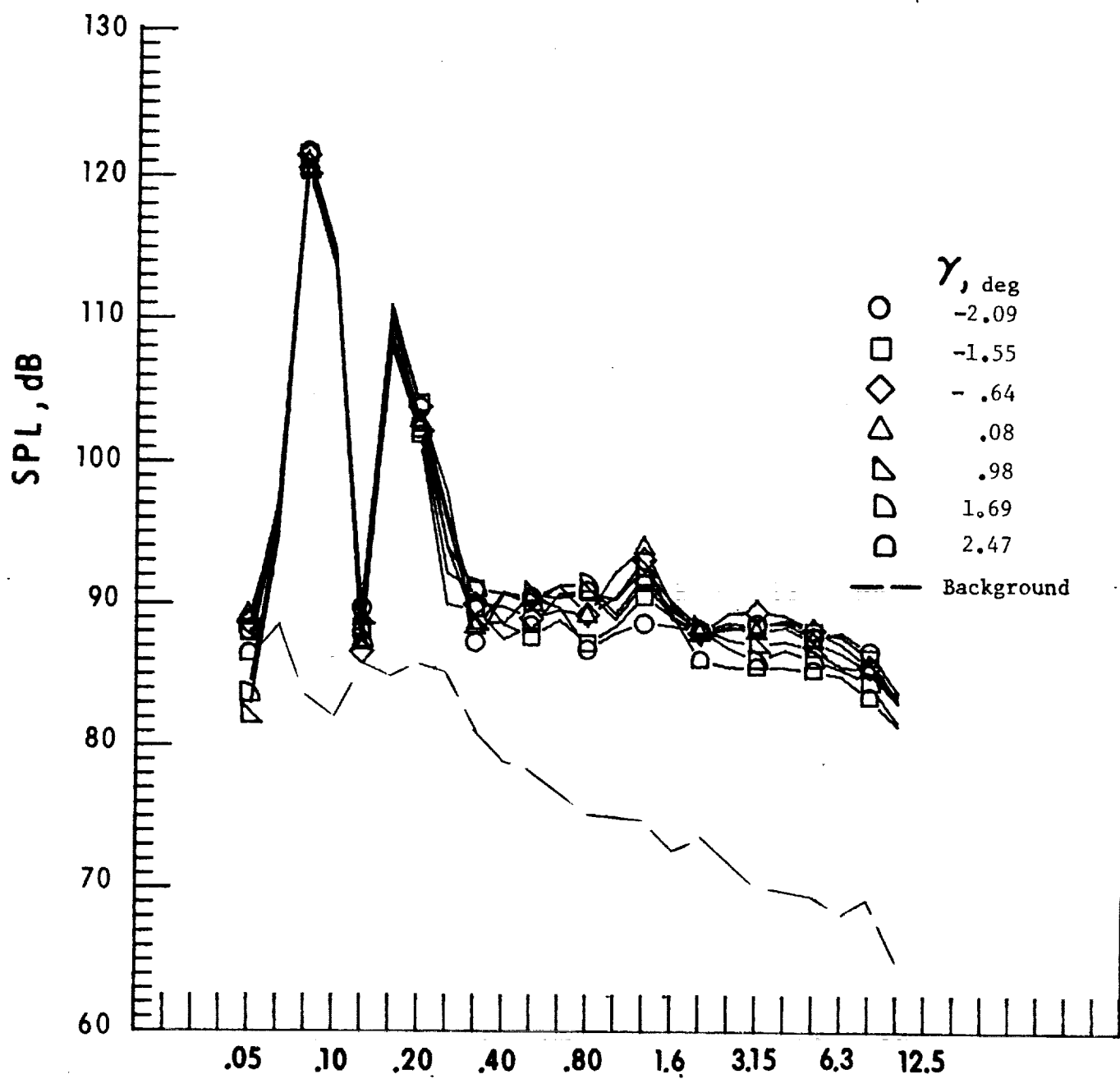
Figure 30. - Concluded.



One-third-octave-band center frequency, kHz

a. Mic. no. 1.

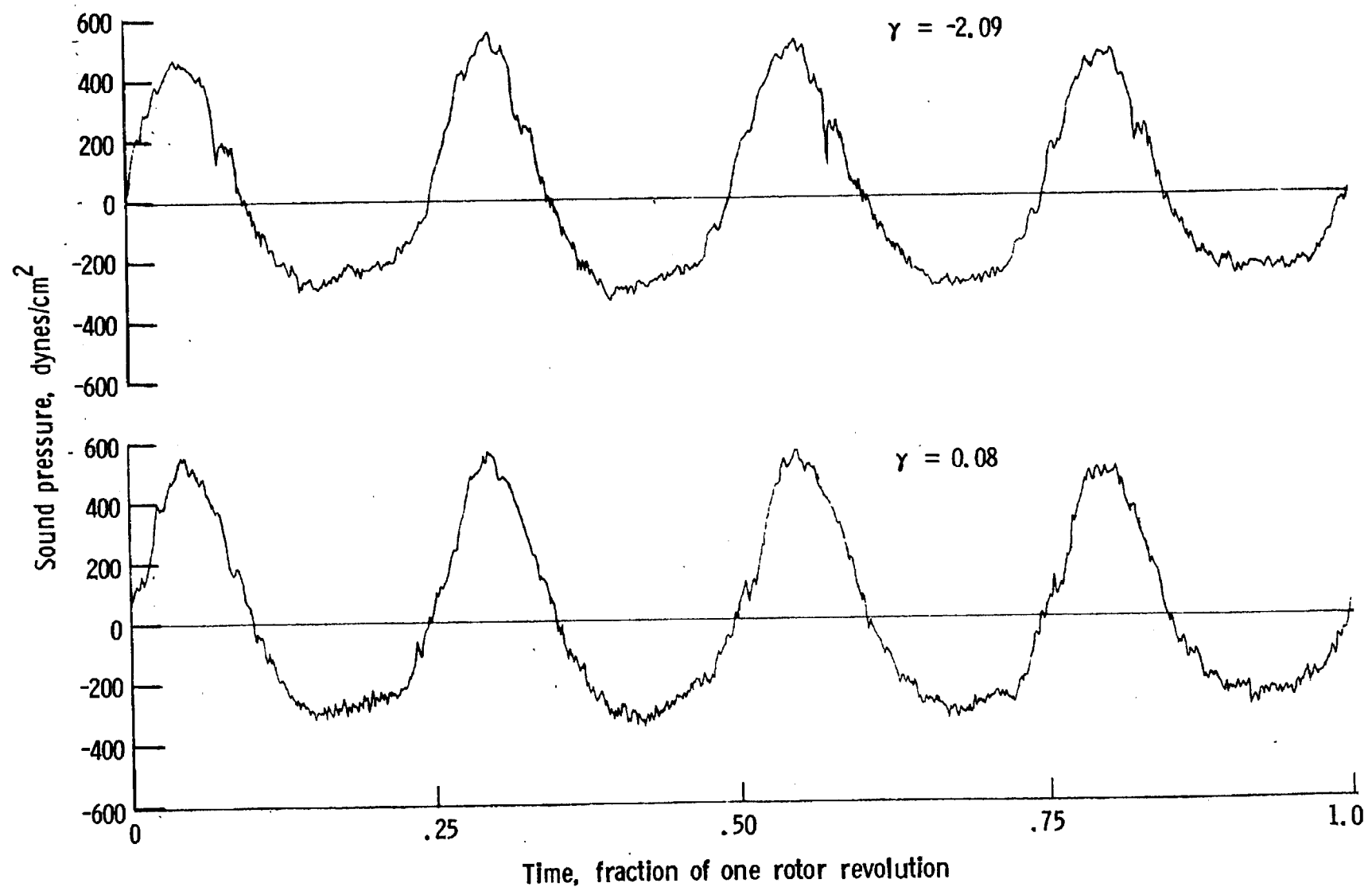
Figure 31. - Effect of descent angle variation on noise generated by helicopter model with ogee tips installed. $V_{\infty} = 70.7$ knots.



One-third-octave-band center frequency, kHz

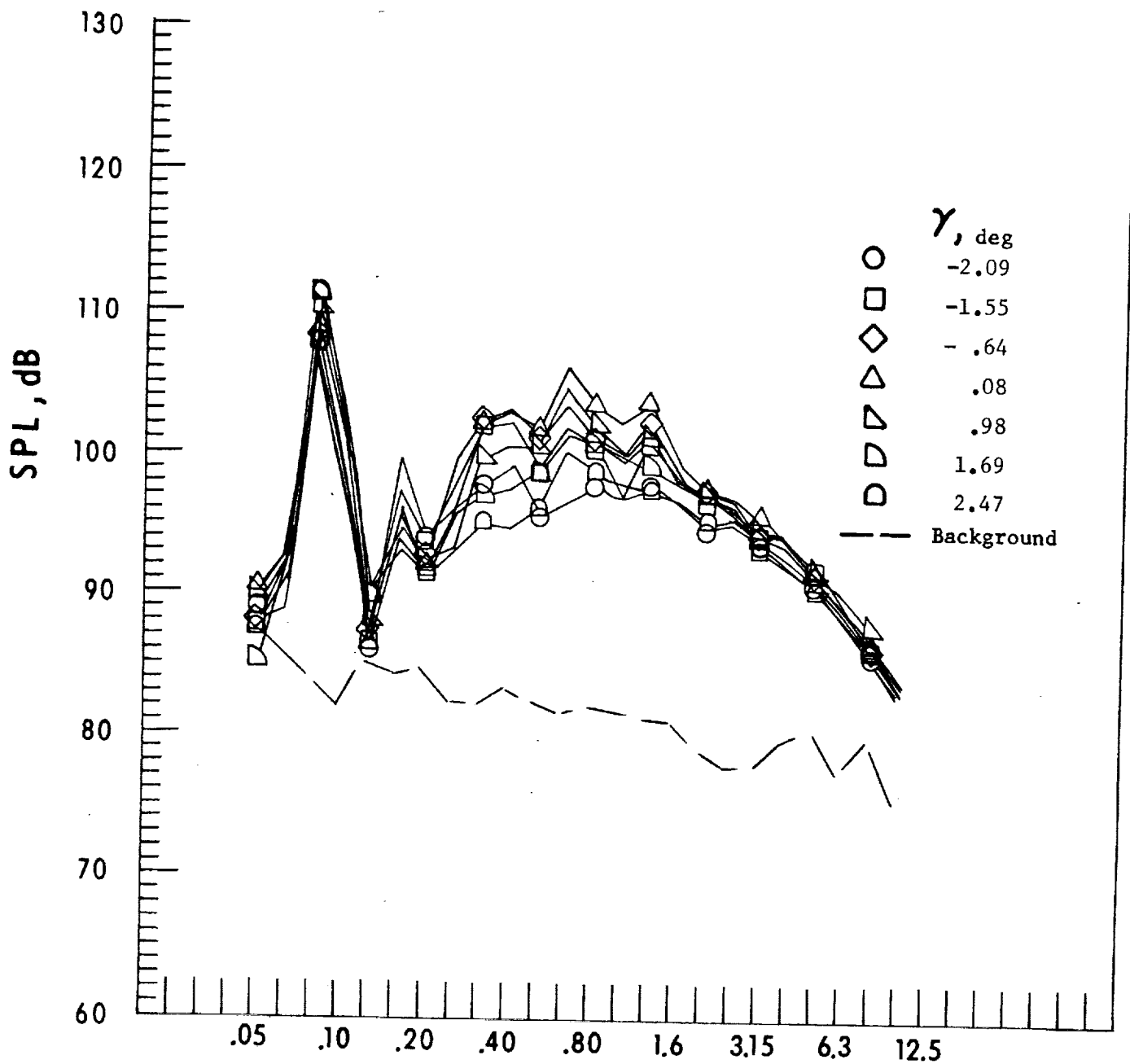
b. Mic. no. 2.

Figure 31. - Continued.



c. Pressure-time histories, Mic. no. 2.

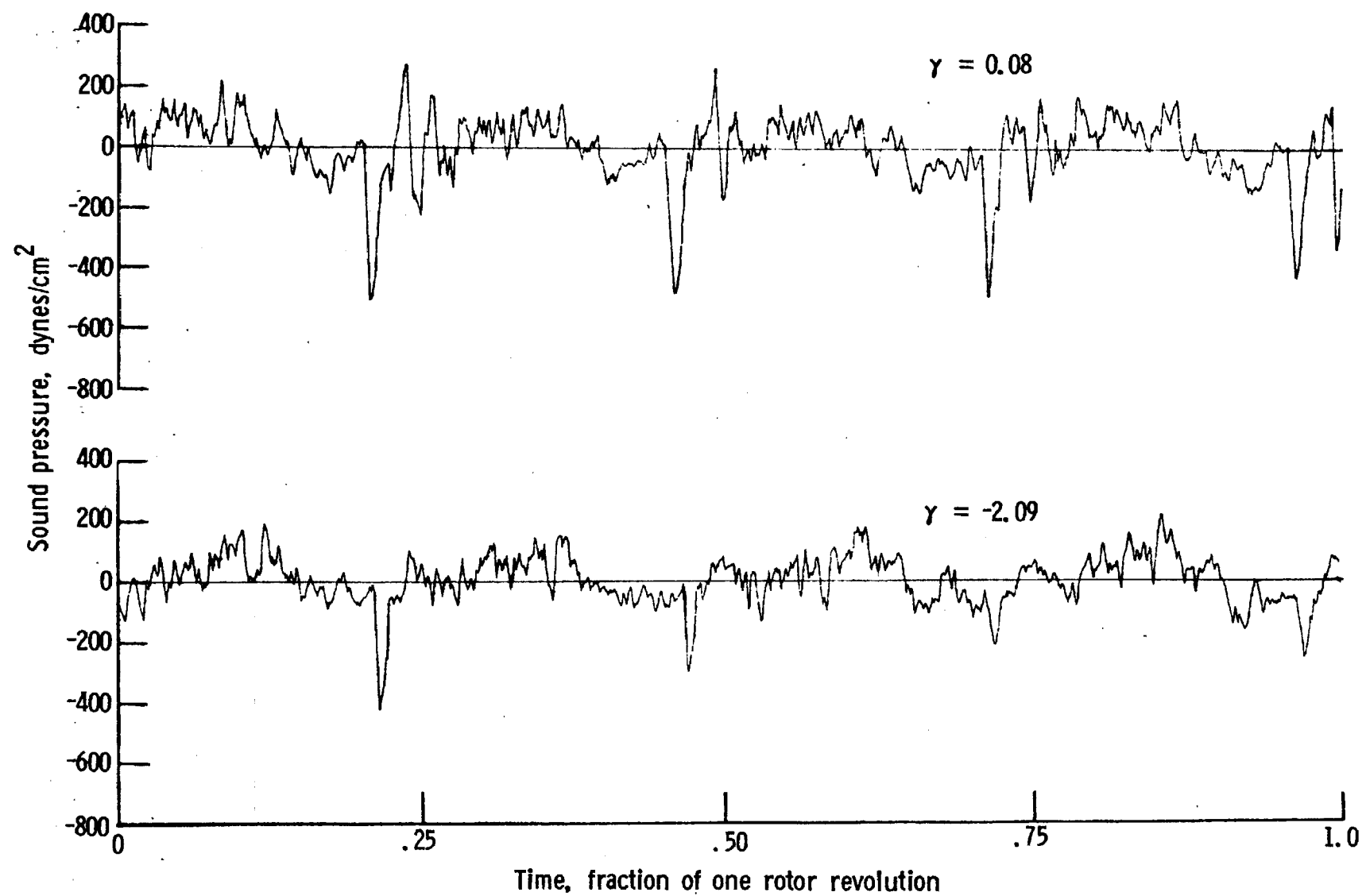
Figure 31. - Continued.



One-third-octave-band center frequency, kHz

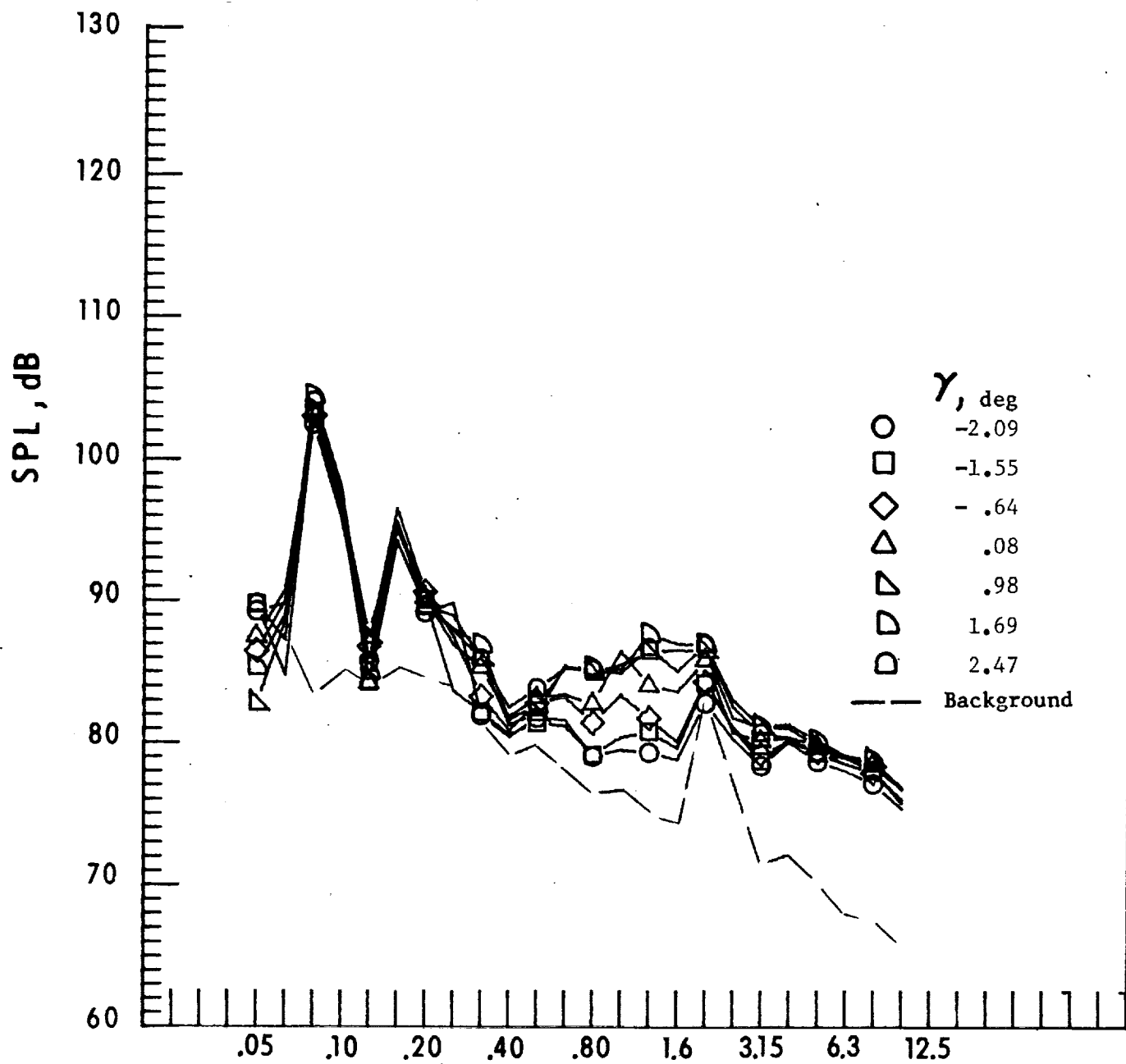
d. Mic. no. 3

Figure 31. - Continued.



e. Pressure-time histories, Mic. no. 3.

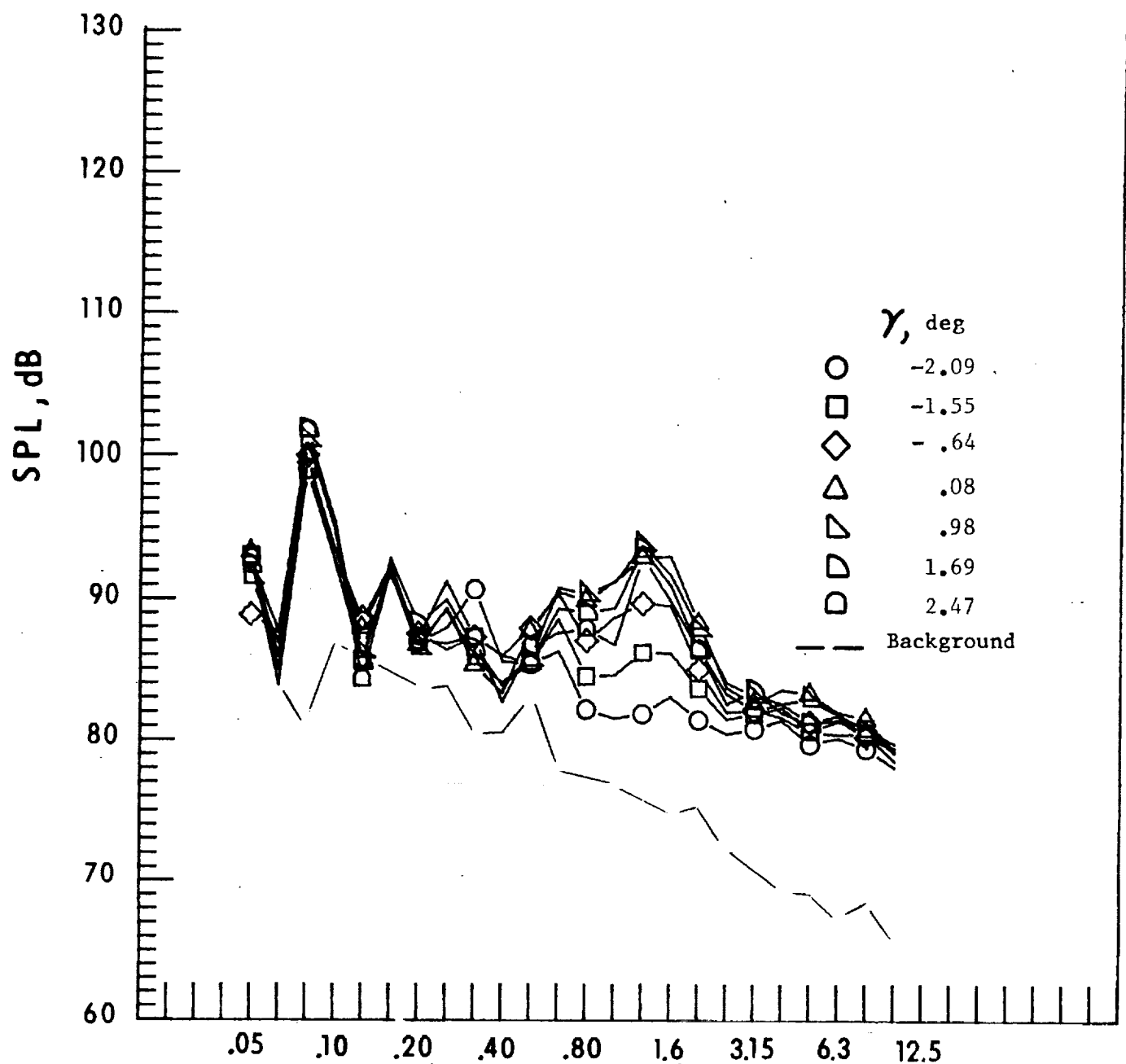
Figure 31. - Continued



One-third-octave-band center frequency, kHz

f. Mic. no. 4.

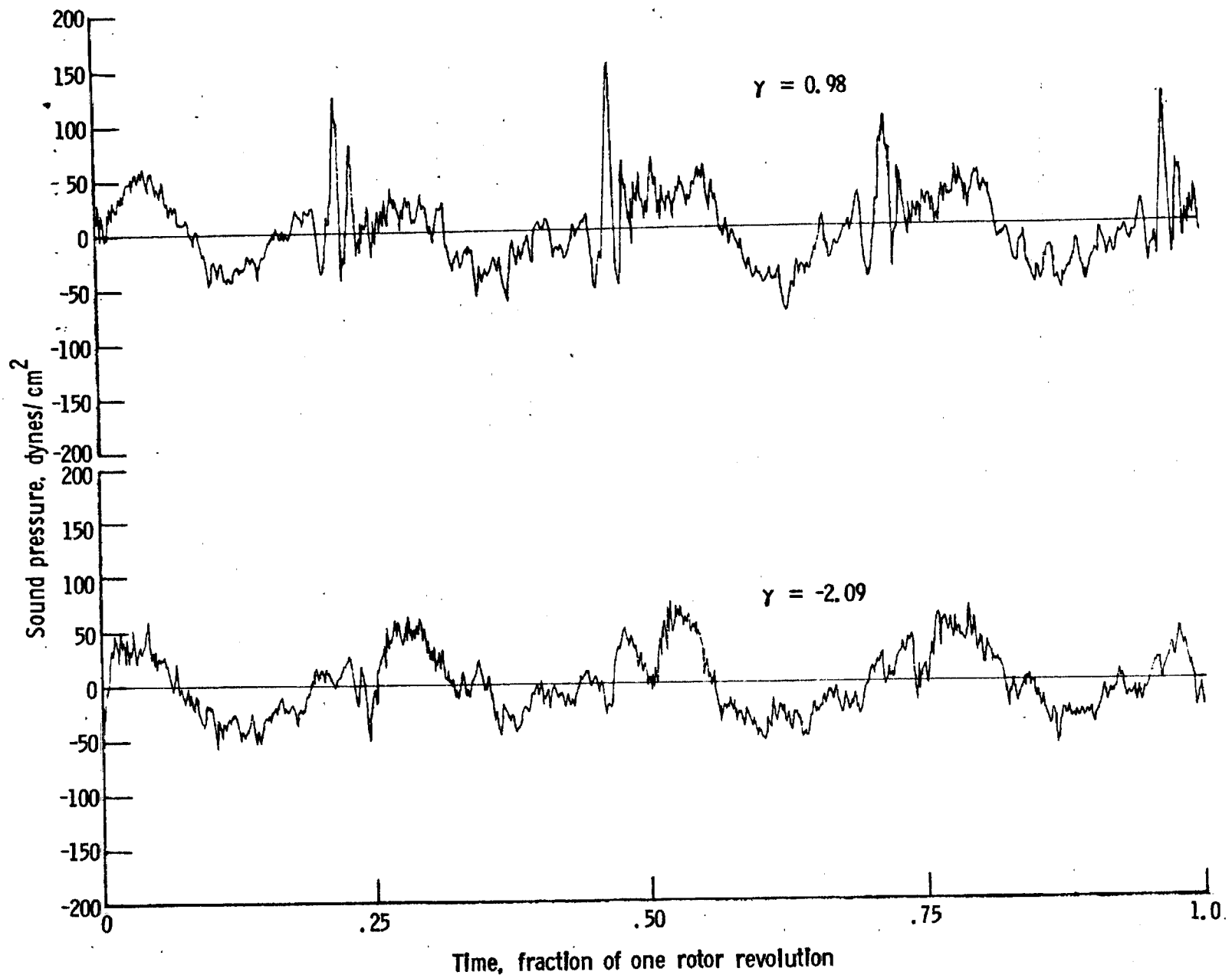
Figure 31. - Continued.



One-third-octave-band center frequency, kHz

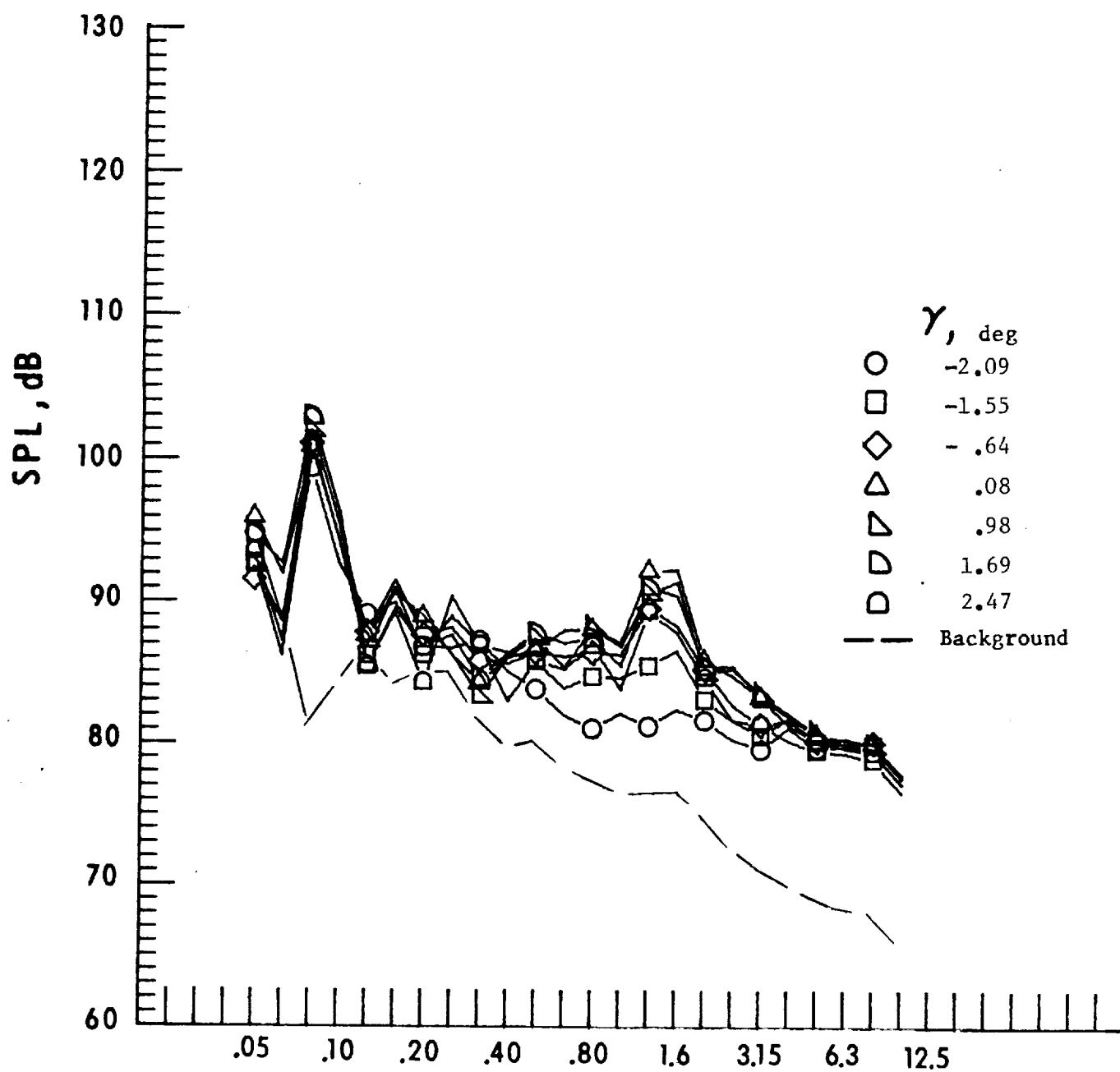
g. Mic. no. 5.

Figure 31. - Continued.



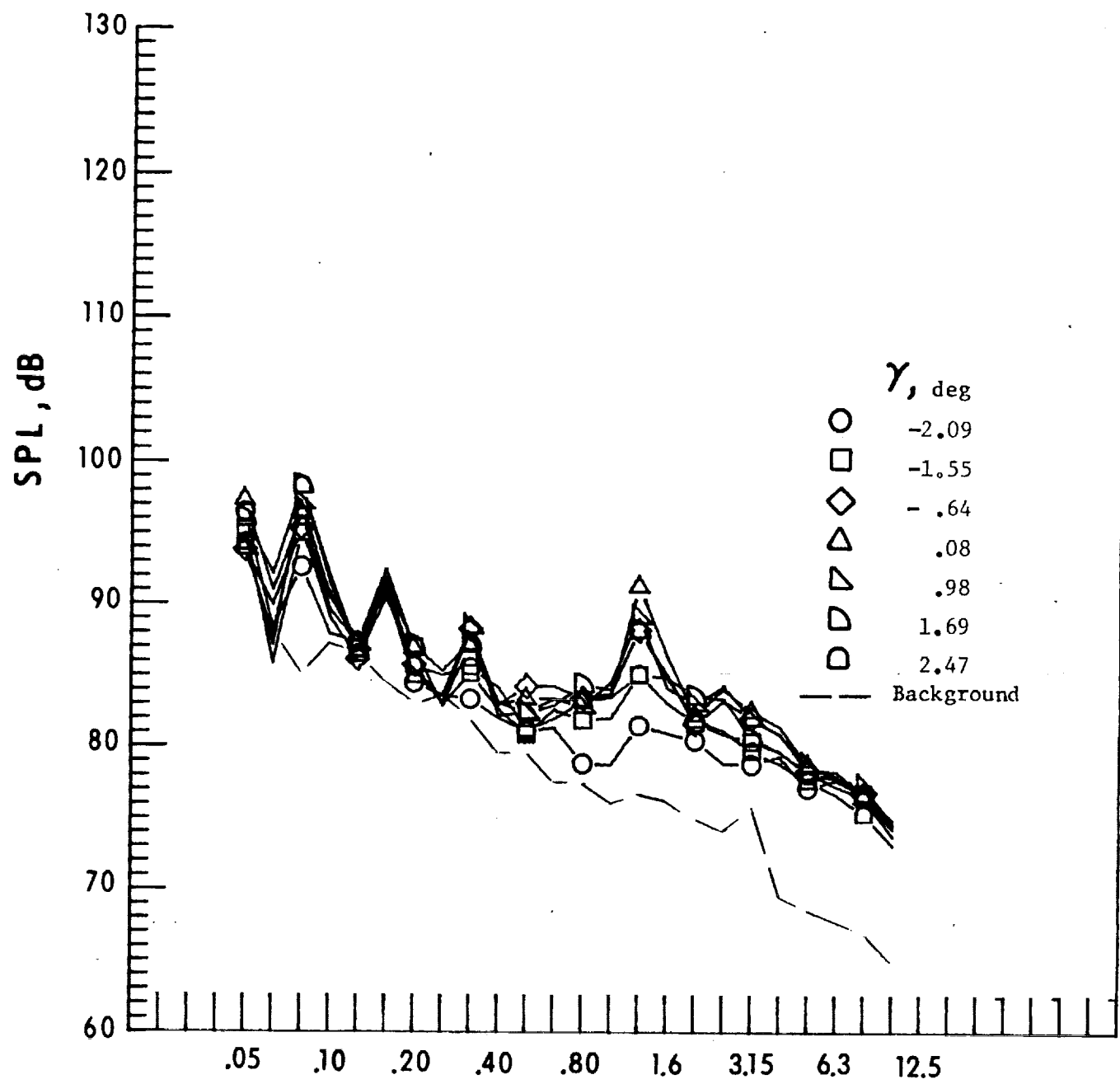
h. Pressure-time histories, Mic. no. 5.

Figure 31. - Continued.



i. Mic. no. 6.

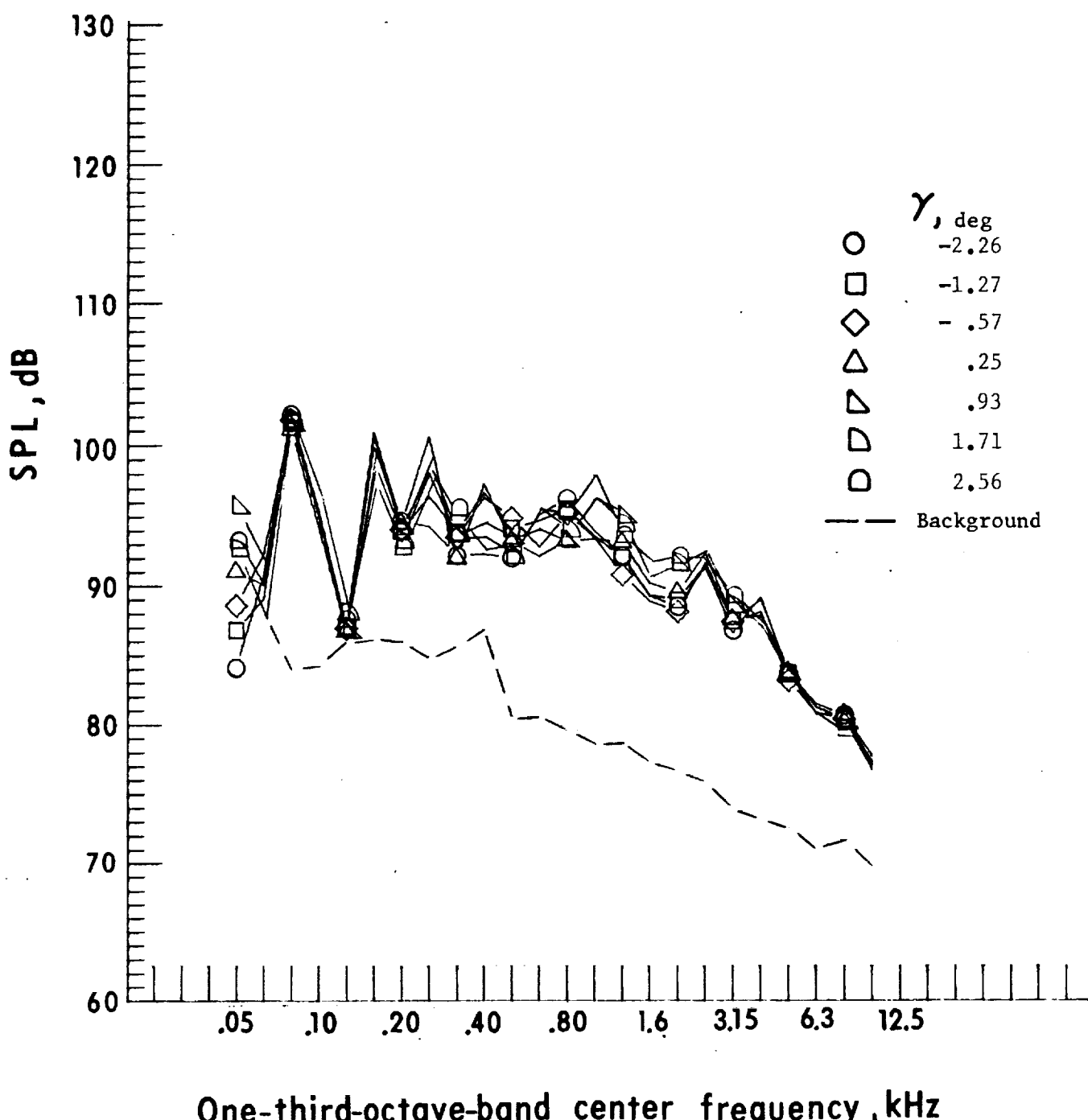
Figure 31. - Continued.



One-third-octave-band center frequency, kHz

j. Mic. no. 7.

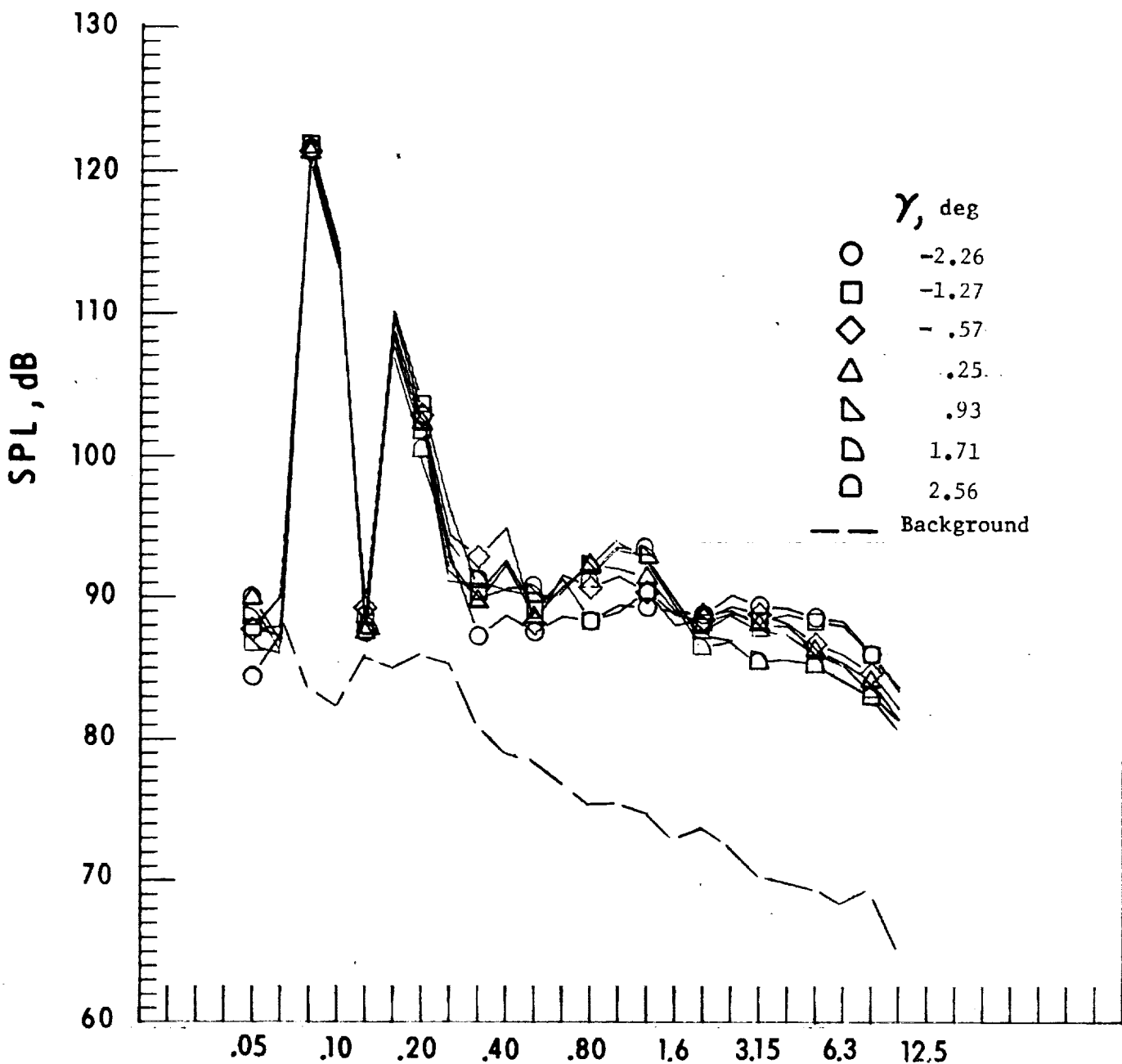
Figure 31. - Concluded.



One-third-octave-band center frequency, kHz

a. Mic. no. 1.

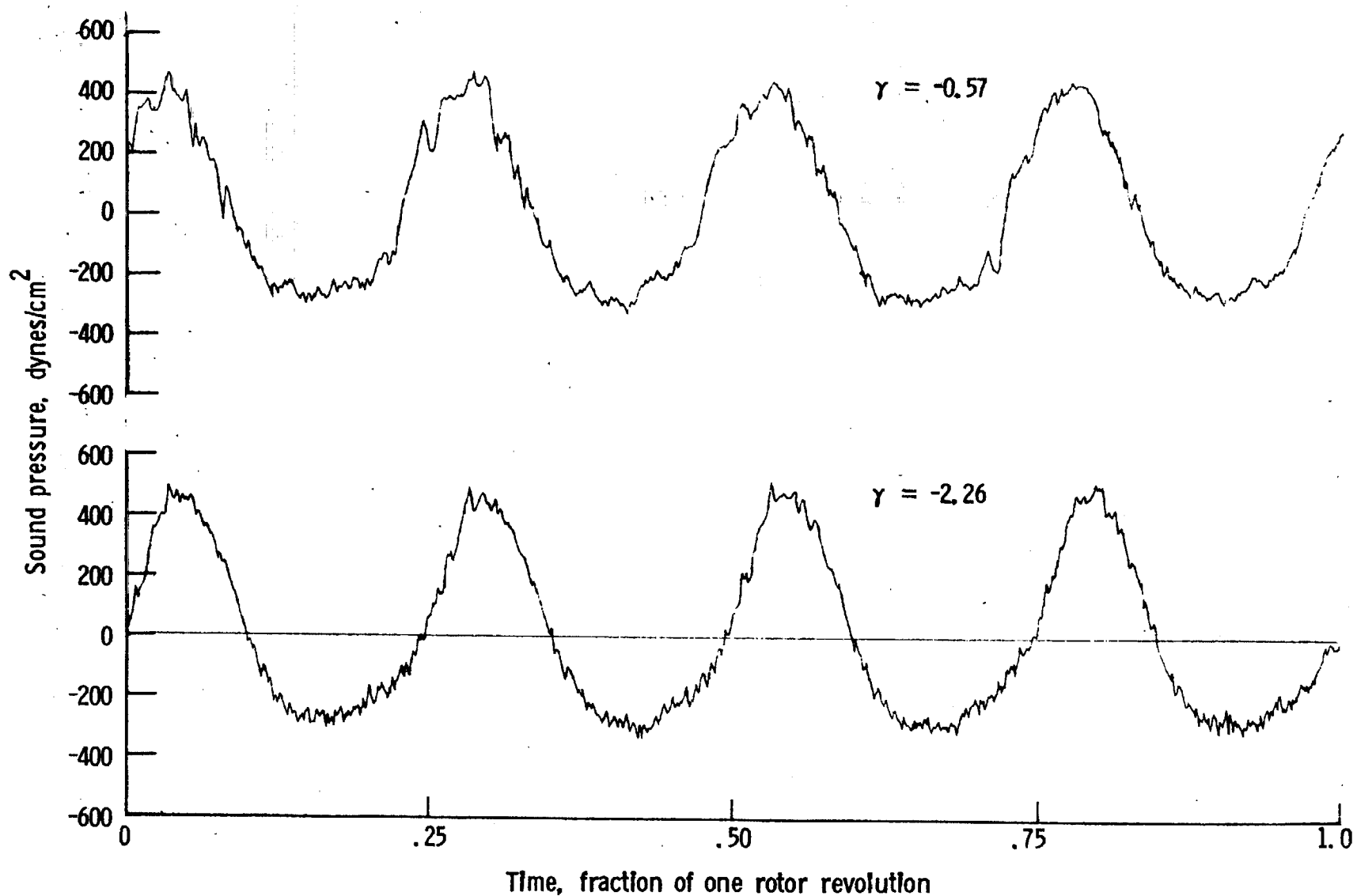
Figure 32. - Effect of descent angle variation on noise generated by helicopter model with sub-wing tips installed. $V_\infty = 71.2$ knots.



One-third-octave-band center frequency, kHz

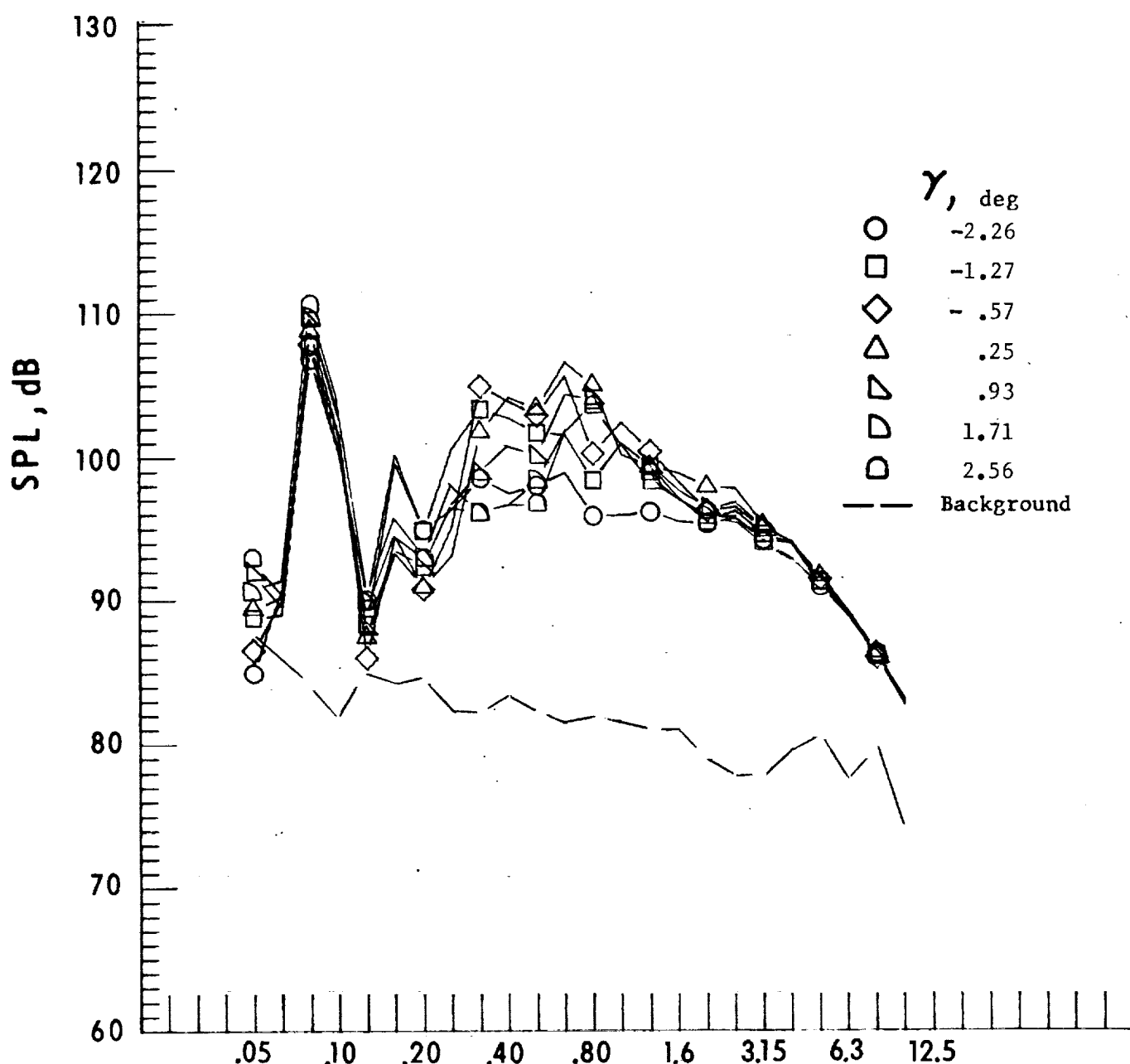
b. Mic. no. 2.

Figure 32. - Continued.



c. Pressure-time-histories, Mic. no. 2

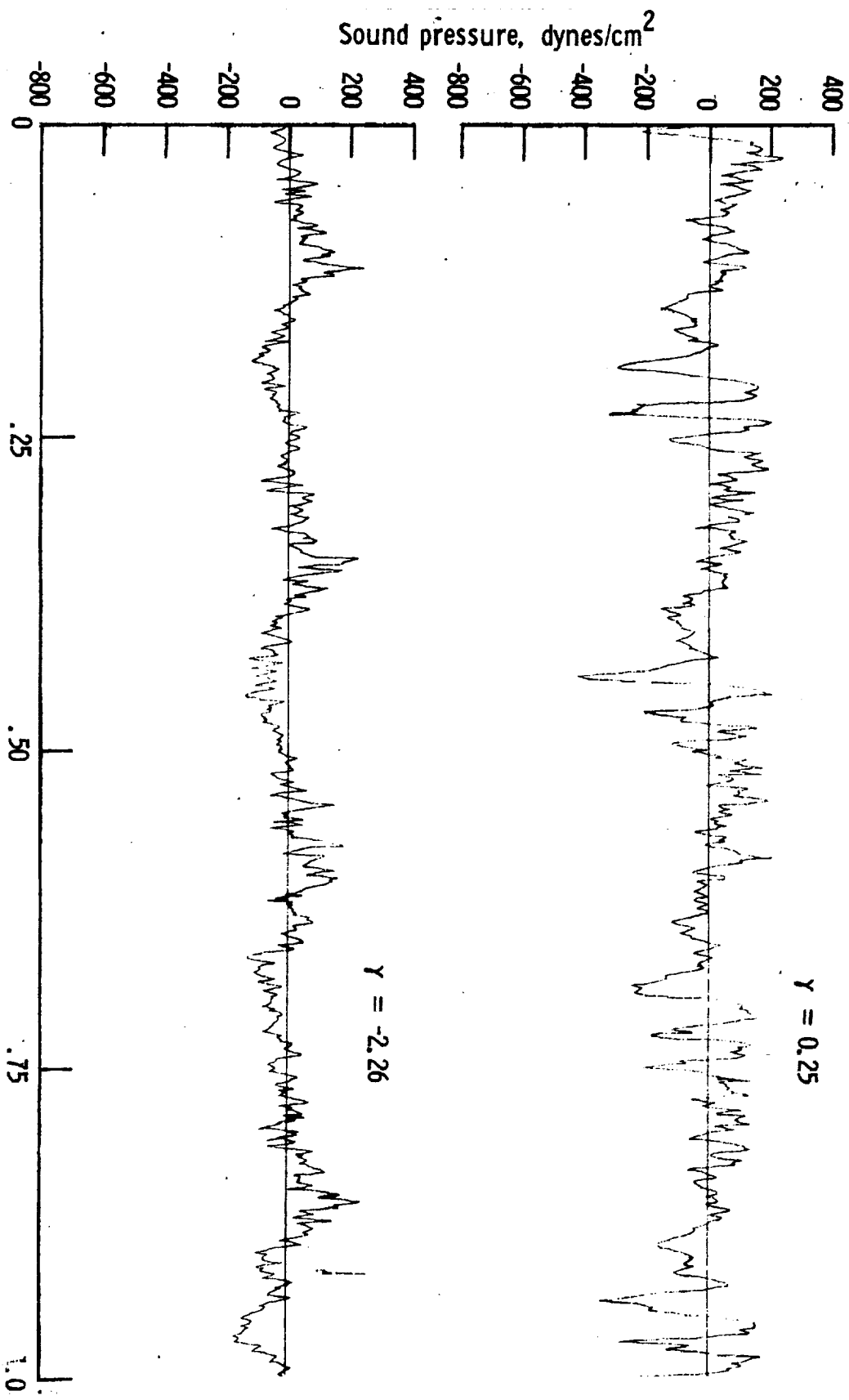
Figure 32. - Continued.



One-third-octave-band center frequency, kHz

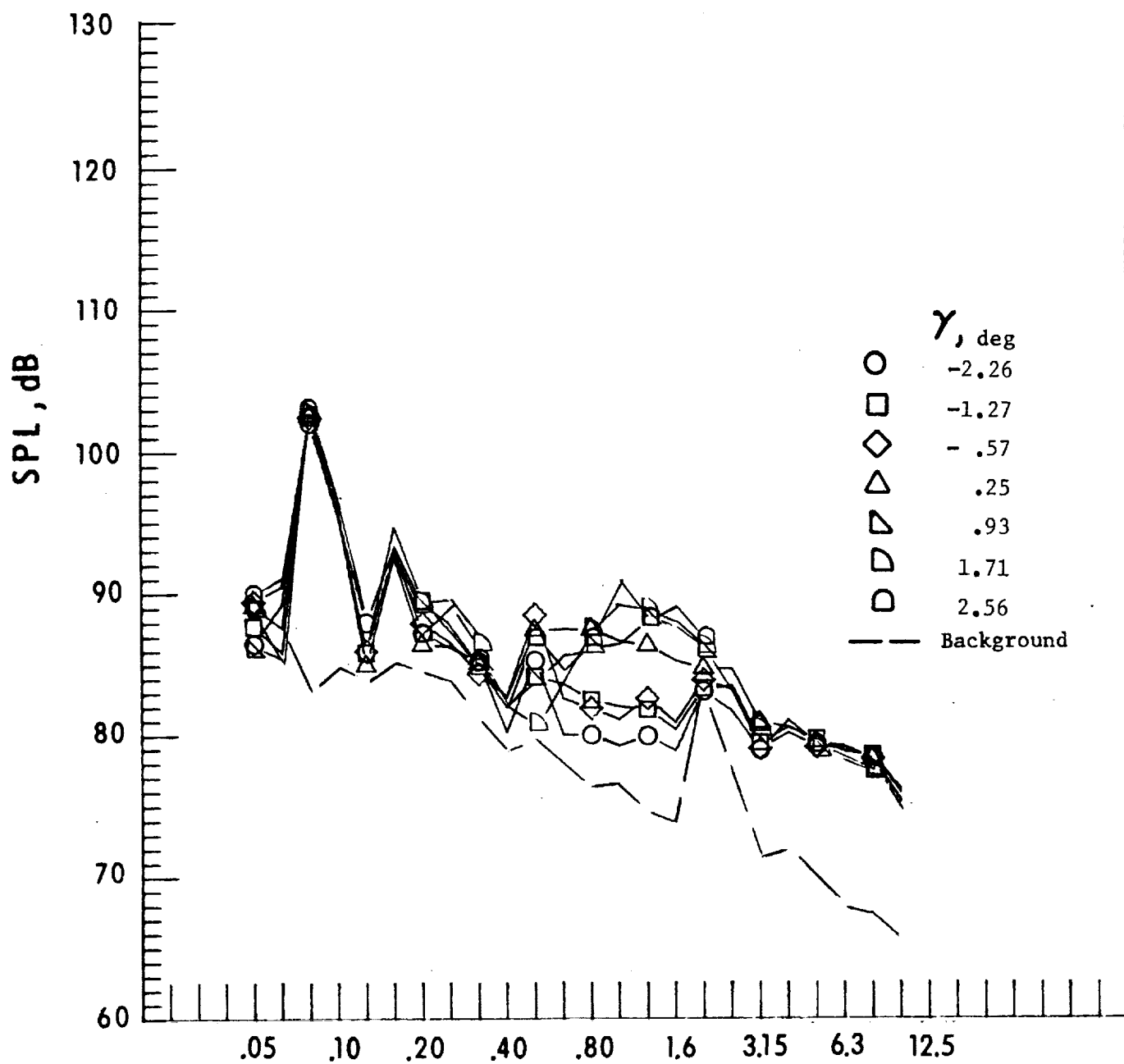
d. Mic. no. 3.

Figure 32. - Continued.



e. Pressure-time-histories, Mic. no. 3

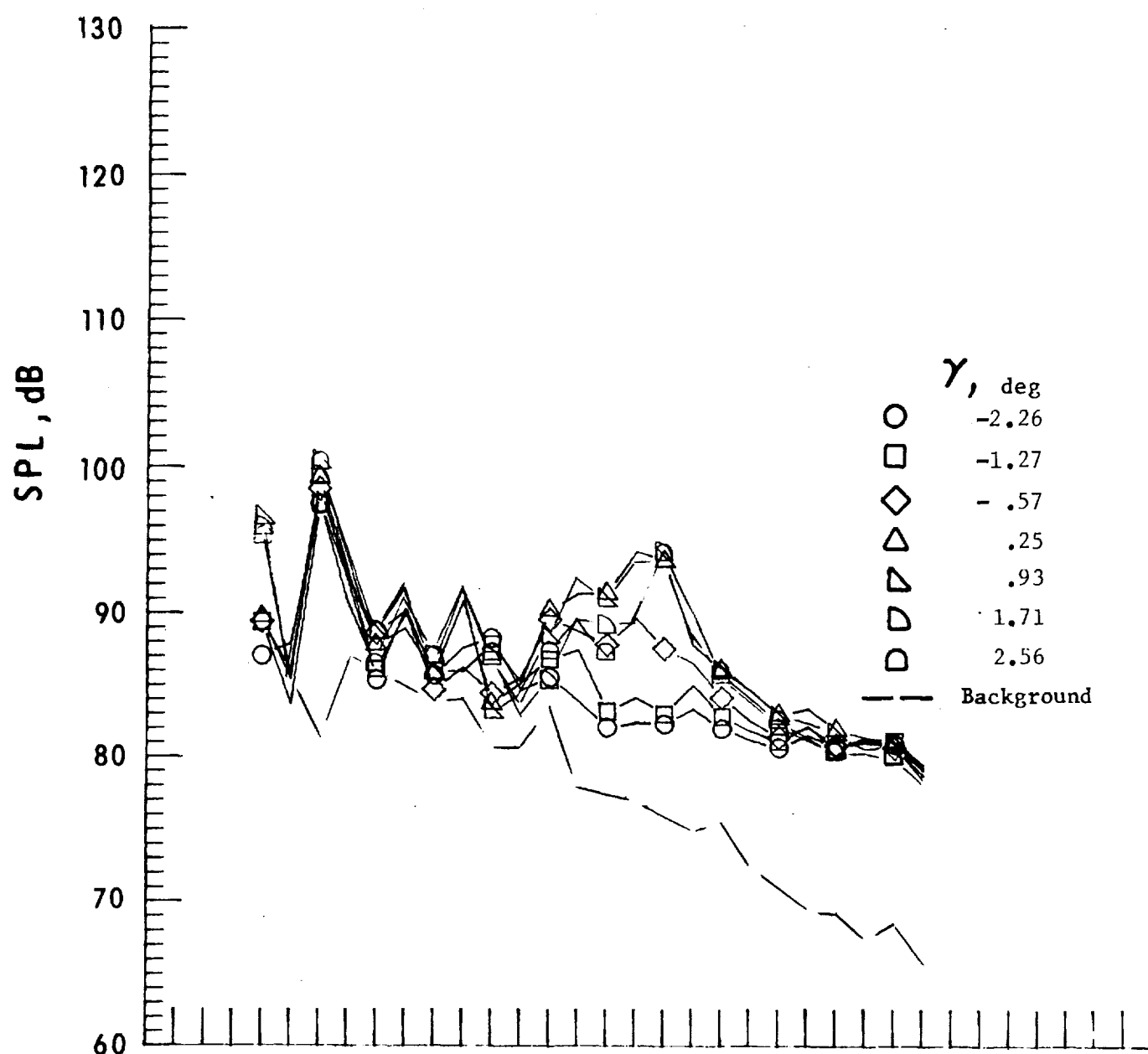
Figure 32. - Continued.



One-third-octave-band center frequency, kHz

f. Mic. no. 4.

Figure 32. - Continued.



One-third-octave-band center frequency, kHz

g. Mic. no. 5.

Figure 32. - Continued.

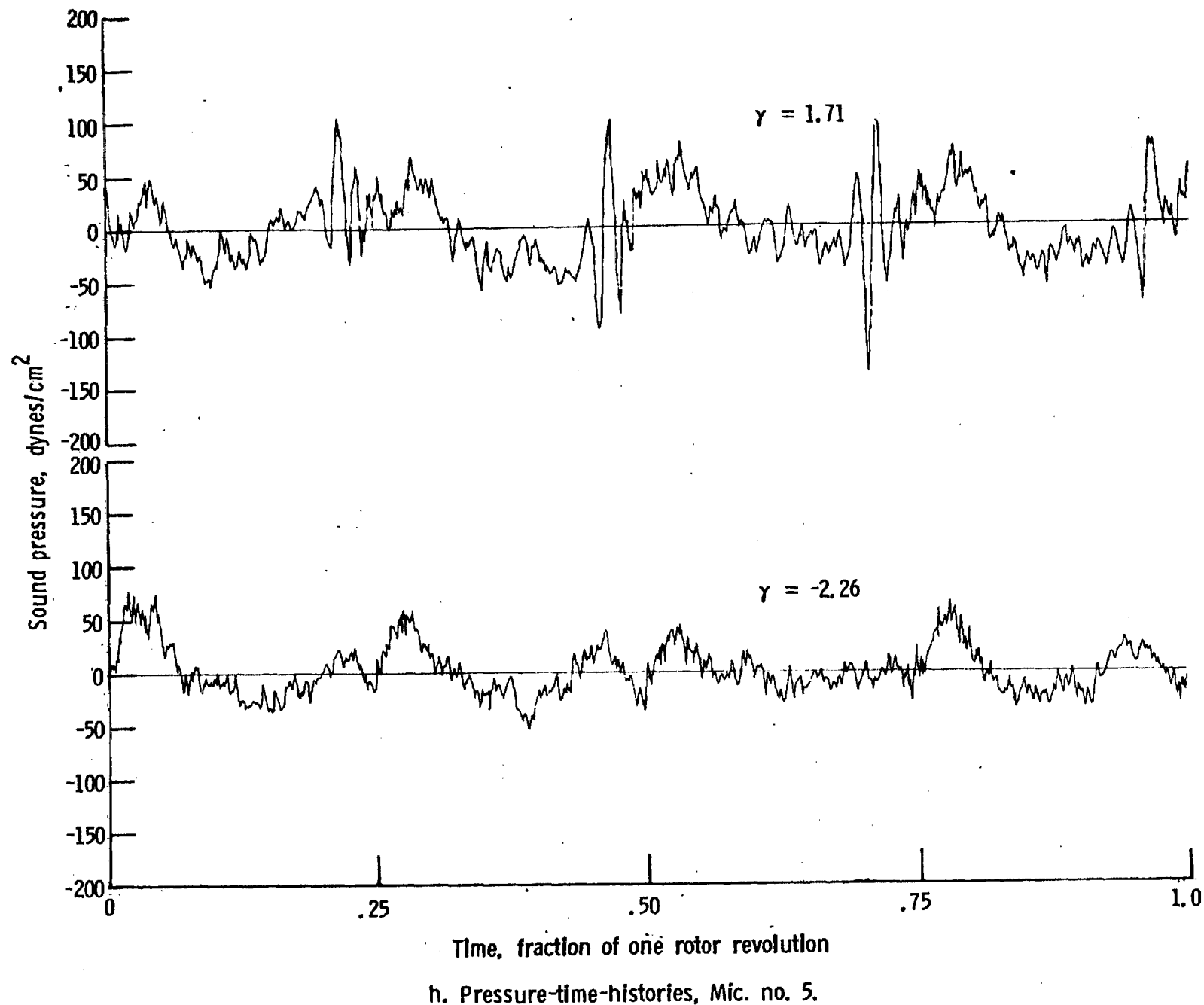
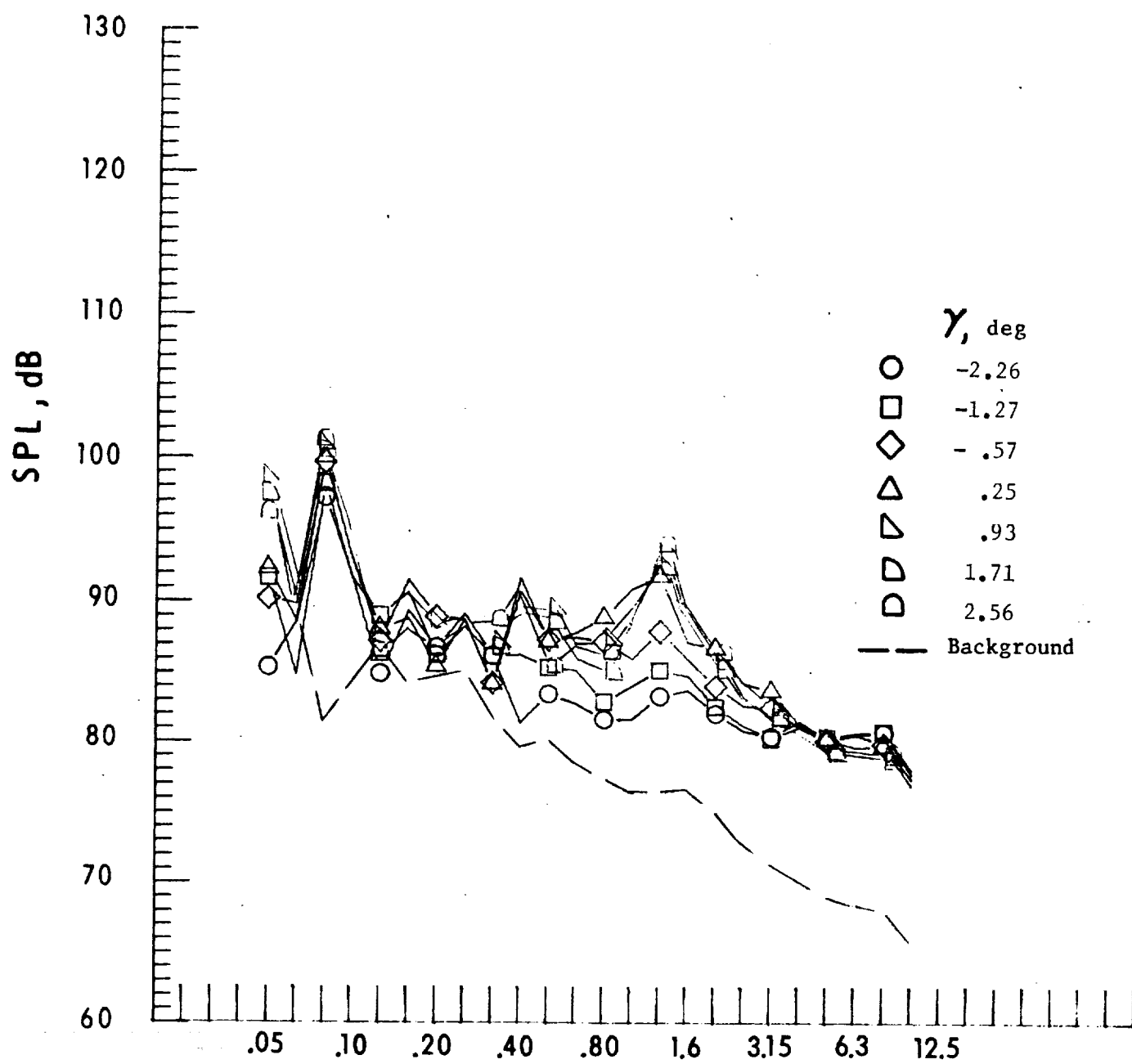


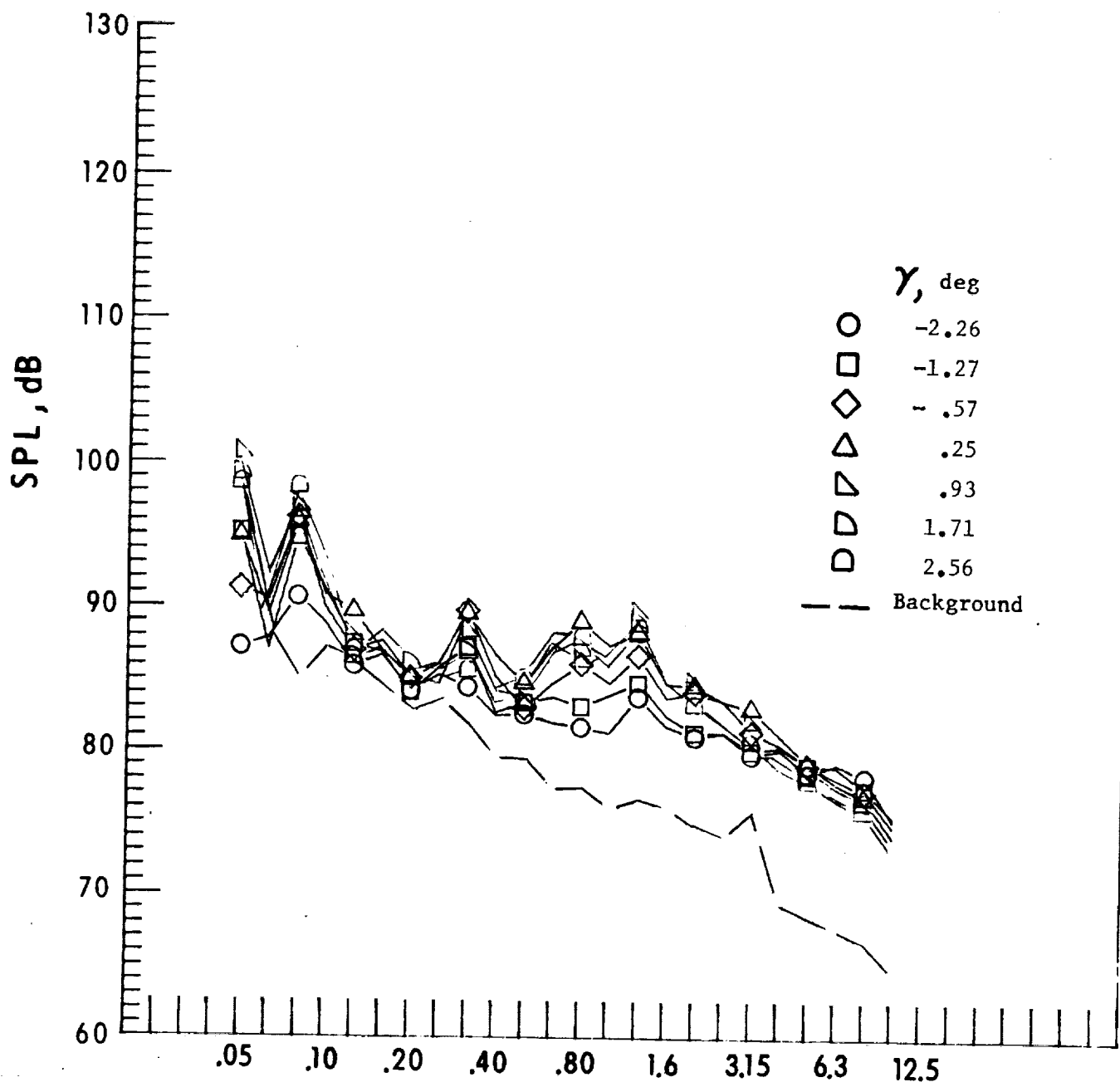
Figure 32. - Continued.



One-third-octave-band center frequency, kHz

i. Mic. no. 6.

Figure 32. - Continued.



One-third-octave-band center frequency, kHz

j. Mic. no. 7.

Figure 32. - Concluded.

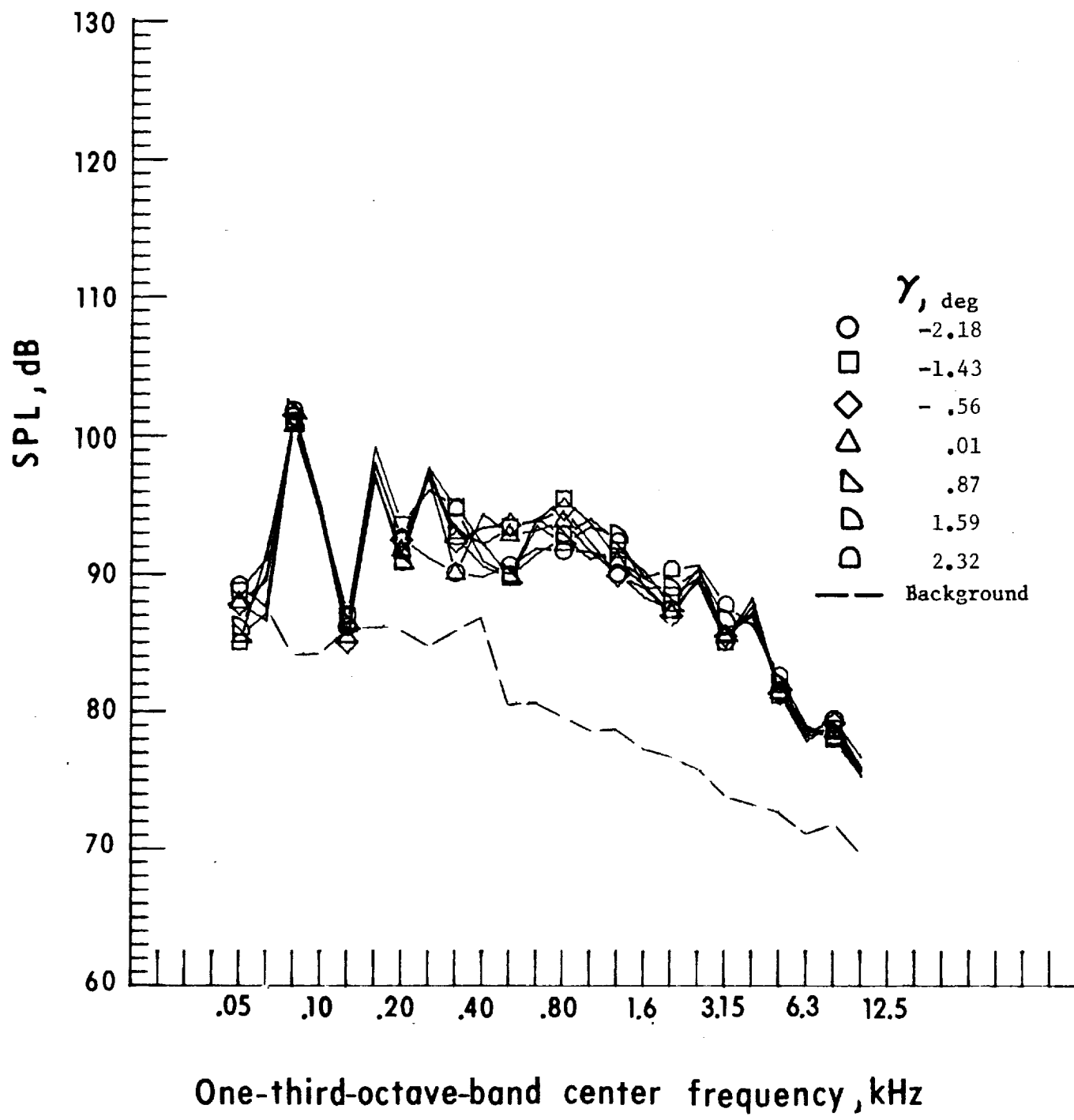
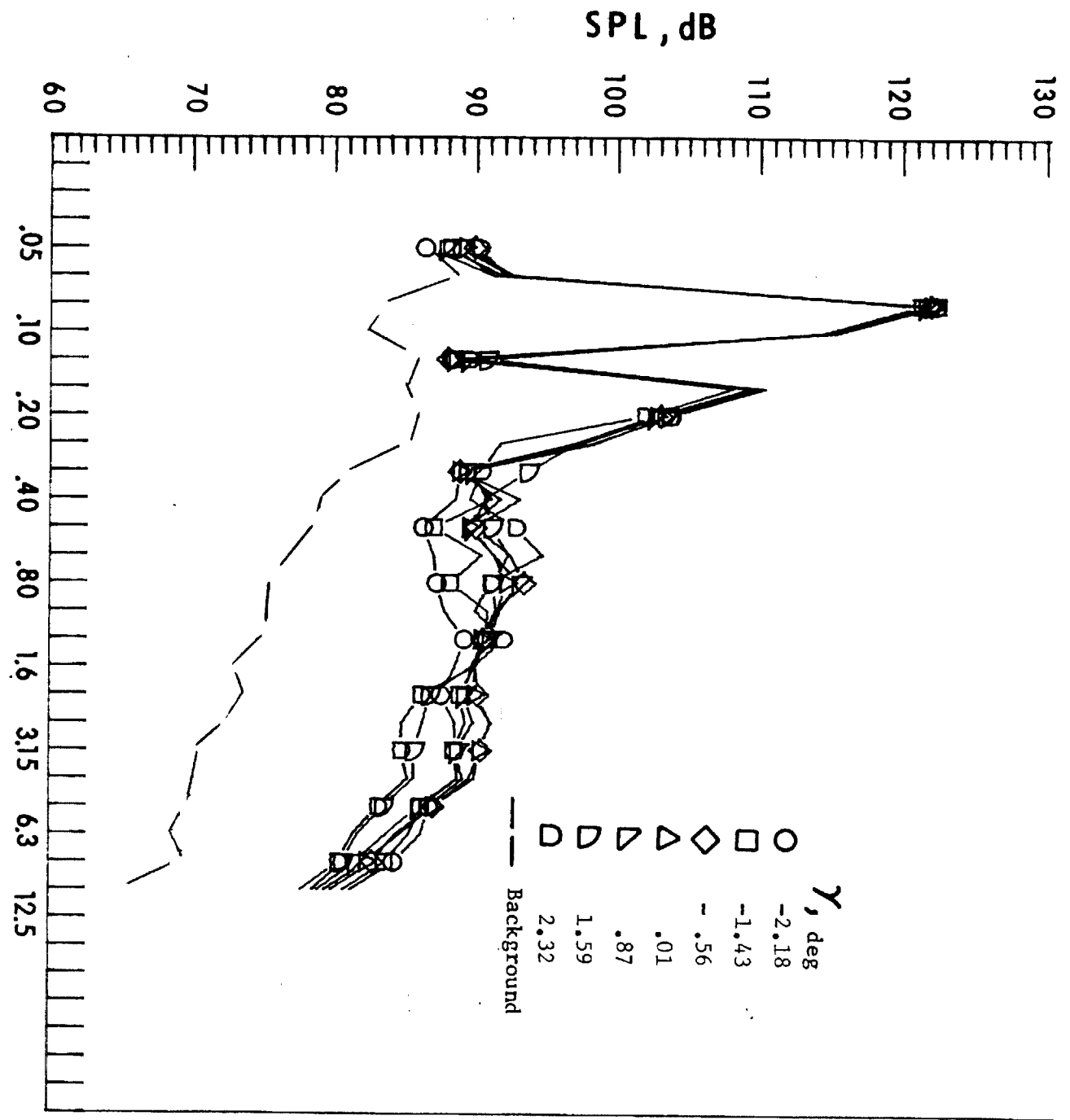


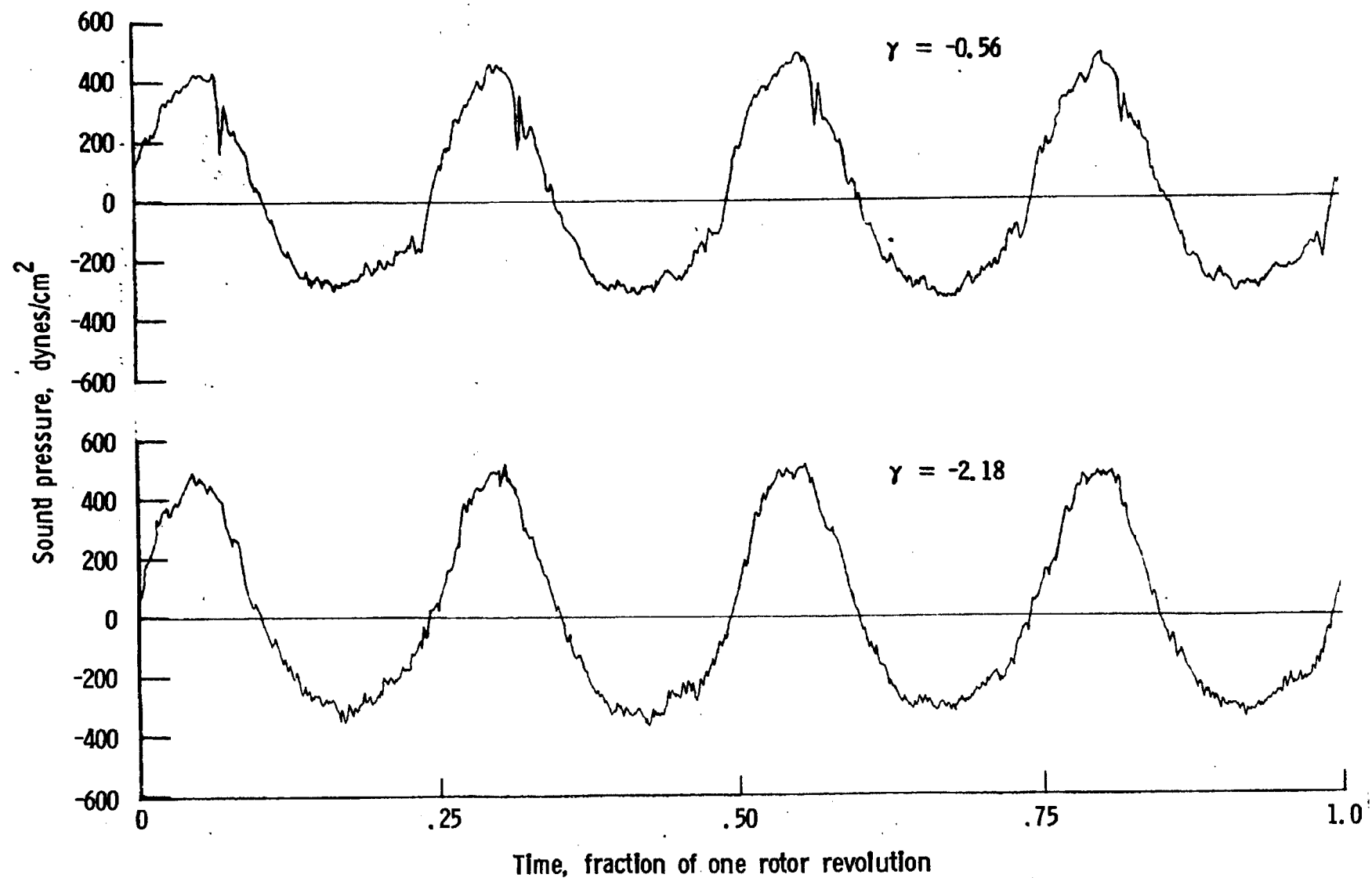
Figure 33. - Effect of descent angle variation on noise generated by helicopter model with swept-tapered tips installed. $V_\infty = 70.9$ knots.



One-third-octave-band center frequency, kHz

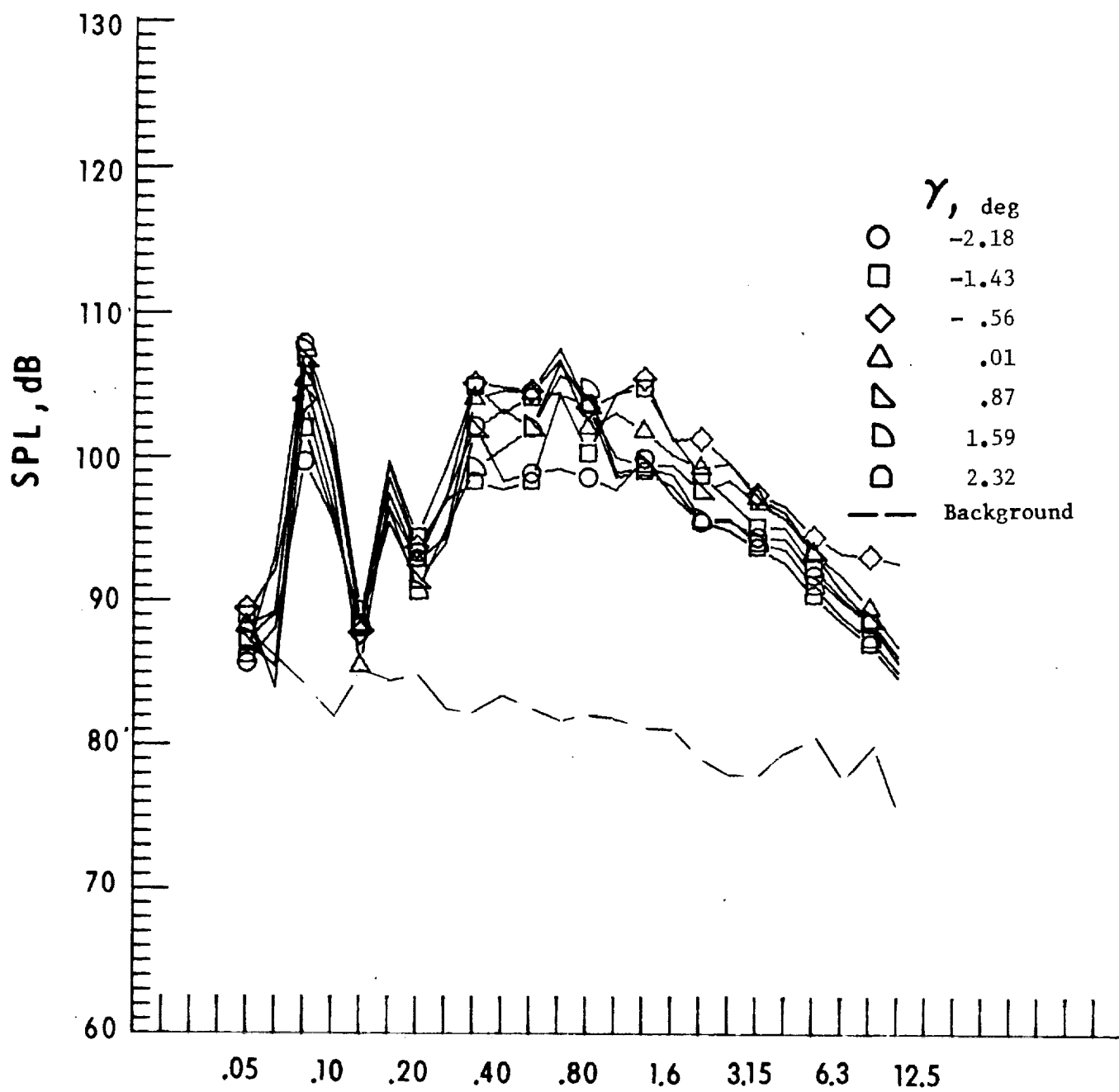
b. Mic. no. 2.

Figure 33. - Continued.



c. Pressure-time-histories, Mic. no. 2.

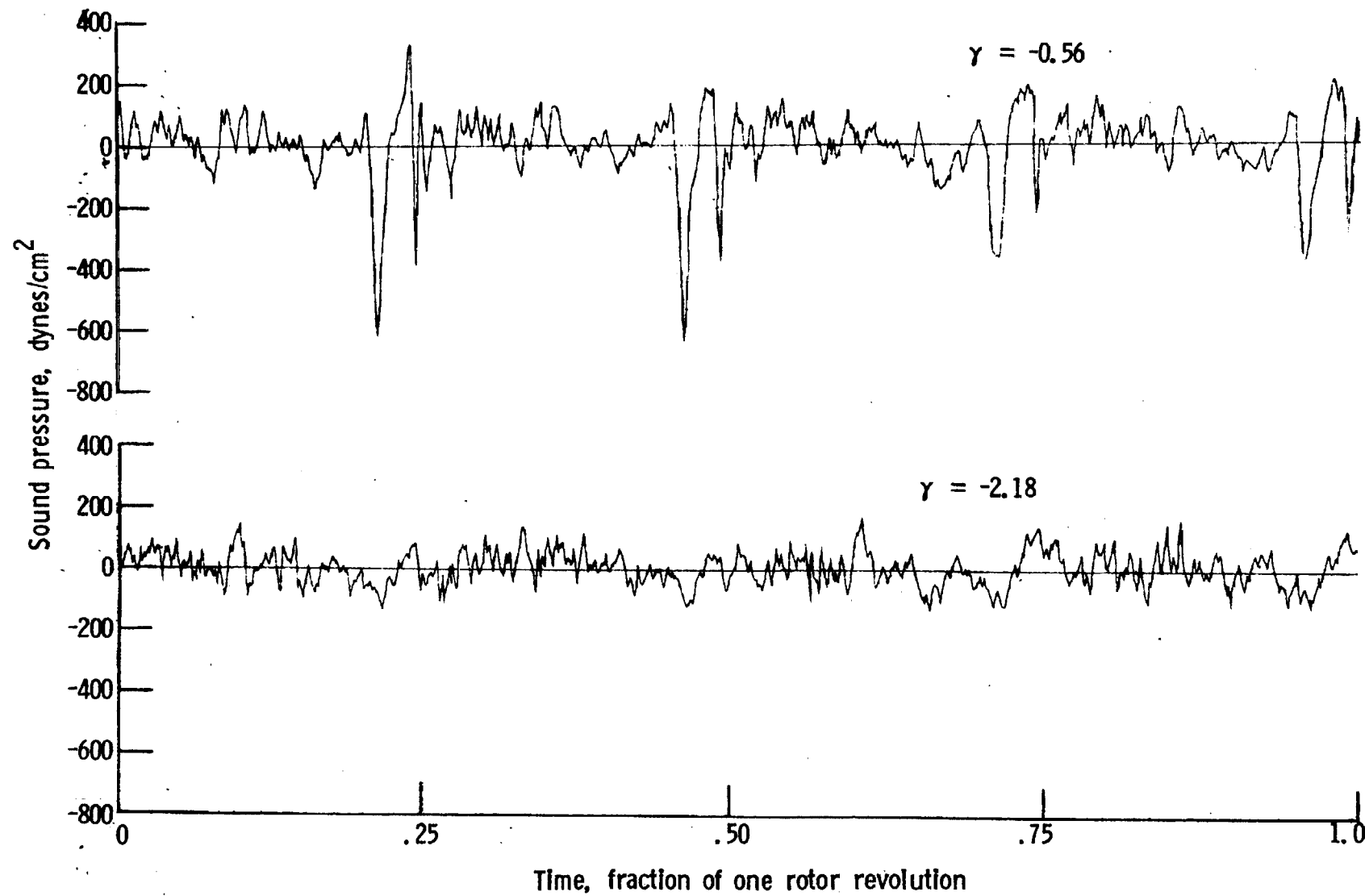
Figure 33. - Continued.



One-third-octave-band center frequency, kHz

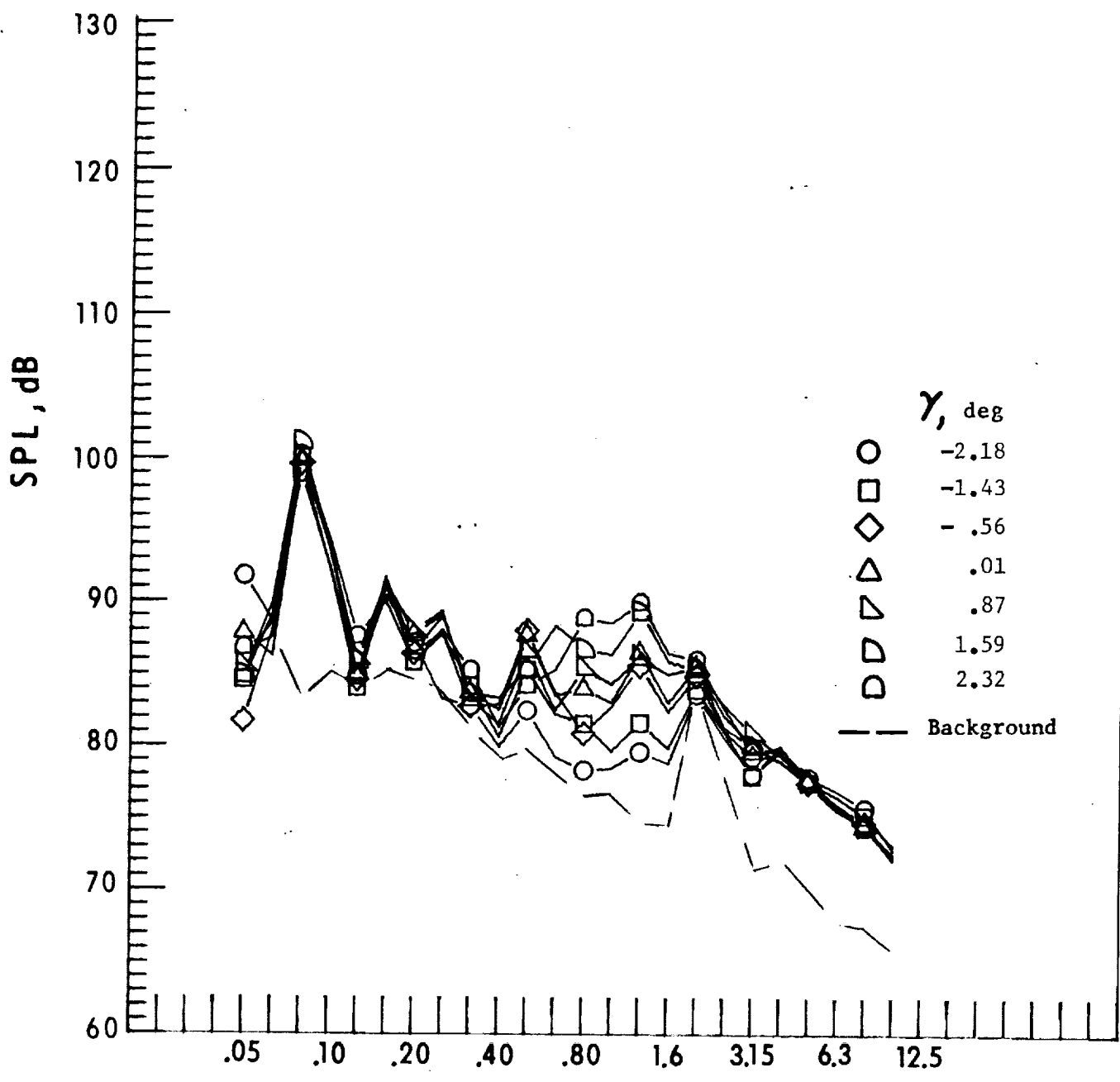
d. Mic. no. 3.

Figure 33. - Continued.



e. Pressure-time-histories, Mic. no. 3

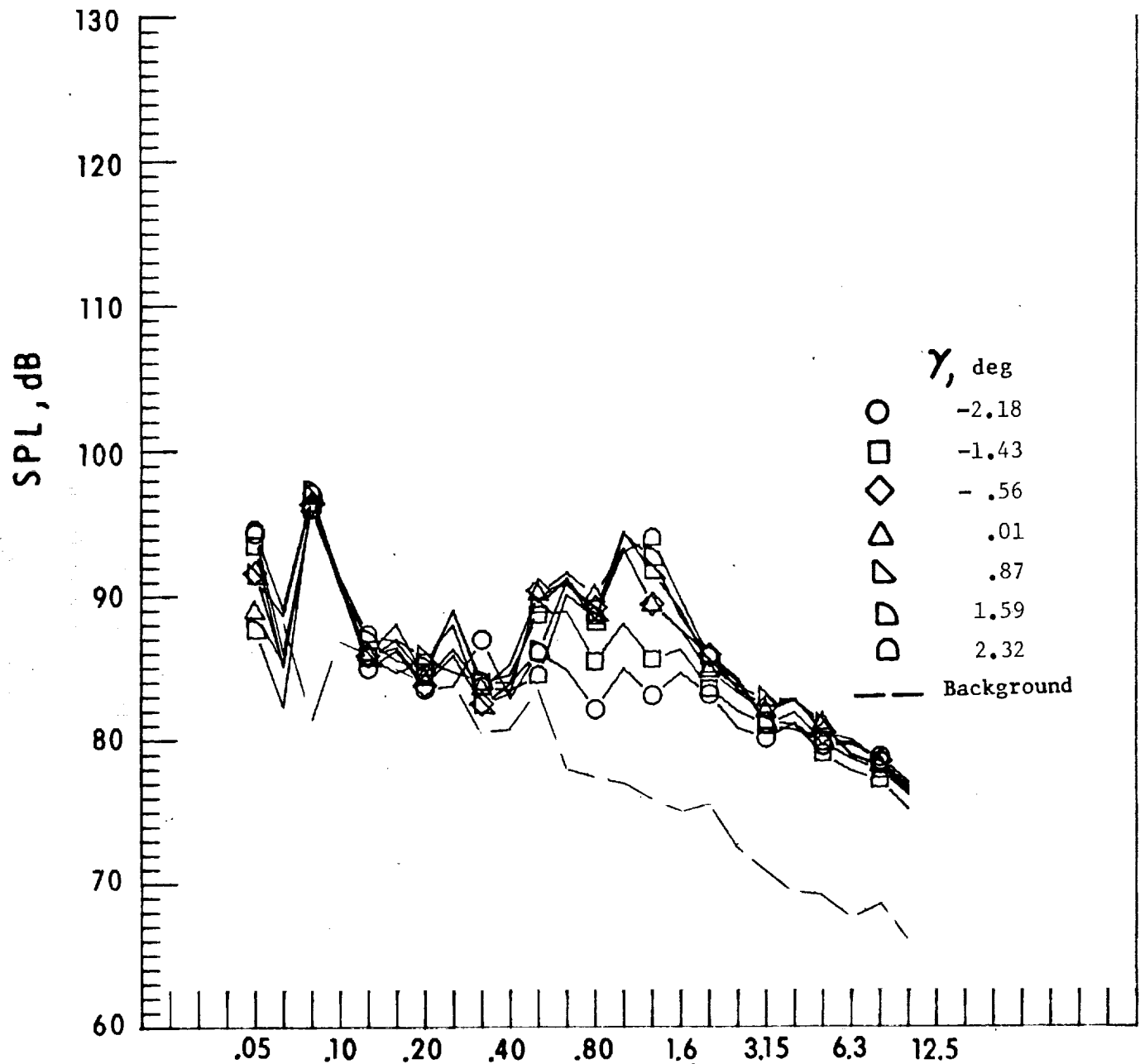
Figure 33. - Continued.



One-third-octave-band center frequency, kHz

f. Mic. no. 4.

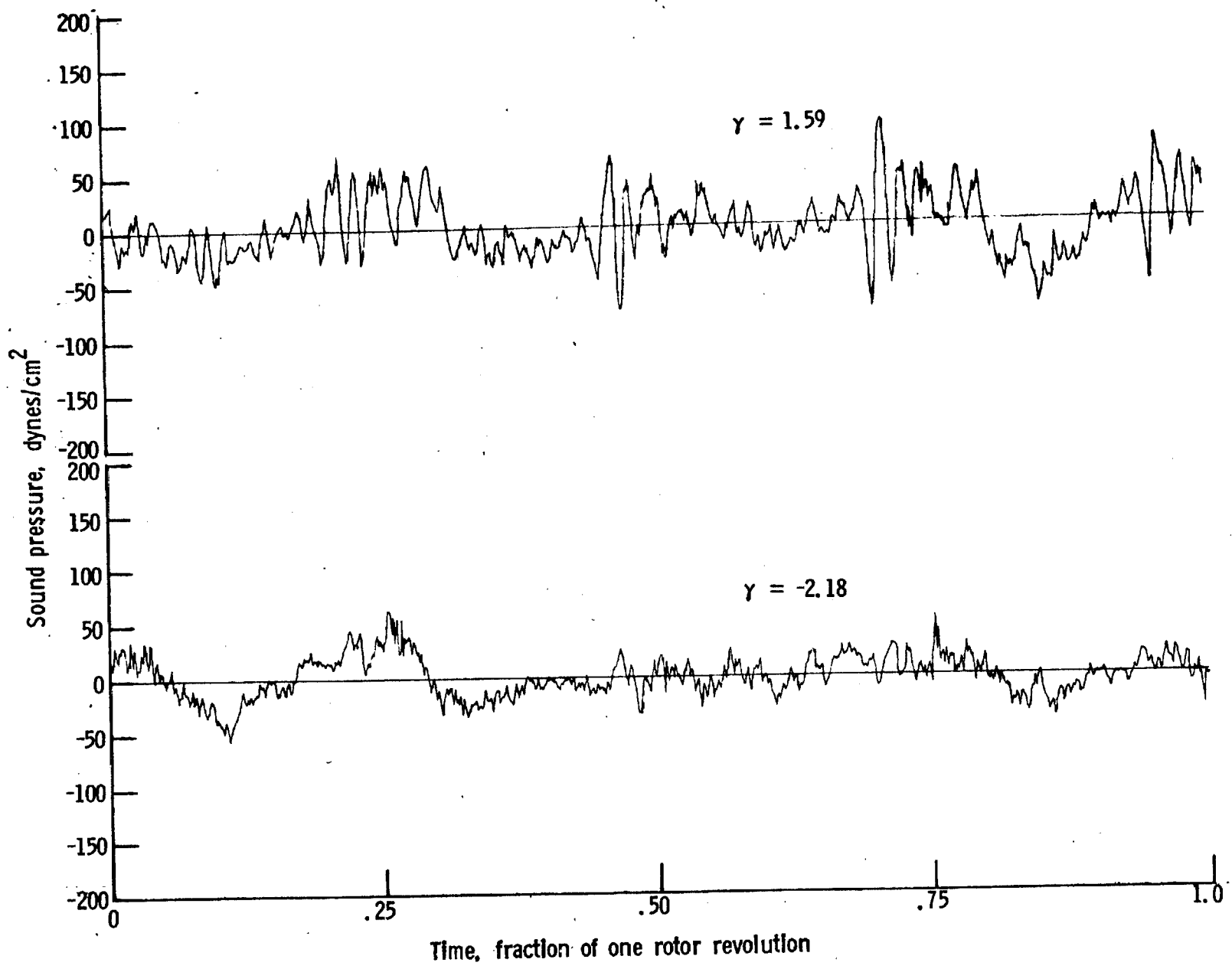
Figure 33.-Continued.



One-third-octave-band center frequency, kHz

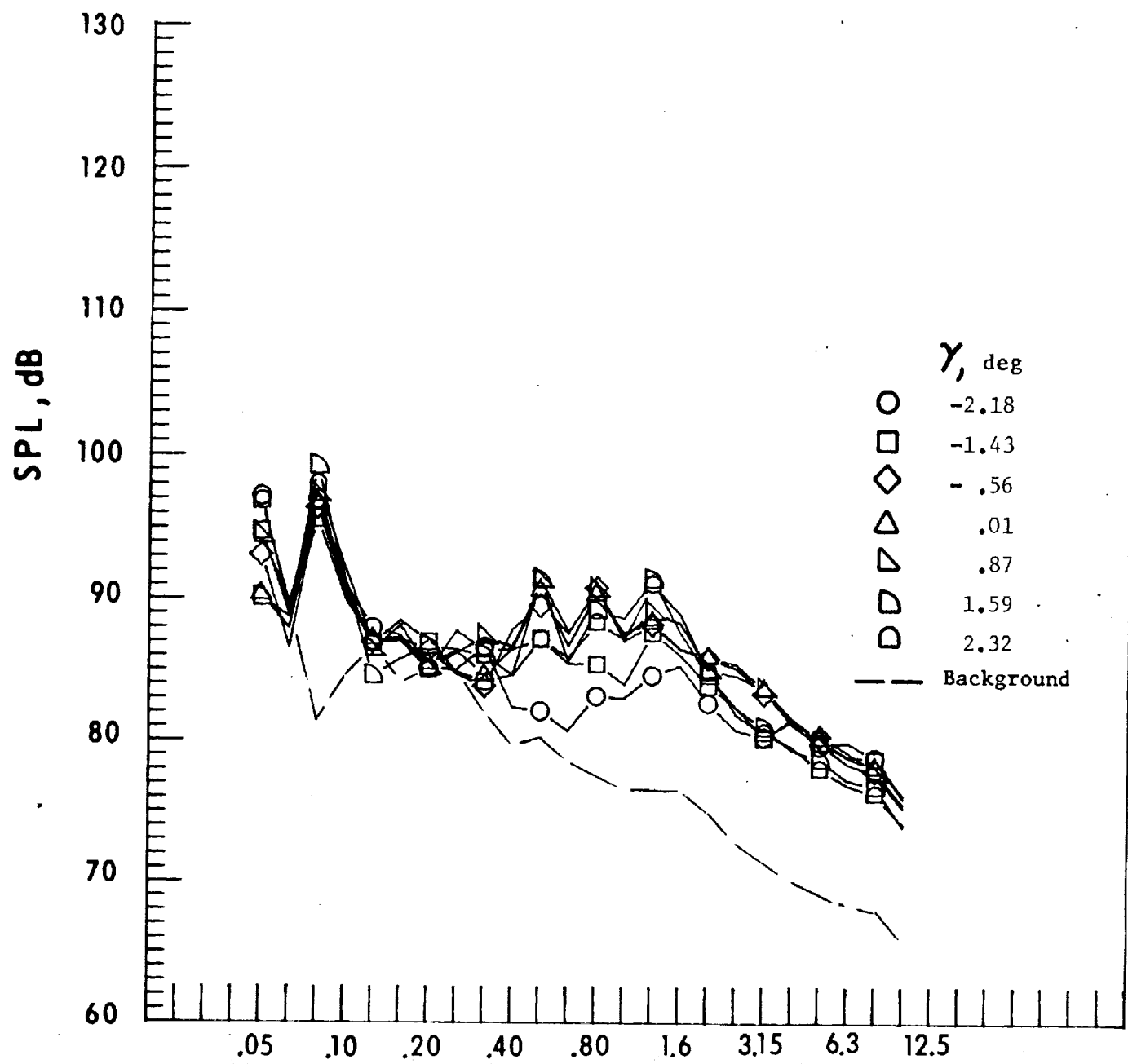
g. Mic. no. 5.

Figure 33. - Continued.



h. Pressure-time-histories, Mic. no. 5.

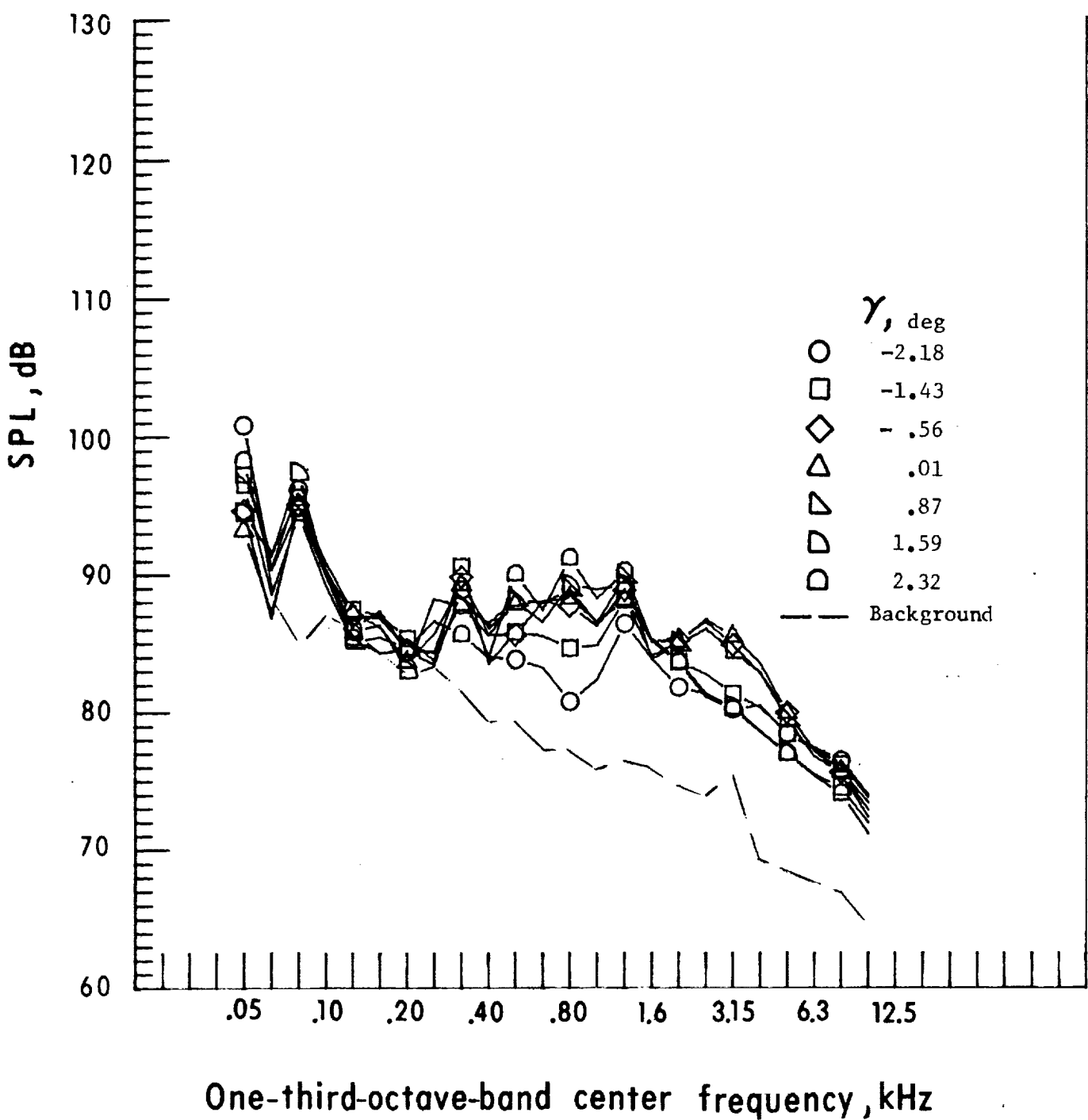
Figure 33. - Continued.



One-third-octave-band center frequency, kHz

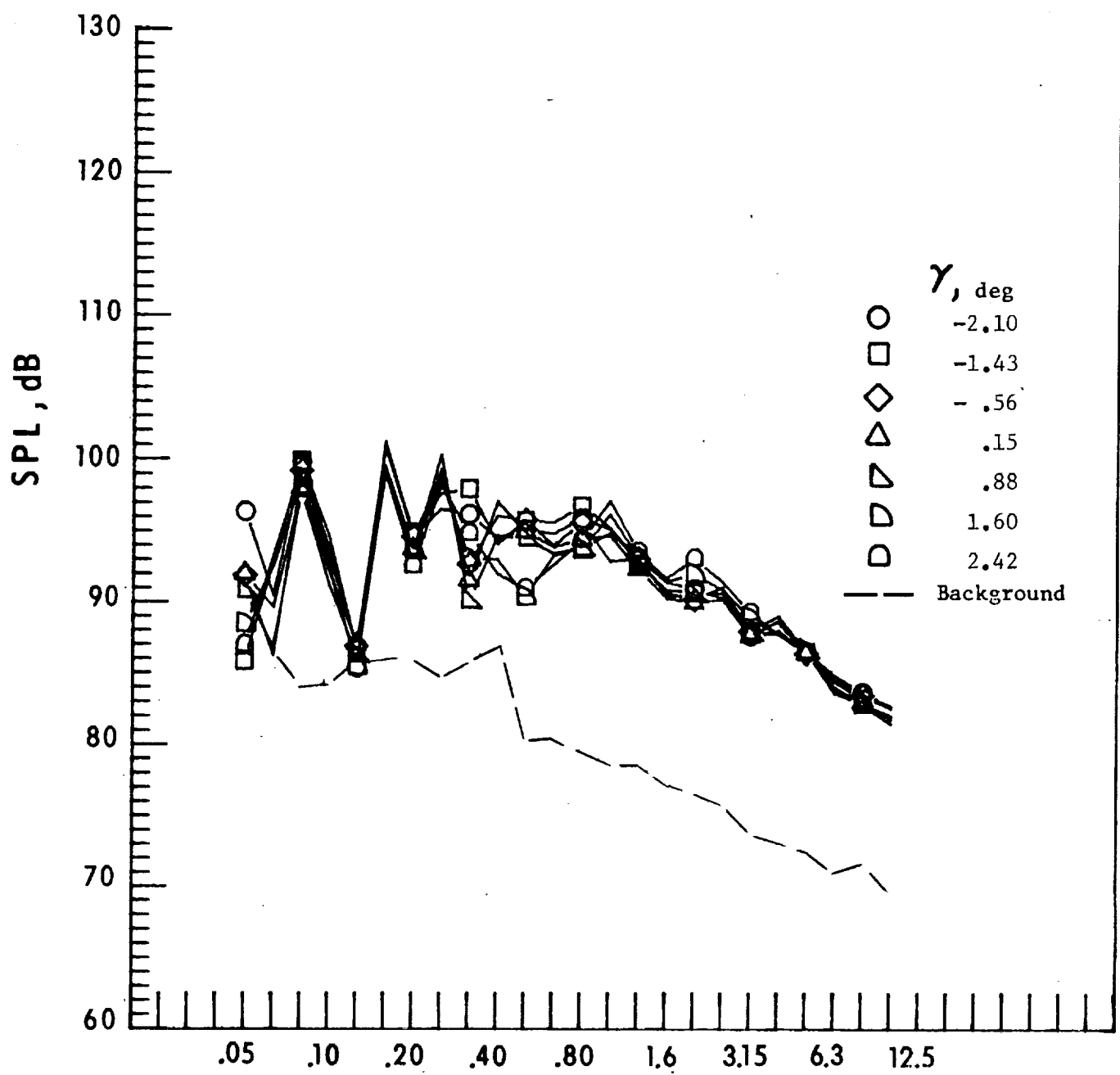
i. Mic. no. 6.

Figure 33. - Continued.



j. Mic. no. 7.

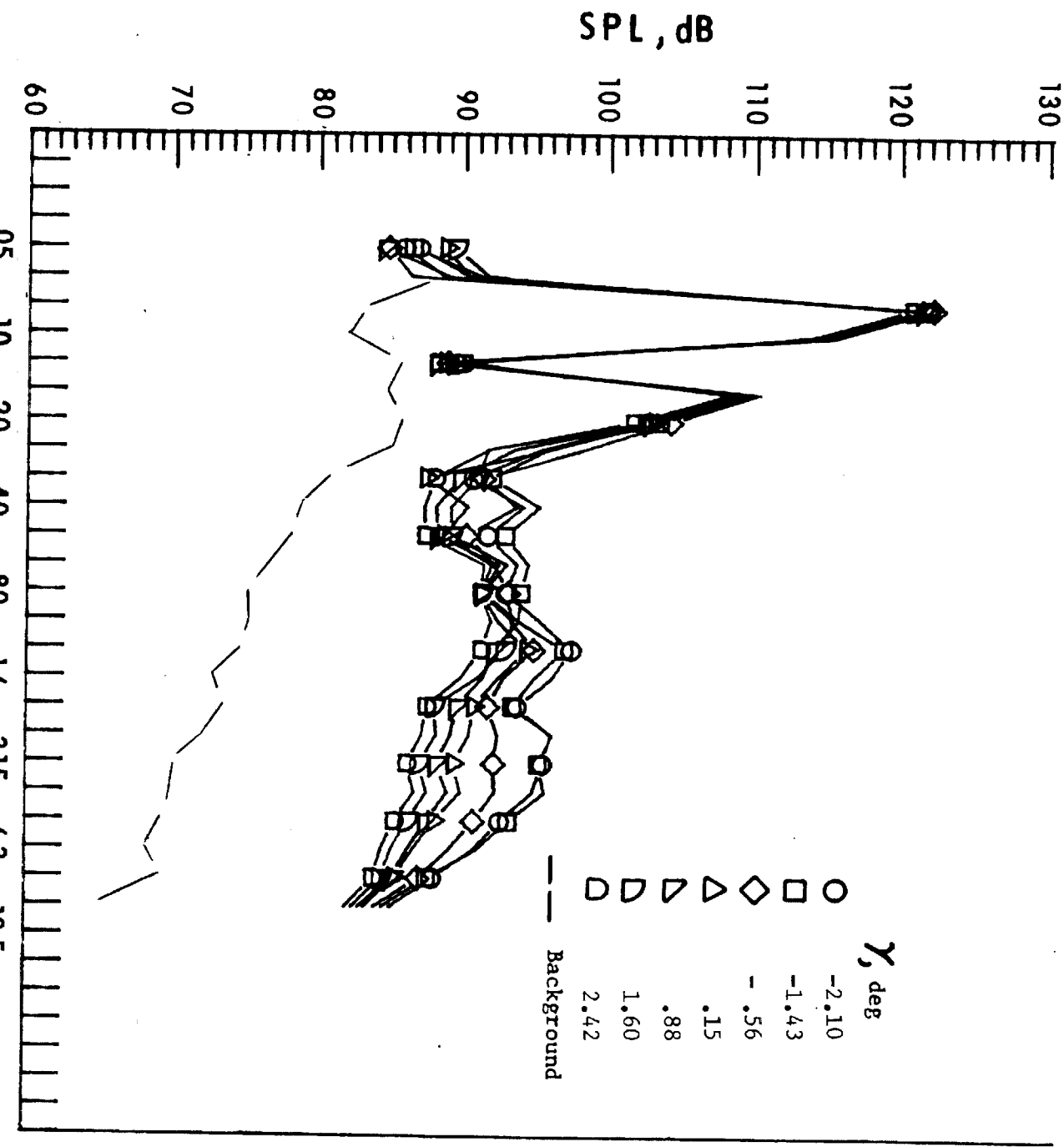
Figure 33. - Concluded.



One-third-octave-band center frequency, kHz

a. Mic. no. 1.

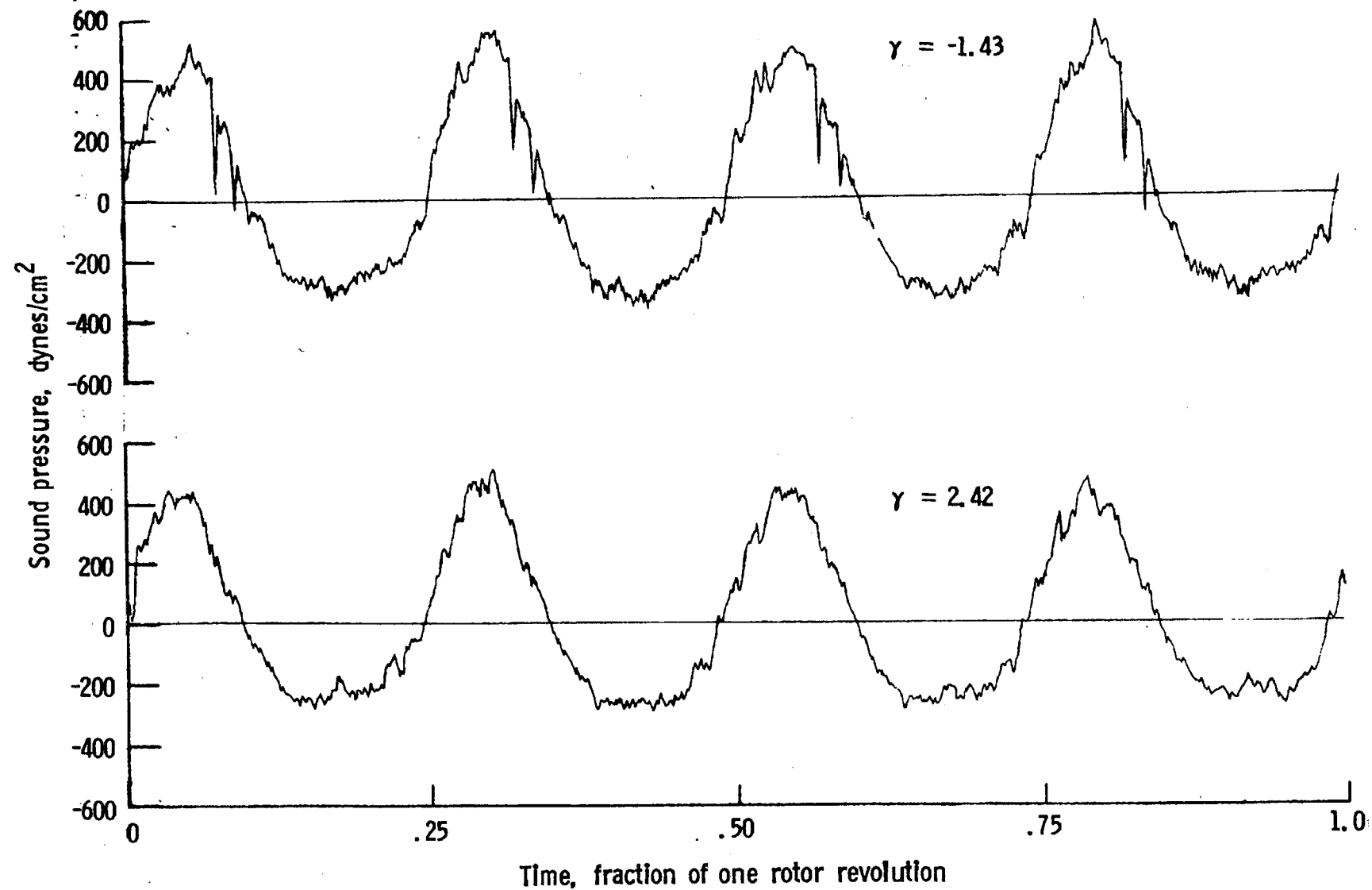
Figure 34. - Effect of descent angle variation on noise generated by helicopter model with end-plate tips installed. $V_\infty = 71.2$ knots.



One-third-octave-band center frequency, kHz

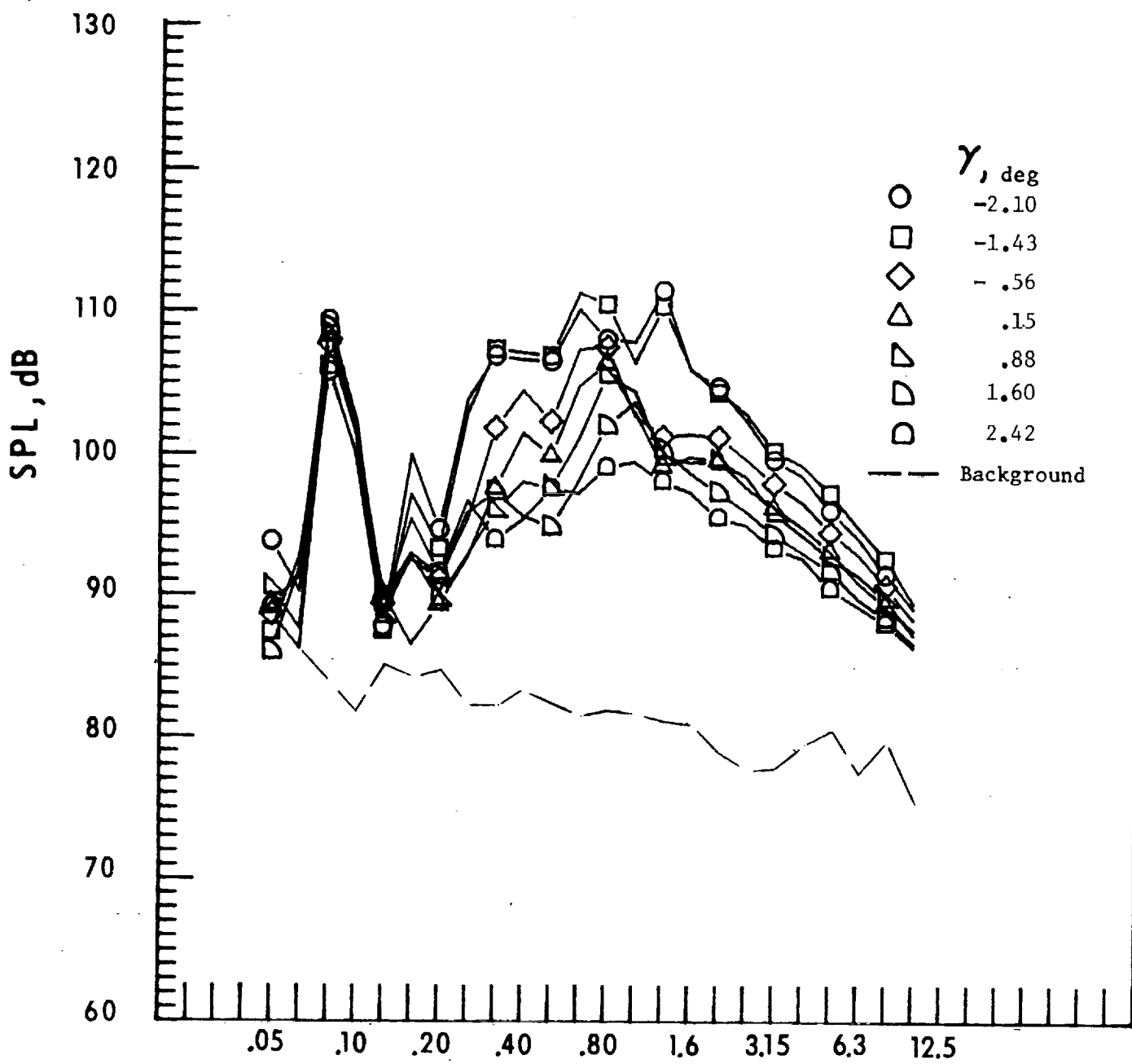
b. Mic. no. 2

Figure 34. - Continued.



c. Pressure-time-histories, Mic. no. 2.

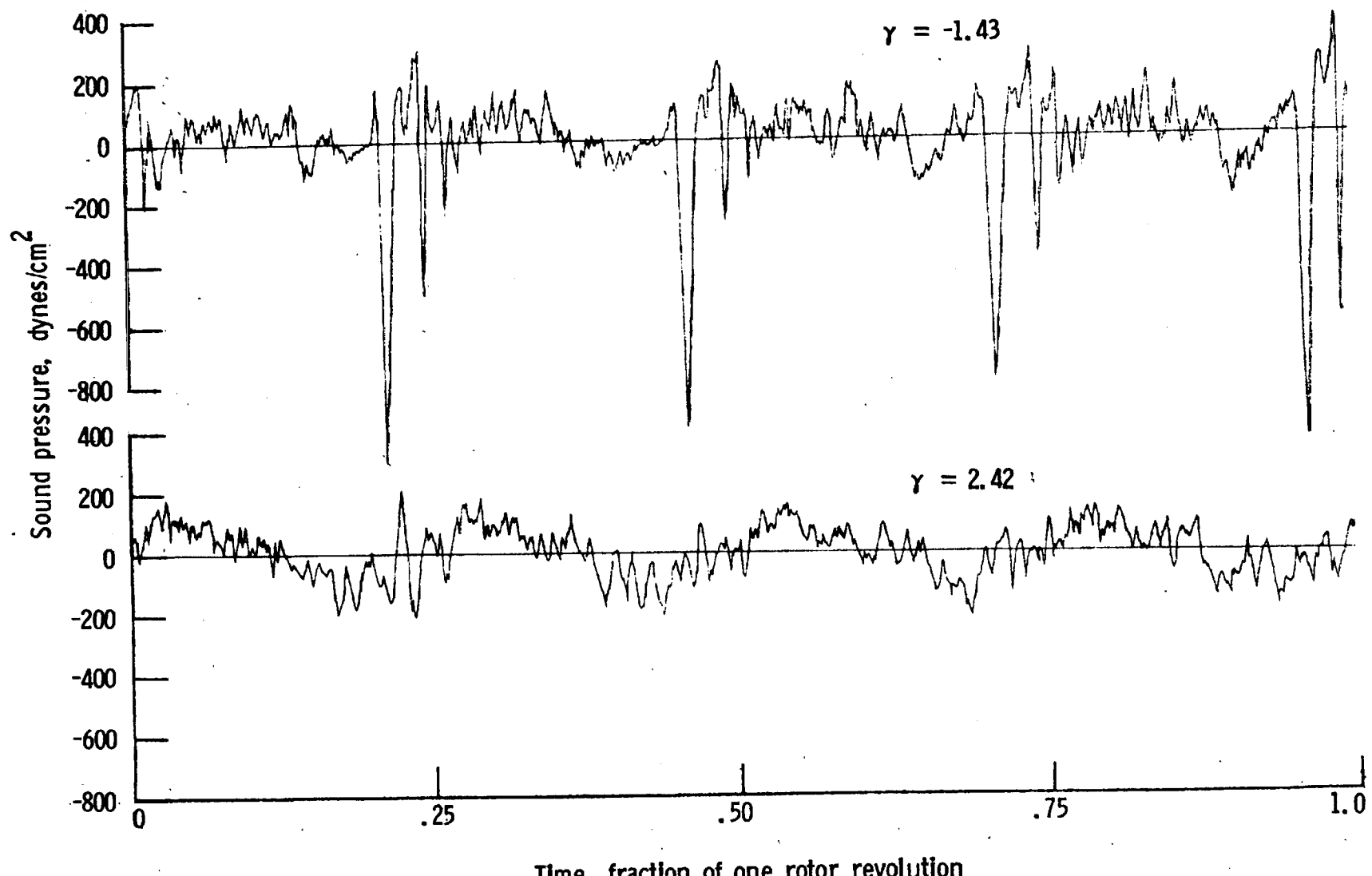
Figure 34. - Continued.



One-third-octave-band center frequency, kHz

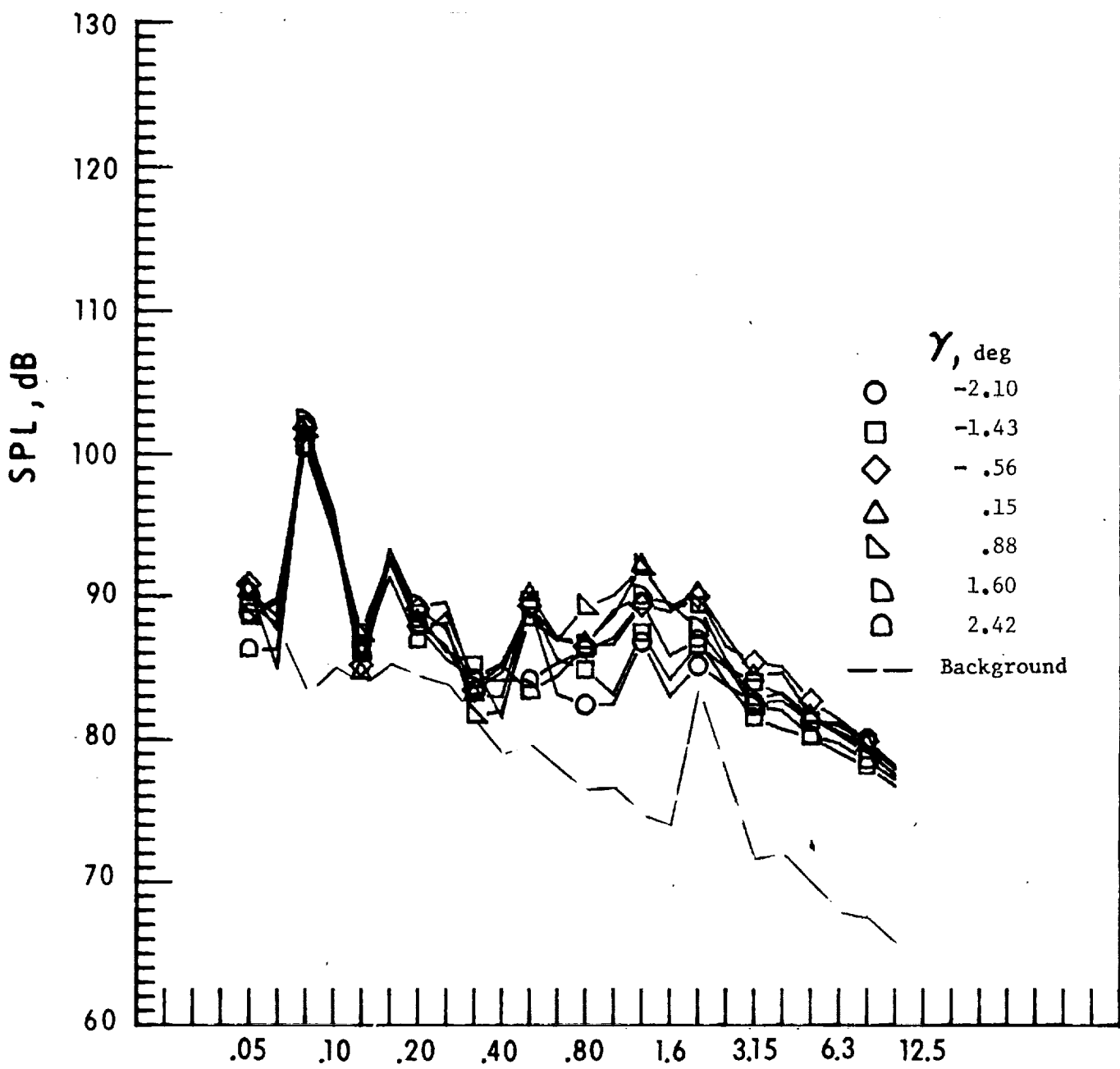
d. Mic. no. 3.

Figure 34. - Continued



e. Pressure-time-histories, Mic. no. 3.

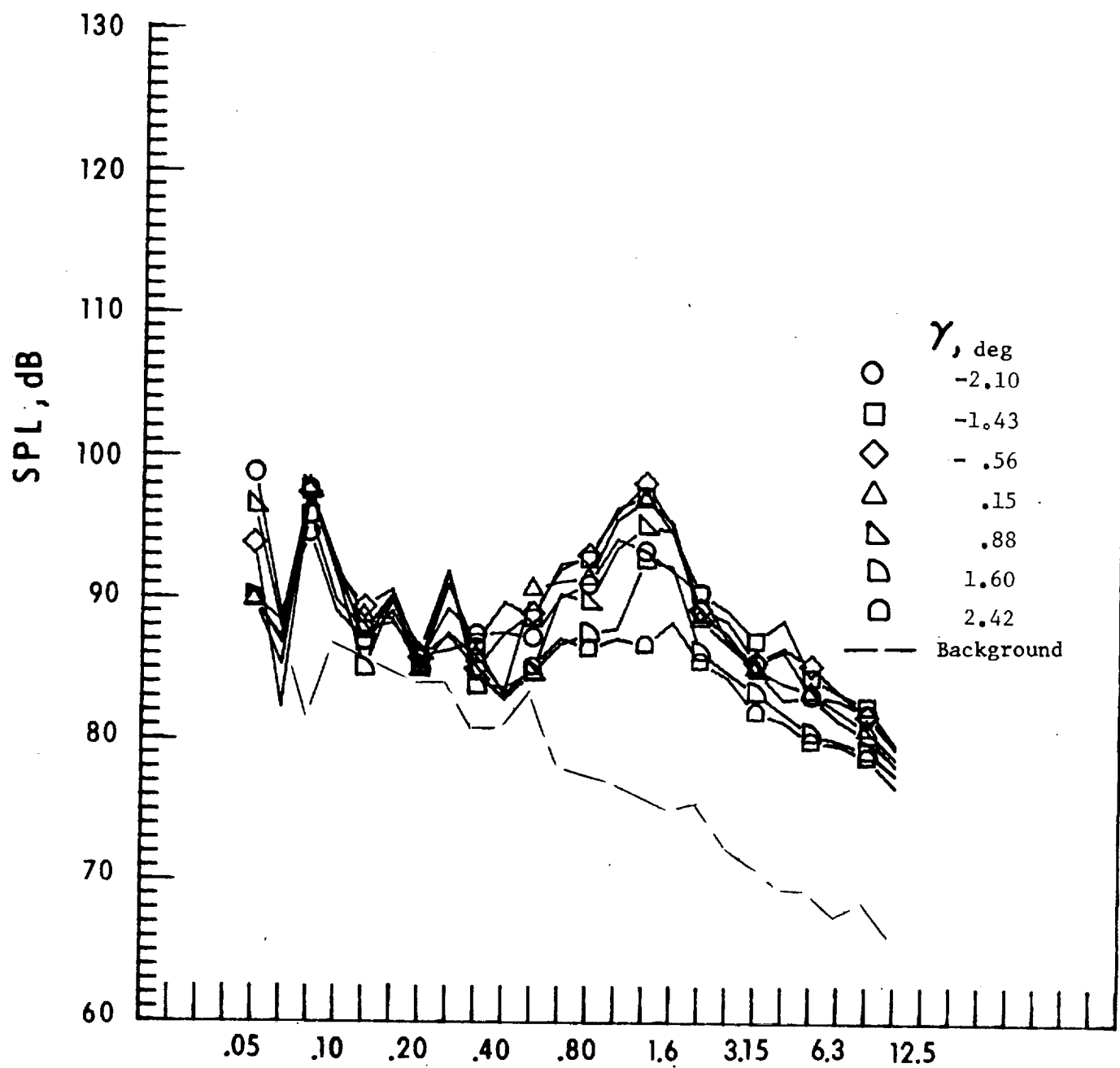
Figure 34. - Continued.



One-third-octave-band center frequency, kHz

f. Mic. no. 4.

Figure 34. - Continued.



One-third-octave-band center frequency, kHz

g. Mic. no. 5.

Figure 34. - Continued.

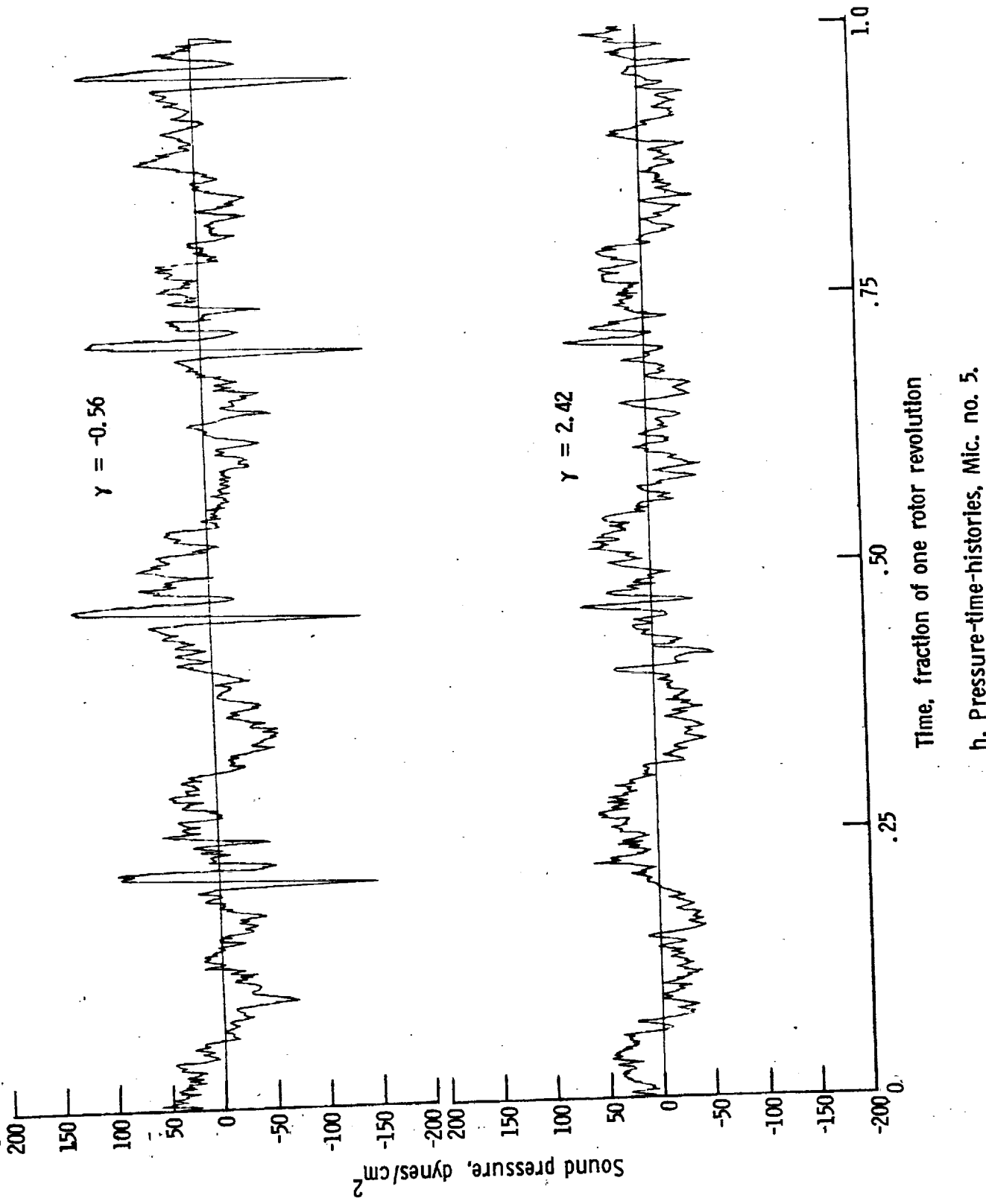
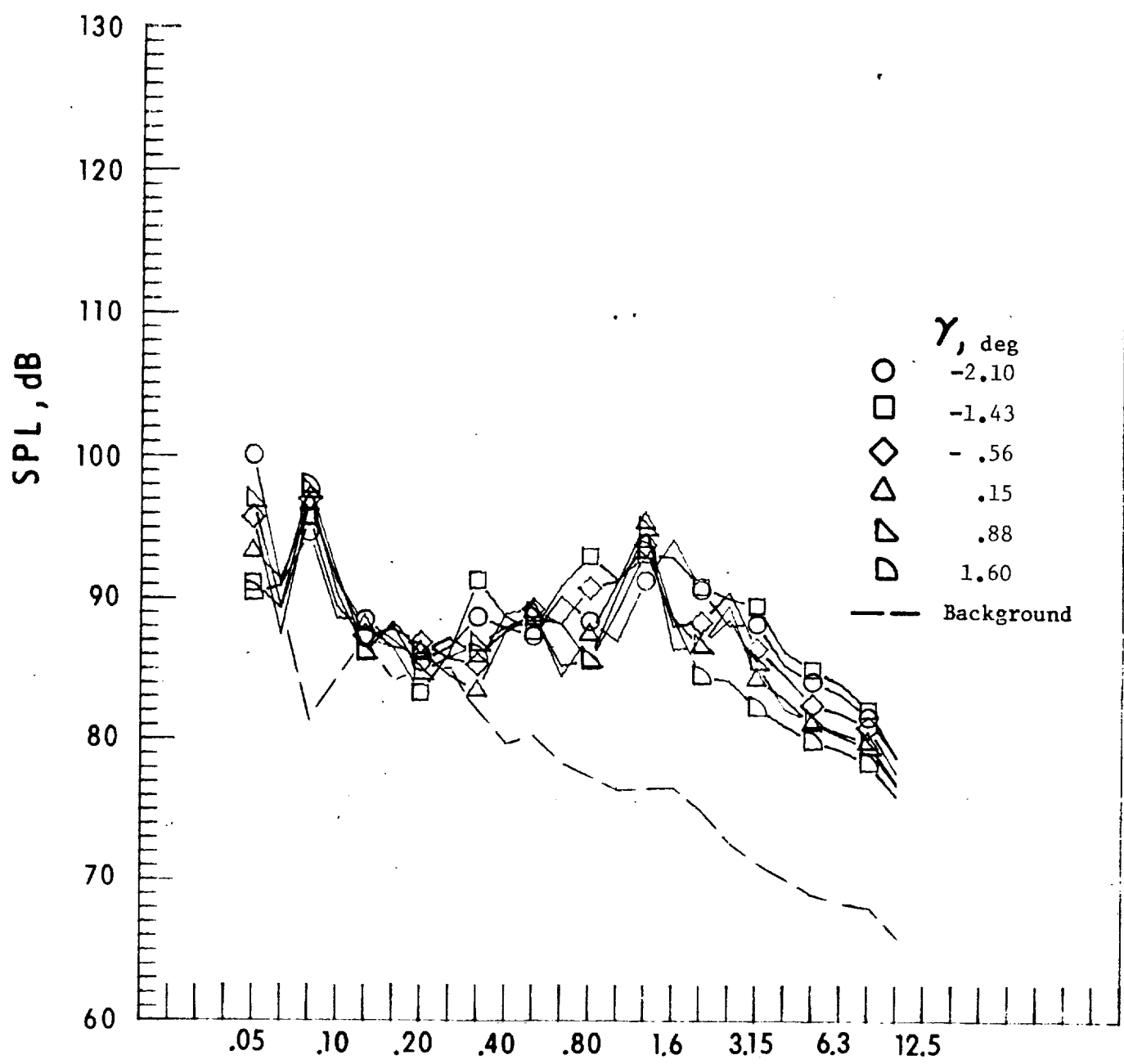


Figure 34. - Continued.

h. Pressure-time-histories, Mic. no. 5.

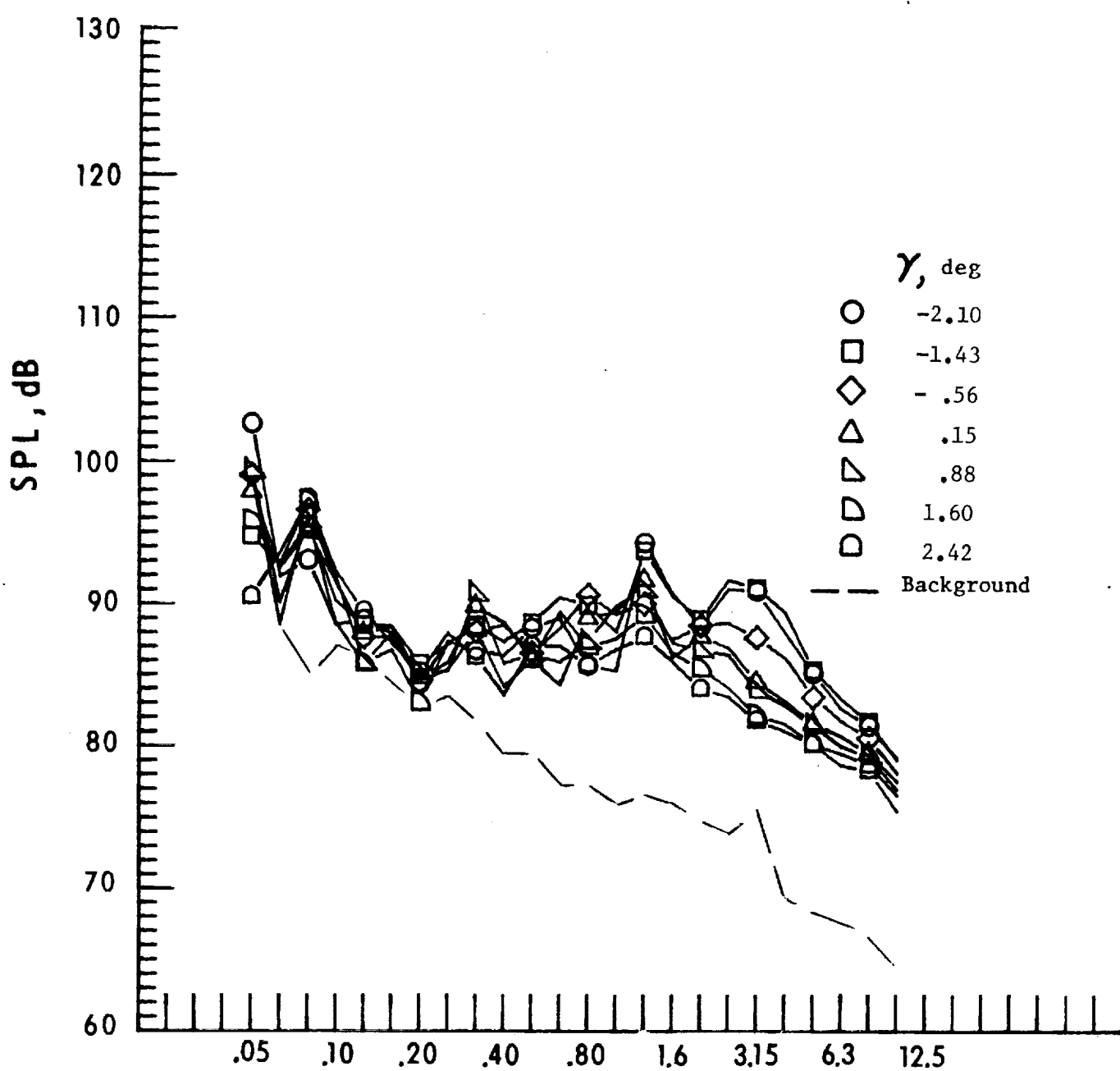
Time, fraction of one rotor revolution



One-third-octave-band center frequency, kHz

i. Mic. no. 6.

Figure 34. - Continued.

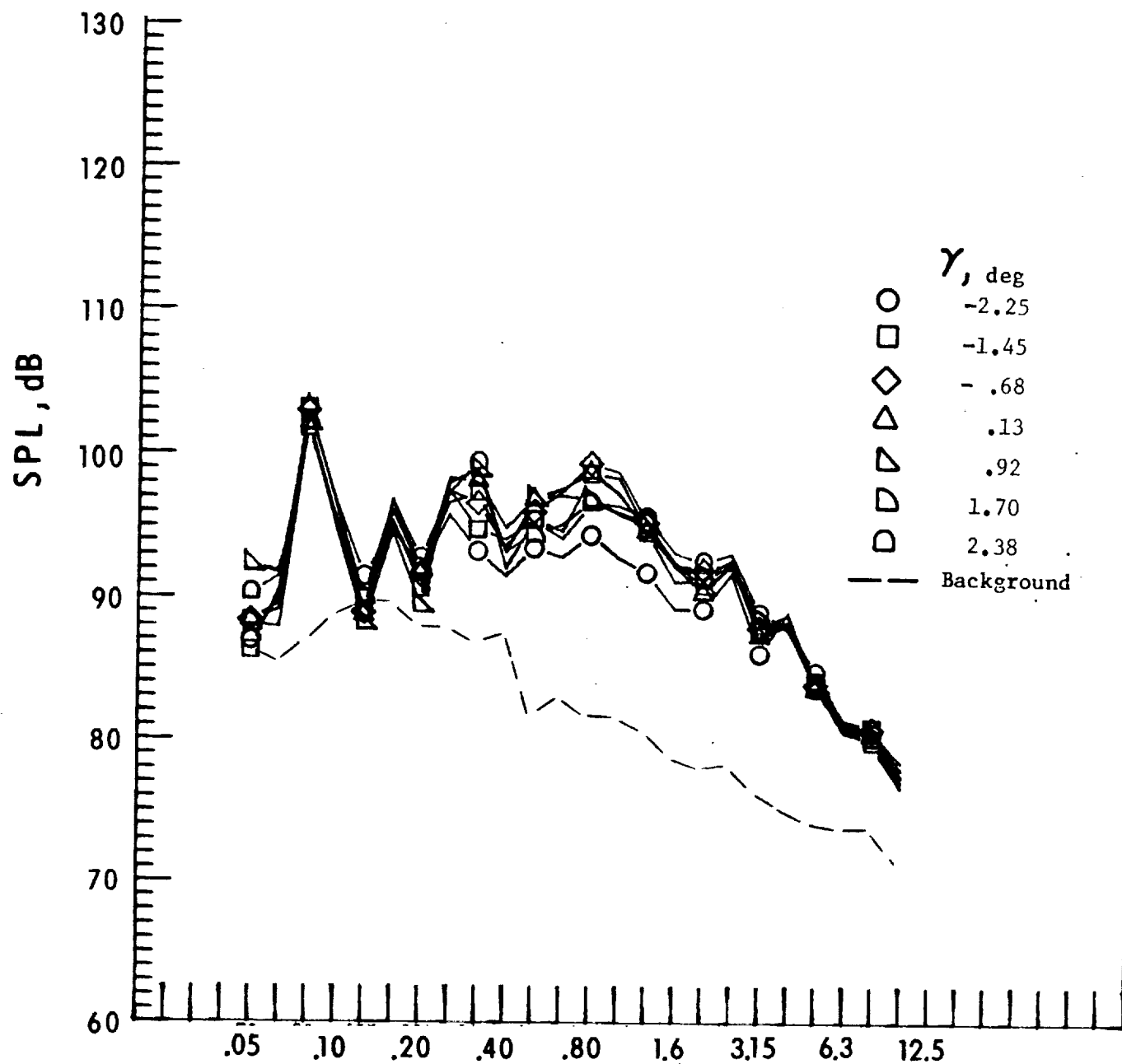


One-third-octave-band center frequency, kHz

j. Mic. no. 7.

Figure 34. - Concluded.

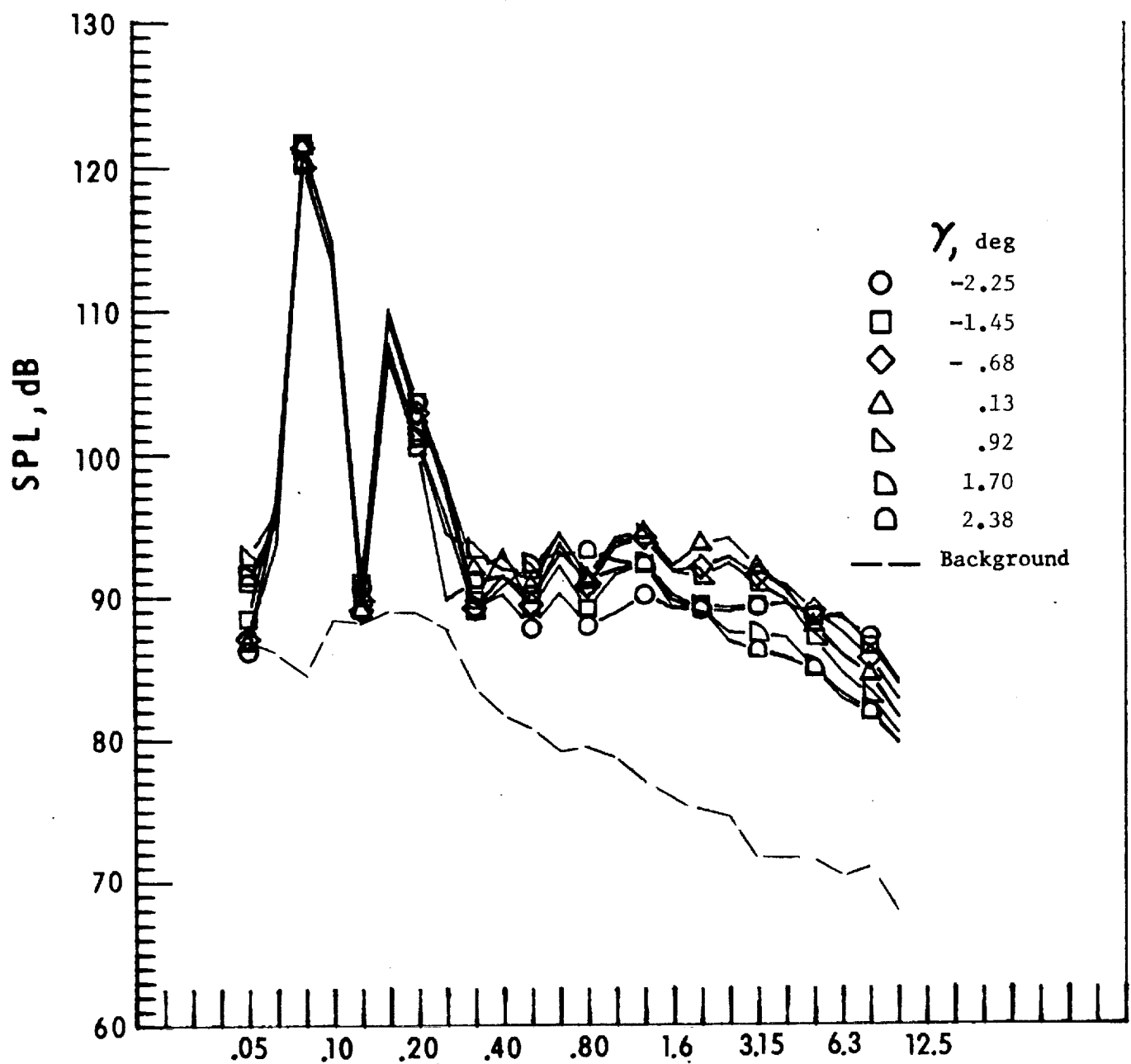
MIC POS I 595-601 75.9



One-third-octave-band center frequency, kHz

a. Mic. no. 1.

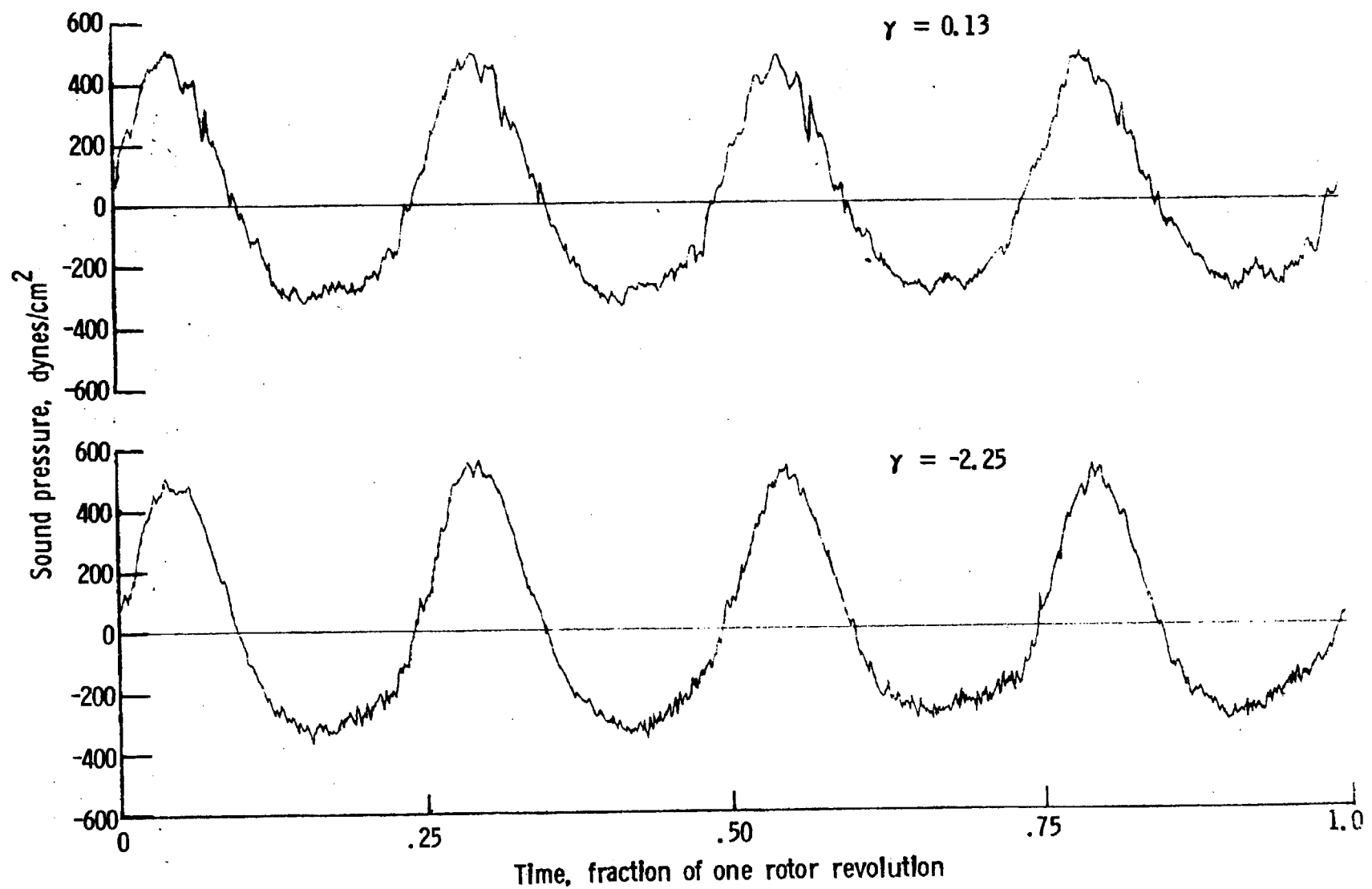
Figure 35. - Effect of descent angle variation on noise generated by helicopter model with square tips installed. $V_\infty = 75.9$ knots.



One-third-octave-band center frequency, kHz

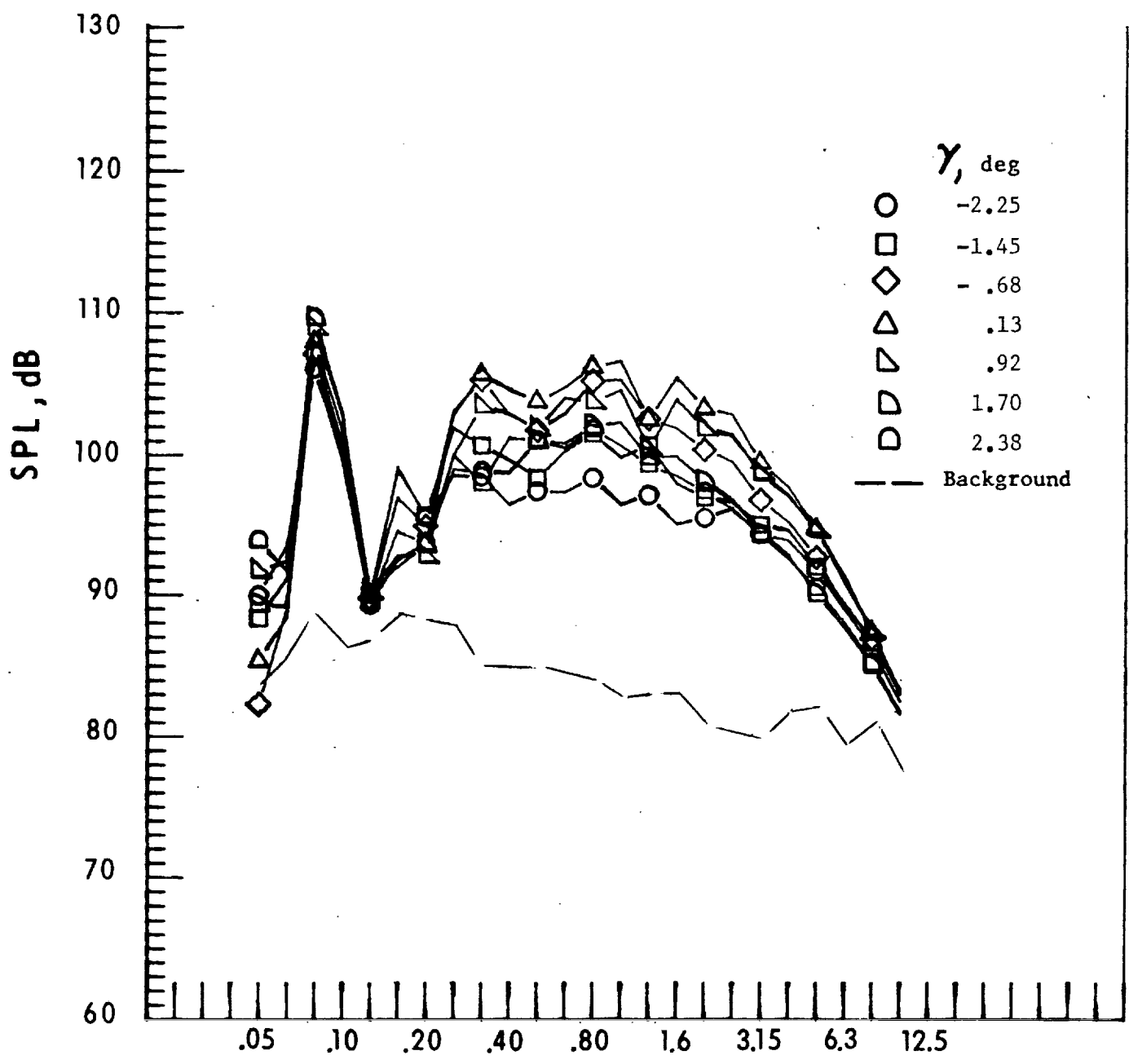
b. Mic. no. 2.

Figure 35. - Continued.



c. Pressure-time histories, Mic. no. 2.

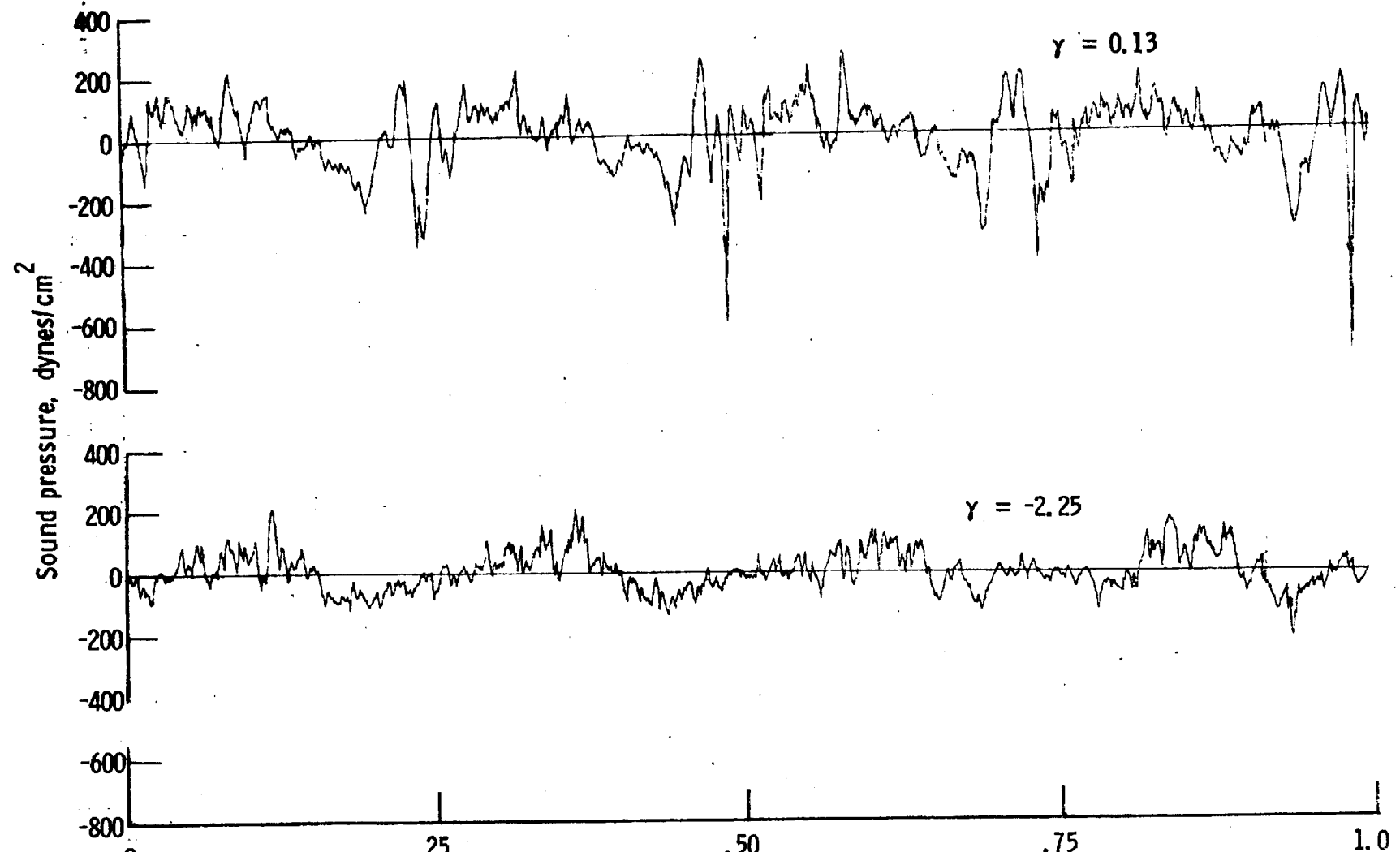
Figure 35. - Continued.



One-third-octave-band center frequency, kHz

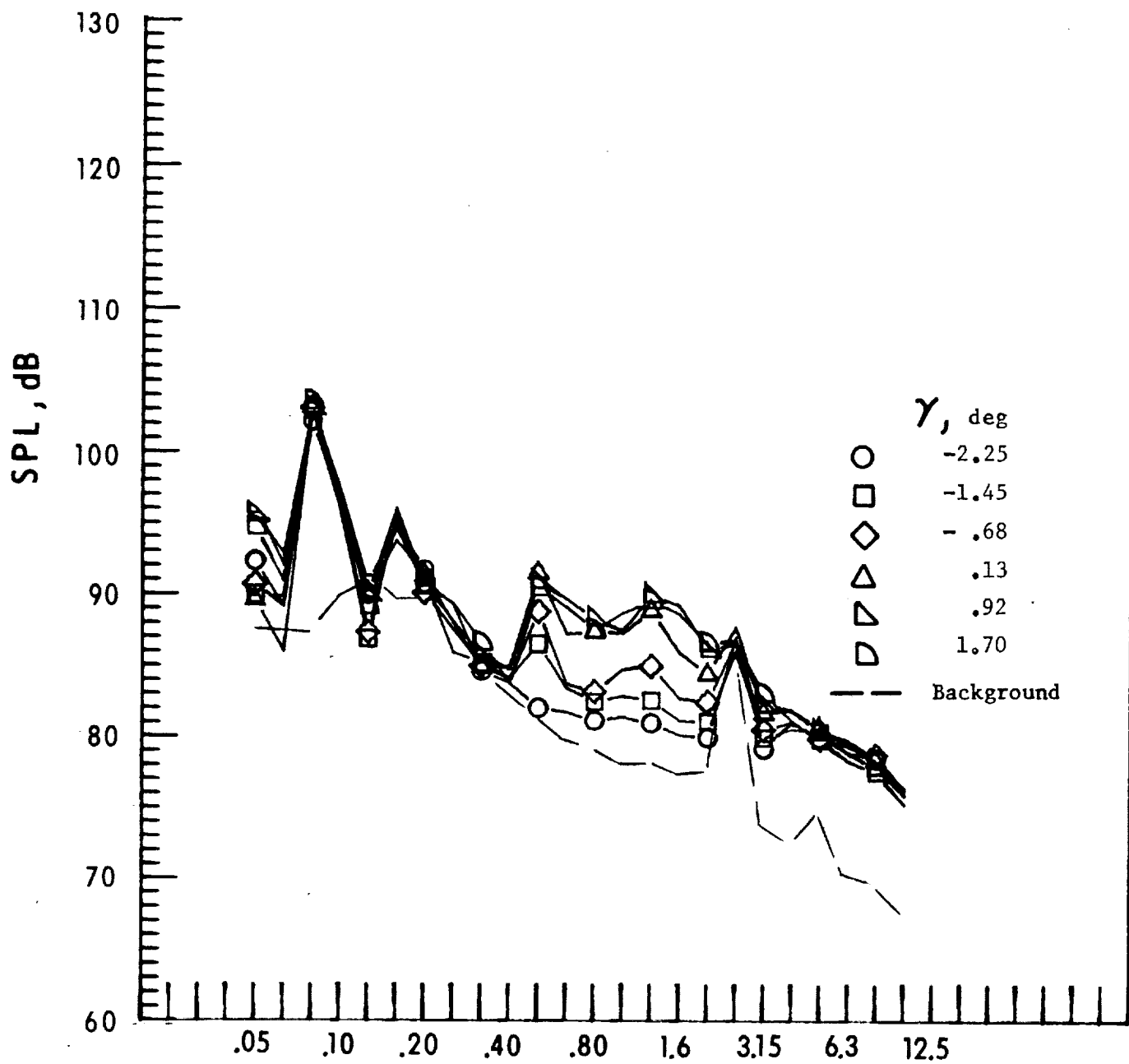
d. Mic. no. 3.

Figure 35. - Continued.



e. Pressure-time histories, Mic. no. 3.

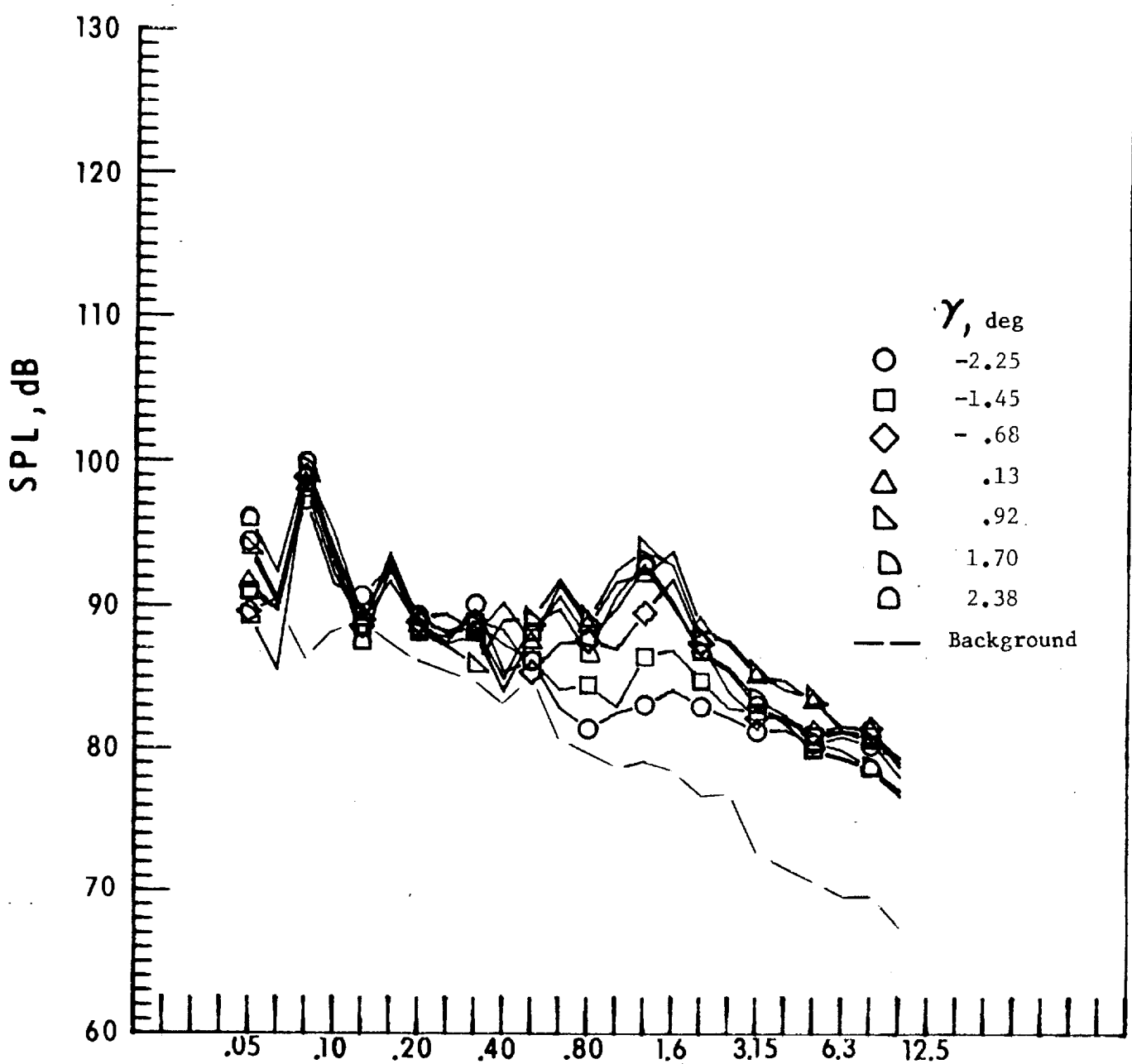
Figure 35.-Continued.



One-third-octave-band center frequency, kHz

f. Mic. no. 4.

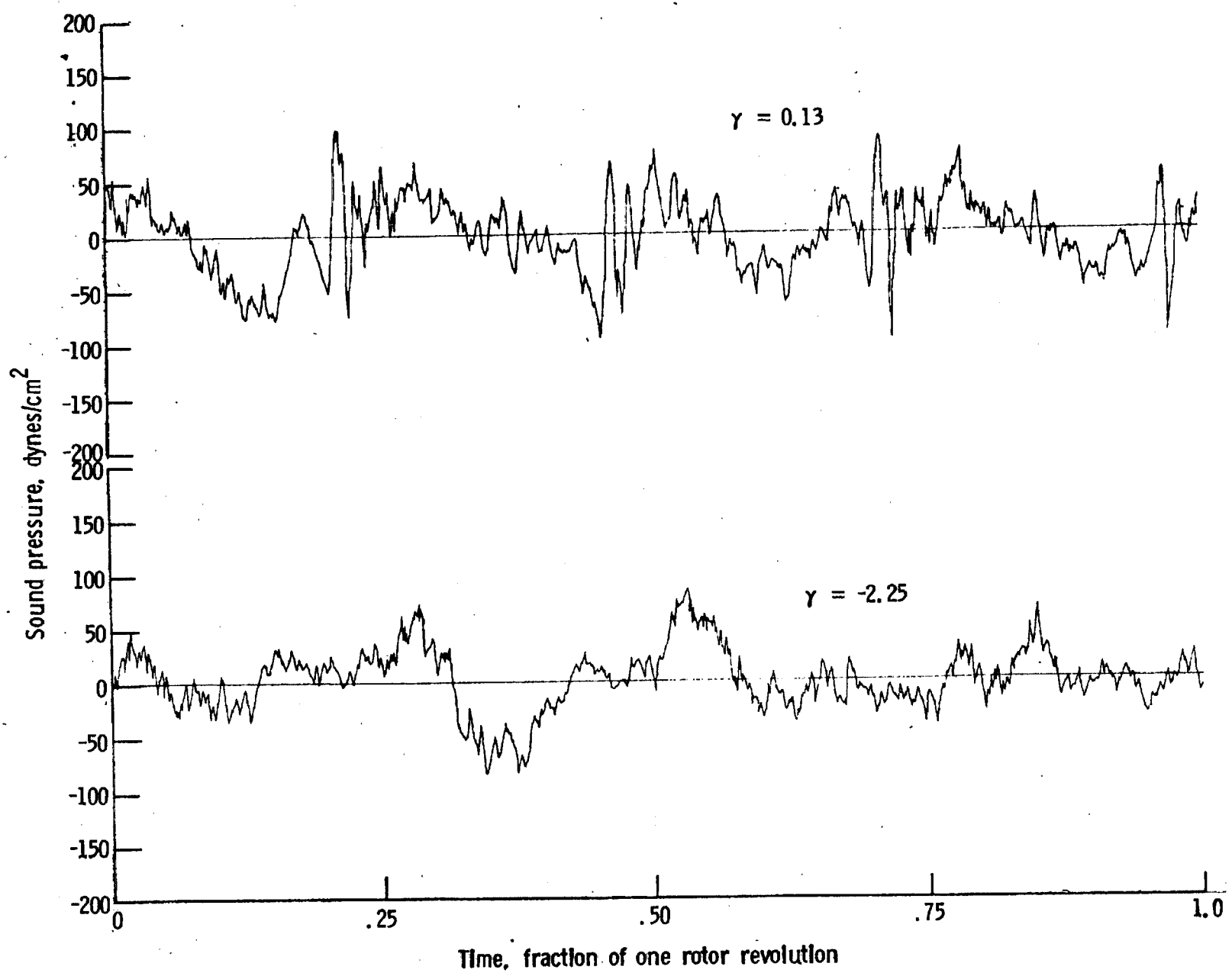
Figure 35. - Continued.



One-third-octave-band center frequency, kHz

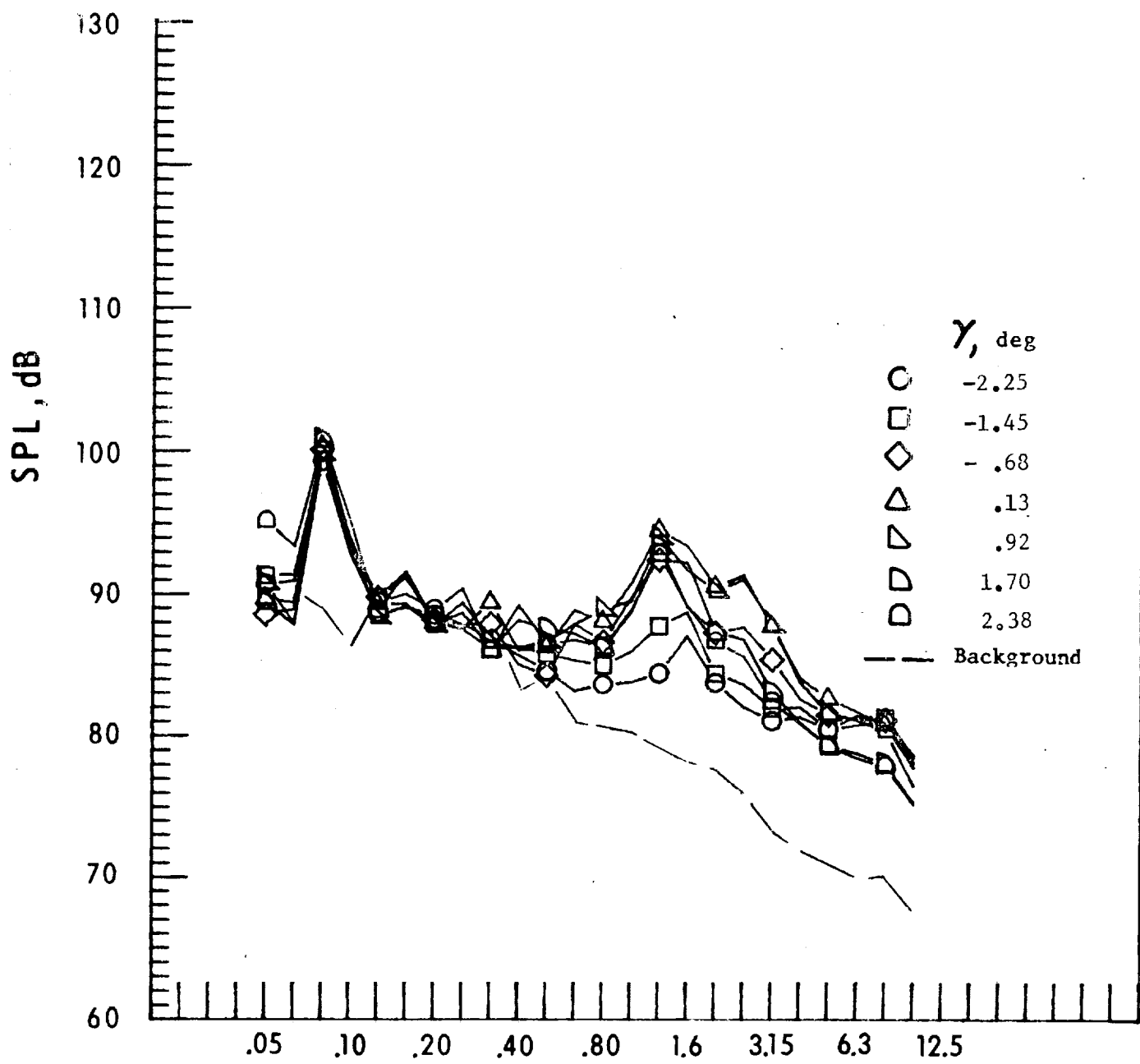
g. Mic. no. 5.

Figure 35. - Continued.



h. Pressure-time histories, Mic. no. 5.

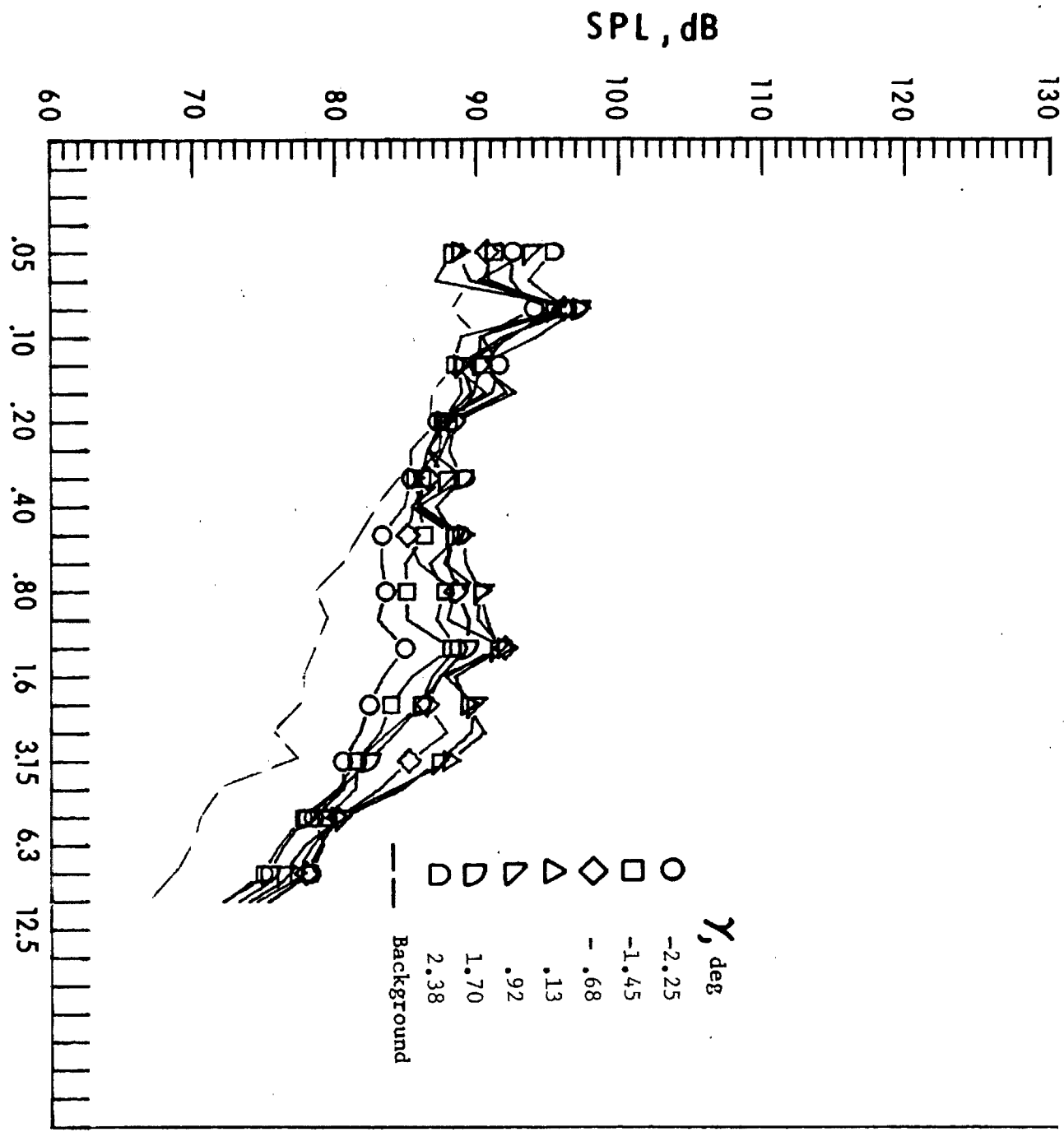
Figure 35. - Continued.



One-third-octave-band center frequency, kHz

i. Mic. no. 6.

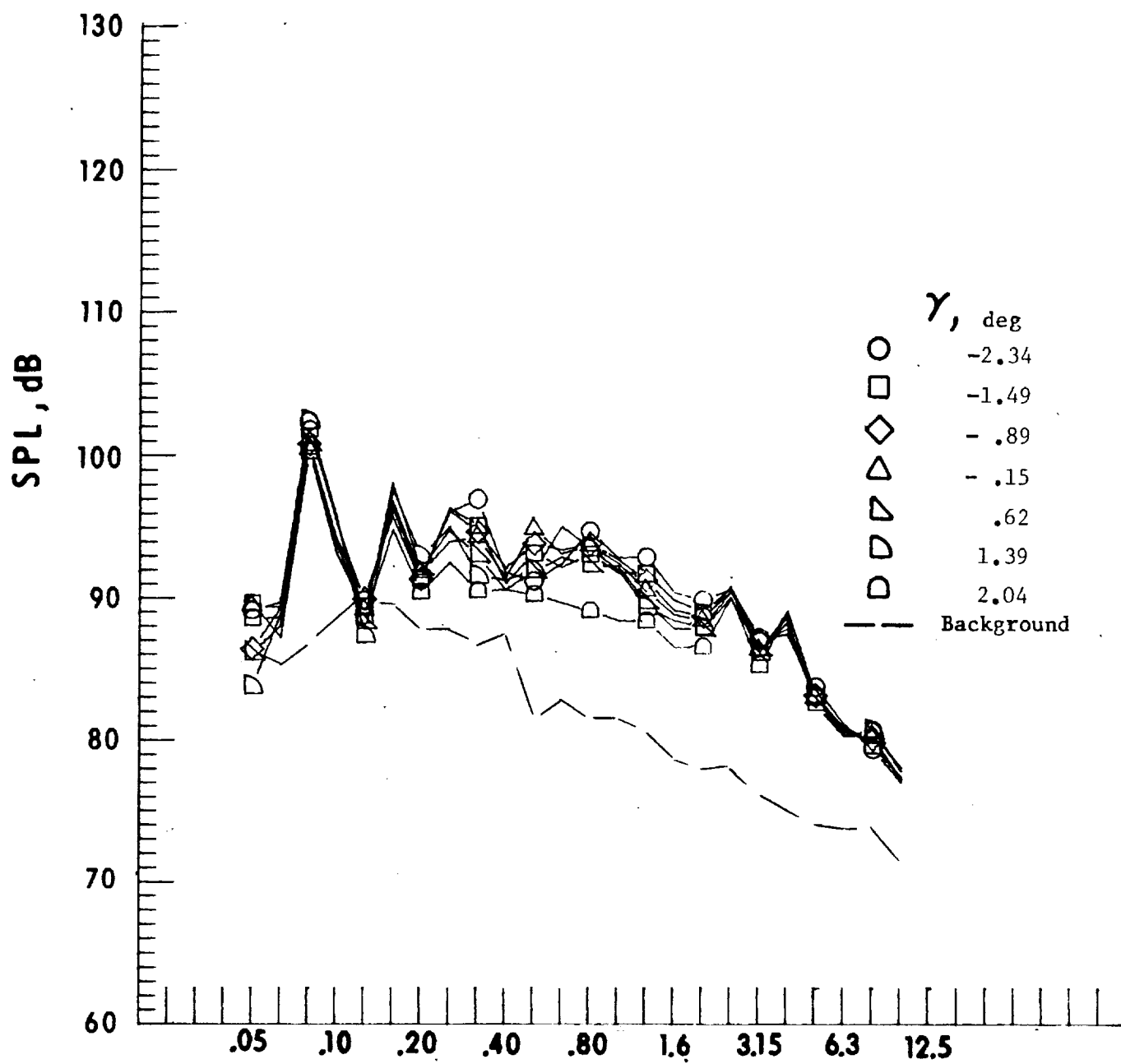
Figure 35. - Continued.



One-third-octave-band center frequency, kHz

j. Mic. no. 7.

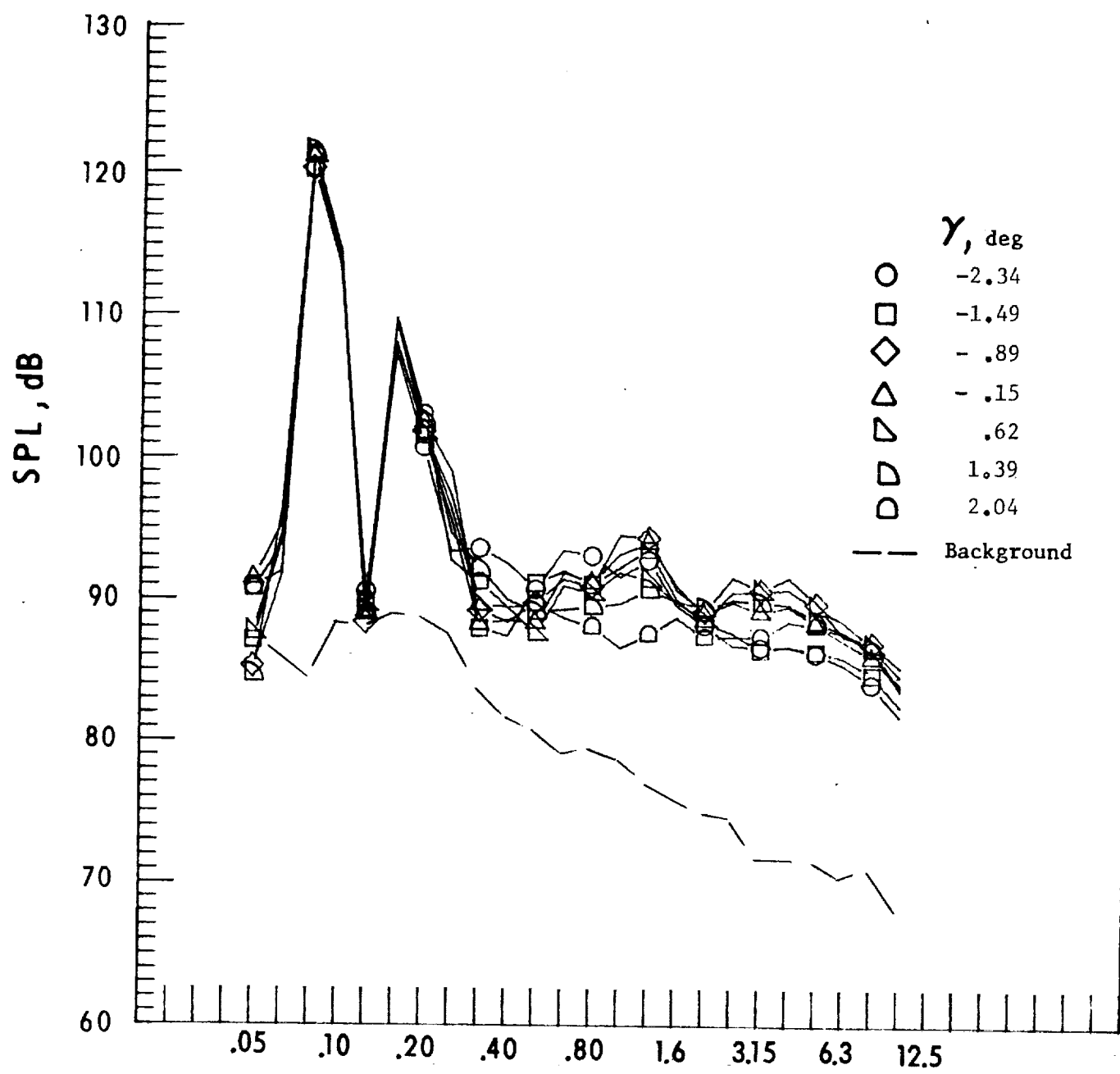
Figure 35. - Concluded.



One-third-octave-band center frequency, kHz

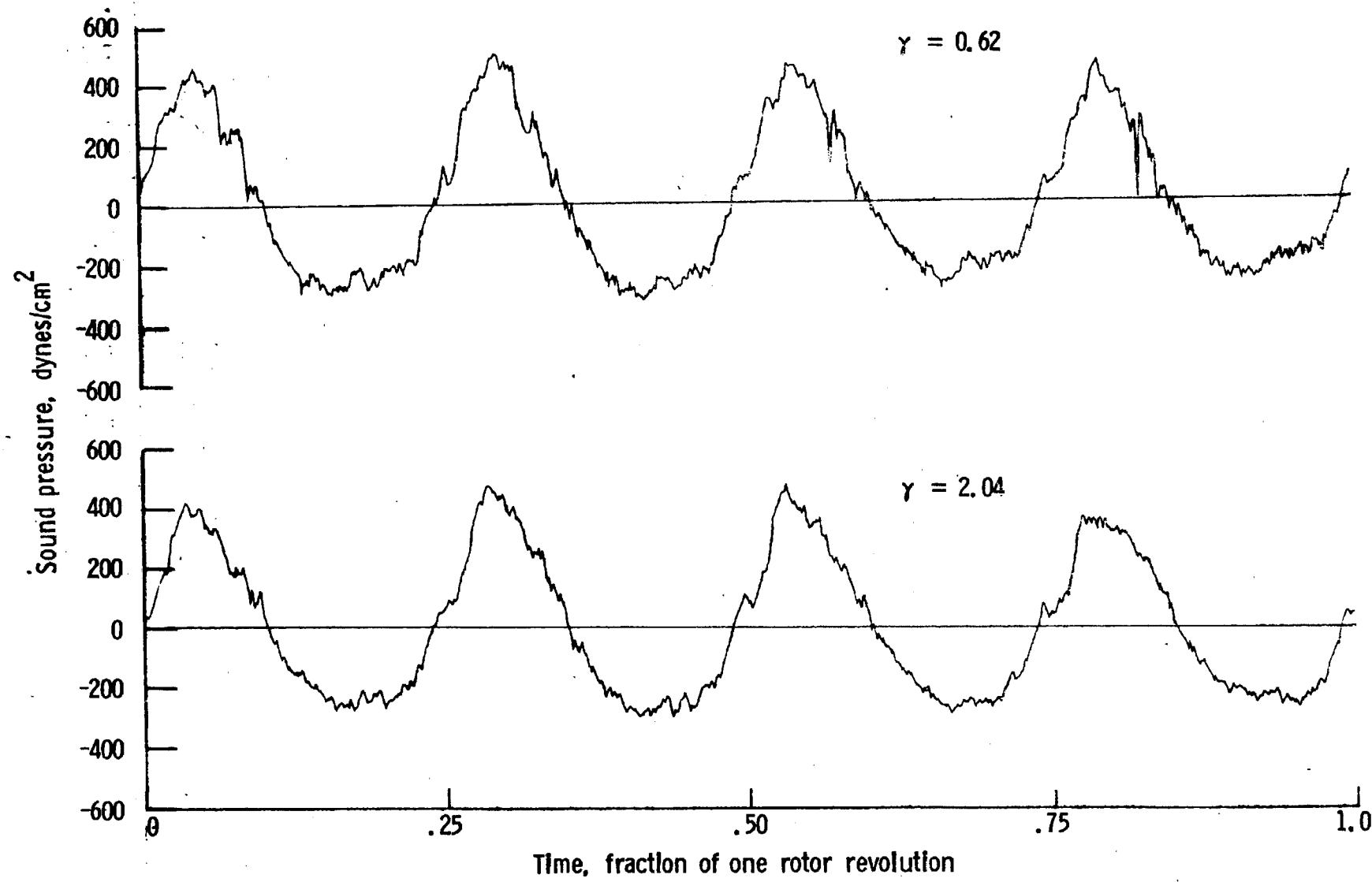
a. Mic. no. 1.

Figure 36. - Effect of descent angle variation on noise generated by helicopter model with ogee tips installed. $V_{\infty} = 76.0$ knots.



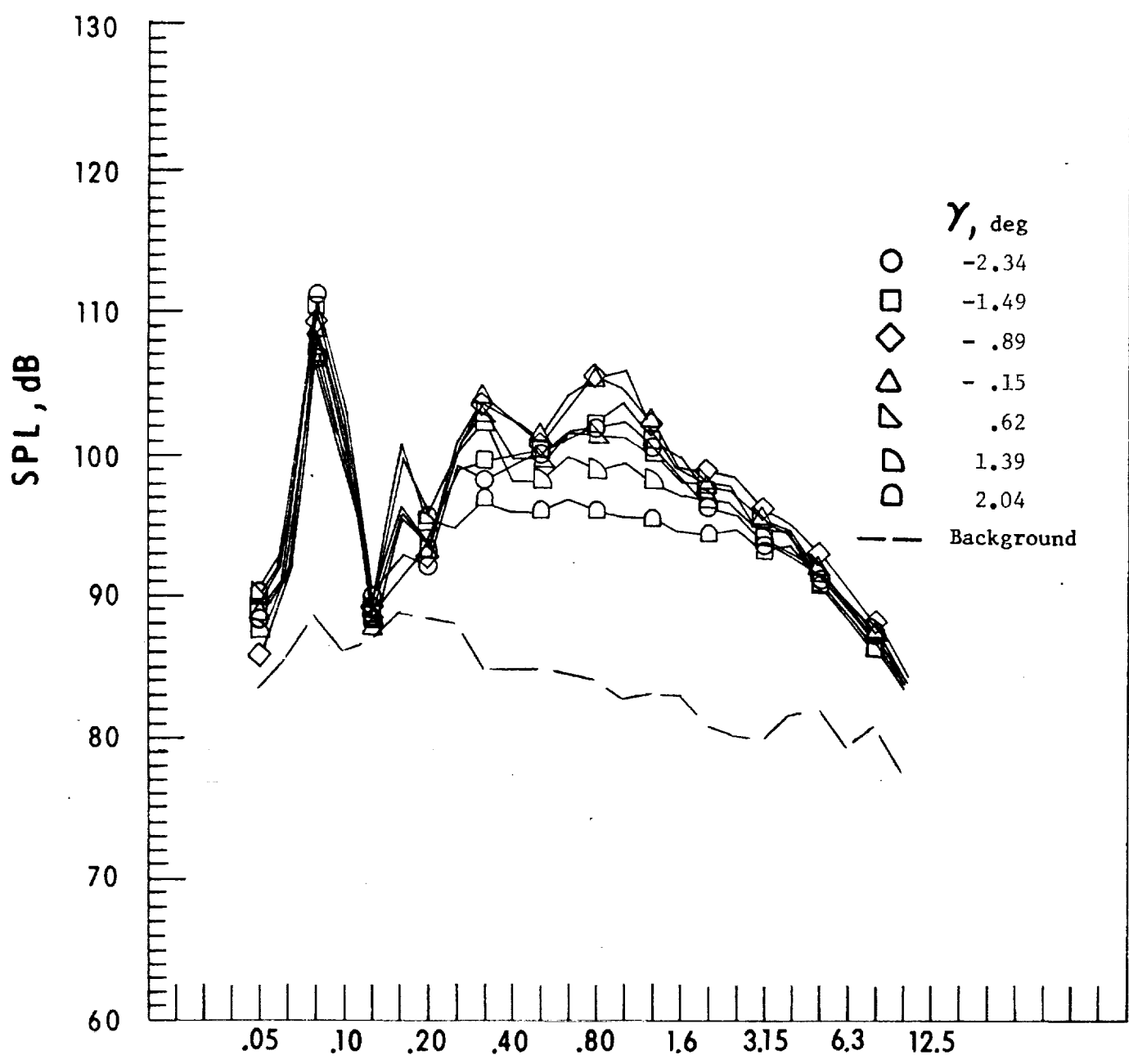
b. Mic. no. 2.

Figure 36. - Continued.



c. Pressure-time histories, Mic. no. 2.

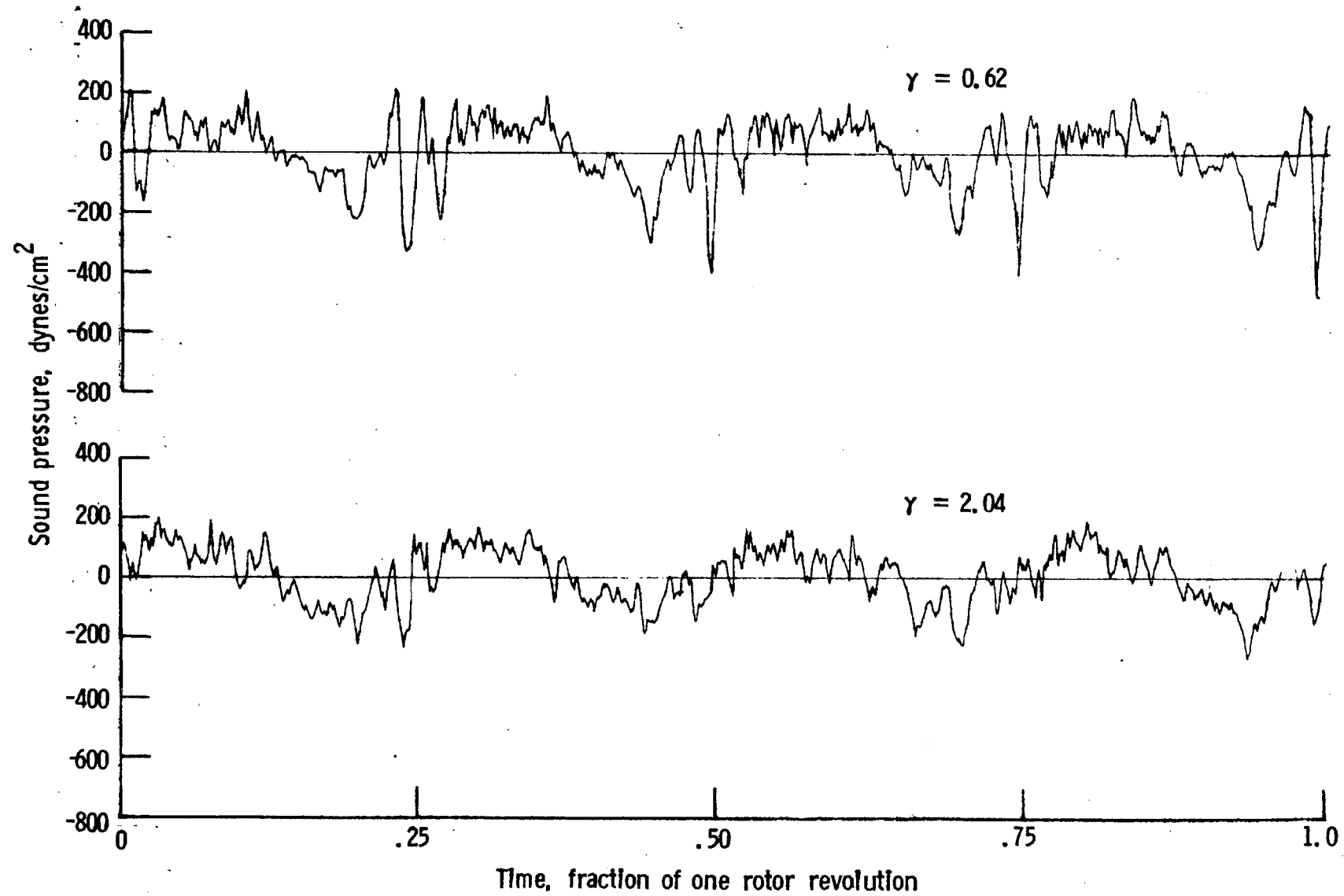
Figure 36. - Continued.



One-third-octave-band center frequency, kHz

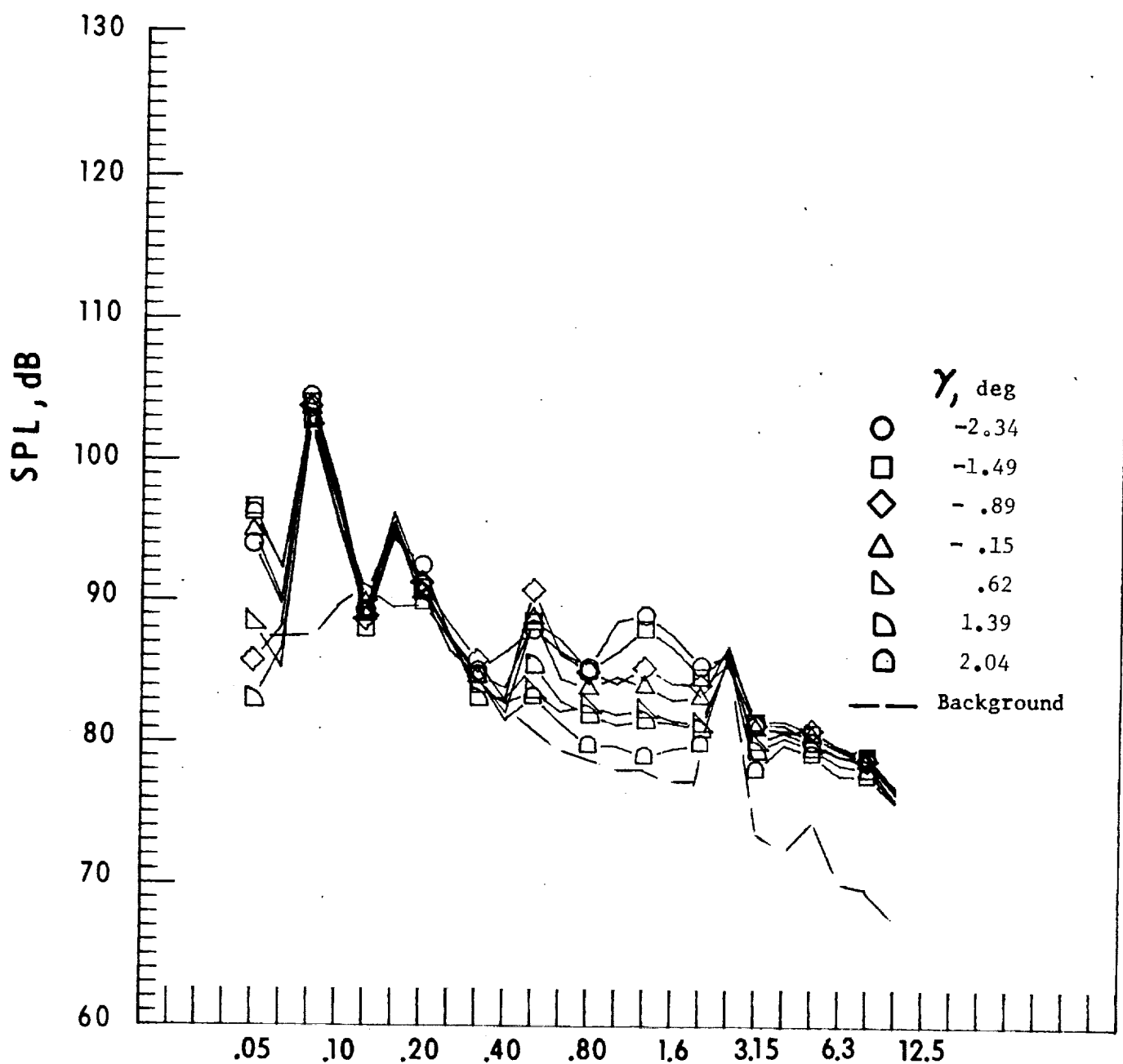
d. Mic. no. 3.

Figure 36. - Continued.



e. Pressure-time histories, Mic. no. 3.

Figure 36. - Continued.



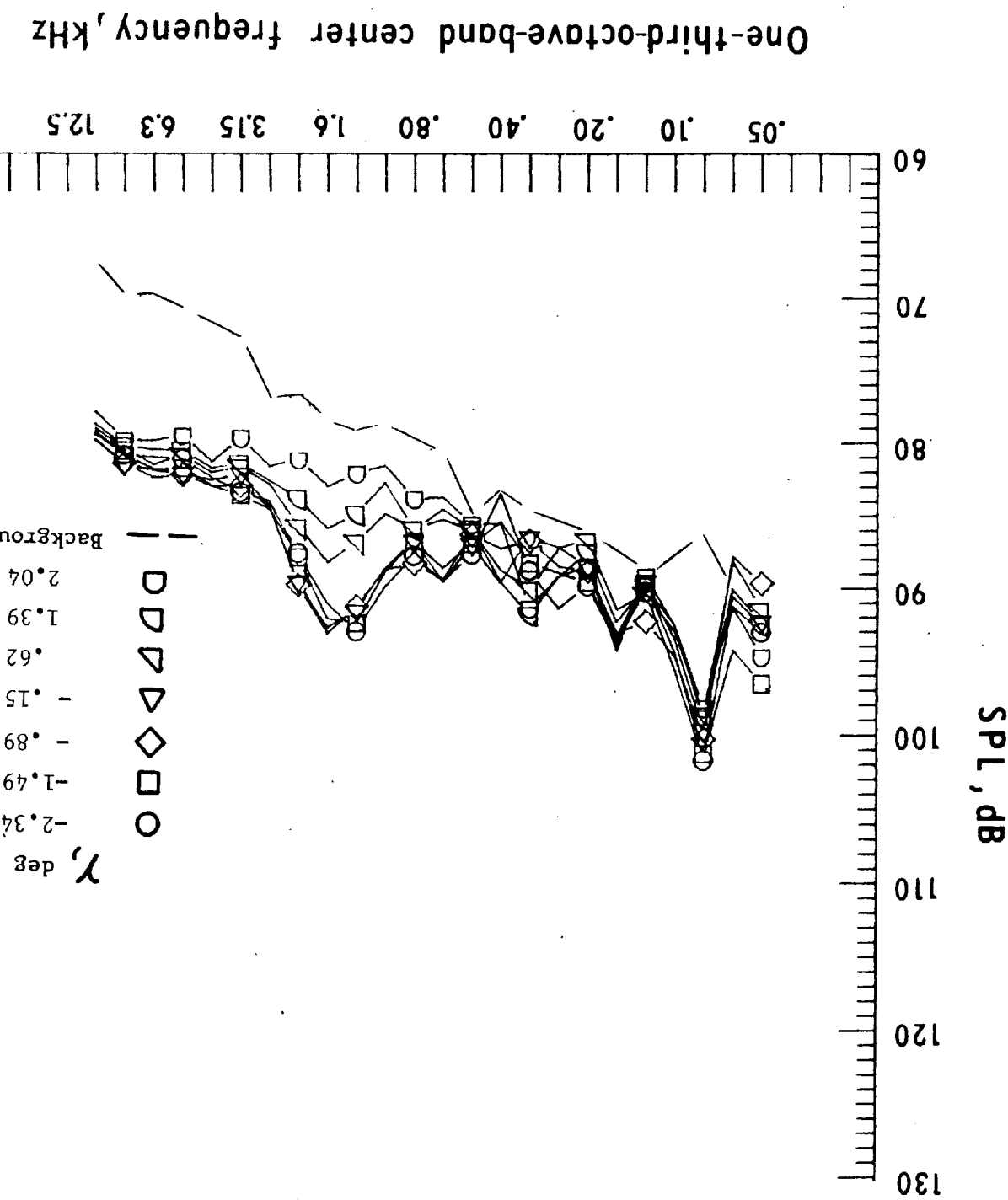
One-third-octave-band center frequency, kHz

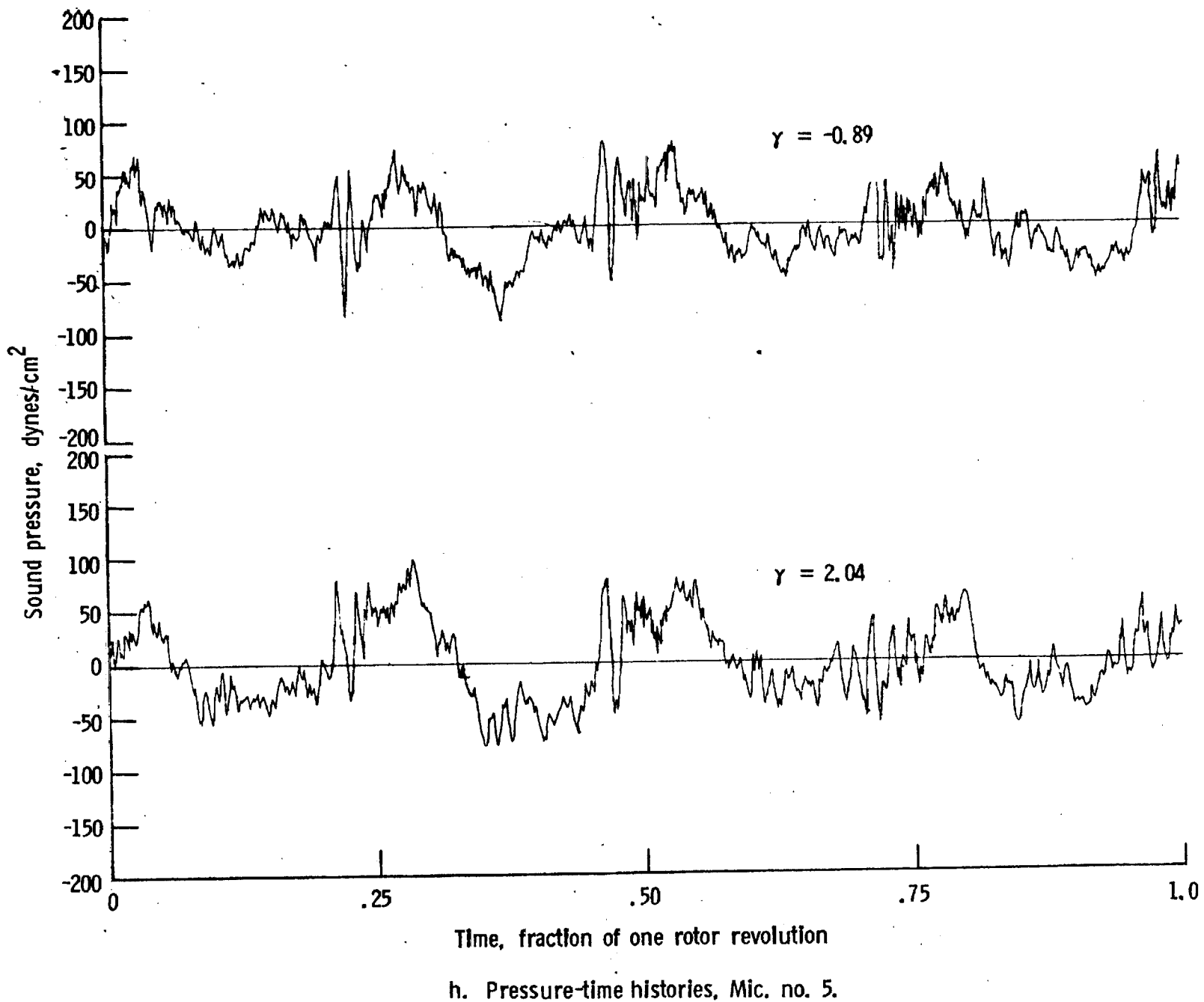
f. Mic. no. 4.

Figure 36. - Continued.

Figure 36. - Continued.

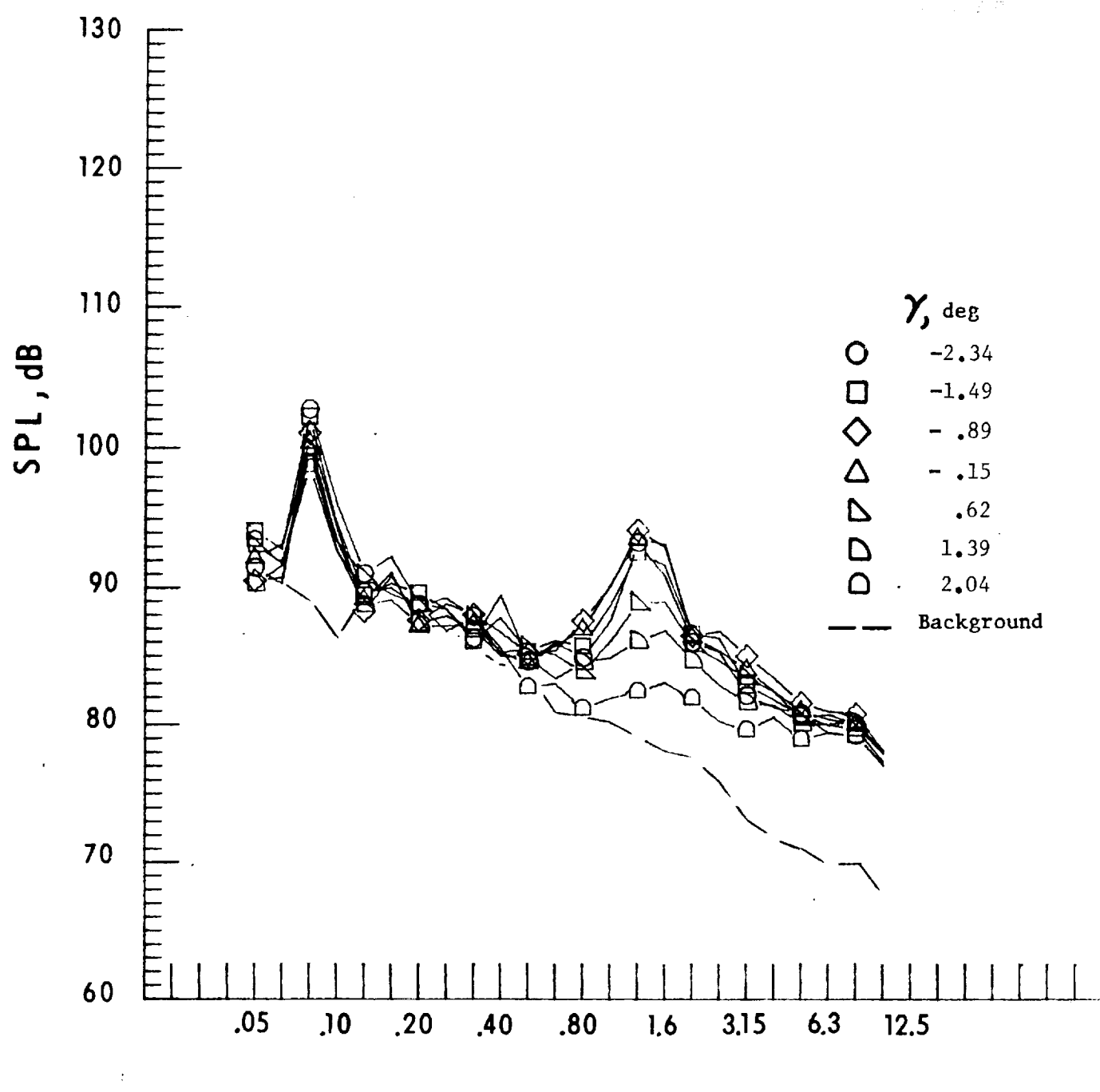
g. Mic. no. 5.





h. Pressure-time histories, Mic. no. 5.

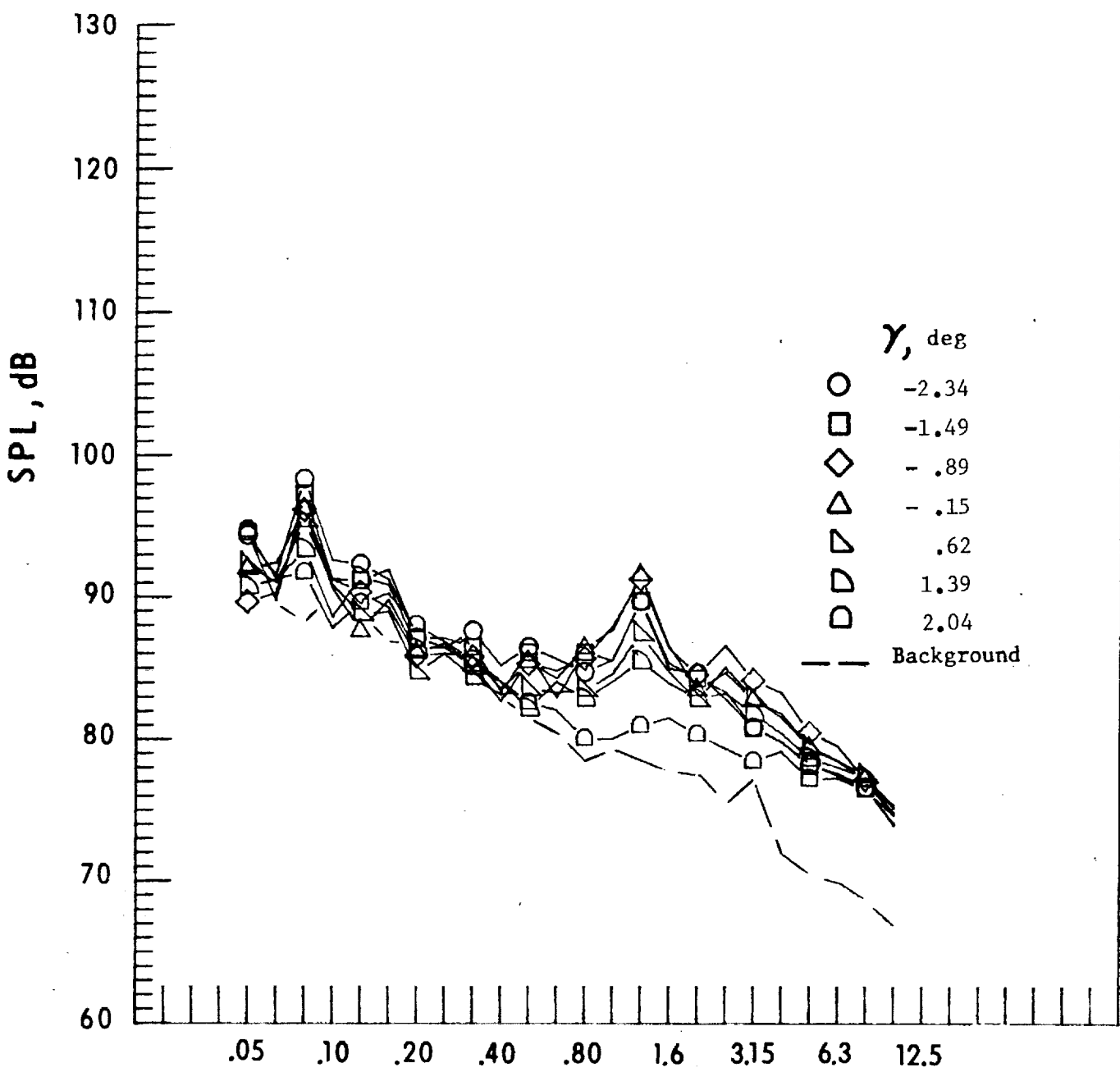
Figure 36. - Continued.



One-third-octave-band center frequency, kHz

i. Mic. no. 6.

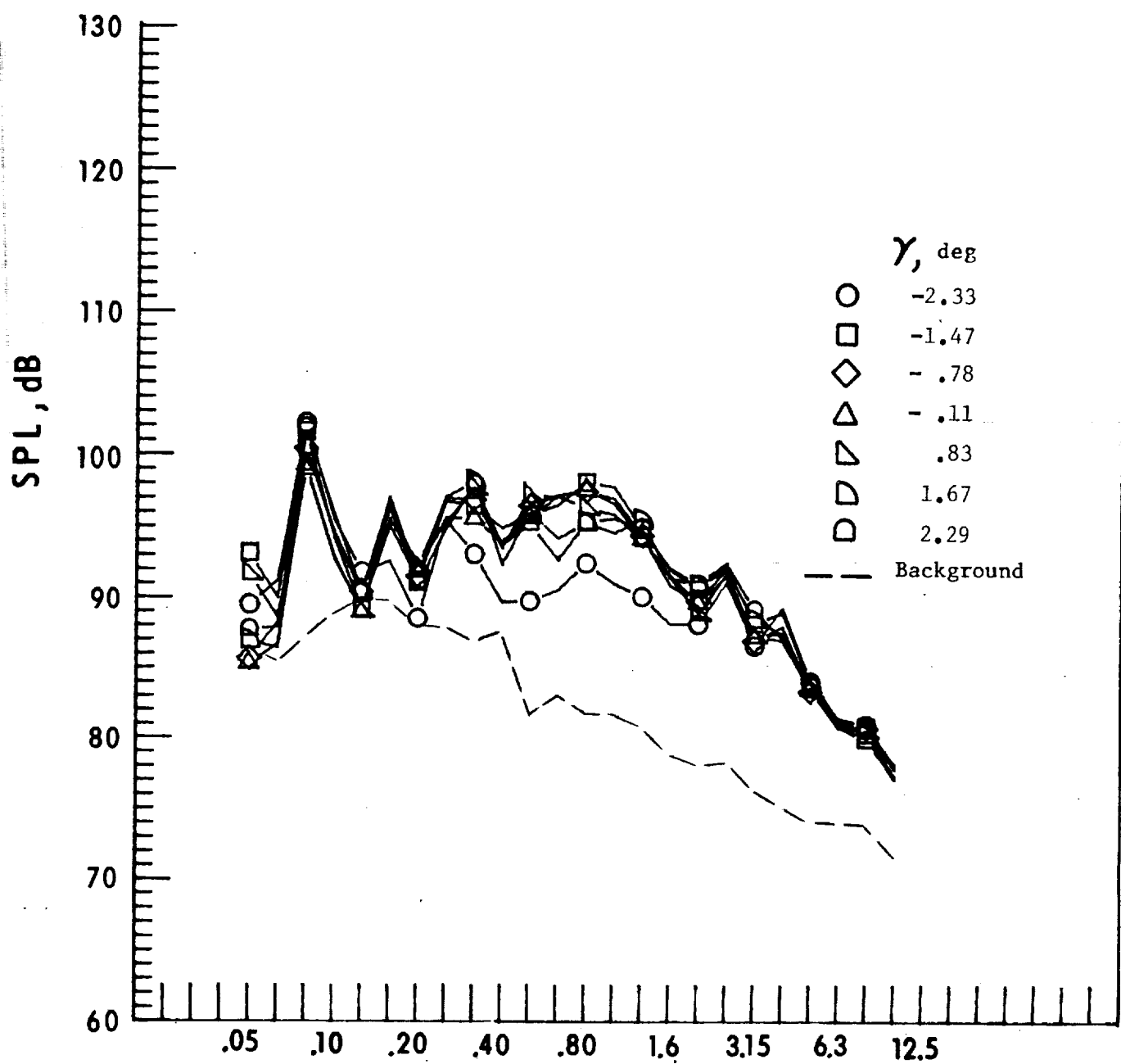
Figure 36. - Continued.



One-third-octave-band center frequency, kHz

j. Mic. no. 7.

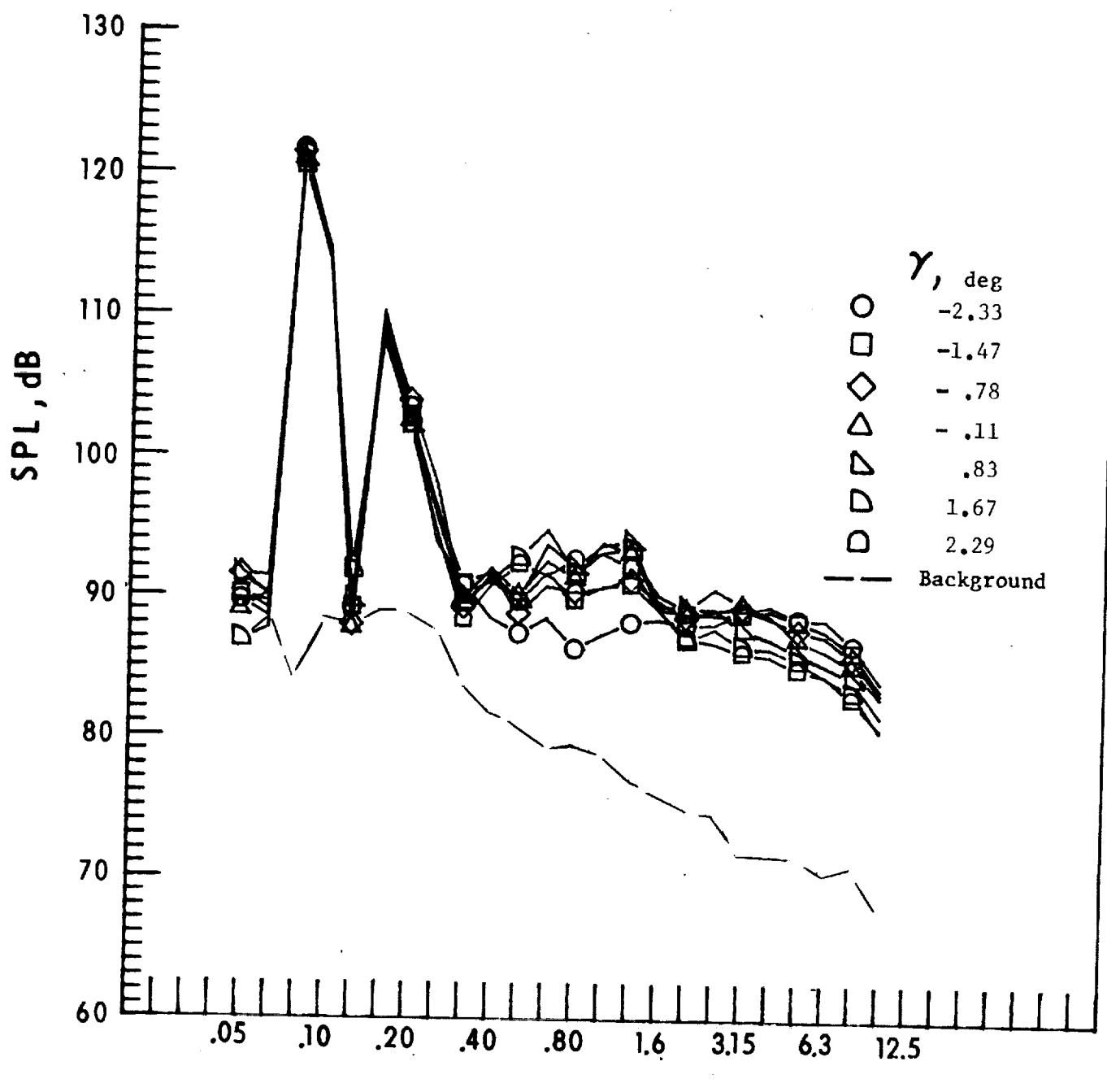
Figure 36. - Concluded.



One-third-octave-band center frequency, kHz

a. Mic. no. 1.

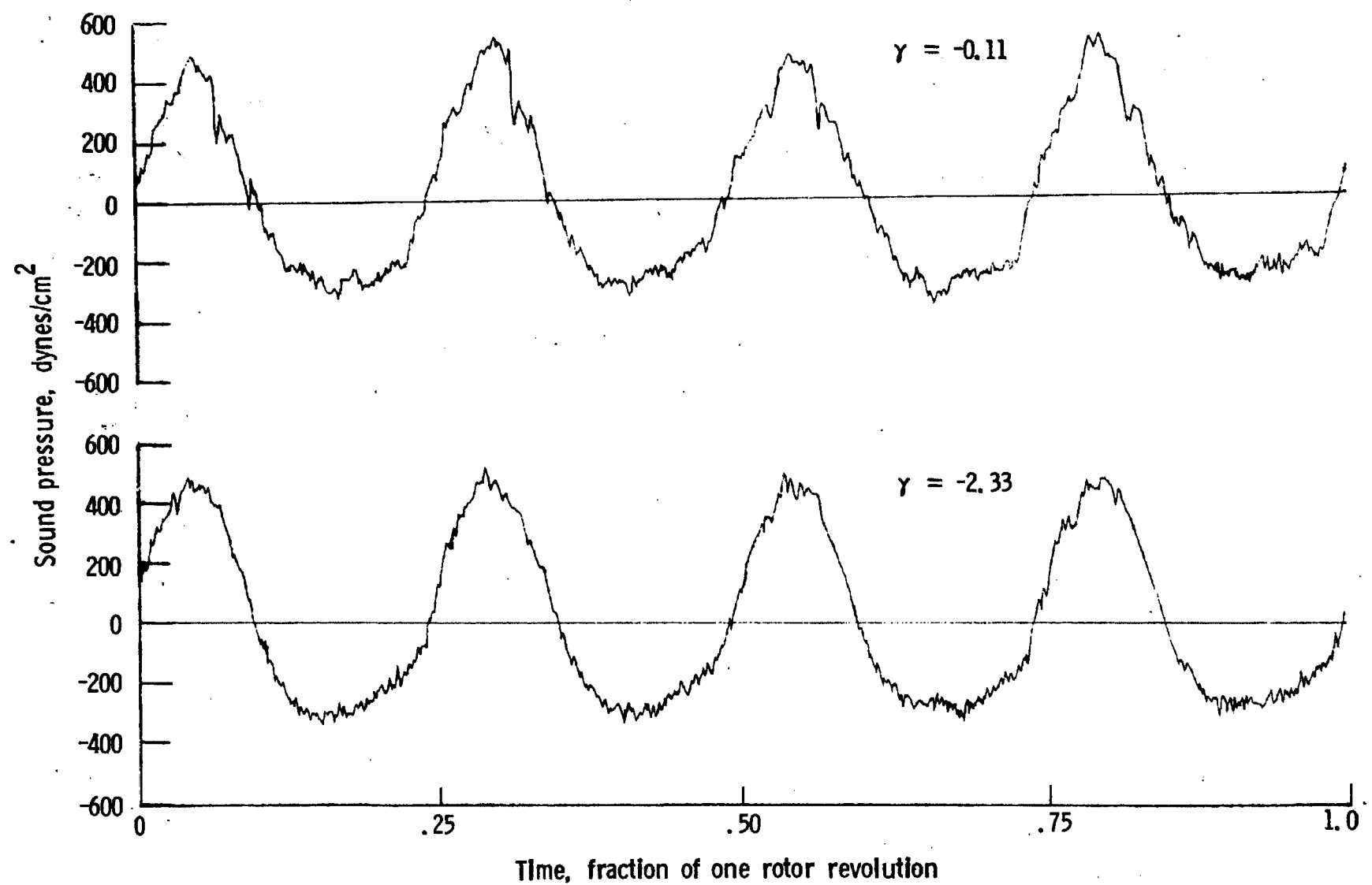
Figure 37. - Effect of descent angle variation on noise generated by helicopter model with sub-wing tips installed. $V_{\infty} = 75.9$ knots.



One-third-octave-band center frequency, kHz

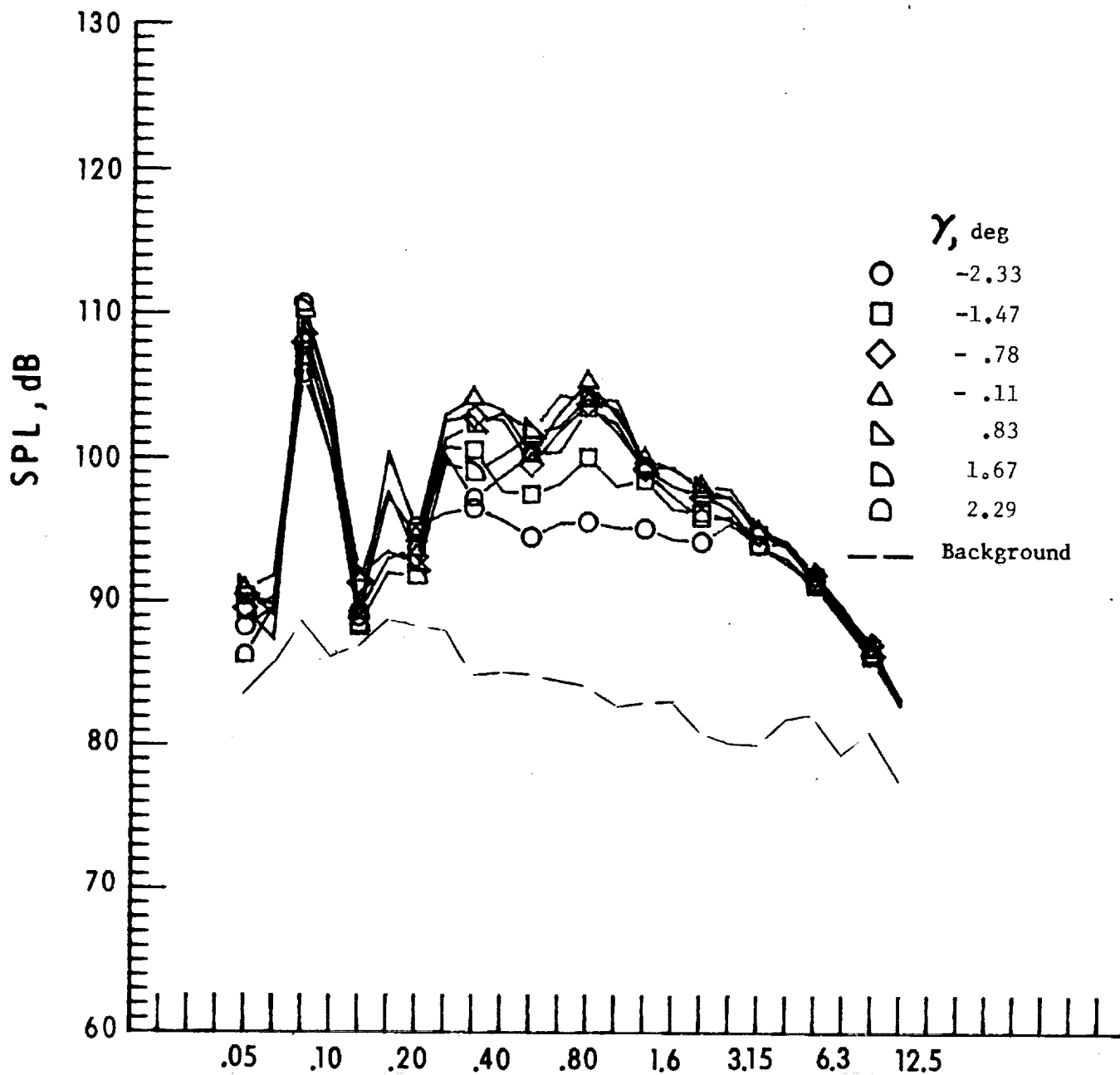
b. Mic. no. 2.

Figure 37. - Continued.



c. Pressure-time histories, Mic. no. 2.

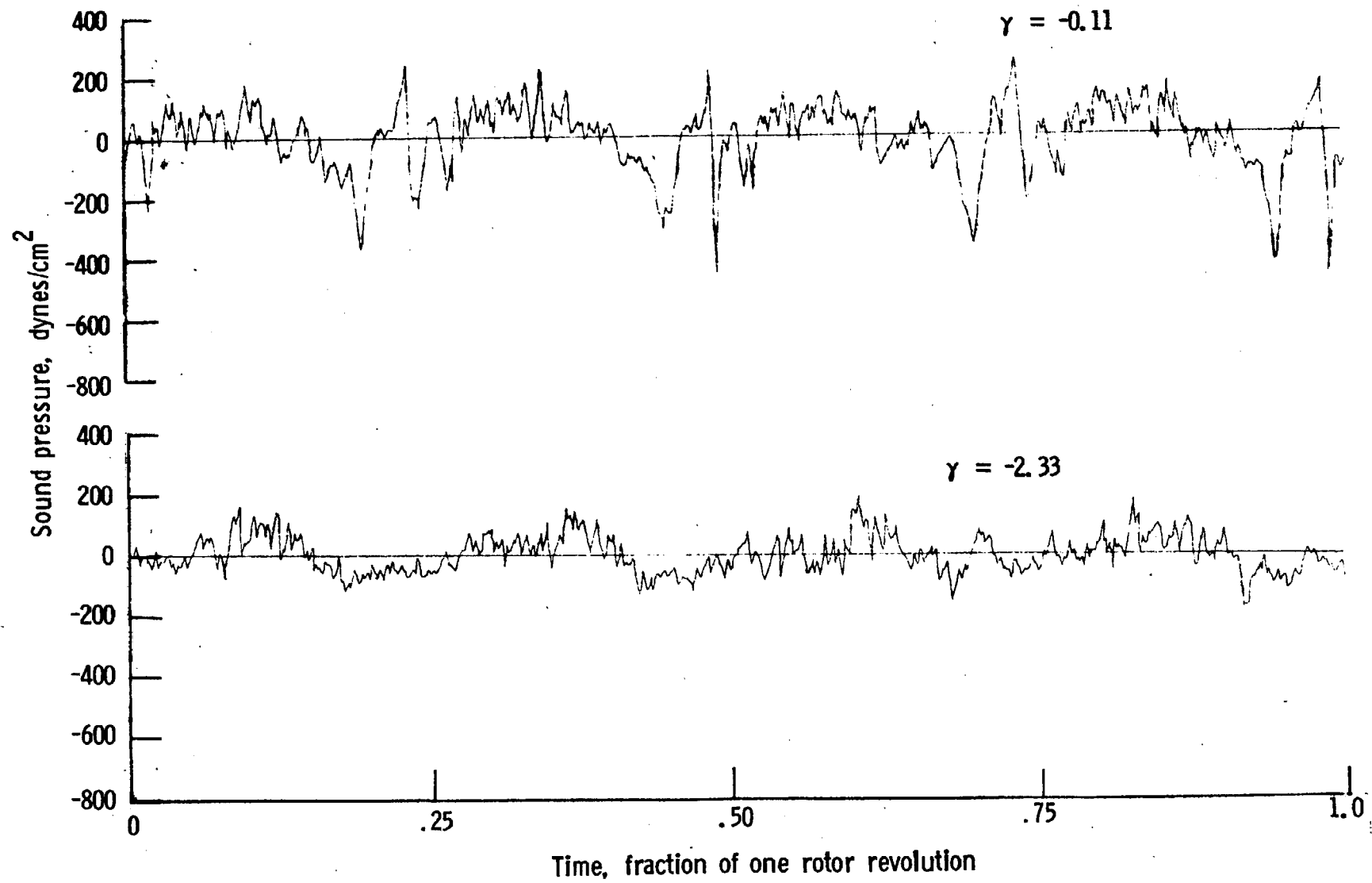
Figure 37. - Continued.



One-third-octave-band center frequency, kHz

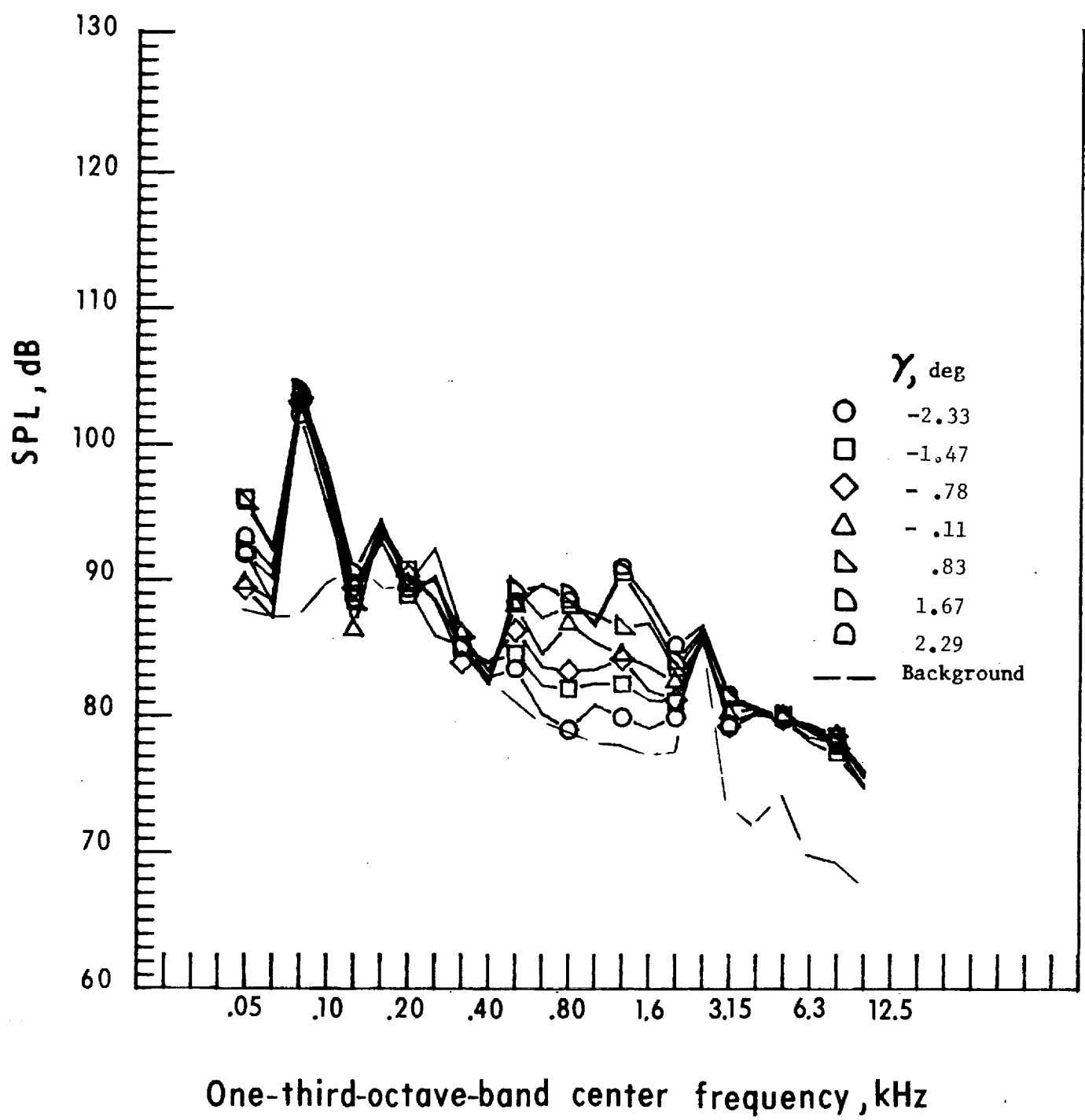
d. Mic. no. 3.

Figure 37. - Continued.



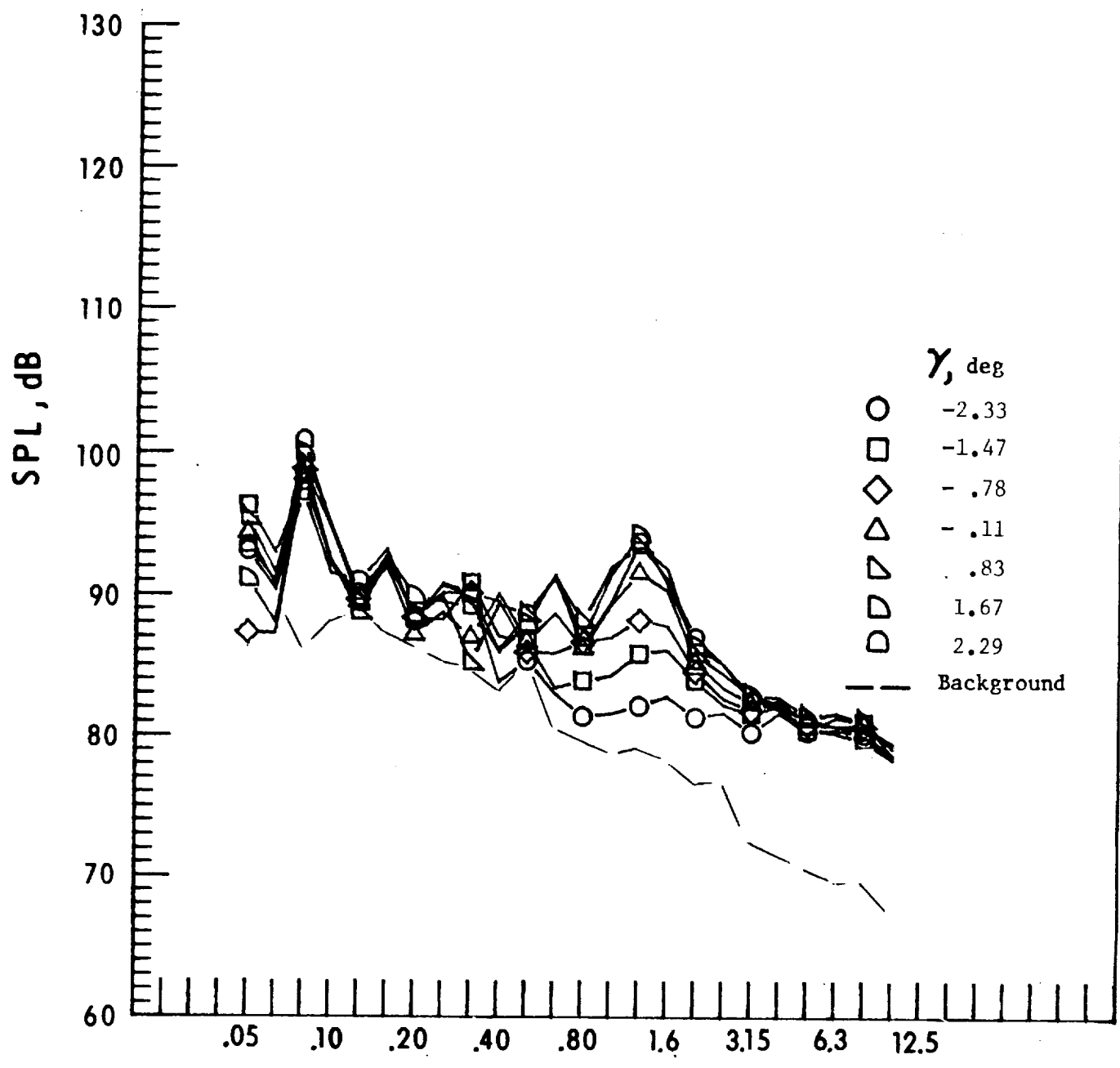
e. Pressure-time histories, Mic. no. 3.

Figure 37. - Continued.



f. Mic. no. 4.

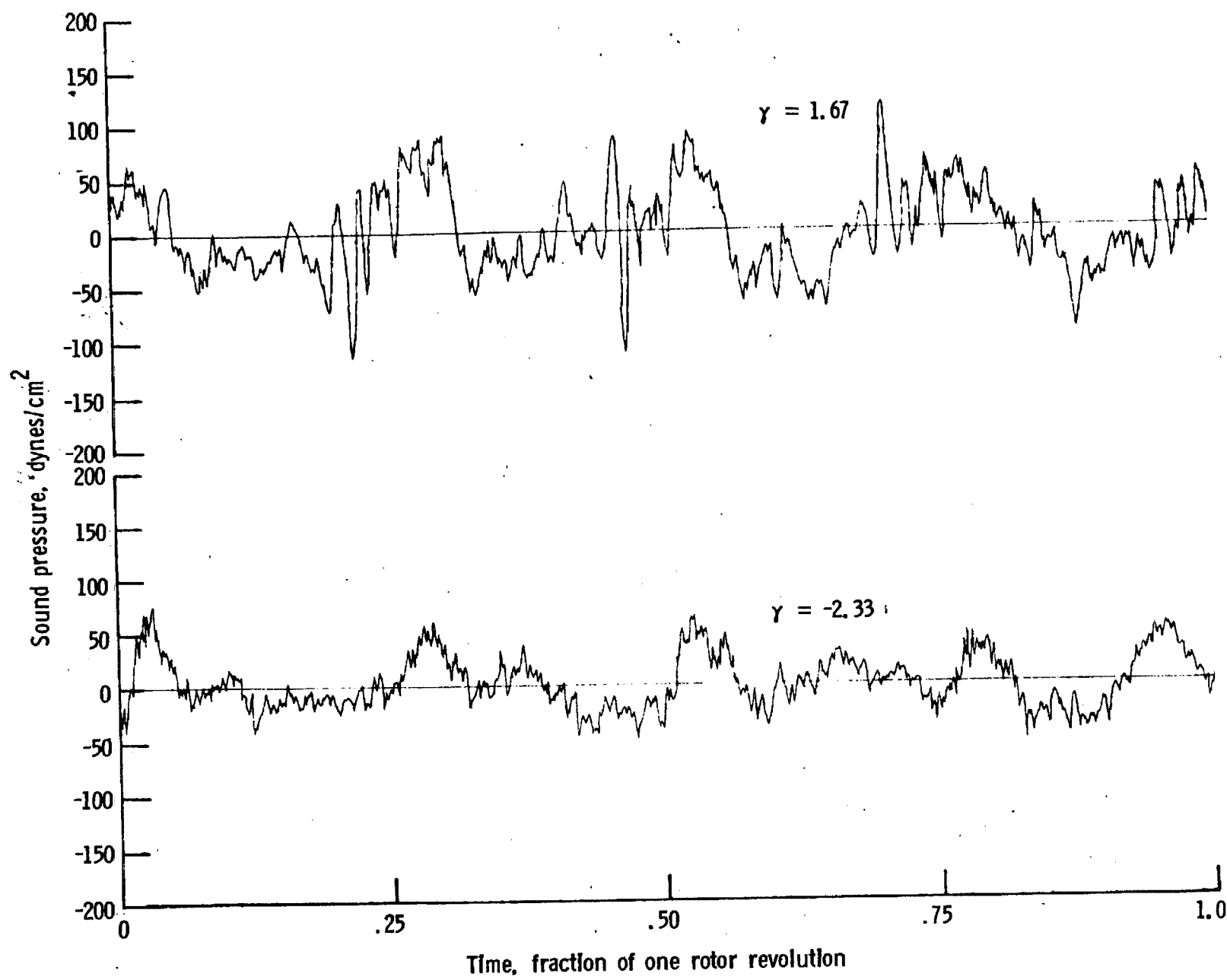
Figure 37. - Continued.



One-third-octave-band center frequency, kHz

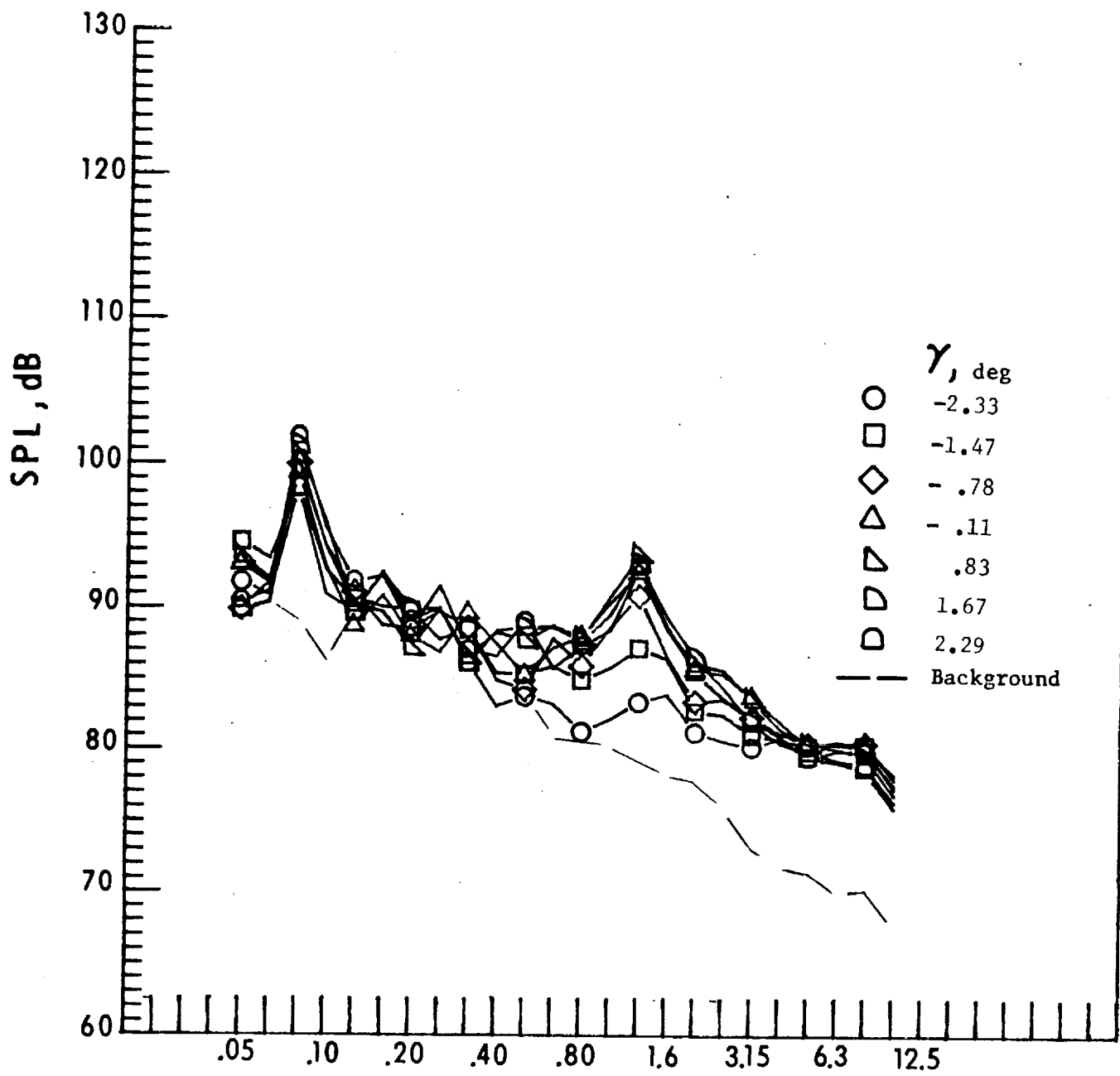
g. Mic. no. 5.

Figure 37. - Continued.



h. Pressure-time histories, Mic. no. 5.

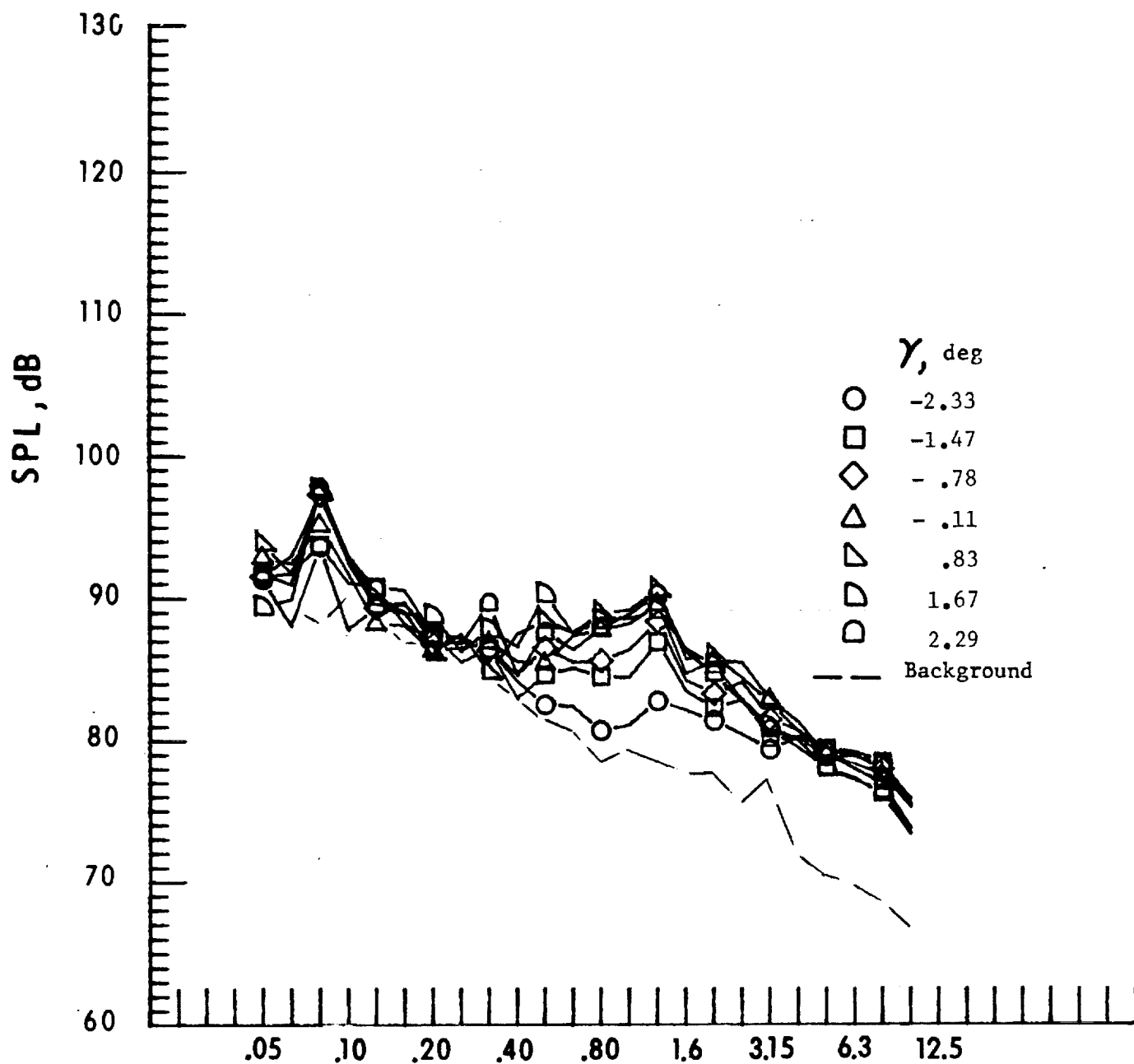
Figure 37. - Continued.



One-third-octave-band center frequency, kHz

i. Mic. no. 6.

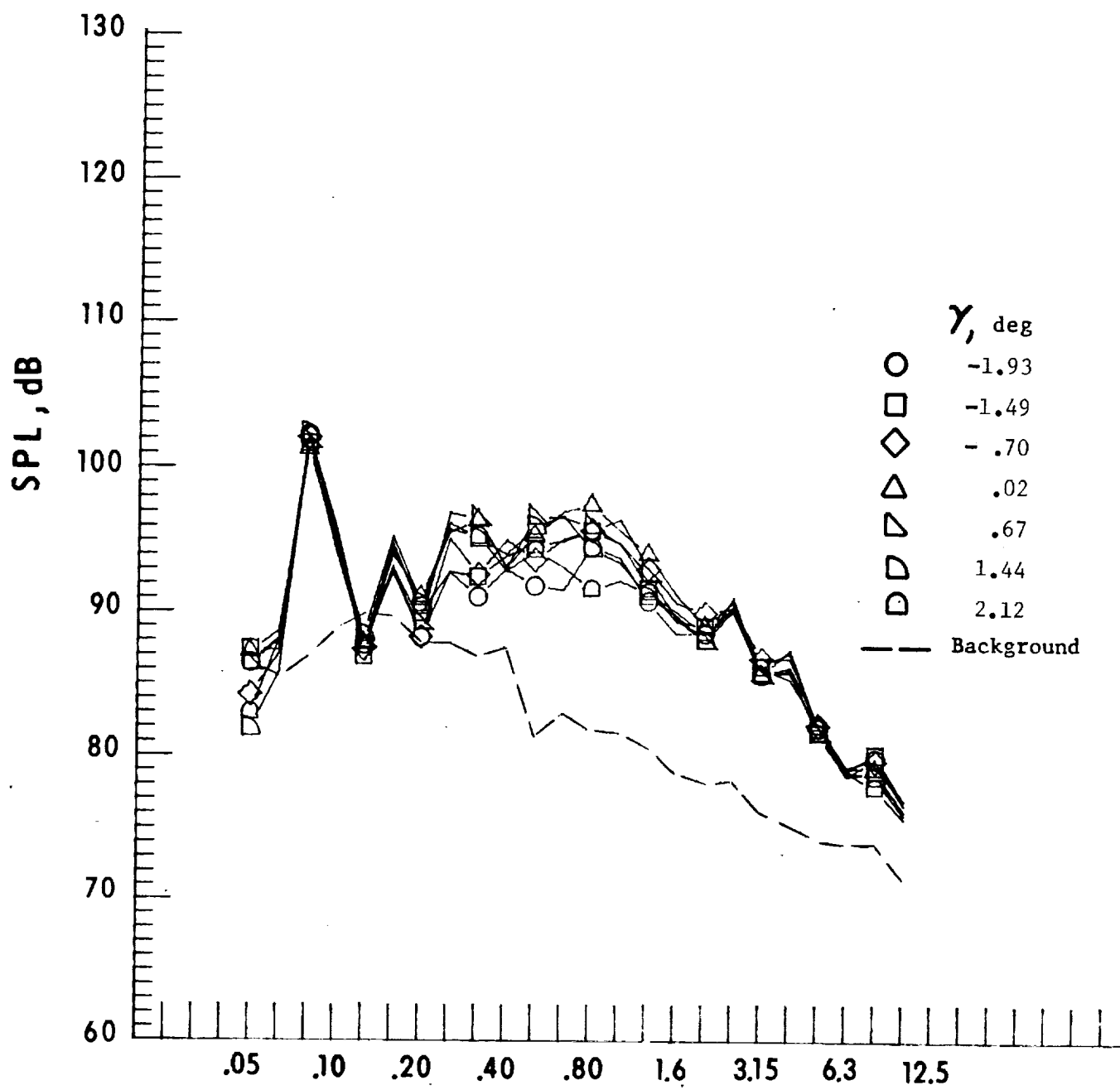
Figure 37. - Continued.



One-third-octave-band center frequency, kHz

j. Mic. no. 7.

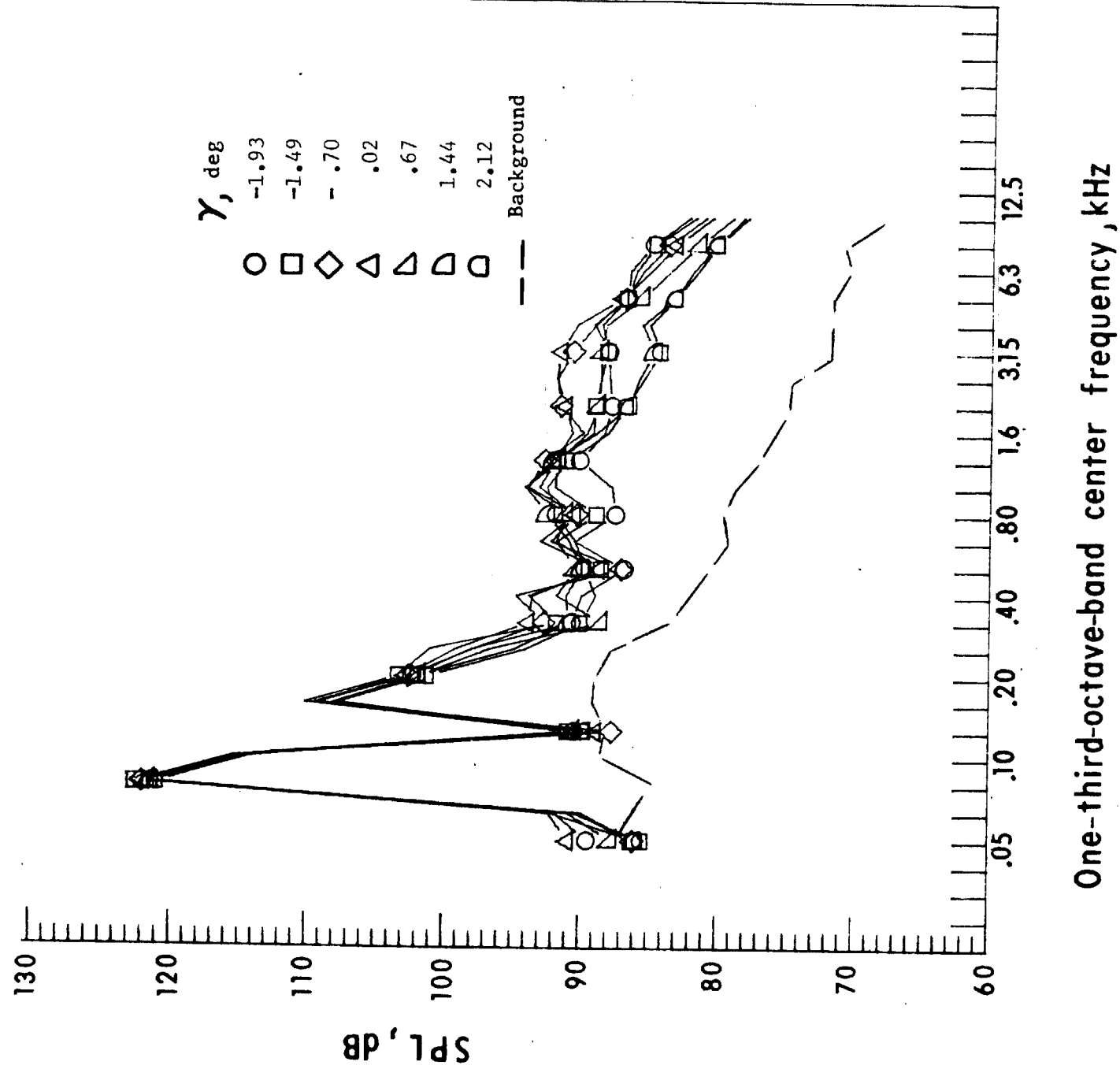
Figure 37. - Concluded.



One-third-octave-band center frequency, kHz

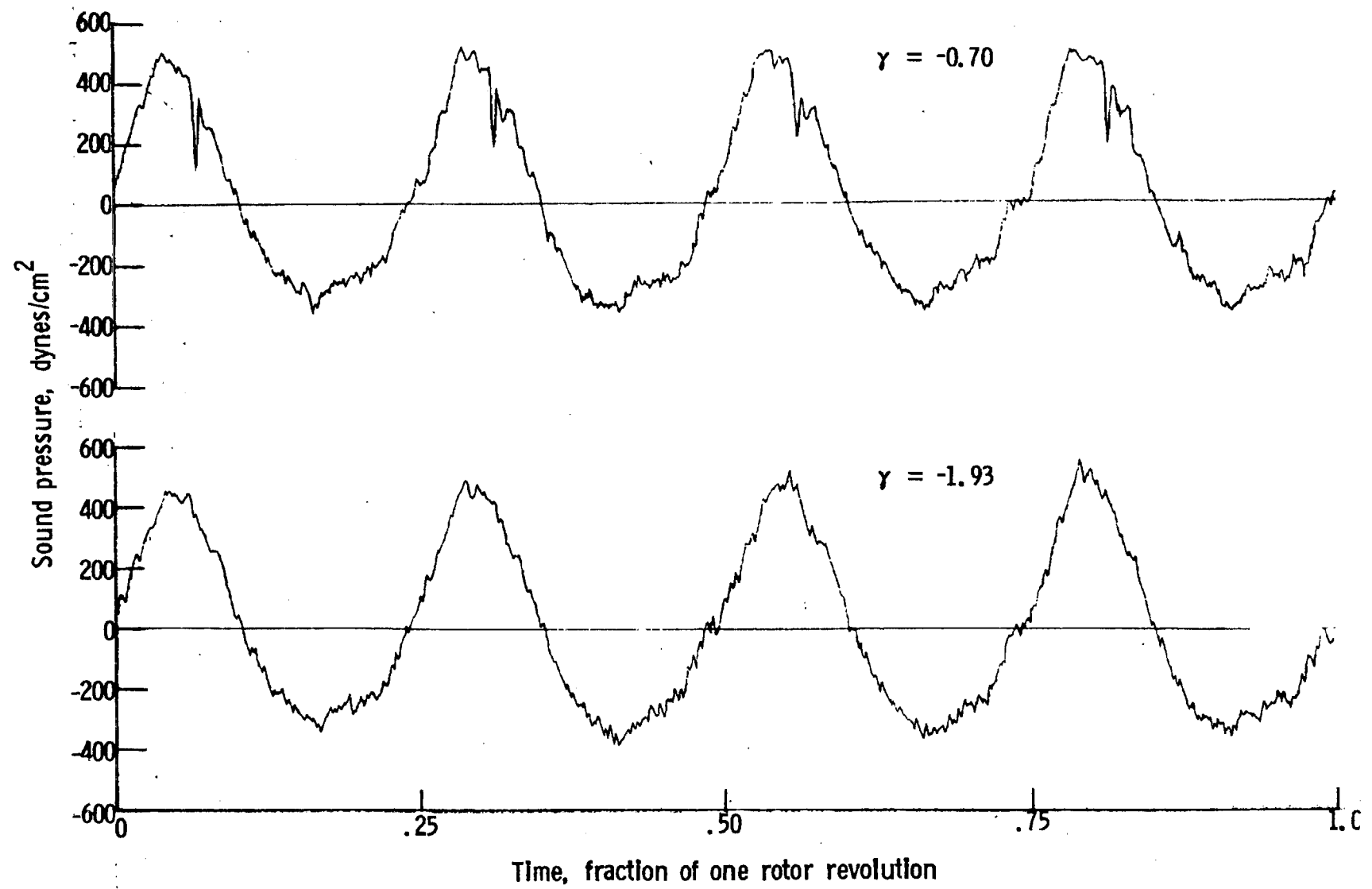
a. Mic. no. 1.

Figure 38. - Effect of descent angle variation on noise generated by helicopter model with swept-tapered tips installed. $V_{\infty} = 75.9$ knots.



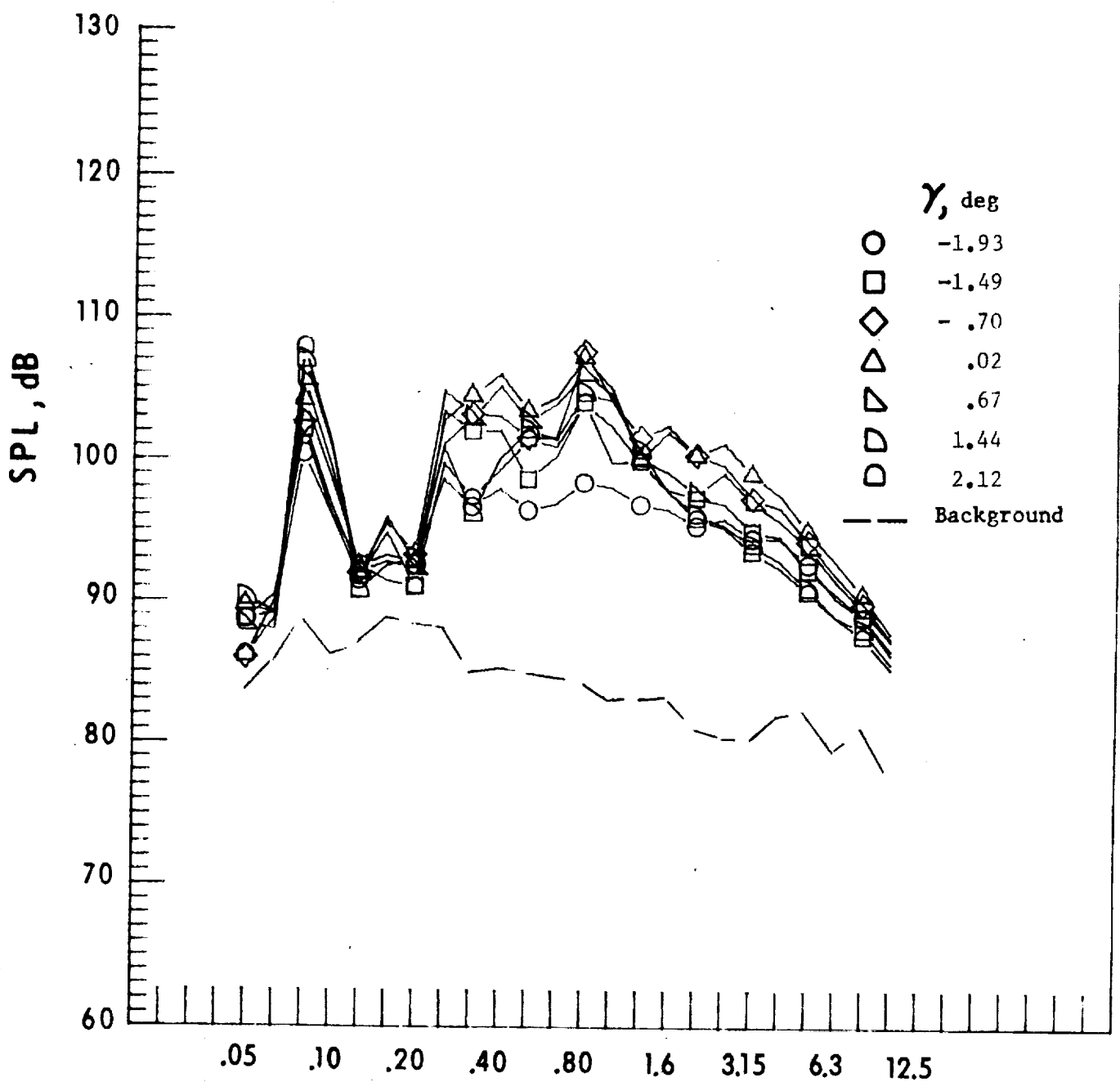
b. Mic. no. 2.

Figure 38_o. - Continued.



c. Pressure-time histories, Mic. no. 2.

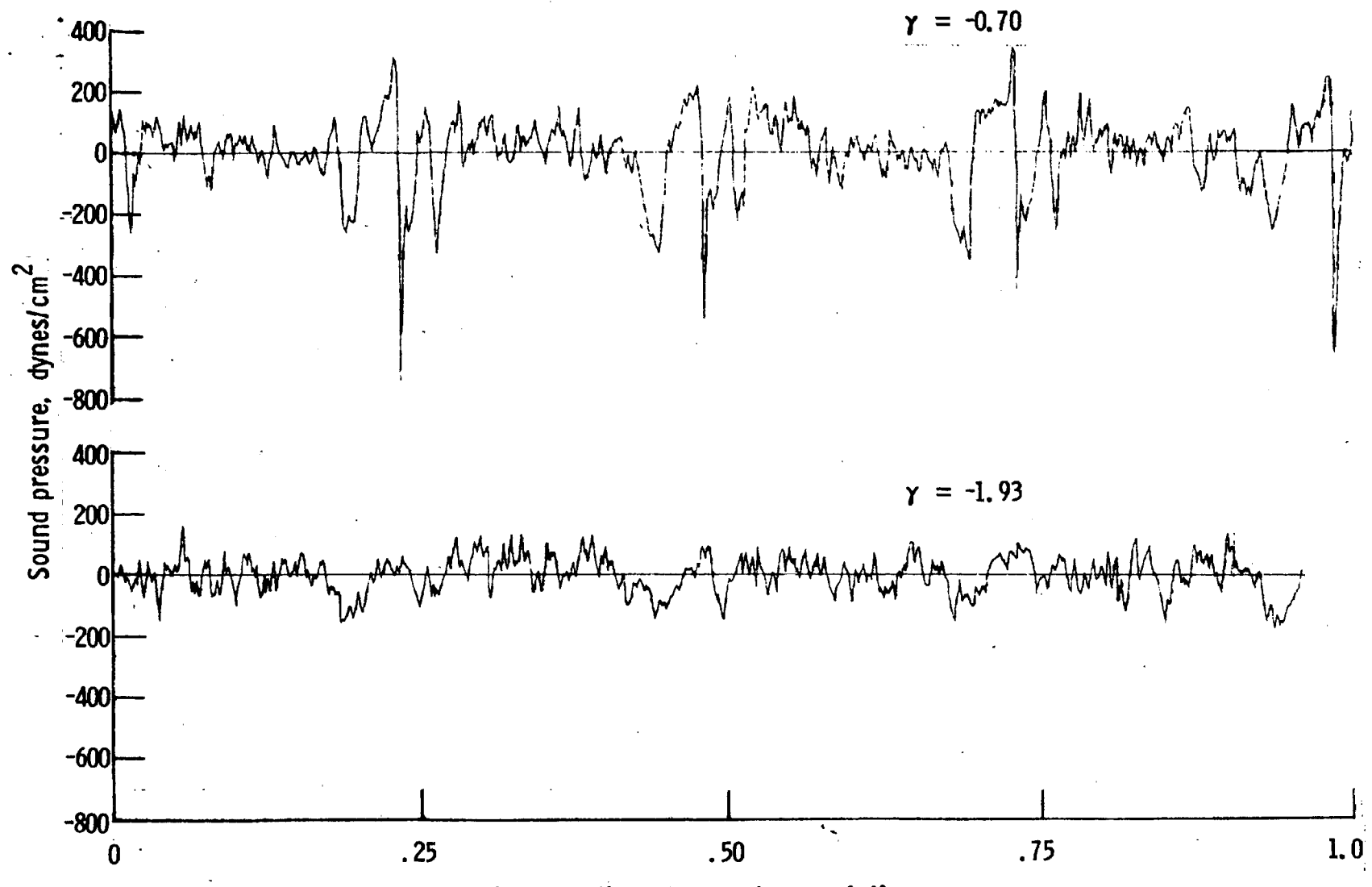
Figure 38. - Continued.



One-third-octave-band center frequency, kHz

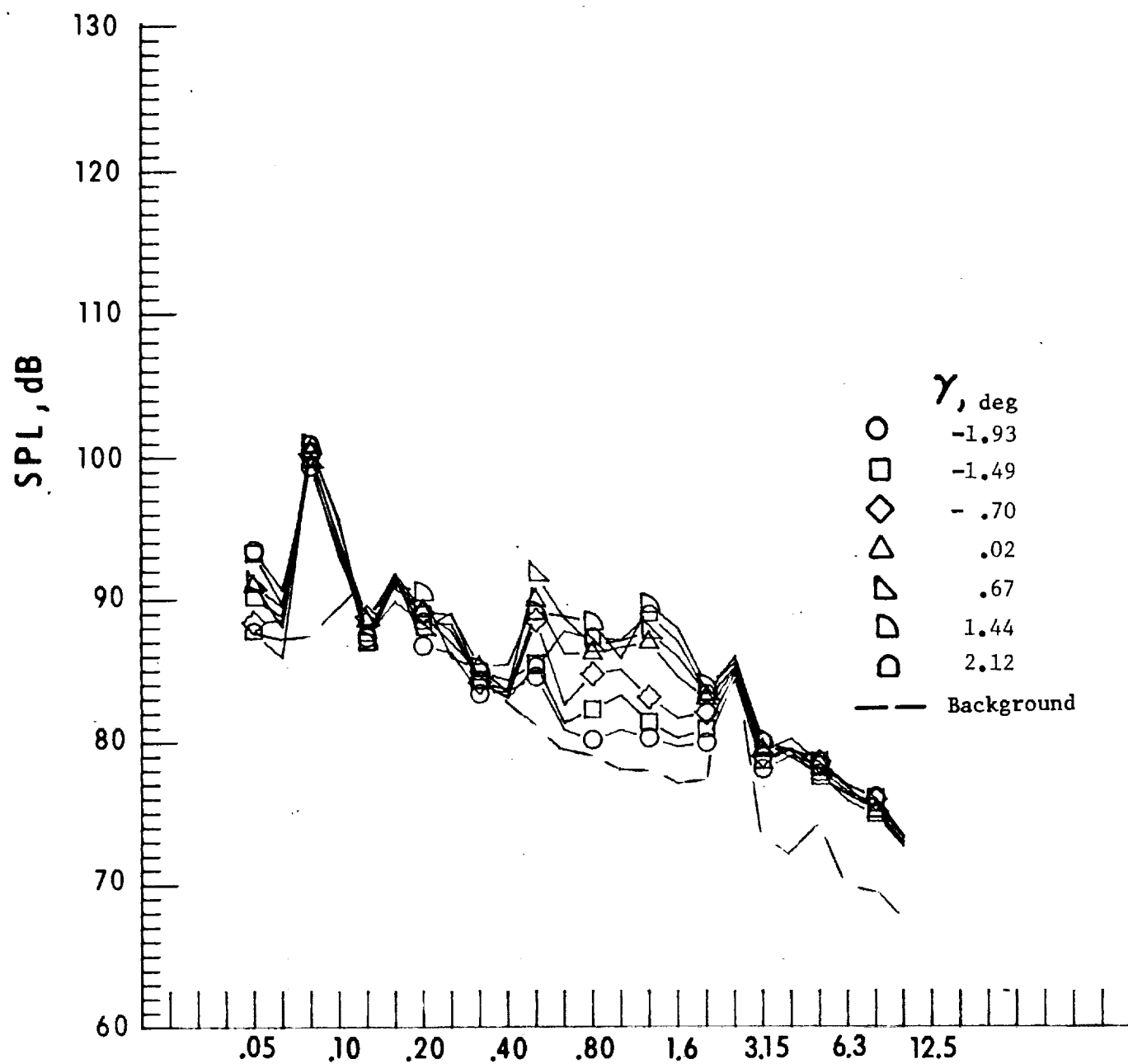
d. Mic. no. 3.

Figure 38. - Continued.



e. Pressure-time histories, Mic. no. 3.

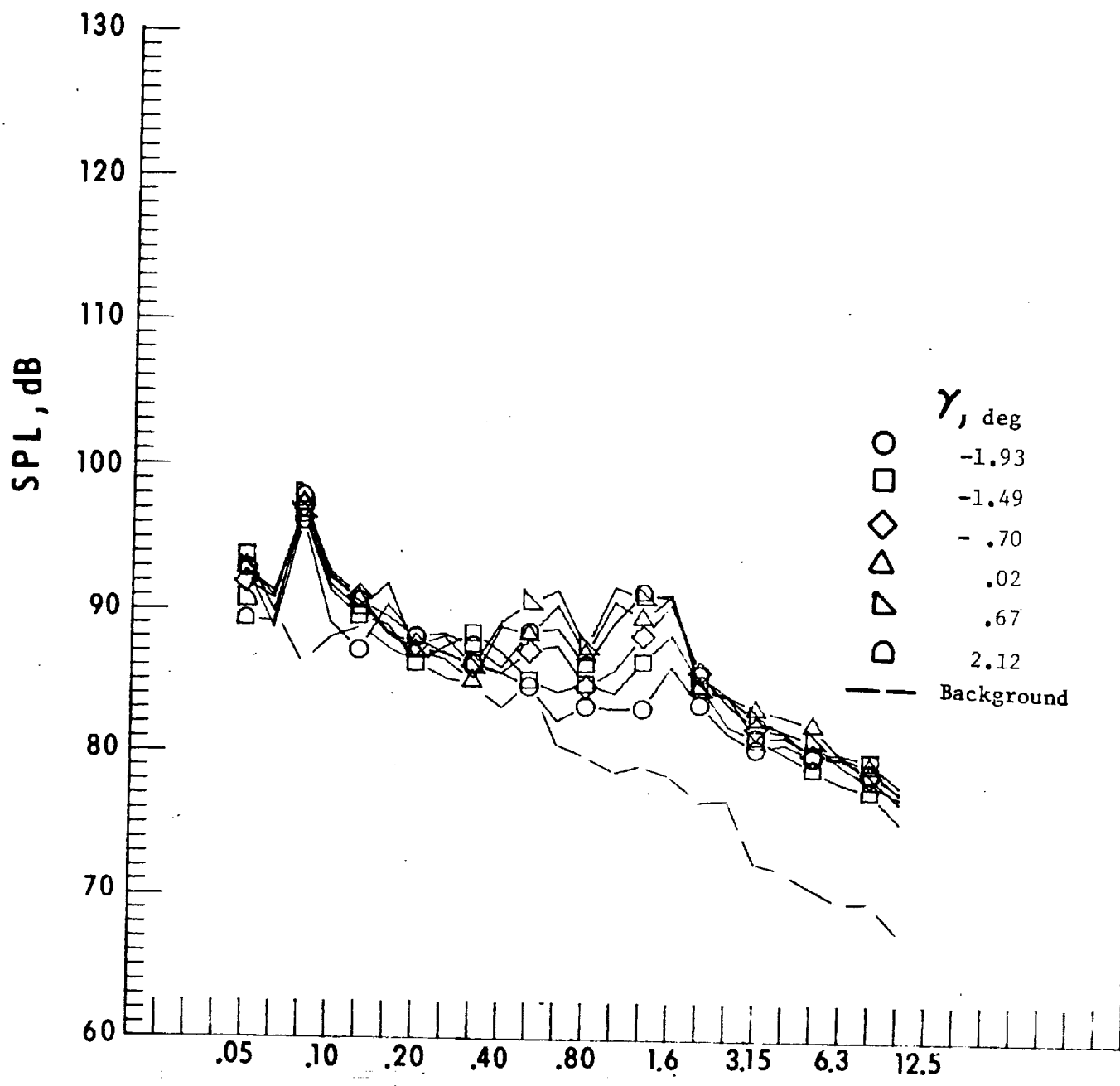
Figure 38. - Continued.



One-third-octave-band center frequency, kHz

f. Mic. no. 4.

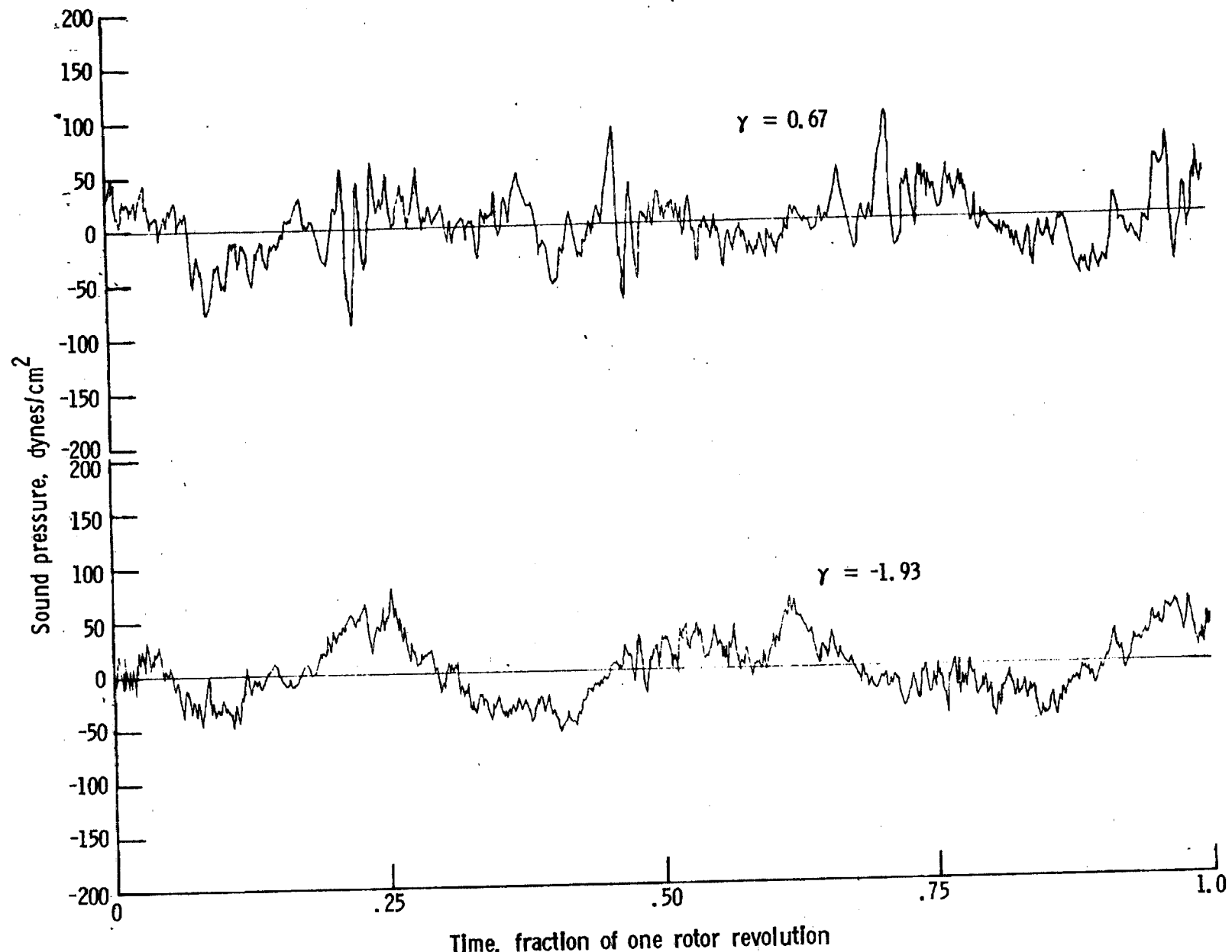
Figure 38. - Continued.



One-third-octave-band center frequency, kHz

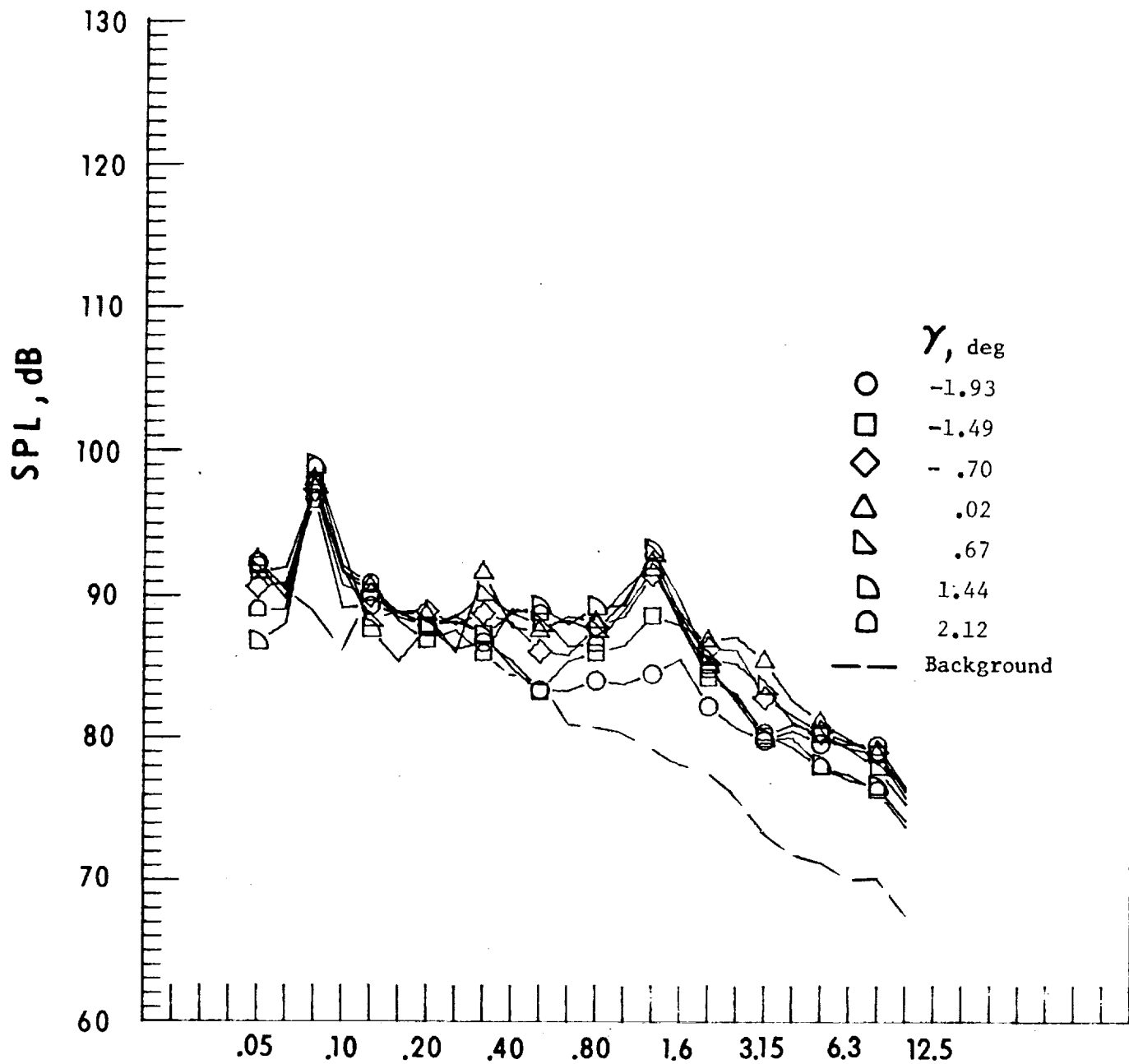
g. Mic. no. 5.

Figure 38. - Continued .



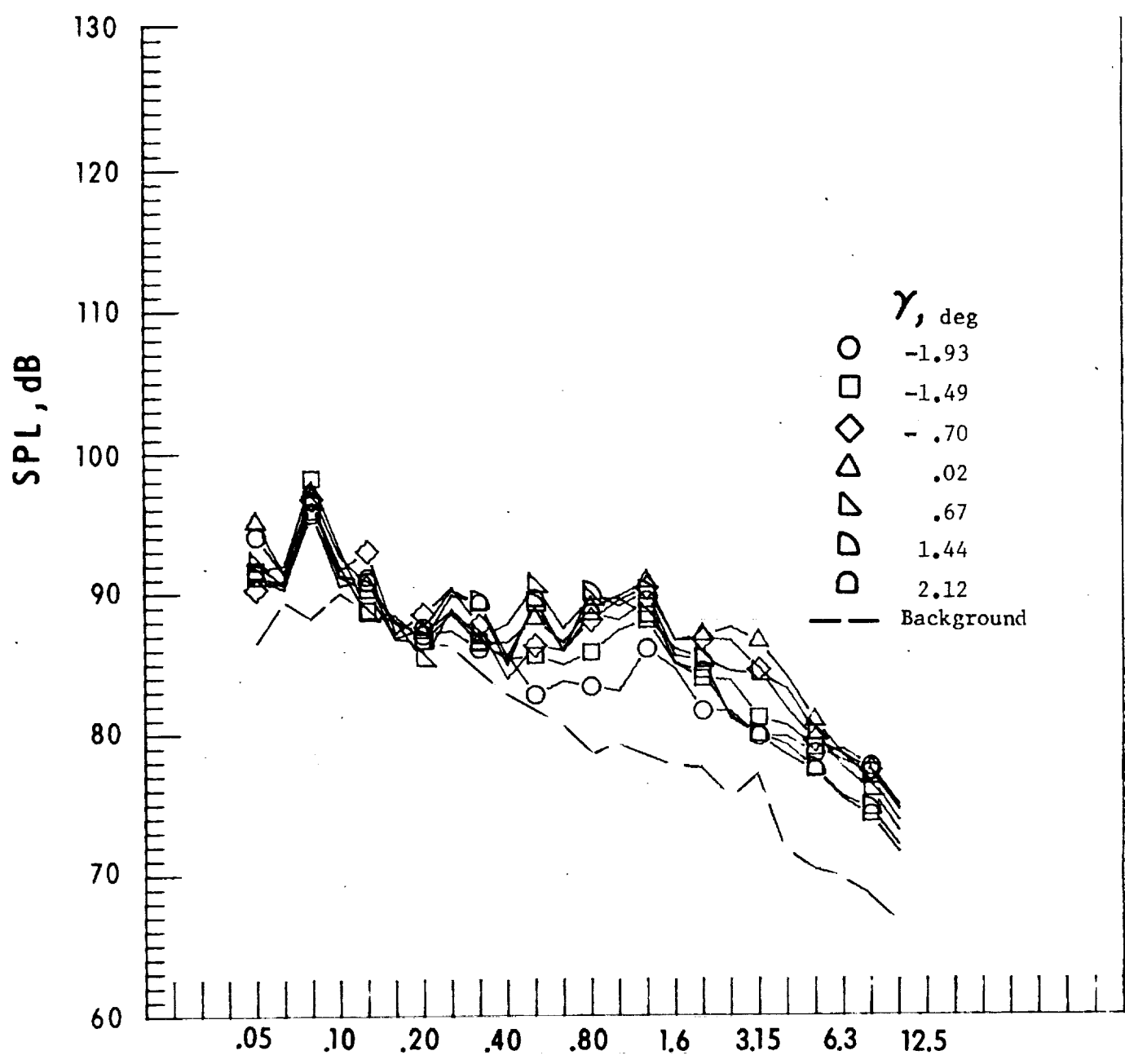
h. Pressure-time histories, Mic. no. 5.

Figure 38. - Continued.



i. Mic. no. 6.

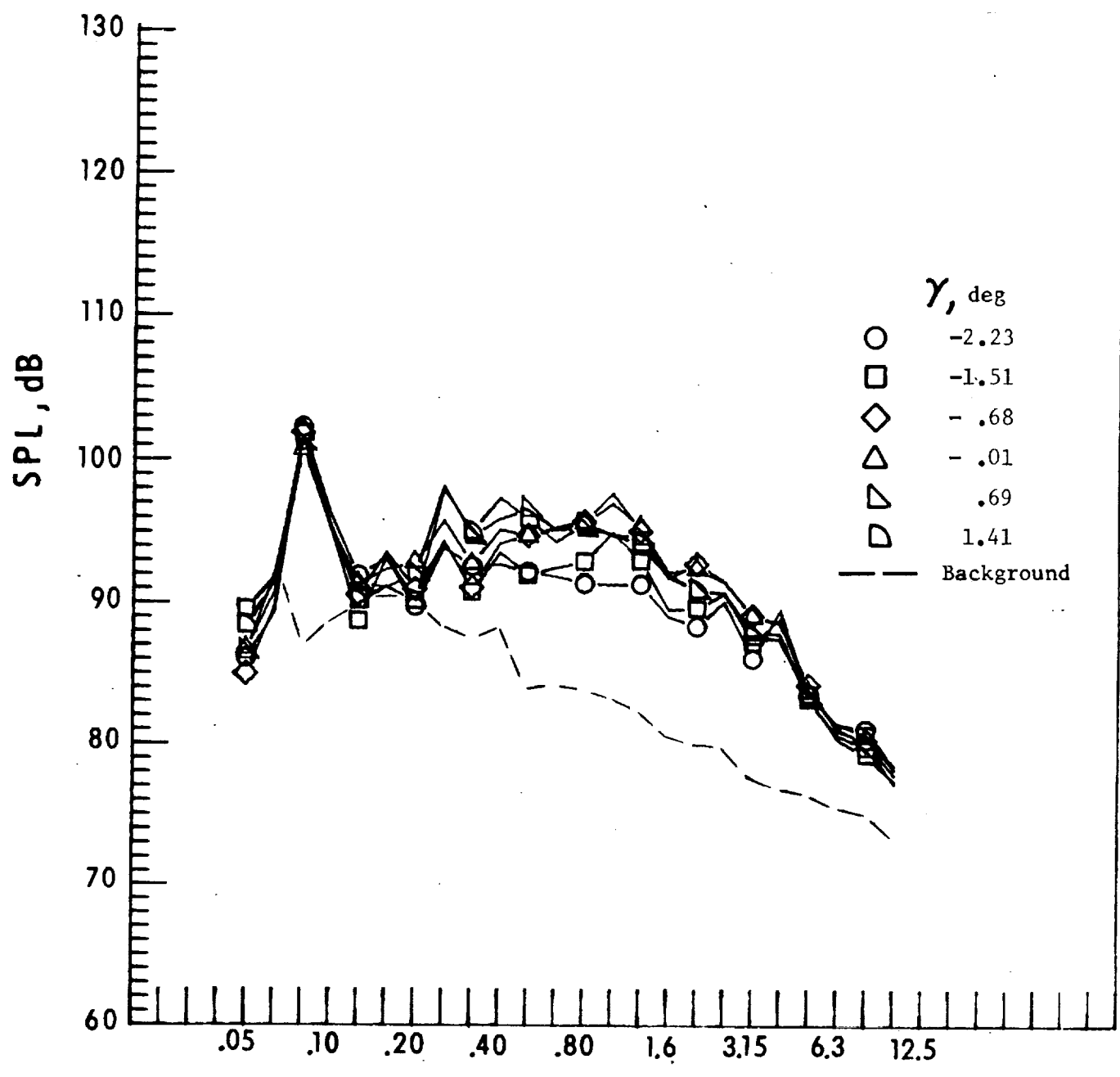
Figure 38. - Continued.



One-third-octave-band center frequency, kHz

j. Mic. no. 7.

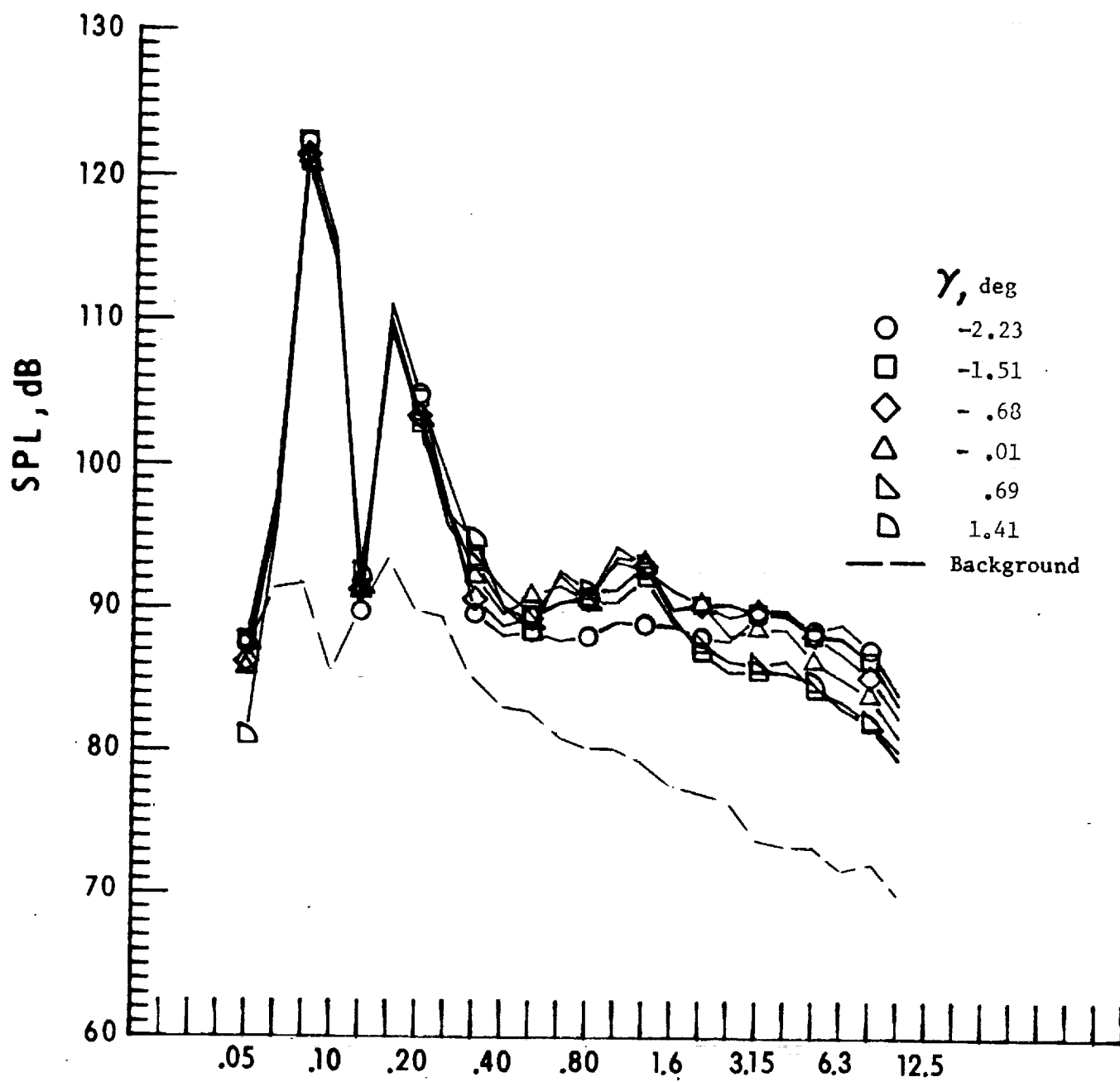
Figure 38. - Concluded.



One-third-octave-band center frequency, kHz

a. Mic. no. 1.

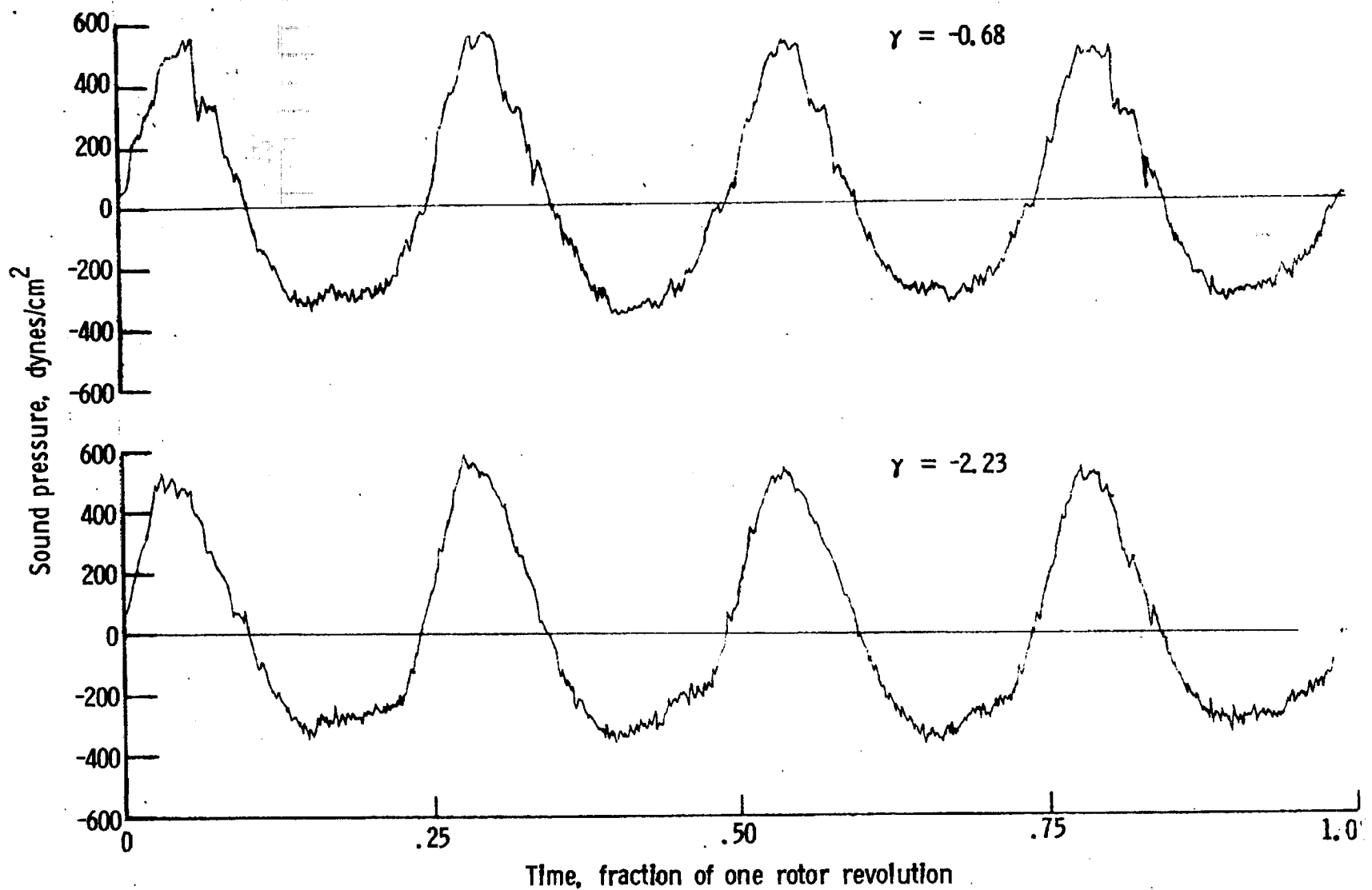
Figure 39. - Effect of descent angle variation on noise generated by helicopter model with square tips installed. $V_\infty = 81.8$ knots.



One-third-octave-band center frequency, kHz

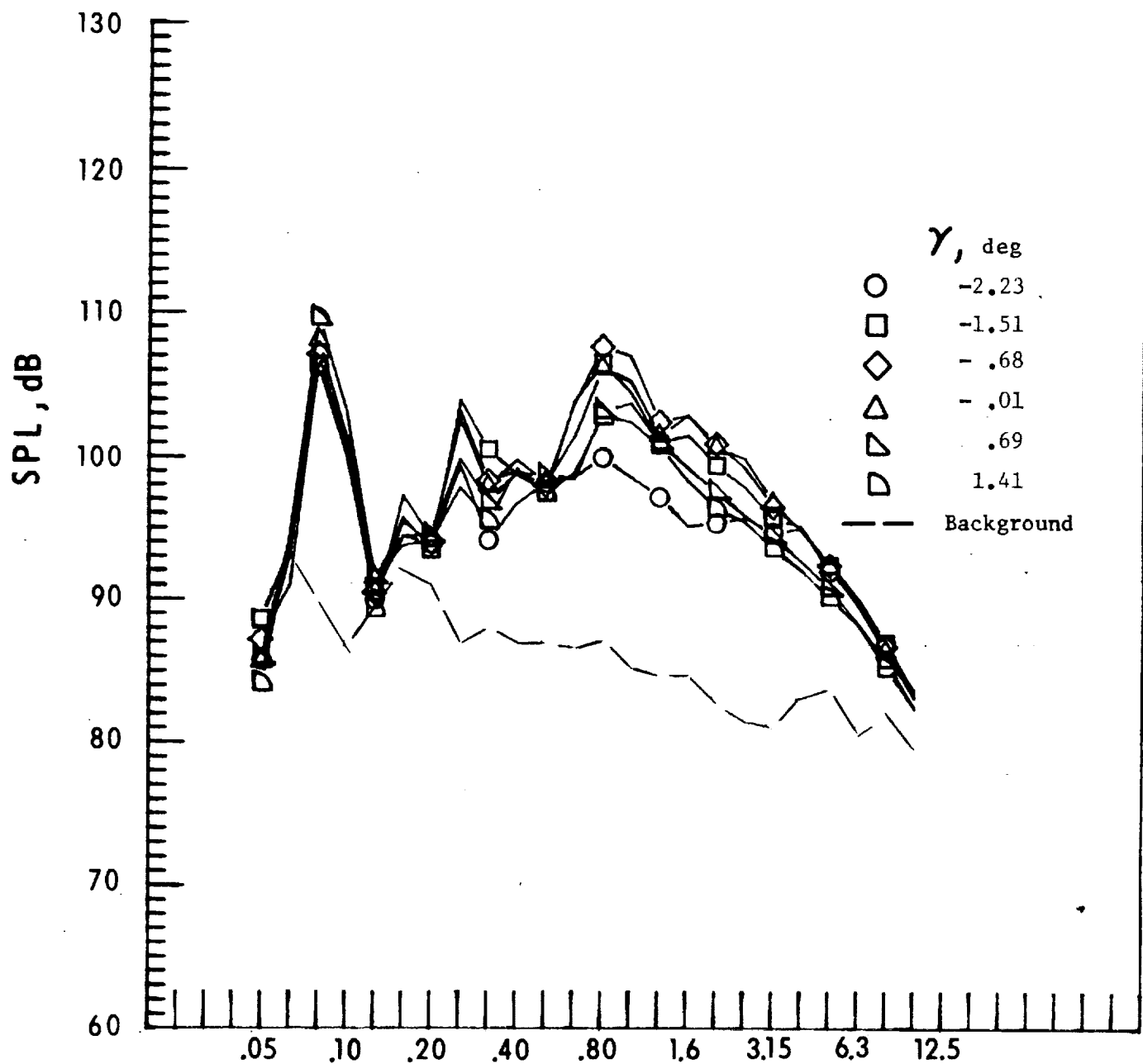
b. Mic. no. 2.

Figure 39. - Continued.



c. Pressure-time histories, Mic. no. 2.

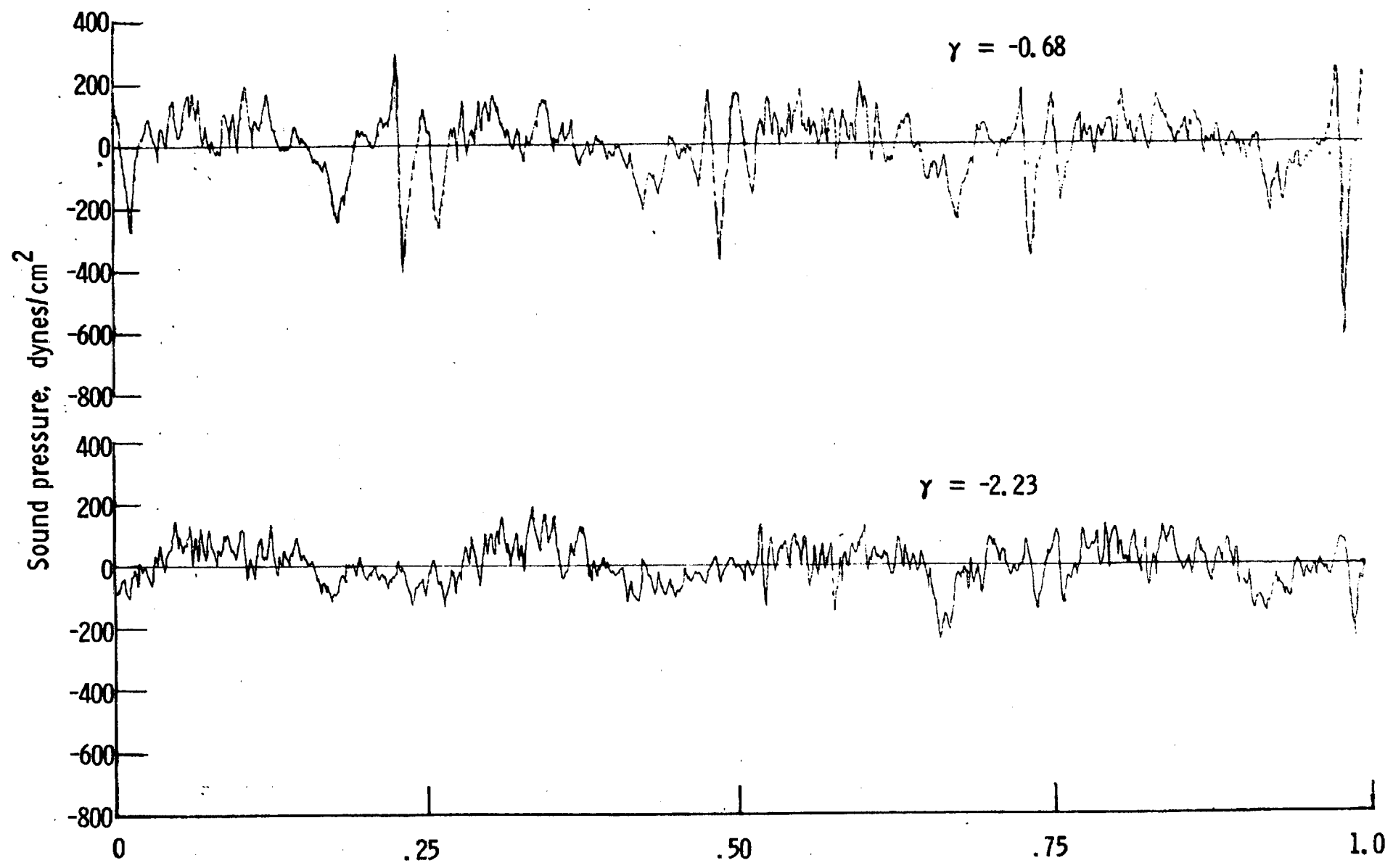
Figure 39. - Continued.



One-third-octave-band center frequency, kHz

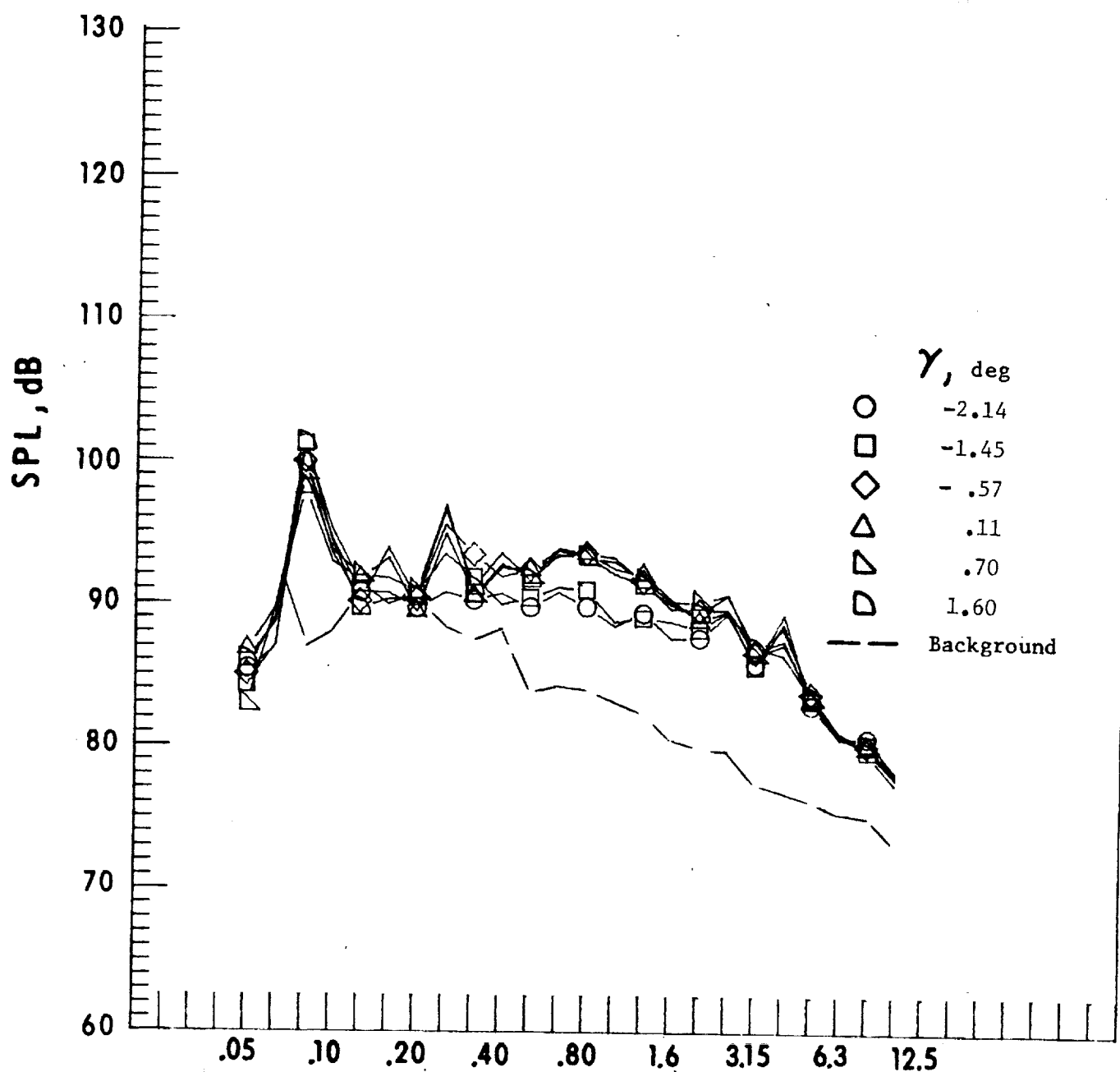
d. Mic. no. 3.

Figure 39. - Continued.



e. Pressure-time histories, Mic. no. 3.

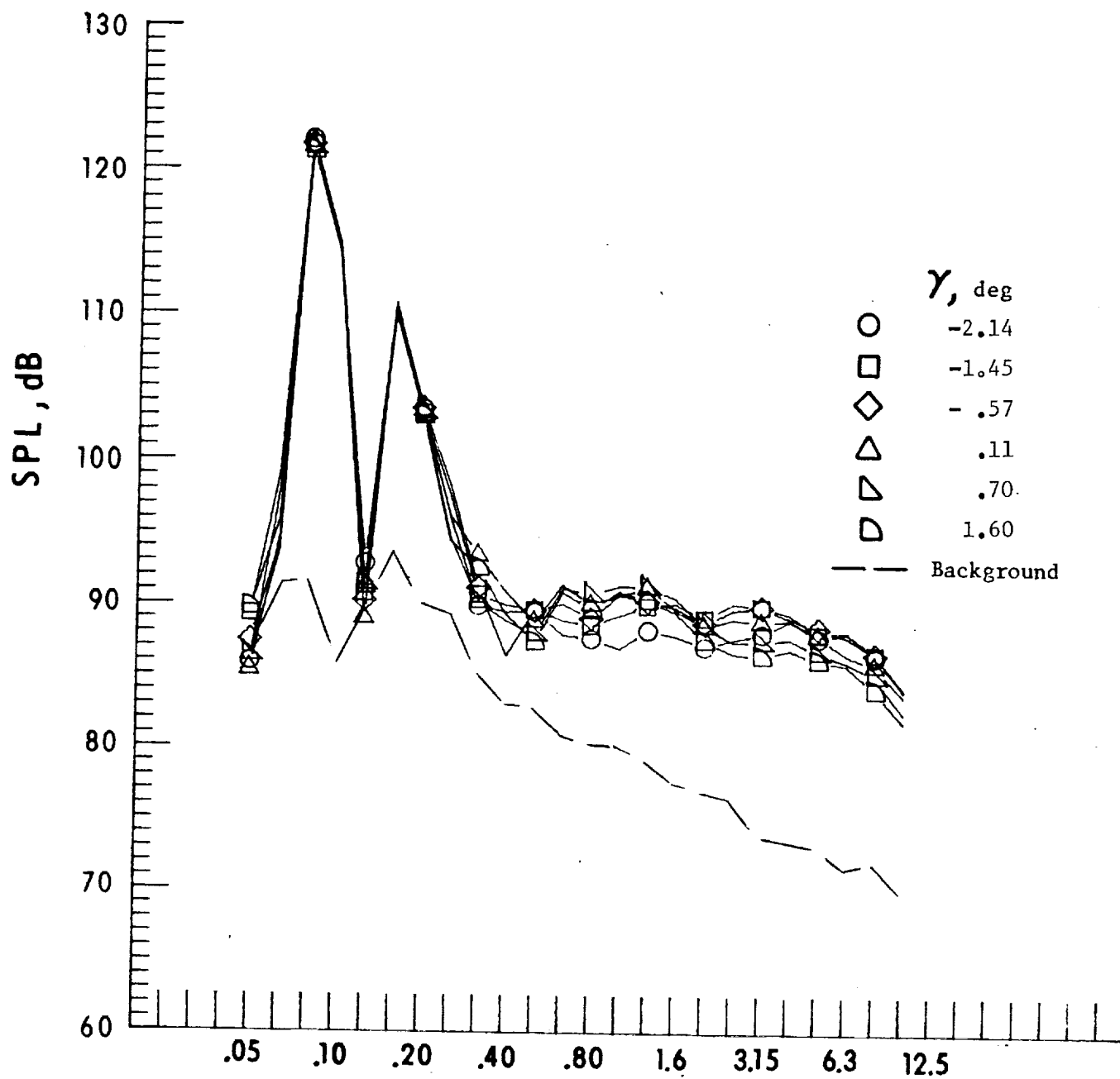
Figure 39. - Concluded.



One-third-octave-band center frequency, kHz

a. Mic. no. 1.

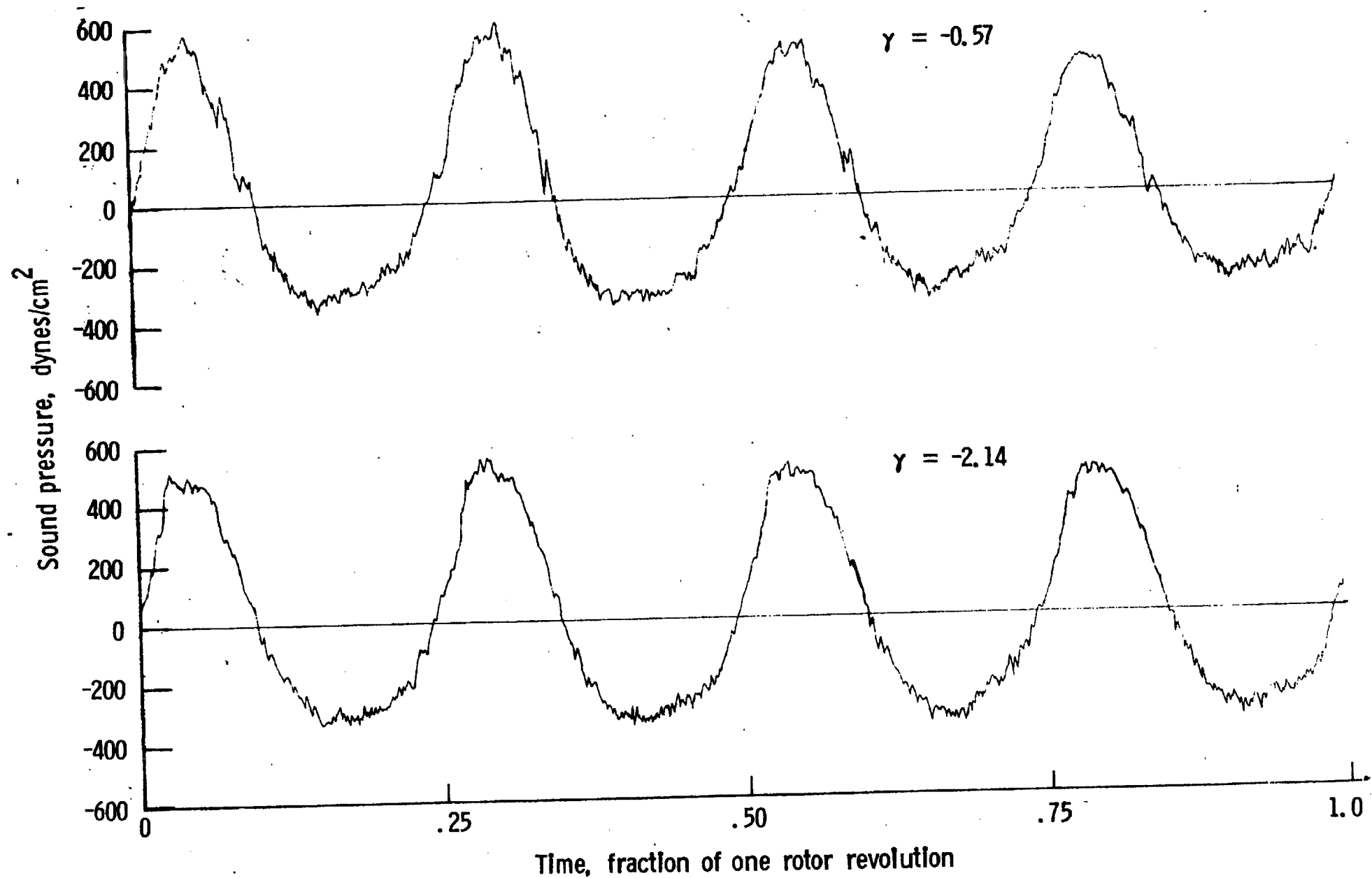
Figure 40. - Effect of descent angle variation on noise generated by helicopter model with ogee tips installed. $V_{\infty} = 81.8$ knots.



One-third-octave-band center frequency, kHz

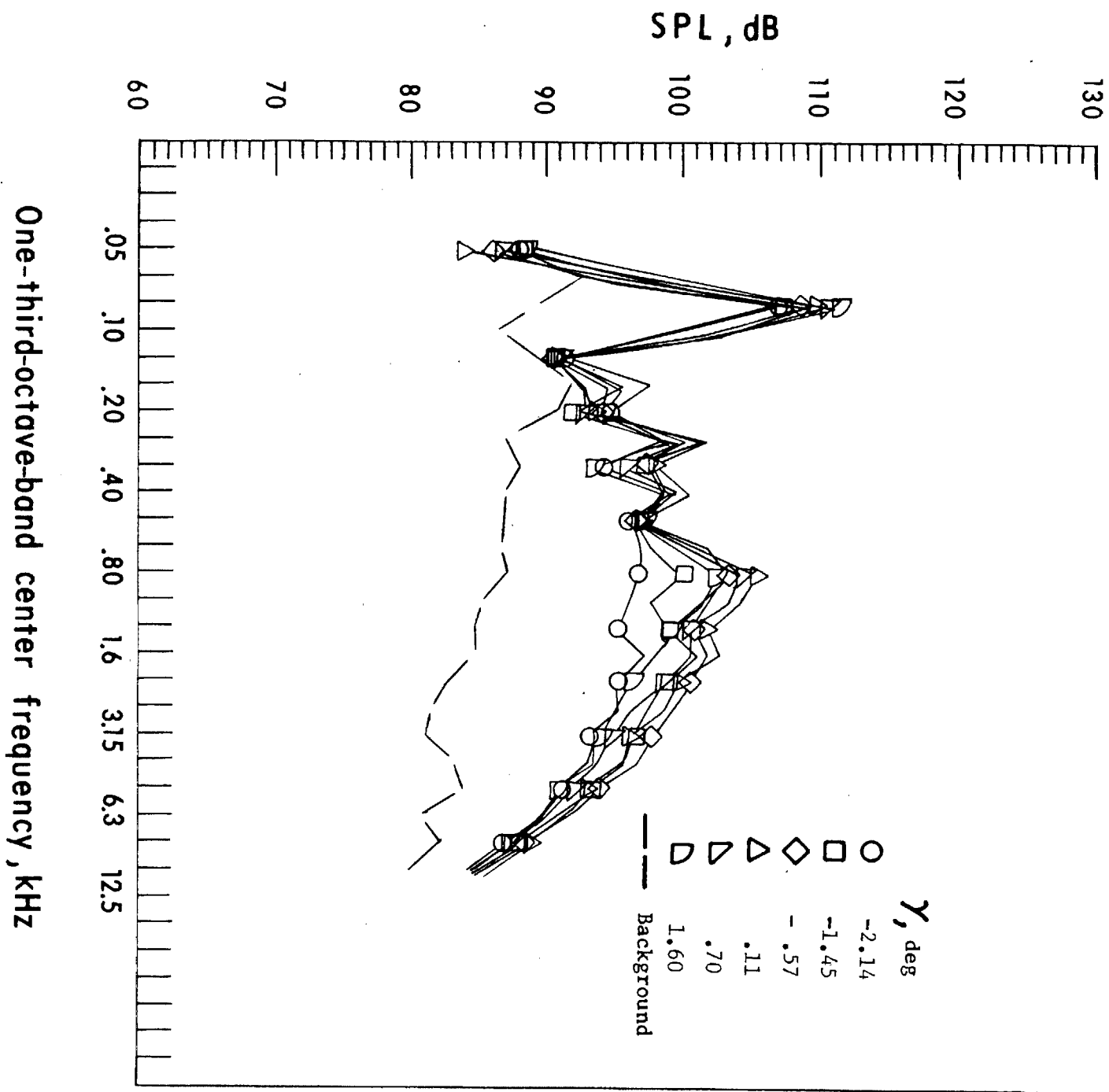
b. Mic. no. 2.

Figure 40. - Continued.



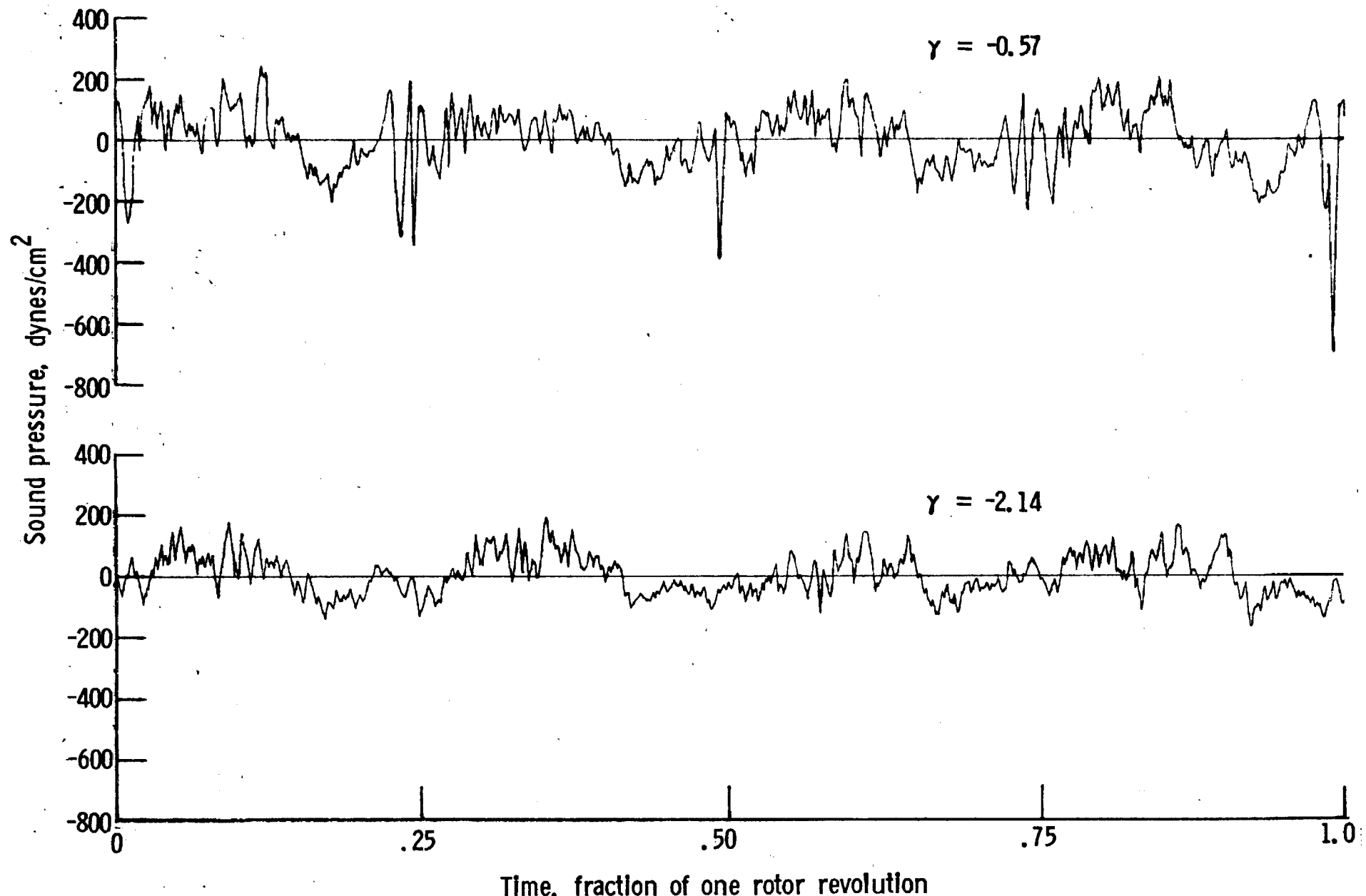
c. Pressure-time histories, Mic. no. 2.

Figure 40. - Continued.



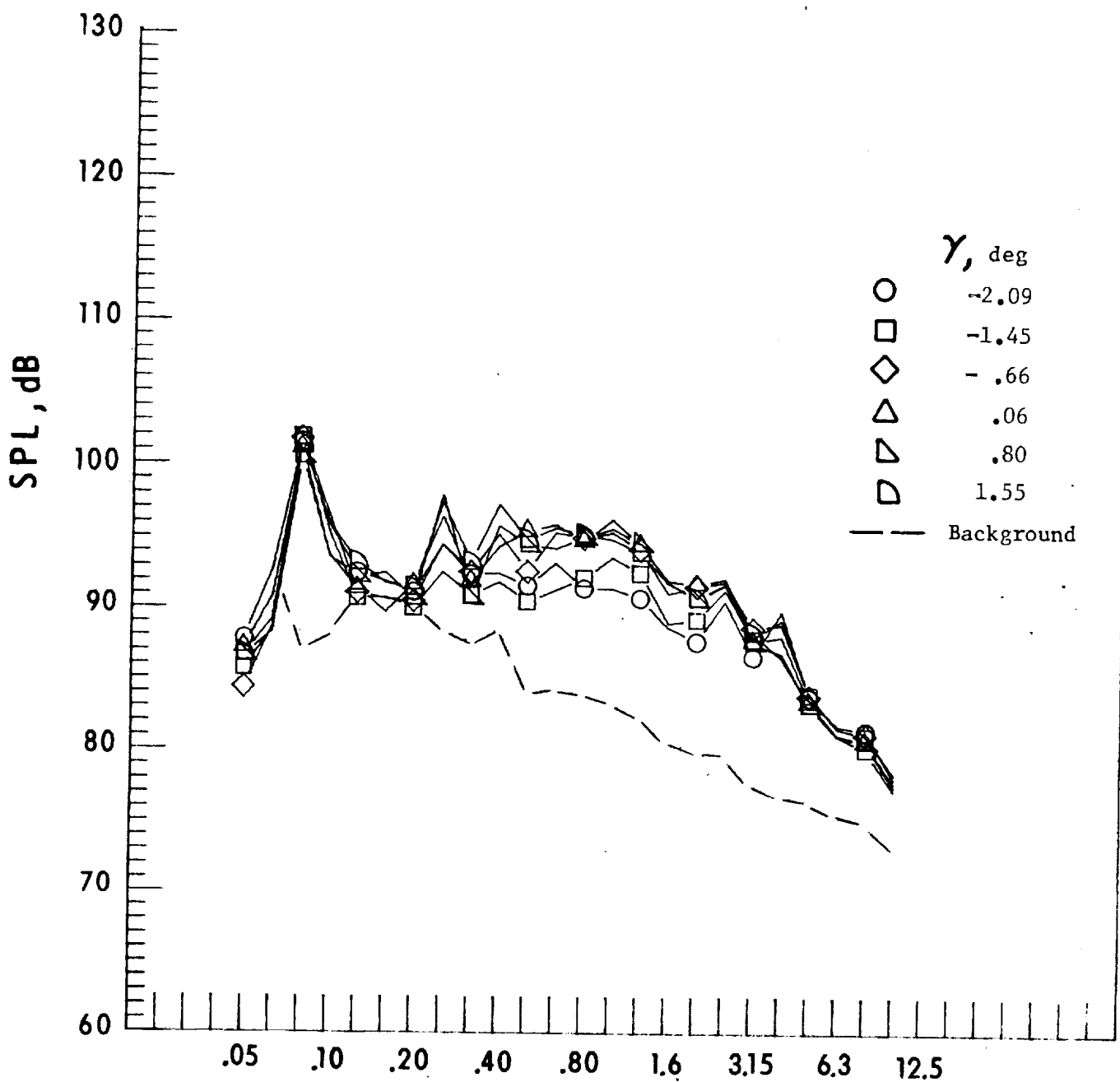
d. Mic. no. 3.

Figure 40. - Continued.



e. Pressure-time histories, Mic. no. 3.

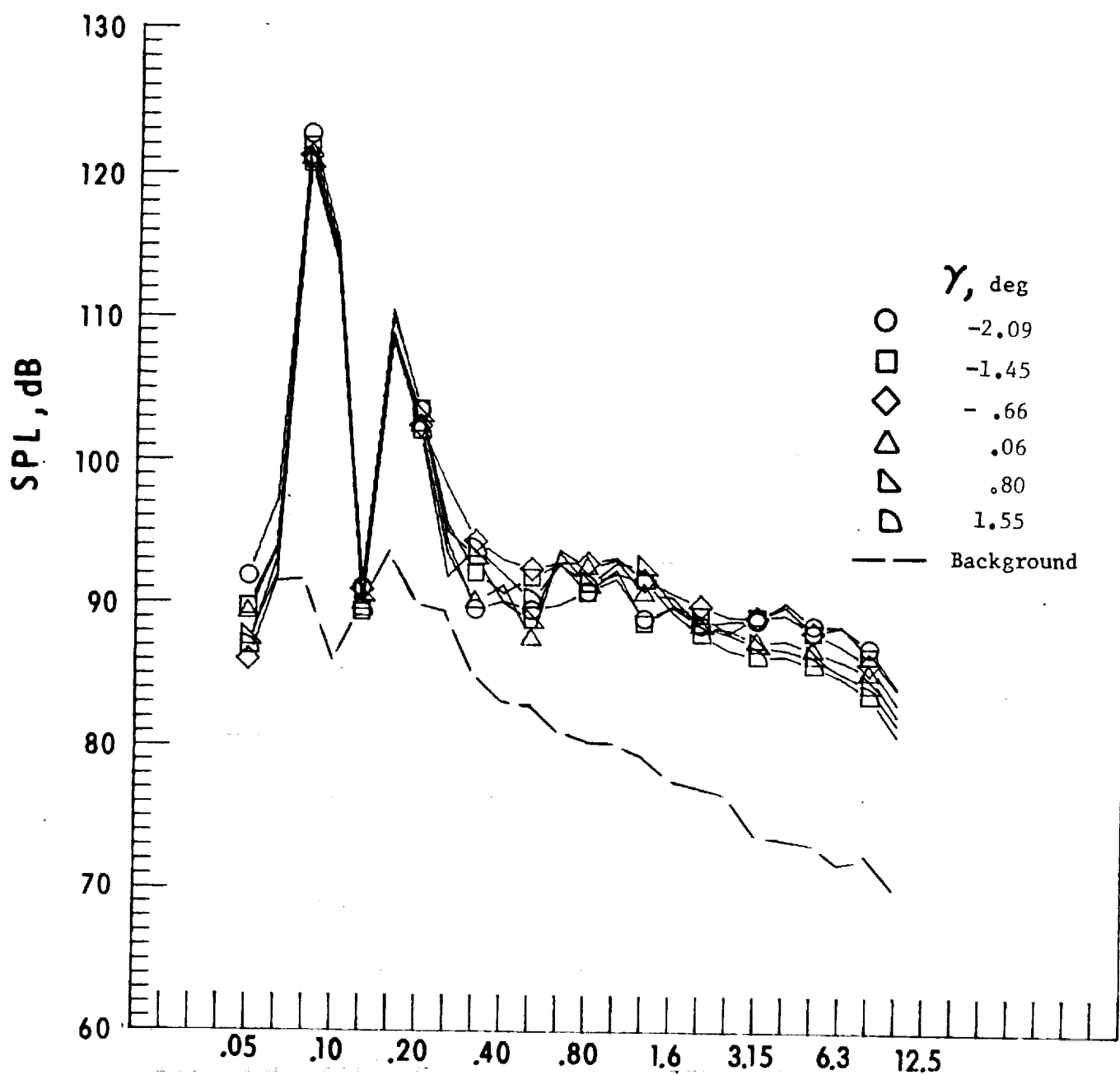
Figure 40. - Concluded.



One-third-octave-band center frequency, kHz

a. Mic. no. 1.

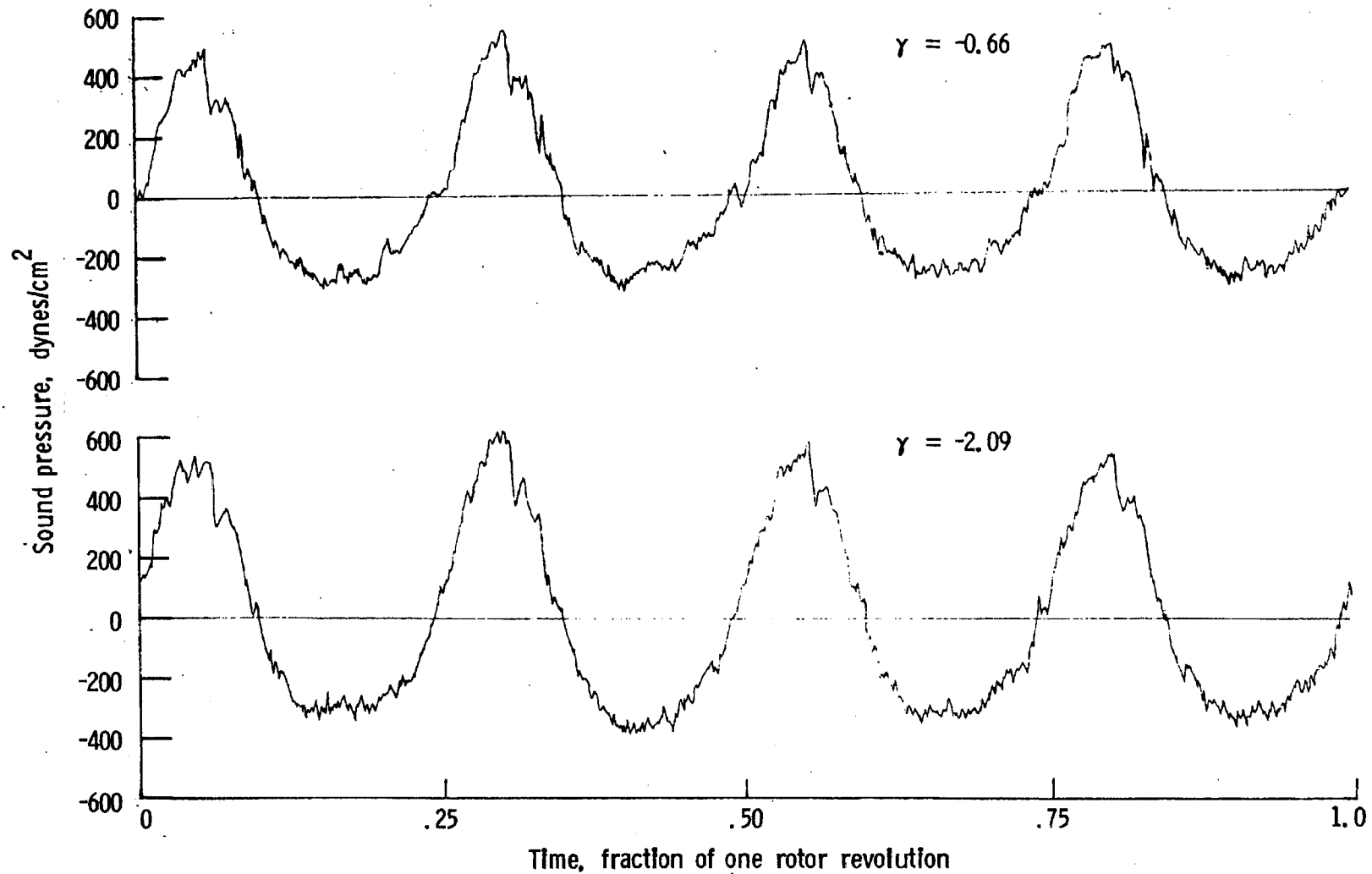
Figure 41. - Effect of descent angle variation on noise generated by helicopter model with sub-wing tips installed. $V_{\infty} = 82.0$ knots.



One-third-octave-band center frequency, kHz

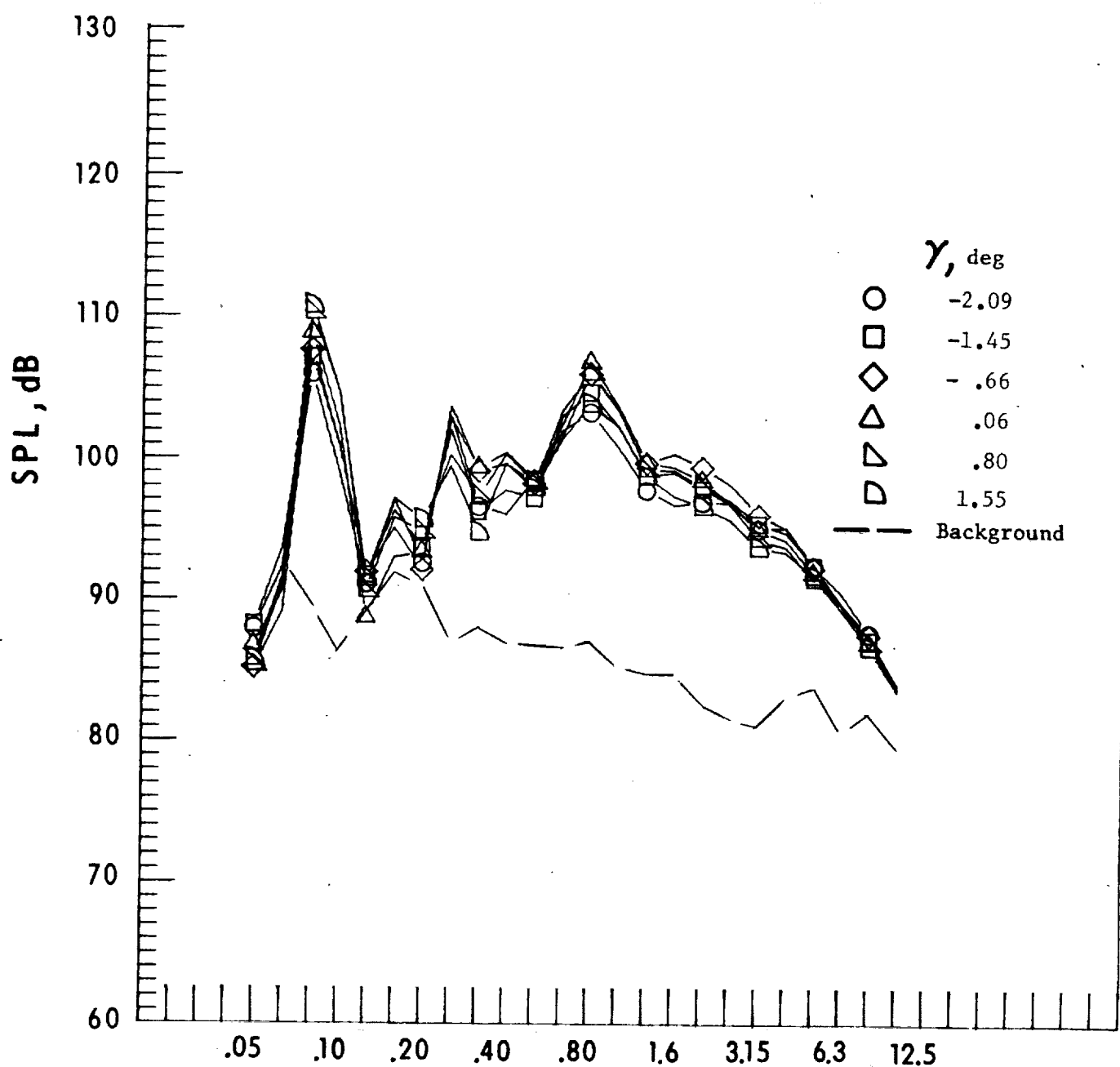
b. Mic. no. 2.

Figure 41. - Continued.



c. Pressure-time histories, Mic. no. 2.

Figure 41. - Continued.



d. Mic. no. 3.

Figure 41. - Continued.

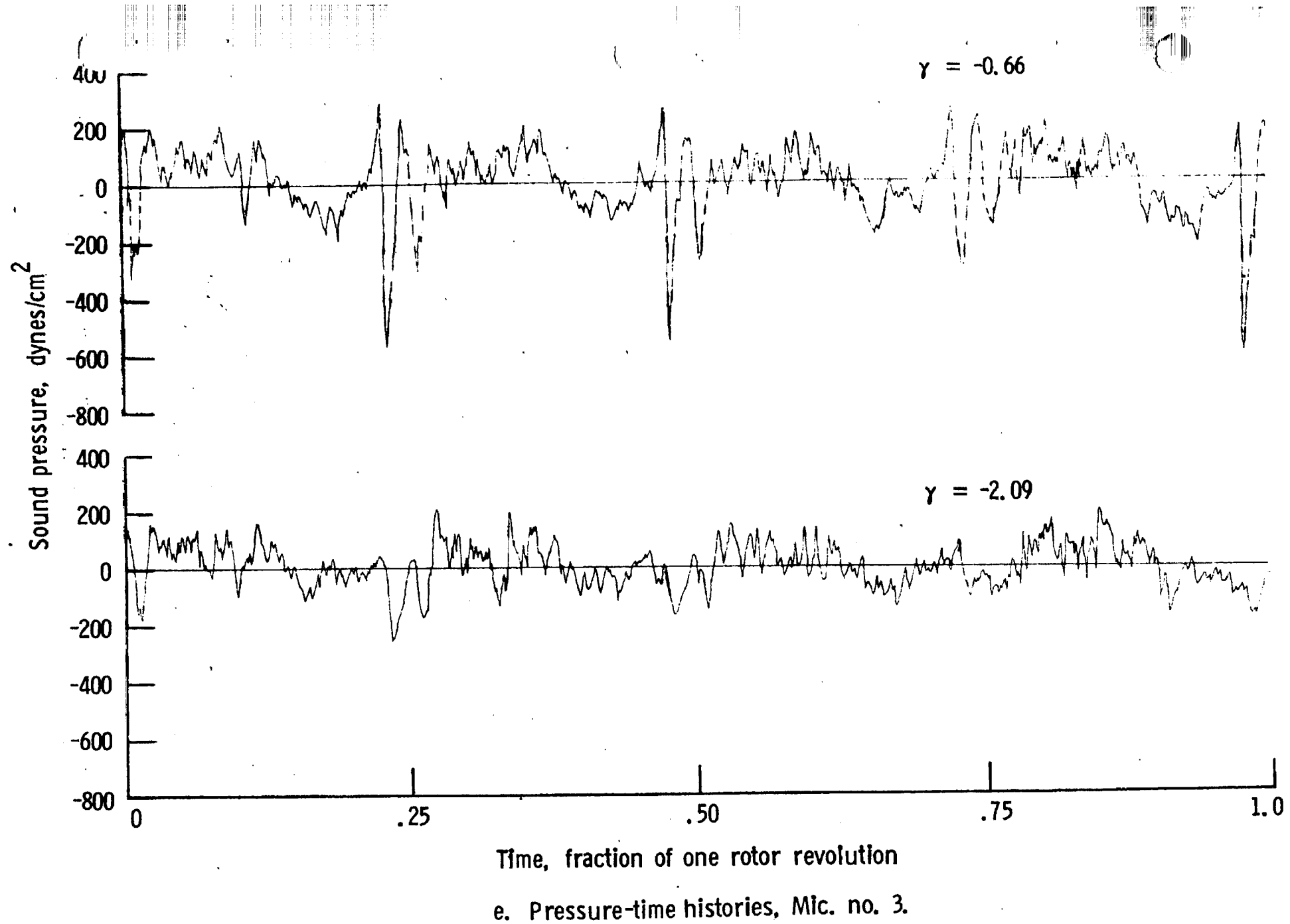
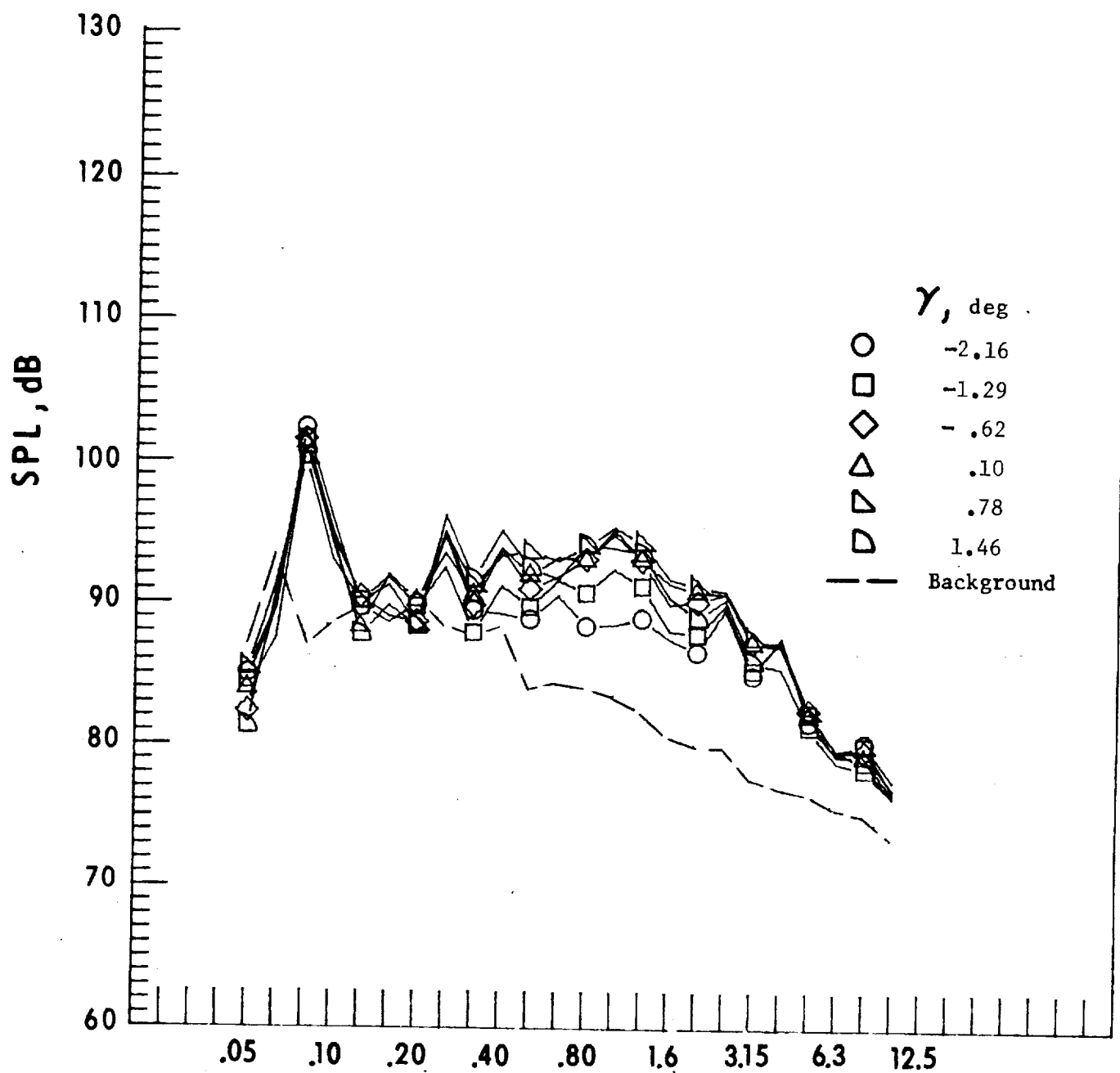


Figure 41. - Concluded.



One-third-octave-band center frequency, kHz

a. Mic. no. 1.

Figure 42. - Effect of descent angle variation on noise generated by helicopter model with swept-tapered tips installed. $V_\infty = 81.6$ knots.

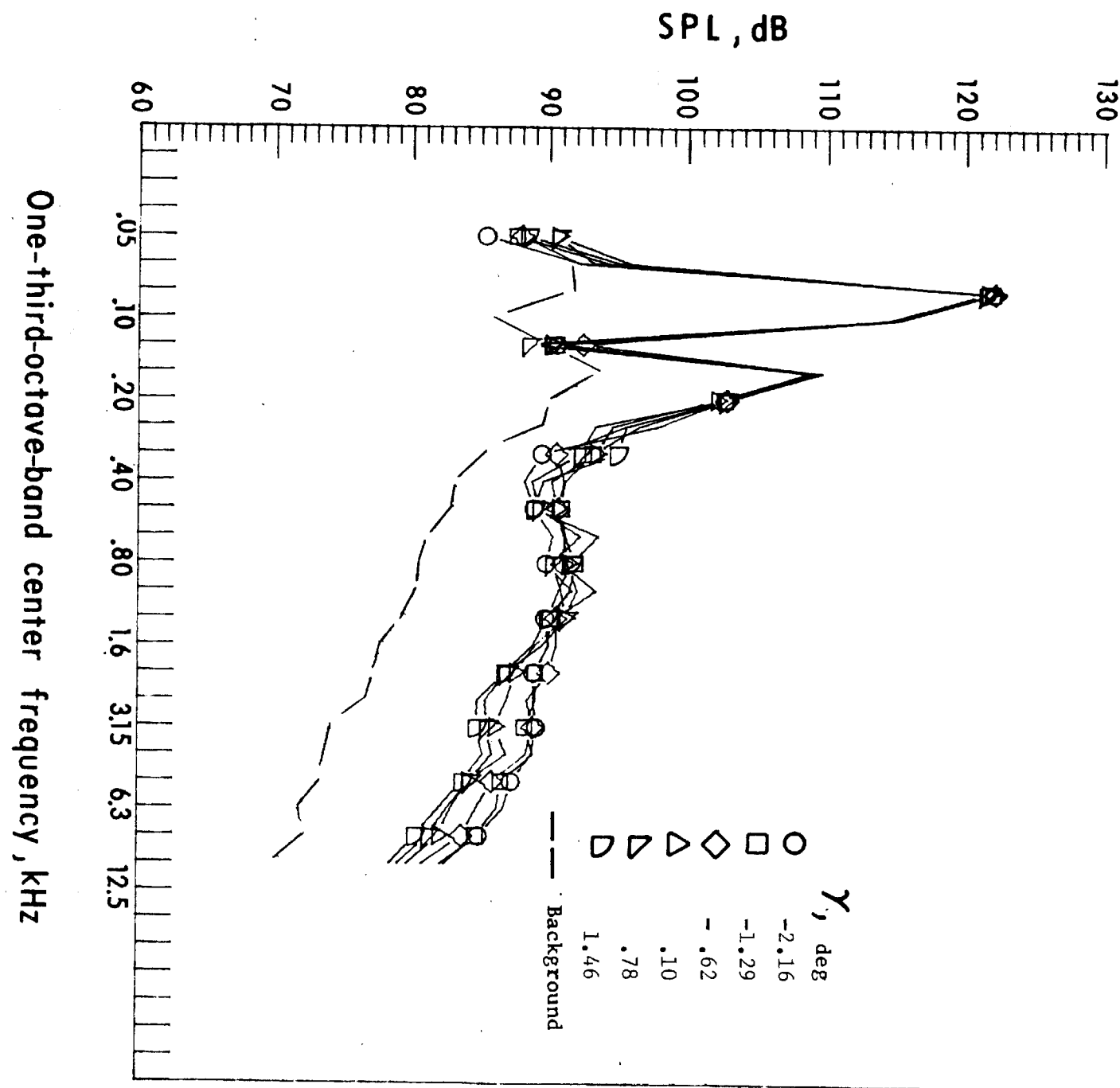
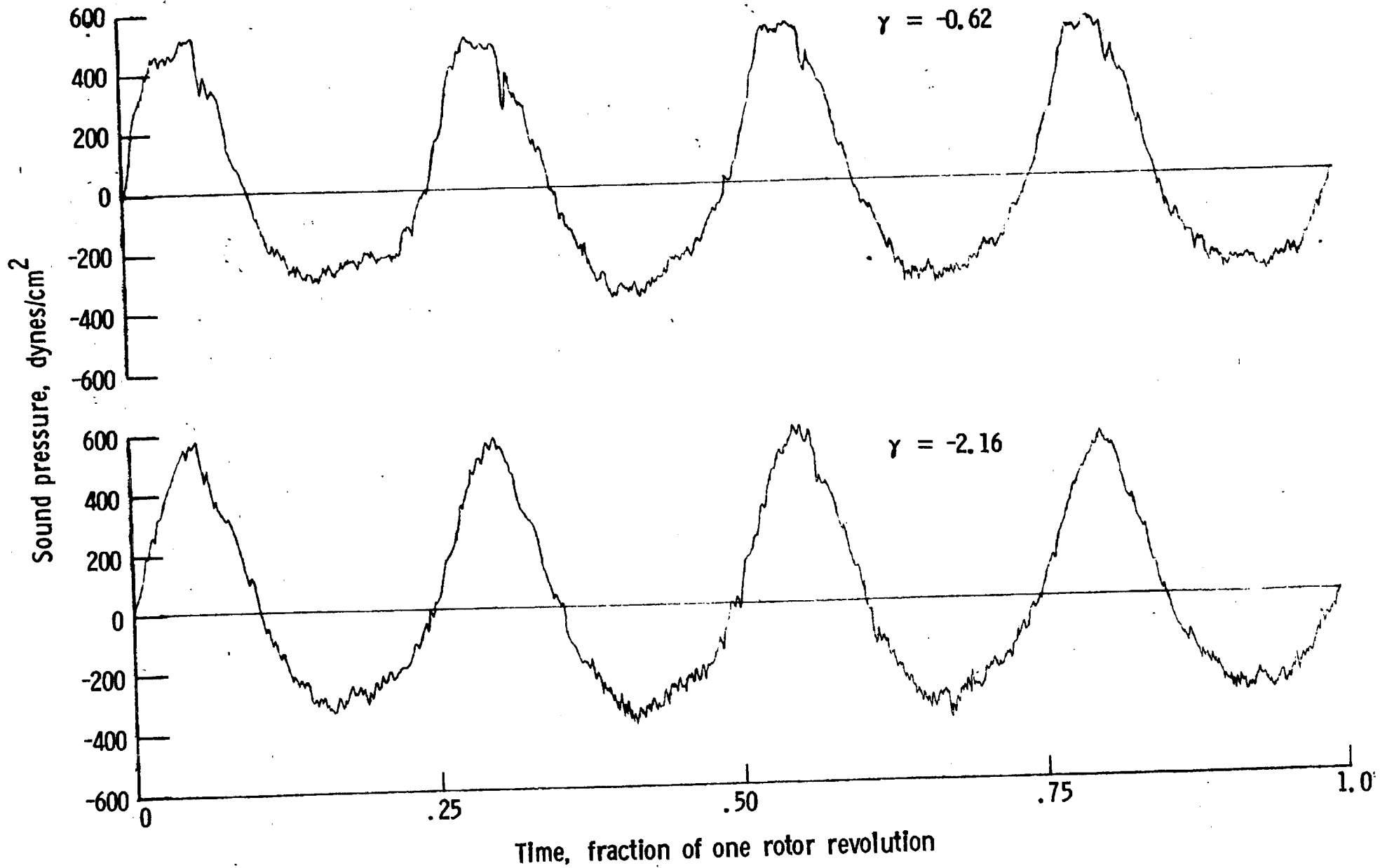


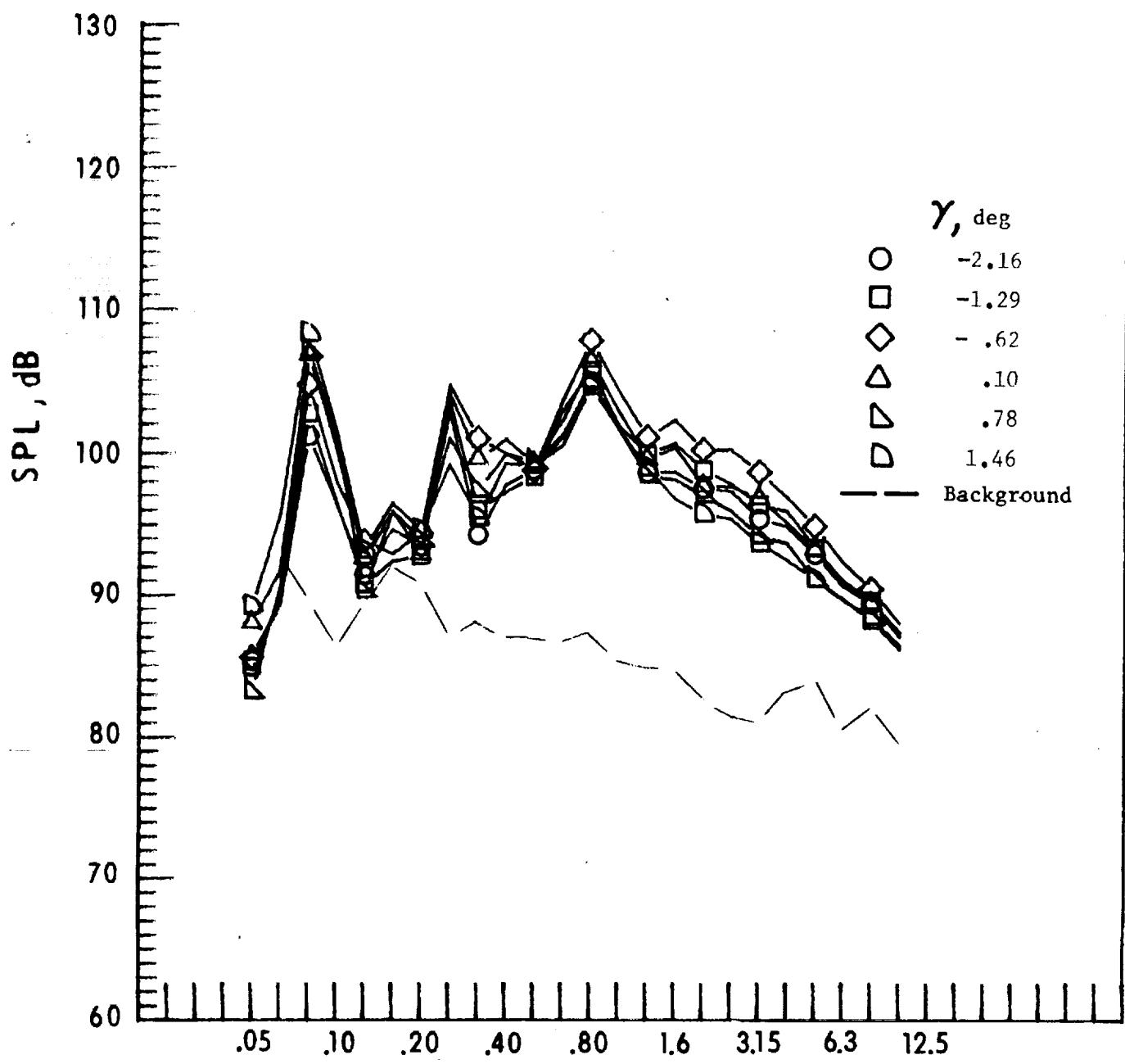
Figure 42. - Continued.

b. Mic. no. 2.



c. Pressure-time histories, Mic. no. 2.

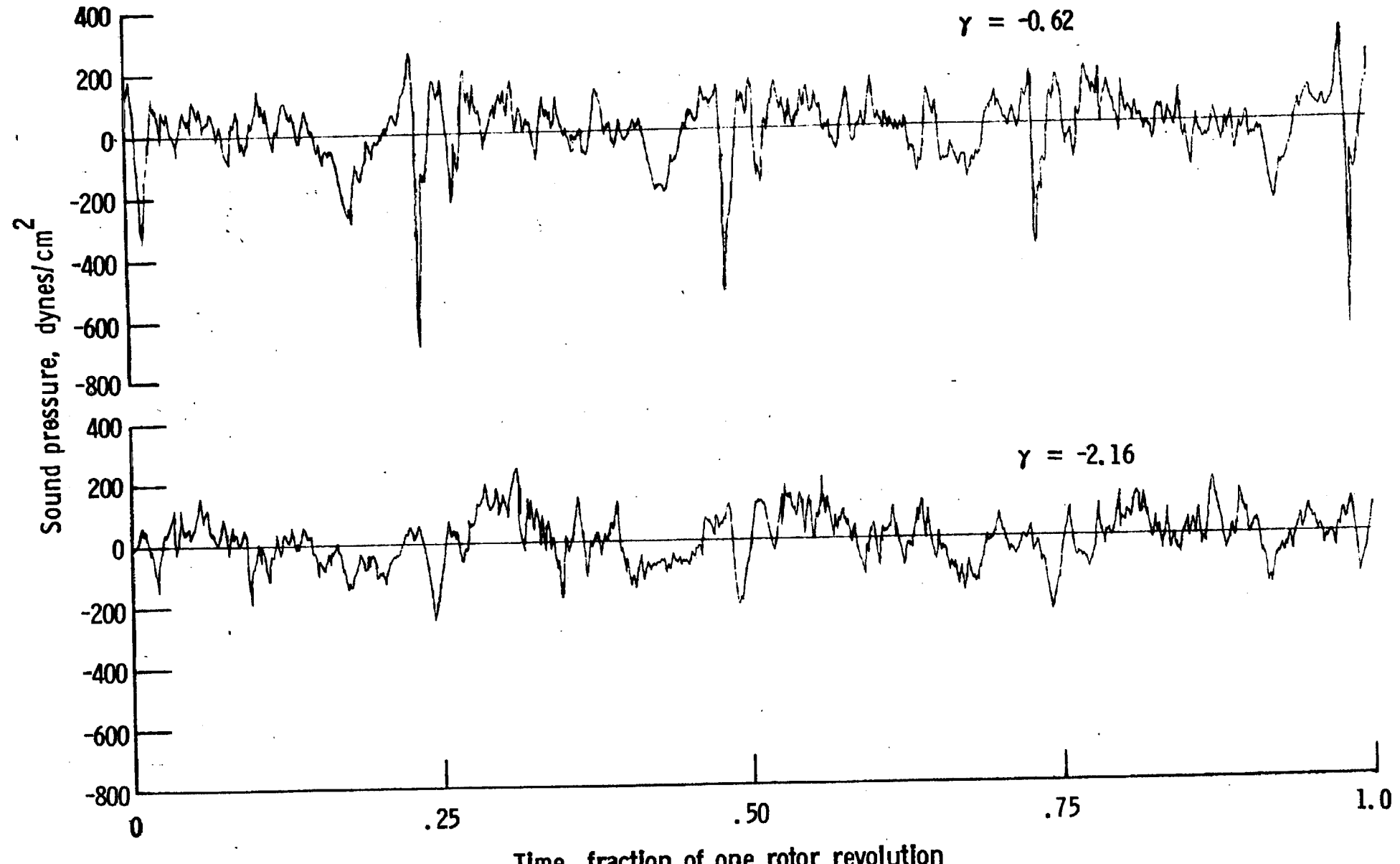
Figure 42. - Continued.



One-third-octave-band center frequency, kHz

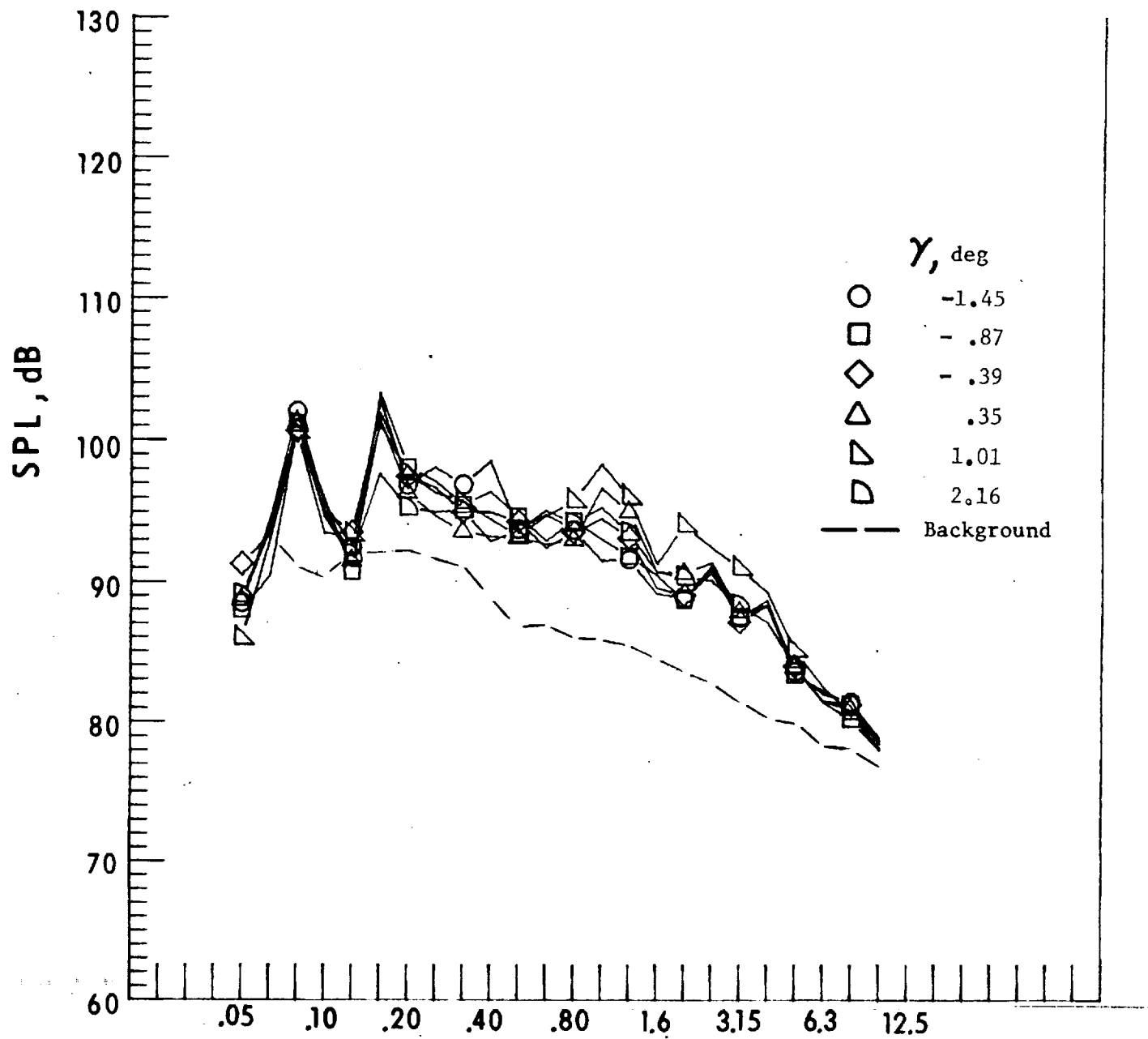
d. Mic. no. 3.

Figure 42. - Continued.



e. Pressure-time histories, Mic. no. 3.

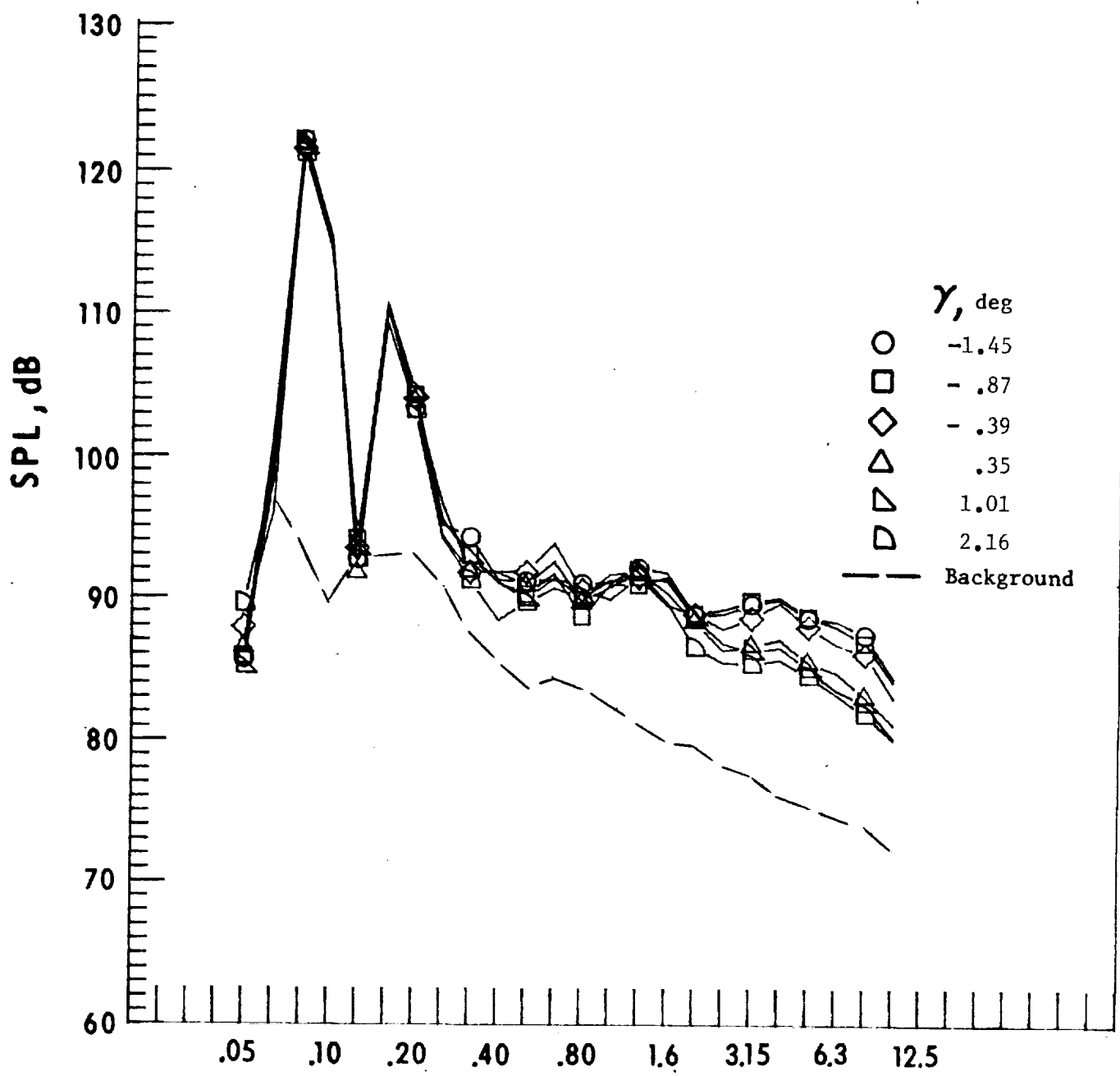
Figure 42. - Concluded.



One-third-octave-band center frequency, kHz

a. Mic. no. 1.

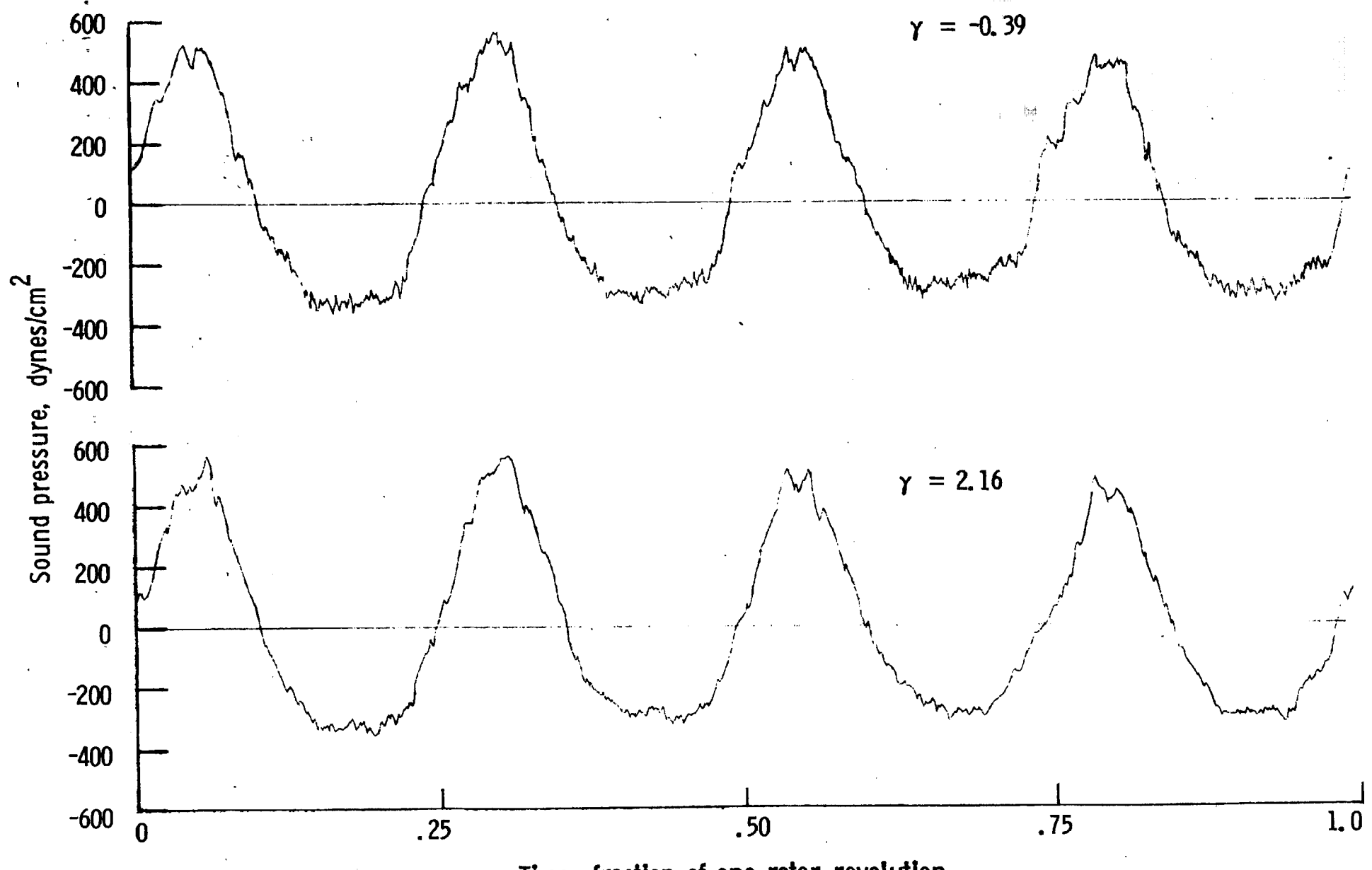
Figure 43. - Effect of descent angle variation on noise generated by helicopter model with square tips installed. $V_\infty = 91.5$ knots.



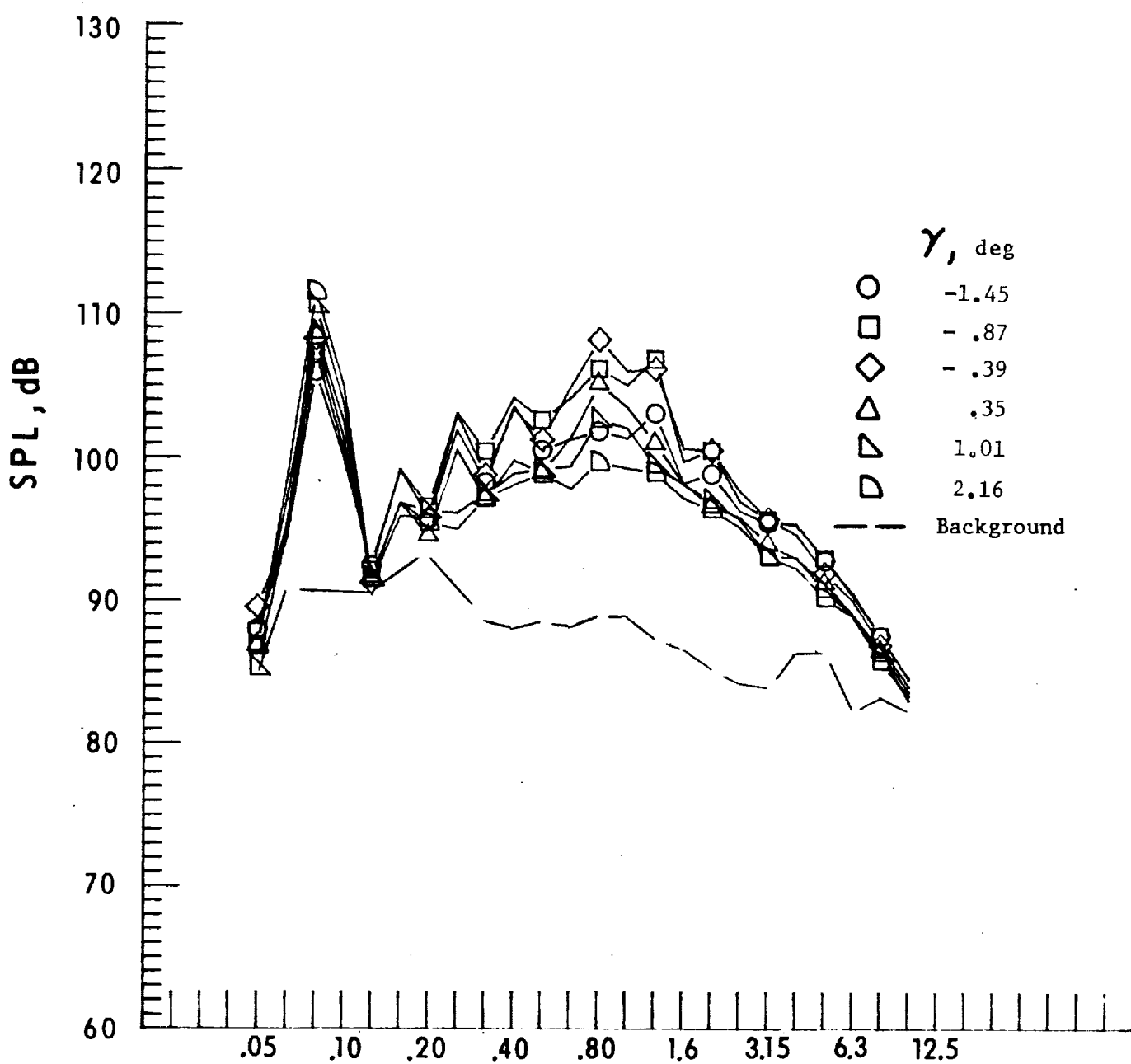
One-third-octave-band center frequency, kHz

b. Mic. no. 2.

Figure 43. - Continued.



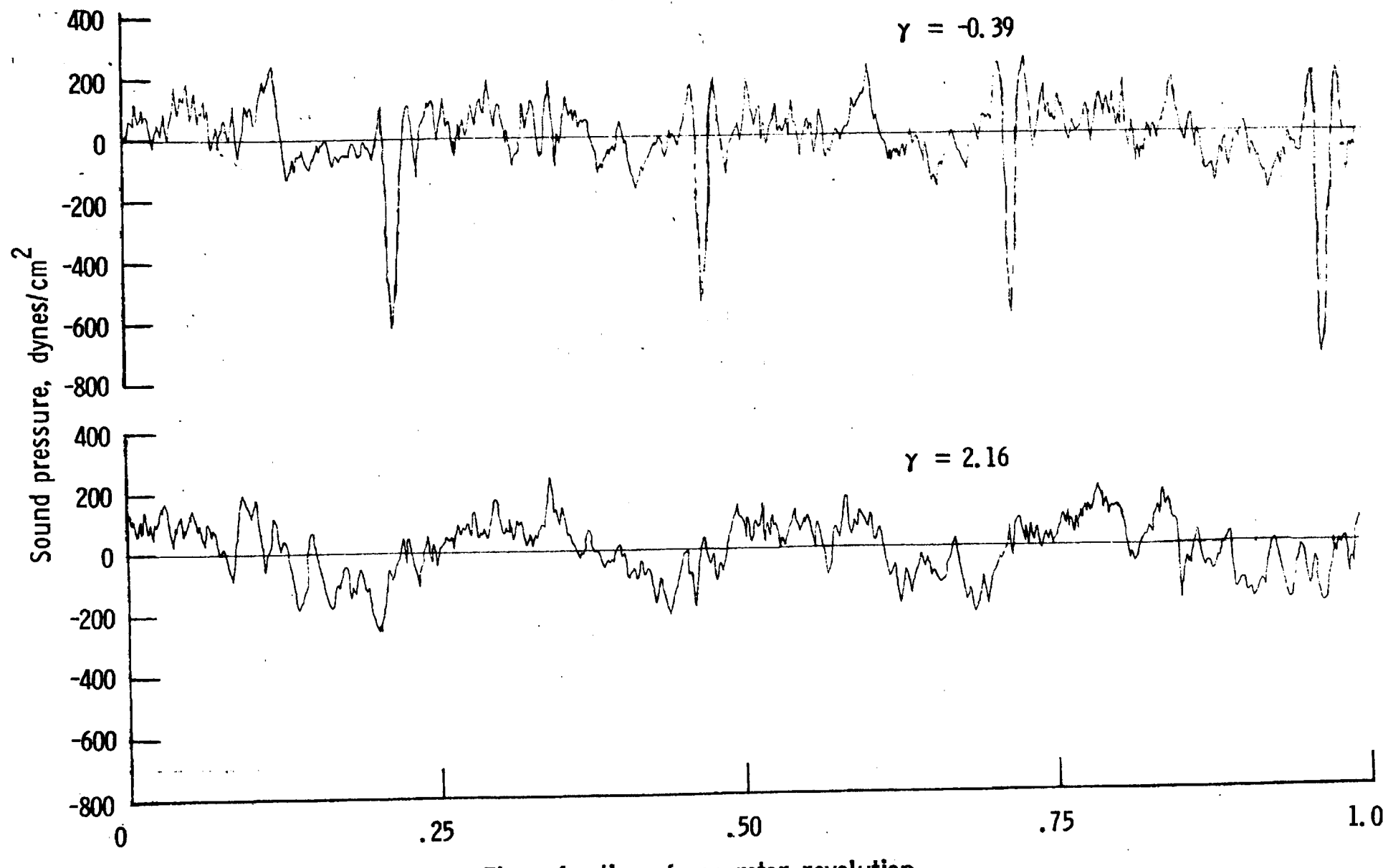
c. Pressure-time histories, Mic. no. 2.



One-third-octave-band center frequency, kHz

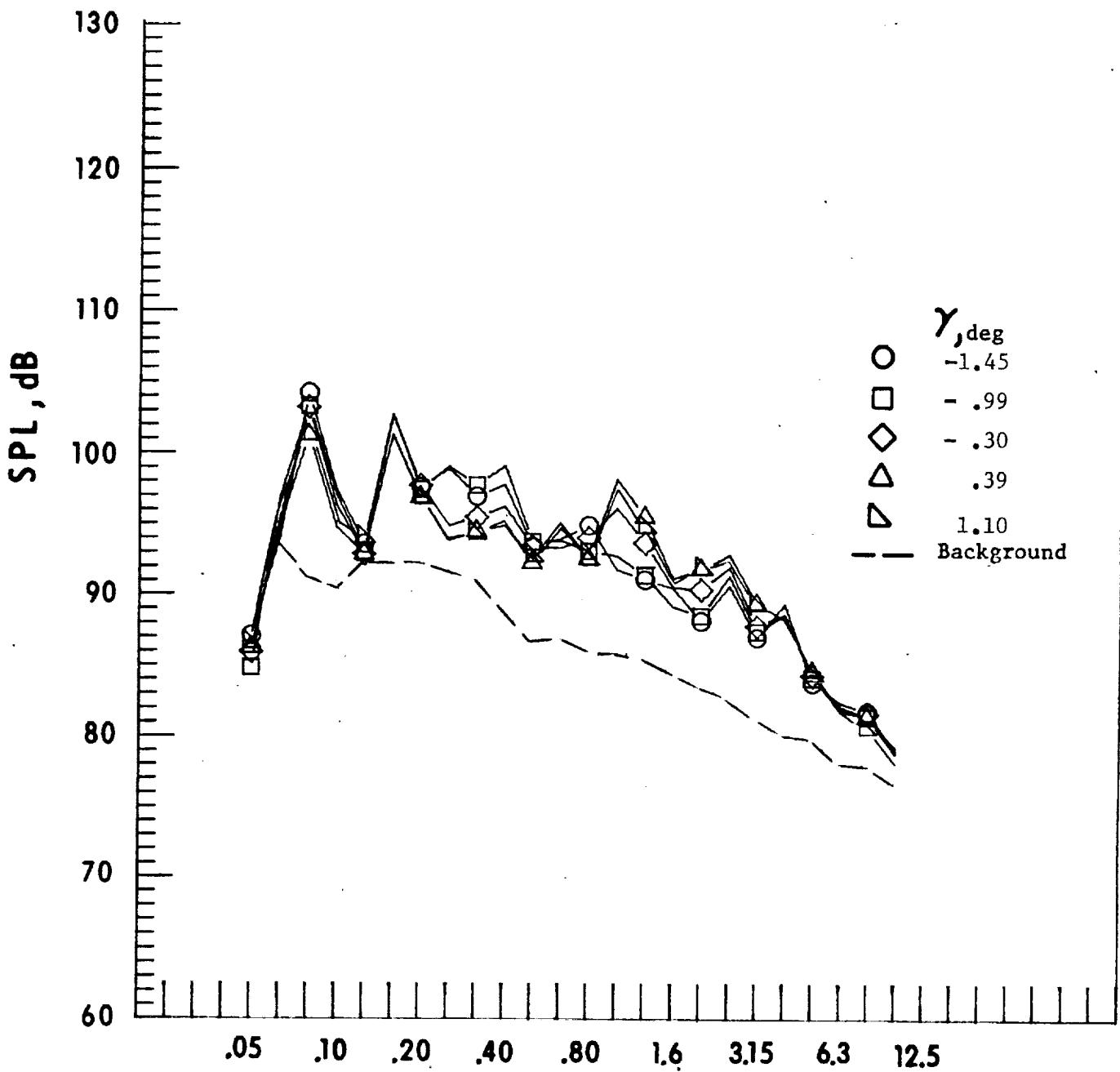
d. Mic. no. 3.

Figure 43. - Continued.



e. Pressure-time histories, Mic. no. 3.

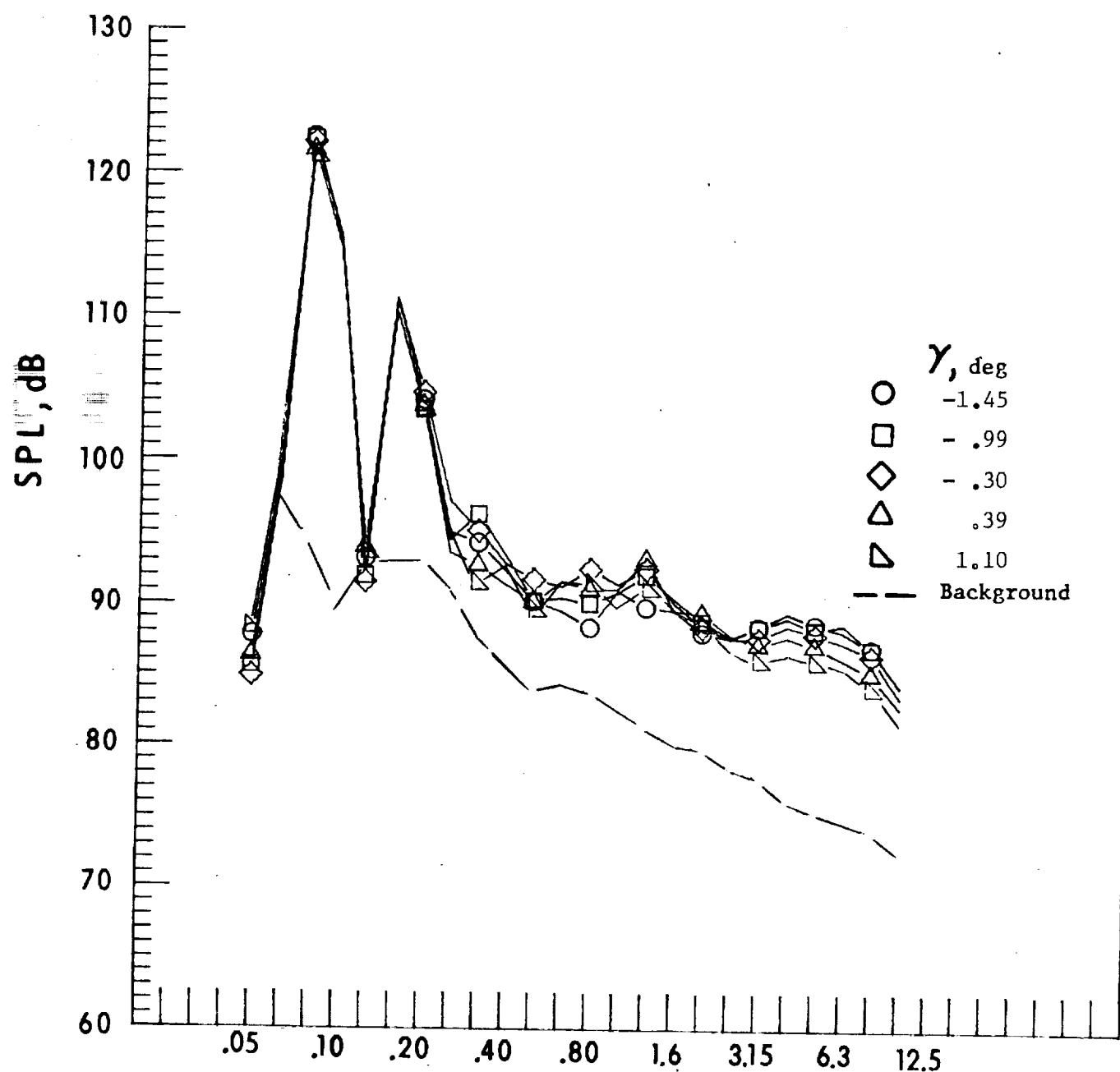
Figure 43. - Concluded.



One-third-octave-band center frequency, kHz

a. Mic. no 1.

Figure 44. - Effect of descent angle variation on noise generated by helicopter model with sub-wing tips installed. $V_{\infty} = 91.6$ knots.



One-third-octave-band center frequency, kHz

b. Mic. no. 2.

Figure 44. - Continued.

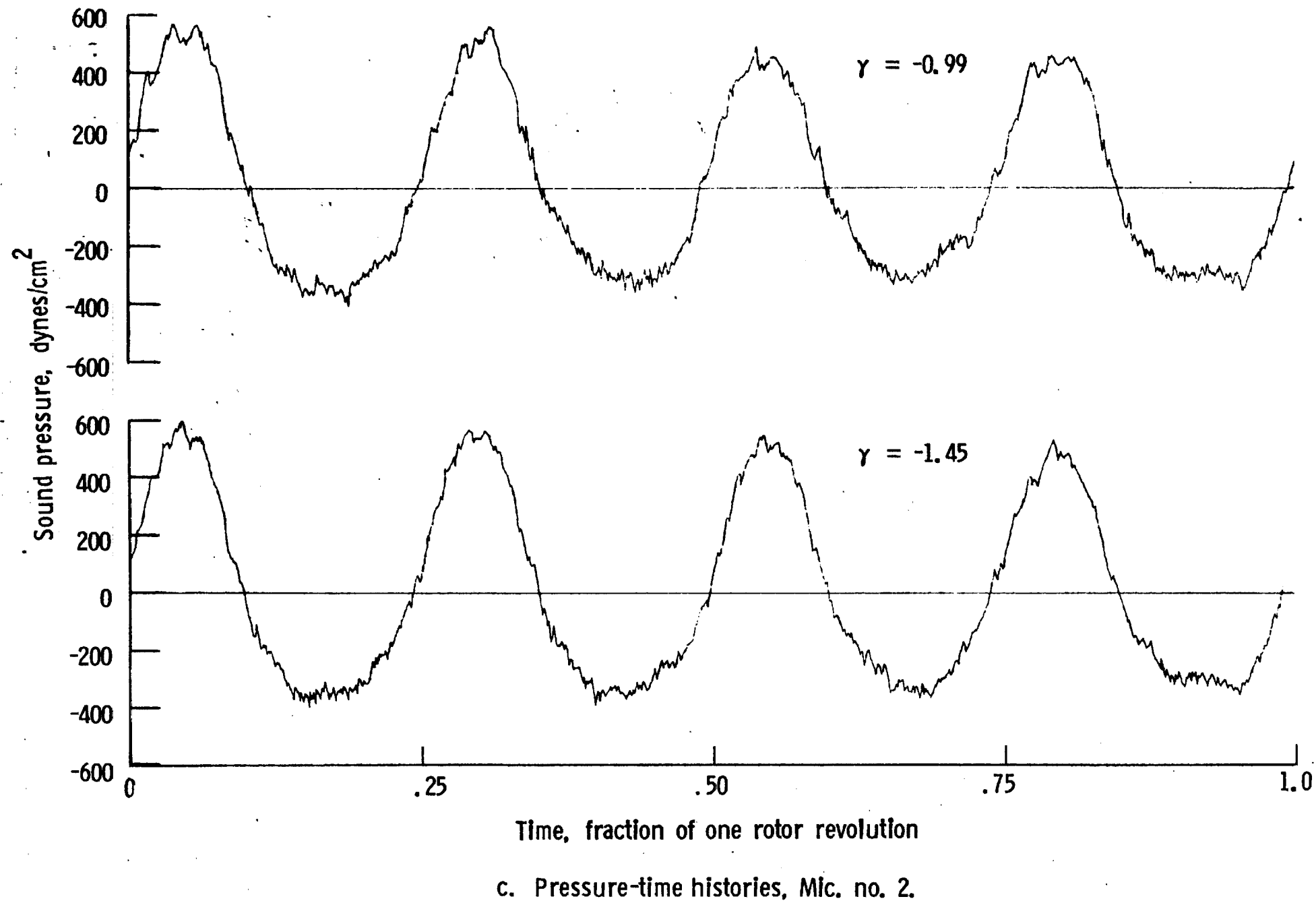
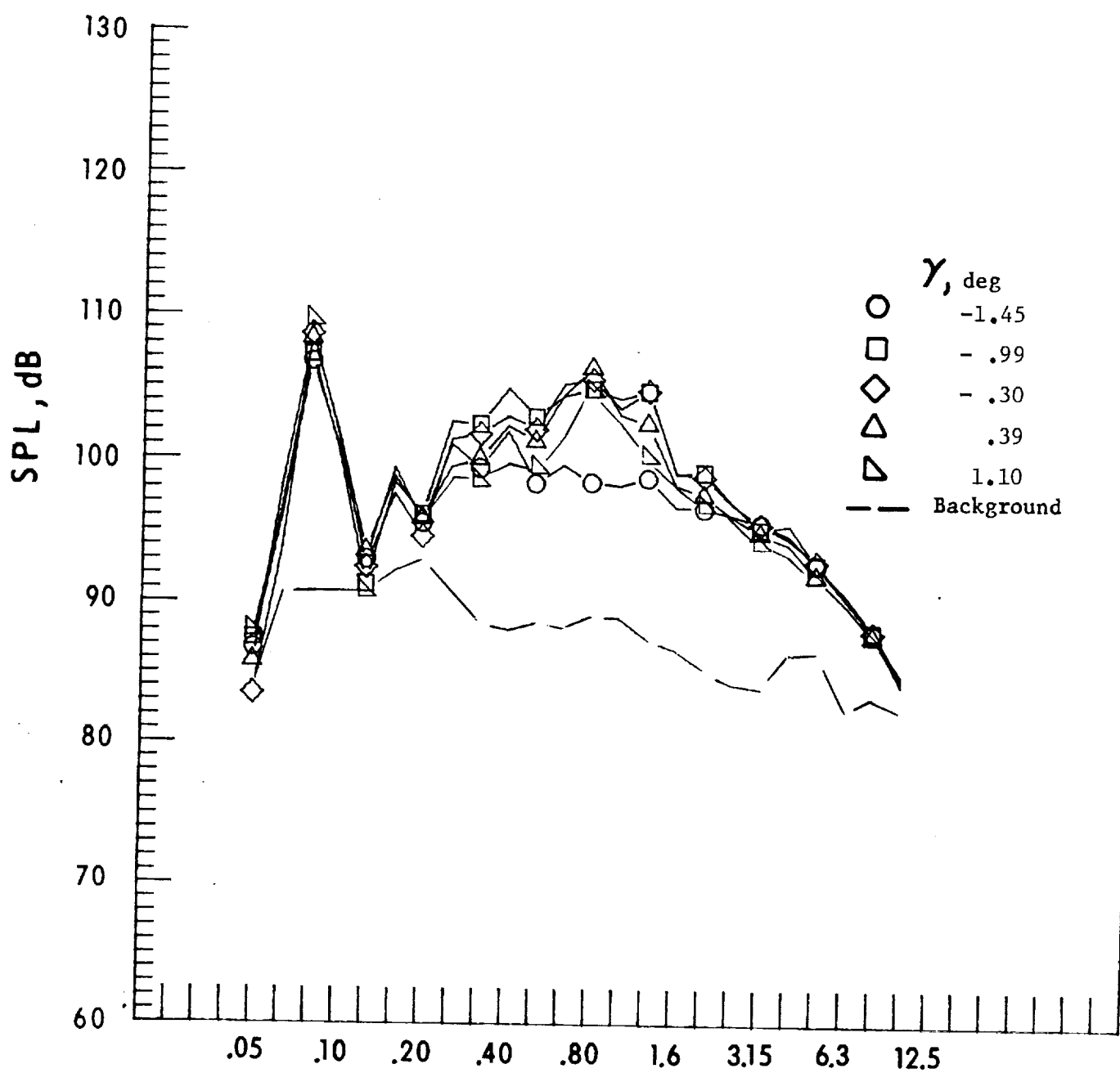


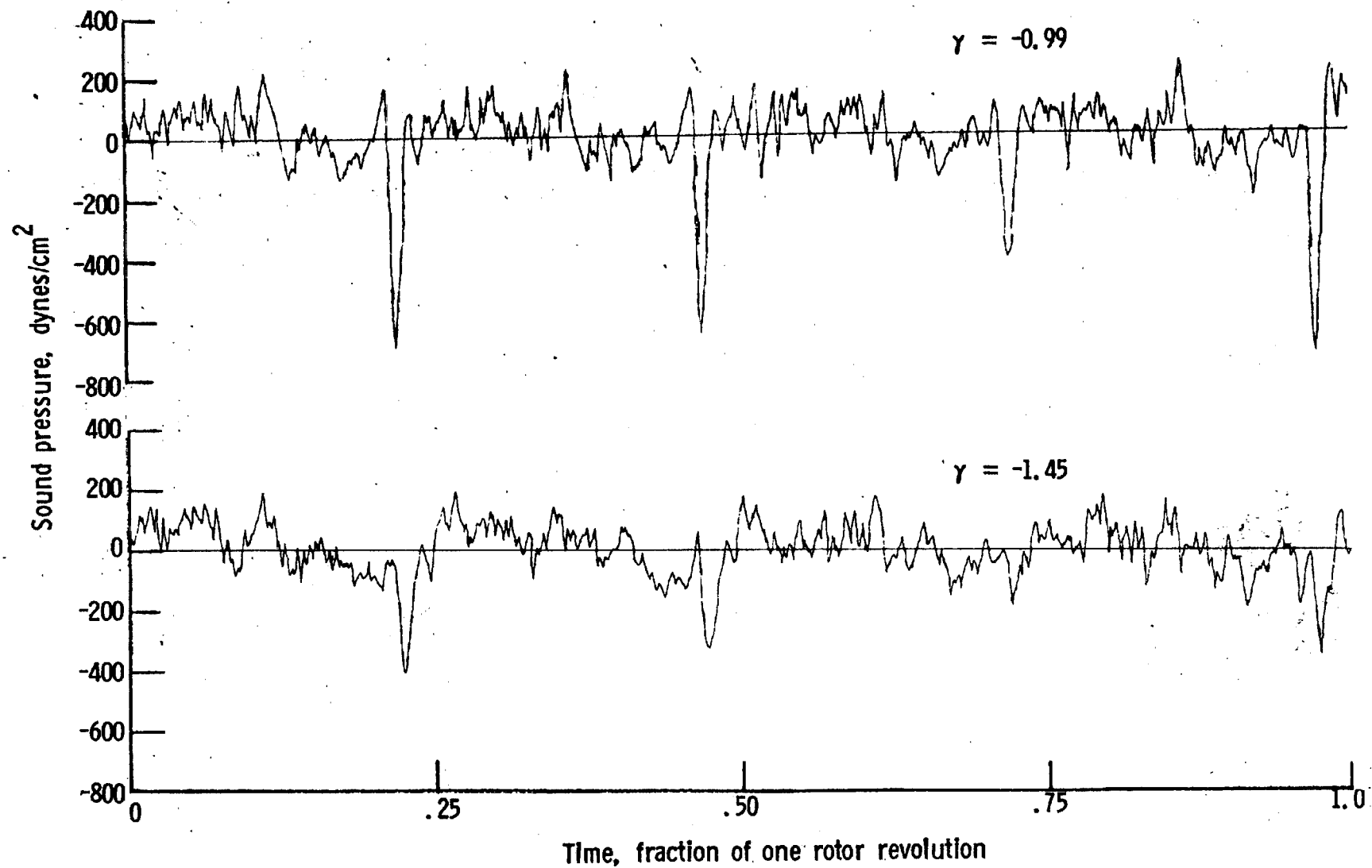
Figure 44. - Continued.



One-third-octave-band center frequency, kHz

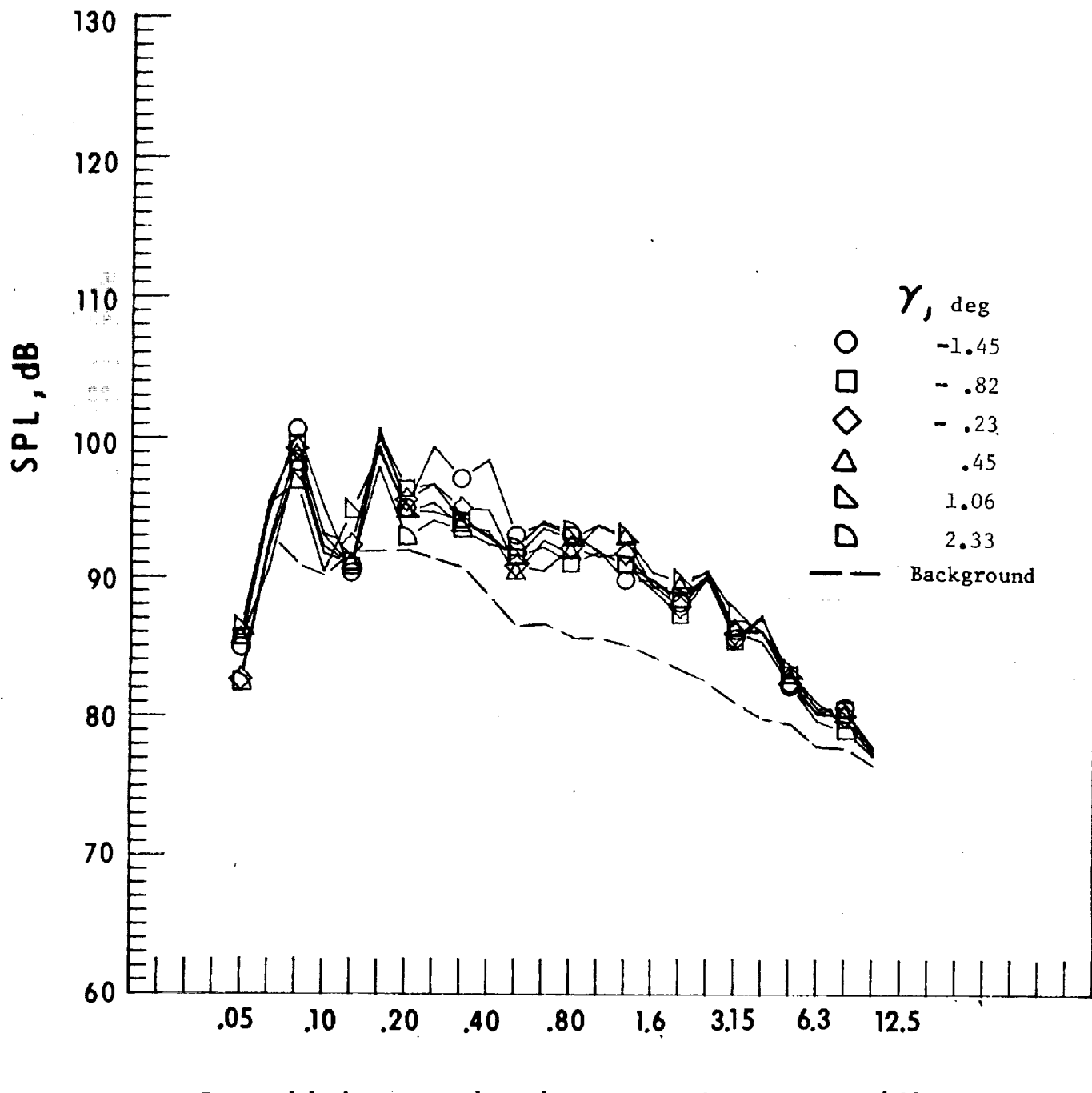
d. Mic. no. 3.

Figure 44. - Continued.



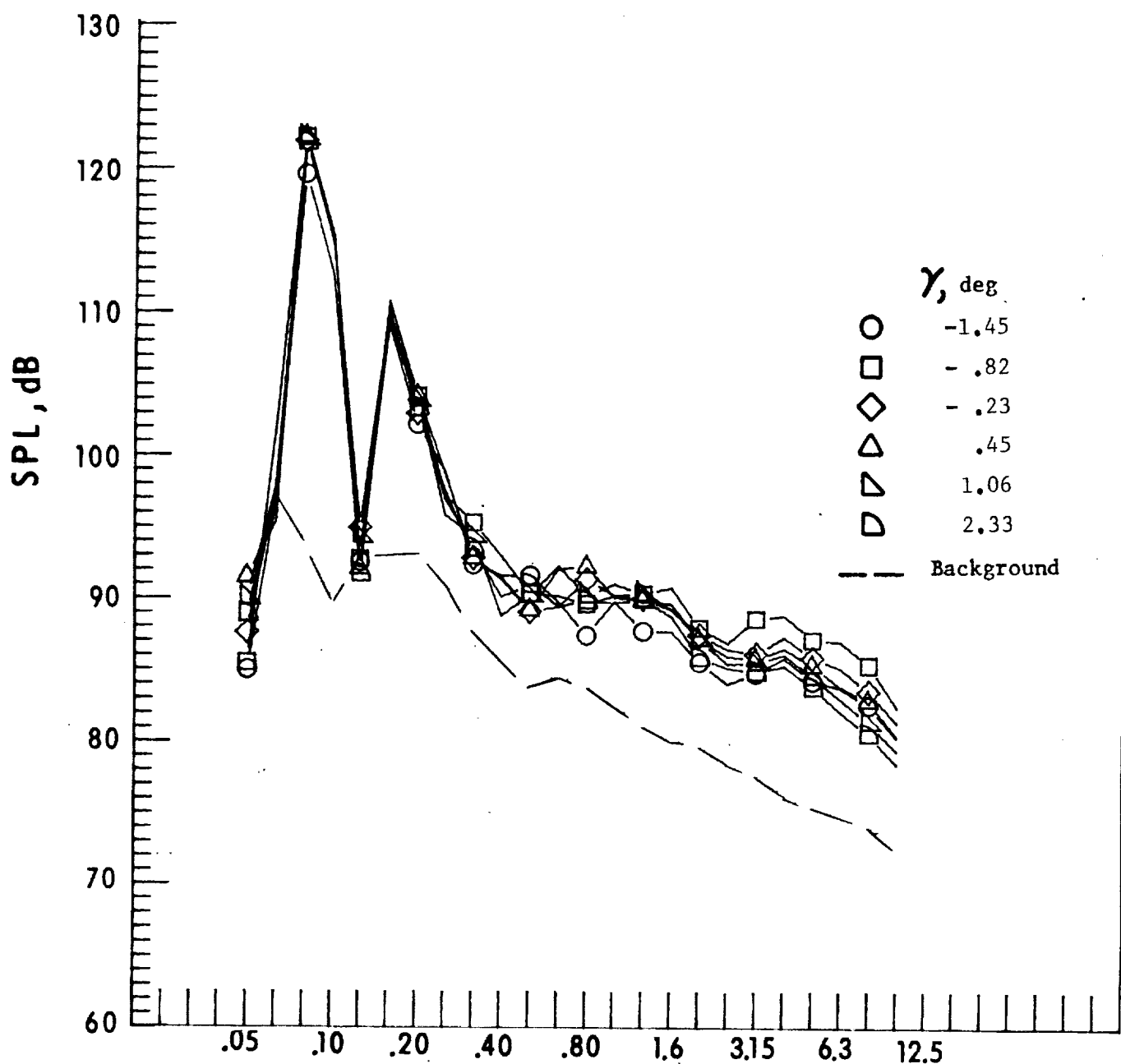
e. Pressure-time histories, Mic. no. 3.

Figure 44. - Concluded.



a. Mic. no. 1.

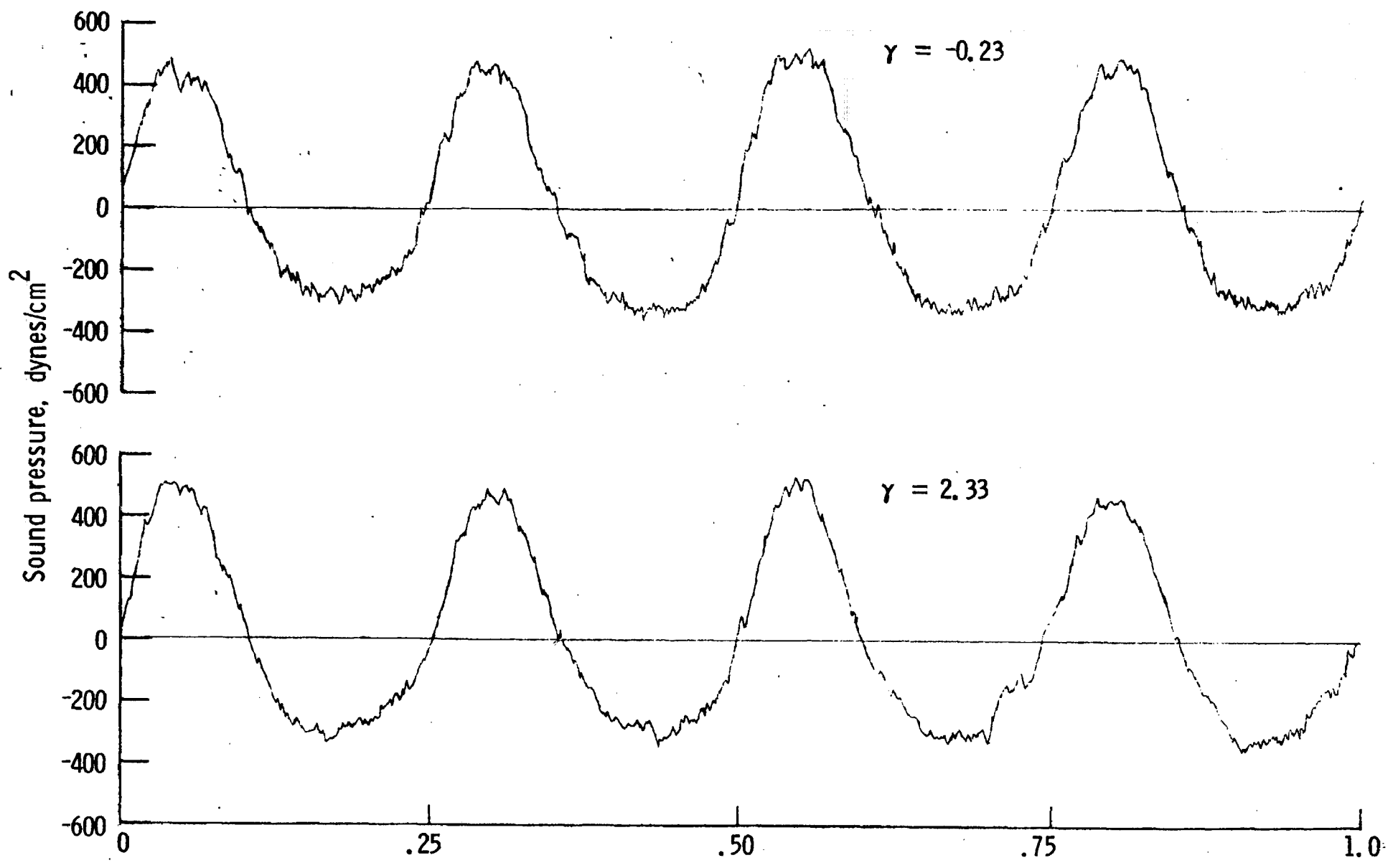
Figure 45. - Effect of descent angle variation on noise generated by helicopter model with swept-tapered tips installed. $V_\infty = 91.1$ knots.



One-third-octave-band center frequency, kHz

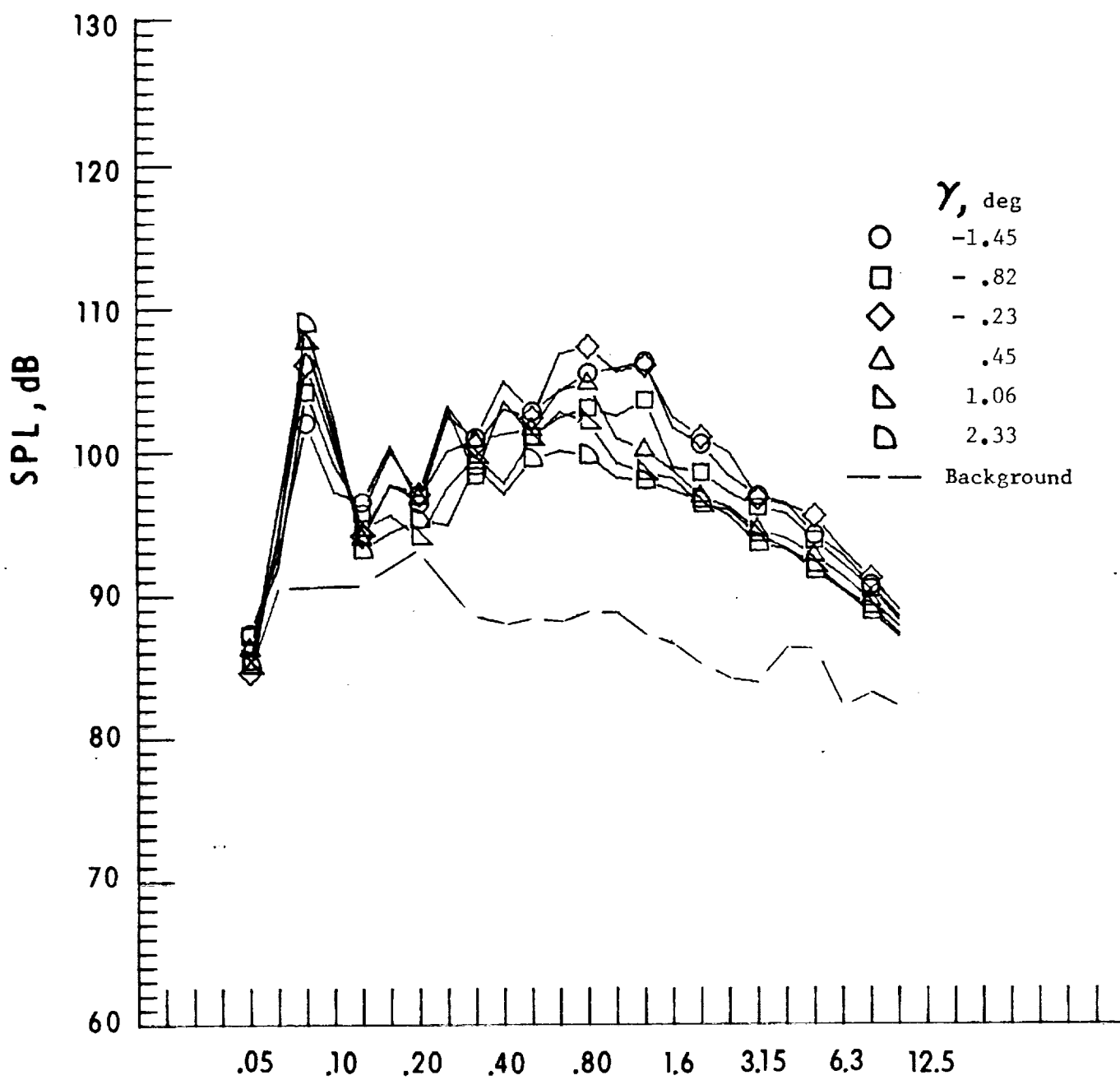
b. Mic. no. 2.

Figure 45. - Continued.



c. Pressure-time histories, Mic. no. 2.

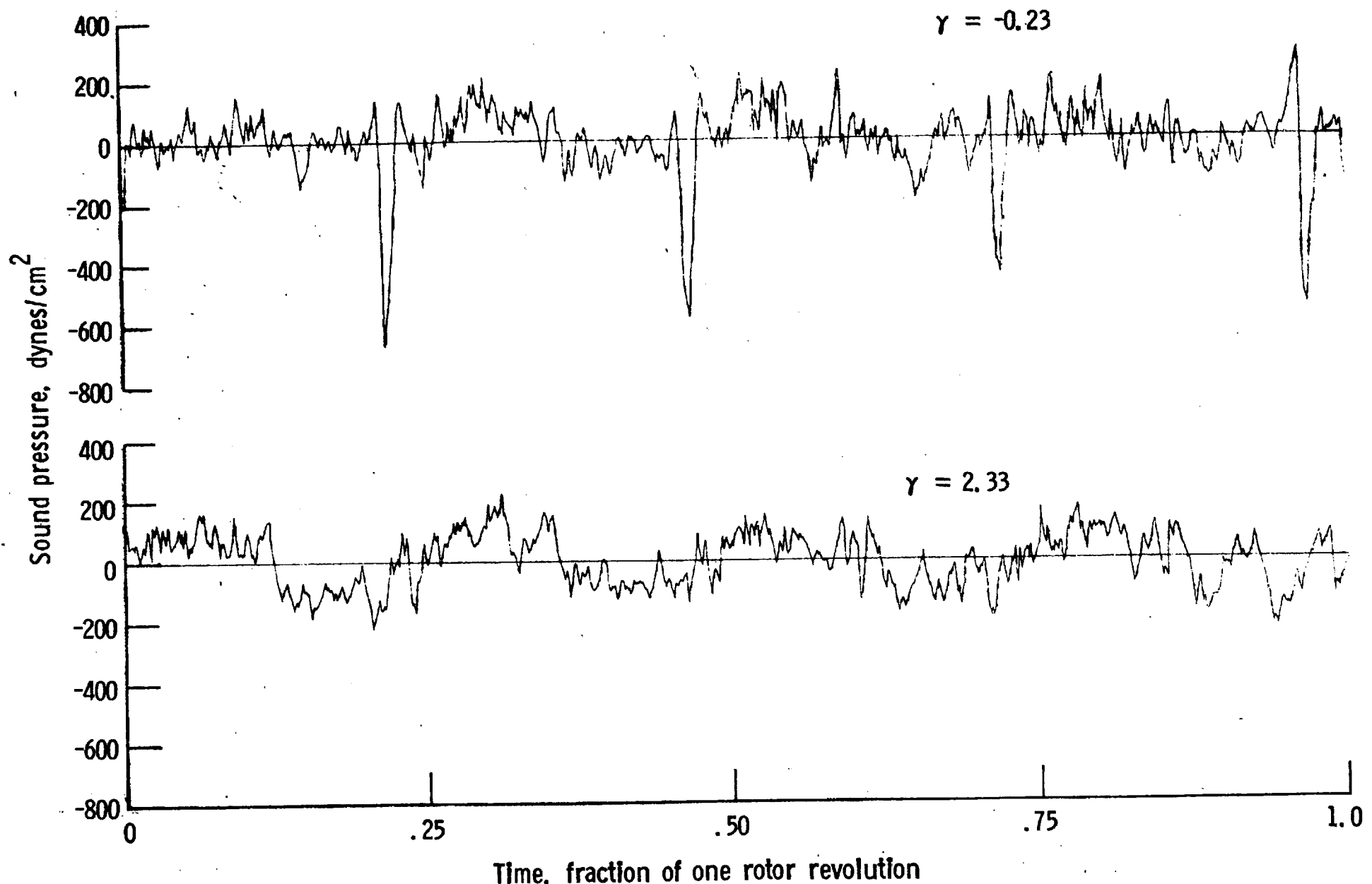
Figure 45. - Continued.



One-third-octave-band center frequency, kHz

d. Mic. no. 3.

Figure 45. - Continued.



e. Pressure-time histories, Mic. no. 3.

